T E R T I A R Y O P H I O L I T E - R E L A T E D

S E D I M E N T A T I O N I N S. W. T U R K E Y

Anthony Bryan Hayward (B.Sc. Aston)

Thesis submitted for the degree of

Doctor of Philosophy

University of Edinburgh

1982

To Dianne - Thank you

How many years can a mountain exist
Before its washed to the sea?
Yes, 'n' how many years can some people exist
Before they're allowed to be free?
The answer, my friend, is blowin' in the wind,
The answer is blowin' in the wind.

Bob Dylan, 1962.

DECLARATION

This thesis has been composed by myself and, except where specifically stated, is my own work.

Anthony Bryan Hayward

12.1.82

ABSTRACT

The Lycian Tauride mountains of S. W. Turkey comprise a central relatively autochthonous carbonate platform unit bordered by two allochthonous units, the Lycian Nappes to the west and the Antalya Complex to the east. From these allochthons thick sequences (~1,000 m) of clastic sedimentary rocks were shed during the Miocene into a basin floored by the subsided carbonate platform.

The Miocene sediments, exposed over ca. 2,500 km^2, have been mapped at 1:25,000 scale; several hundred sedimentary logs have been measured. Three new formations are recognised; the Kemer and Salir Formation of Lower Miocene age, and the Kasaba Formation of Middle to Upper Miocene age. Individual sedimentary facies are dominated by coarse grained ophiolite-derived sediments of which redeposited and subaerial conglomerates, and sandstones are the most widespread.

Along the western margin of the basin closest to the Lycian Nappe front, the Kemer Formation consists of conglomerates and sandstones deposited within a fan-delta. More distal sequences pass basinwards into small submarine fan systems. The overlying Kasaba Formation was deposited as an alluvial fan which prograded into a shallow sea. Proximal alluvial fan deposits consist of dominantly clast-supported massive conglomerates. These pass downslope into well defined conglomerate-sandstone-mudstone fining-upward units. Shallow marine shelf deposits are the lateral equivalents of this distal fan/braidplain succession. Small patch reefs were developed in the marine sequence during periods of reduced sediment supply.

In more central parts of the basin a thick (~800 m) sequence of redeposited bioclastic breccias was derived from a contemporaneous shallow water carbonate build-up. In the south, limestone conglomerates, calcareous sandstones and mudstones, deposited in a submarine fan environment document the uplift and subaerial exposure of a large area of the older carbonate platform.

Along the eastern margin of the basin the Salir Formation mainly comprises conglomerates and sandstones deposited by sediment gravity flows on small submarine fans. Above is a conglomerate dominated sequence deposited on a fan-delta.

Palaeocurrents and downslope facies transitions demonstrate that the ophiolitic sediments of the Kemer Formation were derived from the Lycian Nappe ophiolitic unit to the west. Emplacement of this unit

onto the carbonate platform in Lower Miocene times evidently resulted in irregular subsidence, with uplift and subaerial exposure of areas of older carbonate platform rocks. The western margin of the basin was progressively overthrust until the nappes finally came to rest in the Late Miocene. The regressive-upwards sedimentary sequence reflects both progressive basin infilling and Late Miocene lowering of sea level.

Along the eastern margin, palaeocurrent analysis and downslope facies transitions show that the Antalya Complex was emplaced from the east but only advanced a short distance beyond the eastern margin of the basin. This is consistent with strike-slip dominated emplacement of the Antalya Complex in contrast to the gravity driven emplacement of the far travelled Lycian Nappes. As the Lycian Nappes and Antalya Complex approached the basin from opposite directions their respective ophiolite units must have been derived from separate, or at least distinct, ocean basins to the north and south respectively, of the carbonate platform now flooring the Miocene basin between them. The wider plate-tectonic implications of this conclusion are investigated briefly.

Türkiye nin Güneybutisinda ofiyolitlerle iliskili olarak olusmus Tersiyer çökelimi

Güneybati Türkiye deki Lusiyen Toros dağlari, merkezi durumdaki görece allokton karbonat platformu birliği ve de bunun batisindaki Lusiyen naplari ile doğusundaki Antalya Karmasiği allokton birliklerinden olusur. Tabani, göcmüs karbonat platformundan olusan çanağa, Miosende bu kalin (~1.000 m) kirintili çökel istiflerinden türeyen matiemeter döküImustür.

2.500 km^2 den fazla bir alani kaplayan Miosen çökelleri 1/25.000 lik ölçekte haritalanmis, yüzlerce çökel kesiti ölçülmüştür. Alt Miosen - Miosen yasli Kemer ve Salir Formasyon - lari ve örta-ust Miosen yasli Kasaba Formasyonlari gibi 3 yeni formasyon ayirtlan-mistir. Her bir çökel fasiyesinde, ofiyolitlerden turemis malzemelerin yeniden çökelmesinden olusmus kalin-kirintili çökellen egemendir. Bunlar aroninda en yaygin olanlari Karasal çakiltaşlari ile kumtaşlaridir.

Lusiyen Naplari cephesine en yakin olan; çanağin bati kenari boyunca; çakitasi ve kumtaşlarindan olusan Kemer Formasyonu fan (Velpaze)-delta ortaminda olusmustur. Daha ince taneli istifler çanak doğrultusunda kücük deniz ici fan sistemlerine gecis gösterirler. Üstteki Kasaba Formasyonu sığ deniz içine doğru ilerlemis bir alüvyon fani şeklinde olusmustur. Kalin taneli aluvyon olusuklari genellikle tane-destekli masif çakil-taşlarindan olusurlar. Bunlar yokuş-asağı doğrultu da iyi gelişmiş, yukari doğru incelen Çakitaşi - Kumtaşi - Çamurtaşi birliklerine dönüşürler. Sığ deniz sahanliği olusuklari, ardalanma gösteren bu ince taneli (distal) fan olusuklari ile, derin deniz duzlukleri olusuklarinin yatay karşiliklaridir. Kücük yama resifleri çökel malzemenin azaldiği dönemlerde deniz istifleri içerisinde olusmustur.

Ganağin daha merkezi yerlerinde kalin (~800 m) biokinntili breşler olusmustur. Bunlari olusturan malzemeler ayni zaman suresinde olusmakta olan sig deniz karbonatlarindan deusirilmişlerdir. Güneyde bir deniz ici fan ortaminda olusmus kirectasi çakiltaşlari, karbonat kumtaşlari ve çamurtaşlari daha yaşli genis karbonat platformu alanlarinin yükselimini ve de karada mostra verdigini belgelemektedir. Çanağin doğu kiyisi boyunca olusmus Salir Formasyonu genellikle; kücük deniz içi fanlari üzerine çökel cekim kaymalari sonucu olusmus çakiltaşlarindan ve kumtaşlarindan meydana gelir. Daha üstte ise içerisinde çakiltasi egemen olan istif bir fan-delta üzerine depolanmiştir.

Eski akinti yönleri ile yokus asagi fasiyes degismeleri ofiyolitik çökellerden olusan Kemer Formasyonunun batidaki Lüsiyen Napi ofiyolitik birligiginden devsirildigini gösterir. Bu birligin Alt Moisende karbonat platformu üzerine yerlesimi muntazam olmayan göçmeyle birlikte daha eski karbonat platformu bölgelerinin yükselmesine ve karada mostra vermesine yol açti. Çanagin bati kenari üzerine gelen sariyajlanmalar naplarin üst moisende durmasina kadar devam etti. Yukari dogru regresif özellikte olan istif: çanagin surekli doldugunu ve ayni zamanda deniz seviye-sinin sürekli bir sekilde alcaldiginida göstermektedir.

Çanagin dogu kiyisi boyunca eski akinti analizleri ve de yokus asagi fasiyes degismeleri Antalya Karmasiginin dogu istikametinden gelerek yerlestigini göstermektedir. Ancak bu yerlesme çanagin dogu kenarindan öteye az bir mesafe katetmistir. Bu genelde Antalya Karmasiginin dogrultu-atimli yerlesim biçimiyle tutarlilik gösterir ki bu durum çekim kaymalari sonucu uzun mesafeler kateden Lusiyen Naplari yerlesimine zit bir durumdur. Lusiyen Naplari ile Antalya Karmasiginin çanaga zit yönlerden yaklasmalari onlarin içerdigi ofiyolitik birliklerin ayri okyanus ortamlarindan türedigini gösterir. Bu ortamlarin Lusiyen Naplari için; bu gün Moisen çanaginin tabanini olusturan karbonat platformunun kuzfyinde; Antalya Karmasigi için ise ayni platformun Güneyinde olmasi gerekir. Bu sonuçlara bagli olarak daha genis anlamda diger plaka-tektonigi iliskileri kabaca arastirilmistir.

Frontispiece

The Lycian Nappes viewed from the Susuz Dağ (waterless mountain). The peak of Ak Dağ (white mountain) rises to over 2,000 m.
Carbonate platform limestones (C) in the foreground are overlain by Miocene clastic sediments (M). These are overthrust by the Lycian Nappes. The basal unit consists of an Eocene flysch sequence (E), this in turn is overthrust by an ophiolite complex which in this area is composed dominantly of limestones and radiolarites (L).


L
E
M
C

ACKNOWLEDGEMENTS

This work was carried out during the tenure of a studentship from the National and Environmental Research Council. I thank Professors Sir Frederick Stewart and G. Y. Craig for providing facilities at the Grant Institute. The project was viable only through the logistical support and co-operation of the Mineral Research and Exploration Institute (Maden Teknik ve Arama Enstitusü) of Turkey, in particular the assistance of Erdogoan Demirtaşli. I am also grateful to Necdet Ozgul, Bilsel Keçeli, Reşat Kengil, Mustufa Şenel and Kutlu Tanner for logistical help at various stages during my time in Turkey.

Special thanks go to my supervisor, Alastair Robertson, for his constant encouragement, enthusiasm, help and advice during my stay in Edinburgh.

Technical help and expertise in Edinburgh were provided by Geoff Angell, John Miller, Flo Coxon, Diana Baty, Kenny Cameron, Jim Goodall and Peder Aspen. Colin Chaplin spent many hours of his time assisting with the photographs. Thea Grieve made the library feel like a second 'home'.

Without the results provided by a large number of palaeontologists the project would not have reached fruition. They are: Geoff Adams, Brian Rosen, G. Glacon, A. Poignant, M. Neumann, Ibrahim Çakmak, Cihade Kiragli and a number of palaeontologists visiting the M.T.A. Antalya camp in the summer of 1980.

I am extremely grateful to Maureen Fulton who drafted many of the diagrams and helped in numerous ways during the completion of this manuscript. John Boyle, Andy Martin, Dave Winter and Graham Shimmiel exercised able and willing editorial prowess on earlier versions of the manuscript. Gurhan Aktaş translated the abstract into grammatically correct Turkish. The typing was performed rapidly and skilfully by Lucian Begg.

I have benefited from informal discussion with many other scientists, amongst them are: John Waldron, John Martin, Terry Scoffin, John Dixon, Dorrick Stow, David Ince, Bryan Lovell, John Miller, Nigel Woodcock, Roy Gill, Roger Scrutton, Mustufa Şenel, Erdoğoan Demirtaşli, Sait Bolükbaşi, Mike Johnson, John Ridley, Joan Megson, Jerry Jameson, Gurhan Aktaş, John Boyle, Brian Rosen, Jean Dumont, Alan Heward, Gilbert Kelling and Peter Turner.

However, my greatest debt is to the people of Finike and Kaş whose friendliness, hospitality and kindness made every summer in

Turkey a wonderful experience. In particular, I shall never forget Mehmet Soydaş and his family, Bechet Ozkan, and my two drivers Arif Önder and Faruk Fayan who collectively instructed me in the art of speaking and living the Turkish way of life to the full.

CONTENTS

CHAPTER 3 (continued)

PART IV - CONCLUSIONS

LIST OF TABLES

LIST OF FIGURES

PART I

INTRODUCTION

PART I

INTRODUCTION

CHAPTER 1 INTRODUCTION

CHAPTER 1

1.0 Introduction

1.1 Rationale

It is widely accepted that vast areas of the Alpine-Mediterranean-Himalayan mountain fold belt comprise structurally complex areas of autochthonous and allochthonous rock units. These units are generally interpreted to have formed in environments analogous to present day ocean basins and margins. Large ophiolite terrains include oceanic crust generated at some form of fossil constructive margin. Associated sedimentary sequences formed along rifted continental margins, and as pelagic sediments overlying the oceanic crust. This assemblage of igneous and sedimentary rocks record the history of an ancient ocean basin, the Tethys, which was largely destroyed during the Mesozoic to Tertiary northward drift of Africa (Dewey *et al.*, 1973). The majority of the ophiolites preserved in the Alpine-Mediterranean orogenic belt represent oceanic crust formed during the Jurassic and Cretaceous and emplaced during the Cretaceous and Tertiary. They are therefore probably related to the separation of microcontinental fragments along the margin of Tethys, rather than to spreading within the central part of the ocean (Smith, 1973).

Palinspastic reconstruction of this *"Neo-Tethys"* ocean in the Mesozoic and Tertiary are particularly dependant on knowledge of the direction and timing of emplacement of tectonically transported allochthonous units. Diametrically opposed solutions are still being put forward, particularly for the Hellenides (e.g., Barton, 1975 and discussion) and the Taurides (Dumont *et al.*, 1972a, b; Brunn *et al.*, 1973; Ricou *et al.*, 1974, 1979; Brunn, 1976; Robertson and Woodcock, 1981a; Woodcock and Robertson, 1981b). Most of the arguments are based on regional lithostratigraphical correlation and comparison and detailed analysis of structural style in the allochthonous units.

In this study an alternative approach is adopted: *the determination of emplacement direction by detailed facies analysis of in situ sedimentary sequences in autochthonous blocks adjacent to and underlying the allochthons.* These deposits, the majority of which are derived from the allochthonous units, record the *timing*

and *direction* of emplacement in sequences which have not been subsequently much deformed.

In southwestern Turkey (Fig. 1.1) the debate is whether the Mesozoic rocks of the Antalya allochthon have been transported far from the north *internally* over a contemporaneous carbonate platform, or alternatively whether the rocks were rooted *externally*, that is to the south in the area of the present Mediterranean Sea. The local carbonate platform autochthon (Fig. 1.2) passes up into a thick sequence mostly of mid-Tertiary clastic sediments, which yield critical data on timing, mechanism and direction of emplacement.

The primary objective of this study was therefore to relate variations in *sedimentary facies* within the autochthonous sequence to the large scale emplacement of the allochthonous units. This objective was achieved at a relatively early stage in the study and emphasis changed from a regional approach to a more detailed study of a small, laterally variable sedimentary basin. With the aim to reconstruct the sedimentological history of the basin from its inception in Lower Miocene times to its termination in Upper Miocene times.

In addition the Tertiary sedimentary sequence reveals well exposed sections through dominantly two coarse grained depositional environments: the *alluvial fan* and associated sedimentary system, and the *submarine fan* and its associated facies. The transition between these two environments in areas where they are closely related geographically remains poorly understood. During the course of this study it became evident that this area provides an opportunity to relate the two, and this work is one of the few three dimensional studies of alluvial fans that pass downslope into submarine fans.

1.2.0 Methods and Organization

1.2.1 Fieldwork

Fieldwork was carried out over three summer field seasons totalling approximately 9 months. An area of approximately 2,500 km^2 was mapped in reconnaissance at a scale of 1:25,000, a geological map, reduced to 1:50,000 and cross-sections are included in the back of this thesis, the grid on the map is identical to that on the Turkish Government Topographic maps. During mapping use was made of

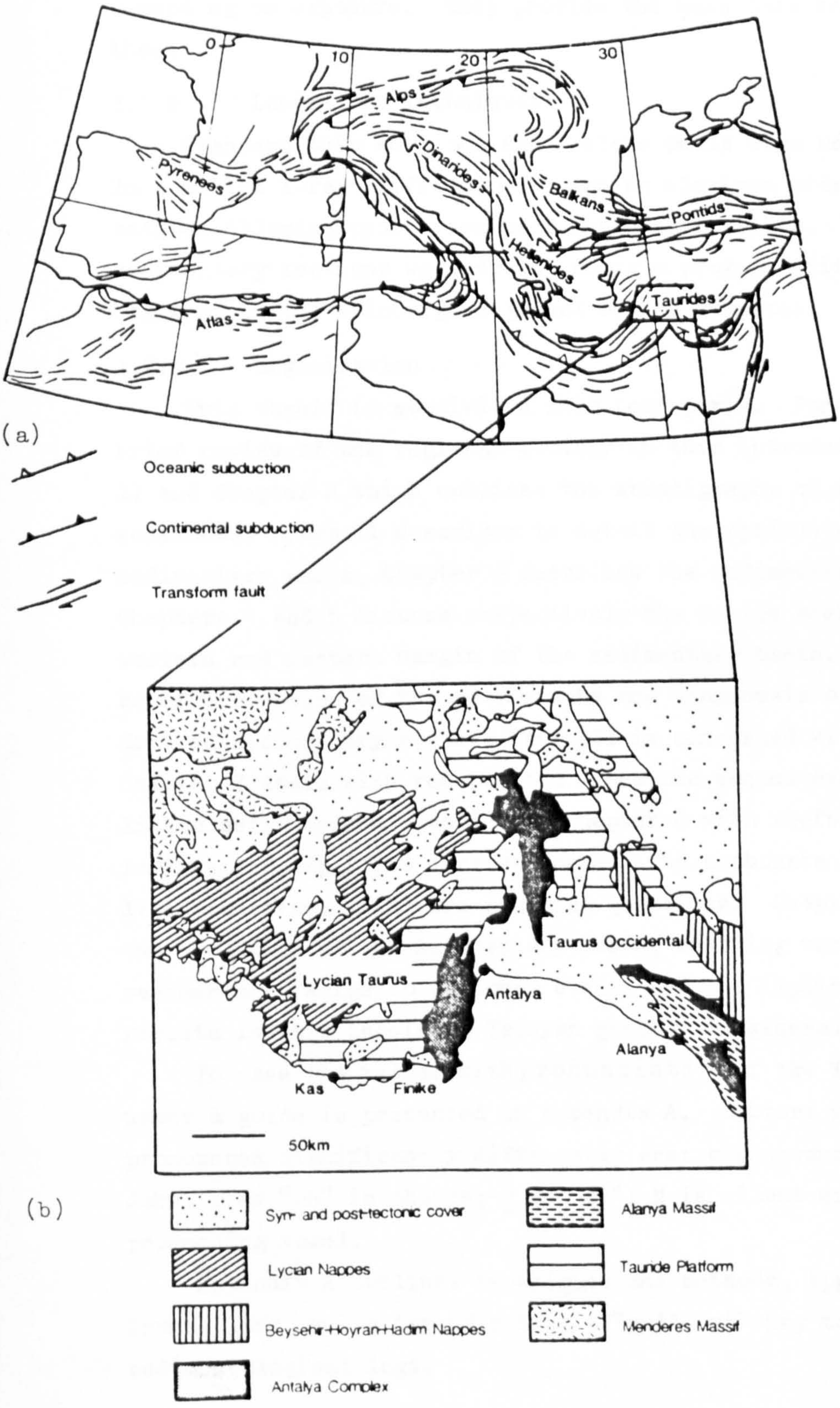

Fig. 1.1 Location map showing the structural trends and plate boundaries of the alpine orogenic belt (a) and the main structural units in southwest Turkey (b).

aerial photographs. Pace and compass sketch maps were made of several critical areas.

Much of the time was spent measuring sections. Approximately 350 sedimentological sections were measured at various scales, depending on exposure. They provide the main data base for this thesis.

1.2.2 Laboratory Techniques

Standard thin sections and acetate peels were used extensively. In addition X-ray diffraction, scanning electron microscopy and cathode illuminescence were used where appropriate. Some of the sedimentary sections were drawn, using a program written by J. W. F. Waldron, on the Edinburgh Regional Centre Computer.

1.2.3 Organization

This thesis is subdivided into four parts. Part I comprises a brief review of the regional geology in this introduction (Chapter 1) and Chapter 2 which outlines the stratigraphy of the Miocene sediments. Part II describes in detail the ophiolite-derived sedimentary units, Chapter 3 describes the sedimentary facies present, Chapters 4 and 5 discuss respectively the facies associations of the western and eastern margin of the sedimentary basin. Chapter 6 is a brief discussion of the petrography and diagenesis of the ophiolite-derived sedimentary rocks. Part III is concerned with carbonates. Chapter 7 deals with redeposited limestone sequences, both lithoclastic and bioclastic and Chapter 8 with reefs. Chapter 9 reviews and amplifies earlier work on the carbonate platform. Part IV is concerned with more regional questions. Chapter 10 summarises the evolution of the sedimentary basin, relating variations in sedimentary facies to tectonic events and the implications of results in this thesis to Tethyan geology in general.

To ease the reader with pronunciation of the Turkish place names a guide is presented in Appendix A. Letters which are pronounced significantly differently are: c pronounced as "j", as in John; ç as "ch" in church; ş as "sh"; ğ is silent extending the proceeding vowel.

Appendix A outlines techniques and methods, Appendix B is a faunal list, while Appendix C is a "pull-out" key to the sedimentological logs.

1.3.0 Regional Geology

The Taurides form an extensive mountain chain that lies south of the Anatolian plateau and runs for some 1500 km between the Aegean Sea and Iran. The mountains form an extension of the Alpine Orogenic belt into southwestern Turkey. The Western Taurides (Fig. 1.1) form an arcuate belt divided into two limbs either side of the Gulf of Antalya. East of Antalya the Taurus Occidental extends for 600 km to Anamur (Fig. 1.1). In the west the Lycian Taurus run from Antalya to the Aegean Sea. Their junction north of Antalya is termed the "Coubure d'Isparta" (or "Isparta Angle") (Blumenthal, 1963). This area has been the subject of a recent study by Waldron (1981).

1.3.1 Taurus Occidental

To the east of Antalya the Taurus Occidental comprises a series of paraautochthonous slices dominated by Mesozoic shallow water carbonates. Erosion to a deep structural level reveals that the carbonates are underlain by a Triassic sequence including thick turbiditic sandstones and shales resting on Palaeozoic sedimentary rocks. Resting upon these slices are the Beysehir-Hoyran-Hadim nappes (Fig.1.1)(Brunn *et al.*, 1971; Monod, 1977a). These nappe units contain an ophiolite unit together with a diverse assemblage of Mesozoic and Permian sedimentary rocks, including shallow water carbonates, flysch and volcanoclastic sandstones overlain by Mesozoic pelagic limestones. The nappe's root zone lies to the northeast beneath a thick cover of Neogene fluvial and lacustrine sediments of the Anatolian Plateau. These nappes were emplaced during the Eocene and are now preserved along the axis of a later gentle syncline (Fig. 1.1).

1.3.2 Lycian Taurus

The Lycian Taurus is considered an extension of the Hellenide orogenic belt of Greece (Brunn *et al.*, 1976; Bernoulli *et al.*, 1974; Ozgul and Arpart, 1973). On a regional scale the Lycian Taurus consists of a central paraautochthonous unit, the "Tauride autochthon" (Brunn *et al.*, 1970, 1971; Dumont *et al.*, 1972a, b) either side of which lie two allochthonous ophiolite units, the *Lycian Nappes* to the northwest (Fig. 1.1) and the *Antalya Complex* to the east.

The *Lycian Nappes* comprise a regionally extensive series of allochthonous sheets (ca. 120 x 150 km) believed to have been

transported from the northwest towards the southeast in a number of phases during the early Tertiary era. Within the Lycian Nappes several distinct stratigraphic sequences of Mesozoic to early Tertiary age are recognised (Brunn *et al.*, 1970, 1971; Poisson, 1977). Sedimentary facies range from shallow water "platform" carbonates through redeposited slope breccias to pelagic limestones and cherts. Some of the sequences terminate in a flysch sequence of Eocene age (Poisson, 1977). Along the eastern front of the nappes (Fig. 1.2) this unit occurs at the lowest structural level tectonically intercalated between the underlying autochthon and overlying allochthonous limestones and cherts. It records the initial tectonism and subaerial emplacement of the Lycian Nappes.

The whole assemblage has been interpreted by Delaune-Mayere *et al.* (1974) as different parts of a Mesozoic continental margin which was subsequently emplaced during late Cretaceous and early Tertiary orogenic events. Ophiolitic units in the Lycian Nappe consist of slices of peridotite and diabase intercalated between the nappes. In the Fethiye area (Fig. 1.1) the uppermost structural unit is capped by a peridotite nappe consisting mainly of hartzburgite cut by pyroxenite and dolerite dykes (Brunn *et al.*, 1971; Graciansky, 1972).

To the northwest of the Lycian Nappes lie the Menderes massif, a complex multiple domal structure composed of granitic gneisses, mica-schists and paragneisses overlain by Mesozoic marbles and a thin metamorphosed flysch sequence (Durr *et al.*, 1977). Dates of metamorphism are mainly Tertiary (22 mys) (Brinkmann, 1976) although older dates (570-160 mys) probably indicate the presence of Palaeozoic and Pre-Cambrian rocks at depth. Continental margin sequences within the Lycian Nappes are generally considered to be contemporaneous with marble sequences in the Menderes massif (Durr *et al.*, 1977) and it is widely believed that the root zone of the Lycian Nappes lie to the north and west of the Menderes massif in the area of the present Aegean Sea.

The *Antalya Complex* (Woodcock and Robertson, 1977a) formerly the Antalya Nappes (Lefevre, 1967; Brunn *et al.*, 1971; Graciansky, 1972; Poisson, 1977) comprises a wide variety of Mesozoic sedimentary facies, including turbiditic sandstones, pelagic limestones, radiolarites, redeposited limestones and ophiolite derived sandstones.

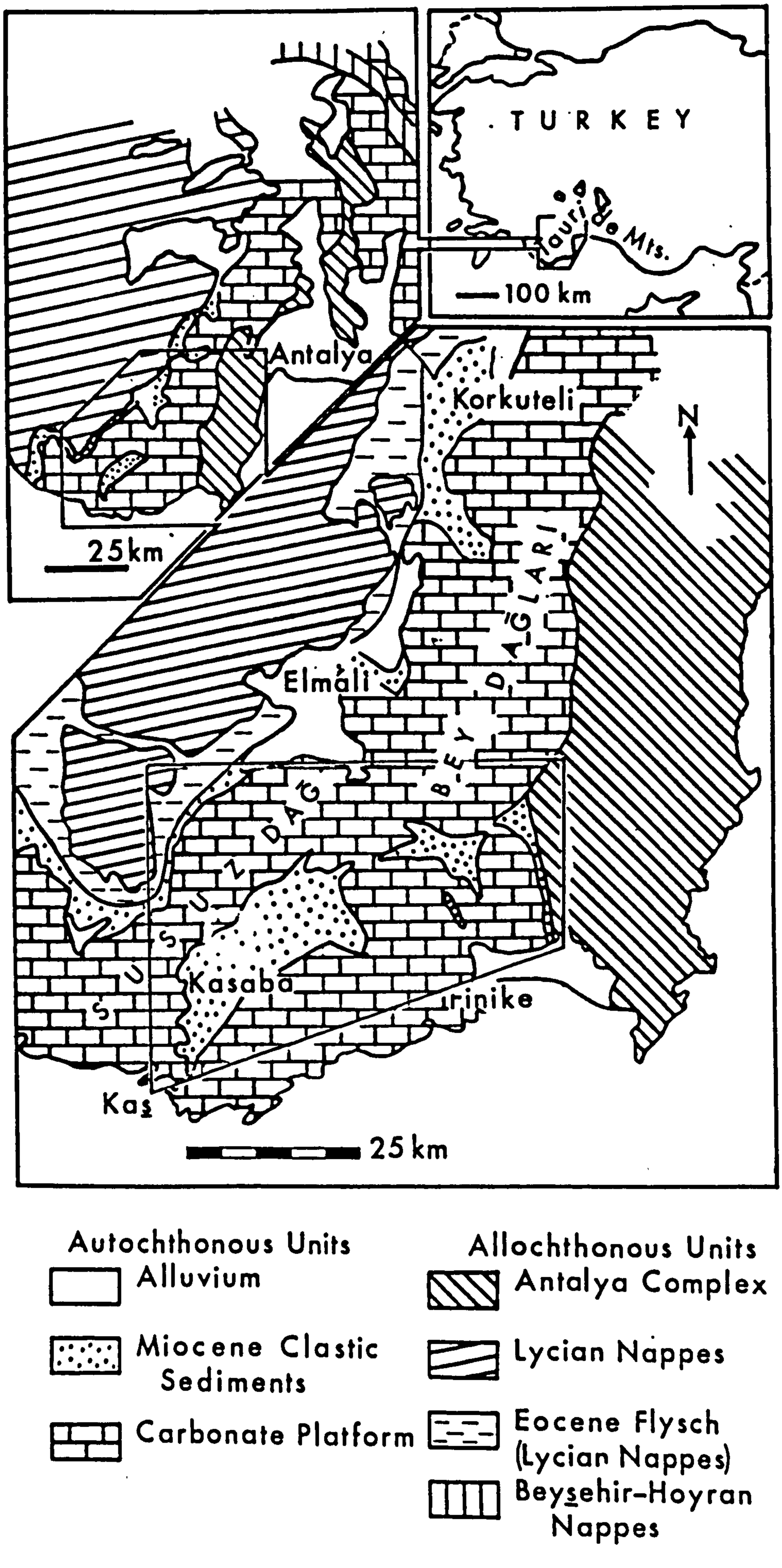

Fig. 1.2 Location map showing distribution of Miocene clastic sediments. Box encloses study area.

Massive shallow water limestones also occur overlying Ordovician to Permian sandstones, mudstones and limestones (Brunn *et al.*, 1971; Marcoux (in Delaune-Mayere *et al.*, 1977); Allasainoz *et al.*, 1974; Kalafatcioglu, 1973; Monod, 1977a, 1978; Dumont, 1976a; Robertson and Woodcock, 1981a, b, c). In addition the ophiolite suite is represented by pillow lavas, dolerites, gabbros, diorites and peridotites (Juteau, 1975). Minor occurrences of metamorphic rocks are also known (Juteau, 1975; Woodcock and Robertson, 1977b).

On the basis of sedimentary correlation throughout the area of the Antalya Complex (Fig. 1.2) Brunn *et al.* (1971) distinguished three nappe units. However, no structural continuity is demonstrated between the various isolated tectonic slices. Woodcock and Robertson (1981a, b, c) have recently reinterpreted a number of the thrust contacts of Brunn *et al.* (1971) as stratigraphic contacts and recognise a number of *en echelon* tectonic zones separated by steeply dipping structures with a strike-slip component of movement. Five N-S trending zones can be distinguished within the Complex. From west to east the tectonic zones record the transition from the Mesozoic carbonate platform (Bey Dağlari and Susuz Dağ, see below 1.5.3 and Fig. 1.4) across Mesozoic continental margin sediments, into oceanic crust formed during the initial stages of continental rifting (Woodcock and Robertson, 1981; Robertson and Woodcock, 1981 in press). Zonesfurther east are tectonically displaced with respect to the western zones. They consist of carbonate platform and basement lithologies and portions of Late Cretaceous ocean crust (Juteau *et al.*, 1977; Robertson and Woodcock, 1980a).

Taken as a whole the Antalya Complex records the initiation, construction and later tectonic disruption of part of the continental margin of a small Mesozoic-Cainozoic oceanic basin (Woodcock and Robertson, 1981; Robertson and Woodcock, 1980b).

The central unit of the Lycian Taurus comprises the *Taurus autochthon*. A regionally extensive paraautochthonous unit of shallow water limestones of a carbonate platform ranging in age from Liassic to Lower Miocene (Aquitanian) with several non-sequences in the Lower Tertiary (Poisson, 1977; Dumont *et al.*, 1972b). This unit forms the limestone massifs of the Susuz Dağ and Bey Dağlari which trend southwest to northeast for 180 km from the coastline of southwestern Turkey (Fig. 1.2) into the region of the Coubure

d'Isparta. In this area the platform sequence spans Upper Jurassic to late Miocene, although in the area north of Antalya platform sequences are known to rest on continental basement lithologies (Dumont, 1972).

A thick sequence of Miocene clastic sediments which unconformably overlie the carbonate platform limestones is the main subject of this thesis.

1.4 Previous Research

This is not intended to be an exhaustive literature review but merely a brief outline of the major studies. For a more detailed review of earlier work (pre-1964) the reader is referred to Brunn *et al.* (1970) and Monod (1977a). Waldron (1981) gives an exhaustive summary of most of the readily available literature on the entire Western Taurides published between 1964 and 1980. Early studies of the Lycian Nappes by Colin (1962), Bassaget (1966), Maitre (1967) and Sarp (1976) have been followed by the more regional studies of Poisson (1968a, b, 1974a, c, 1976, 1977), Bronniman *et al.* (1970) Graciansky (1967, 1968, 1972, 1973), Graciansky and Lys (1968) and Graciansky *et al.* (1967, 1970).

The relationship between the Menderes massif and the Lycian Nappes is speculated on by Boray *et al.* (1973). Bremer (1971) summarises much of the earlier work. The most recent field based study is that of Onalon (1980).

Lefevre (1967) first identified the Antalya Complex as a separate group of allochthonous rocks. Since that time this unit has been the subject of an extensive study by the Orsay team, from Paris, lead by Professor J. H. Brunn. The principal stratigraphic and structural results of the Orsay team are summarised by Brunn *et al.* (1970, 1971) and Gutnic *et al.* (1979), and interpreted in terms of continental evolution by Monod *et al.* (1974) and Delaune-Mayere *et al.* (1977). More recently sedimentological and structural work by Robertson and Woodcock (1980a, b, 1981a, b, c), Robertson (1981) and Woodcock and Robertson (1977, 1981, in press) has established a zonal scheme for the southwestern segment of the Complex adjacent to the Bey Dağlari, and demonstrated that strike-slip faulting played an important part in its emplacement.

North of Antalya the relationship of the Antalya Complex to the Bey Dağlari massif and Lycian Nappes is described by Gutnic and

Poisson (1970) and Allasainoz *et al.* (1974). The area in the centre of the Isparta angle has been studied by Akbullut (1977) and more recently Waldron (1981) has produced a detailed structural and sedimentological history of the area south and east of Lake Eğridir (Fig. 10.1). Gutnic (1977), Gutnic *et al.* (1979) and Dumont *et al.* (1980) also describe this area of the Antalya Complex.

The autochthonous limestone sequence has been the subject of an extensive biostratigraphical study by Poisson (1967a, b, 1974b, 1977), Poisson and Poignant (1974) and Jaffrezo *et al.* (1978). By comparison, the overlying Miocene clastic sediments have been given only cursory attention by Poisson (1977), Onalon (1980), Pisoni (1967), Tolun (1965), Zaralioğlu (1976) and Şenel (1980).

Despite the number and detailed nature of many of the studies controversy continues to surround the origin and emplacement of the Antalya Complex. Dumont *et al.* (1972a, b) propose an *origin to the south* of the Tauride platform units, followed by northward emplacement in late Cretaceous times. In contrast a *northern origin* on the margins of the main Tethyan ocean is favoured by Ricou *et al.* (1974, 1975, 1979) and Argyriadis *et al.* (1980). The main arguments for both theories are summarised by Brunn (1974) and Brunn *et al.* (1973). Alternative models involving strike-slip faulting are proposed by Monod (1976a, b) and by Dumont (1976b). Robertson and Woodcock (1980a, 1981a, b, c) and Woodcock and Robertson (1981, in press) put forward convincing evidence to suggest that the Antalya Complex represents a virtually *in situ* passive continental margin sequence that was affected by extensive strike-slip faulting during Cretaceous to Miocene times. Waldron (1981) invokes northeastward directed thrusting orientated at 90° to strike-slip fault movement in the south as an emplacement mechanism for the northeastern area of the Antalya Complex (Fig. 1.2).

On a more regional scale the relationship between the Taurides and other areas of the Tethys Ocean has been speculated on by a number of authors, amongst them, Bernoulli *et al.* (1974), Auboin *et al.* (1976), Argyriadis *et al.* (1976), Brunn (1976), Brunn *et al.* (1976), Izdar (1976), Durr (1976), Durr *et al.* (1977), Monod (1977b), Robertson and Woodcock (1980b) and Şengor and Yilmaz (1981).

1.5.0 Structure

This section outlines the structure of the autochthon in the study area (Fig. 1.2). The detailed structure of the allochthonous units (Lycian Nappes and Antalya Complex) is outside the scope of this thesis. However, their general structure in the region adjacent to the study area (Fig. 1.2) is briefly discussed.

1.5.1 Autochthon

The autochthon comprises a structurally simple domal tectonic unit. The largest scale structures within the carbonate massif comprise broad open to closed anticlines and tight synclines. The folds have wavelengths of several hundred metres to several tens of kilometres, amplitudes are ten to hundreds of metres. Axial planes are steep to upright (classification of Fleuty, 1964). Fold attitude ranges from upright horizontal to inclined and plunging. The Miocene clastic sediments that lie within large synclines (e.g. Kasaba syncline) and along both flanks of the two major anticlines (Susuz Dağ and Finike anticline, Fig. 1.2) are largely unaffected by folding. Where present, gentle megascopic folds are upright with a wavelength and amplitude of a few tens of metres. Fold axis orientation is parallel to the larger scale structures.

Axial traces of major folds in the autochthon (drawn from aerial photographs and direct field observations) are shown in Fig. 1.3. The eastern area of the carbonate massif (Fig. 1.3) is dominated by N-S trending folds which are often asymmetrical to the west. The central and northwestern areas comprise mainly NE-SW trending folds, that are rarely asymmetrical to the southeast.

<u>Discussion</u> Axis orientation and fold style suggests that the minor folds within the Miocene sediments are parasitic to the larger scale structures. On a regional scale the interference patterns between the two fold axes orientations (Fig. 1.3) indicate that the NE-SW trending structures post-date N-S trending structures. In the eastern area of the massif fold orientation parallel to the thrust front of the Antalya Complex, and asymmetry suggests these folds may be related to the final stages of emplacement of the Antalya Complex. By contrast, in the western area fold axes are orientated parallel to the thrust fold of the Lycian Nappes, suggesting these folds may be related to the later stages of emplacement of the Lycian Nappes.

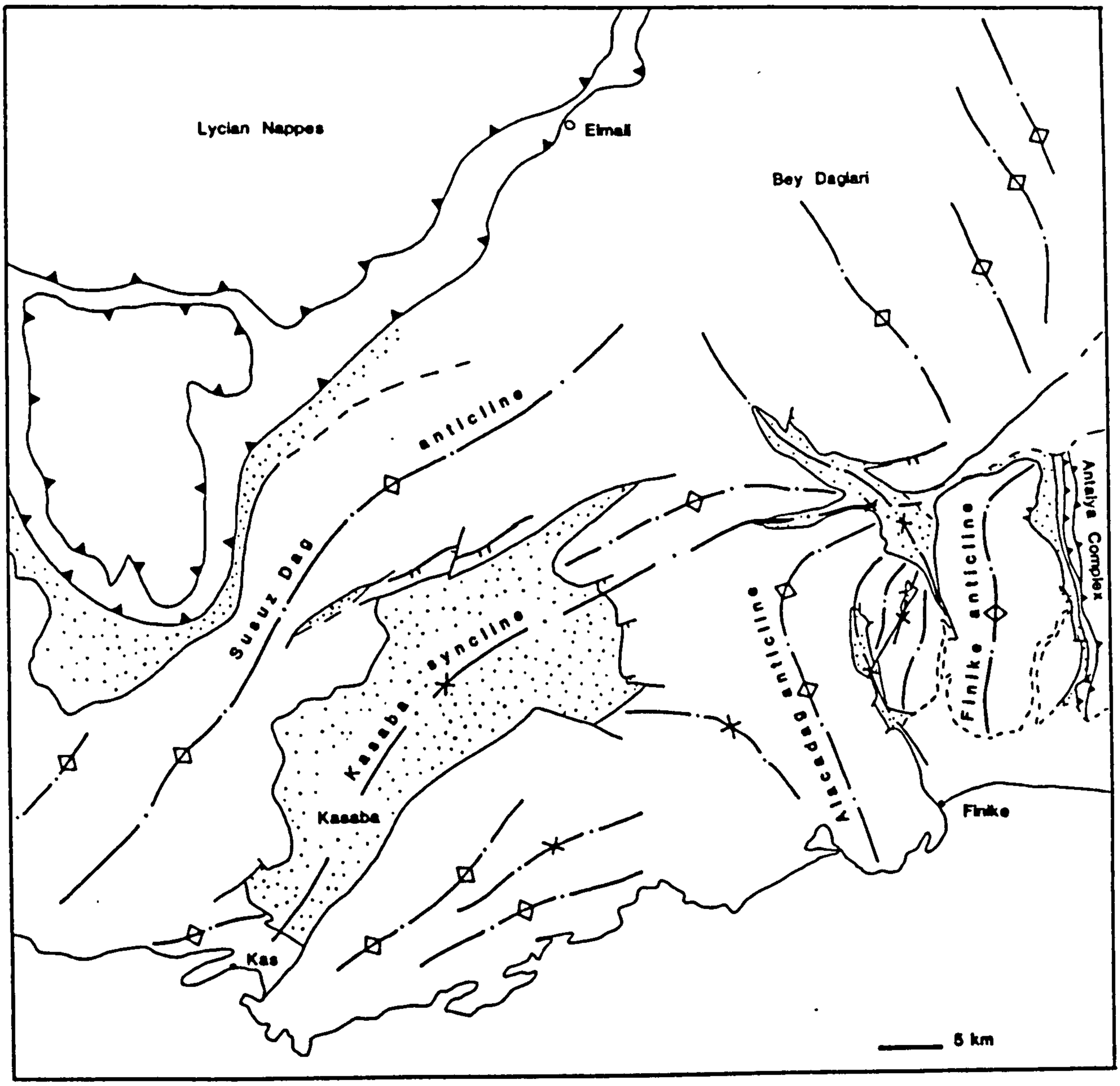

Fig. 1.3 Main structural trends and lineaments over the Susuz Dağ and southern Bey Dağlari (single tick indicates normal fault, double tick reverse fault). Miocene clastic sediments are dotted, for more details of the structure see maps and sections in the back of the thesis.

Joints Regular joint sets are ubiquitous in the carbonate platform limestone, their orientation has not been investigated systematically but they are probably related to the folding. Joints are only rarely present in more competent beds in the overlying clastic sequence.

Faults A number of high angle normal faults are present in the carbonate massif, they are generally orientated in a NE-SW or E-W direction. The majority of the faults are probably related to the late stage (Neogene?) regional uplift following Miocene deformation. In some areas (e.g. Çağman, Chapter 7) earlier faults that were active during the deposition of Miocene clastic sediments, were apparently reactivated during this late stage of uplift.

Several northeast-southwest trending faults along the southern limb of the Susuz Dağ syncline (Fig. 1.3) preserve clastic sediments of Upper Miocene age. Dip on the faults cannot be determined accurately in the field, although, in most places, they are apparently vertical or dip steeply to the north. They are here interpreted as reverse faults, possibly formed during the final stages of emplacement of the Lycian Nappes from the northwest (Chapter 10).

1.5.2 Lycian Nappes

The structure of the Lycian Nappes is dominated by low-angle to horizontal reverse and thrust faults. In the area south of Elmali (Fig. 1.2) the nappes can be broadly subdivided into two tectonic units. The tectonic contact between the upper limestone and radiolarite unit and underlying redeposited Eocene sandstone sequence forms a prominent break in slope that can be followed parallel to topography over a considerable distance.

The structurally underlying Eocene sandstone sequence is cut by a large number of low-angle (0-20°) shear planes, marked by brecciation and rarely intense, localised deformation. The absence of marker horizons prohibits the detailed structural study of this unit, however, it would appear to consist of a series of imbricate slices. The contact with the underlying autochthonous Miocene sediments is a reverse fault which dips at between 10° and 15°.

1.5.3 Antalya Complex

In the area adjacent to the Bey Dağlari, the Antalya Complex is subdivided into four structural units by Robertson and Woodcock (1980b) (Fig. 1.4). Immediately adjacent to the Bey Dağlari, the

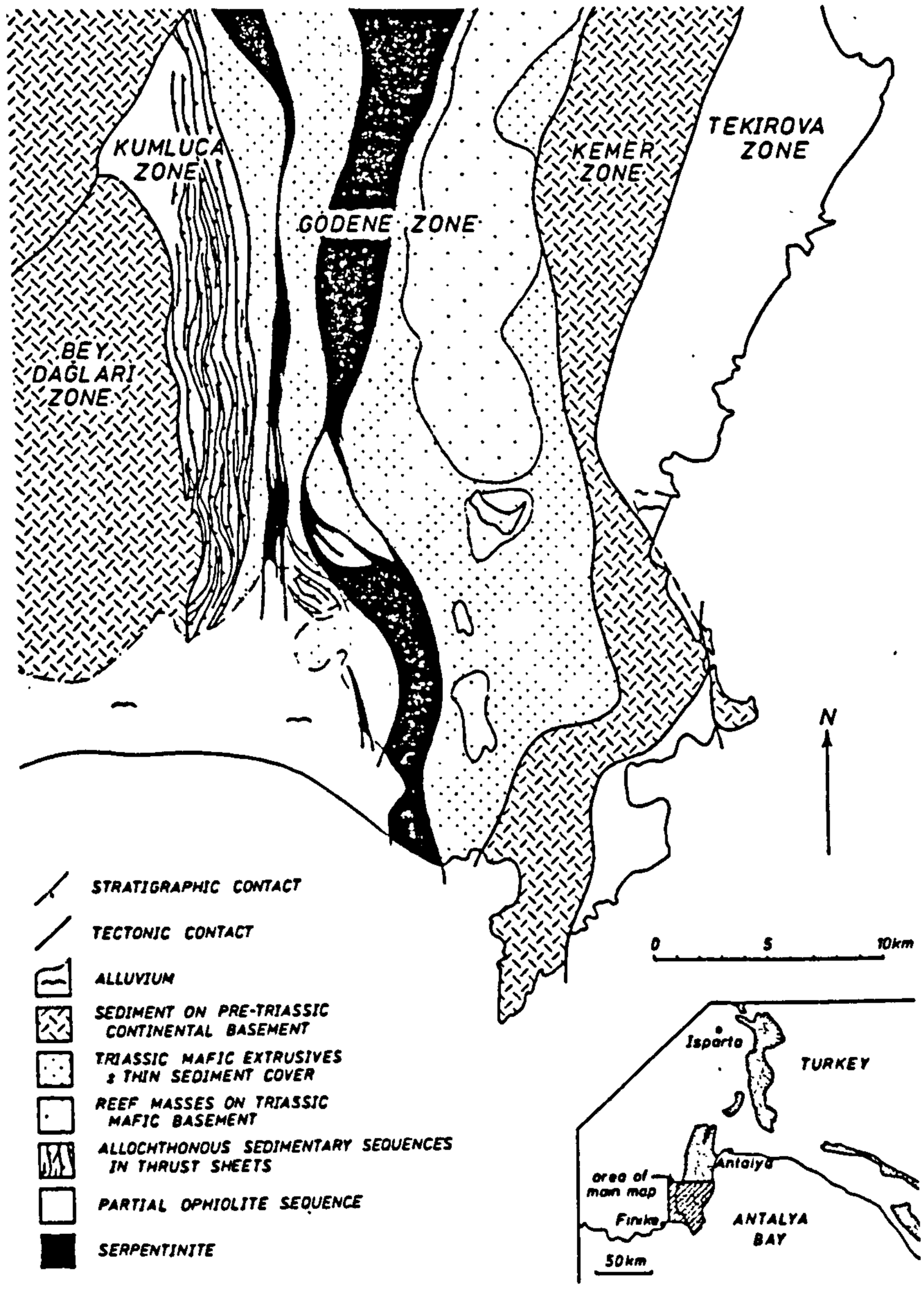

Fig. 1.4 Structure of the Antalya Complex adjacent to the Bey Dağlari (after Woodcock and Robertson, 1981a).

Kumluca Zone consists of Triassic to Cretaceous sandstones, redeposited limestones and radiolarites of a Mesozoic continental margin. The sediments of the Kumluca Zone are deformed by west vergent folds and imbricate thrusts. The contact with the structurally underlying autochthonous Miocene sediments is a low-angle reverse fault that overlies a tectonic melange. The melange is up to 70 m thick and comprises blocks of mainly Kumluca Zone rocks in a matrix of disrupted ophiolite-derived sediments.

East of the Kumluca Zone, the *Godene Zone* is characterised by a thick sequence of Triassic lavas overlain by a sequence of Triassic to Cretaceous sandstone, hemipelagic limestones and radiolarites. The zone is cut by north-south trending high-angle serpentinite belts enclosing fragments of basic and ultrabasic plutonic rocks.

The *Kemer Zone* consists of a series of north-south orientated slices of Mesozoic platform and slope carbonates resting on Palaeozoic basement. In some areas carbonate slope breccias can be traced onto lava basement of the adjacent Godene Zone. The Kemer Zone is interpreted as a series of off-margin carbonate platforms constructed on blocks of continental basement.

The *Tekirova Zone*, furthest east, consists of a well preserved partial ophiolite sequence extending from upper mantle hartzburgite to the base of the sheeted dyke complex (Juteau, 1975; Juteau *et al.*, 1977). The suite is dated as Upper Cretaceous in age by Thiuzat and Montigny (1979). The structure of the southwestern segment of the Antalya Complex, adjacent to the Bey Dağlari is shown in Fig. 1.4 (after Woodcock and Robertson, 1981a).

CHAPTER 2 STRATIGRAPHY OF THE MIOCENE CLASTIC SEDIMENTS

CHAPTER 2

2.0 Stratigraphy of the Miocene Clastic Sediments

2.1 Introduction

In this chapter the stratigraphy of the Miocene clastic sediments is outlined. The revised stratigraphy conforms with the principles laid down by Hedberg (1976) in the International Stratigraphic Guide.

Each formation is a mappable unit (at 1:50,000) with a precisely defined type section. Previously used names are retained wherever possible, e.g. those defined by Pisoni (1967), Poisson (1977), Onalon (1980), Senel (1980), Tölun (1965) and Zaralioğlu (1967). New terms have only been introduced where they are essential to conform with the International Guide, and to take into account the present more detailed study of the sedimentary succession. In some instances the rank of a formation has been changed, either upgrading it to a group or downgrading it to a member.

Before the exploratory study of Poisson (1977) a number of informal stratigraphies had been erected for the Miocene sequence in different areas over both the Bey Dağlari and Susuz Dağ (Fig. 1.2) (Pisoni, 1967; Tölun, 1965; Zaralioğlu, 1967). More recently Onalon (1980) and Senel (1980) have proposed *ad hoc* stratigraphies for various parts of the Miocene sequence. In most cases no type section was defined.

During the course of the present regional study, it became obvious that the local informal stratigraphies could not be easily correlated and that a new stratigraphy encompassing the entire Miocene sequence was required.

The new stratigraphy outlined below (and Figs. 2.2 and 2.3) comprises the Karakus Tepe Group within which three formations and five members are defined (Figs. 2.2 and 2.3). This nomenclature reduces the number of stratigraphic units and recognises the sedimentary interdigitations of several distinct lithologies, all of which occur as mappable units (1:50,000 scale) within the Miocene succession.

2.2 Karakus Tepe Group

New group comprising of Kemer, Salir and Kasaba Formations.

Name and Type area. The Group is named after the Karakus Tepe southwest of Korkuteli (Fig. 1.2).

Synonymy. Originally the Karakus Tepe Formation (Poisson, 1977). Upgraded to group rank to encompass newly defined formations. The name is retained to provide continuity in the revised stratigraphy (Hedburg, 1976, p. 44).

Subdivision. The Karakus Tepe Group is subdivided into three formations; the Salir Formation, Kemer Formation and Kasaba Formation.

2.3.0 Salir Formation

The Salir Formation was first defined by Tölun (1965) and Senel (1980). It consists of ophiolite-derived conglomerate and sandstone, mudstone, chalk and limestone breccias.

Name. The formation is named after the village of Salir 25 km by road northeast of Finike. (Fig. 2.1).

Synonymy. Salir Formation (Tölun, 1965), Karakus Tepe Formation in part (Poisson, 1977), Salir Formation (Senel, 1980).

Type Section. Previous workers did not establish a type section. For the first time a type section is defined in a road cutting 1 km northwest of Salir, (Fig. 2.1, Section 1). The lower 35 m consist of green calcareous mudstone, structureless and parallel-laminated thin (3-20 cm) sandstone and very thin (1-3 cm) white chalk. These rocks pass upwards into a sequence of thick (.30 m-1 m) to very thick (1-3 m) pebble, cobble and boulder conglomerates interbedded with fine, medium and coarse buff-grey sandstone, green mudstone and white chalk. The sandstone shows well developed turbidite sedimentary structures. The polymict conglomerates are both clast- and matrix-supported; well-rounded clasts consist of most members of an igneous ophiolite assemblage and the associated sedimentary cover. The majority of the sequence consists of coarse sandstones and conglomerates between 5 m and 15 m thick interbedded with thin-bedded sandstone, mudstone and chalk. Massive beds (to 5 m) of white bioclastic limestone breccia, which occur sporadically throughout the sequence, make up less than 10% of the total thickness.

Regional Characteristics. The Salir Formation is everywhere dominated by coarse sandstones and conglomerates, which form between 60% and 80% of the sequence. Individual units are laterally discontinuous on both the scale of an exposure and over several hundred metres. Beds of bioclastic limestone breccia increase in

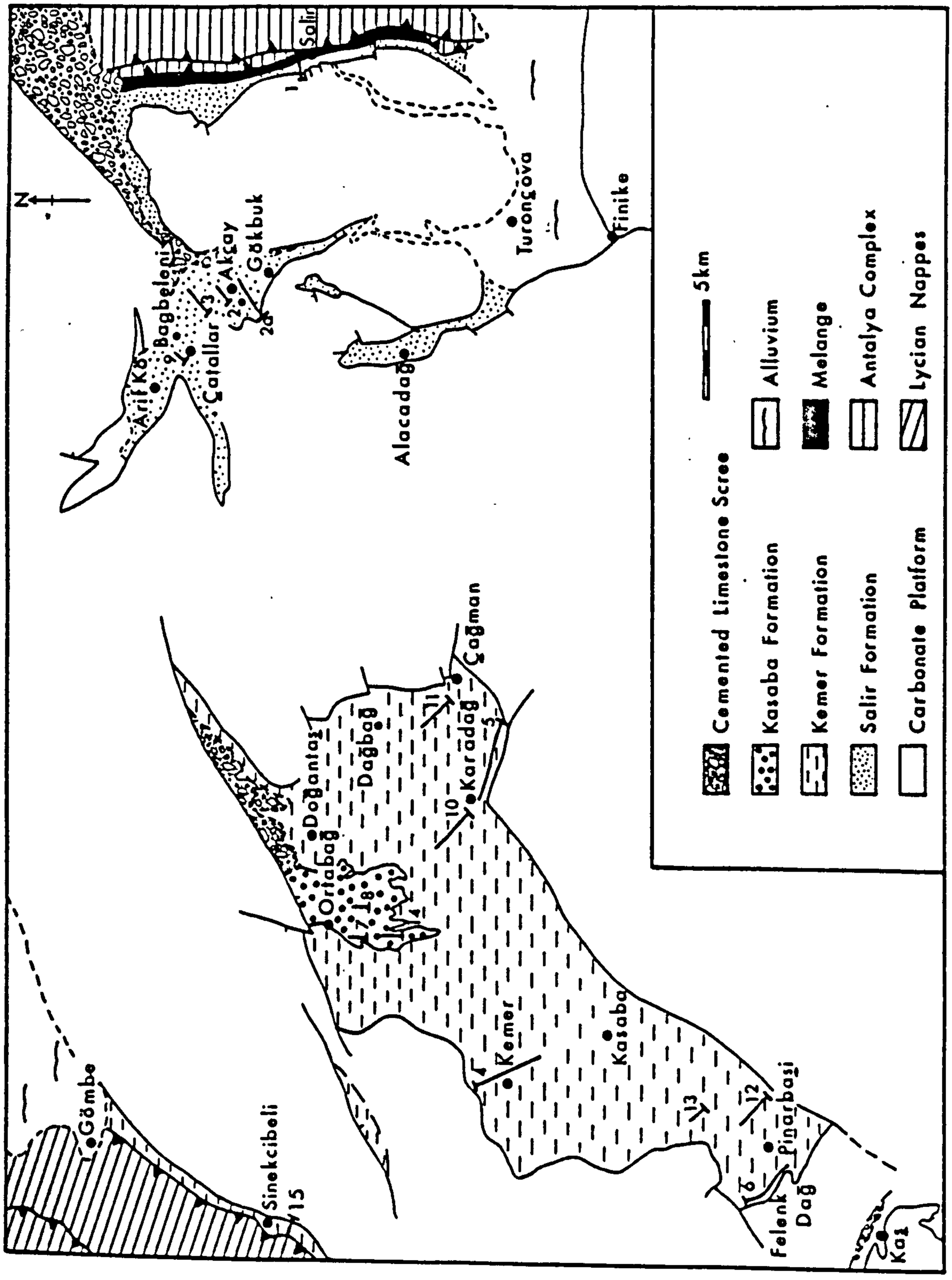

Fig. 2.1 Outcrop of the Miocene clastic sediments over the Susuz Dağ and south Bey Dağlari showing location of type sections, and reference sections referred to in the text.

frequency and thickness northwards.

In the Akçay area, to the west (Fig. 2.1), the Formation is represented by a sequence of ophiolite-derived sandstones and mudstones overlain by a considerable thickness of conglomerate here distinguished as the Akçay and Bağbeleni Members respectively (Fig. 2.2).

Lower and Upper Boundaries. In the type section the base lies unconformably on thin-bedded pelagic limestones; the top is marked by a transitional contact to a tectonic melange of Middle Miocene age (Langhian - Serravallian). Elsewhere (e.g. Akçay area) the base lies unconformably on green calcareous mudstone.

Age. The base of the Salir Formation is assigned to the Lower Miocene (Burdigalian?) on the basis of a foraminiferal assemblage that includes *Miogypsina, Eulepidra, Nepholepidra, Rotalia* cf *viennati, Elphidium,* and *Austrotrallira.* The highest fossiliferous horizons contain *Praeorbulina glomerosa* indicating a Middle Miocene (Langhian) age.

2.3.1 Akçay Member

Status. New member, consists of interbedded ophiolite-derived sandstone, pebbly mudstone, mudstone, chalk, limestone breccia and detached limestone blocks.

Name. The Member is named after the village of Akçay, (Fig. 2.1) 20 km by road north of Finike and 5 km southeast of Arif Köy.

Synonymy. None.

Type Section. No complete section is exposed; the type section is a composite one correlated lithologically 2 km along strike (Fig. 2.1, Section 2a, 2). The basal part is defined along a track which runs east-west 1 km north of Gökbuk; the higher parts of the sequence are well exposed in a stream section directly northeast of Akçay (Fig. 2.1).

The lower part (200 m) consists of laterally continuous thin-bedded buff-grey sandstones with scattered carbonaceous material, green mudstone and white chalk. The sandstones are graded and show well developed turbidite sedimentary structures. Above this lenticular sandstones become abundant; they show turbidite structures and occur interbedded with thin- and medium-bedded (10-30 cm)

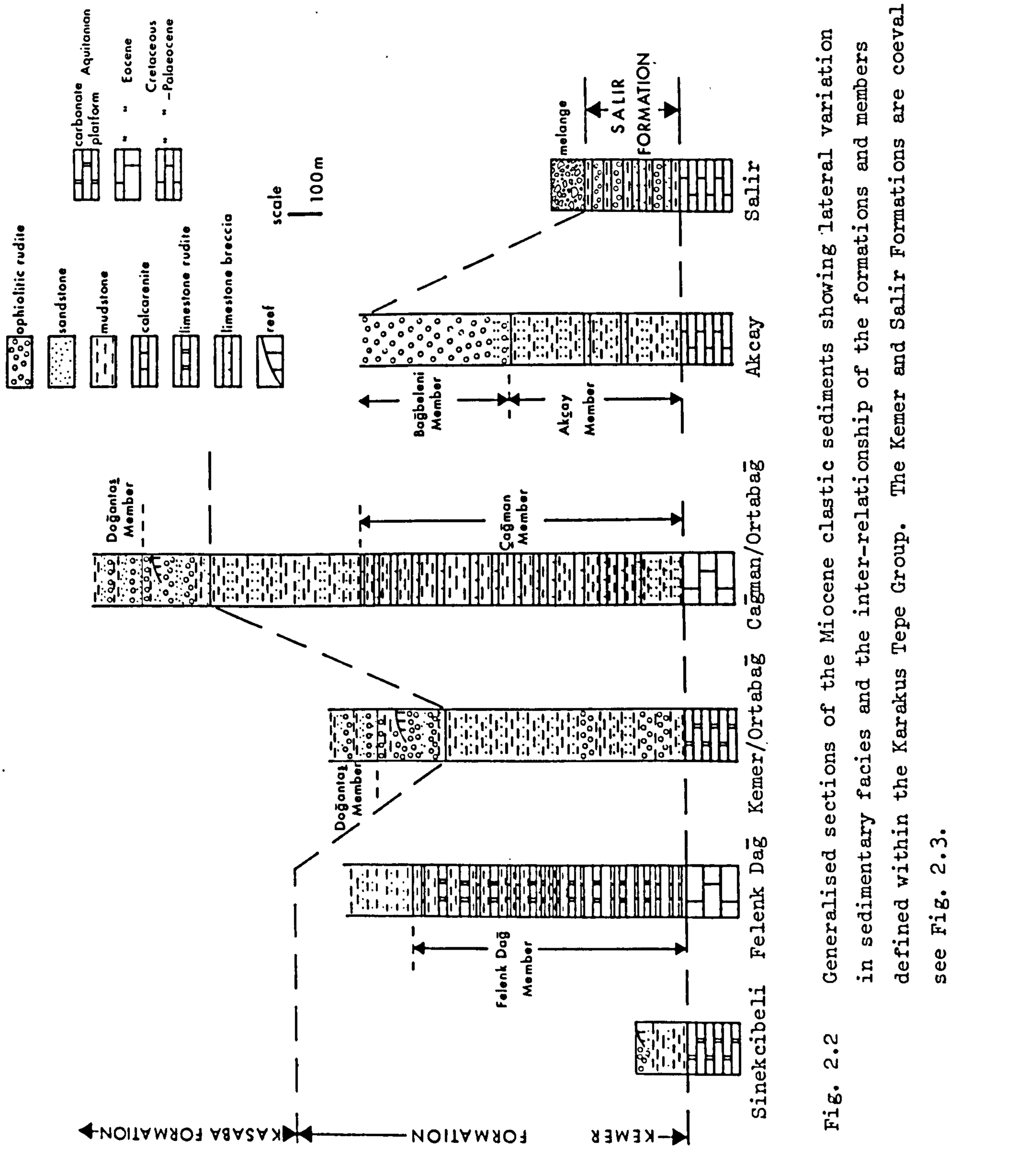

Fig. 2.2 Generalised sections of the Miocene clastic sediments showing lateral variation in sedimentary facies and the inter-relationship of the formations and members defined within the Karakus Tepe Group. The Kemer and Salir Formations are coeval see Fig. 2.3.

sandstones, mudstones and chalk. Thick (30 cm-1 m) grey calcarenites with normal grading and turbidite sedimentary structures occur sporadically throughout and make up approximately 10% of the sequence. The total thickness of the Akçay Member in the type section is 500 m.

Regional Characteristics. The Akçay Member is dominated in most areas by the lithologies seen in the type section, but other lithologies are also important. In summary these are:
(i) Laterally discontinuous ophiolite-derived pebble and cobble mudstones (clasts of pebble and cobble size supported in a mud matrix);
(ii) Limestone breccias with poorly developed normal grading occur as beds between 2 m and 5 m thick. Both of the preceding lithologies are well exposed in a reference section directly north of Çatallar (Fig. 2.1, Section 9).
(iii) Large (up to 15 m across) detached blocks of platform limestone. These are restricted to the middle of the sequence and are well exposed on the road between Akçay and Çatallar (Fig. 2.1).

Lower and Upper Boundaries. Mudstones and sandstones at the base of the member lie disconformably on green calcareous mudstone. The boundary with the overlying Bağbeleni Member is placed where the first clast-supported conglomerates occur.

Age. The base is dated as Lower Miocene (Burdigalian) by the presence of the planktonic foraminifera *Globigerinoides sicanus*, *Globigerinoides trilobus* and *Globigerinoides irregularis* (Poisson, 1977). The benthonic foraminifera *Miogypsina*, *Eulepidina*, *Alveolina*, *Rotalia* cf *viennati* and *Nephrolepidina* confirm this date. The highest fossiliferous horizon is dated by the occurrence of *Praeorbulina* as Middle Miocene (Langhian).

2.3.2 Bağbeleni Member

Status. New member, consists of ophiolite-derived conglomerate, subordinate sandstone, mudstone and calcrete (carbonate palaeosol).

Name. The Member is named after the village of Bağbeleni 3 km southwest of Arif Köy and 23 km by road north of Finike (Fig. 2.1, Section 3).

Synonymy. None.

Type Section. The type section is defined in a stream 2 km southeast of the village of Bağbeleni. The lowermost 50 m consist

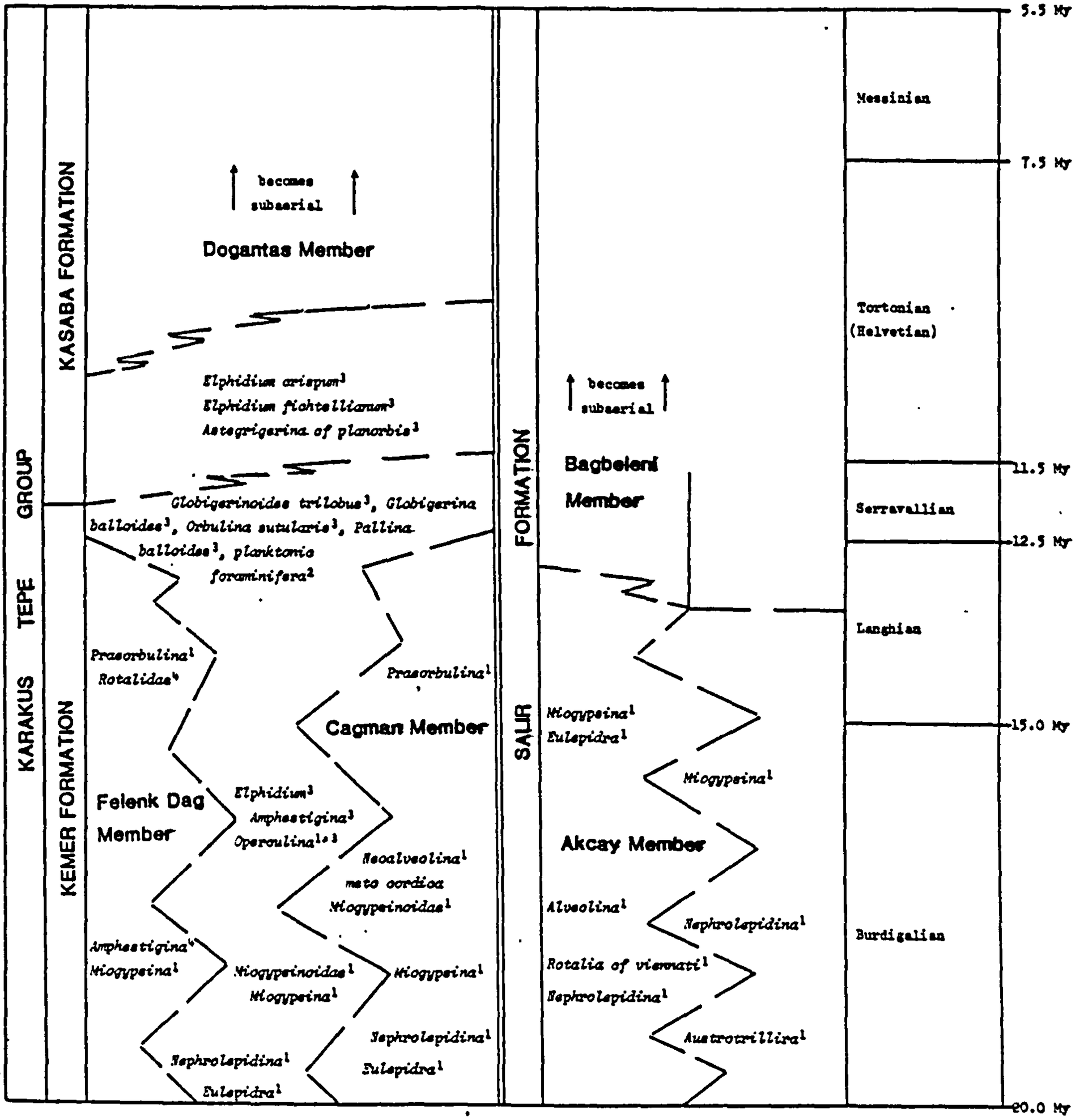

Fig. 2.3 Stratigraphy of the Karakus Tepe Group, showing principal palaeontological determinations

[1]This study
[2]Poisson (1977)
[3]Onalan (1980)
[4]Pisoni (1967)

of massive clast-supported pebble and cobble conglomerate. These are interbedded with medium to coarse sandstone, green mudstone and white chalk. The overlying 100 m comprises of poorly stratified and massive cobble and pebble conglomerate interbedded with laterally discontinuous very coarse sandstone and rare siltstone horizons. The remainder of the sequence consists of horizontally stratified, frequently lenticular, pebble, cobble and boulder conglomerate interbedded with lenticular coarse sandstone, thin mudstone and rare calcrete horizons. The estimated thickness of the Bağbeleni Member in the type area is 300 m.

Regional Characteristics. Lithologies in the Bağbeleni Member are everywhere similar to those of the type section, although in some areas the uppermost parts of the sequence have been removed by erosion (e.g. in the area north of Alaçadağ, Fig. 2.1).

Lower and Upper Boundaries. In most areas the base is the transition from sandstone and mudstone of the Akçay Member to conglomerate, although locally the member lies with an angular contact against pelagic limestones of the carbonate platform (e.g. Alaçadağ area, Fig. 2.1). The top is overlain unconformably by cemented limestone screes.

Age. The base is dated as Middle Miocene (Langhian) by the presence of *Praeorbulina*. The upper parts of the sequence are devoid of fossils but are probably Middle Miocene in age.

2.4.0 Kemer Formation

Status. New Formation, consists of interbedded ophiolite-derived conglomerate, sandstone, mudstone, green calcareous mudstone and chalk.

Synonymy. Karakus Tepe Formation in part (Poisson, 1977), Sinekcibeli Formation in part (Onalon, 1980).

Type Section. The type section is exposed in several road cuttings immediately north and south of Kemer (Fig. 2.1, Section 4).

The basal 40 m consists of 10 m of calcareous mudstone overlain by 30 m of interbedded thin dark green mudstone and buff green sandstone. The sandstones are graded and show turbidite sedimentary structures. Above this, the section, with a combined thickness of 200 m, comprises two conglomerate horizons between 15 m and 25 m

thick interbedded with medium to coarse turbidite sandstone, mudstone and rare very thin white chalk. The uppermost 300 m of the sequence consists of medium- and thin-bedded sandstone, which are in many places graded with turbidite sedimentary structures, and thin-bedded dark green mudstone. In the type section the upper parts of the sequence are poorly exposed, but are well seen in a reference section north of Kara Dağ (Fig. 2.1, Section 10). In the top 100 m of this section occasional pebbly mudstones and lenticular conglomerate horizons are seen interbedded with sandstone and mudstone. The mudstones contain an abundant shallow marine fauna of bivalves and gastropods.

Lower and Upper Boundaries. In the type section the base lies conformably on shallow water limestones. The top is marked by the lowest conglomerate beds of the Kasaba Formation.

Age. The base is dated as Burdigalian (Lower Miocene) by the presence of *Globigerinoides trilobus*, and *Globigerinoides sicanus*. Poisson (1977, p. 162) listed an abundant planktonic foraminiferal assemblage of Burdigalian age. The central and upper parts of the sequence span Langhian to Serravallian as indicated by the presence of the planktonic foraminifera *Praeorbulina* (Langhian) and *Globoratalia mageri*, and *Globaratalia periphenor* (Serravallian) (Poisson, 1977). Benthonic foraminifera present include *Miogypsina*, *Miogypsinoidae*, *Amphestigina*, *Elphidium* and *Operculina*.

Regional Characteristics. In most areas the Kemer Formation comprises lithologies similar to those in the type section but several other lithologies form sedimentary intercalations: these are distinguished as members (see below).
Briefly the additional lithologies are:
(i) Redeposited bioclastic limestone breccias, calcarenites and mudstones, distinguished as the Çağman Member.
(ii) Redeposited limestone conglomerate, calcarenites and mudstones, distinguished as the Felenk Dağ Member.

2.4.1 Çağman Member

Status. New member, comprises redeposited limestone breccias, calcarenites and mudstones.

Name. Named after the village of Çağman 5 km south of Dağbağ, 8 km east of Kara Dağ (Fig. 2.1).

Type Section. The type section is exposed in a track 4 km southwest of Çağman (Fig. 2.1, Section 5). The basal 40 m consist of light green calcareous mudstone with rare medium bedded calcarenites. Above this buff brown calcareous sandstones with turbidite sedimentary structures interbedded with dark green mudstones form a unit 120 m thick. This is overlain by approximately 800 m of bioclastic limestone breecias, interbedded with grey/white calcarenites, green calcareous mudstones and white chalks. Individual breccia beds are up to 22 m thick. The breccias decrease in thickness and frequency upwards and are progressively replaced by calcarenites with turbidite sedimentary structures interbedded with calcareous mudstones and white chalks.

Regional Characteristics. The Çağman Member consists everywhere of lithologies present in the type section. In a reference section northeast of Çağman (Fig. 2.1, Section 11) the thickness of individual limestone breccias is greatly reduced from an average of 15 m in the type section to 5 m. Laterally the member passes into the Kemer Formation.

Lower and Upper Boundaries. The base of the member is always marked by shallow water nummulitic limestone. The top of the member, well exposed in the type section, is transitional to the ophiolitic sandstones and mudstones of the Kemer Formation. The top is taken above the highest calcarenite horizon.

Age. The base is dated as Burdigalian by the presence of an abundant planktonic foraminiferal assemblage, which includes *Globigerinoides trilobus*. *Praeorbulina* from directly above the highest calcarenite horizon dates the top of the member as Langhian (Middle Miocene).

2.4.2 Felenk Dağ Member

Status. New member, consists of limestone conglomerate, calcarenites, calcareous mudstone and chalk.

Name. Named after Felenk Dağ 12 km northwest of Kaş.

Synonymy. Felenk Dağ Conglomerates in part (Pisoni, 1967), Pinarbaşi Formation in part (Pisoni, 1967).

Type Section. The type section is exposed in road cuttings along the north eastern side of Felenk Dağ (Fig. 2.1, Section 6).

The lowermost 90 m consist of calcareous mudstone, interbedded with calcareous sandstone with turbidite sedimentary structures; white chalks occur as very thin beds. Above this, thick to very thick (1-3 m) redeposited limestone conglomerates form laterally continuous beds throughout much of the sequence. In the upper part of the sequence, mudstone and sandstone predominate. The approximate thickness of the Felenk Dağ Member is 750 m.

Regional Characteristics. The lithology of the Felenk Dağ Member is everywhere similar to that of the type section. In some areas carbonate conglomerate and calcareous sandstone form the basal unit; this is well seen in a reference section 2 km east of Pinarbaşi (Fig. 2.1, Section 12). Elsewhere, the thickness of the basal mudstone and calcareous sandstone unit increase to approximately 300 m and only two conglomerate horizons are present in a well exposed section 5 km southwest of Kasaba (Fig. 2.1, Section 13). Laterally the Felenk Dağ Member passes into ophiolite-derived sandstone and mudstone of the Kemer Formation.

Lower and Upper Boundaries. The base of the member is everywhere taken as the transition from underlying shallow-water bioclastic limestone. In the type section the top is not exposed but is seen in a reference section 5 km southwest of Kasaba (Fig. 2.1, Section 13). There calcareous sandstone and mudstone pass transitionally upwards into ophiolite-derived sandstone and mudstone of the Kemer Formation.

Age. A Lower Miocene (Burdigalian?) age is indicated for the base of the member by the presence of *Rotalidae*, *Amphestigina* and *Miogypsina*. *Praeorbulina* from just below the highest calcareous sandstone confirms a Langhian (Lower/Middle Miocene) age for the top of the member.

2.5.0 Kasaba Formation

Status. Formation defined by Zarioğlu (1967), Onalon (1980). Clast-supported conglomerate, sandstones, mudstone, reefal limestones and calcretes (carbonate palaeosols).

Name. The Kasaba Formation is named after the village of Kasaba 15 km northeast of Kaş.

Synonymy. Kasaba Formasyonu (Zaralioğlu, 1967; Onalon, 1980).

Type Section. Previous workers did not define a type section. It is here defined in the side of a gorge 2 km southeast of Ortabağ (Fig. 2.1, Section 7). The lowest part of the section consists of thick to very thick clast-supported cobble and pebble conglomerates interbedded with medium to coarse, in a few places trough-cross-stratified, grey to brown sandstones and very fossiliferous dark green mudstones. The section is 300 m thick, the upper 100 m which comprises cross-stratified conglomerate, sandstone and red and green mudstone is here defined as the Doğantaş Member (see below).

Regional Characteristics. The Kasaba Formation in most areas is dominated by lithologies similar to the type section, but reef limestones also form important intercalations. In a reference section 4 km south of Ortabağ (Fig. 2.1, Section 14), these limestones are well exposed, interbedded with conglomerate. The reefs consist of *in situ* corals (*Tarballastraea sp.*, *Montastrae sp.* and *Favites sp.* being the most important) which form mounds between 6 m and 8 m high. Associated sediments include calcarenites and very coarse limestone breccias which thin away from the reef complex.

Lower and Upper Boundaries. The base is taken as the lowest conglomerate horizon, the top is transitional to the Doğantaş Member which is marked by the lowest red mudstone horizon.

Age. The planktonic foraminifera *Globorotalia meyeri*, *Globorotalia periphero ronda*, *Globigerinoides trilobus* and *Orbulina suturalis* (Poisson, 1977) give a Serravallian age for the base of this Formation. Onalon (1980) records an abundant benthonic foraminiferal assemblage, from the highest fossiliferous horizons (base of the Doğantaş Member). Benthonic forams present include *Rotalia breccarii*, *Elphidium crispum*, *Elphidium fichtellanium*, *Asterigerina* cf *planorbis*, these give an Upper Miocene (Tortonian-Helvetian) age for this part of the sequence.

2.5.1 Doğantaş Member

Status. New Member, consisting of stratified conglomerate, sandstone, green and red mudstone and calcretes (carbonate palaeosols).

Name. The member is named after the village of Doğantaş 25 km by road northeast of Kasaba and 4 km east of Ortabağ (Fig. 2.1).

Synonymy. None.

Type Section. The type section is defined in the eastern side of a gorge 5 km southwest of Doğantaş (Fig. 2.1, Section 8). The entire section comprises massive and cross-stratified conglomerate interbedded with coarse to fine sandstone, red and green mudstone and calcretes.

The lithologies are arranged in distinct fining-upward units between 12 m and 22 m thick. The base of each unit is marked by a conglomerate which passes upwards, through progressively finer grained sandstone, to mudstone which are in many places reddened at the top. Calcretes are associated with the red mudstones. The thickness in the type section is 150 m.

Lower and Upper Boundaries. The base is taken as the lowest red mudstone horizon; the top is overlain unconformably by cemented limestone screes.

Age. The Doğantaş Member is devoid of any fossils; the immediately underlying and laterally equivalent sequences (in the Kasaba Formation) are dated as Tortonian-Helvetian; this member is assumed to be the same age or slightly younger.

PART II

OPHIOLITE-DERIVED SEDIMENTS

PART II

OPHIOLITE-DERIVED SEDIMENTS

CHAPTER 3 SEDIMENTARY FACIES OF THE OPHIOLITE-DERIVED SEDIMENTS

CHAPTER 3

3.0 Sedimentary Facies of the Ophiolite-derived Sediments

3.1.0 Introduction

Comparison of the ophiolite-derived sediments over the area of study reveals individual sedimentary facies to be similar. To avoid unnecessary repetition by discussing the sequence formation by formation, a sedimentary facies scheme is developed that can be applied to all the ophiolite-derived sediments. The detailed sedimentary facies described in this chapter are used as the basis for the discussion of facies association and interpretation of depositional environment presented in Chapters 4 and 5.

The interpretation of each facies type is based on field evidence in the light of sedimentation processes reported from laboratory experiments and comparison with published work on modern sedimentary environments and, where relevant, ancient sequences.

3.1.1 Historical Background

The analysis of sedimentary sequences is increasingly sophisticated. Publications of the early 1960's (e.g. Duff and Walton, 1967; Allen, 1965; Merriam, 1964) were based on the search for, and recognition of, an ideal or normal cyclothem. This was followed by the development of the facies and facies association approach, typified by the publications of De Raaf *et al.* (1965), Elliot (1968) and Collinson (1969). This provided an improved descriptive method for sediments, emphasising the variability of sequences and exploding the myth of ideal cyclothems. However, much of its usefulness was lost in an often bewildering amount of terminology and "facies types" or significant and important parts of the sequence were "distilled out" in the need to fit every type of sediment into one or other of the 'erected boxes'.

There are currently two approaches to detailed, field, clastic sedimentological studies, facies analysis as outlined below and summarised by Teichert (1958), Krumbein and Sloss (1963), Reading (1978) and Walker (1979a), and the vertical sequence style of analysis (e.g. Heward, 1976, 1978a, b) where individual depositional units are assigned to an environment, or depositional sequences to a geomorphic body (e.g. alluvial fan).

In this thesis the two approaches are combined to produce the

most complete picture of the sedimentary environment at any time (i.e. facies approach) and to document the change in sedimentary environment with time (i.e. vertical sequence analysis).

3.1.2 Sedimentary Facies

Definition. In this study facies is the sum total of all primary characteristics of a rock. In the case of a sedimentary rock it is determined by grain size, composition, colour, texture, sedimentary structure, fossils and chemical or other parameters; based on the measurement of vertical sections and lateral profiles. Reading (1978b) states:

> "a facies should ideally be a distinctive rock that forms under certain conditions of sedimentation reflecting a particular process or environment".

Significance of Facies. Walthers Law of Facies (1894, in Middleton, 1973) states that:

> "the various deposits of the same facies area and similarly the sum of the rocks of different facies areas were formed beside each other in space, but in the crustal profile we see them lying on top of each other".

Hence, facies occurring in a conformable vertical sequence were formed in laterally adjacent environments and facies in vertical contact are the product of geographically neighbouring environments (Reading, 1978b). However, this only applies to a succession without a break (Middleton, 1973). A break in the succession marked by an erosional or sharp contact may represent the passage of any number of environments that have subsequently been removed. Even when erosion cannot be demonstrated sharp contacts indicate the facies may have been formed in depositional environments widely separated in space (Reading, 1978b). Therefore within a sedimentary sequence boundaries between different units are critical to the understanding of the sequence and overall depositional environment.

The degree to which a unit of rock is subdivided into a number of facies types is dependant both on the type of study and on the abundance of physical and biological structures in the rock (Walker, 1979a).

3.1.3 Sedimentary Environments.

The identification of ancient sedimentary environments is based on all possible data, e.g. lithology, process, preceeding, succeeding, and lateral environments, nature of preservation, diagenesis, etc.

Potter (1967) states:

> "A sedimentary environment is defined by a set of values of physical and chemical variables that correspond to a geomorphic unit of stated size and shape".

However, as emphasised by Walker (1979) some environments are defined geomorphologically (e.g. alluvial fan) and others by process (e.g. aeolian), it is therefore important to recognise both the environment and the range of processes operating in them.

3.1.4 Facies Scheme

The facies (facies is here synonymous with lithofacies) scheme outlined below and in Tables 3.1, 3.2, 3.3, 3.4, 3.5 and 3.6, is based primarily on sedimentary structures, grain size and composition. It is comparable to those used by Miall (1977, 1978), Rust (1978), Martin (1981) and Surlyk (1978) in the discussion of braided fluvial, glacio-fluvial and redeposited submarine sediments respectively.

Methods and Parameters

The establishment of any facies scheme is dependent initially on the raw data collected.

Database. In the present work a large number (ca. 350) of sedimentological sections were measured at a variety of scales dependant on exposure. Where exposure permitted the sections were measured at 90° to bedding. In areas of good exposure lateral as well as vertical sections were measured and photographed and lateral facies transitions recorded.

In the field no attempt was made to subdivide rock units into the well defined facies units shown here. Instead the parameters which are used in the facies subdivisions were carefully noted, namely; grain size, grain size variation, sedimentary structures, biogenic features and composition.

Grain Size. The grain size scale used is that introduced by Wentworth (1922). In this scale the gravel/sand boundary lies at 2 mm (-1.00ϕ) and the sand/clay boundary at 0.0625 mm (4.00ϕ). The average grain size was recorded and estimated to within a Wentworth grain size class.

Conglomerates. In describing conglomerates the average grain size was recorded, along with the average of the ten largest clasts after the exclusion of any outsize clasts. Visual estimates of the

percentage of conglomerate size clasts, roundness, sphericity and angularity were made from comparison with standard charts (Odell, 1977) (Fig. A.1, Appendix A). In cases where a sediment exhibited a marked bimodal grain size distribution, the average and maximum clast size of both modes was estimated. The presence and approximate percentage of mud (clay and silt) was also recorded.

In drawing up sedimentological logs of conglomerates, the average of the ten largest clasts was used and simplified into one of the Wentworth grain size classes. In some instances the maximum clast size is plotted to the right of the log.

Composition. Except where specifically stated the scheme is independent of composition. The sandstones and conglomerates range from ophiolitic litharenites to bioclastic limestones containing less than 15% terrigenous clastic material (Chapter 6).

Sediment Body Geometry. The terms used for stratification and thickness are after Reineck and Singh (1973) and Allen (1963).

3.2.0 Subaerial Sedimentary Facies

3.2.1 Introduction

Subaerial sediments are restricted to the upper parts of both the Salir Formation (Bağbeleni Member) and the Kasaba Formation (Doğantaş Member) where they are particularly well developed.

3.2.2 Conglomerate Facies

3.2.3 Matrix-rich Conglomerate (Gmr)

Description. This facies comprises of poorly sorted, rounded to subangular (R1-R3), pebble, cobble and boulder conglomerate. It is restricted to the lower proximal parts of the Kasaba Formation (Doğantaş Member) (Fig. 4.20) and parts of the Bağbeleni Member. Grain size and texture are very variable. This facies lacks the well developed clast framework and imbrication typical of facies Gm. Clasts vary in size from coarse sand to boulders up to .80 m in diameter, which in some cases are supported in silty muddy matrix. Lenticular horizons of matrix support pass laterally and vertically into clast-supported horizons.

Structure. Beds between .80 and 2.50 m thick have non-erosive planar bases and planar or irregular sharp tops. Clasts may be aligned parallel to the basal surface or a-axes are rarely imbricated

FACIES	GRAIN SIZE	EXTERNAL CONTACTS	INTERNAL STRUCTURE	GEOMETRY
Massive cgl. Gm	pebble-boulder cgl.	U. gradational or planar and sharp L. erosive, sharp	massive, a-axes imbrication normal to flow	sheet
Trough-cross-strat. cgl. Gt	vc sst.-boulder cgl.	U. gradational L. erosive sharp	trough-cross-strata tangential to lower bounding surface	scour fills or lenticular wedges
Planar-cross-strat. cgl. Gp	vc sst.-boulder cgl.	U. sharp planar L. slightly erosional undulatory	planar-cross-strata oblique to lower bounding surface	wedge
Matrix-rich cgl. Gmr	vc sst.-boulder cgl.	U. planar, irregular sharp L. non-erosive, sharp	structureless, areas of matrix-support	sheet

TABLE 3.1 Summary Table of Subaerial Conglomerate Facies.

upcurrent. Interbedded sandstone lenses are rarely cross-stratified.

Matrix. Matrix is generally a silty medium sand with a moderate to low clay content.

Interpretation

Processes. The absence of a well developed clast framework and imbrication suggests that this conglomerate did not form as a result of bedload transport in a unidirectional flow (cf Facies Gm). Sediments similar to this have been attributed to debris floods or mudflows (debris flows). Clasts in gravitationally unstable positions and protruding from the tops of some beds suggest matrix strength during deposition.

Modern Analogues. Conglomerates similar to this have been described from modern semi-arid alluvial fans in Arizona (Blissenbach, 1954). In this area mudflows deposit poorly sorted coarse bouldery material, with a random clast orientation which lacks a well developed clast framework. The term mudflow is misleading as the actual mud content may be less than 10% (Lustig, 1965; Miall, 1970). Sharp and Nobles (1953) use the term debris flood to describe similar recent catastrophic events. Mudflows on Recent alluvial fans in California (Bull, 1963) vary between matrix-supported mud-rich deposits, and clast-supported mud-poor deposits. The type of deposit reflects the fluid (water) content of the flow.

In conclusion this facies was deposited by debris flows or mudflows, with variable water content, which develop at the present day as a result of rapid run-off in semi-arid areas (10-20 inches per annum, Blissenbach, 1954).

3.2.4 Massive Conglomerate (Gm)

Description. This facies comprises of pebble, cobble and boulder clast-supported conglomerate (grain size varies from 0.10-1.50 m). Grain size varies both laterally and vertically, where present crude stratification parallel to bedding is delineated by variations in the average grain size or by a higher concentration of larger clasts (Fig. 3.1). Discontinuous clay, silt and cross-stratified sandstone lenses are commonly interbedded within the conglomerate so that individual depositional events are difficult to recognise.

Fig. 3.1

Massive conglomerate (facies Gm).
Note presence of crude stratification, sandstone-siltstone lenses and well developed imbrication.
Palaeoflow was to the right and out of the photograph.
Clast (a) is 40 cm across.
Conglomerate facies association, Kasaba Formation (Doğantaş Member).
GR. 517369.

Fig. 3.2

Trough-cross-stratified conglomerate (facies Gt) infilling broad scour in underlying sandstone/mudstone sequence, section parallel to flow.
Note alignment of clasts down foresets.
Unit is 2 m thick.
Conglomerate-sandstone association (fluvial braidplain)
Kasaba Formation (Doğantaş Member). GR. 520355.


a

Structure. The base of individual conglomerate units is often strongly erosive (Fig. 4.23); scours at the base are frequently filled with trough-cross-stratified conglomerate (Gt). Tops to conglomerate units are generally gradational to overlying conglomerate or sandstone, or are planar and sharp.

Imbrication. Contact imbrication of the clast a-axes normal to the inferred current flow is often a prominent feature (Fig. 3.1).

Matrix. The most common matrix is a muddy silty medium sandstone. The percentage of matrix varies both laterally and vertically, in some places areas of conglomerate are matrix-free.

Interpretation

Bed lenticularity and the poor segregation of sand and gravel is consistent with a fluvial origin (Clifton, 1973). Associated facies which include reddened oxidized horizons, formed subaerially, and calcrete palaeosols are in agreement with this.

Processes. Clast a-axes imbrication normal to palaeoflow in framework-supported conglomerate is formed as a result of bedload transport in response to unidirectional flow (Rust, 1972b), and is evidence for the individual response of particles to a flow mechanism (Harms *et al.*, 1975).

Approximations of flow strength and critical tractive force, from clast size, for very similar conglomerates (gravels) (Church, 1978; Martin, 1981) indicate that transport took place mainly under upper flow regime conditions, although this conglomerate probably encompasses a wide range of flow strengths and variable sediment concentrations. The absence of cross-stratification indicates that bedform resistance did not cause flow separation and the depth of flow was probably shallow (Church and Gilbert, 1975; Rust, 1975; Saunderson, 1975).

Most of this conglomerate accreted as planar sheets (Rust, 1972a), although where present lenses of trough-cross-stratified conglomerate suggest greater flow depths.

Modern Analogues. Conglomerates similar to facies Gm are found in modern alluvial environments (Smith, 1970; McDonald and Bannerjee, 1971; Rust, 1972; Church, 1972), where longitudinal bars are the dominant depositional features. These bars are formed by unconfined flow during the flood stage. They may be stable at maximum flood

or form as a result of decreased flow strength at falling stage (Leopold and Wolman, 1957; Rust, 1975; Bluck, 1979). As in most ancient deposits bar morphology is not distinguishable within facies Gm and the detailed morphological classification of bar types used in modern alluvial environments (Smith, 1970; Rust, 1979) cannot be applied.

Conclusion. Facies Gm was deposited by mainly widespread unconfined sheet-flood flow, with a high poorly sorted sediment load, in the form of diffuse sheets or within low relief bed forms (Smith, 1974; Eynon and Walker, 1974; Hein and Walker, 1977; Rust, 1978, 1979).

3.2.5 Trough-cross-stratified Conglomerate (Gt)

Description. Sets of trough-cross-stratified conglomerate form units between 0.60 and 3 m thick (Fig. 3.2). Grain size varies between very coarse sand and boulder gravel. This facies is distinguished from facies Gp by the geometry of the cross-strata.

Structure. In sections parallel to inferred flow, cross-sets frequently infill large scours, between 1 m and 2 m deep and 3 m and 6 m across (Fig. 4.23) cut into the underlying mudstone/ sandstone unit. In sections normal to flow (Fig. 4.24) scours are consistently narrower but of a similar depth. The base of each unit is strongly erosional.

Cross-strata are markedly heterogenous composed of poorly sorted openwork conglomerate, separated by pebbly sand and sandy units (Fig. 3.2). Upwards and laterally trough-cross-sets pass transitionally into massive conglomerate (Gm) of a similar grain size (Fig. 4.23). Dip on the foresets is generally low between 10° and 15°, within the smaller troughs, however it may be as high as 25°. In many instances facies Gm contains small cross-stratified lenses of facies Gt. In these areas cross-stratification is difficult to distinguish from well developed imbrication, this is particularly true for poorly exposed parts of the Bağbeleni Member.

Matrix. The matrix is generally a medium to coarse, silty sandstone, as in Gm the percentage of matrix varies laterally and vertically and some areas are matrix-free. Analogues and interpretation of this facies are discussed below (3.2.9).

3.2.6 Planar-cross-stratified Conglomerate (Gp)

Description. Planar-cross-stratified conglomerate forms sets between 0.40 and 2.50 m thick. This facies which is of limited occurrence is distinguished from facies Gt by the geometry of cross-stratification (Figs. 3.3 and 5.31). Grain size varies from very coarse sand to boulder conglomerate, the average falls in the cobble class.

Structure. Heterogeneous cross-strata are composed of poorly sorted conglomerate concentrations separated by pebbly sand and very coarse sandy units. The lower bounding surfaces are either undulose or slightly erosional. Upper surfaces are indistinct as they are generally overlain by other conglomerate facies, normally Gm (Fig. 3.3). Only rarely are they overlain by sand, in which case they are sharp.

In section wedge shaped geometry is characteristic, conglomerate foresets commonly lensing out downcurrent into coarse and medium sand laminae (Fig. 5.31). In sections normal to flow units have a planar or slightly concave lower bounding surface.

Interpretation of Facies Gp and Gt

Calcrete palaeosols and reddened oxidised horizons, formed subaerially, interbedded with this facies, suggest deposition in a fluvial environment.

Processes. Cross-stratification is formed by flow separation caused by the presence of bed roughness elements of "form drag" origin (e.g. migrating dunes) or of aggradational origin such as delta wedges or scour fills (Jopling, 1965). Minimum flow depth can be estimated from thickness of sets. For trough-cross-sets formed by migrating mega-ripples water depth is equal to at least twice set height (Harms *et al.*, 1975). Tabular sets however may form as the result of a shallow flow expanding into a standing body of water of any depth (Jopling, 1965, 1966).

The size (generally less than 3 m), and lateral and vertical facies associations (Chapters 4 and 5) which indicate deposition in a totally fluvial environment, of both types of cross-strata are not consistent with origin as coarse grained delta foresets which are characteristically much larger (e.g. Gilbert, 1885, 1890; Church and Gilbert, 1975; Collinson, 1978).

Fig. 3.3

Planar-cross-stratified conglomerate (Facies Gp) passing transitionally into massive conglomerate (facies Gm).
Note undulose slightly erosional base to unit.
Cross-sets are 1.5 m high.
Conglomerate-sandstone association (fluvial braidplain).
Kasaba Formation (Doğantaş Member). GR. 522362.

Fig. 3.4

Massive sandstone (s), red mudstone (m) and calcrete horizon (c).
Fine grained overbank facies (fluvial braidplain),
Kasaba Formation (Doğantaş Member).
Lenticular conglomerate horizon formed by minor channel during flood.
Face is 3 m high. GR. 520358.

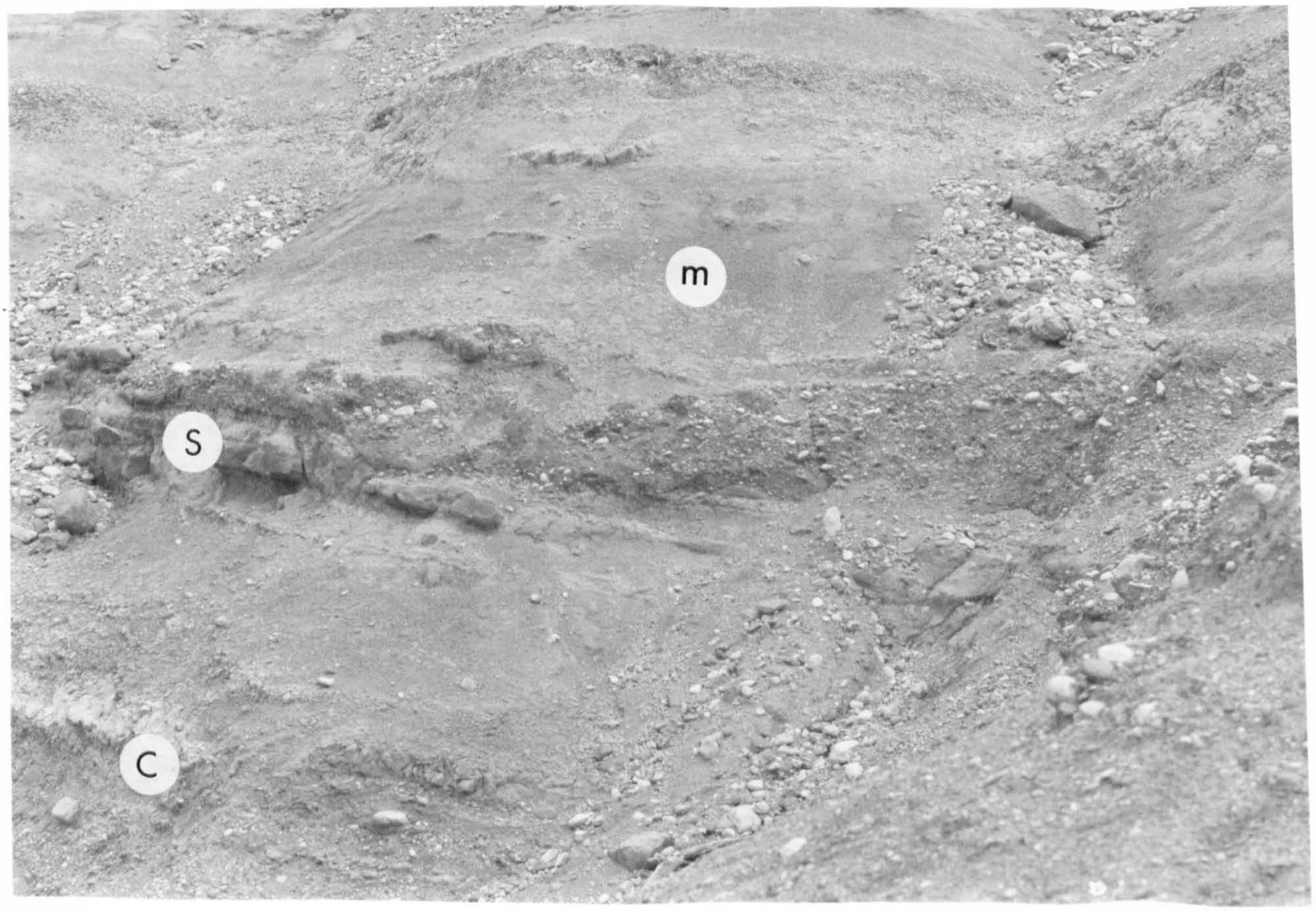
m
S
C

Hein and Walker (1977) and Eynon & Walker (1974) propose the downstream migration of transverse bars with distinct slip faces to deposit facies Gp. Miall (1977), however, considers that gravel cross-strata are restricted to deep channel flood stage deposits.

Modern Analogues. Sedimentary structures from modern gravelly braided fluvial deposits are not well documented, although it is known that gravel bars rarely show trough-cross-stratification (Miall, 1977; Rust, 1978).

Conclusion. Trough-cross-stratified conglomerate infilling scours above a sharp erosional surface are interpreted as the result of scour and channel-fill features. The scours may be related to local vortices developed around obstructions, or to channels formed by avulsion at high water stage (Miall, 1977). Laterally discontinuous trough-cross-stratified conglomerates are the deposits of migrating bedforms within channels formed at high flood stage (Martini, 1977).

Transitional gradational contacts between facies Gt and Gm is consistent with transport as diffuse sheets or within low relief bedforms (Smith, 1974; Eynon and Walker, 1974; Hein and Walker, 1977; Rust, 1978). Facies Gp may have formed as a result of migrating bedforms at high flood stage (Eynon and Walker, 1974) or more likely as the lateral modification of longitudinal bars during falling stage, when flow diverges away from the bar axes (Rust, 1978; Bluck, 1979).

3.2.7 Sandstone Facies

Within the subaerial sequences sandstones make up a relatively minor amount of the sedimentary succession (see Chapters 4 and 5).

3.2.8 Cross-stratified Sandstone (Sp and St)

Description. Both facies generally comprise of medium to coarse sandstone with occasional scattered granule conglomerate clasts. Cross-stratification is delineated by slight variations in grain size, by higher concentrations of larger clasts or slight mineralogical variations.

Structure. The sandstones occur in two modes:

(1) as sheets and wedges bounded by conglomerate units, in which trough and planar cross-sets are present. Units are up to .70 m

FACIES	GRAIN SIZE	EXTERNAL CONTACTS	INTERNAL STRUCTURE	GEOMETRY
Planar-cross strat. sst. Sp	med. to coarse sst.	U. gradational or sharp, planar L. gradational or erosive	planar-cross-strata oblique to basal surface	wedge
Trough-cross-strat. sst. St	med. to coarse sst.	U. gradational or sharp, planar L. erosive	trough-cross-strata tangential to basal surface	wedge
Parallel-strat. sst. Sl	med to coarse sst. with scattered granules	U. sharp or gradational L. gradational, or sharp planar	horizontal strat. 2-20 mm thick	sheet
Low angle cross-strat. sst. SL	med. to fine sst.	U. gradational or sharp L. sharp, planar gradational, rarely erosive	irregular low-angle-parallel strat. dip less than 10^{o}	sheet
Rippled sst. Sr	(medium), fine to very fine sst.	U. gradational L. gradational	assymetric troughs	sheet

TABLE 3.2 Summary Table of Subaerial Sandstone Facies.

thick and 10 to 15 m in lateral extent;
(11) as slightly dipping sheets or wedges within massive and parallel stratified sandstone, up to .50 m thick, these are generally finer grained and transitional to facies Sl.

In the former planar cross-strata predominate, in the latter trough geometry is dominant; both are of the order of 10 to 20 cm thick. Dip on the cross-sets varies between 5 and 20°, but is commonly 10-15°.

Interpretation

Bedforms such as those observed have been produced in flume experiments (Harms and Fahnestock, 1965; Harms *et al.*, 1975) and can be interpreted in terms of stream flow velocity (Miall, 1977). Both types are formed under low flow regime conditions (Harms and Fahnestock, 1965; Harms *et al.*, 1975).

Modern Analogues

Sp within conglomerate units: Tabular sand wedges and sheets are deposited at gravel bar margins at low or falling stage (e.g. Boothroyd and Ashley, 1975, Fig. 17). They generally have inclined or horizontal topsets and steep avalanche faces (Bluck, 1979).

Sand sheets are formed by the progradation of rippled sand into deep water and occur in side channels or form levees at channel margins (Bluck, 1979). This style of cross-stratification produced is of small scale and less heterolithic than that produced by migration of sand bars (Bluck, 1979). This is consistent with the style of cross-stratification observed here and lenticular sand sheets within conglomerate units are interpreted to be the result of low flow stage aggradation of sand wedges adjacent to gravel bars.

Sp within fining-upward cycles above conglomerate units: Sand waves and small dunes are known to deposit multiple sets of planar and trough cross beds less than 30 cm thick in shallow areas at low flow velocities (Cant, 1978). The cross-strata are much smaller in scale than those formed in channel bars (Cant and Walker, 1978; Cant, 1978) and comparable with those described here.

St within fining-upward cycles above conglomerates: Multiple trough-sets are the result of scour formation in conjunction with megaripple dune migration under uniform or non-uniform flow (Harms and Fahnestock, 1965; Harms *et al.*, 1975; Miall, 1977). Megaripples active during flood may be preserved as a result of the reduction of

trough depth with falling stage (Cant, 1978). Facies St was therefore probably deposited by migrating megaripples.

3.2.9 Parallel-stratified Sandstone (Sl)

Description. This facies comprises horizontally stratified medium to coarse sand and occasional scattered granule conglomerate clasts. Stratification is delineated by slight variations in grain size. This facies occurs as horizontal sheets and lenses within conglomerate units and more commonly as beds associated with cross-stratified sandstone overlying conglomerate units. Depositional dip is rarely greater than 5°.

Interpretation

The presence of continuous strata of conglomerate and sand suggests transport transitional between upper and lower flow regimes (Harms and Fahnestock, 1965; Walker, 1977). Flow velocity fluctuations on a plane bed result in sporadic downstream movement of gravel sized clasts. Where granule conglomerate predominates deposition was probably in the upper flow regime flat bed field (Harms *et al.*, 1975). In beds dominated by finer grain sizes deposition was in the lower flat bed field.

3.2.10 Low-angle cross-stratified Sandstone (SL)

Description. This facies comprises low angle (less than 10°) cross-stratified medium to fine sandstone. Cross-strata are irregular, concave or convex down and rest on broad flat to shallow scours.

Interpretation

Processes. Stratification of this type has been described from a variety of other deposits (Cant and Walker, 1978; Miall, 1977; Rust, 1978; Martin, 1981). These authors suggest shallow high velocity flow into low relief scours.

Modern Analogues. Similar low angle cross-stratified units have been recorded by Singh (1977) from within large low amplitude fluvial bars. The low angle cross-stratification of these bars is comparable to beach cross-stratification but contrasts with steeper sets of slipface bound bars (e.g. Cant, 1978; Cant and Walker, 1978).

3.2.11 Rippled Sandstone (Sr)

These facies form only a small percentage of the subaerial sandstones, and are confined to the braidplain association of the Kasaba Formation. Their structure is not easily seen in the partially cemented faces of most of the rock units described here.

Description. Ripple-cross-stratified sandstones are consistently finer grained than the other stratified sandstones. Cross lamination is asymmetric and trough-shaped with rounded crests. They are associated with, and pass laterally into, parallel laminated and massive sandstone. Contacts between sets are gradational.

Interpretation

Processes. Linguoid ripples produce cross-lamination of this type (Allen, 1963). The asymmetric nature of the ripples suggests they were formed under conditions of unidirectional current flow (Reineck and Singh, 1975, p. 27). Allen (1970) and Harms *et al.* (1975) have shown that a whole range of sedimentary structures, including ripples are produced by currents of low flow velocity transporting material of different grain size. Experimental studies suggest velocities between 0.2-0.7 ms^{-1} for current ripple generation (Harms *et al.*, 1975). However, relationship between bedform stability fields is complicated, and it is common to find ripples, megaripples and plane laminations in close association (cf Martin, 1981) suggesting non-uniform flow conditions.

Modern Analogues. During low flow stage ripples and small dunes are observed to migrate across bar surfaces in modern fluvial systems, forming small scale cross-stratification (Miall, 1977, p. 36; Smith, 1970).

3.2.12 Fine Grained Facies

Thick development of these facies types is restricted to the braidplain sequence of the Kasaba Formation (Chapter 4, Fig. 4.24). Elsewhere as in the Bağbeleni Member (Salir Formation) (Chapter 5, Fig. 5.29) these facies occur as thin laterally discontinuous drapes overlying coarse sandstone and conglomerate units.

3.2.13 Massive Sandstone (Sm)

Description. In outcrop this facies is characterised by its unbedded or poorly bedded homogeneous texture (Figs. 3.4, 4.23).

Bed thickness ranges from .15 m to 2.50 m. Grain size varies from very fine to coarse, mud content is generally high. Red colouring and green mottling and 'veining' is often characteristic of this facies, this is discussed below (3.2.15). Evidence of bioturbation is seen in mottled and green-grey variable grain sized areas in an otherwise homogeneous sandstone. Rare isolated ripples up to 3 cm high and 7-10 cm across and slightly coarser sand laminae are also observed. Dessication cracks and calcretes are intimately associated with this facies.

Interpretation

Lack of current structures, indicates deposition from suspension in standing water. Ripples and winnowed sand laminae suggest periods of slight current activity alternating with periods of quiescence (cf the flaser, wavey and lenticular bedding of Reineck and Singh, 1973). Dessication cracks and calcretes are consistent with periods of subaerial exposure.

3.2.14 Mudstone (Mm)

Description. This facies is of variable composition, estimated clay contents range from 80% to less than 30%.

Structure. Two members are recognised:

(I) Thick, to very thick (.50-4.0 m) mudstone units forming the upper parts of fining-upward cycles as in the Kasaba Formation (Figs. 4.23, 4.24). Structureless units sometimes contain indistinct coarse silt laminae up to 1 cm thick, which are continuous over several metres. Colour is red or green. Generally the mudstones are unbedded (Fig. 3.4) with a homogeneous texture. In thin section they are extremely poorly sorted, with a textural inhomogeneity on a microscopic scale, varying from silty claystones and claystones to clayey sandstones. Rare rootlet horizons, dessication cracks and calcretes occur in association with this facies.

(II) Thin (1-10 cm) laterally discontinuous drapes overlying conglomerate and coarse sandstone units as in the Baǧbeleni Member (Salir Formation) (Chapter 5). These are composed of faintly laminated clay rich mudstone and silt laminae, often with abundant carbonaceous material.

Interpretation

The general absence of sedimentary structures indicative of

current flow suggests deposition in standing water. Dessication cracks, rootlets and calcretes are consistent with intermittent subaerial exposure. Microscopic inhomogeneous textures may be produced by sediment mixing from bioturbation.

Thin laminated horizons within conglomerate-sandstone sequences document periods of quiescence in an otherwise active environment, and indicate a time of reduced sediment supply probably associated with low water level.

3.2.15 Calcrete (Cp)

Description. Pedogenic carbonates (calcretes) occur in two forms:
(I) Horizons of rounded, nodular, pale red to grey/white carbonate (carbonate nodules similar to this are termed glaebules by Allen, 1974a) within mudstones and fine sandstones towards the top of individual fining-upward cycles. They are laterally continuous over tens of metres and up to 20 cm thick. Nodules make up between 20% and 60% of the rock by volume. Individual nodules are 0.5-3.0 cm across and are sometimes elongate parallel to bedding.
(II) Nodular and brecciated layers (Figs. 3.4, 4.22) are 10-20 cm thick and laterally continuous over up to 100 m, although they may be truncated by erosional based overlying conglomerate or sandstone. They occur either with reddened mudstone, or more commonly as caps to conglomerates or very coarse sandstones (Fig. 4.22), where they reach their thickest development. Bases to layers are irregular and commonly comprise only 30% carbonate, this increases uniformly upwards to a maximum of 80% carbonate at the tops which are often brecciated and infilled with red siltstone. In thin section the nodules and layers are composed of micrite, within which are scattered detrital grains (Fig. 3.5). Microspar has crystallised to sparite in patches, which now enclose detrital grains (Fig. 3.5). Chert and quartz grain margins are frequently corroded and surrounded by coarser grained micrite (Fig. 3.6, see also 6.2.5). In some instances quartz has been extensively preferentially corroded parallel to crystallographic axes (Fig. 3.6). Crystalline and amorphous haematite is patchily distributed throughout the rock (Fig. 3.5) producing a red hue. The carbonate horizons are normally unveined, occasionally small scale (0.01 mm) fracture patterns occur. Irregular patches of fine grained silt material may represent burrows.

Fig. 3.5

Photomicrograph of calcrete showing finely dispersed detrital grains within a micrite matrix. The micrite has recrystallised to sparite in patches (s) which now enclose detrital grains. Irregular inhomogeneous texture and areas of finer grained silt (b) are the result of bioturbation.
Field of view 2 cm. Spec. 205a/80 Kasaba Formation (Doğantaş Member). GR. 521360.

Fig. 3.6

(a) S.E.M. photograph of quartz grain in calcrete.
The quartz (q) is being replaced and invaded by stubby prismatic calcite crystals (c).
Spec. 205a/80 Kasaba Formation (Doğantaş Member).
GR. 521360.

(b) Preferential corrosion and replacement of quartz (q) by calcite (c) parallel to crystallographic axes. Calcrete horizon.
Spec. 205a/80 Kasaba Formation (Doğantaş Member)
GR. 521360.

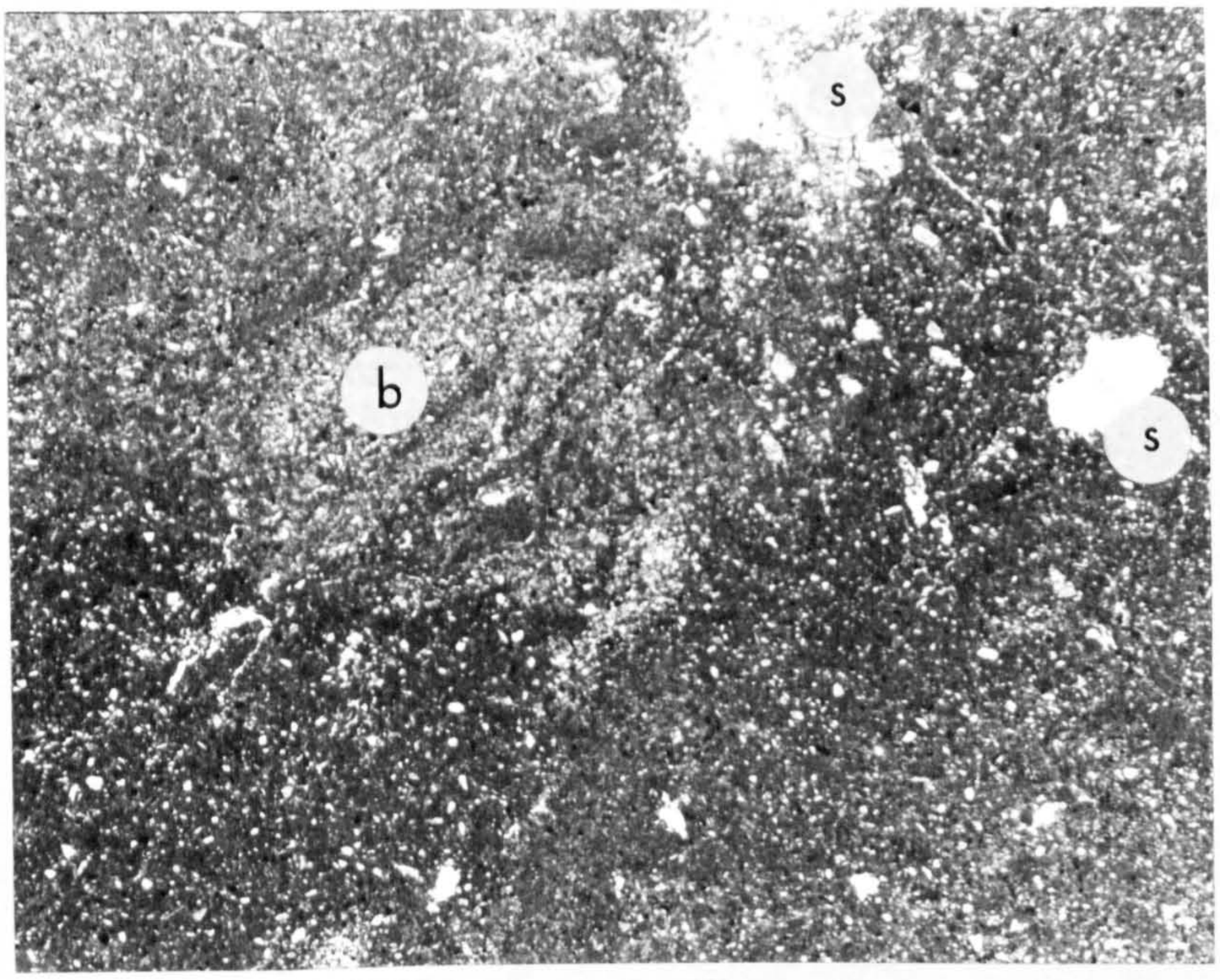
s
b
s

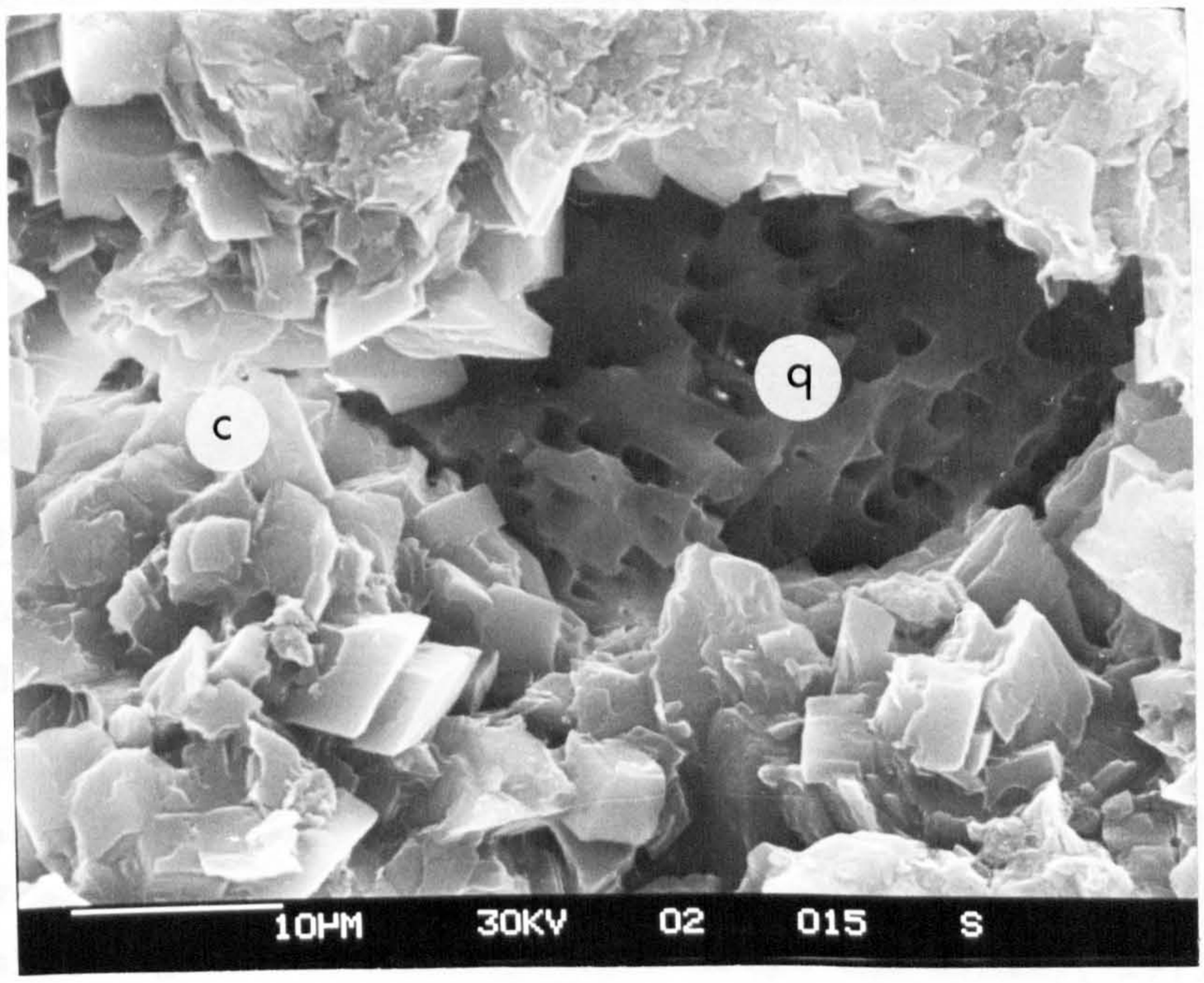
q
c
10HM 30KV 02 015 S

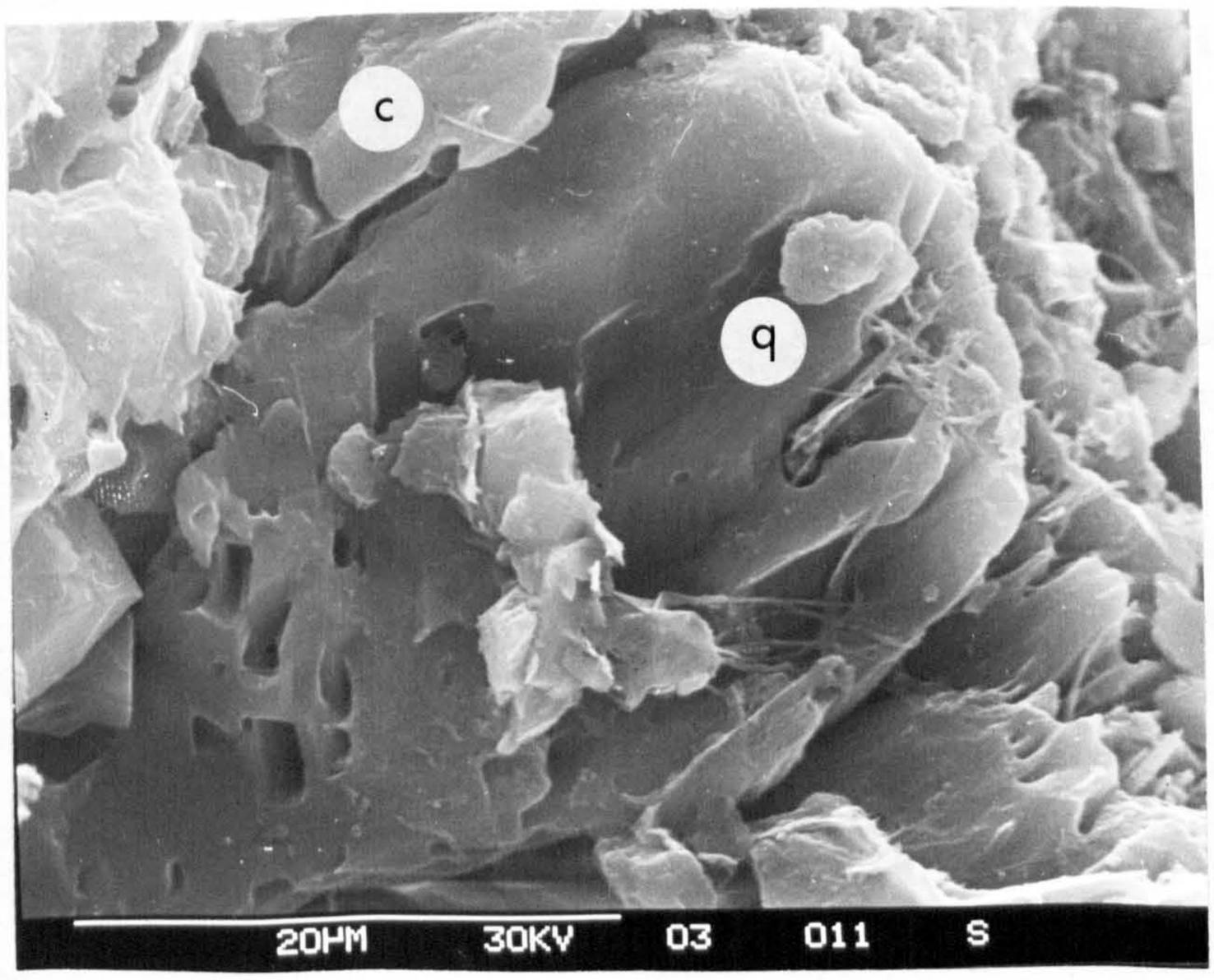
c
q
20HM 30KV 03 011 S

Interpretation

From their mode of occurrence, composition replacive and displacive internal growth structure the carbonate horizons are interpreted as penecontemporaneous features developed in subaerially exposed overbank sites prior to the deposition of the next fluvial cycle (Allen, 1974a, b; Leeder, 1975; McPherson, 1979).

These carbonates are closely comparable in texture and composition to modern pedogenic carbonates (Goudie, 1973). Calcretes form at the present day in pedocal soils of hot semi-arid regions (Reeves, 1970; Goudie, 1973). They are formed by illuviation in the soil profile, upper zone solubles are carried downwards and precipitated when soil moisture is removed by evaporation (Gile *et al.*, 1966; Gile, 1970; Reeves, 1970; Goudie, 1973). Calcretes of this nature are best developed in areas of mean annual precipitation of less than 500 mm, a very seasonal distribution, low soil surface relief required to prevent excessive run-off, and reduced ground water leaching (Reeves, 1970; Goudie, 1973). The relevance of this to the regional palaeo-climatic interpretation and sedimentary model is discussed more fully in Chapter 4.

3.2.16 Modern Analogues of the Fine Grained Facies

Overbank Deposits. Fine grained overbank sediments in modern fluvial sequences have received scant attention when compared with the associated active channel sediments (cf Miall, 1977, 1978; Rust, 1978). Modern braided streams are not characterised by large areas of floodplain, however, many do have abandoned areas with variable vegetation cover (Williams and Rust, 1969; Miall, 1977). In humid regions extensive vegetation develops (Boothroyd and Ashley, 1975; Miall, 1977), in arid regions reddened oxidised horizons and calcretes are formed (Allen, 1974a, b; Steel, 1974; Rust, 1979).

Deposition in the inactive areas is primarily by vertical accretion of fine sediment (Williams and Rust, 1969; Rust, 1979) and washover from active channel areas. Inactive areas are only covered by water at highest flood stage, the deposition of fine sediment is encouraged by the slow flow velocities, produced by the shallow depths and friction due to vegetation (Miall, 1977). In modern examples these sediments are characterised by small scale current structures and bioturbation or plant growth (Williams and Rust, 1969; Boothroyd and Ashley, 1975; Rust, 1979).

Silt Drapes. At low water level pools of water are left in abandoned channels, fine silt and mud settling from suspension forms lenticular drape deposits (Miall, 1977). The reactivation of most channel areas results in drapes of this nature having a low preservation potential (Cant, 1978).

3.3.0 Shallow Marine Sedimentary Facies

3.3.1 Introduction

Shallow marine sedimentary facies form only a small percentage of the total sedimentary succession. The best development is in proximal parts of the Kemer Formation around Sinekcibeli (Fig. 4.1) in marine parts of the Kasaba Formation (Fig. 4.20) and in the transition zone in the Bağbeleni Member (Salir Formation) (Fig. 5.29). In these sequences shallow marine macro-faunas and *in situ* coral reefs (Chapter 8) attest to deposition in a shallow marine environment. Some of the sandstones also contain abundant benthonic and occasional scattered planktonic foraminifera. In some sequences, as in the Bağbeleni Member, the distinction between marine and non-marine sediments is unclear. This is a common problem in coarse grained conglomeratic sequences where shoreline facies are not well developed (A. Heward, pers. comm., 1979). Table 3.5 compares principal sedimentary features of conglomerate facies from the three sedimentary environments (i.e. subaerial, shallow marine, deep marine (redeposited facies)).

Coarse grained conglomeratic shorelines and shallow marine deposits are very poorly documented, the only detailed studies of modern environments are those of Clifton *et al.*, 1971; Clifton, 1973 and Clifton, 1981.

3.3.2 Stratified Conglomerate-sandstone (Gst)

Description. This facies consists of laterally continuous horizons of regularly interstratified conglomerate and medium to coarse sandstone (Fig. 3.7). Individual beds are typically 20-50 cm thick, conglomerate clasts are aligned parallel to the bedding. Sandstones are moderately to well sorted with a very low mud/silt content. Contacts with underlying and overlying sediments are gradational. Two end members can be distinguished:

(I) conglomerate - consists of 80%+ conglomerate; pebbles, cobbles and granules form laterally continuous horizons interstratified with

FACIES	GRAIN SIZE	EXTERNAL CONTACTS	INTERNAL STRUCTURE	GEOMETRY
Stratified cgl-sst. Gst	cobble cgl. -c sst.	U. gradational L. gradational	regularly interstratified cgl. and sst.	sheet
Massive conglomerate G	pebble to boulder cgl.	U. sharp, planar or gradational L. non-erosive, sharp or gradational	structureless, random clast orientation	sheet
Trough-cross-strat. sst. ST	med. sst.- granule cgl.	U. sharp, planar often burrowed L. sharp, planar	trough-cross sets, tangential to lower surface	wedge
Plane laminated sst. Spl	med.- coarse sst.	U. sharp to gradational L. sharp to gradational	Laminations 3-10 mm thick	wedge/sheet
Mudstone Mm	silt-clay	U. sharp, planar L. sharp planar, rarely drapes underlying bedform	structureless homogeneous	sheet

TABLE 3.3 Summary Table of Shallow Marine Sedimentary Facies.

very coarse to medium sandstone;
(II) sandstone - consists of very coarse sandstone with laterally discontinuous pebble and granule conglomerate stringers. The sandstones are well sorted with heavy mineral concentrations. This facies is transitional to plane laminated sandstone.

Interpretation

The well developed segregation of sand and conglomerate into discrete laterally continuous horizons (Fig. 3.7) suggests wave reworking in a shallow marine environment (Clifton, 1973). This facies requires currents of varying velocity over a period of time and may indicate periods of locally slow sedimentation over a large area.

3.3.3 Massive Conglomerate (G)

Description. This facies is characterised by its clast support, lack of stratification and random orientation of clasts.

Two members are recognised:
(I) pebble, cobble and boulder conglomerates with randomly orientated clasts, and abundant silty sandstone matrix (Fig. 3.8). They are very poorly sorted with non-erosive bases and sharp planar or gradational tops;
(II) randomly orientated pebble, cobble and boulder conglomerate, with a moderately to well sorted coarse to very coarse sandstone matrix, with a very low mud/silt content. Non-erosive or gradational bases and sharp or gradational planar tops.

Interpretation

Those units with high mud/silt content are restricted to the near shore area of the Kasaba Formation (Chapter 4, Fig. 4.20). They show no evidence of reworking by marine processes and are interpreted as being deposited as poorly sorted sheets by fluvial channels entering a shallow sea (4.8.2). In this environment the presence of patch-reefs offshore protects the shoreface from marine reworking. Beds with a sandstone matrix which is well sorted and a low mud/silt content suggests partial reworking by marine processes. The absence of bedforms and stratification suggest low current velocities that were unable to transport material coarser than medium to coarse sand.

In the absence of other criteria (fossils etc.) it is often

Fig. 3.7

Stratified conglomerate-sandstone (facies Gst).
Note well developed separation and lateral continuity of conglomerate and sandstone horizons, parallel to bedding.
Beds dip to the left.
Proximal Kemer Formation (near Sinekcibeli).
Stick is 1 m long. GR. 370405.

Fig. 3.8

Massive conglomerate (facies G), with characteristic random clast orientation.
Note high mud content, non-erosive bases paralleling underlying beds and total lack of sedimentary structures.
Interbedded mudstones (m) contain an abundant *in situ* shallow marine fauna of bivalves and gastropods.
Kasaba Formation.
Face is approximately 25 m high. GR. 502336.

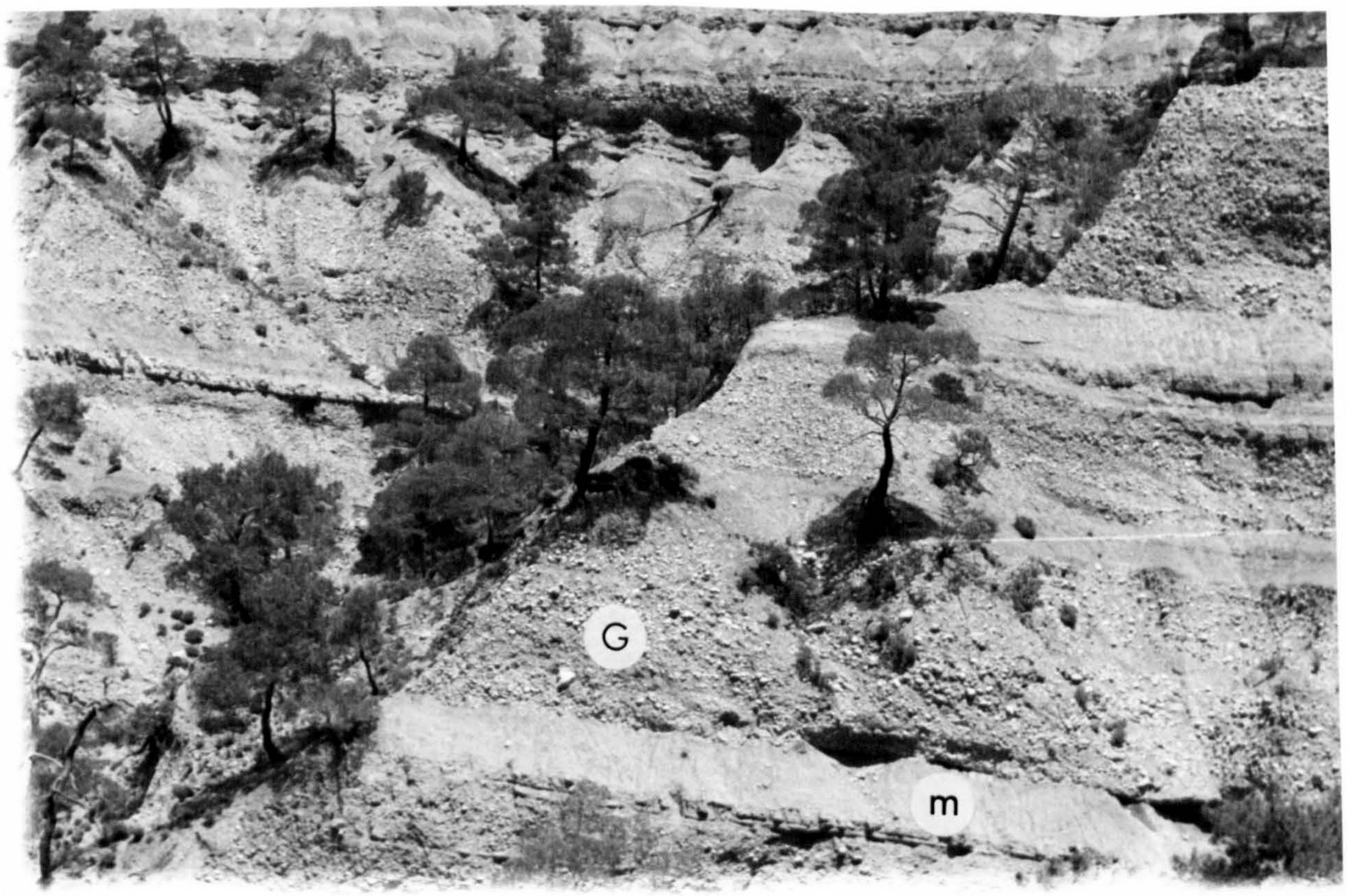
G
m

difficult to distinguish this facies from subaerial massive conglomerate. Table 3.5 outlines the basic differences between the two facies.

3.3.4 Trough-cross-stratified Sandstone (ST)

Description. This facies consists of well sorted clean, often calcareous medium sandstone to granule conglomerate. Cross-sets between 20 and 30 cm thick form wedge or sheet units. Internal contacts are gradational, trough sets often passing downcurrent into plane-laminated sandstone. External contacts are normally sharp, granule or pebble lags occur at the base, tops to units are often burrowed (Fig. 4.29).

Interpretation

Sets of trough-cross-strata indicate currents capable of moving granule sand in dune bedform (Harms *et al.*, 1975). Similar facies have been described by Clifton *et al.* (1971) and Clifton (1981) from areas of wave build-up and surf where rip-currents and longshore currents continually rework sediment. Davidson-Arnott and Greenwood (1974) describe trough-cross-strata from a gently sloping shoreface, where deposition was by longshore currents parallel to the shoreline. This can be excluded in the present case on the basis of palaeocurrent evidence which has a wide scatter (Fig. 4.19, Chapter 4). The sporadic occurrence of this facies throughout the present sequence suggests that this facies may have been produced when storms augmented normal sedimentary processes (cf. Sellwood, 1972). The exact interpretation of this facies is difficult without considering facies associations, these are outlined in Chapter 4.

3.3.5 Plane-laminated Sandstone (Spl)

Description. Consists of medium to coarse, moderately to well sorted sandstone. Laminations on a scale of 3-10 mm are delineated by slight variations in grain size and changes in composition between laminae rich in limestone clasts and those poor in limestone clasts, some heavy mineral concentrations also occur. Beds up to 1.5 m thick pass laterally into trough-cross-strata and massive sandstone. External contacts are sharp to gradational.

Interpretation

Plane-laminated or horizontally stratified sandstone deposited

in a shallow marine environment have been likened to hummocky cross-stratification (Harms *et al.*, 1975). These bedforms are interpreted to be the result of strong wave surge which are unsteady in velocity and varied in direction. Deposition was probably under upper flow regime (flat bed) conditions (Harms *et al.*, 1975). Unidirectional flow is not implied. These beds may have formed when storms augmented normal marine processes.

3.3.6 Mudstones

Description. Massive, completely homogenised dark grey calcareous mudstone contains an abundant marine fauna of gastropods (*Conus sp.*, *Ancilla sp.*) and bivalves (*Lutrania sp.*, *Venus sp.*). See Appendix B for complete faunal list. Grain size varies from silty clay to muddy fine sands. Laterally discontinuous thin granule conglomerate and shell debris horizons are between 5 and 10 cm thick.

Interpretation

The mudstone was homogenised by biological activity indicating an environment where the rate of bioturbation exceeded the rate of production of sedimentary features (Clifton, 1981).

Thin granule conglomerate and shell debris horizons are interpreted as lag deposit layers and indicate occasional periods of high wave activity probably associated with storms.

3.4.0 Redeposited Sedimentary Facies

These facies types are well developed in both the Kemer and Salir Formations. Associated facies and the abundance of marine fauna both macro and micro, indicate deposition in a fully marine environment.

3.4.1 Redeposited Conglomerates

Introduction

The presence of different grading types, the imbrication of clast (a) long axes into the palaeoflow, generally disorganised fabric and almost total lack of features indicative of deposition by traction current transport as a bed load (e.g. cross-stratification) suggests deposition of the conglomerates by subaqueous mass-flow mechanisms.

Recent work on redeposited subaqueous conglomerates has adopted three approaches. *Firstly*, the discussion of theoretical and

experimental models centred on the mode of transport and deposition of sediment gravity flows (Hampton, 1972; Carter, 1975; Middleton and Hampton, 1973, 1976; Lowe, 1976a, b; Naylor, 1981); *secondly*, the types of ancient deposits inferred to have resulted from such flows (Hendrey, 1973; Davies and Walker, 1974; Walker, 1975, 1977; Surlyk, 1978; Kelling and Holroyd, 1978; Nemec *et al.*, 1980); and *thirdly*, facies modelling of the submarine setting in which the sediments were deposited (see Chapters 4 and 5) (Walker, 1975; Carter and Norris, 1977; Long, 1977; Surlyk, 1978; Rupke, 1977; Stanley, 1980; Stow *et al.*, in press). Despite the abundant literature, the processes and mechanisms of deposition of redeposited conglomerate are still not fully understood.

In the current study a wide range of redeposited conglomerates are recognised, in a well controlled sedimentary environment (Chapters 4 and 5). Prior to the field description a brief summary is given of the mechanisms that may operate in the redeposition of an unstable sediment downslope under the influence of gravity.

3.4.2 Theoretical Considerations

The general term sediment gravity flow (sediment flow) encompasses all subaqueous mass transport mechanisms (e.g. turbulent flow, grain flow, density modified grain flow, debris flow), it refers to the flowage of sediments or sediment fluid mixtures in which gravity acts directly on the sediment grains to drive them downslope (Middleton and Hampton, 1973).

Sediments will remain at rest on the seafloor provided the combined forces of shear resistance are greater than the shear stress imposed by gravitational acceleration (Terzaghi, 1956; Shephard and Dill, 1966). The shear strength of granular materials can be calculated from the coulomb model of shear failure.

For a potential shear plane within a pile of water saturated sediment the Coulomb equation can be written:

$$S = c + (\gamma_s Z - U_w) \tan\phi \qquad \text{(after Terzaghi, 1956).}$$

γ_s = submerged unit weight of the sediment;
Z = the depth below the free surface of the sediment;
U_w = the excess pore water pressure at the point of stress;
S = shear strength;
c = interparticle forces due to cohesion;
ϕ = angle of internal friction (normally 28-42° for cohesionless coarse sands and silts).

The applied shear force (T) to a potential shear plane within the sediment pile is the downslope component of gravitational force, hence:

$$T = Pv \sin \theta$$

θ = angle of slope on which the sediment rests;

Pv = applied gravitational force.

Failure of the sediment pile occurs if the shearing resistance S is decreased below the applied shear force. This may take place in a number of ways:

(1) By thixotropic changes in cohesive properties as the result of an applied shock.

(2) If the sediment accumulated with metastable grain packing, an applied shock may result in the collapse of this packing and the temporary production of excess pore water pressure, mobilisation by liquefaction will follow (Terzaghi, 1956; Lowe, 1976b). Such behaviour is commonly associated with sands and silts (Terzaghi, 1956; Shephard and Dill, 1966; Lowe, 1976b), and the presence of very coarse sand and gravel may act to prevent complete liquefaction.

(3) An upward flow of fluid through the sediment may produce a continuing excess pore water pressure; mobilisation is then by fluidisation (Reynolds, 1954). Lowe (1976b) has shown that sediments mobilised by fluidisation will move only a short distance before coming to rest, and this mechanism is insignificant in contributing to the accumulation of most sedimentary sequences. Although it may produce locally massive sandstones.

(4) The slope the sediment rests on is increased or more sediment is added above, both processes increase the effective shear stress, the former will also decrease the effective normal force and hence shear strength (Carter, 1975).

Following mobilisation the sediments may move by various sediment gravity flow mechanisms (after Middleton and Hampton, 1973; Lowe, 1976a, b):

(1) turbidity currents where the sediment is supported mainly by the upward component of fluid turbulence;

(2) grain flow in which the sediment is supported by direct grain to grain interaction and in which the fluids interstitial to the dispersed grains is the same as the ambient fluid;

(3) density modified grain flows in which the sediment is supported by direct grain to grain interaction and where the density of the interstitial fluid is greater than that of the ambient fluid and aids significantly in maintaining the dispersion of the grains;
(4) debris flows where the sediment is supported by a matrix, a mixture of interstitial fluid and fine sediment which has a finite yield strength;
(5) liquified flows, where as a result of liquefaction, a loosely packed sediment collapses so that the grains temporarily lose contact with each other and settle within their own pore fluid. The particles fall a short distance, fluid is displaced upward, and a more tightly packed grain-supporting framework is established.

Of the above mechanisms density modified grain flows, debris flows and to a lesser extent turbidity currents are the most important in the downslope transport of coarse sand and gravel. The following paragraphs discuss grain flows and debris flow in detail, turbidity currents are covered more fully in the section on redeposited sandstone.

Grain Flows. The concept of grain flows was first applied in geology following Bagnolds (1954) experimental work on the properties of concentrations of cohesionless grains in a Newtonian fluid under shear. This showed that a force called the dispersive pressure was exerted normal to the mean flow direction and was of sufficient magnitude that an appreciable part of the moving grains are in equilibrium between it and the force of gravity (Bagnold, 1954). The dispersive pressure comprises a component due to intergranular collision and a component due to statistically ordered shear-velocity-changes as one grain passes near another (Carter, 1975).

The initial work of Bagnold (1954 and 1956) defined grain flow in two regions:
(1) *Grain flow in the inertial region* where the viscosity of the continuous phase is low (generally when it is water) and movement is from dispersal pressures resulting from the actual impacts of the dispersed phase; the continuous phase has no strength and deforms as a Newtonian fluid.
(2) *Grain flow in the viscous region* where the continuous phase has a high viscosity and the dispersive pressure generated from ordered shear velocity changes as dispersed grains approach one

another, and a further dilatent effect introduced by non-Newtonian behaviour of the fine grained clay suspension (Metzner and Whitlock, 1958).

This earlier work has been considerably refined in recent years. Lowe (1976a) has shown that grain flow (*sensu stricto*, inertial region of Bagnold), where the interstitial fluid is the same as the ambient fluid (i.e. for cohesionless equidimensional sand grains in water), can only operate on slopes at or near the angle of repose and generally only produces deposits 5 cm or less in thickness.

Flows in which the density of the interstitial fluid is greater than that of the ambient fluid are termed *density modified grainflows* (Lowe, 1976a). Within these flows the buoyant affect of the interstitial fluid aids dispersive pressure in maintaining the dispersion against gravity.

If the clay content of the interstitial fluid exceeds a few percent the mixture becomes plastic and can no longer be treated as a fluid. The increasing presence of dense plastic mud interstitial to the clasts, reduces the effects of dispersive pressure by grain-grain interaction and the buoyancy and finite yield strength of the continuous phase become important. This results in a *debris flow* mechanism (Middleton and Hampton, 1973).

Debris Flows. The occurrence and nature of debris flows have been known for a considerable time (e.g. Blackwelder, 1928), but only recently have descriptions been superseded by an analytical and theoretical approach (e.g. Hampton, 1972; Middleton and Hampton, 1973; Rodine and Johnson, 1976; Enos, 1977; Naylor, 1981).

Early workers described debris flows as highly viscous Newtonian fluids. Johnson (1970) and Hampton (1972) showed that a visco-plastic (coulomb viscous model) is more appropriate to the rheological behaviour of debris flow. Using this model the internal shear stress during flow is

$$\tau_{int} = \underset{\text{cohesion or yield strength}}{K} + \underset{\text{coulomb frictional term}}{\sigma_n \tan\phi} + \underset{\text{viscous term}}{\eta\varepsilon}$$

σ_n = normal stress; ϕ = internal friction angle;

η = viscosity; ε = shear strain rate.

For a given flow on a constant slope this can be simplified to a Bingham plastic model (Johnson, 1970):

$$(\tau) = K_2 \eta b \varepsilon.$$

This model indicates that flow will not occur below a minimum internal shear stress. At incipient flow, $\varepsilon = 0$, thus flow can only occur if:

$$\tau_{int} > K + \sigma_n \tan \phi \qquad (a)$$

Theoretical applications of this model (Hampton, 1972; Middleton and Hampton, 1973; Naylor, 1981) place two constraints on debris flow development and behaviour:

(1) There is a minimum thickness required for flow. For a debris flow of thickness T, on slope θ, with a submerged density of ρ' (= $\rho d - \rho w$) (Fig. 3.9), shear stress at the base of the debris flow is due to the downslope component of its submerged weight. For an element of length L and width W parallel to the slope,

$$\text{weight component} = \rho' g \, TLW \sin \theta$$

dividing by the area L, W

$$\tau = \rho' g \, T \sin \theta \qquad (b)$$

Combining (a) and (b) for flow

$$\rho' g \, T \sin \theta > K + \sigma_n \tan \phi$$

in the case of wet sediments where $\phi = 0$,

$$\rho' g \, T \sin \theta > K$$

or $$T_{crit} = \frac{K}{\rho' g \sin \theta}$$

(2) All debris flow will have a rigid plug or non deforming central region.

For materials flowing in channels, regions exist where the applied shear stress is less than the strength of the materials (Fig. 3.9). A moving debris flow travels mainly by laminar shear within a circumferential zone where shear strength has been exceeded, and carries with it a rigid plug (Hampton, 1972) in the top centre of the flow. After a critical thickness has been exceeded, movement will commence by shear along the boundary surface, where flowing material is in direct contact with the substrate. In the case of subaqueous flows, due to interface friction +ve shear operates at

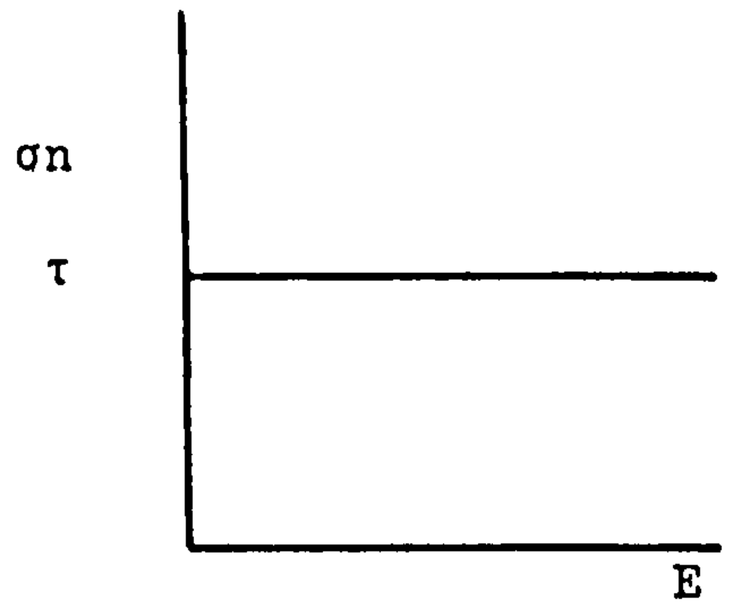

a) plastic

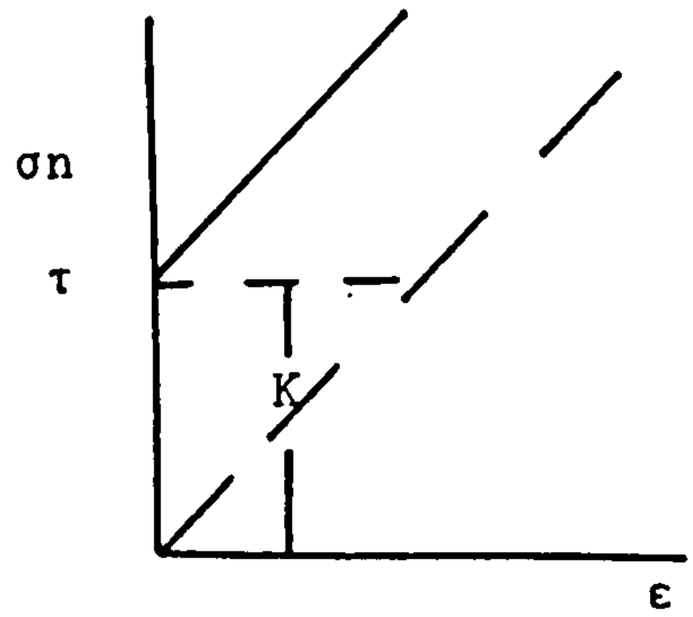

b) Bingham plastic

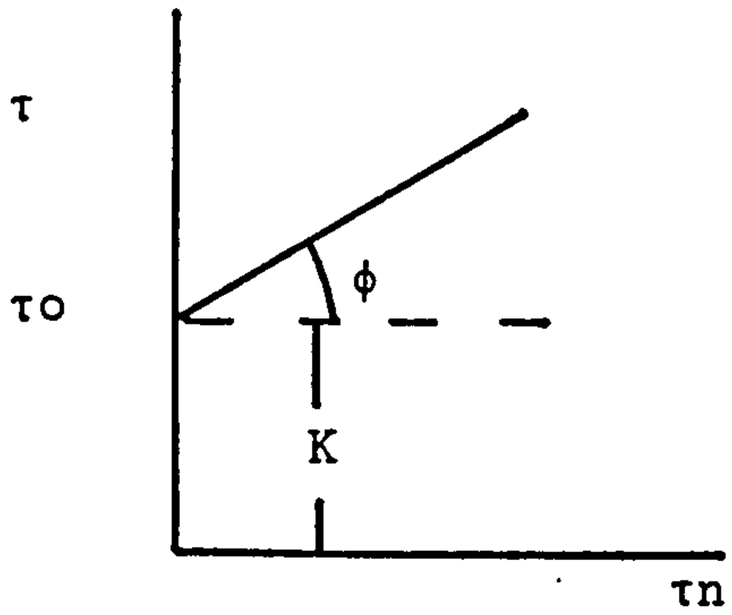

c) Coulomb Frictional

σn normal stress

τ normal shear stress

τ_{int} internal shear stress

E strain

ε shear strain rate

ϕ internal friction angle

K cohesion or yield strength

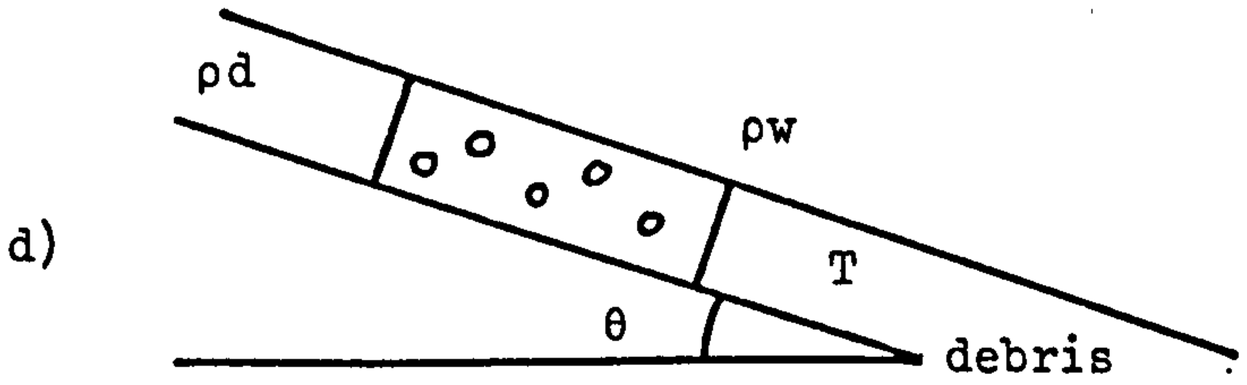

d) Definition diagram for debris, thickness T, density ρd, in water of density ρw, on slope θ.

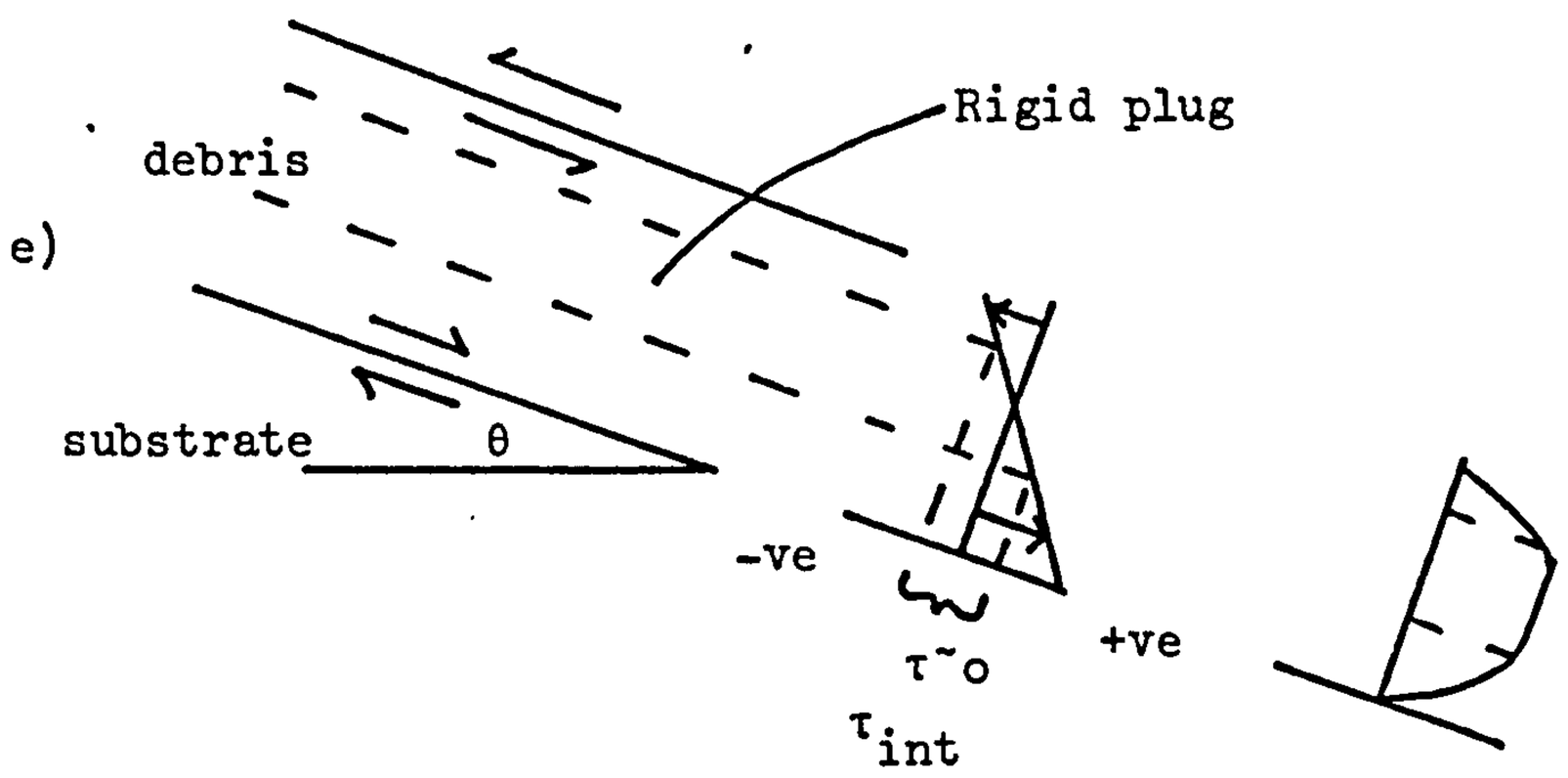

e)

Fig. 3.9 Mechanical models (a-c) and definition diagrams (d and e) for debris flows.

the base of the base and -ve shear at the top. In Fig. 3.9 it can be seen that this results in an intermediate region of very low or zero shear stress. In these zones, where $\tau_{int} < K+\sigma_n \tan \phi$ no flow can occur, since matrix yield strength is not exceeded. The resultant rigid plug is symmetrical about the int = 0 line (Naylor, 1978). As the flow travels farther from source, or as the amount of material fed into it decreases, the thickness diminishes to a point where the thickness of the plug is equal to the thickness of the flow and the flow freezes *in situ*.

Clasts in a debris flow are supported by the yield strength of the mud matrix and by enhanced buoyancy as a result of being immersed in mud and not water. The major controls of competence are clay:water ratio, clay type and cation content of the water (Hampton, 1975). Strength, and hence competence falls as the amount of water in the slurry increases.

3.4.3 Modern Analogues

Only a few descriptions exist of recent subaqueous sediment gravity flow deposits. To date no subaqueous mass-flow event has been recorded occurring and all records are from cores of previous events and photographs of the submarine floor.

Subaqueous debris flows. The best documented 'Recent' flows are those on the Lower Continental rise west of the Canary Isles (Embley, 1976). In this area multiple amalgamated debris flows occurred on slopes of as little as 0.1^{o}, travelled over a distance of several hundred kilometres and cover an area of 30,000 km^2. The flows are characterised by a pebbly mudstone fabric, sharp angular contacts and an undulatory surface. They are interpreted to have been generated by large sediment slides. Deposits similar to this, related to large slump scars are known from the Amazon Cone, Gulf of Mexico and from the Wilmington Canyon on the eastern seaboard of the U.S.A. (Stanley, 1974) and the northwest Africa continental margin (Jacobi, 1976). In all these areas there is abundant mud present and redeposition is apparently by a debris flow mechanism.

Recent deposits where other sediment gravity flow mechanisms may have operated have been described by Bouma and Shephard (1964) who document sandy gravel from the head of San Jose Canyon on the eastern seaboard of the U.S.A., and also by Piper (1975) from the Laurentian fan also on the eastern seaboard of the U.S.A. Sand and

gravel in both these areas are interpreted to have been deposited by mainly turbidity currents.

This paucity of information on recent subaqueous sediment gravity flows has resulted in much of the current understanding being derived from the study of subaerial debris flows.

Subaerial debris flows. Although many similarities exist between subaerial and subaqueous flows the two are not directly analogous. Subaerial flows are initiated by water saturating talus (Curry, 1976). Water lowers the debris strength and permits flow. Secondary strength loss may occur by remoulding and further water incorporation (Naylor, 1978). Flow stops as a result of water loss by seepage or evaporation. By comparison, submarine sediments are already water saturated, initiation of failure is by one of several mechanisms, all of which involve either strength loss or slope steepening. Submarine sediment gravity flows are generally thought to halt because of a decrease in slope, or an increase in substratum roughness (Naylor, 1978; Middleton and Hampton, 1976).

3.4.4 Field Description

In the following section a description of the main types of redeposited conglomerate recognisable in the field and an interpretation of the mechanism of transport is given based mainly on the fabric and texture of the conglomerate.

3.4.5 Disorganised Conglomerate (Dsg)

Description. This comprises clast-supported pebble, cobble and boulder conglomerate (Fig. 3.10). Grain size varies irregularly both laterally and vertically. Beds are between .50 m and 4.50 m thick and laterally continuous over distances of up to 100 m. Muddy, medium to coarse sandstone matrix comprises up to 25%. Bases may be erosive and channelled (Fig. 3.10), with scours up to 2 m deep and between 5 and 10 m across. Occasional rip-up clasts of sandstone and mudstone are concentrated along the base of the bed. Tops are gradational or planar. Rare isolated imbrication of the a-axes parallel or inclined to the flow direction is observed (Fig. 3.10).

This facies is well developed in large conglomerate channel fills in the Kemer Formation (Figs. 4.10, 4.11) and in proximal parts of the submarine fan sequence of the Salir Formation (Fig. 5.11).

FACIES	GRAIN SIZE	EXTERNAL CONTACTS	INTERNAL STRUCTURE	GEOMETRY
Disorganised conglomerate Dsg	pebble-boulder cgl.	U. gradational or sharp and planar L. erosive and scoured	structureless, rare a-axes imbrication parallel or inclined into flow	sheet or wedge
Normally graded cgl. Ng	granule to boulder cgl.	U. sharp planar L. erosive scoured	normal grading,(coarse tail and distribution grading),a-axes imbrication inclined into or parallel to flow	sheet or wedge channel-fill
Normally graded stratified cgl. Ngst	cobble cgl. to coarse sst.	U. gradational to sst. L. erosive, irregular channelled	graded base parallel-stratified cgl.-sst. in upper part of bed	sheet wedge channel-fill
Inverse to normally graded cgl. Ign	pebble to boulder cgl.	U. sharp or gradational to overlying sst. L. slightly or non-erosive planar	coarse plug conc. in centre of bed	sheet or wedge
Inversely graded cgl. Ig	pebble to boulder cgl.	U. sharp to gradational, planar L. non-erosive, planar	inverse grading as concentration at top of bed, or uniform distribution grading	sheet or wedge
Mud-supported congl. Msp	pebble to boulder cgl.	U. sharp, planar or irregular L. non- or slightly erosive	rare a-axes imbrication into flow	sheet or wedge
Sand-supported cgl. (pebbly sst.) Ssp	pebble to cobble cgl.	U. sharp and planar L. non- or slightly erosive, planar	struct., rare a-axes imbrication into flow	sheet or wedge

TABLE 3.4 Summary Table of Redeposited Conglomerate Facies.

Fig. 3.10

Disorganised conglomerate (facies Dsg), deposition was by debris flow mechanism.
Note non-erosive, planar base, imbrication of clasts and large clast rafted parallel to the base of the flow, suggesting laminar flow conditions. Palaeoflow was to the right.
Salir Formation (inner fan association, 5.4.0).
Markings on hammer are at 10 cm intervals. GR. 516384.

Fig. 3.11

Normally graded conglomerate. Cobble and boulder conglomerate at the base (b) grades to very coarse sand at the top (t). This is overlain by a massive structureless redeposited sandstone unit. Scour (s) is the result of erosion by the overlying conglomerate unit.
Salir Formation (inner fan association, 5.4.0).
Scale is 20 cm long. GR. 517393.

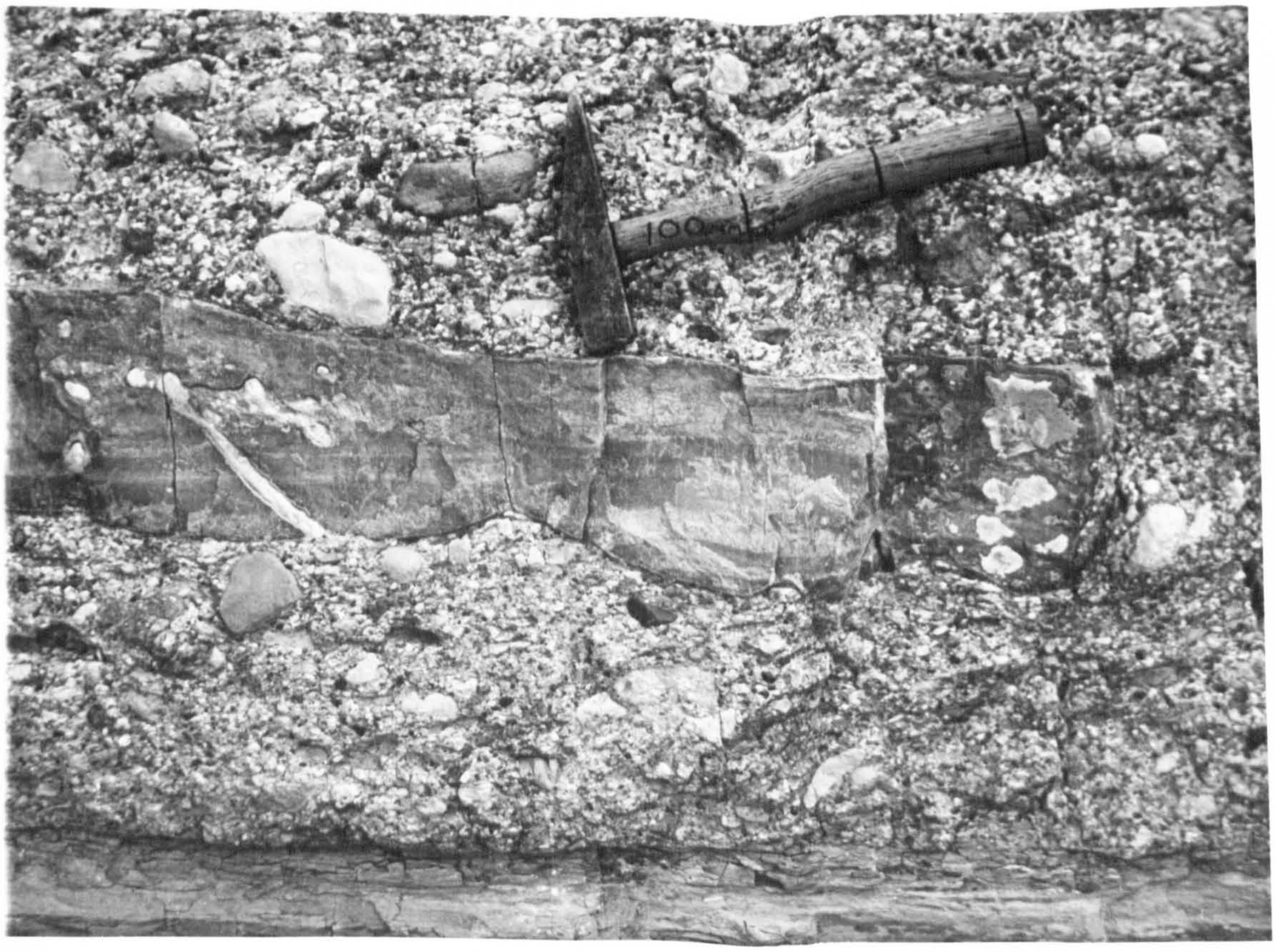

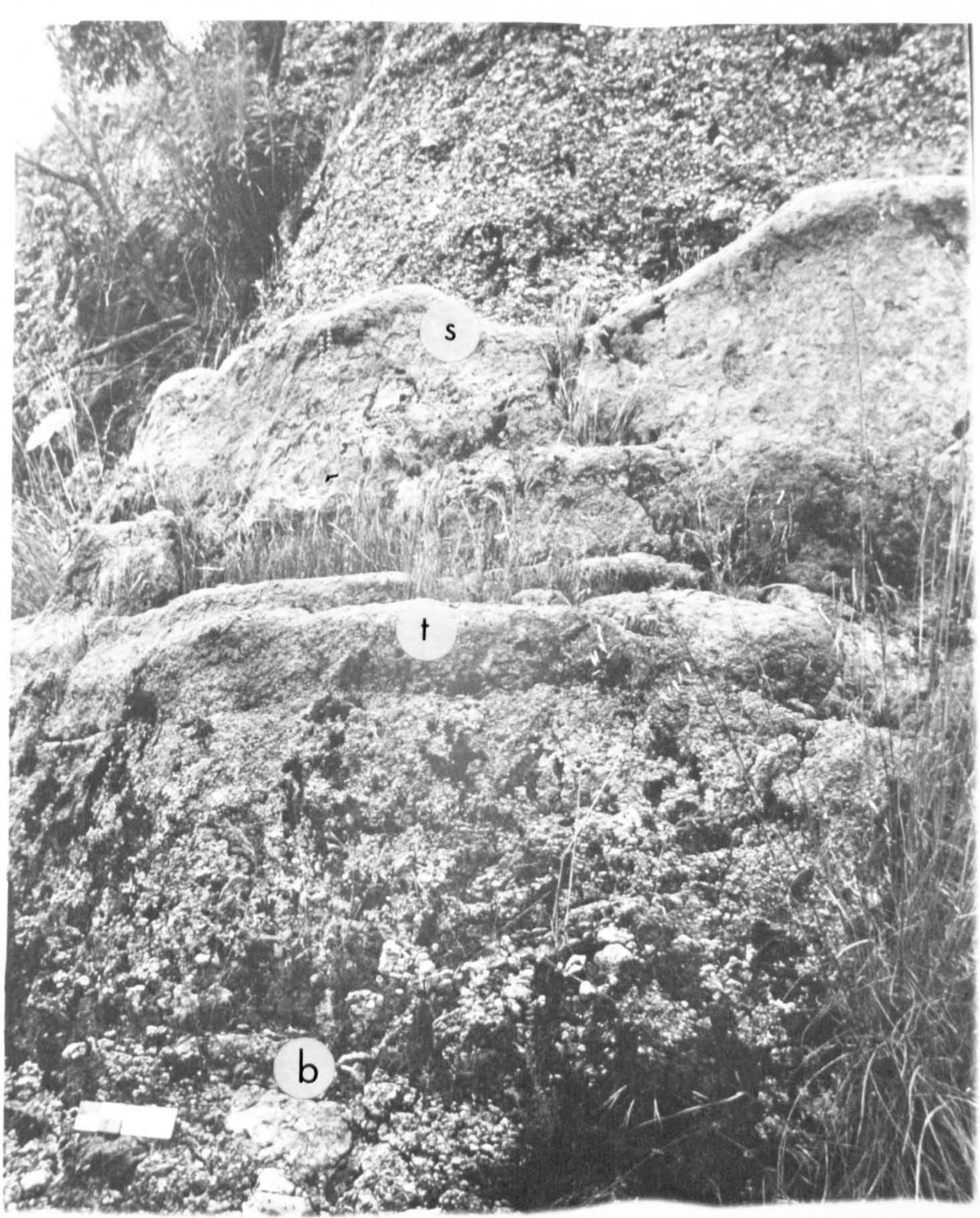
S
t
b

Interpretation

The general lack of fabric and texture suggest that the clasts moved little in relation to one another during transport.

The absence of matrix support excludes a solely debris flow origin and it is likely that dispersive pressure produced by clast interaction was the main supporting mechanism, this is consistent with the development of occasional imbrication. Alternatively the imbrication may be the result of the migration of the rigid plug and associated shear zones within a debris flow (Hampton, 1975).

In conclusion, deposition was by density modified grain flow, transitional to sandy debris flow where dispersive pressure was aided by matrix strength and buoyancy.

3.4.6 Normally Graded Conglomerate (Ng)

Description. This comprises clast-supported boulder, cobble, pebble and granule conglomerate which may grade to sand at the top of a bed (Figs. 3.11, 3.17). This facies forms ca. 50% of all graded beds. Average bed thickness is 2 m. Grain size variation may be extreme, e.g. boulders grading to coarse sand or minimal granule gravel grading to coarse sand. This facies is well developed in proximal parts of the Salir Formation (Fig. 5.3) and in the transition zone at the base of the Bağbeleni Member (Fig. 5.30). Three grading types occur: (I) beds with weak grading in the top with only clasts of the largest size absent; (II) beds which show a uniform grading from bottom to top of the bed. These first two are the coarse tail grading of Middleton (1967), with an upward decrease in the mean grain size of the coarsest fraction accompanied by a much less pronounced grading/non-grading of the finer fractions. (III) beds which exhibit a strong grading with the uniform decrease in the average grain size and the total disappearance of clasts coarser than sand in the upper parts of the bed (distribution grading of Middleton, 1967). Basal surfaces of conglomerate beds may be slightly or non-erosional or strongly channelled. Channelling is on several scales and discussed more fully in sections 4.4.6 and 5.4.2. Channelised conglomerates generally have a complex geometry resulting from repeated erosion and infilling of channels (Figs. 4.10 and 5.5). Imbrication of clast a-axes is parallel or inclined into the flow direction. Mudstone rip-up clasts concentrated along the base of beds are

orientated parallel to the base of the bed or inclined upcurrent.

Interpretation

The presence of normal grading suggests that the clasts were allowed to move freely within the flow (Walker, 1975) and that lateral and vertical clast size segregation operated. The occurrence of isolated imbrication suggests that dispersive pressure may have played an important supportive role. The lack of imbrication in some flows is more a function of clast shape than the mechanism of transport. In many of the gravels clasts have a sphericity of three or more (Odell, 1977); long axis imbrication results from the tilting of the principal clast axis during the collision of clasts (Rees, 1968), with equidimensional clasts such as these no imbrication will develop. In some beds well rounded clasts possessing no fabric pass laterally into elongate clasts with a well developed fabric.

In conclusion, it is likely that the depositional mechanism was intermediate between a sandy debris flow and full turbulent flow. In the matrix-rich examples the former was more important and matrix strength and buoyancy were the dominant supporting mechanisms, dispersive pressure caused by clast-clast interaction playing only a subordinate role. Grading in subaqueous debris flows is a common feature and is thought to result from a lower sediment concentration due to dilution of the flow by water intake (Walker, 1975). In the matrix-poor examples fluid turbulence was the main supporting mechanism.

3.4.7 Normally Graded Stratified Conglomerate (Ngst)

Description. This facies comprises approximately 30% of all graded beds with an average thickness of 1.70 m. It is particularly well developed in proximal parts of the Salir Formation submarine fan system (Figs. 5.3, 5.8, 5.9). Grain size variation is generally pebble to coarse sand or more rarely cobble to coarse sand. Typically the upper third of the bed is ungraded consisting of interstratified granule conglomerate and coarse sand as parallel-stratified units (Fig. 3.13), or more rarely low angle cross-stratified units (Fig. 3.14). Bases are erosive and channelled with scours up to 1.5 m deep and 15 m across. Rip-up clasts of sandstone and mudstone are concentrated along the base of the bed. Tops are gradational to sandstone. Isolated imbrication of the clast a-axes parallel or inclined into the palaeoflow is common in the coarser

Fig. 3.12

Normally graded conglomerate bedding vertical.
Cobbles and boulders at the base (b) grade to granule conglomerate at the top.
Deposition was by turbulent flow.
Note presence of imbrication shown by hammer orientation.
Base of Bağbeleni Member (fan-delta, base of slope association, 5.9.2).
Hammer is 34 cm long. GR. 405418.

Fig. 3.13

Normally graded stratified conglomerate.
Note well developed stratified appearance, pebble conglomerate trains, sandstone lenses and prominent imbrication of larger clasts.
Flow was to the left.
Salir Formation (inner fan association, 5.4.0).
Scale is 20 cm long. GR. 518370.


b

clast sizes. Where present matrix is a generally coarse or medium sand.

Interpretation

This facies is generally finer grained than all other conglomerate facies and is the only one to contain consistently well developed stratification.

For conglomerate similar to this Davies and Walker (1974) suggest that the granules were moving into their final position by bedload traction, but that the sand was deposited directly from suspension. Calculations of the shear velocity required to initiate granule transport on the bed suggest that it will be sufficient to maintain low concentrations of sand in suspension. Slight fluctuations in current velocity would create interstratified pebble conglomerate and coarse sand. Cross-stratified sandstones (Fig. 3.14) produced by migrating mega-ripples are consistent with an interpretation involving bedload traction in contrast to the pure gravity transport mechanisms of other conglomerates.

In conclusion, these conglomerates were deposited in the final stages of turbulent flow where bedload traction had become increasingly important (cf. Davies and Walker, 1974, p. 1214).

3.4.8 Inverse to Normally Graded Conglomerate (Ign)

Description. This facies is sporadically developed in proximal parts of both the Salir (Figs. 5.3, 5.8, 5.9, 5.10) and Kemer Formations (Fig. 4.10). It comprises 15% of all graded beds with an average thickness of 1.5 m. Two grading types occur; beds which show a gradual change in average clast size, and beds in which a coarse plug is concentrated in the centre (Fig. 3.15). Both are of the coarse tail type of grading. In the former isolated imbrication of the a-axes parallel or dipping up palaeoflow occurs throughout the bed. In the latter a similar imbrication occurs outside the plug zone. Within the plug clasts generally have a random orientation. Bases are generally slightly or non-erosive, rip-up clasts are rare. Tops are sharp or sometimes gradational to an overlying sandstone.

Interpretation

The presence of grading and imbrication of clasts indicate that the clasts moved freely with respect to each other, allowing the

lateral segregation of clast sizes within the flow. Inverse grading at the base of the bed is attributed to size-sorting within a concentrated layer of clasts, maintained above the bed by dispersive pressure (Bagnold, 1954). To maintain sufficient dispersive pressure the applied shear stress must be high. Walker (1975) made the correlation between inverse grading steep slopes (necessary to produce a high shear stress) and proximal environments. This has not been demonstrated in the field (Walker, 1975; Nemec *et al.*, 1980). In the present study area no evidence for this relationship is found, inverse to normally graded conglomerates being continuously interbedded with all other redeposited conglomerate facies (e.g. Salir Formation, Fig. 5.3).

In some of the more matrix-rich conglomerates the observed grading may be the result of the migration of the rigid-plug-boundary (see Fig. 3.9) within a debris flow (Hampton, 1975). In the debris flow model (Hampton, 1975), coarser grain sizes will be concentrated within the rigid central plug and the finer grains within the zones of shear. Continued movement of the rigid plug boundary will produce a gradual transition in grain size across the shear zone.

3.4.9 Inversely Graded Conglomerate (Ig)

Description. This facies comprises less than 5% of all graded beds. Pebble, cobble and boulder clast-supported conglomerate has a mean bed thickness of 1.20 m. Examples of this facies are recorded from proximal parts of the Salir Formation (Figs. 5.3, 5.8, 5.9, 5.10). Grading comprises either uniform distribution grading through the bed, or beds with a concentration of coarser clasts at the top of the bed. Isolated imbrication of clasts inclined into or parallel to flow direction is sometimes well developed. Mudstone rip-up clasts are rare. Matrix is a medium to coarse sandstone. Bases are generally non-erosive, tops are sharp to gradational.

Interpretation

The presence of grading indicates that the clasts moved freely within the flow (Walker, 1975). Dispersive pressure generated by clast collision (Bagnold, 1954) was the main supporting mechanism aided by matrix strength and buoyancy. A mechanism capable of producing inverse grading is the kinetic sieve effect (Middleton, 1970), where smaller clasts fall between larger clasts as the flow proceeds.

Fig. 3.14

Ripple cross-lamination (m), low angle cross-lamination and pebble-granule conglomerate horizon.
Top of graded-stratified conglomerate unit.
Flow was to left.
Salir Formation (inner fan association, 5.4.0).
GR. 517384.

Fig. 3.15

Non-erosive planar base to inversely graded conglomerate.
Mean clast size increases upwards.
Note well developed imbrication, flow was to the right.
Salir Formation (inner fan association, 5.4.0).
GR. 521378.

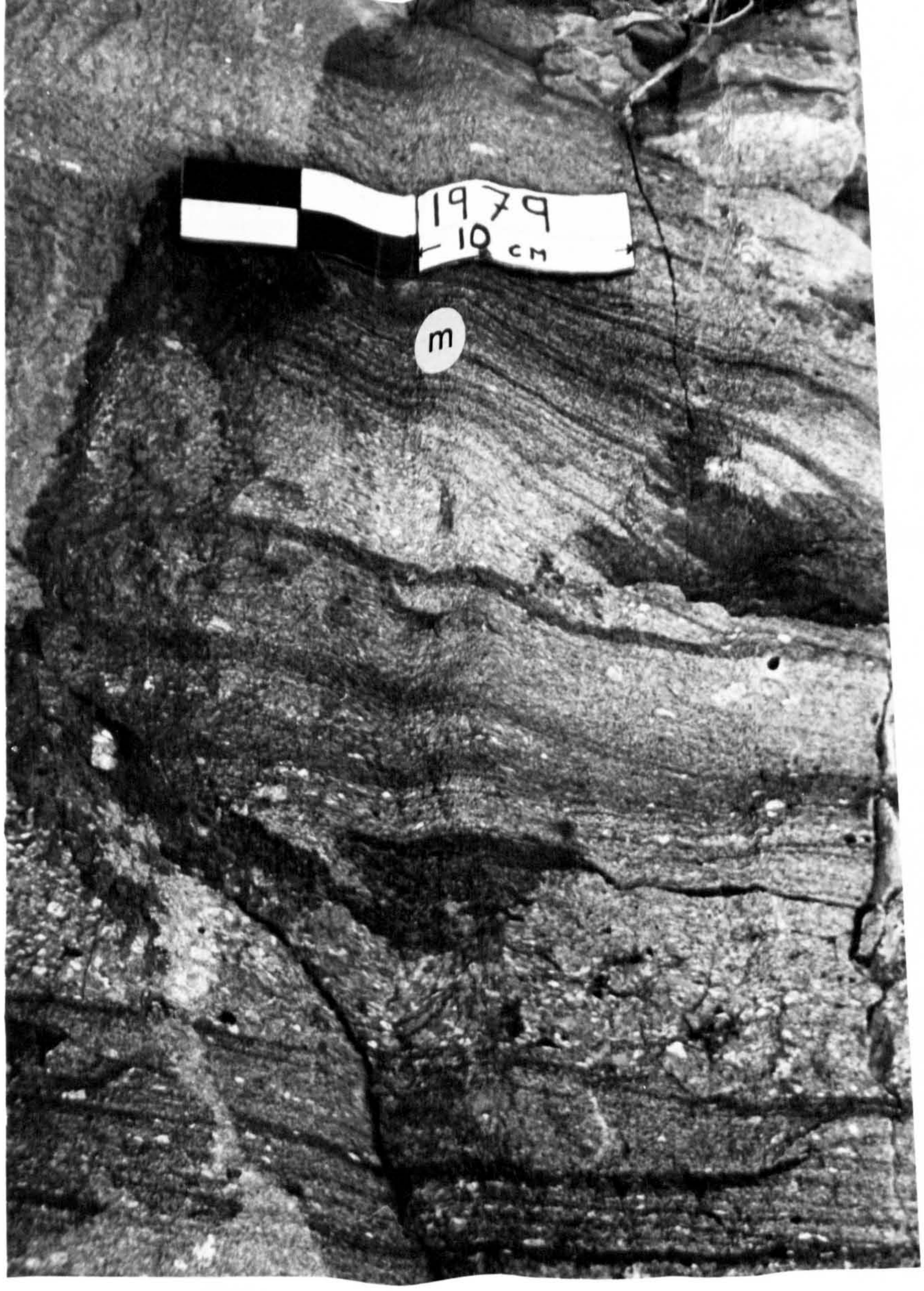
1979
10 cm
m


1979
10 cm

Nemec *et al.* (1980) find a close correlation between bed thickness and maximum clast size implying a close balance between discharge and competence. The limited data set for this type of conglomerate here prevents any such conclusion, although the correlation between maximum clast size, inverse grading and hence proximality (Nemec *et al.*, 1980) is not apparent in the present study area.

These conglomerates probably originated from density modified grain flows where inverse grading may be the result of high dispersive pressure.

3.4.10 Matrix-Supported Conglomerates (Msp)

This facies is subdivided into two; those conglomerates in which the matrix is dominantly mud and those in which it is sand.

3.4.11 Mud-Supported Conglomerate

Description. Thick sequences of this facies are well exposed in the north of the Akdere valley within the Salir Formation (5.7.1, Fig. 5.26), and also in upper parts of the Kemer Formation. Massive structureless disorganised units consist of boulders, cobbles and pebbles supported in a mudstone matrix. Bed thickness ranges from .50 m to 4.50 m. Clast percentages range from less than 5% to 25%. Sorting is very poor, clasts are angular to rounded, some are in gravitationally unstable positions. This facies is characterised by occasional outsize clasts up to 5 m in diameter. Angular intraclasts of sandstone and mudstone do not show evidence of aggradation. Bases are non-or slightly-erosive, or more rarely channelled. Tops are irregular, clasts may protrude from the top of the bed. Rare imbrication of clast a-axes dip into the inferred palaeoflow, at the base of beds a-axes may be orientated parallel to the flow direction. In some instances clast orientation changes through the bed. In basal parts clasts are orientated parallel to flow, this passes into a central zone with random orientation. Only rarely are units graded, both irregular and normal grading are of the coarse tail type.

Interpretation

Matrix support, non-erosive bases and the presence of unbroken fragile sandstone-mudstone intraclasts all indicate deposition by a debris-flow mechanism. Clasts in gravitationally unstable positions

Fig. 3.16

Mud-supported conglomerate (facies Msp), deposited by debris flow mechanism.
Note non-erosive planar base and rare imbrication of larger clasts.
Flow was to the right.
Salir Formation (inner fan association, 5.4.0).
Stick is 1 m long. GR. 521384.

Fig. 3.17

Complete Bouma cycle Ta-e. Graded base (A) with mudflake rip-up clasts, passes up into parallel laminated B division, ripple laminated C division, parallel laminated D division and very thin structureless E division.
Note small flutes on overlying bed.
Mixed terrigenous bioclastic sandstone.
Salir Formation (mid-fan association, 5.5.0).
Pen is 14 cm long. GR. 422393.

and protruding from the top of beds is evidence for matrix strength during transport and deposition. It is unlikely that such a poorly sorted sediment would originate by turbulent or density modified grain flow. Lack of rounding of clasts during transport, clast orientation parallel to bounding surfaces and non-erosive bases is consistent with laminar flow and hence debris-flow deposition.

3.4.12 Sand-Supported Conglomerate (pebbly sandstone, Ssp)

Description. This facies is present in inner submarine fan sequences in the Salir Formation (Figs. 5.3, 5.8, 5.9, 5.10) and in large conglomerate filled channels in the Kemer Formation (Fig. 4.10). Disorganised beds between .50 m and 2.70 m thick comprise pebbles and cobbles in a sandstone matrix (Fig. 3.15). Beds are laterally persistent for up to 50 m. Clast percentages range from less than 5% to 25%. Rarely clasts are aligned parallel to the inferred flow direction. Bases are only slightly or non-erosive, tops are sharp and planar. Beds are generally non-graded, where developed both normal and inverse grading are of the coarse tail type.

Interpretation

The presence of matrix-support, only occasional imbrication and clasts in unstable positions are all evidence for a debris-flow mechanism. Matrix strength and buoyancy were the main agency in maintaining clasts in dispersion during transport.

3.4.13 Discussion

Textural Transitions. The similarity in textures and close relationships in the field indicates that a complete transition probably exists between debris flows and other sediment gravity flows, in particular density modified grain flows and turbulent flows. As stressed by other authors (e.g. Middleton, 1970; Carter, 1975), all intermediates are possible between the end members of this spectrum, and a gradational sequence probably develops during a single sediment gravity flow event, changes occurring with time and from one point to another within the flow (e.g. Walker, 1975; Carter and Norris, 1977; Stanley, 1980). As a general rule sediments with good internal organisation, e.g. graded-stratified units, are indicative of a far travelled flow (Walker and Davies, 1974; Carter and Norris, 1977; Walker, 1975), whereas those with no internal organisation are generally indicative of a less travelled flow.

In the Kemer Formation there is a general increase downslope in the percentage of normally graded conglomerate units that show good internal organisation (Fig. 4.13), accompanied by a decrease in massive disorganised beds. In the Çağman Member (7.1) massive redeposited carbonate breccias that can be traced downslope over a distance of several kilometres, show a progressive change to more internally organised units away from source. In most cases (e.g. Salir and Kemer Formation sequences), however, individual beds cannot be traced for any distance downslope.

Source area control. The type of initial sediment gravity flow that occurs and the downslope textural transitions that may occur are greatly dependant on material in the source area and depositional setting. A critical aspect is the availability of fine matrix and mud necessary for a debris flow mechanism to operate. Redeposited conglomerate facies in the majority of the sequences discussed here (Chapters 4 and 5) are characterised by clast-support, coarse sandstone matrix and a low mud content. They were deposited in the main by density modified grain flows and turbulent flows. Debris-flows *sensu stricto* account for only a small percentage of the total sequence (with the exception of parts of the Salir Formation, see below). This reflects derivation from a fan-delta depositional environment, where abundant, well sorted, wave reworked coarse sand and gravel with a very low mud content was available for redeposition. Sequences of this type have also been documented by Nemec *et al.* (1980), Surlyk (1978) and Carter and Norris (1977). By contrast, in parts of the Salir Formation (e.g. northern part of the Akdere valley, 5.7.1) a thick sequence of mud-supported conglomerates were deposited by debris flows. This sequence is interpreted (5.7.1) to have been derived from the Antalya Complex in a submarine environment. The debris flow mechanism of deposition reflects abundant mud in the source area and the lack of well sorted sand and gravel. Sequences dominated by conglomerates deposited by debris flow mechanisms are common where intra-basin submarine source areas are present, as in large scale slumping of continental margins (e.g. Recent margin of Africa, Embley, 1976; Dingle, pers. comm. 1981; ancient - Palambino limestone, Naylor, 1978).

TABLE 3.5 Summary Table of Conglomerate Facies deposited in different sedimentary environments, but with common textural features. This emphasises the difficulty in distinguishing the depositional environment of conglomerate facies in the absence of other criteria (fauna, associated sediments, etc.).

FACIES	TEXTURE	SEDIMENTARY STRUCTURES	BOUNDARY SURFACES	DEPOSITIONAL ENVIRONMENT AND INTERPRETATION
Massive conglomerate Gm	clast-supported poor-mod sorting, lenses silt and sst. some lenses cgl. matrix-free	horizontal stratification, a-axes normal to flow, scours infilled by cross-strata	U. gradational or sharp L. scoured erosional	subaerial fluvial, deposition by unconfined sheet-flood
Massive conglomerate G	clast-supported v. poorly sorted, high percentage coarse muddy sand matrix	struct. random clast orientation	U. gradational L. non-erosive paralleling underlying sediment	shallow marine deposition as poorly sorted sheets, by fluvial channels entering a shallow sea
Stratified cgl.-sst. Gst	clast and matrix support, good sorting and finer (pb) cgl c sst matrix	stratified or massive pebble cgl. inter-stratified with c sst.	U. gradational L. gradational	shallow marine reworking by wave and storm action
Disorganised conglomerate Dsg	clast-supported poorly sorted muddy sst. matrix	rare a-axes imbrication parallel to flow	U. gradational or sharp and planar L. erosive and scoured	'deep' marine redeposited under gravity by density-modified grain flow-debris flow

3.4.14 Redeposited Sandstones

3.4.15 Introduction

Of the five redeposited sandstone facies recognised, three facies which together form greater than 90% of the total are attributable to deposition either directly or indirectly by turbidity currents.

History. The recognition of turbidity currents dates back to the work of Forel (1885, not seen in Middleton, 1970) on the undercurrent formed by the Rhone river entering Lake Geneva. They were first introduced into geology by Daly (1936), who suggested that such currents may be responsible for the erosion of submarine canyons. Johnson (1938) introduced the term turbidity current, but it was not until the 1950's (Keunen, 1950; Keunen and Migliori, 1950; Heezen and Ewing, 1952) that the transportational rather than erosional powers of turbidity currents were first studied. The theoretical studies that followed are reviewed by Middleton (1969, 1970).

Bouma (1962) first distilled the many and varied sedimentary structures seen in turbidities into the classical Bouma sequence. This is now interpreted in terms of decreasing flow regimes (Harms and Fahnestock, 1965; Walker, 1965).

3.4.16 Thick-bedded Graded Sandstones

Description. Distinctive grading is a feature of this facies (Fig. 3.17). Grain size varies from pebble and granule conglomerate present as lenticular lags at the base of beds (Fig. 3.18), to medium or fine sandstone. Bed thickness ranges from .30 to 2.75 m. Parallel, ripple and convolute laminations are common (Fig. 3.19, 3.20). Flutes, grooves and rare gutter casts are present on the base of sandstone beds (Fig. 3.21), along with load marks (ball and pillow structs.). Individual beds are laterally continuous or lenticular over tens of metres (Fig. 5.15). Bases are markedly erosional into underlying mudstone and pelagic chalk, rip-up clasts are concentrated along the base of beds. Amalgamated sandstones may form channel fill features. The channels are generally symmetrical, only rarely do overlying sandstone beds cut into underlying units. These are discussed fully in Chapter 5 (5.4.3, 5.5.1).

FACIES	GRAIN SIZE	BASAL CONTACT	INTERNAL STRUCTURE	GEOMETRY
Thick-bedded sst.	pebble cgl. to med. sst.	erosive, scoured flutes, grooves and rare 'gutter' casts	Tabcde, Tabcd, Tbc, Tbcd	lent./laterally continuous
Thin bedded sst.	medium to fine sst.	sharp,slightly erosive rare flutes and grooves	Tcde, Tde	laterally continuous
Graded, struct. sst.	pebble cgl. to coarse sst.	erosive, scoured flutes, grooves	struct, graded	lenticular
Struct sst.	coarse-med. sst.	sharp, slightly erosive	struct, ungraded	lent. or laterally continuous
Thin-bedded c sst.	coarse to v. coarse sst.	sharp, erosive, rare flutes and grooves	struct.	v lenticular
Inversely graded sst.	med. to coarse sst.	non-erosive, sharp, slightly scoured	distribution grading	lent/laterally continuous
Inverse to normally graded sst.	coarse to med. sst.	sharp, non-erosional	grading	lent. or laterally continuous

TABLE 3.6 Summary Table of Redeposited Sandstone Facies

Fig. 3.18

Lenticular conglomerate horizon at base of thick turbiditic sandstone (A division). Majority of clasts are ripped-up mudflakes.
Note presence of well developed imbrication.
Flow was to the left.
Salir Formation (inner fan facies association, 5.4.0). GR. 518385.

Fig. 3.19

Ripple cross-lamination (C division of Bouma cycle overlying parallel laminated B division). Structures delineated by alignment of heavy minerals (magnetite, spinel, chromite) along ripple foresets.
Salir Formation (inner fan facies association, 5.4.0). GR. 519385.


1979
10 cm

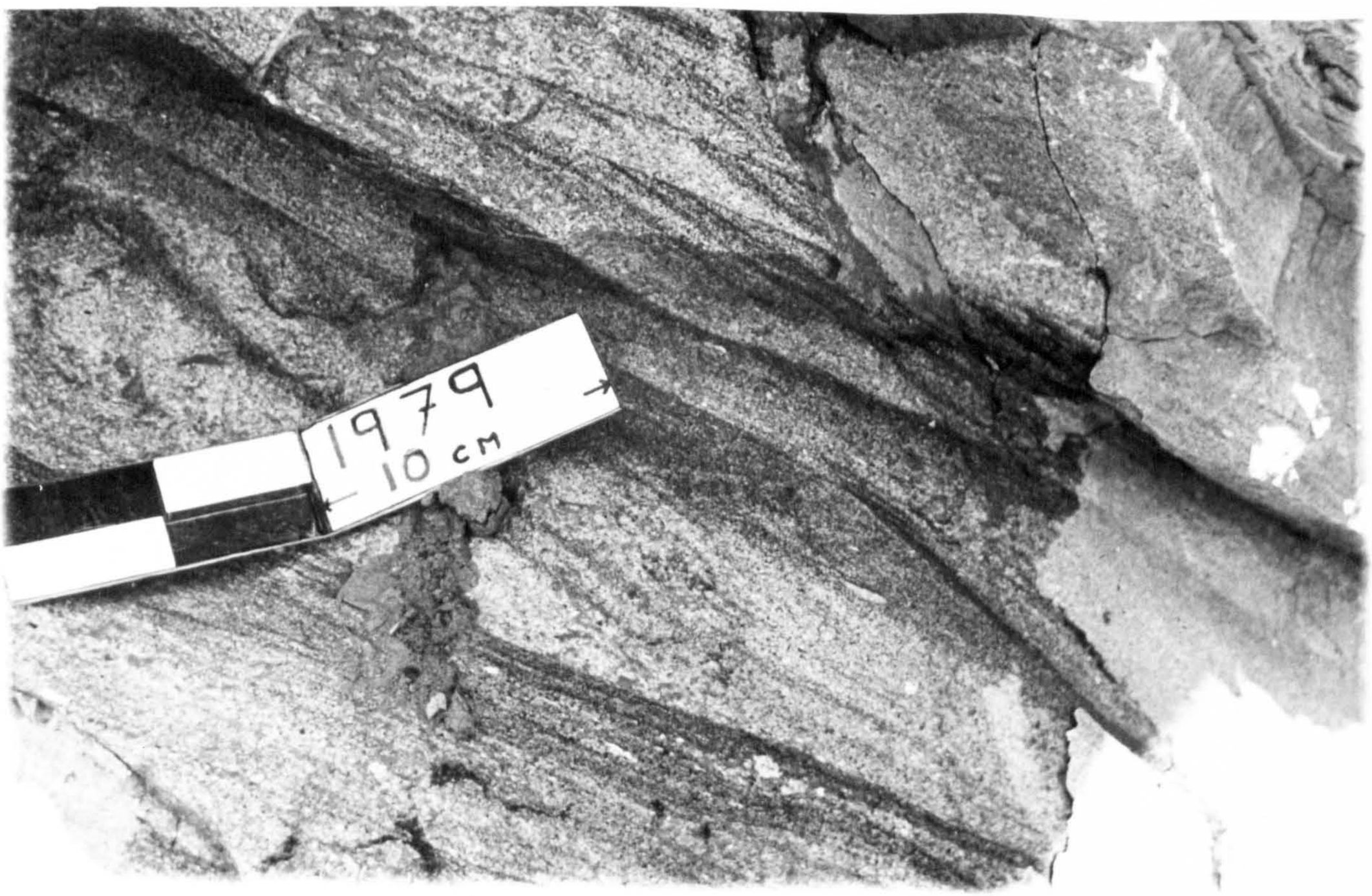
1979
10 cm

Fig. 3.20

Convolute (c) and ripple laminations (r). C division of a Bouma turbidite cycle. Convolute laminations were produced by dewatering as a result of very rapid deposition.
Note the presence of parallel laminated B and D divisions also.
Salir Formation, mid-fan association (5.5.0).
Lens cap is 7 cm across. GR. 421390.

Fig. 3.21

Well developed flute marks on base of thick turbidite bed.
Current was left to right.
Salir Formation, mid-fan association (5.5.0).
Stick is 1 m long. GR. 420400.

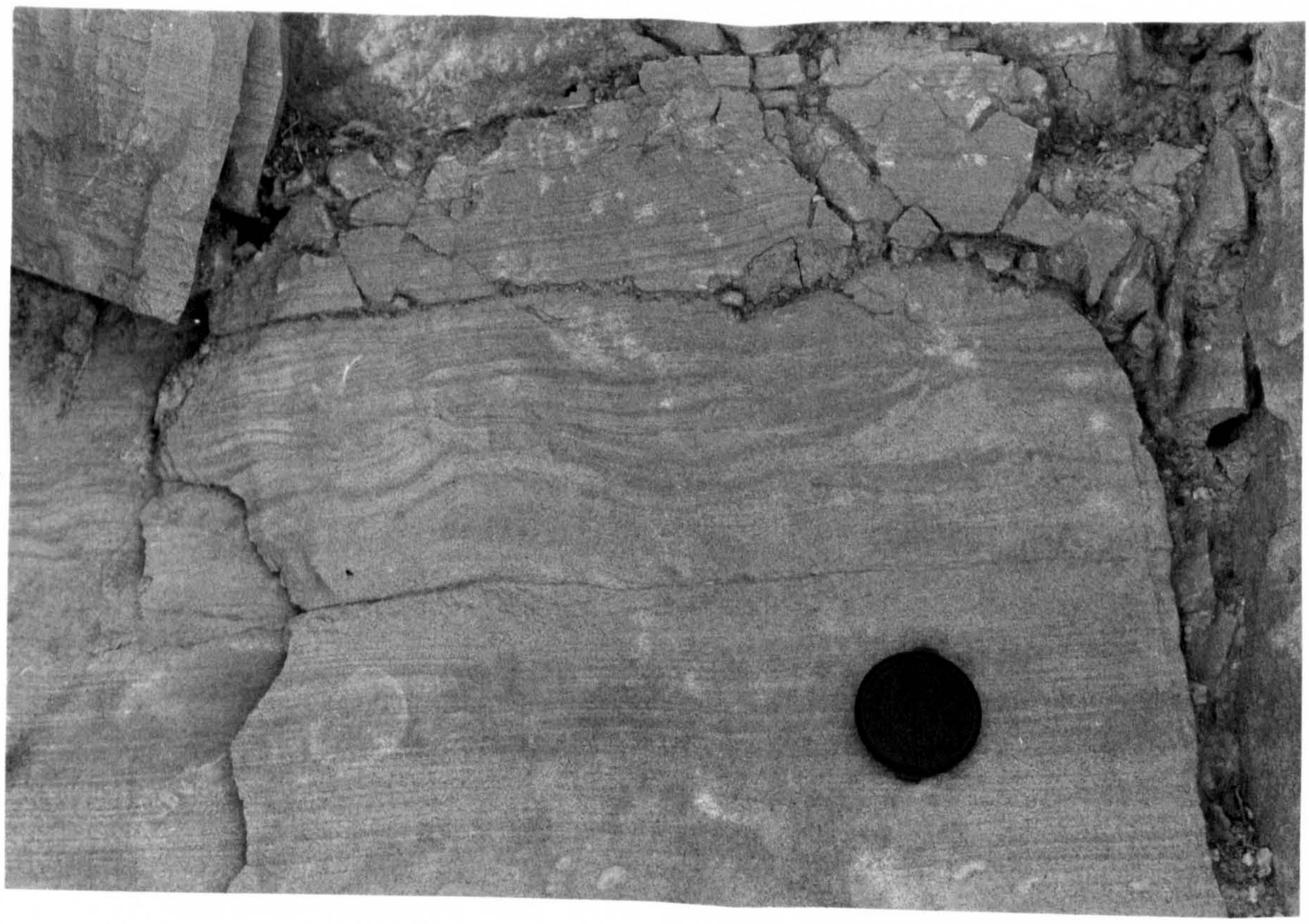

Interpretation

Deposition was by high density 'classical' turbidity currents. Features consistent with this are:

(I) Well developed internal organisation into Bouma cycles, characterised by the development of the a) massive, and b) parallel laminated, divisions of the Bouma sequence;

(II) Thickness of individual depositional units (beds) which average .70 m, and grain size;

(III)Abundant and often large flute and tool marks which suggest large flows with strong erosive power. Bottom structures are consistent with deposition from turbulent flow.

3.4.17 Thin-bedded Facies

Description. Thin-bedded sandstones are 0.03-30 cm thick, medium to fine grained laterally continuous with sharp bases and gradational tops (Fig. 3.22). Flute and groove marks are rare. Carbonaceous laminae are often present in the top of the bed.

Two members are recognised:

(I) Graded: Beds grade from medium to fine sand or silt, often with ripple and parallel laminations and more rarely convolute laminations;

(II) Ungraded: Fine to very fine grained sandstones show parallel ripple and convolute laminations or are structureless.

Interpretation

Sedimentary features which suggest deposition by low density turbidity currents are:

(I) Sharp bases and flat tops;

(II) Lateral continuity of individual depositional units (beds);

(III)Grain size (medium to fine) and bed thickness (average 10-15 cm);

(IV) Internal organisation into "base absent" Bouma sequences, e.g. T_{cde}, T_{de}, T_{ce};

(V) Small flutes, tool marks and bottom structures consistent with a turbulent current with minimal erosive power.

Where size sorting is not apparent, but sedimentary structures are developed, weak flows transporting a previously well sorted sediment are invoked. Structureless ungraded beds may be the result of syndepositional liquefaction (Lowe, 1976b) (see Section 3.4.2).

Fig. 3.22

Interbedded turbiditic sandstone (s), mudstone (m) and pelagic chalk (c). Chalks represent hemipelagic 'rain type' sedimentation. Detailed bed-by-bed measurements of sections similar to this can provide estimates of sedimentation rates (e.g. 5.6.).
Salir Formation (mid-fan association, 5.5.0).
Stick is 1 m long. GR. 421394.

Fig. 3.23

Normally-graded structureless sandstone, very coarse sandstone at the base grades to coarse sandstone at the top.
Salir Formation inner submarine fan environment.
Markings on stick are at 10 cm intervals. GR. 519374.

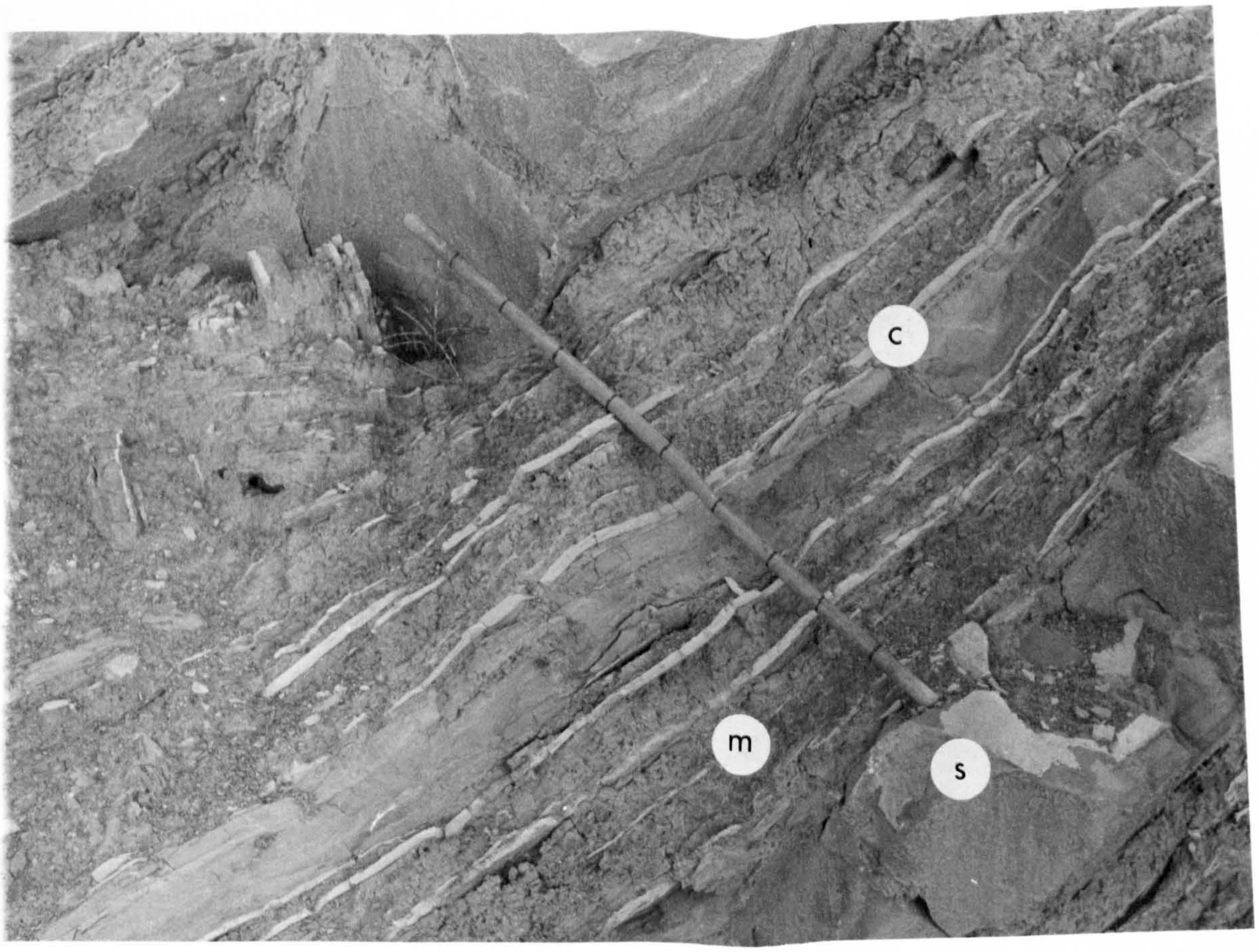
C
m
s

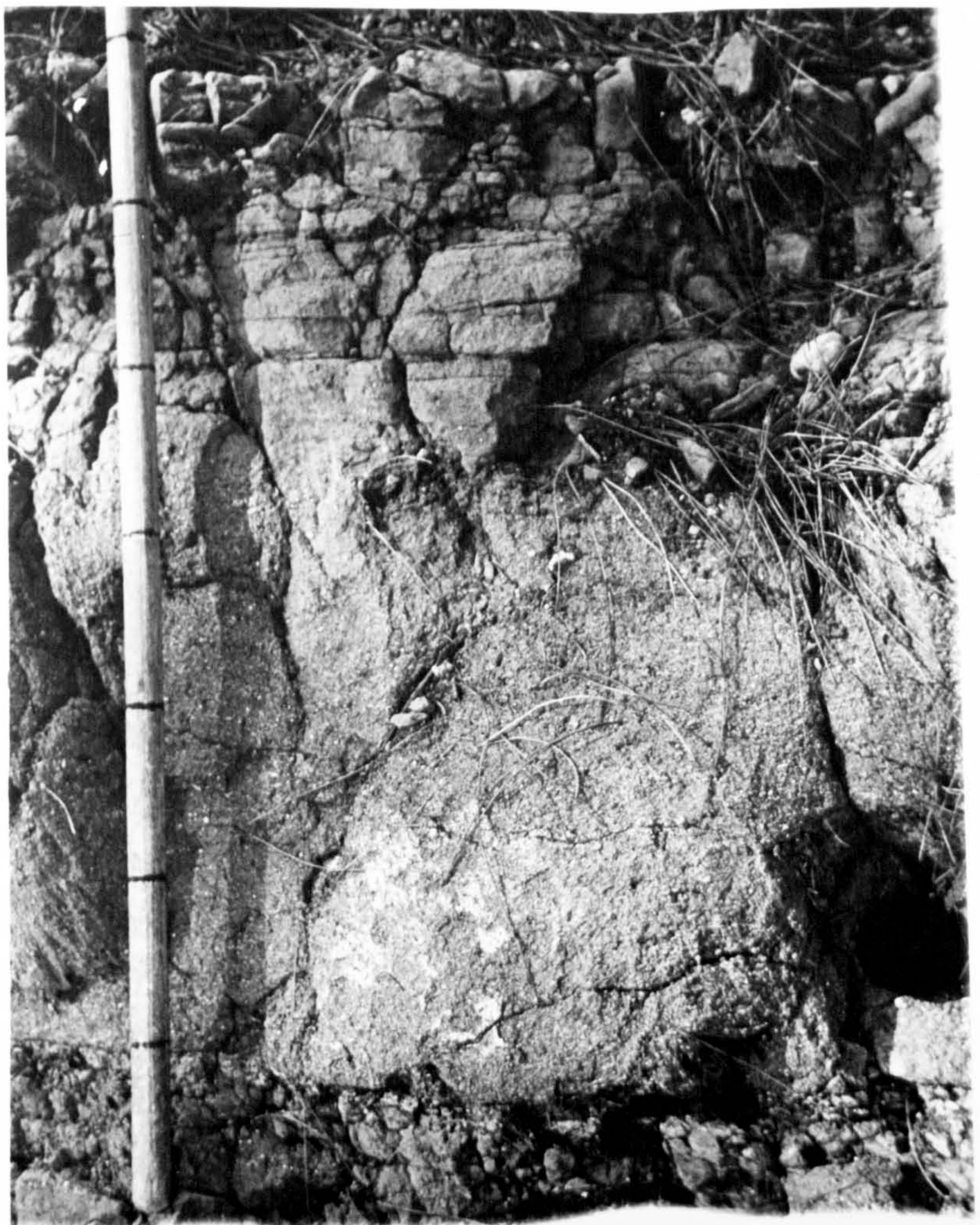

3.4.18 Graded Structureless Sandstone

Description. This facies forms beds between .70 m and 2.20 m thick. Grain size varies from granule or pebble conglomerate occurring as discontinuous layers at the base of beds, to coarse sandstone (Fig. 3.23). Beds are markedly lenticular over several tens of metres. Bases are erosive with scours flute and groove marks, rip-up clasts are abundant.

Interpretation

The presence of grading indicates that grains were free to move in relation to one another during deposition (see section 3.4.6). Flute and tool marks suggest a turbulent erosive current. Absence of sedimentary structures (ripple and parallel laminations) indicative of deposition by turbidity currents may be due to the coarse grain size and 'proximal nature' of the sandstones. They may represent only the 'A' division of a Bouma cycle. Deposition was probably by flows intermediate between 'classical high density' turbidity currents and sediment gravity flows responsible for the deposition of graded stratified conglomerate (section 3.4.7).

3.4.19 Structureless Sandstone Facies

Description. Beds between .45 m and 1.90 m thick vary from coarse to medium sandstone. Many beds contain pebble and granules that are either scattered throughout the bed or form thin layers concentrated towards the base of a unit. Bases to beds are sharp and slightly erosive, tops are sharp and planar. Grooves and flute marks are rare, rip-up clasts are concentrated along the base of beds. Individual beds are laterally continuous over 50 m+. This facies occurs most commonly in association with redeposited conglomerates.

Interpretation

Beds with pebbles and granules concentrated at the base (coarse tail grading) may have resulted from syndepositional fluidisation. Rapid deposition from a turbidite can result in the upward flow of interstitial fluid through the sediment, producing excess water pressure and momentary mobilisation of the sediment (Reynolds, 1954; Middleton, 1967; Lowe, 1976b). This effectively destroys any primary sedimentary structure and remixes a graded sand unit (cf. Swarbrick, 1979). Larger clasts at the base are not remixed into the overlying sediment.

Beds with randomly scattered pebbles and granules, indicate poor size sorting and non-turbulent flow. Deposition was probably by sandy debris flow transitional to density modified grain flow (3.4.2).

3.4.20 Thin-bedded Coarse Grained Sandstones

Description. Beds between .03 and .10 m thick are lenticular over 10-20 m. Rarely beds to .30 m thick occur. Grain size is coarse to very coarse sandstone. Bases are sharp and generally erosive with rare flute and groove marks, tops are sharp and sometimes slightly concave.

Interpretation

Coarse grained sandstones of this type may have been deposited as lags from larger turbidite events, and as such are indicative of turbidity current by-pass, or in some cases represent spill-over from channel areas.

The following facies are of restricted occurrence and form less than 5% of the redeposited sandstone facies types.

3.4.21 Inversely Graded Sandstone

Description. Beds between .45 m and 1.30 m thick are laterally continuous over 40 m+. Grain size varies from medium to coarse sandstone, grading is of the distribution type. Bases are non-erosive or slightly scoured. Tops are planar and sharp.

Interpretation

Inverse grading in sandstone has been attributed to two mechanisms:

(I) Dispersive pressure generated by interparticle collision (Bagnold, 1954; Carter, 1975). Where particles of a mixed grain size are sheared together, the larger grains drift to the zone of least shear (top of the flow) and smaller grains migrate to the areas of greatest shear.

(II) Kinetic sieving. In this mechanism small grains pass through the interstices between larger grains when agitated, displacing the larger grains upwards.

Both of these have only been demonstrated for cohesionless sand, and imply deposition by a density modified grain flow mechanism where dispersive pressure caused by clast-clast interaction was the main supporting mechanism.

3.4.22 Inverse to Normally Graded Sandstone

Description. This facies forms beds between .60 m and 1.5 m thick. Grain size varies between very coarse and medium sandstone, generally an area of coarse sandstone forms a laterally continuous central zone. Bases are sharp and non-erosional, tops are planar and sharp.

Interpretation

By analogy with redeposited conglomerates (3.4.2) inverse grading at the base may be the result of size sorting within a concentrated layer of clasts maintained above the bed by dispersive pressure (Bagnold, 1954). Normal grading in the upper half of the bed is the result of size sorting and gravitational settling within the flow (Walker, 1965). Deposition was probably by density modified grain flow.

3.4.23 Cross-stratified Sandstone Facies

This facies is restricted to a few occurrences in proximal environments of the Salir Formation submarine fan sequence (Chapter 5).

3.4.24 Small Scale Cross-stratification

Description. Planar-cross-stratification occurs as small (2-50 cm thick), wedge shaped units infilling erosive scours up to 5 m across. Grain size is medium to coarse sand. Cross-laminations dip at angles between 10 and 20°, and are discordant on the irregular lower surface. Upper surfaces are flat and planar.

Interpretation

Geometry of the cross-strata and their localised occurrence within scour fill features suggests an aggradational origin (Jopling, 1965). This facies may have formed by deposition from the base of a waning turbidity current. Movement over irregularities such as scours would cause flow expansion, reduce flow velocity with consequent deceleration and abandonment along a subaqueous slope, with the subsequent formation of foreset lamination. Facies similar to this have recently been described by Calella (1979) from a flysch sequence of Miocene age.

3.4.25 Large Scale Cross-stratification

Description. This facies is only well developed in one locality (Fig. 5.31), as a wedge shaped unit 3 m thick. Steeply inclined foresets pass downcurrent into parallel stratified sandstone. Individual cross-strata delineated by slight variations in grain size are between 2 and 10 cm thick and tangential to the lower bounding surface. Abundant mudstone rip-up clasts are aligned down the foresets (Fig. 5.31). The upper surface which has a partially preserved geometry (Fig. 5.31) is overlain by a matrix-supported conglomerate.

Interpretation

The presence of cross-stratification suggests deposition by some form of traction current. Facies similar to this have been described by Winn and Dott (1977, 1979) from the axial regions of a large submarine fan channel. These authors suggest the reworking of previously deposited sediment gravity flows by large turbulent flows. Movement of the clasts was by rolling, sliding and saltation at the base of a later low to moderate density, turbidity current.

The apparent dune geometry (Fig. 5.31) and downcurrent transition to plane beds described here is consistent with this origin. Estimates of the velocity required to rework pebble conglomerate (Walker, 1975; Winn and Dott, 1979) suggest velocities of 700-800 cm s^{-1}, which compare well with those observed from deep sea channels (Komar, 1970) which predict velocities of 600 cm s^{-1} for low density turbidity currents. Associations of this unusual facies are described in Chapter 5 (Section 5.4.1).

3.4.26 Mudstone and Pelagic Chalk Facies

These two facies occur intimately interbedded.

3.4.27 Mudstone

Description. The mudstones are a ubiquitous green colour. In thin section they are silty with a low clay content. The partially lithified brecciated nature in outcrop makes the recognition of any sedimentary structures difficult. Unit thickness ranges from .04 cm to 1.5 m (average 5 cm), the latter represents amalgamation of individual beds. A general appearance is one of faintly laminated to massive, with occasional evidence of grading from silt to clay. In thin section silt laminae with sharp slightly scoured bases grade

into clay over 2-3 cm. Weakly developed parallel and very low angle ripple laminations are sometimes developed.

Interpretation

Deposition was by very dilute turbidity currents. In some instances partial reworking by bottom currents cannot be ruled out (see below).

3.4.28 Pelagic Chalk

Description. White to cream chalk horizons are between 5 and 40 mm thick, laterally continuous and well indurated (Fig. 3.22). In thin section silt grains, planktonic and rare benthonic forams are dispersed in a micrite matrix. Grains of terrigenous material form between 5% and 60%. Examination using the S.E.M. shows the micrite matrix to be composed of equigranular calcite crystals (Fig. 3.24), with poorly preserved coccolith plates and planktonic foraminifera fragments (Fig. 3.24).

Bases to beds are sharp, planar or irregular or transitional. Tops are generally sharp and planar. Many of the beds are structureless and homogeneous. Sedimentary structures observed in the field are limited to lenticular, 0.5-1 cm thick silt flasers, drawn out asymmetric fading ripples (Stow and Shanmugan, 1980), and occasional small (2 mm) mudstone rip-up clasts. Only rarely is there any evidence of bioturbation.

In thin section a range of small scale sedimentary features are observed:

(I) Cross-laminated silt (5-10 mm thick) pass downcurrent into parallel laminated silt (Fig. 3.26).

(II) Micro-graded discontinuous laminae wisps with sharp bases and gradational tops (Fig. 3.26).

(III)Cut-and-fill features less than 5 mm across (Fig. 3.26) with graded fills and transitional tops (Fig. 3.26).

Interpretation

The composition of this facies, in marked contrast to the mudstones, reflects initial deposition by hemi-pelagic fall out sedimentation. Subsequent reworking to produce the sedimentary structures observed was by one of two processes:

(I) Partial reworking, or partial initial deposition by dilute turbidity currents;

Fig. 3.24

(a) S.E.M. photograph of authigenic calcite growing on calcareous nanofossil, in a mixed matrix of equigranular calcite and clays (mainly authigenic). Chalk horizon, Salir Formation (mid-fan association). Spec. 946. GR. 527336.

(b) Photomicrograph of structures within pelagic chalk horizon.
(a) Small scale cut-and-fill structure, note presence of micrograding and carbonaceous lamellae.
(b) Wispy silt lamination with scoured base.
Field of view is 2 cm.
Spec. 9122. GR. 425369.
Salir Formation (mid-fan association).

Fig. 3.25

Pelagic chalk horizon (c) draping irregular top to redeposited conglomerate (disorganised conglomerate Dsg).
Salir Formation (inner fan association, 5.4.0).
GR. 513412.
Lens cap is 7.5 cm in diameter.

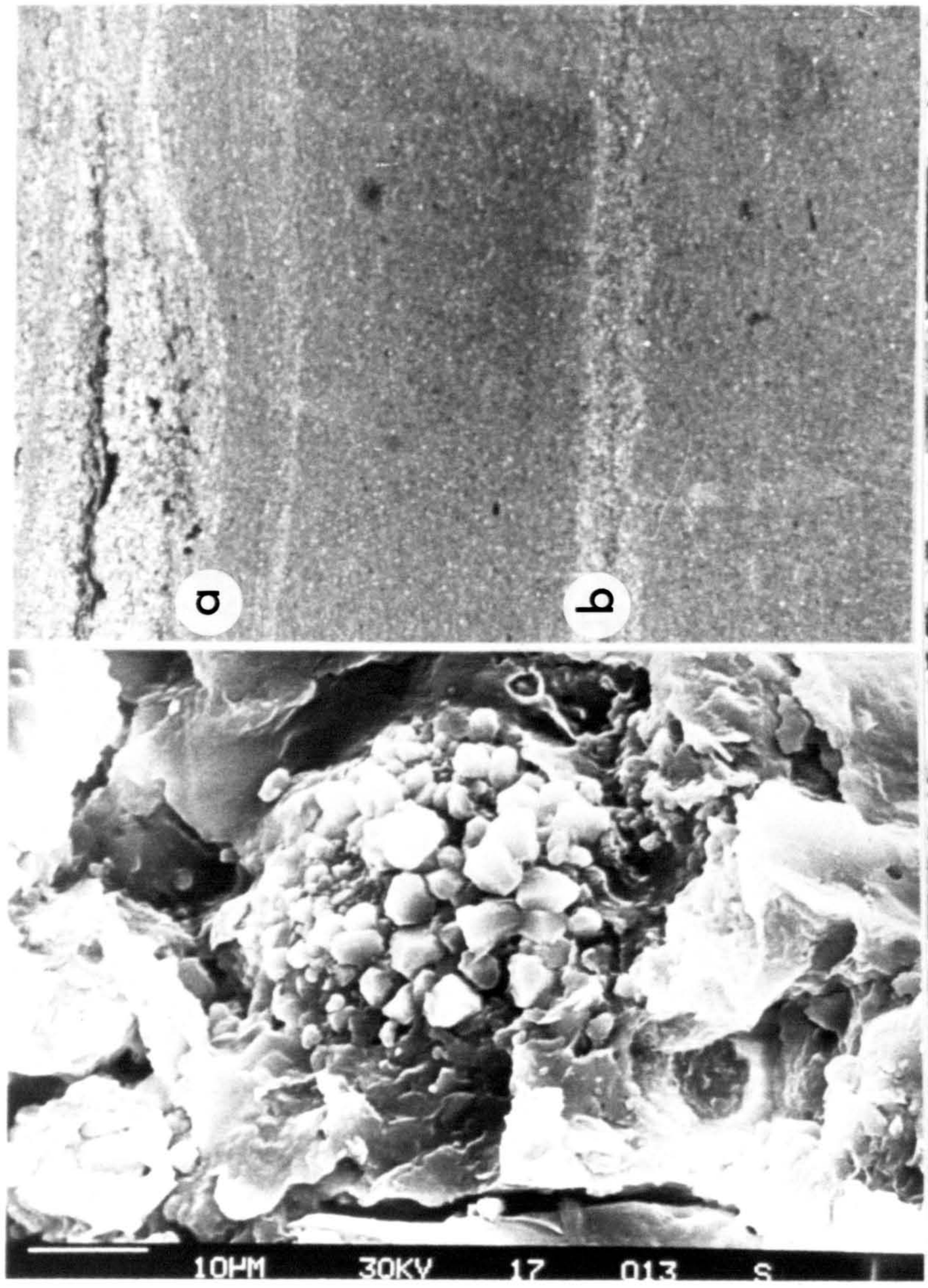
a
b
10HM 30KV 17 013 S

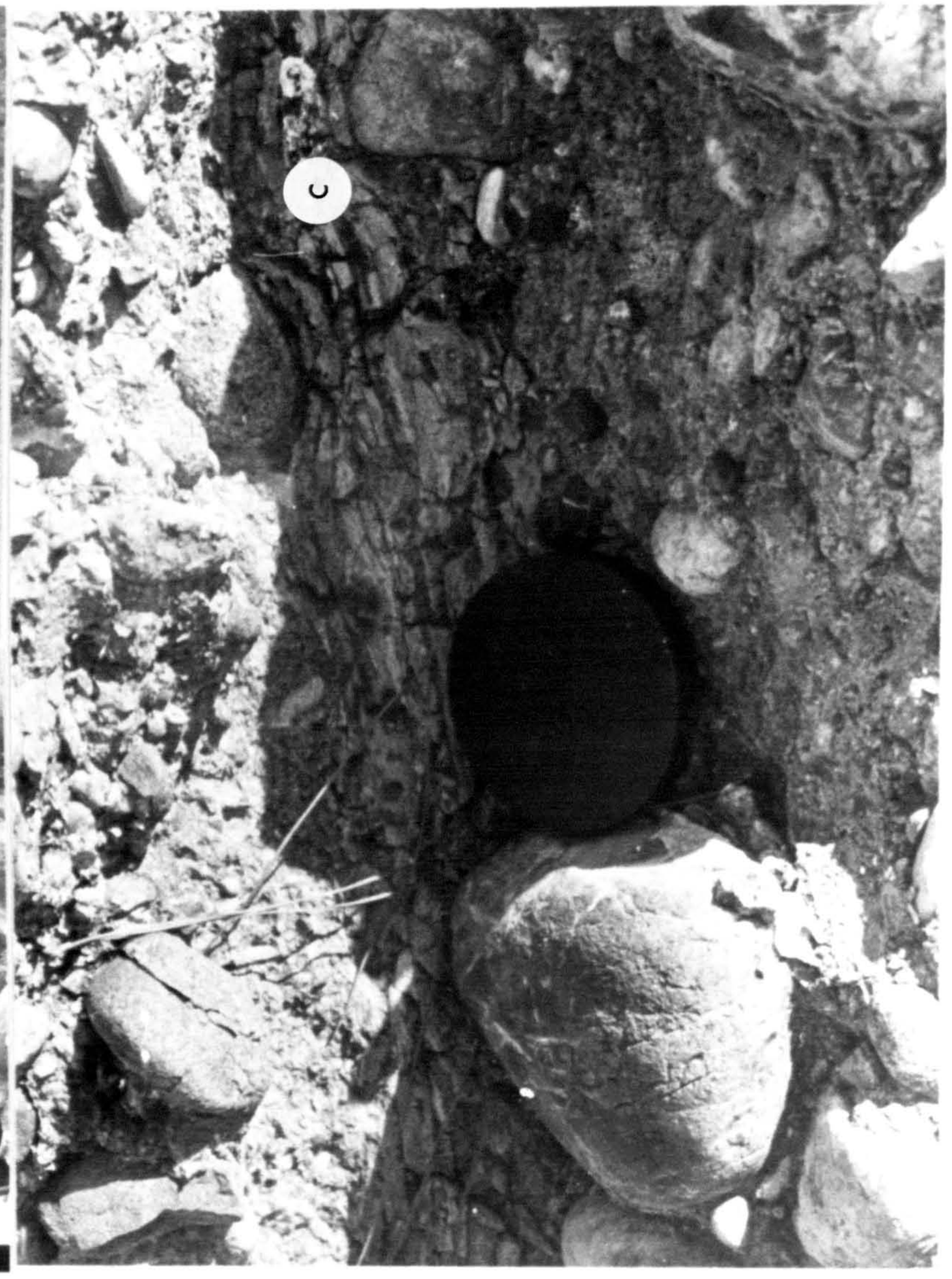
c

Fig. 3.26 Structures in pelagic chalk horizons
(a) fading-ripple lamination
(b) small scale cut-and-fill structure with planktonic foraminifera and laminations
(c) pinch and swell silt lamination (d) scoured base wispy silt lamination

(II) Reworking by bottom currents.

Following the recognition of 'contour currents' (Heezen and Hollister, 1964) a variety of sedimentary structures have been claimed to be distinctive of the reworking of fine grained deep marine sediments by bottom currents (Piper and Brisco, 1975; Rupke and Stanley, 1974; Hesse, 1975; Nelson *et al.*, 1975; Piper, 1978; Stow, 1979).

Many of the sedimentary features observed here are characteristic of both contourites and turbidites (Stow, 1979). However, the type sedimentary sequence for fine grained turbidites erected by Stow and Shanmugan (1980) is not distinguished and most of the chalk beds show features more easily ascribable to bottom current reworking of slowly deposited hemipelagic rain-out sediments. Particularly diagnostic are the often homogeneous chalk horizons, produced by micro-bioturbation of the very slowly deposited pelagic sediment and the ubiquitously high $CaCO_2$ content.

A sedimentary feature known to have been produced by currents flowing parallel to the continental margin, was drilled recently on the Blake Outer Ridge on the Eastern seaboard of the U.S.A. (D.S.D.P. Leg 76). Sediments recovered were found to consist of completely structureless homogeneous nanoplankton ooze and mudstone (Robertson, pers. comm. 1981) with few characteristic sedimentary structures.

In conclusion, deposition was by hemipelagic "rain" sedimentation subject to occasional reworking by impersistent bottom currents.

CHAPTER 4 WESTERN MARGIN SEDIMENTARY FACIES ASSOCIATIONS

Colour Plate 1

Kasaba Formation (Doğantaş Member).
Conglomerate-sandstone association deposited on an alluvial braidplain showing three fining-upward units (photograph taken from the top of the lowest conglomerate unit). Trough-cross-stratified conglomerate (Gt) infills scoop-shaped scours at the base of conglomerate units and passes upwards into massive conglomerate (Gm).
Note the thickness of fine sandstone and mudstone overbank sediments in the lowest fining-upward unit (M).
The section is transverse to palaeoslope, palaeocurrents were into the photograph.
Tree left of centre is 5 m high.

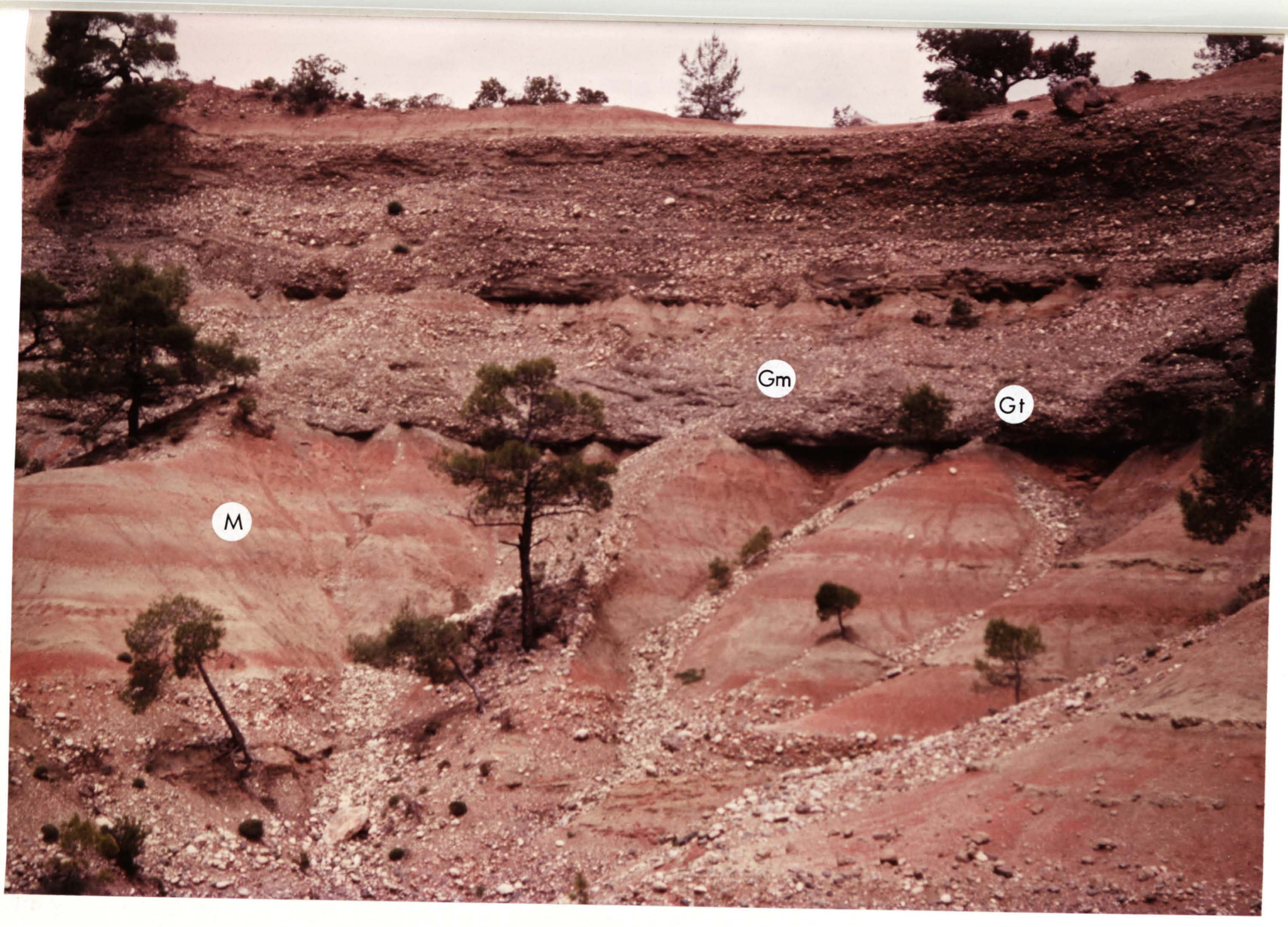
Gm
Gt
M

CHAPTER 4

4.0 Western Margin Sedimentary Facies Associations

4.1 Introduction

Sedimentary facies in Chapter 3 were described mainly in terms of depositional processes; depositional environments were mentioned only briefly. A facies association is a group of facies that are genetically related to one another and have some environmental significance (Collinson, 1969).

In this chapter, and the succeeding one (Chapter 5), facies associations of the Kemer, Kasaba (this chapter) and Salir Formations (Chapter 5) are analysed in terms of their sequential (vertical) and lateral distribution, with a view to reconstructing their depositional environment and developing facies models for each sedimentary sequence (cf Walker, 1979).

4.2 Kemer Formation

Provenance. The composition of the conglomerate and sandstone, discussed more fully in Chapter 6, indicate a mixed igneous ophiolite and ophiolite-related sediment source area. Bioclastic content varies between 0% and 40%. Palaeocurrent measurements of clast imbrication in conglomerates (Fig. 4.2) sole marks and ripples in sandstone (Fig. 4.2) and rare slump folds (palaeoslope indicators) indicate a general northwest to southeast dispersal pattern. The Kemer Formation was derived from the Lycian Nappes (1.3.2) to the northwest of the Kasaba basin.

4.3 Initiation of Terrigenous Clastic Sedimentation

In the north of the basin, around Sinekçibeli, Gömbe and Kemer (Fig. 4.1) the shallow water carbonate realm, stable throughout the Aquitanian (Poisson, 1977) (9.2.5) passes upwards into a thin-bedded turbidite sequence. The transition occurs over approximately 70 m (Fig. 4.3) and is marked by a gradual upward increase in terrigenous material and decrease in carbonate and associated shallow-water faunas (gastropods and bivalves). Algal limestones pass upwards into a distal flysch sequence, comprising interbedded fine to medium sandstone (T_{de}), mudstones and rare pelagic chalks. Redeposited turbiditic algal calcarenites, interbedded with calcareous marls decrease in thickness and size upwards; reflecting the termination of shallow-water carbonate deposition on local basement highs and

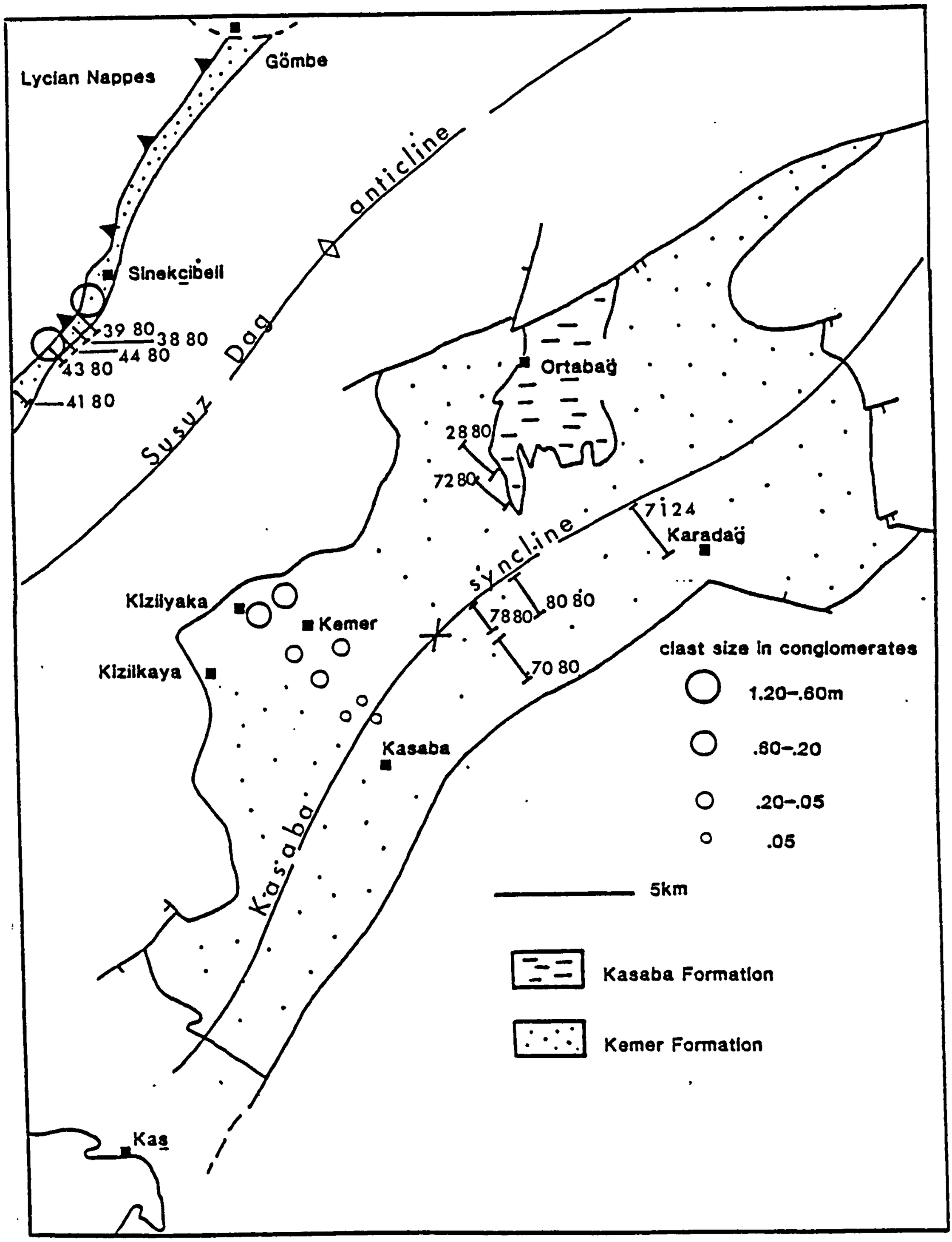

Fig. 4.1

Outcrop area of the Kemer and Kasaba Formations, showing locations mentioned in text and position of sedimentological logs.
Clast size variation refers only to the Kemer Formation.

Palaeocurrent readings for Kemer Formation

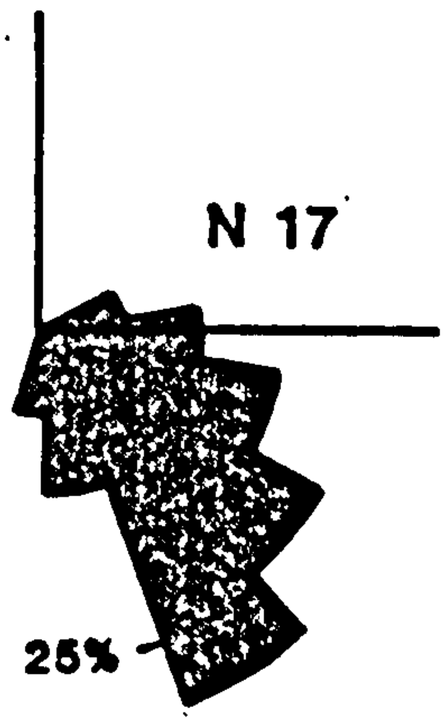

flutes and grooves

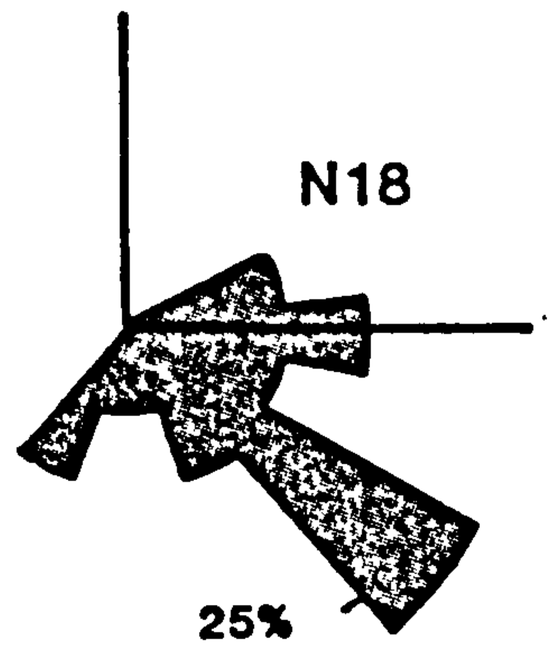

ripple laminations

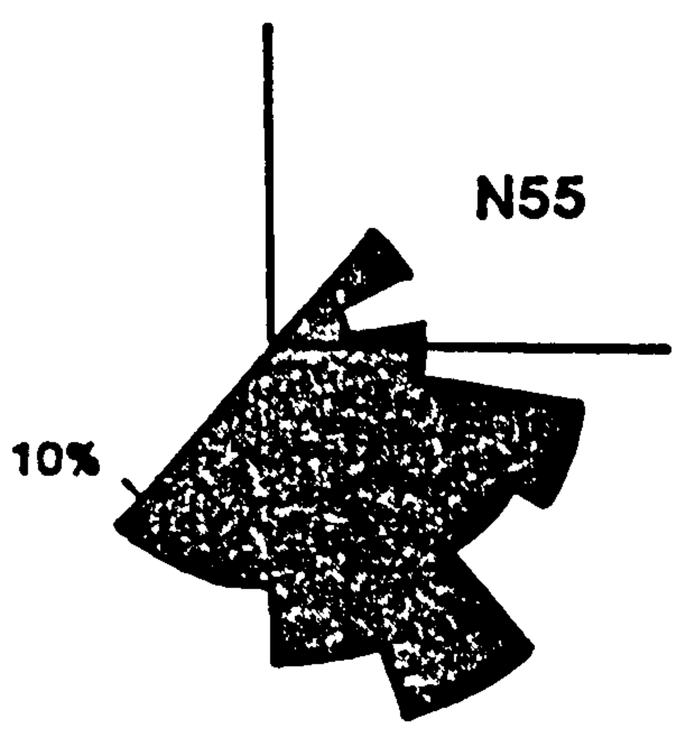

imbrication in conglomerate

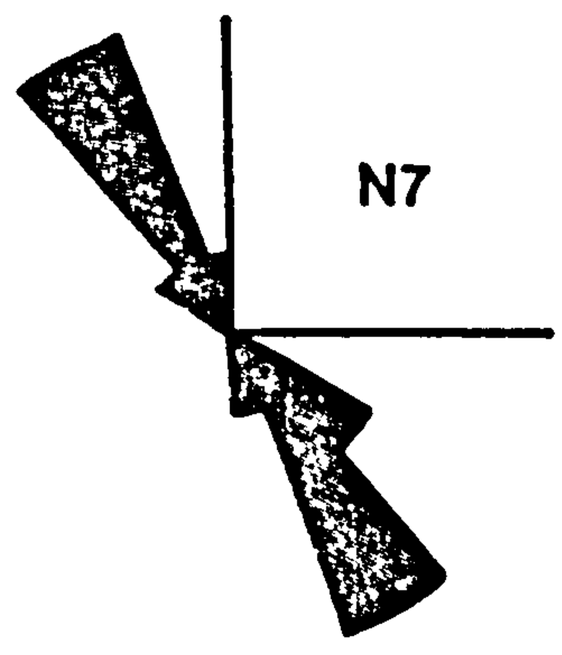

channel axes

Fig. 4.2

Palaeocurrent readings for the Kemer Formation.

N refers to number of readings, % percentage of total readings.

around the margins of the basin. Southwards around Kasaba (Fig. 4.1) Aquitanian limestone is absent (9.2.5); the transition is sharp. Eocene shallow water nummulitic limestone is overlain disconformably by a distal turbiditic sequence of interbedded thin sandstones (T_{de}), mudstones and abundant pelagic chalk horizons.

The transition from very shallow water carbonate deposition and exposed carbonate platform (9.2.5), through a marl sequence deposited in shallow water (from faunal evidence) into a terrigenous flysch sequence deposited in deeper water, reflects the *initial Miocene* emplacement of the Lycian Nappes onto the margin of the carbonate platform (see 10.2.2). Loading and the subsidence that followed are discussed in 10.2.3.

4.4.0 Sedimentary Facies Associations

The Kemer Formation is characterised by vertical and lateral facies variations. It is initially subdivided into proximal and distal facies associations based on palaeocurrent evidence (Fig. 4.2) and clast size trends (Fig. 4.1).

4.4.1 Proximal Facies Association

Coarsening-upward sequence. Proximal facies are well exposed in the Sinekçibeli and Gömbe area (Fig. 4.1), where a marked coarsening-upward sequence is observed (Fig. 4.3). Thin-bedded turbiditic sandstones (T_{de}) and mudstone → thick-bedded turbiditic sandstone (Tcde, de) and mudstone → massive conglomerate (Fig. 4.3).

4.4.2 Sandstone-Mudstone Facies Association

Fine to medium grained turbiditic sandstones (Tcde, de) are sharp based and laterally continuous. Layer thickness plots show irregular increase in bed thickness upwards; the sequence is generally non-cyclic. Slump horizons indicate a NW to SE palaeoslope (Fig. 4.3); palaeocurrents measured from flute and groove marks are consistent with this (Fig. 4.2).

Interpretation

This sequence represents the first pulse of terrigenous clastic sedimentation into the area. Fine grain size suggests a distal or low relief source. On regional grounds the former is considered more likely (see 10.2.2). Lack of traction current structures is consistent with deposition below wave base. The overall

coarsening-upward sequence represents progradation of the sedimentary system and probable uplift in the source area.

4.4.3 Conglomerate Association

Conglomerate and coarse sandstone crop out discontinuously beneath the sole thrust of the Lycian Nappes (Fig. 4.3). Their greatest occurrence near Sinekçibeli (Fig. 4.3) comprises a section 60 m thick.

The transition from medium to coarse turbiditic sandstone (Tcde) and mudstone to conglomerate occurs abruptly over 7.5 m. The base of the conglomerate unit is marked by erosional scours 3 m deep and 10-20 m across. Units of massive and stratified (Gst) conglomerate are interbedded with very coarse sandstone and mudstone (Fig. 4.4). Structureless, poorly sorted dark green cobble and boulder conglomerates form coarsening-upward sequences 6-10 m thick (Fig. 4.4). Well rounded (R2-3) clasts are up to 1.20 m in diameter. Large (to 3.50 m) disorientated coral blocks are present in the conglomerate. Green-grey subordinate sandstones (<10%) are structureless or rarely plane-laminated. Massive silty dark green mudstones form less than 5% of the sequence. They contain an abundant shallow marine fauna of gastropods and bivalves.

Southwest of Gombe (Fig. 4.1) a unit of massive pebble and cobble conglomerate forms a fining-upward lenticular (over 80 m) channel feature (Fig. 4.5). Abundant disorientated coral blocks are present in the conglomerate.

Interpretation

Abundant *in situ* marine macro-fauna and disorientated coral blocks indicate deposition in a marine environment. Stratified conglomerate sandstone (Facies Gst) is consistent with reworking by marine processes (3.3.2). Large clast size, general lack of structure and poor sorting in the coarse (cobble-boulder) conglomerates suggests deposition close to source, possibly at the mouth of high-gradient gravel-bedload streams entering a shallow sea. The conglomerates represent the submarine toe of an alluvial fan undergoing slight reworking by marine processes. Most material finer than coarse sand is reworked out of the sediment. The absence of sedimentary structures such as cross-stratification is the result of the dominantly coarse grain size and low energy environment.

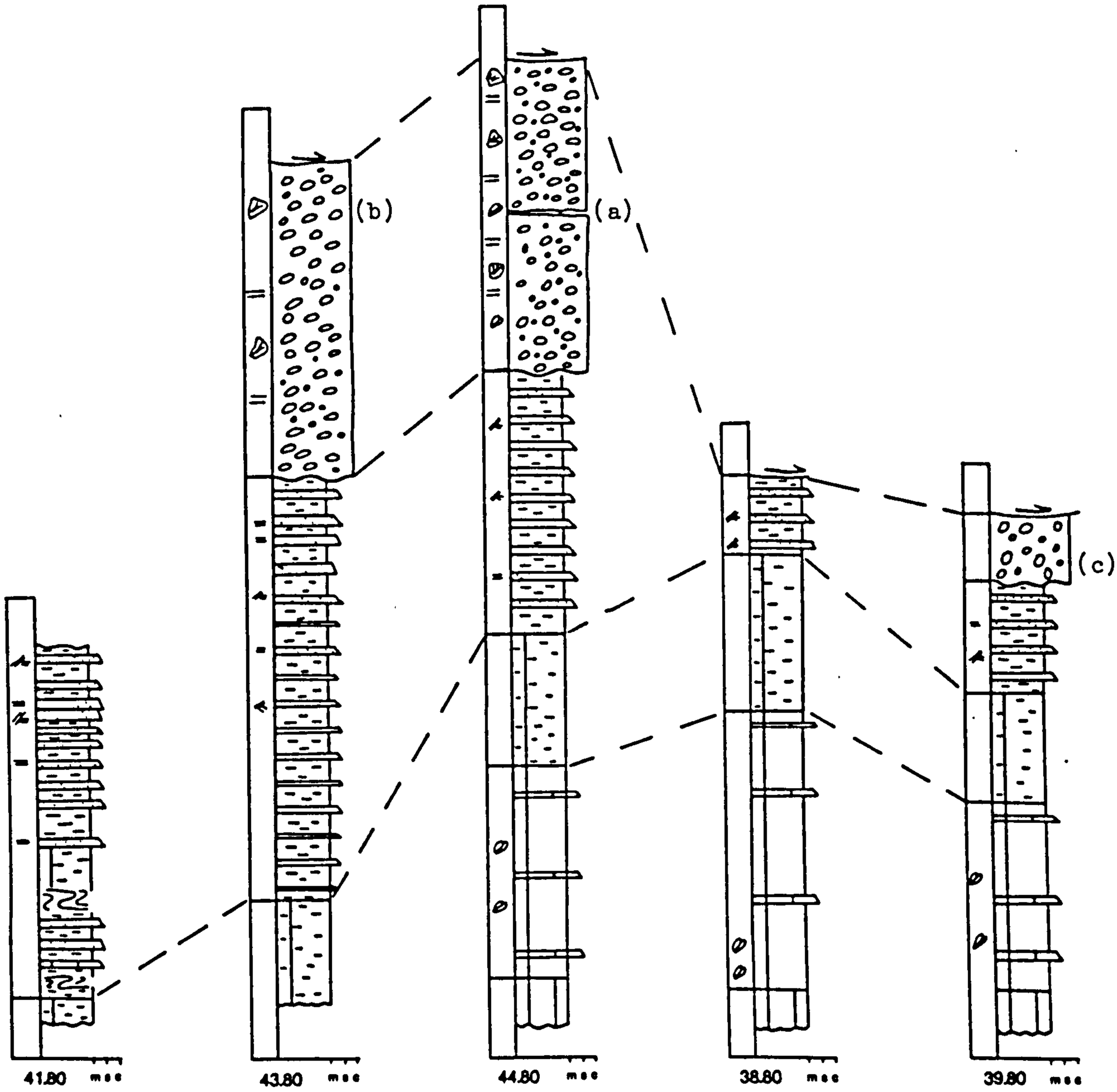

Fig. 4.3

Sedimentological logs measured in proximal sequences in the Kemer Formation. For location of logs see Fig. 4.1. The majority of sections are truncated by the overthrust Lycian Nappes.
Note general coarsening-upward sequence. Age range is Burdigalian to Langhian, (Appendix C for key).
Letters refer to location of detailed logs in Fig. 4.4.

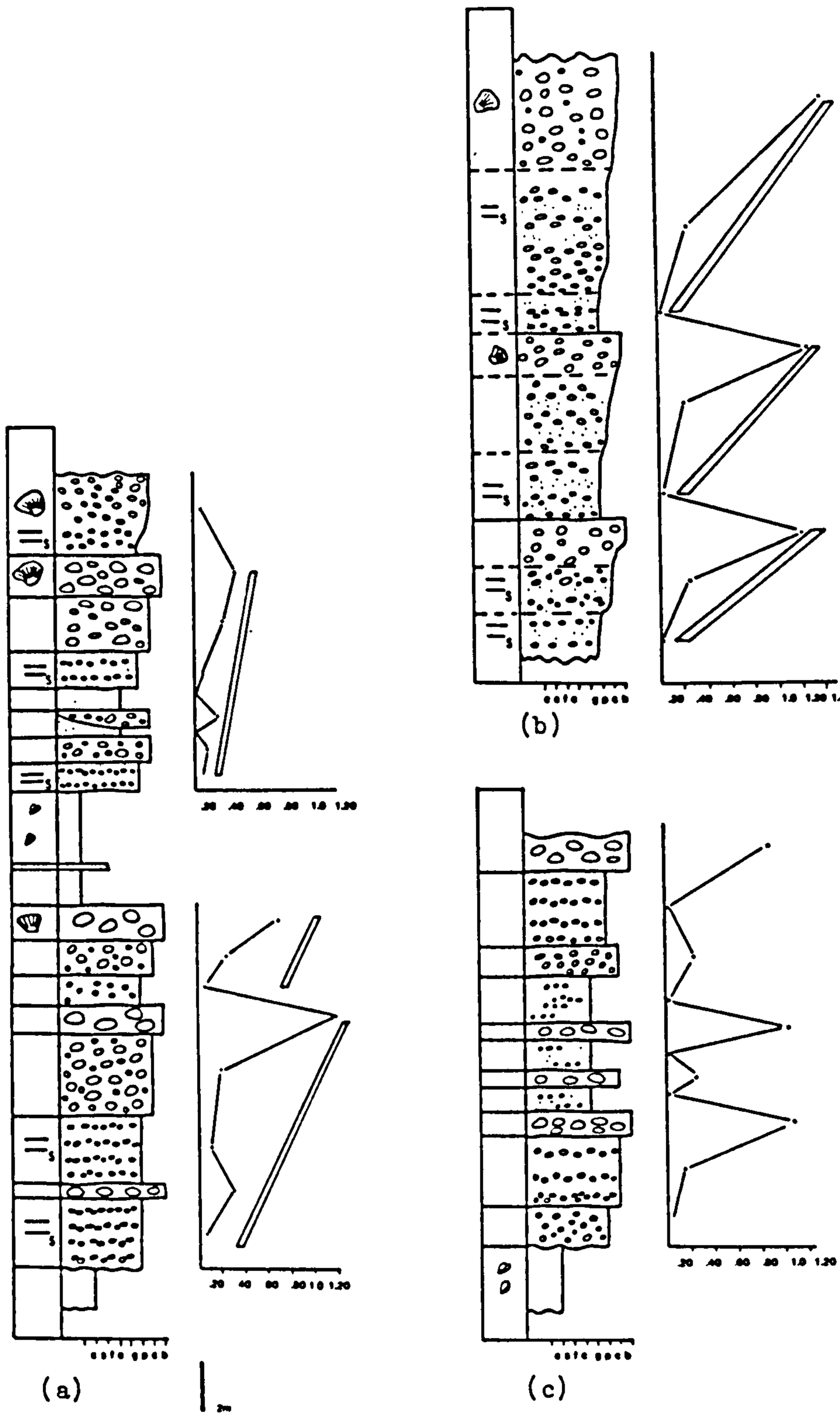

Fig. 4.4

Detailed sedimentological log in proximal 'fan-delta' sequence, Kemer Formation. Note small coarsening-upwards units produced by the local progradation of a fan-delta. For location of sections see Fig. 4.3 (Appendix C for key).

Fig. 4.5

Clast-supported channel fill conglomerate, submarine fan-delta association, exposed southwest of Gombe (Fig. 4.1).
The conglomerate contains abundant disorientated coral blocks.
Stick is 1 m long. GR. 390448.

Fig. 4.6

Conglomeratic fill to submarine fan channel.
The conglomerates deposited by a variety of sediment gravity flows, erode up to 8 m into the underlying sandstone/mudstone sequence.
Submarine fan channel association, Kemer Formation.
Stick is 1 m long. GR. 440287.

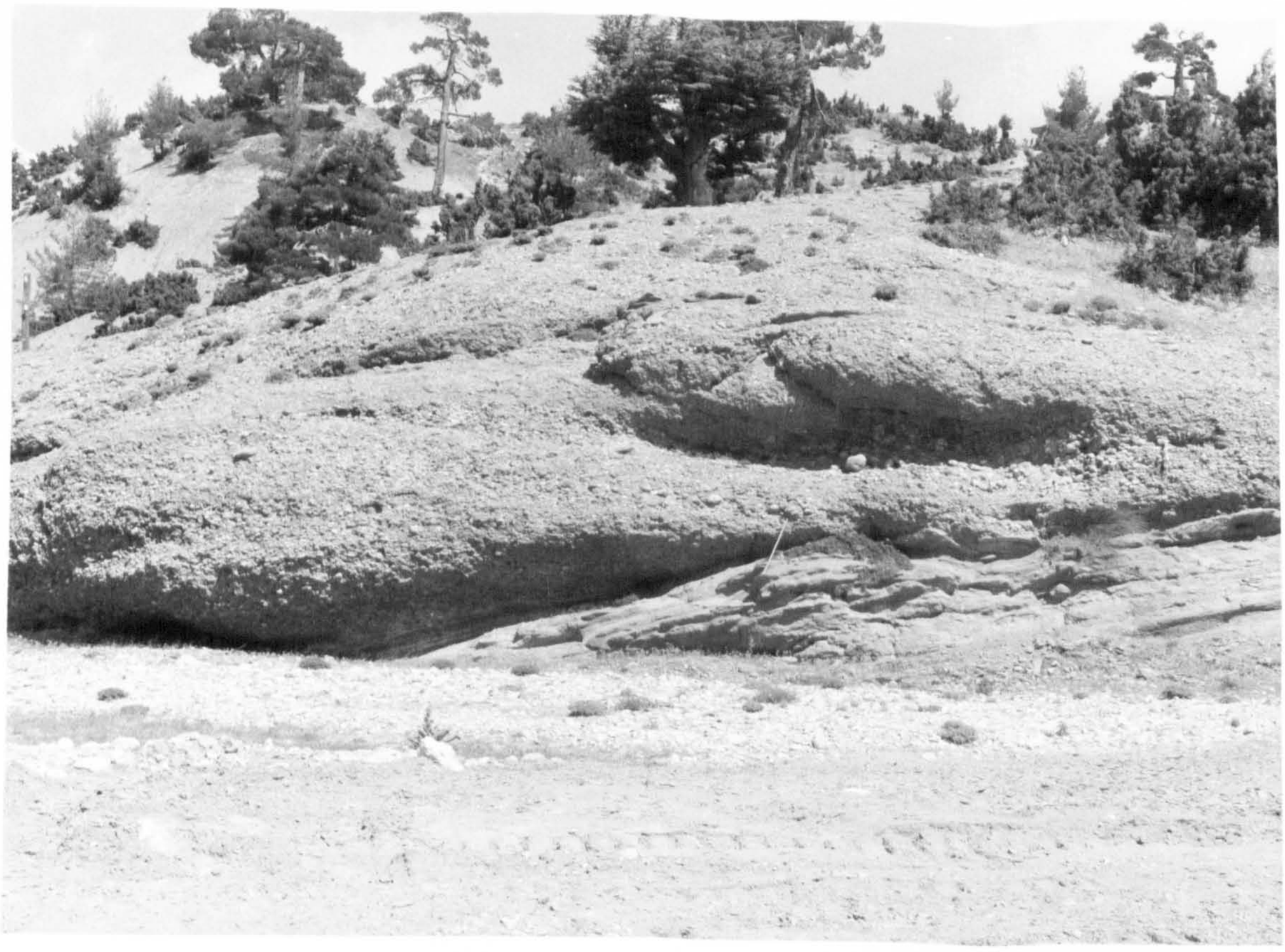

Deposition may have been below wave base. Reworking occurred when storms increased wave energy and lowered wave base. Small scale coarsening-upward cycles probably represent local progradation of the alluvial fan (cf Heward, 1978a).

4.4.4 Distal Facies Association

The 'proximal' sedimentary sequence (described above) exposed in the northwest is not continuous across the Susuz Dağ anticline (Fig. 4.1). However, identical ages, similar sedimentary facies and palaeocurrent dispersal patterns (Fig. 4.2) indicate the clastic sequence exposed in the Kasaba syncline (Fig. 4.1) can be correlated with the sequence in the northwest and represents a development of more basinal sedimentary facies.

Pelagic chalk horizons and benthonic foraminifera assemblages (G. Adams, pers. comm. 1980) suggest water depths in excess of 500 m.

In the central area, e.g. around Kemer and Kasaba (Fig. 4.1), a similar transition to the northwest marks the initiation of clastic sedimentation. Carbonate platform limestone (Chapter 9) pass up into calcareous marls and then into a distal turbiditic sandstone and mudstone sequence. In this area the sequence is not truncated by the Lycian Nappes.

4.4.5 Sedimentary Facies Associations

Conglomerate-sandstone association. Within the Kemer Formation a number of conglomerate-sandstone horizons are present. Amalgamated units are between 10 and 25 m thick. Beds of dark green to buff conglomerate are between .50 and 3.50 m thick (Fig. 4.7), poorly sorted. They comprise moderately to well rounded clasts (R2-3) up to .60 m in diameter. Both conglomerates and sandstone show no evidence of deposition by traction currents.

Textures in the conglomerates indicate deposition by a variety of sediment gravity flows (refer to 3.4). Redeposited conglomerate facies present are: (I) Disorganised (45%); (II) normally graded (25%); (III) matrix-supported (sand matrix) (20%); and (IV) inversely graded (10%). Mechanisms of deposition are discussed in 3.4. Imbrication of clast long axes indicate W-NW to E-SE palaeocurrent flow (Fig. 4.2).

Sandstones are thick-bedded, graded (Tab) or structureless, with erosional bases and flat or truncated tops.

Amalgamated conglomerate-sandstone units have the appearance of sheets. However, when traced laterally they are lenticular over several kilometres across palaeoslope and interfinger with interbedded sandstone, mudstone and pelagic chalk horizons (Fig. 4.7). On the basis of this and other evidence outlined below these units are interpreted as large channels aligned in a general NW-SE orientation.

4.4.6 Submarine Channels

Channel morphology. Of the two channel bodies in the Kemer area (Fig. 4.8), the upper one is best exposed, both laterally and down palaeoslope, and affords opportunity for a detailed study. Sections measured at various localities from the axial region to the margin of the channel are shown in Figures 4.7 and 4.9.

Bases to the channels are concave and irregular, conglomerates at the base are erosive into the underlying mudstone-sandstone up to 8 m (Fig. 4.6). Within 'proximal' channel fills no vertical internal organisation exists (Fig. 4.7). Clast size and bed thickness vary randomly (Fig. 4.7). No sequential upward transition in conglomerate facies is observed. In 'distal' channel sequences, occasional poorly defined fining-and thinning-upward sequences are present (Fig. 4.13) (see below).

Central parts of the channel are characterised by complex lenticular, wedge-shaped conglomerate and coarse sandstone beds produced by the truncation of underlying beds by successive depositional events (4.10). Across palaeoslope individual beds are rarely laterally continuous over 10 m (Fig. 4.10). Down palaeoslope, where exposure permits, they may be traced up to 100 m. Thin mudstone, siltstone and rare pelagic chalk horizons within conglomerate units are also laterally discontinuous as a result of erosional truncation. Towards channel margins clast size and bed thickness in conglomerate decreases (Fig. 4.9). Conglomerate and coarse sandstone interfinger with thin-bedded sandstone and mudstone (Fig. 4.8). Conglomerate textures pass from massive disorganised beds (Dsg), to normally graded beds (Ng), to massive sandstone beds with scattered pebbles and cobbles (Fig. 4.7).

Channel margins. Nowhere in the area is a complete margin exposed. Fig. 4.9 is a simplified reconstruction of the best exposed conglomerate unit. Conglomerate and sandstone thin laterally

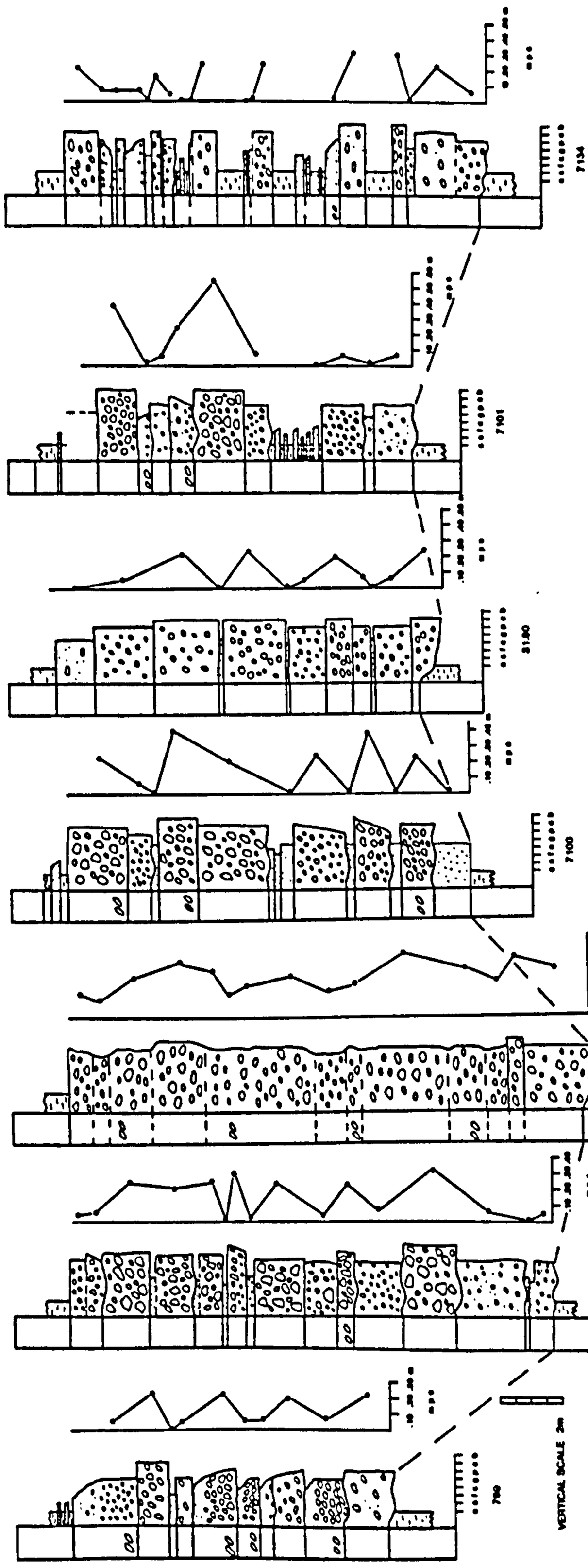

Fig. 4.7 Detailed sections across strike, in conglomerate fill to submarine fan channel, in Kemer Formation.
See Fig. 4.8 for location of sections and Fig. 4.9 for simplified section and horizontal scale (Appendix C for key).

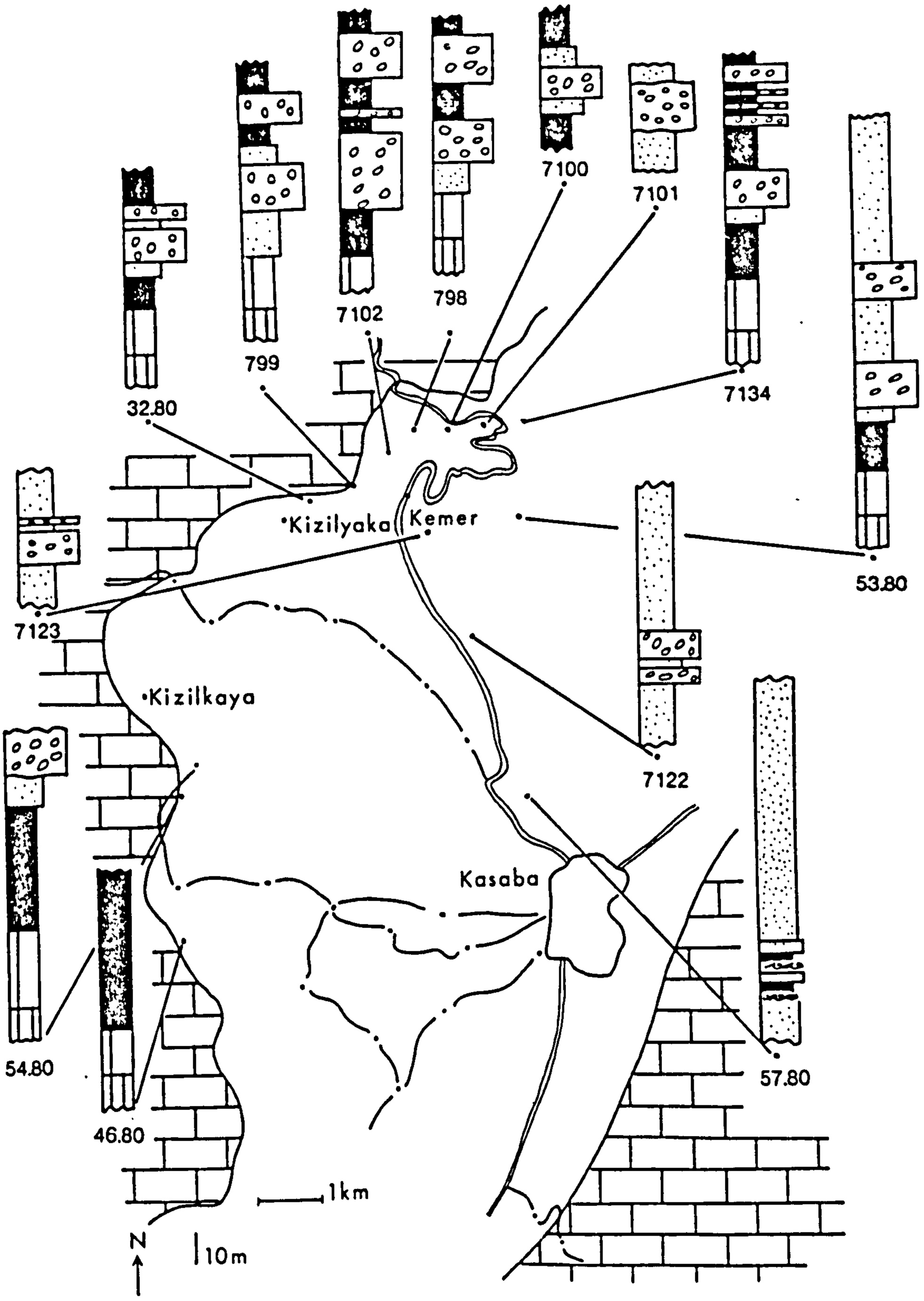

Fig. 4.8

Location map for sections in conglomerate channel (Figs. 4.7 and 4.9), and generalised sections through two superimposed channel-fill sequences.

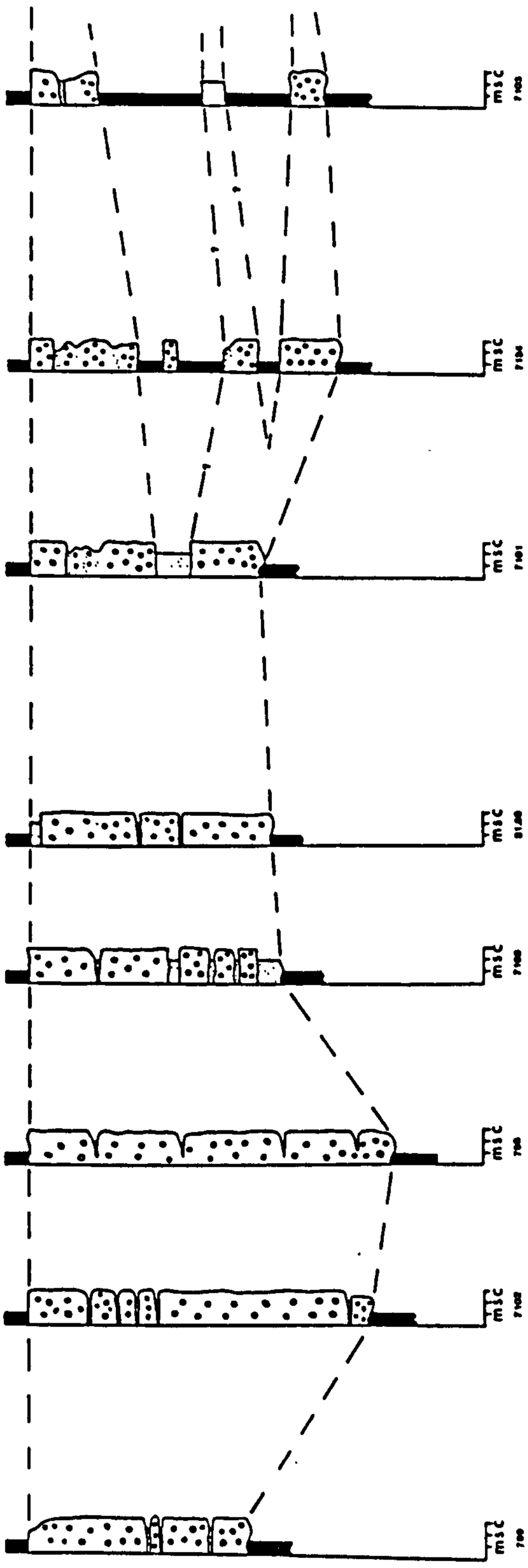

Fig. 4.9 Simplified sections, drawn to scale, showing vertical and lateral variations in submarine fan channel, Kemer Formation.
Note interfingering (on the right) of conglomerates deposited within the channel, and mudstone-sandstone deposited in overbank areas.
See Fig. 4.8 for location of sections (Appendix C for key).

(a)

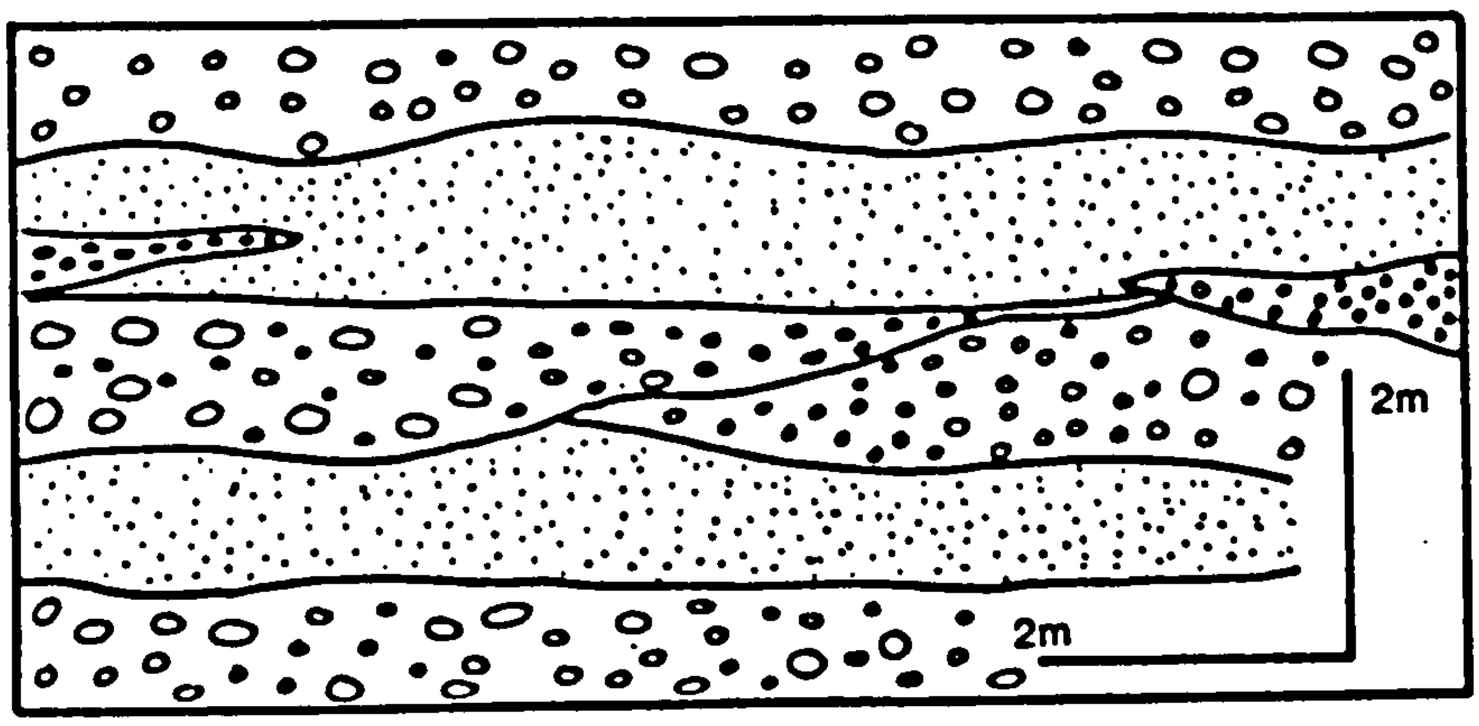

(b)

Fig. 4.10
Sketches of central parts of submarine fan channel in proximal area north of Kemer, GR. 442287.
Note erosion at base of channel in (a) and marked lateral discontinuity of individual beds as a result of erosive truncation of underlying beds produced by successive depositional events.

Figs. 4.11 and 4.12

Base of submarine fan channel ('mid-channel' area) well exposed in cliff face south of Kemer, GR. 444267. Note only slight erosion at base of channel, generally finer grain size when compared with more proximal channel fill sequences (Fig. 4.6), also erosional truncation within channel-fill and soft sediment loading as shown below. Face is 15 m high.

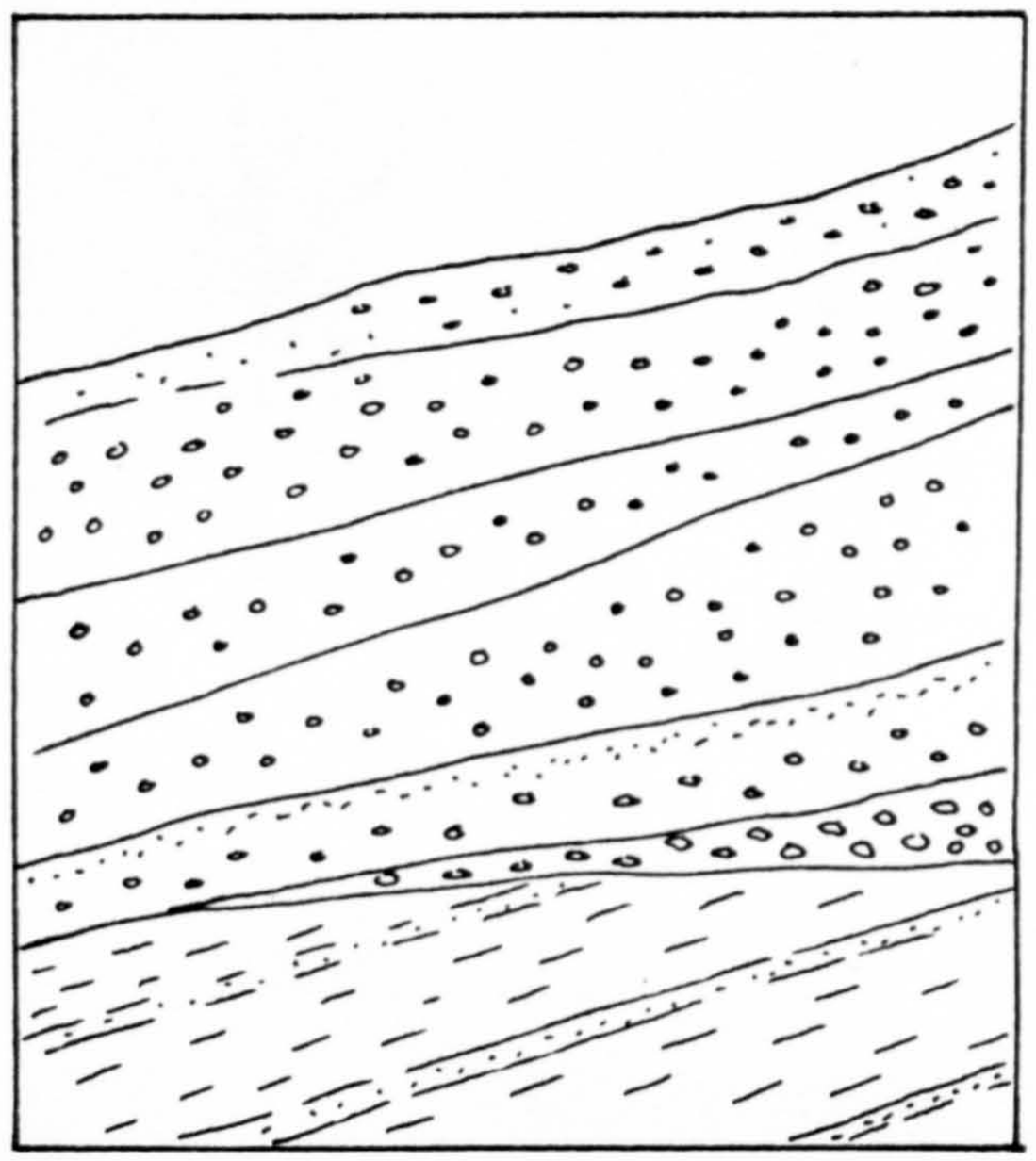

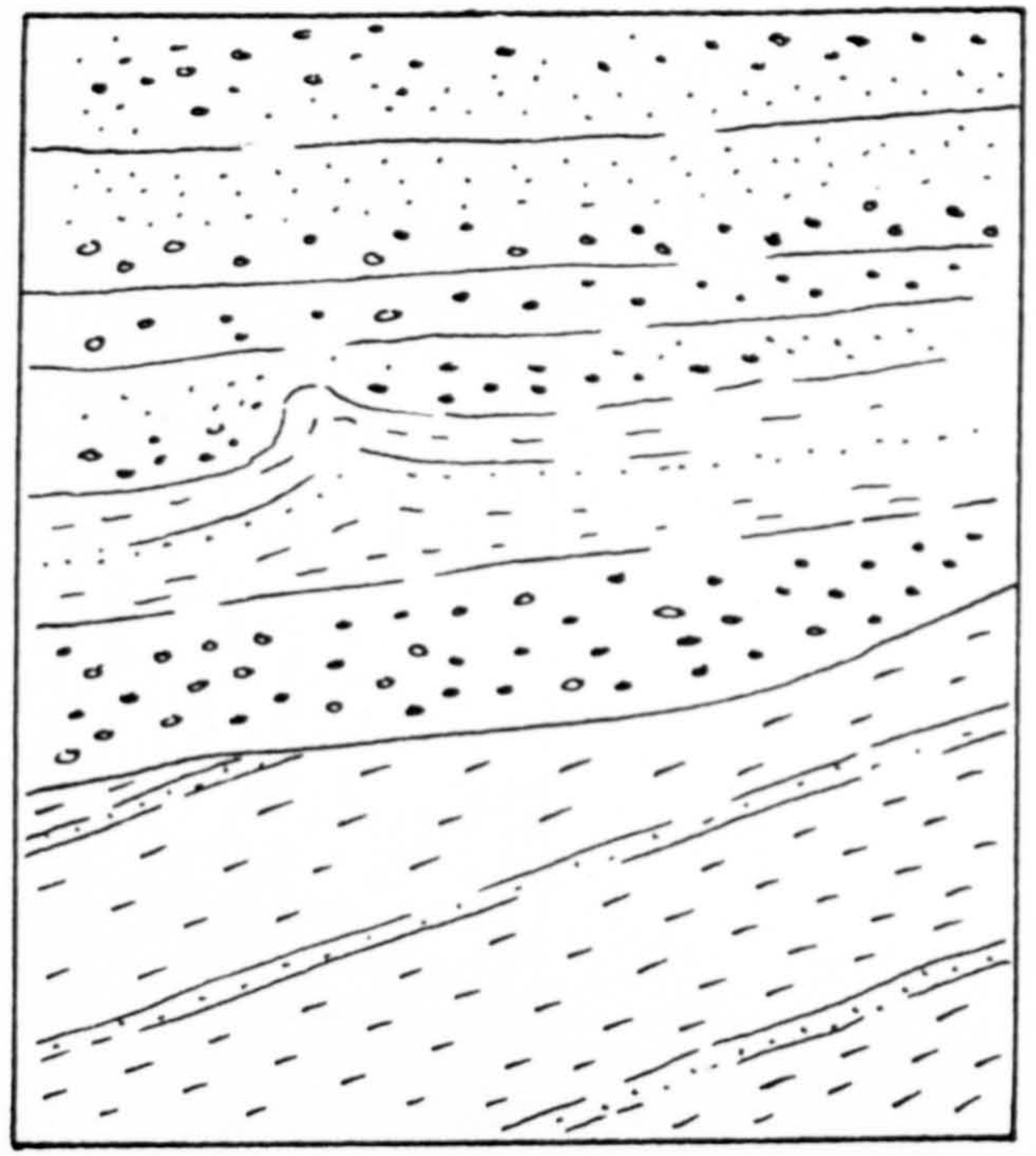

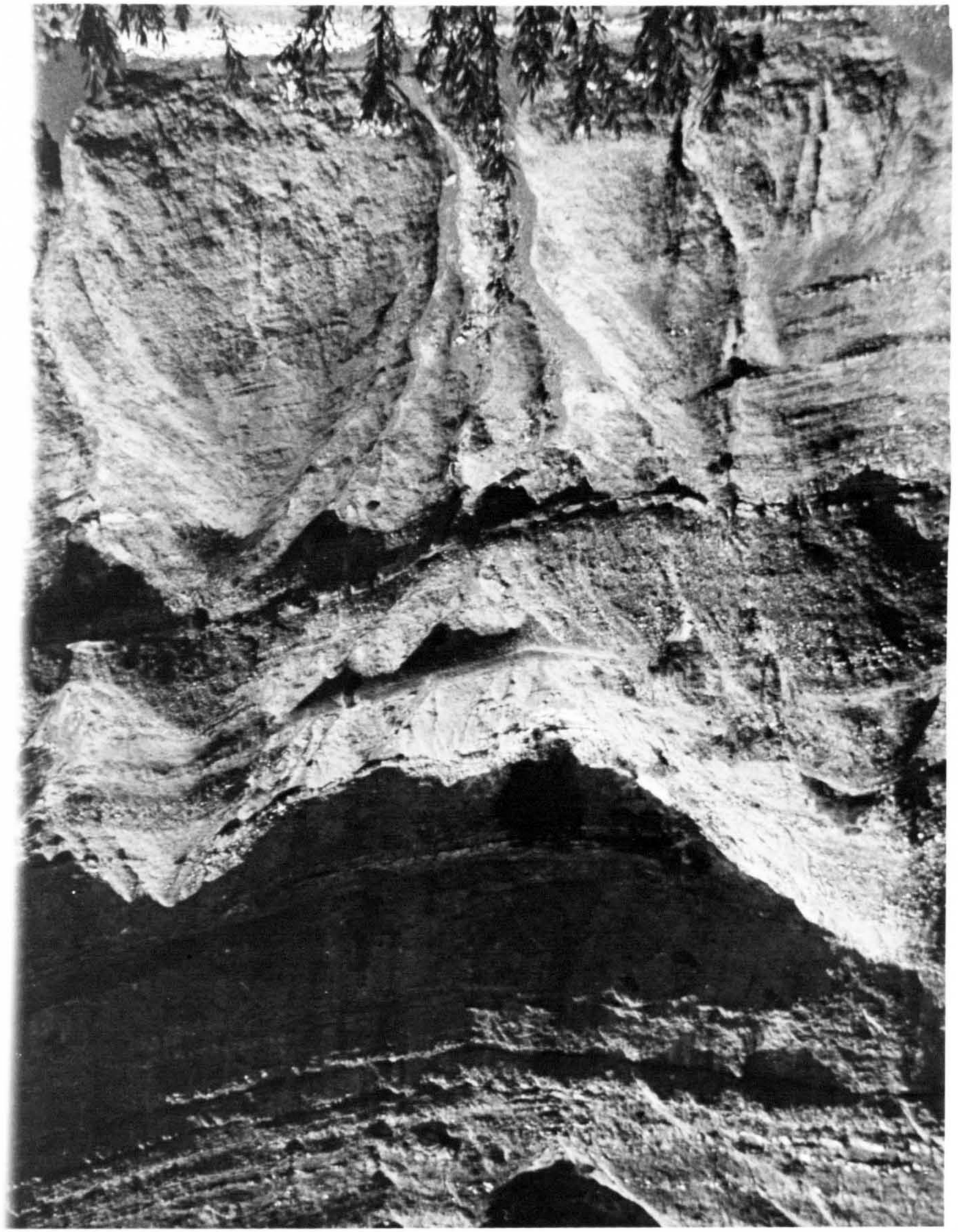

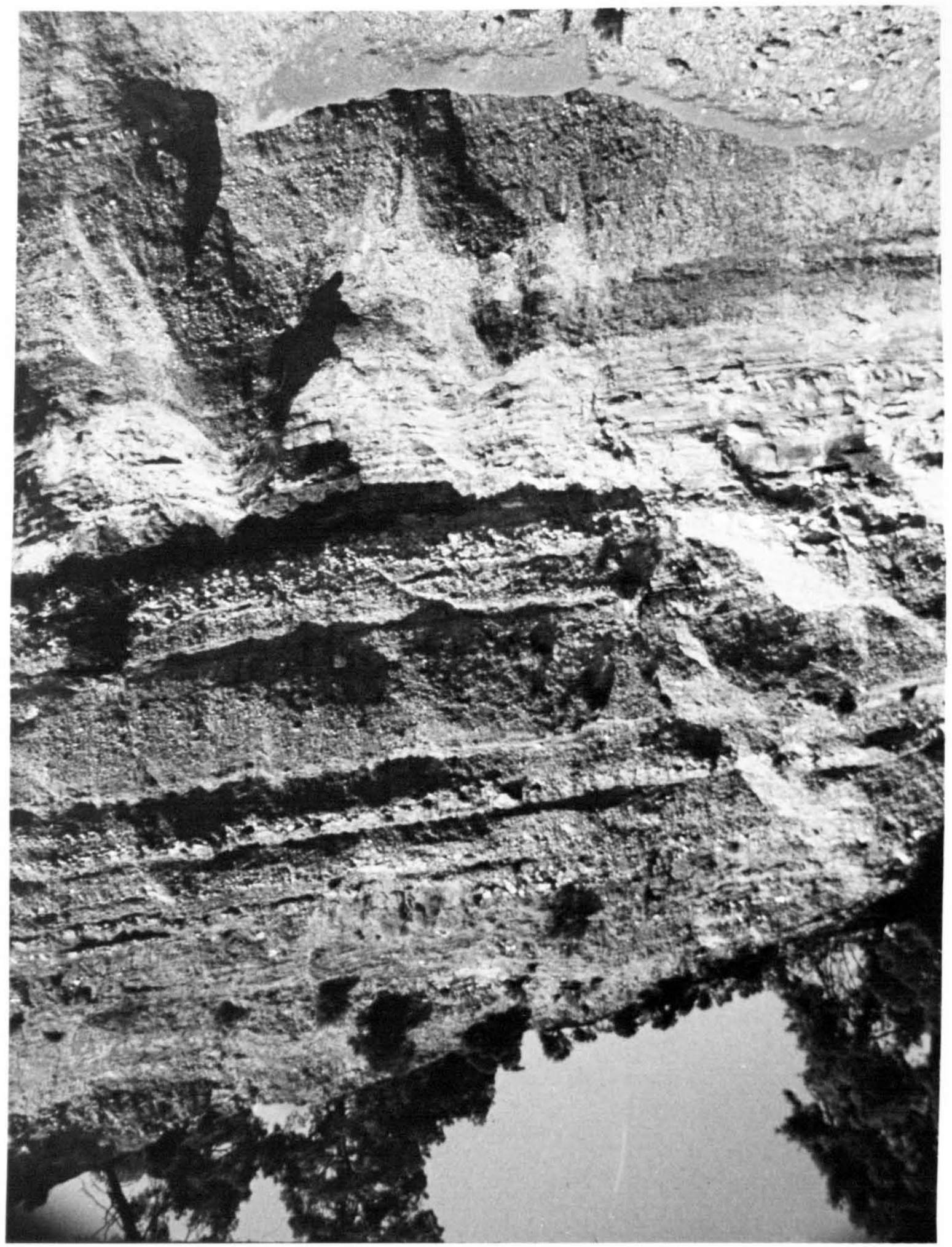

eastwards and interdigitate with thin-bedded sandstone and mudstone.

Submarine channel morphology is produced in one of three ways (Nelson and Kulm, 1973):

(I) Erosional channels - channel walls are formed by erosion into previously deposited, consolidated or partially consolidated sediment.

(II) Depositional channels - channel walls are constructed by the deposition of fine grained material deposited marginally to the main channel, resulting in the formation of subaqueous levees, similar in nature to subaerial levees formed by river channels.

(III)Depositional-erosional channels - channels of this sort are constructed by a combination of erosion in axial regions, and limited deposition by overflow of turbidity currents and other mass flow events on to channel margins.

Depositional-erosional channels are the most common deep sea channels at the present day (Nelson and Kulm, 1973). They may not be directly applicable to this sequence as most of the channels described are from much larger sedimentation systems at the base of continental slopes. Modern channels of this sort are thought to originate as a depositional system that is modified by erosional downcutting at a later date (Normark, 1970; Griggs and Kulm, 1970; Nelson and Kulm, 1973). Features of depositional-erosional channels that may be recognised in the ancient, are (after Nelson and Kulm, 1973):

(I) Their position may be controlled by topographic lows in the underlying basement.

(II) Levees occur on both sides of the channel.

(III)Truncated beds may occur against both walls and levees.

Modern channels of this sort often have steep axial gradients (1:600); channel relief may exceed 300 m (Nelson and Kulm, 1973).

In the present example erosion of the underlying sandstone/mudstone sequence to a minimum depth of 8 m can be demonstrated in axial parts of the channels (Fig. 4.6). On the margins channel deposits clearly interfinger with, and do not abut abruptly against, overbank deposits (Fig. 4.9). The channels are interpreted to have formed by a combination of coeval erosional and depositional events, both playing an equal part in confining the channel. Levee deposits cannot be recognised in the field, although Winn and Dott (1979) have demonstrated that even where thick levee deposits are present they are difficult to recognise in ancient sediments as a result of

differential compaction between channelled conglomerate/sandstone units and thin sandstone and mudstone of levees.

Deposition in the channels was by a variety of sediment gravity flows (3.4) ranging from debris flow, to density modified grain flow and turbulent flow. Erosional contacts, scouring and conglomerate facies (mainly clast-supported beds) suggest turbulent flows may have been dominant. In central parts of the channels many of the contacts are gradational, and individual units difficult to delineate. This may be the result of immediate post-depositional mobilisation and partial homogenisation (cf Carter and Norris, 1977) of the channel fill. The large channel features contained an anastomosing series of smaller channels (Fig. 4.18), resulting in lateral discontinuity and lenticular geometry to conglomerate beds (Figs. 4.12, 4.13, 4.14). They are often modified by erosion from overlying beds (Figs. 4.10, 4.12).

In conclusion, channel walls probably had only low relief and conglomerate deposition was in a shallow complexly channelled central region with no well defined channel margins, allowing frequent overflow into marginal overbank areas.

4.4.7 Channel trends down Palaeoslope

Channelled conglomerate and sandstone are best exposed in the Kemer area (Fig. 4.1) and to the west around Kizilkaya (Fig. 4.1). Up palaeoslope the entire clastic sequence is removed by erosion. Downslope control between well exposed sections is poor. General downslope trends observed are (Fig. 4.13):

(I) Decrease in the average clast size of the conglomerate (Figs. 4.1, 4.13);

(II) Decrease in the conglomerate:sandstone ratio and increase in the sandstone: mudstone ratio within the channels (Fig. 4.13);

(III) Increase in the percentage of matrix-supported conglomerate.

Conglomerates within channels die out and are progressively replaced by coarse sandstone and mudstone over a distance of 5-7 km (Fig. 4.16) down palaeoslope.

4.4.8 Mid-distal Channel Sequences

Sandstone-mudstone association. Within the mid-to distal-channel sequence (Fig. 4.13), well exposed north of Kasaba (Fig. 4.1) several highly disorganised slump horizons occur (Fig. 4.13). Orientation of the slumps is oblique to the main NW-SE trend of the channel.

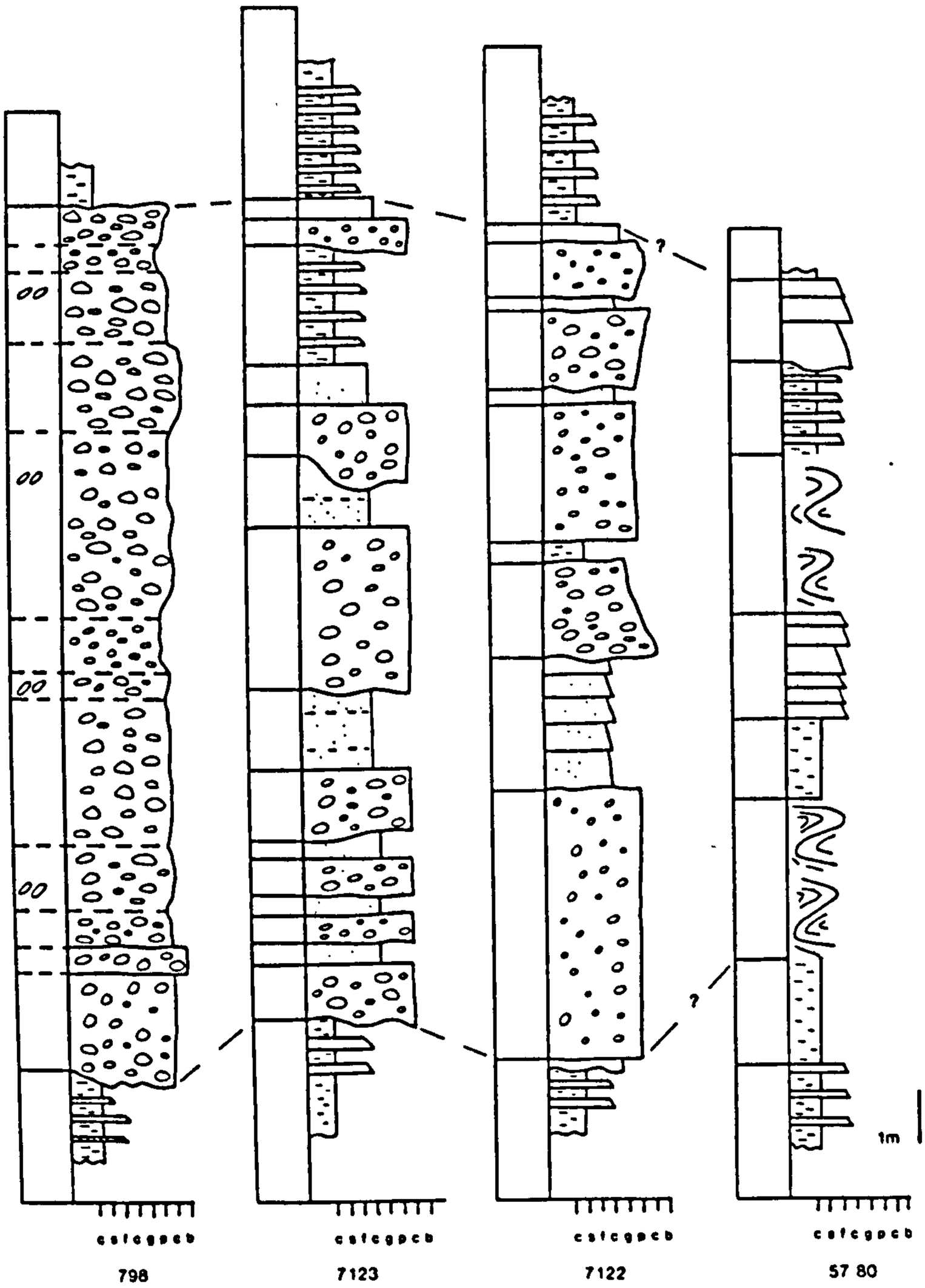

Fig. 4.13

Detailed sedimentological logs showing progressive down channel variation in sedimentary facies in submarine fan channel.
Note progressive decrease in percentage of conglomerate and change from disorganised to organised conglomerate beds.
See Fig. 4.8 for location of logs. Kemer Formation.

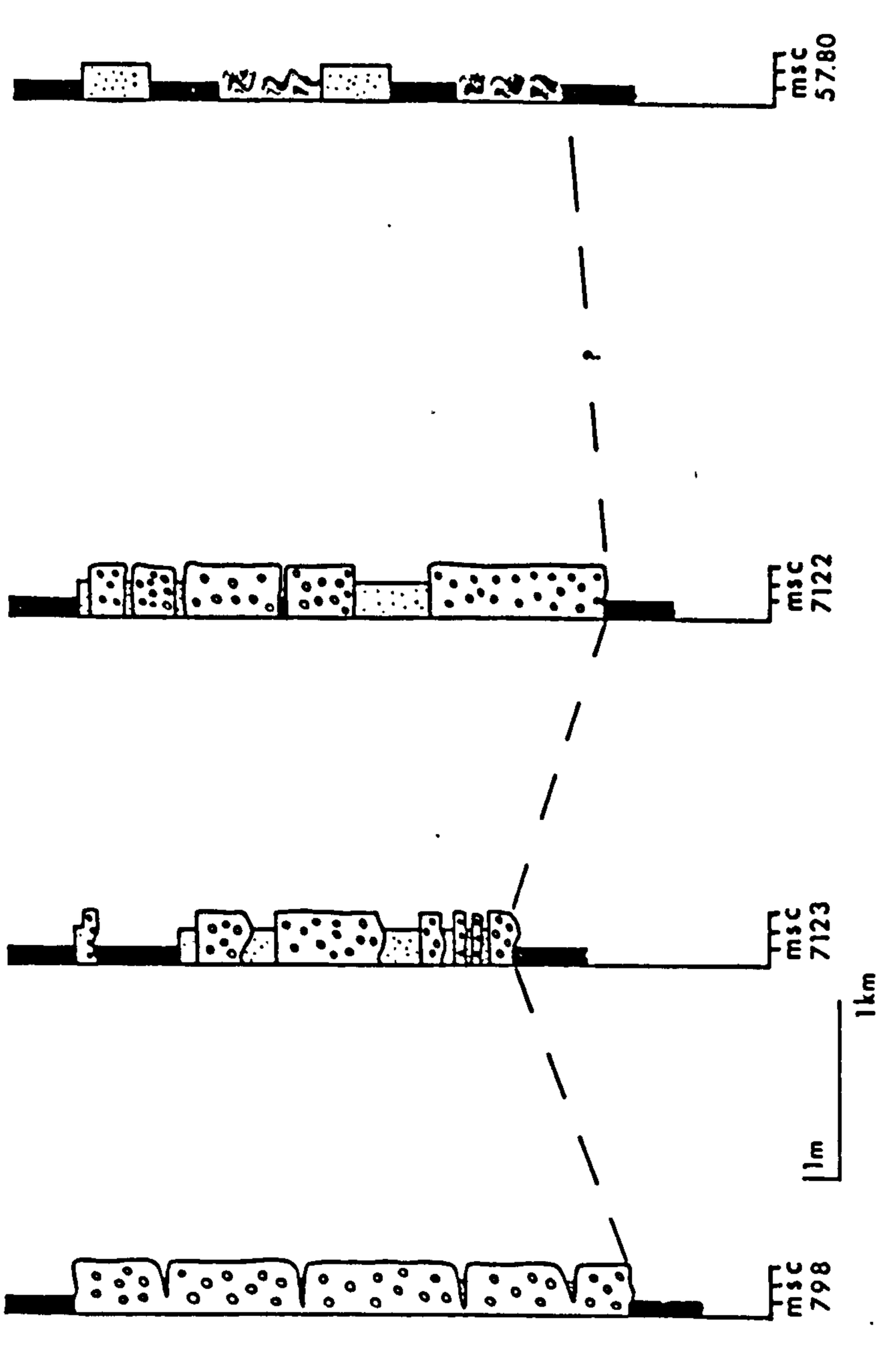

Fig. 4.14 Generalised sedimentological logs, drawn to scale, showing progressive down channel variation in sedimentary facies (based on Fig. 4.13).

Interbedded structureless and graded (Tab, abc) coarse sandstones form amalgamated units between 2.5 m and 5.0 m thick. The units have erosive bases and a wedge-shaped geometry. Within units poorly defined fining- and thinning-upwards cycles are observed (Fig. 4.13). Rare matrix-supported (mud) pebble conglomerates (Msp) also occur interbedded with mudstone and occasional pelagic chalk horizons.

Interpretation

Slump orientation broadly to the south suggests that slumping may have been from marginal areas towards axial channel areas. Fining- and thinning-upward cycles were produced by the lateral migration of small channels within the larger system (cf Ricci Lucchi, 1975a, b). Mud-supported pebble conglomerates represent 'distal' debris flows. Down palaeoslope from the above sequence, poorly exposed sections near Kasaba consist of lenticular, thick, structureless (Sst) and graded (Tab) sandstones interbedded with laterally persistent thin sandstone (Tde, cde), mudstone and chalk. The sequence which comprises 70% sandstone is non-cyclic.

In poorly exposed distal areas to the channels, southeast of Kasaba, conglomerate and coarse sandstone are entirely absent. The sequence comprises interbedded thin sandstone (Tcde, de), mudstone and chalk. Rare flute and groove marks, and ripples suggest a southeasterly-directed palaeocurrent.

4.4.9 Channel Location and Migration

The presence of two conglomerate-sandstone units in the Kemer area (Fig. 4.8) both representing a channel feature, indicates either channel migration or periodical supply of coarse grained material. The lenticular superimposed nature of the channels and absence of any form of fining-upward channel fill, produced by the lateral migration of the channel, suggest the periodic supply of coarse grained material rather than the migration of the channel.

The location of present day submarine channels is a result of:

(I) Initial alignment along a pre-existing basement lineament;

(II) Relict river channels, eroded at low sea level stand;

(III)Slumping at the break of slope between the shelf and continental slope;

(IV) Large slump scars at the site of rapid deposition at the foot of deltas.

In the Kemer Formation the immediate 'up-channel' parts of the sequence have been removed by erosion. However, more proximal sequences of massive conglomerate units (Fig. 4.4) are interpreted to have been deposited on the submarine toe of a coastal alluvial fan. In this environment initial channel location may have been the site of large slump scars produced by sediment overloading as a result of very rapid deposition.

Once initiated it requires a major change in the locus of sedimentation on the alluvial fan, effectively reducing sediment supply to one area and directing it to another, to produce channel migration.

In conclusion, the site of subaerial and shallow marine deposition exerted strongest control on submarine channel location. Catastrophic events which resulted in the movement of the locus of sedimentation on the alluvial fan, produced channel switching in the submarine sequence.

4.4.10 Lateral Variation in Sedimentary Facies

Thin-bedded sandstone-mudstone-chalk association. Sediments exposed laterally away from the main channels are composed of thin-bedded, sharp based laterally persistent sandstone (Tcde, de), dark green mudstone and pelagic chalk. Sandstone and mudstone are the result of overflow of fine grained turbidity currents from channel areas or turbidity currents emanating from other points on the basin margin.

Local variations. Conglomerate-sandstone channels in the Kemer area (Fig. 4.1) are traced laterally several kilometres east (Fig. 4.10). To the west near Kizilkaya (Fig. 4.1) poorly exposed lenticular conglomerate-sandstone units form two channellised bodies. They cannot be correlated with channels in the Kemer area and represent separate depositional units. Orientation of these channels is NNW to SSE; they cannot be traced downslope. Across slope dimensions are comparable to channels in the Kemer area.

The main area of deposition was in the Kemer, Kizilkaya, Kasaba region; away from here conglomerates are absent, sandstones become thinner and are progressively replaced by mudstone. Layer-thickness plots show symmetrical cycles of variable wavelength, they correlate most closely with the basin plain cycles of Ricci Lucchi (1975a, b). However, caution must be exercised in applying sedimentological

models developed for large submarine fan systems developed at the base of the continental slope (e.g. models of Walker and Mutti, 1973; Ricci Lucchi, 1975a, b) to small immature sedimentation systems developed in tectonically active ensialic basins. This problem is discussed more fully in Chapter 5.

Regional variations. Fine grained, thin-bedded sandstones (Tcde, de), mudstone and pelagic chalk interdigitate with bioclastic limestone breccias of the Çağman Member (7.2) to the south east, and with carbonate conglomerates and calciturbidites of the Felenk Dağ Member (7.12.0) to the southeast.

4.5.0 Sedimentary Model : Summary

Evidence for a northwest-southeast palaeoslope is:

(I) Overall palaeocurrent dispersal trends (NW-SE) (Fig. 4.2);

(II) General decrease in clast size (Fig. 4.1);

(III) Increasingly more basinal aspects of the sedimentary sequence from NW to SE (e.g. pelagic chalk horizons, lack of macrofauna).

Proximal sequences show a coarsening-upwards tendency, turbiditic sandstones are overlain abruptly by a thick conglomerate unit (Fig. 4.3). Following rapid subsidence at the end of the Aquitanian (10.2.3), this sequence represents a shallowing-upwards, produced by the infilling of the sedimentary basin and progradation of the shoreline, in return related to the advance of the Lycian Nappe front (10.2.2).

Within the conglomerates a marine fauna of bivalves and gastropods and disorientated coral blocks indicate deposition in a shallow marine environment. This sequence is interpreted to have been deposited at the submarine toe of an alluvial fan. The lack of shallow marine sedimentary structures (cross-stratification, strand lines, seaward dipping imbrication) suggests deposition in a low energy micro-tidal environment, probably below wave base. Stratified conglomerate and sandstone, formed by wave reworking, may be the result of storm-induced currents, when wave base was lowered.

The immediate down palaeoslope sequence has been removed by erosion. Distal facies equivalents of the shallow marine sequence are large channels of a 'submarine fan' produced by a combination of deposition and erosion. Within the channels, conglomerate sandstone units were deposited by a variety of sediment gravity flows (3.4) in

a complexly channelled braided system (Fig. 4.18). The general model is shown in Fig. 4.18. Major channels are 3-5 km across and extend up to 10 km downslope. Down channel conglomerate and sandstone are successively replaced by sandstone and mudstone (Fig. 4.14).

Sandstone occurs in small (~5 m) fining upward units, the result of deposition in a minor braided channel system (Ricci Lucchi, 1975a,b). Southwards in more distal areas bundles of sandstones are laterally continuous and non-cyclic. This part of the sequence, exposed around Kasaba (Fig. 4.1) forms the depositional lobes of classical submarine fan nomenclature (Mutti and Ricci Lucchi, 1972; Normark, 1974, 1978). The lack of any well defined cyclicity (coarsening-and thickening-upwards etc.) within the sequence (cf Mutti and Ricci Lucchi, 1972; Walker and Mutti, 1973; Mutti, 1974; Ricci Lucchi, 1975a, b) produced by the ordered progradation of the system, may be the result of the migration and low confinement of channels, allowing both the wide spread of individual turbidity currents and the overlap of several lobes.

Marginal to the area of channel deposition thin-bedded sandstone (Tde) mudstone and pelagic chalk were deposited.

4.5.1 Analogous Sequences

Studies of modern submarine fans and channels have concentrated on two types of sedimentation systems:

(I) Deep water, small fans on the Californian continental margin (Normark, 1970, 1974, 1978; Normark *et al.*, 1979);

(II) Very large fans described from deep ocean basins, e.g. Bengal fan (Curray and Moore, 1971), Indus cone (Jippa and Kidd, 1974), Mississippi cone (Huang and Goodell, 1970), Amazon cone (Damuth and Kumar, 1975), Laurentian fan (Stow, 1977, 1979; Uchapi and Austin, 1979; Stow, 1980). Small immature sedimentation systems developed in tectonically active ensialic basins are very poorly known.

In studies of ancient sequences the same is again true. Most studies on which modern submarine fan models are based, particularly those of the Italian school (Mutti and Ricci Lucchi, 1972, 1974, 1975; Ricci Lucchi, 1975a, b) have been based on seemingly mature, stable, base of continental slope, submarine fans deposited in deep axial troughs. Walker's (1976, 1978, 1979b) models combine features developed from both modern and ancient examples. These models are

not generally applicable to small immature sedimentation systems discussed here. However, recent studies by Surlyk (1975a, 1978), Howell and Link (1979) and Stow *et al.* (in press) have produced models for submarine fans developed in tectonically active ensialic basins characterised by immature sedimentation systems. Features of these models are discussed briefly in 5.12.

4.6.0 Vertical Variations in Sedimentary Facies - a regressive upwards sequence

Conglomerate-sandstone channels in both the Kemer and Kizilyaka area are restricted to the lowermost 200 m of the Kemer Formation. Above this coarse to fine grained, poorly sorted, graded sandstone (Tbcde, Tcde, Tde) and thick structureless, poorly sorted muddy sandstones are interbedded with mudstones, pelagic chalk and rare pebbly mudstone. As a result of poor exposure, interpretation of this sequence is restricted to vertical sequence analysis, from a series of pieced together sections (Figs. 4.15, 4.16).

Vertical trends observed subdivide the sequence into two. The basal 200 m is characterised by:

(I) An upward decrease in the frequency of pelagic chalk horizons (Fig. 4.17) completely absent after 100 m;

(II) Upward increase in the mudstone:sandstone ratio;

(III)Upward increase in the number of turbiditic sandstone beds that show evidence of partial reworking of tops by current activity (Figs. 4.15, 4.16). This general fining-upward sequence marks the end of *initial* Miocene emplacement of the Lycian Nappes (10.2.4), relief in the source area having been lowered by erosion. Shallowing-upwards is probably related to eustatic sea level changes during and towards the end of the Serravallian (Vail *et al.*, 1977; Hsu, 1973; Gwirtzmann and Buchbinder, 1977), and the progressive infilling of the sedimentary basin. Both are discussed more fully in 10.2.5.

The upper 100 m of the sequence (Fig. 4.16) is characterised by:

(I) An increase in sandstone:mudstone ratio (Fig. 4.17);

(II) General upward increase in grain size;

(III)The incoming of strongly channellised coarse sandstone and conglomerate horizons (Fig. 4.16), associated with mudstones that contain an abundant shallow marine fauna (Appendix B). Fig. 4.17 shows vertical trends and associations for both parts of the sequence.

Fig. 4.15
Sedimentological logs in middle parts of the Kemer Formation (see Fig. 4.1 for location of sections, Appendix C for key)

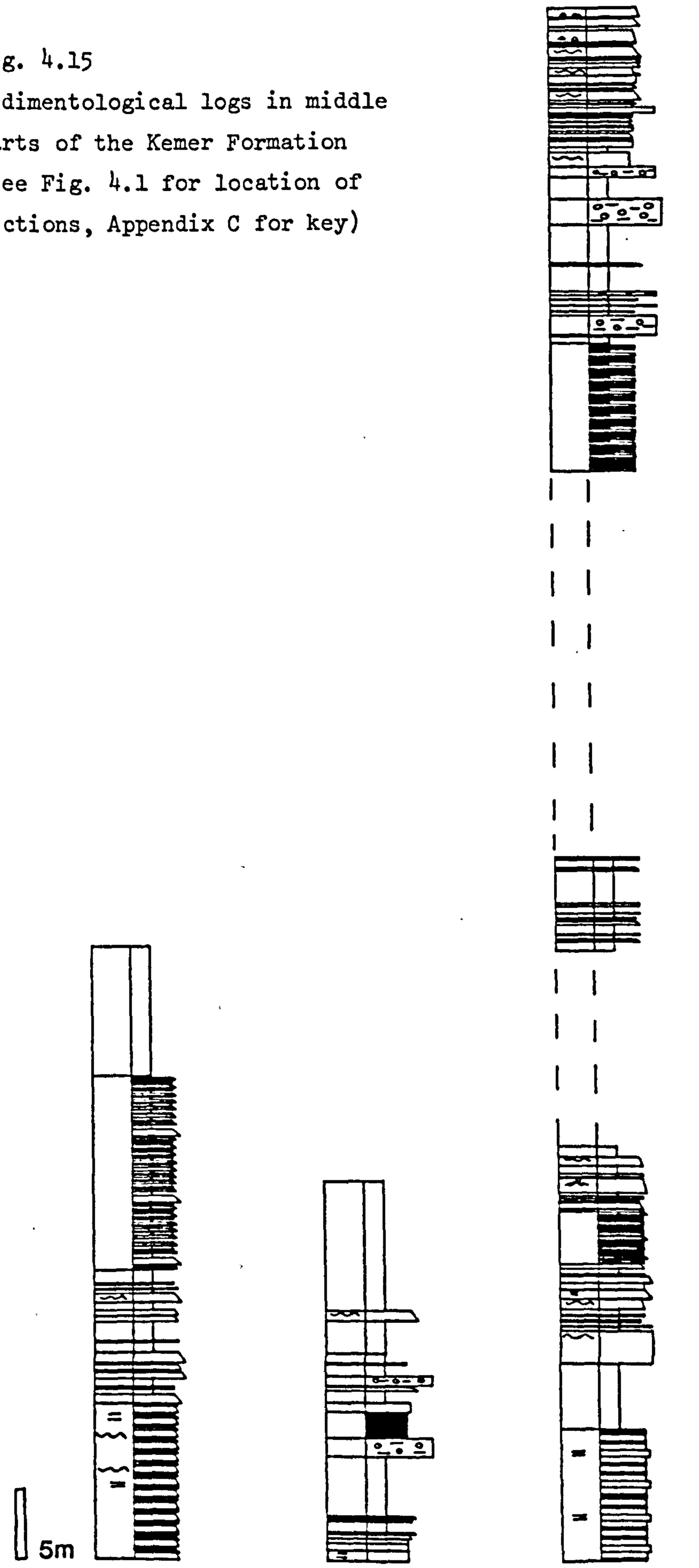

Fig. 4.16
Sedimentological logs in middle and upper parts of the Kemer Formation. See Fig. 4.1 for location of sections (Appendix C for key).

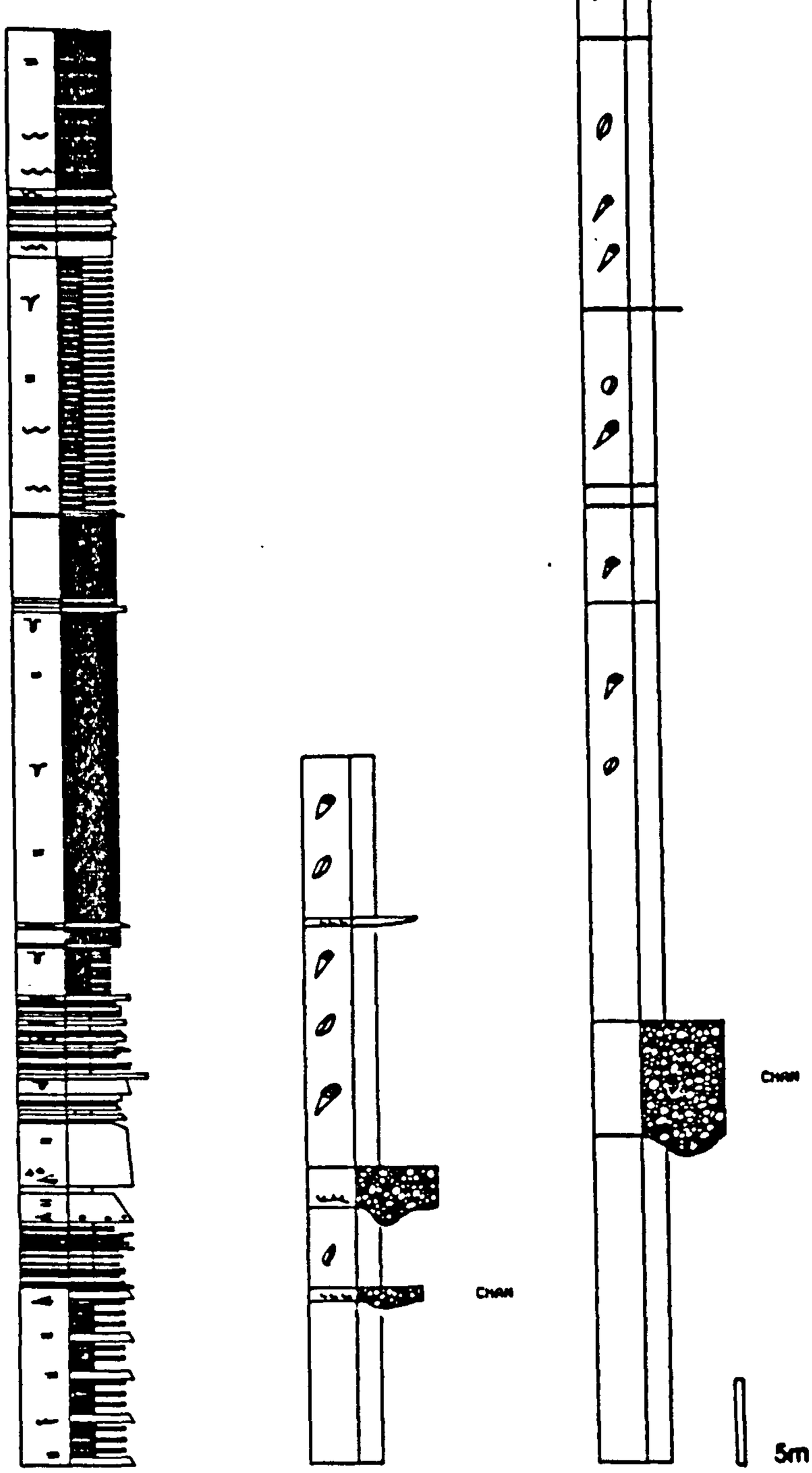

SECTION 7124

SECTION 72 80

SECTION 28.80

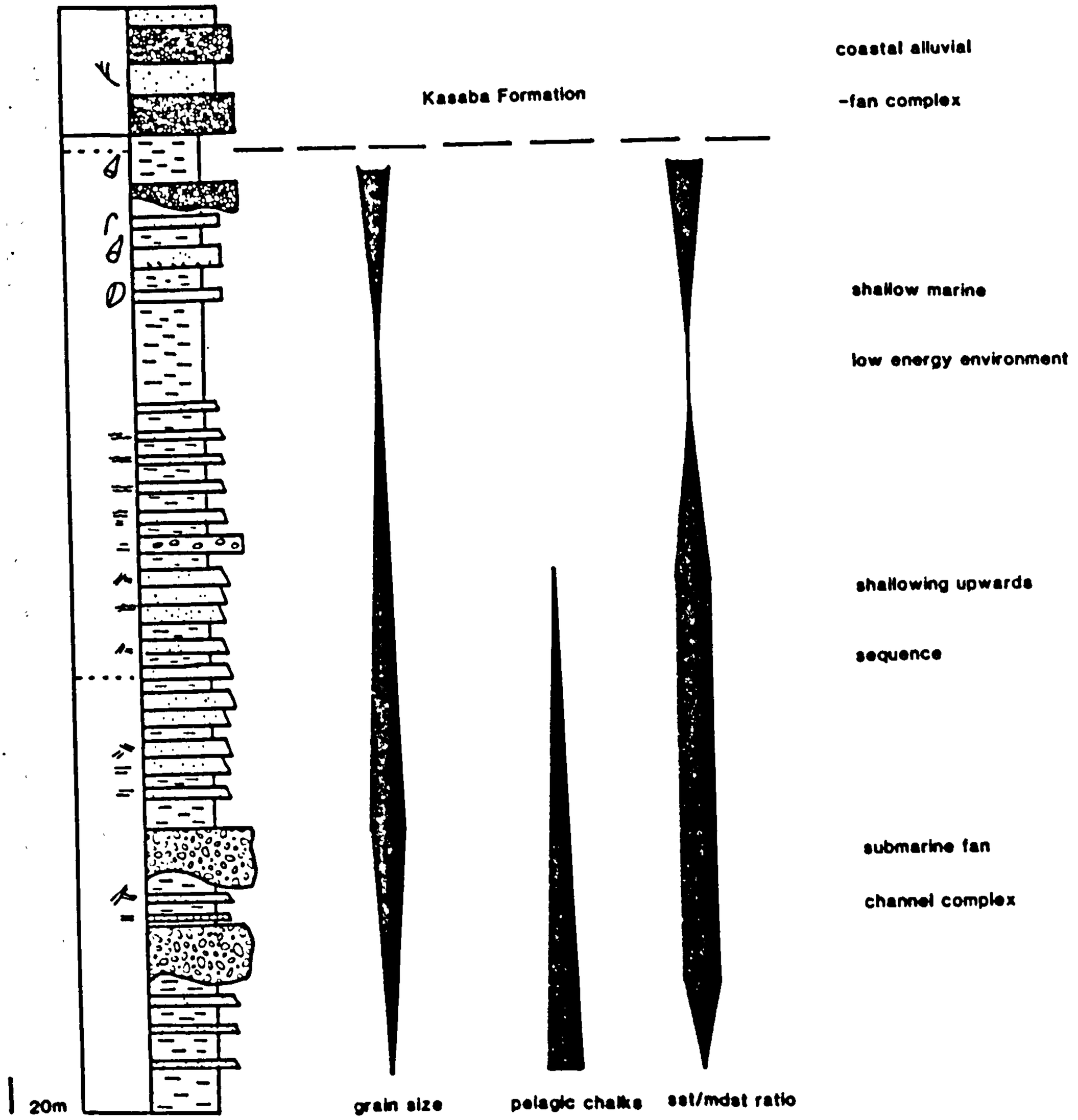

Fig. 4.17

General vertical trends in sedimentary features within the Kemer Formation (Kasaba - Kemer area, see Appendix C for key to sedimentary section).

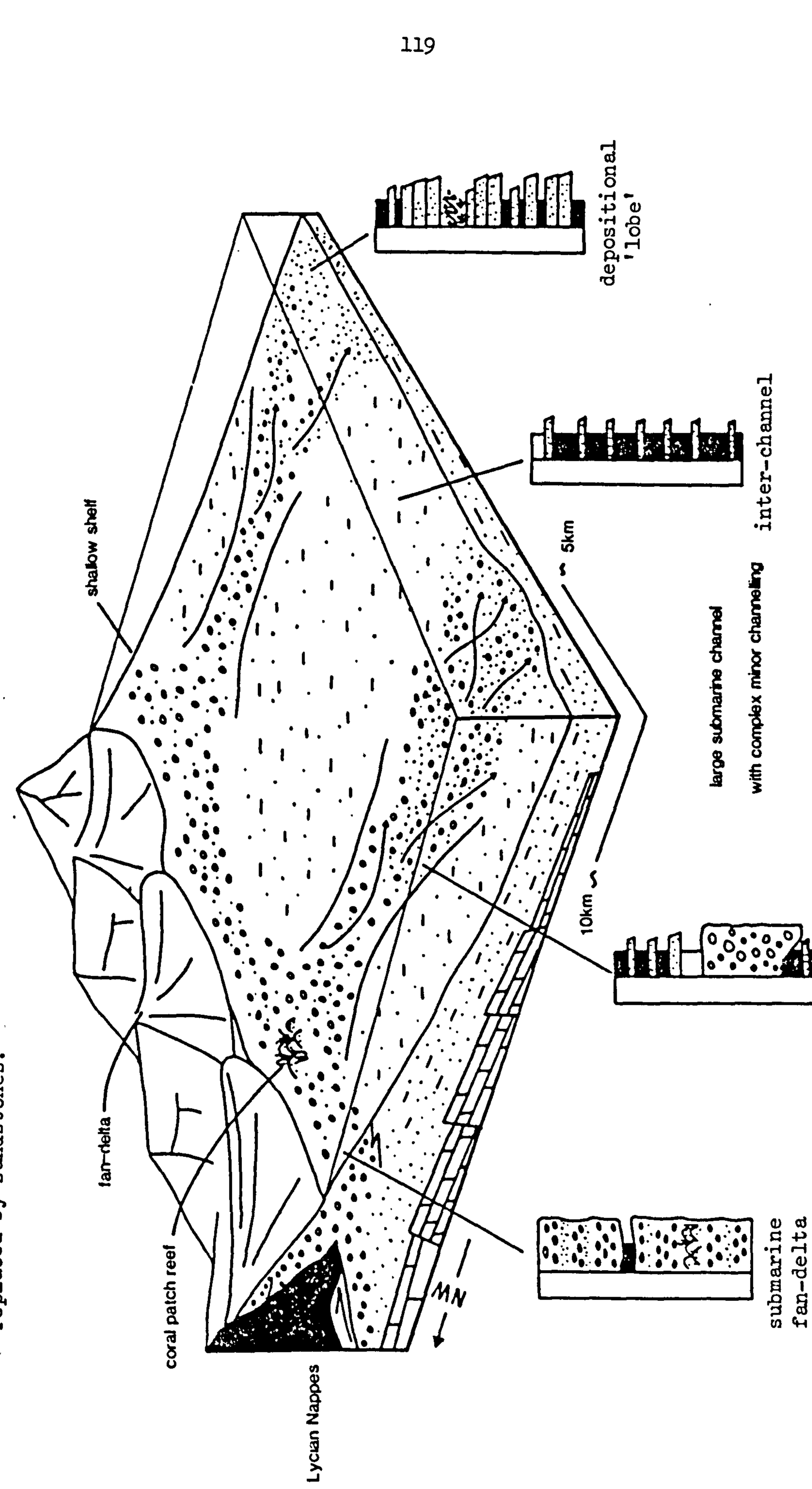

Fig. 4.18 General sedimentological model for the Kemer Formation. Fan-deltas, derived from the Lycian Nappes, pass basinwards into large submarine fan channels. Down channel conglomerates are successively replaced by sandstones.

Rare clast-supported pebble conglomerates are moderate to well sorted, lenticular over 50 m and up to 7 m thick (Fig. 4.16). Bases to units are concave and erosional, thinning- and fining-upwards within units is observed (Fig. 4.16). Interbedded sandstones are medium to fine grained, moderate to well sorted and up to . 25 m thick. Structureless or graded with parallel laminations, they have erosive bases and often contain thick (.10 m) winnowed shell lags. Massive brecciated mudstone which contains an abundant shallow marine fauna (Appendix B) forms greater than 90% of the sequence. Rare (5%), thin (.10 m) calcareous horizons are completely homogeneous.

4.6.1 Interpretation

The graded sandstones with shell lags are comparable to coquinal sands deposited from suspension by decelerating currents produced by storm activity (Johnson, 1978). Mudstone represents predominantly quiet background sedimentation, the presence of abundant fauna suggests a shallow marine environment. Conglomerates were deposited in minor channels cutting through an otherwise muddy, shallow marine sequence. Channel axes are orientated north-south, approximately 90° to the palaeoshoreline, of both the underlying sequence (Kemer Formation) and the overlying sequence (Kasaba Formation). They may be related to rip-currents generated by storm activity or to fluvial channels.

Conglomerates only occur at the top of the sequence, they mark the initial phase of the second pulse of coarse terrigenous clastic sedimentation (see below, 4.7.0).

This sequence clearly represents a continued shallowing-upwards. The absence of coarse terrigenous material in the lower part of the sequence is consistent with a low relief source area.

The transition to the overlying Kasaba Formation occurs abruptly over 20 m, mudstone and sandstone with less than 5% conglomerate horizons are successively replaced by interbedded conglomerate, sandstone and mudstone (Fig. 4.17, see below 4.8.1).

4.7.0 Kasaba Formation

4.7.1 Introduction

The shallow marine (Serravallian) regressive-upwards sequence (above) is overlain by a thick sequence (ca. 350 m) of conglomerates and sandstones, the Kasaba Formation, of Tortonian age (Chapter 2). This represents the second major incursion of coarse terrigenous

clastic sediment along the western margin of the sedimentary basin.

4.7.2 Provenance

Composition. Petrographically the sediments consist of a complete admixture of rock types, (Chapter 6). Clast types in the conglomerate (described in detail in Chapter 6) consist of moderate to well rounded (R2-3) limestone, dolerite, gabbro, chert and subordinate serpentinite and basalt rock fragments. The sandstones are generally poorly sorted; rock fragments again predominate. Serpentinite, chert, dolerite, basalt and subordinate quartz and feldspar are cemented by carbonate (Chapter 6). Bioclastic content ranges from 0%-50%, comprising foraminiferal, algal and shell fragments (Chapter 6).

Palaeocurrents. Cross-stratification in conglomerates and sandstones for most of this formation indicate that palaeocurrents flowed dominantly north to south (Fig. 4.19). Variations related to sedimentary facies are discussed below (4.8.2).

The Kasaba Formation was derived from the Lycian Nappe ophiolitic unit and areas of upfaulted carbonate platform (Chapter 6) to the northwest. The influx of coarse terrigenous clastic material marks the *final* emplacement of the Lycian Nappes onto the carbonate platform (see discussion, 10.2.4).

4.8.0 Sedimentary Facies

The sedimentary sequence can initially be subdivided into sediments deposited in either a continental or marine environment (Fig. 4.20). The continental sediments are characterised by calcretes, dessication cracks and reddened horizons. These are all consistent with subaerial exposure in an arid climate (4.8.3).

4.8.1 Continental Facies Associations

Within the continental sequences two facies associations are recognised:

Conglomerate Facies Association. This consists of laterally extensive poorly sorted reddened conglomerate with subordinate sandstone and red and green mudstone.

The conglomerates which make up more than 80% of the association (Fig. 4.20) comprise poorly to moderately rounded (R1-3, Odell, 1977) pebbles, cobbles and boulders with a maximum clast size of .80-1.30 m.

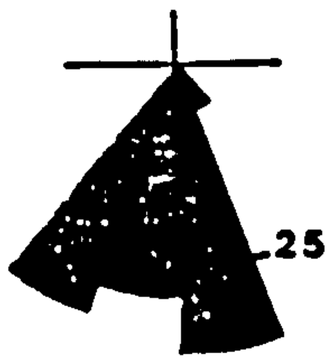

N.16

Proximal
Alluvial Conglomerate

N.38

Distal
Alluvial Conglomerate

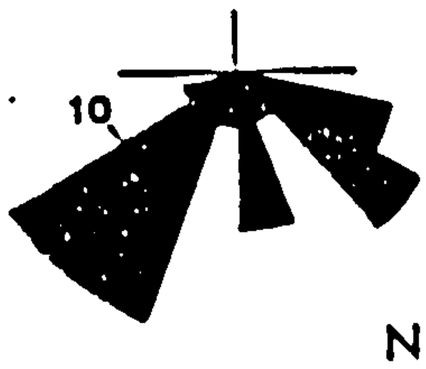

N.24

Distal
Alluvial Sandstone

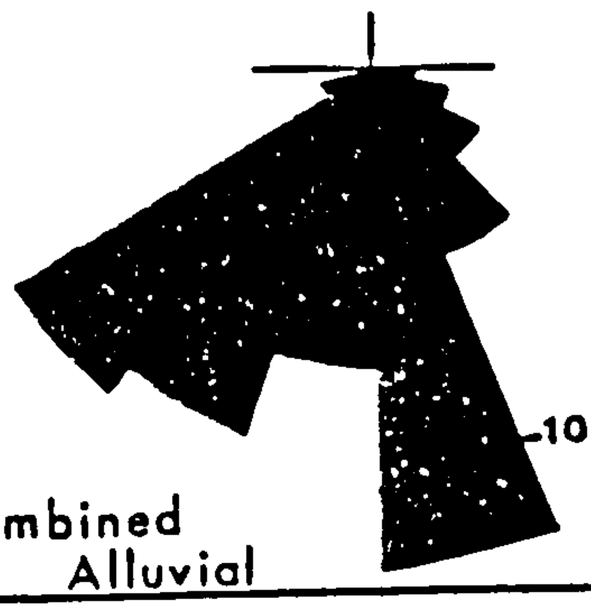

N.74

Combined
Alluvial

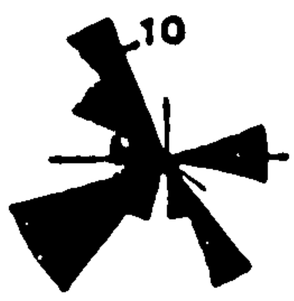

N.23

Marine Sandstone

Fig. 4.19

Palaeocurrent data for the Kasaba Formation.
N = number of readings, 25 = percentage of total readings.
Note consistency in fluvial trends, but wide variation in marine sequence (see text for details).

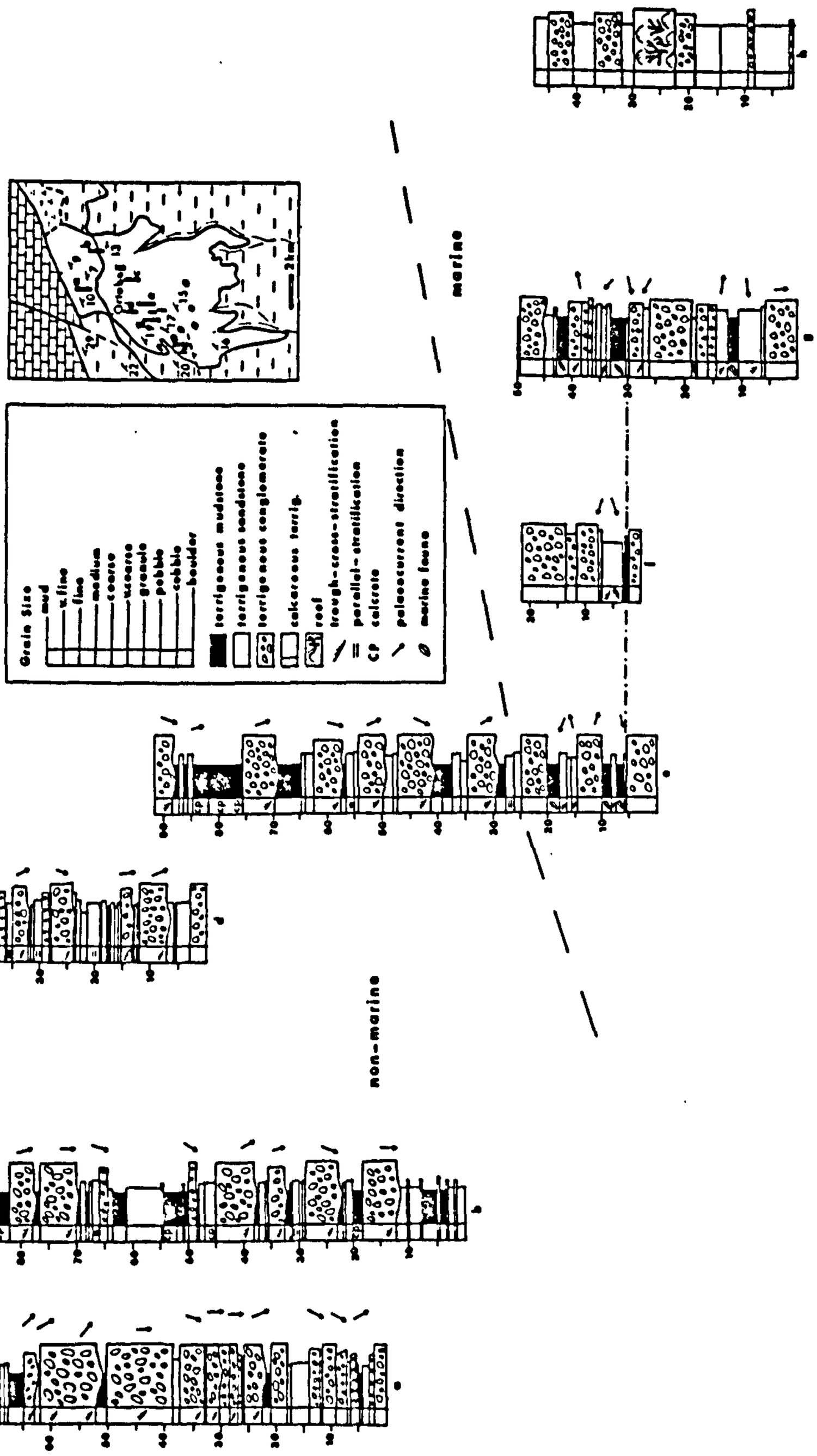

Fig. 4.20 Sedimentological logs measured in the Kasaba Formation. Inset map for loc

The conglomerates are dominantly clast-supported (Gm), although rare (10%) matrix-rich and matrix-supported conglomerates (Gmr) are also present. In the clast-supported conglomerates two facies are recognised: horizontally stratified or massive (Gm) cobble and boulder conglomerate, and volumetrically subordinate trough-cross-stratified (Gt) cobble and boulder conglomerate (3.2.2).

In the former, crude stratification is picked out by variations in the average clast size or by high concentrations of larger clasts. Discontinuous clay, silt and planar-cross-stratified sandstone lenses are commonly interbedded within the conglomerate so that individual depositional events are difficult to delineate.

Trough-cross-stratified units between 0.60 m and 3.0 m thick infill erosive scours, up to 1.5 m deep and 4-5 m across (Fig. 4.21). Upwards and laterally, trough-cross-sets pass into massive conglomerate of similar grain size. Contact imbrication of the clast a-axes normal to flow direction, as determined from associated planar and trough-cross-stratified units, is common.

Subordinate matrix-rich conglomerates (Gmr) which vary between 1.0 and 2.5 m thick, consist of clasts of up to 0.8 m in a silty mudstone matrix. Some beds contain lenticular matrix-supported horizons. Palaeocurrent flow (measured from cross-stratification) was consistently to the south for this facies association (Fig. 4.20).

Interpretation

The high proportion of conglomerate, the clast size and palaeocurrent directions (Fig. 4.19) show that this association is the most proximal.

Reddened horizons within the conglomerates and rare, laterally discontinuous, red siltstone and sandstone horizons are consistent with subaerial oxidation and suggest subaerial deposition in an arid environment.

Bed lenticularity and poor segregation of sand and gravel is consistent with a fluvial origin (Clifton, 1973). The interbedding of debris-flow conglomerates (Gmr) and stream deposited conglomerates (Gm and Gt) is consistent with deposition on an alluvial fan (Bull, 1964, 1972; Wasson, 1977; Rust, 1978; Daily *et al.*, 1980). The low proportion of debris-flow conglomerates precludes deposition on the upper parts of an alluvial fan. Instead this association is interpreted as being the result of dominantly unconfined sheetflood

Fig. 4.21

Conglomerate association (mainly facies Gm) deposited on mid-distal parts of an alluvial fan.
Note thin mudstone horizons (m) and trough-cross-stratified conglomerate (Gt) infilling scours (s).
Face is approximately 8 m high.
Kasaba Formation (Doğantaş Member). GR. 518368.

Fig. 4.22

Nodular calcrete horizon (c) overlying cobble conglomerate (facies Gm). The calcrete is overlain by medium/fine structureless sandstone.
Lens cap is 7 cm in diameter.
Conglomerate-sandstone association deposited on a fluvial braidplain (Kasaba Formation).
GR. 520364.

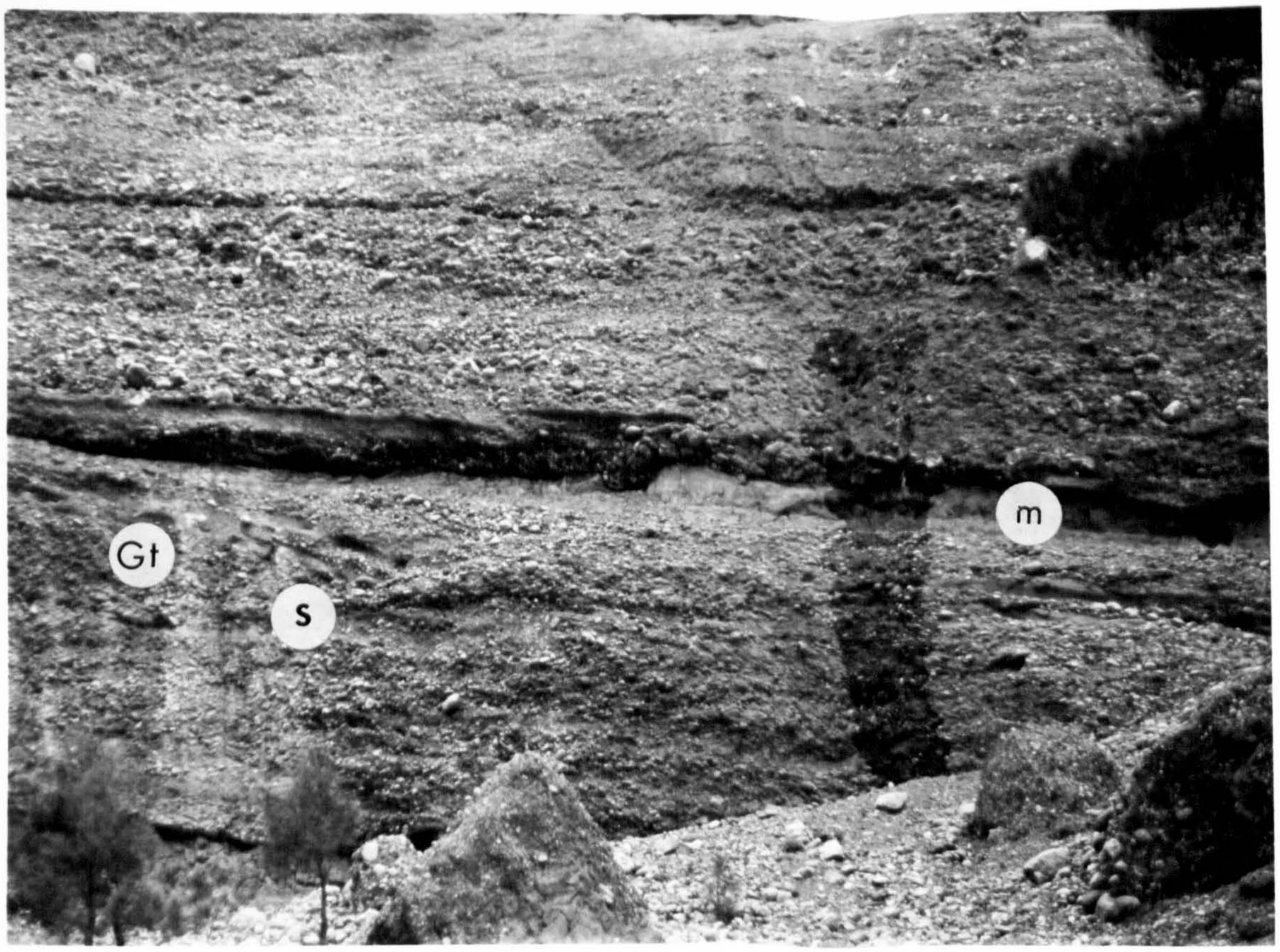
Gt
S
m


C

and channel deposition on the mid to distal parts of an alluvial fan.

Conglomerate-Sandstone Facies Association. This occurs as well defined fining-upward units of the order of 15-20 m thick, (Figs. 4.23, 4.24). Trough-cross-stratified conglomerate (Gt) at the base of a unit infills scours up to 1.5 m deep and 5-7 m across (Figs. 4.23, 4.24). This passes laterally and vertically into massive conglomerate (Gm) of a similar grain size. Maximum clast size varies up to 0.90 m but is commonly 15-35 cm. Within the massive conglomerate clay, silt, cross-stratified sandstone and planar- and trough-cross-stratified conglomerate occur as discontinuous lenses.

The conglomerates form units with an average thickness of 7 m (approximately half of the actual thickness of a complete fining-upwards succession). They occur as laterally continuous sheets over 3-400 m, with irregularly scoured erosional bases. On a scale of several hundred metres bases parallel the underlying sediments (Fig. 4.23). Conglomerates make up less than 50% of the succession (Fig. 4.20, 4.26). Palaeocurrent flow measured from trough-cross-strata in the conglomerate is consistently south-southwest (Fig. 4.19), essentially the same as the proximal deposits.

Two types of fining-upward units can be distinguished (Fig. 4.25). In the majority of the cycles (70%) the conglomerates are overlain by either fine to medium massive (Sm), parallel-stratified (Sl) and low angle cross-stratified sandstone (SL), or directly by calcrete. Red to brown, medium to fine grained, massive and parallel-laminated sandstones pass upwards and laterally into massive (Mm) red and green siltstones and claystones with silt laminae and rare pebble conglomerate horizons (up to 60 cm thick).

Calcretes (Cp) form laterally continuous nodular horizons (Fig. 4.22), 5-15 cm thick, in which very fine sand and silt sized terrigenous grains are dispersed in a micrite matrix. Dessication cracks are associated with calcretes.

In the second cycle type, conglomerates are overlain, and are transitional to, granule conglomerate and very coarse sandstone (Fig. 4.25). Red to brown, poorly sorted granule conglomerate and coarse sandstone form trough-cross-stratified units (Gt, St) comprising shallow troughs, commonly 10-20 cm thick. They are in many places interbedded with, and pass laterally into, parallel stratified (Sl) and rarely planar-cross-stratified (Sp) coarse to medium grained

Fig. 4.23

Conglomerate-sandstone association deposited on a fluvial braidplain.
Section is parallel to inferred palaeoflow direction (flow was left to right).
Trough-cross-stratified conglomerage infills large scoop-shaped scours (Δ) at base of each fining-upward unit.
Note well developed fining-upward cycles and high proportion of fine grained sandstone and mudstone deposited in overbank areas. Thickest conglomerate unit is approximately 5 m thick.
Kasaba Formation (Doğantaş Member). GR. 520355.

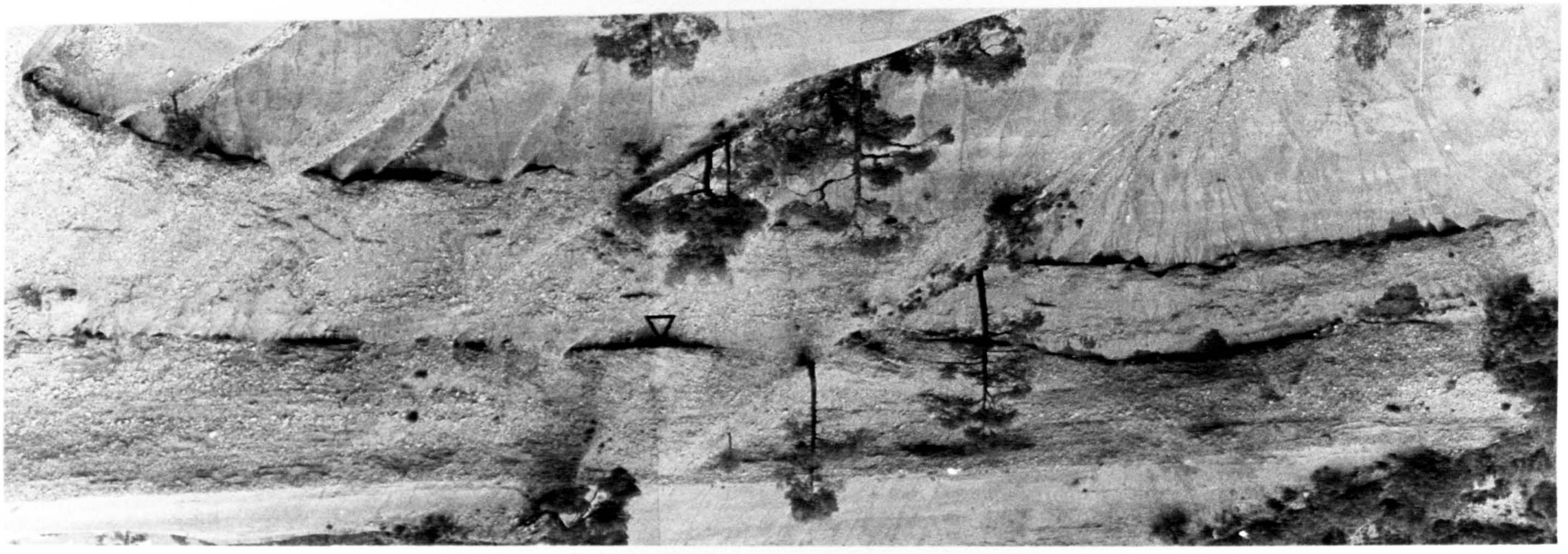

Fig. 4.24

Conglomerate-sandstone association section transverse to inferred flow direction.
Note presence of three well developed fining-upward cycles and
scoop shaped scour-fills at base of conglomerate units (s).
Fine grained sediments deposited in overbank areas comprise structureless
sandstone, mudstone and calcrete horizons (Δ).
Kasaba Formation (Doğantaş Member). GR 520355.

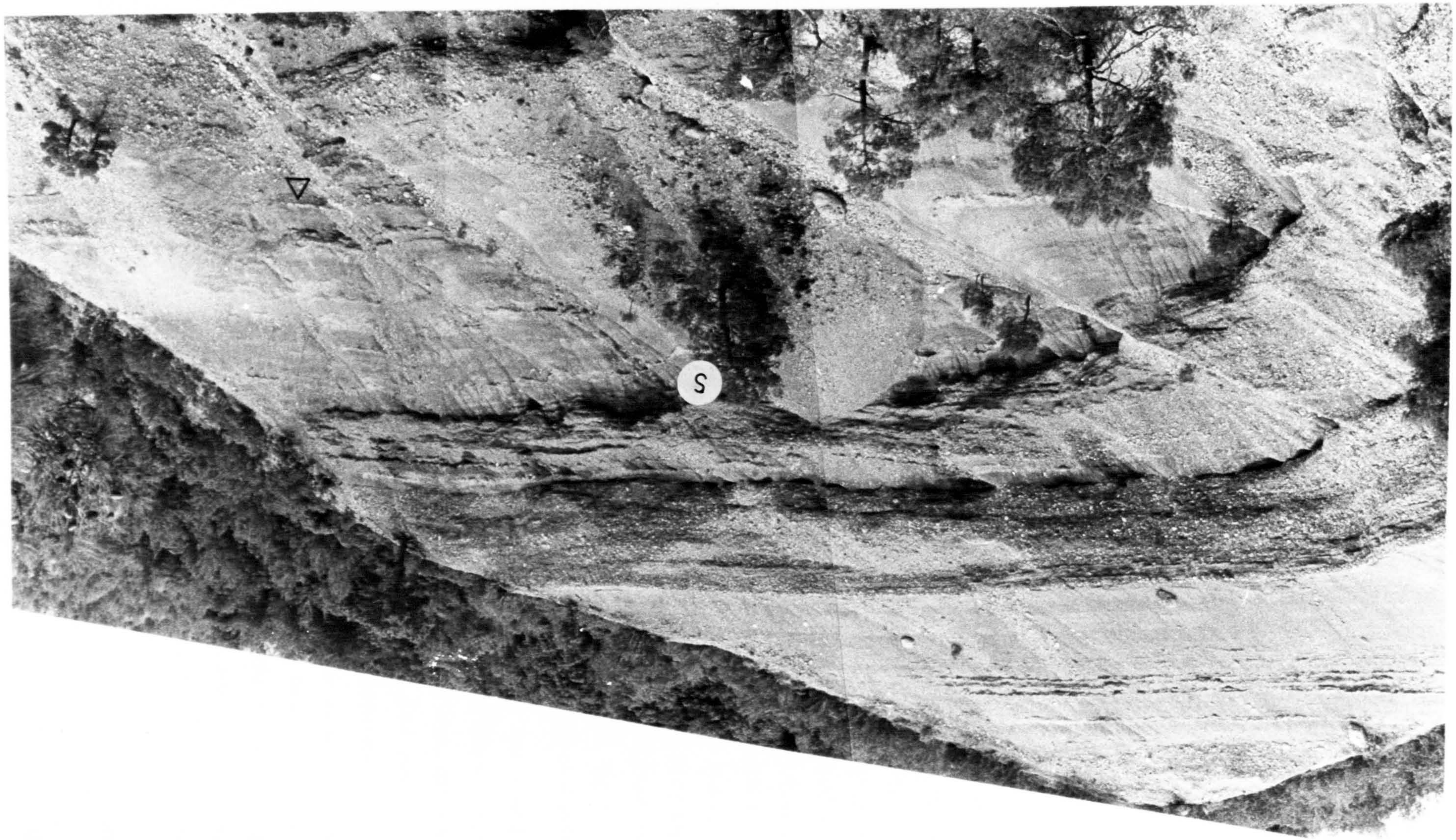
S

sandstone. Planar cross-sets are 10-15 cm thick and dip at shallow (5-10°) angles. The palaeocurrent trends for these sandstones (Fig. 4.19) are consistently southwards, with slight divergence to the SE and SW.

The coarse sandstone passes upwards into fine to medium, moderately to poorly sorted, red and brown, massive and parallel-stratified sandstone and rarely ripple-laminated sandstone (Sr). Occasional trough-cross-stratified sandstone, with mudstone rip-up clasts, display low-angle trough-sets less than 10 cm thick. Palaeocurrent trends are similar to those of the coarse sandstone.

Sandstones of this type are interbedded with, and pass upwards into, red and green claystone with discontinuous siltstone and rare conglomerate horizons. A preferred facies transition diagram for this association (Fig. 4.2.6) emphasises the cyclic nature of deposition.

Interpretation

The conglomerate-sandstone facies association contrasts with the conglomerate association in the well developed internal organisation exhibited by the fining-upward cycles (Figs. 4.23, 4.24 and 4.25). Subaerial exposure is indicated by the occurrence of calcrete and reddened mudstone horizons. The palaeocurrent orientations and the lower mean clast size are all consistent with this association being a distal equivalent of the conglomerate association.

The conglomerates which form the base of individual fining-upward units are related to depositional processes similar to those of the conglomerate association. Trough-cross-stratified, clast-supported conglomerate that occurs infilling scours above a sharp erosional surface (Fig. 4.23) at the base of conglomerate units are the result of scour and channel-fill. Laterally discontinuous trough-sets within conglomerate units are the deposits of migrating bedforms within channels formed at high flood-stage (3.2.5) (Martini, 1977; Rust, 1978).

Trough-cross-stratified conglomerate in all cases passes transitionally into massive conglomerate, suggesting that most of this fluvial conglomerate was transported as diffuse sheets or within low relief bedforms (Smith, 1974; Eynon and Walker, 1974; Hein and Walker, 1977). By analogy with modern braided fluvial

systems, massive conglomerate probably accreted as planar sheets in the form of longitudinal bars during high flood-stage (3.2.4).

In some instances (Fig. 4.25) trough-cross-stratified conglomerates pass upwards through massive conglomerate into trough-cross-stratified and low-angle cross-stratified coarse sandstone, parallel-stratified sandstone and finally into fine sandstone, mudstone and calcrete.

Trough-cross-stratified sandstones are interpreted as dunes formed under low flow-regime conditions (Harms and Fahnestock, 1965) (3.2.8). Low-angle cross-stratified and horizontally stratified sandstones are formed respectively as very shallow scour fills (Miall, 1977) and as plane-beds formed under low-flow regime conditions (Harms and Fahnestock, 1965; Harms *et al.*, 1975) (3.2.9, 3.2.10). This sequence is the result of waning flood and the shallowing of water over actively accreting bars (Williams and Rust, 1969; Miall, 1977, 1978). Mud and fine sand are deposited as the area becomes inactive. Pedogenic calcretes develop as a result of subaerial exposure.

The calcretes which directly overly conglomerates are evidence of a depositional break, prior to deposition of the overlying sandstone, mudstone and calcrete couplets. The red and green mudstone and sandstone are characterised by their fine grain size, lack of current structures, or only occasional small isolated ripples and rare bioturbation. All these features are consistent with deposition in standing water away from the active area of sedimentation.

The sudden change from conglomerate to mudstone is interpreted as the result of a rapid decline in velocity from high flood-stage and an associated fall in water level. The active area of sedimentation becomes localised down the sides of accreted bars, exposing bar tops and marginal terraces subaerially. Deposition in the inactive areas is primarily by the vertical accretion of fine sediment (Williams and Rust, 1969; Rust, 1979) and washover from the active channel area. In humid regions extensive vegetation develops in this area (Williams and Rust, 1969; Miall, 1977; Boothroyd and Ashley, 1975). In arid regions reddened oxidised horizons and calcretes are formed (Allen, 1965; Rust, 1978). In flood minor channels may transport sand and gravel across the inactive area

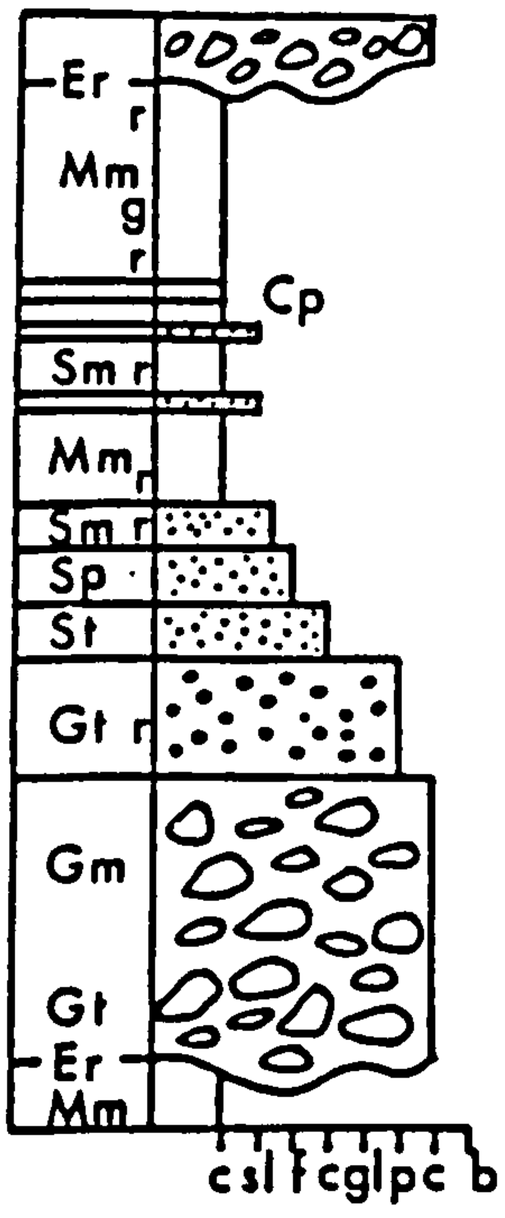

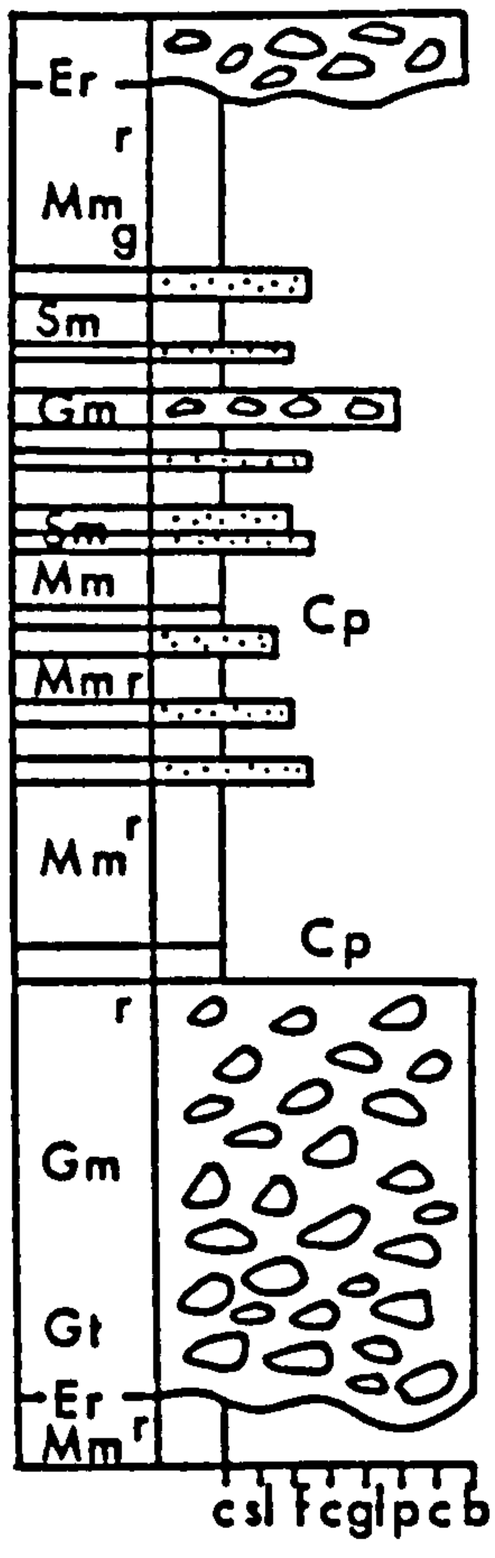

Gm massive conglomerate
Gt trough-cross-strat. cgl.
Sp parallel-strat. sst.
St trough-cross-strat sst.
Sm massive sandstone
Mm massive mudstone
Cp calcrete
Er erosion surface
r red
g green

2m

Fig. 4.25
Generalised sections showing the two types of fining-upward cycles distinguished in the Kasaba Formation (Dogantas Member) conglomerate-sandstone (fluvial braidplain) association

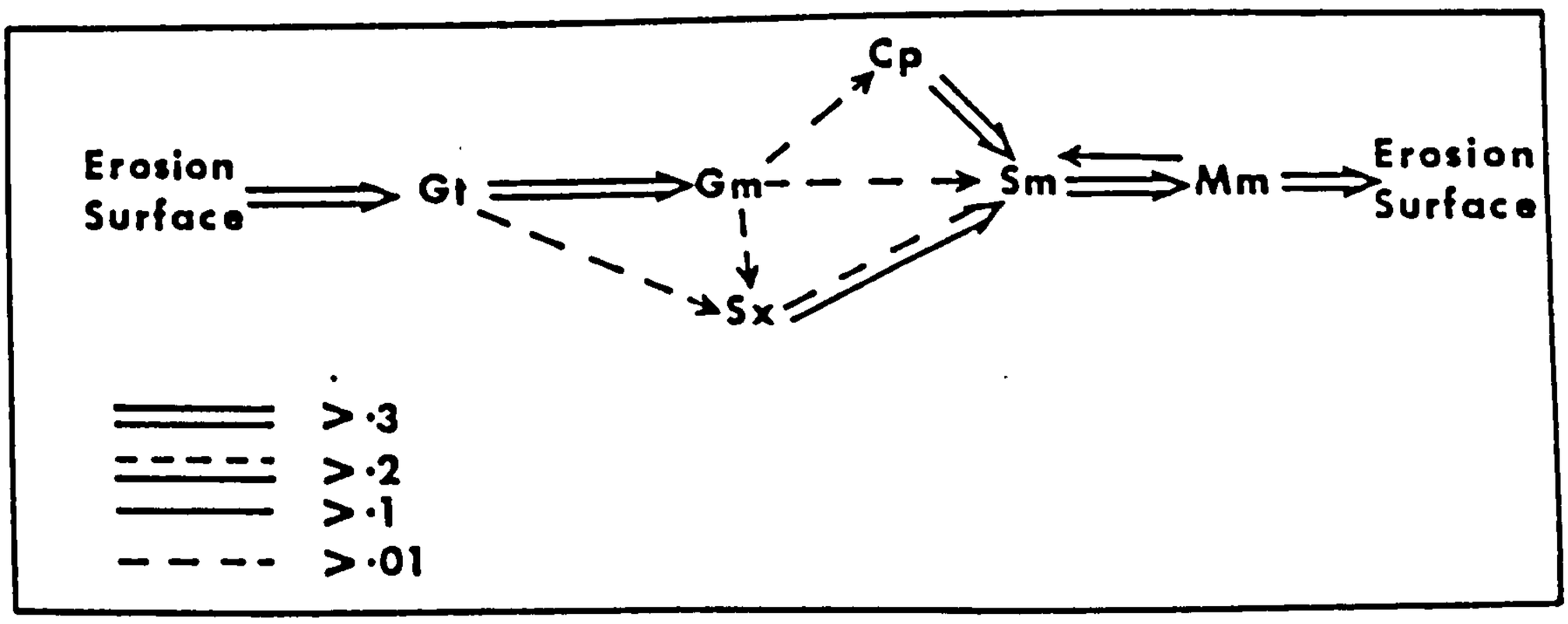

Fig. 4.26
Preferred facies transitions for conglomerate-sandstone (fluvial braidplain) association. Calculated from 188 transitions (method of Walker, 1979a).

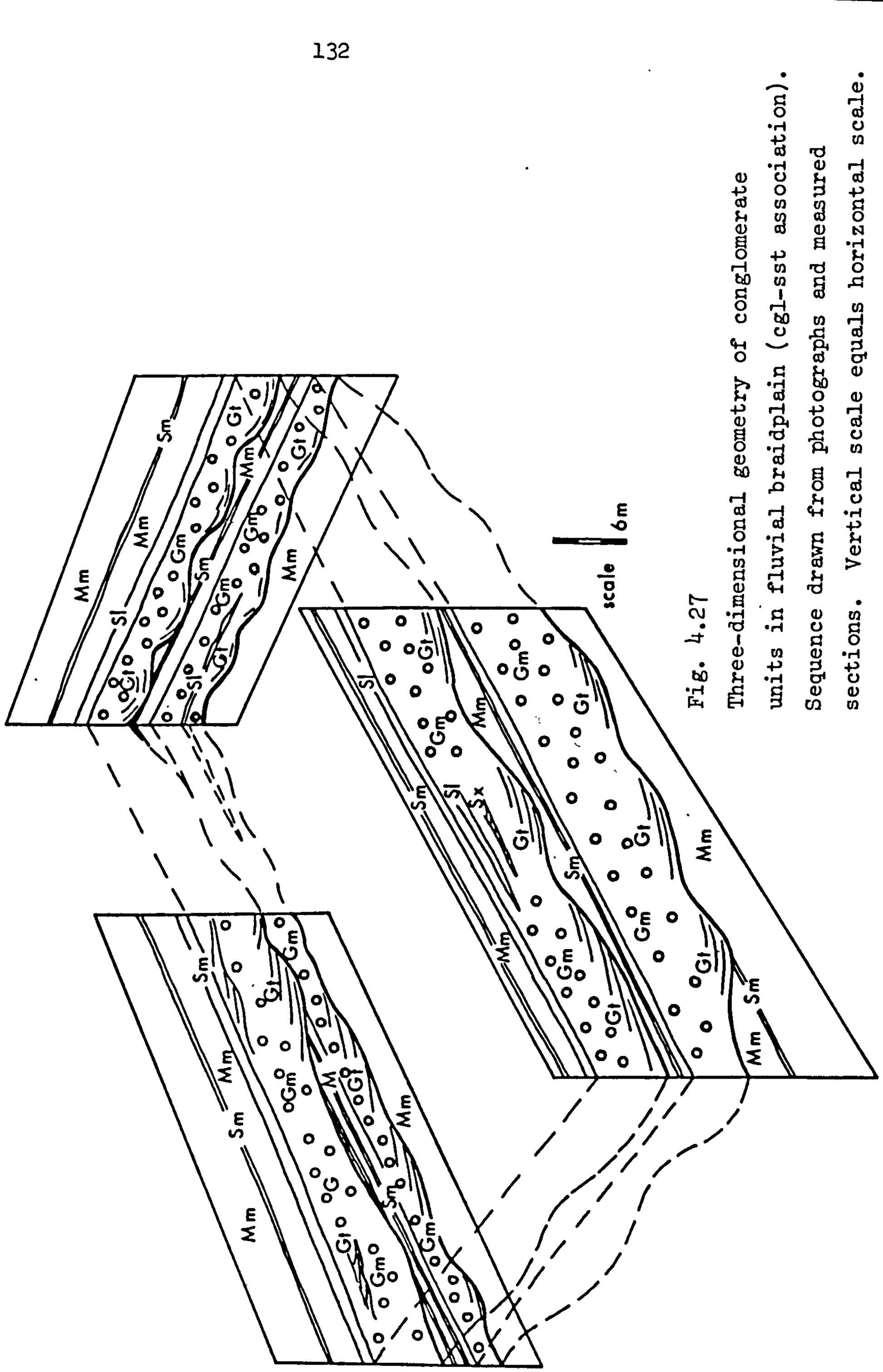

Fig. 4.27
Three-dimensional geometry of conglomerate units in fluvial braidplain (cgl-sst association). Sequence drawn from photographs and measured sections. Vertical scale equals horizontal scale.

(Rust, 1979) producing thin sand and conglomerate lags within the mudstone sequence (Fig. 4.25).

Superficially this association resembles the middle reaches of the Donjek river in Alaska, chosen by Miall (1977) as the modern type example of a distal gravelly braided fluvial system. Similar sequences have also been described by Rust (1979) from the Carboniferous of eastern Quebec. This interpretation is consistent with the depositional environment proposed here. However, a major difference is the proportion of 'active area sediments' (conglomerate and coarse sandstone) to 'overbank sediments' (mudstone, fine sandstone, calcrete). Vertical sequence models in the literature (Miall, 1977, 1978; Rust, 1978, 1979) commonly show proportions of greater than 90% active area sediments (cf 50% in this case). Exceptions to this have been documented by McLean and Jerzkiewicz (1978) and Friend (1978), (see below).

In summary, this association was deposited down palaeoslope from the distal alluvial fan sequence (conglomerate association) on a fluvial braid-plain.

4.8.2 Marine Facies Associations

This comprises interbedded conglomerate, sandstone and mudstone, with an abundant marine fauna, and small coral patch-reefs (Chapter 8). Within this spectrum of deposits two sequence types are distinguished.

In proximal areas (Fig. 4.20) mudstones (Mm) are interbedded with conglomerate (G) and sandstone (ST) forming units between 10 and 15 m thick. To the south (Fig. 4.20) mudstone is absent or subordinate, and conglomerate and sandstone are interbedded with small patch-reefs.

Dark green to buff pebble, cobble and boulder conglomerates have a maximum clast size of 0.50 cm. Bedforms within the conglomerates are rare; where present they consist of poorly defined low-angle ($5-7^{\circ}$) cross-stratification with a set height of 1.0 m. Palaeocurrents are consistent with fluvial trends. However, the conglomerates are generally structureless with non-erosive bases parallel to the underlying sediment, and a random orientation of the clast a-axes (Fig. 4.28).

Green to grey, moderately to well sorted trough-cross-stratified and parallel-stratified sandstone and granule conglomerate comprise

Fig. 4.28

Proximal marine facies association comprising interbedded conglomerate (G), sandstone (ST) and mudstone (Mm) with an abundant *in situ* marine fauna of gastropods and bivalves. In the conglomerate horizon note the poor sorting, absence of sedimentary structures and non-erosive bases parallel to the underlying sediment. Prominent horizon (p) is a well cemented medium grained sandstone.
Kasaba Formation. GR. 505341.
Labelled conglomerate is approximately 5 m thick.


P
ST
G
Mm

up to 20% of this association (Fig. 4.20, sections e, f, g). The trough-cross-sets are 20-30 cm thick. Palaeocurrent trends measured from cross-stratification, and rare primary current lineations show a wide scatter (Fig. 4.19). Burrows within the sandstones consist of U-shaped or vertical tubes which penetrate the top of individual sandstone beds to a depth of 10 cm (Fig. 4.29).

Massive and laminated, dark grey calcareous mudstones form up to 10% of the association (Fig. 4.20, sections e, f, g). The mudstones are burrowed and contain a marine fauna of dominantly bivalves (*Lutraria ablonga, Venus basteroti*) and gastropods (*Turritella tarris, Bursa marginata*) (see also Appendix B).

Southwards, where mudstone is subordinate or absent (Fig. 4.20, section g), interbedded patch-reefs occur on depositional slopes of up to 5°. The patch-reefs described in detail in Chapter 8, consist of a central framework, up to 8 m high and 15-20 m across, composed of *in situ* corals against which is banked reef talus breccia that interfingers with the surrounding coarse grained terrigenous sediment. The latter comprises of interstratified pebble-cobble horizons (Gst), 25-40 cm thick, and coarse sandstone-pebble horizons 40-60 cm thick. The matrix is generally coarse to very coarse sandstone.

Interpretation

An abundant marine macrofauna of gastropods and bivalves, and small patch-reefs indicate that this sequence was deposited in a fully marine environment.

Conglomerates in the nearshore zone (Fig. 4.20, sections e, f, g) show no evidence of being reworked by marine processes.. Rare low-angle cross-stratification is consistent with fluvial trends. The general lack of structure within the conglomerates suggests that they were deposited as poorly sorted sheets by fluvial channels entering a shallow sea.

Offshore, fine conglomerates and coarse sandstones (Gst) which occur in association with patch-reefs, are indicative of reworking by wave processes (Clifton, 1973) (3.3.2).

Trough-cross-stratified coarse sandstone and granule conglomerate have widely scattered palaeocurrent orientations (Fig. 4.19) which differ from fluvial trends. These trends may result from the action of onshore waves which are known to form lunate mega-ripples in the outer rough zone of shorefaces at the present day (Clifton *et al.*, 1971) (3.3.4).

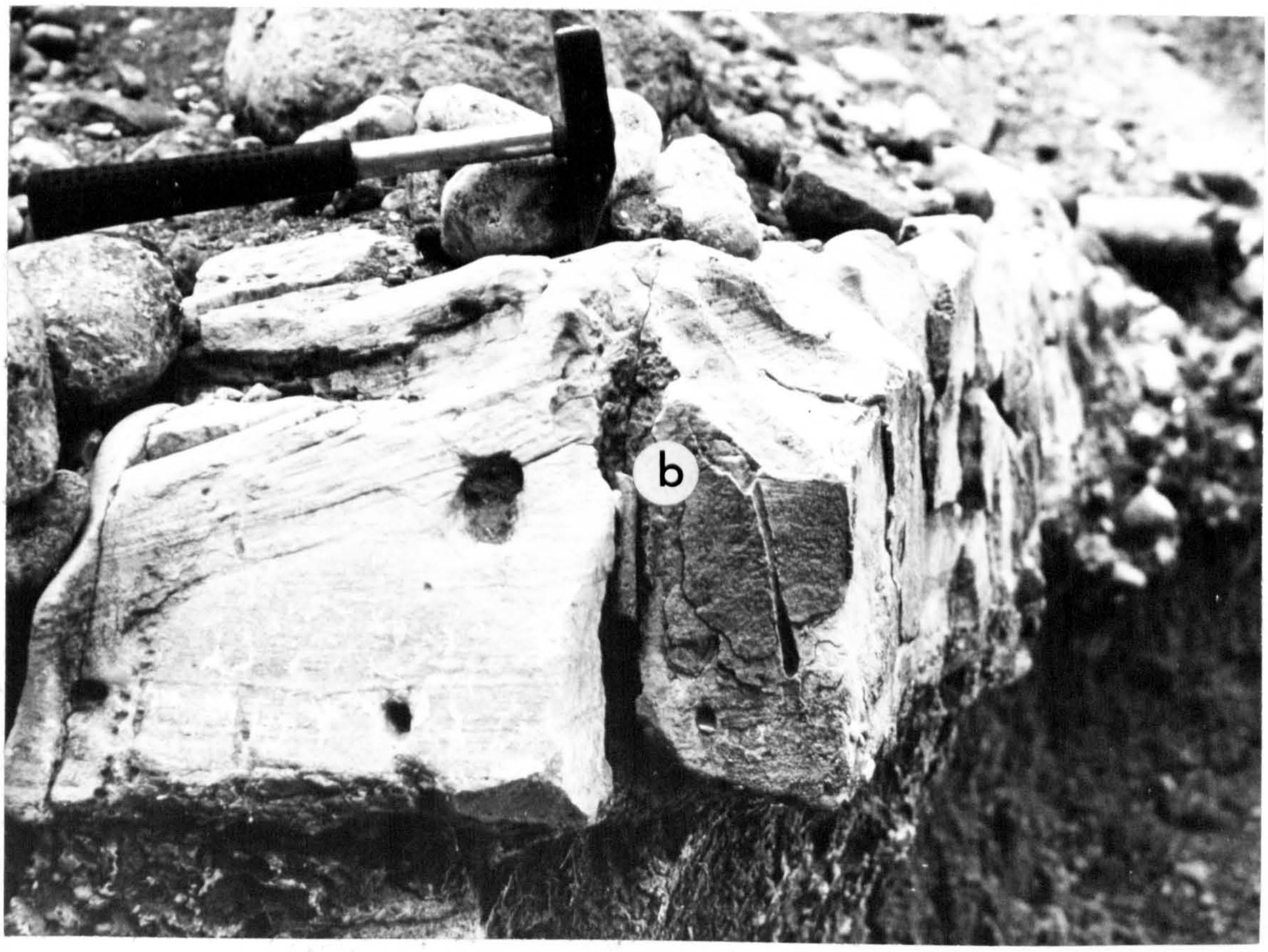

Fig. 4.29

Well sorted trough-cross-stratified sandstone marine facies association (Kasaba Formation).
Note vertical burrows (b) in upper parts of bed.
Deposition was probably by onshore wave action.
GR. 502334.

The paucity of stratification, absence of bipolar cross-stratification and ripples generally considered indicative of tidal currents (Johnson, 1978) suggests that the shoreline was not subject to strong tidal influence. The sporadic occurrence of sedimentary structures indicating marine reworking may suggest that most reworked beds formed when storms augmented normal marine processes (Sellwood, 1972).

In summary, the marine sequence was deposited in a shallow partially enclosed micro-tidal sea. Patch-reefs developed parallel to the shoreline protecting the nearshore and shoreface from extensive reworking by wave processes. Offshore marine processes reworked sand and fine conglomerate.

4.8.3 Upper Miocene Palaeoclimate

Several lines of evidence are used to indicate the palaeoclimate during deposition of the Kasaba Formation.

Calcrete. Calcrete palaeosols occur within the sedimentary sequence (Fig. 4.22). They develop at the present day in hot or semi-arid regions with a mean annual precipitation of less than 500 mm/yr (Goudie, 1973; Reeves, 1970; Watts, 1981). They are best developed in areas of highly seasonal precipitation (Goudie, 1973). Associated red beds are consistent with, but not indicative of, a semi-arid climate (Van Houten, 1973; Turner, 1981) (6.2.6).

Reefs. Coral reefs of the type present in the Kasaba Formation (Chapter 8) are only developed in subtropical and tropical regions at the present day. In these areas surface water temperature is between 18°C and 29°C (Clarkson, 1979).

The Upper Miocene palaeoclimate was semi-arid, developed in the sub-tropical belt with a highly seasonal precipitation.

4.9 General Model : Summary

There is clear evidence of a N-S palaeoslope, as indicated by:

(1) The general decrease in maximum clast size from north to south (Fig. 4.20);

(2) The overall palaeocurrent trend which is uniformly to the south for the non-marine sequences (Fig. 4.19);

(3) The increasing marine influence seen in the sediments from north to south.

Facies associations and downslope transitions indicate deposition on an alluvial fan passing through a fluvial braidplain into a shallow sea. The general model is shown in Fig. 4.30.

The alluvial fan (conglomerate association) with no internal organisation passes over a distance of approximately 2 km (Fig. 4.30) downslope into a sequence with good internal organisation (conglomerate-sandstone association) (Fig. 4.23). In this association fining-upward cycles are characterised by conglomerate units that are laterally continuous up to 400 m down palaeoslope and thick overbank deposits.

This association extends for 3 km down palaeoslope before passing into a shallow marine environment (marine association). The transition zone lacks features such as strand lines or low-angle seaward-dipping imbrication in conglomerates, normally associated with beach environments (Cailleaux, 1945; Bluck, 1967). This is taken to indicate a low energy, probably micro-tidal, marine environment.

The development of patch-reefs parallel to the shoreline partially protected the shoreface from marine processes. The immediate nearshore zone is characterised by very strong fluvial influence, the conglomerates showing no evidence of marine reworking. The lack of large scale cross-stratification typically produced when fluvial currents of high velocity expand into standing water (Rust, 1975; Jopling, 1965) probably indicates that the shoreface and offshore slope was shallow. Offshore, marine processes were more dominant.

Palaeocurrents (Fig. 4.19) in the sandstones of the marine sequence show a wide scatter in marked contrast to the fluvial sequence. This is possibly the result of storm induced currents which are unlikely to be consistently from one direction.

The association of alluvial fans passing directly into a standing body of water has been termed a fan-delta (Gilbert, 1890; Holmes, 1965; Sneh, 1979; Wescott and Ethridge, 1980). For many sequences of this type, the term 'delta' is misleading as terrestial relief is the major control on sedimentation and the fans frequently show no clear relationship to sea base level. In many Recent examples (e.g. Red Sea, Hayward, 1981) there is no break in slope at the sea level line and geomorphic areas of the 'delta' (delta top

Fig. 4.30

General sedimentary model for the Kasaba Formation, showing lateral and vertical sedimentary facies variations.

(a) Down fan change in vertical sequences from alluvial fan - braidplain - nearshore marine - offshore marine.

(b) Interdigitation of the three facies associations, alluvial fan passes downslope into a fluvial braidplain sequence and then into a shallow marine sequence.

(c) 3-D model for the Kasaba Formation. Alluvial fans prograde over a fluvial braidplain into a shallow sea. During periods of low sediment supply patchreefs develop on the submarine toes of the alluvial fan.

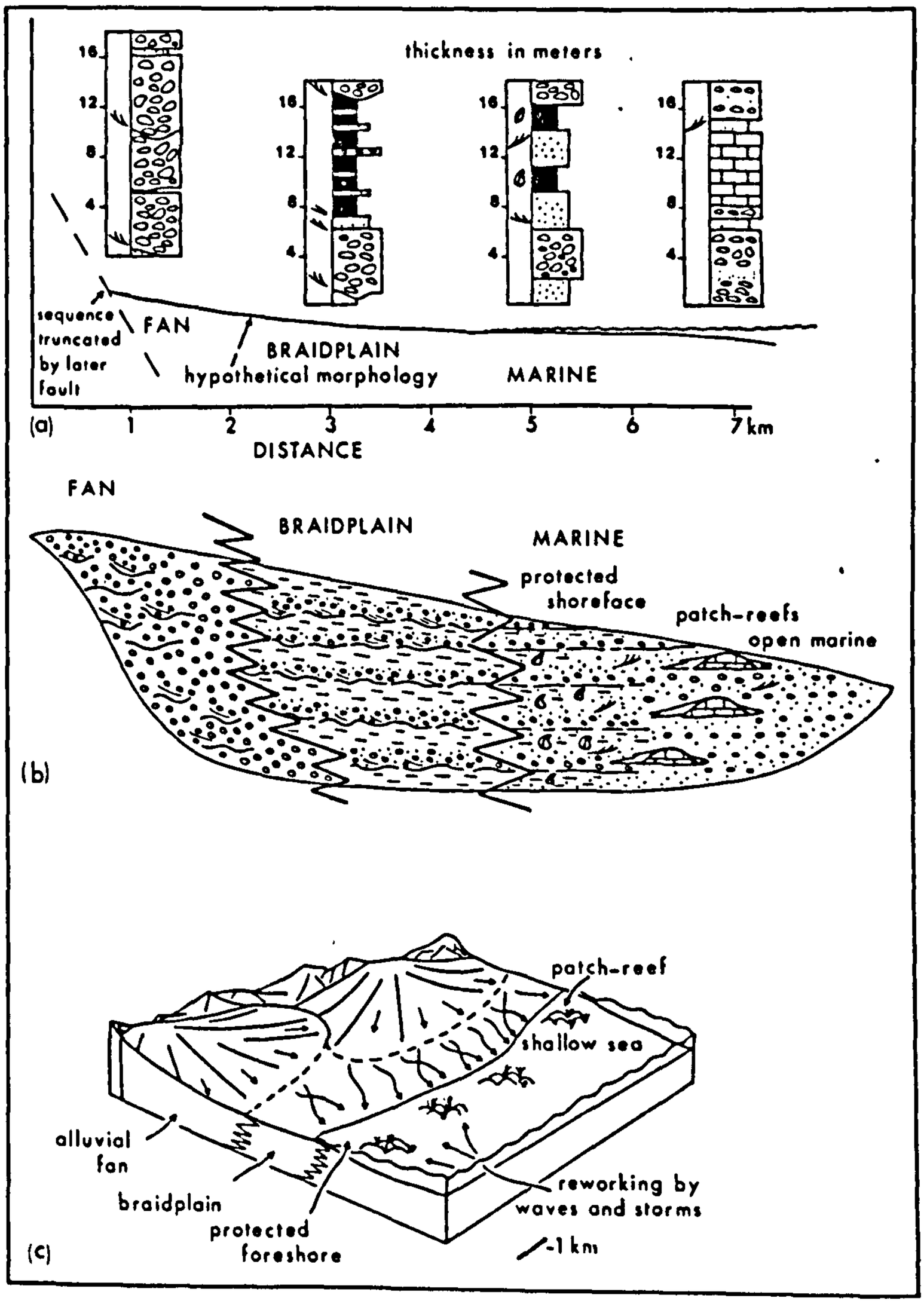
thickness in meters
16
12
8
4
sequence truncated by later fault
FAN
BRAIDPLAIN
hypothetical morphology
MARINE
(a)
1
2
3
4
5
6
7 km
DISTANCE
FAN
BRAIDPLAIN
MARINE
protected shoreface
patch-reefs
open marine
(b)
patch-reef
shallow sea
alluvial fan
braidplain
protected foreshore
reworking by waves and storms
~1 km
(c)

Fig. 4.30

front, etc.) cannot be recognised. Moreover, as in the present case, the submerged parts frequently show little or no evidence of modification by marine processes. In sequences such as the one described here the term coastal alluvial fan is preferable (see also sequences described by Daily *et al.*, 1980); although in many ancient sequences subaerial parts of the fan are only poorly exposed or preserved, geometry and downslope transitions cannot be determined and the general term fan-delta is justified. Fan-deltas are best developed where a high relief area adjacent to the coastal zone is drained by short high-gradient streams that remain braided to the coast (Wescott and Ethridge, 1980). The streams generally drain a small area and have the ability to transport bedload sand and gravel at some time in the year.

The facies association described is relatively rare in the geological record, although occurrences have been described by Dabrio (1975) from the Miocene of Spain, Howell and Link (1979) from the Eocene of S. California, Daily *et al.* (1980) from the Cambrian of S. Australia, and Ricci Lucchi (1981) from the Pliocene of Italy.

4.10 Modern Analogues

Modern analogues of this environment are the braided outwash fans, described by Boothroyd and Ashley (1975), and Boothroyd and Nummedal (1978) from Alaska and the Yallahs 'fan-delta' on the island of Jamaica (Wescott and Ethridge, 1980). Both of these occur in humid environments.

In the Alaskan examples a comparable down-fan transition, between upper- and mid-fan (here termed fan and braidplain), is seen in the vertical sedimentary sequences of the active tract sediments (Boothroyd and Ashley, 1975, Fig. 25), as is observed in the present study (Fig. 4.30), although in this case the braidplain only extended 2-3 km from the base of the alluvial fan (Fig. 4.30) before reaching the coastline, compared with the 15 km of the Alaskan fans. In the latter a complete braidplain succession is developed, gravel fluvial deposits passing downslope into sandy fluvial deposits before reaching the coastline.

Probably the best modern analogue of this sequence in terms of both fan size and climate are the alluvial fans that pass directly into the sea along the Gulf of Aqaba and the Red Sea (Friedman and Sanders, 1978; Gwirtzman and Buchbinder, 1978; Hayward, 1981). Here

alluvial fans and braided fluvial systems drain over a coastal plain which varies in width between 1 km and 7 km. In particular, the Ras Antatur area of the Gulf of Elat (Gwirtzman and Buchbinder, 1978) includes an alluvial fan that passes downslope into a braidplain with a regional dip between 0.5° and 1°; this passes directly into the sea with the development of a large fringing reef and associated patch-reefs along the seaward margin.

4.11 Discussion of Cyclicity within the Fluvial Sequence

Models explaining cyclicity and vertical sequences in alluvial sediments have been the subject of much study in recent years (Beerbower, 1964; Allen, 1964, 1965, 1974b, 1978; Miall, 1977, 1978; Friend, 1978; Leeder, 1978; Rust, 1978; Bridge and Leeder, 1979). The major controls, significance and types of both modern and ancient alluvial sequences are still not fully understood.

Cyclic alluvial sequences occur as a result of mechanisms that can be placed in two broad categories (Beerbower, 1964).

Autocyclic mechanisms require no net change in the total energy and sediment input into a sedimentary system, but simply the redistribution of energy within the system. Examples of this are channel migration, avulsion, crevassing and subsidence due to compaction. Over time, provided no external control is exerted on the system, this will result in equilibrium being approached (Leopold and Wolman, 1957). The cause and effect of this type of cycle have been discussed extensively by Allen (1978) and Bridge and Leeder (1980), who use a computer model to predict vertical sequences developed from a number of stated autocyclic variables. Cycles resulting from autocyclic processes are generally developed on the scale of ten to several tens of metres in thickness. Equivalent cycles are termed "sequences" by Heward (1978a).

Allocyclic mechanisms require a change in the total energy input into the sedimentary system; the sedimentary system is subject to one or more external forces. These can include eustatic variations in sea level, climatic changes, and tectonic controls such as irregular elevation of the source area and spasmodic depression of the basin. Cycles of this type are generally developed on the scale of several hundred metres. They are comparable to the mega-sequences of Heward (1978a).

The fluvial succession described here shows small scale

fining-upward cycles that are comparable with those produced by autocyclic mechanisms. Established models for coarse grained conglomeratic fluvial successions (Miall, 1977, 1978; Boothroyd and Nummedal, 1978; Rust, 1978, 1979) do not fit the data well. Fine grained overbank deposits in the Kasaba Formation frequently form up to 70% of individual cycles (Fig. 4.23, 4.24), whereas in most published models they are often less than 10%.

It has been generally assumed that overbank deposits are of little importance in braided alluvial deposits (Miall, 1978, p. 603) and current models of vertical sequences, based mainly on studies of modern alluvial environments, emphasise channel processes (Miall, 1977, 1978; Boothroyd and Ashley, 1975; Boothroyd and Nummedal, 1978; Rust, 1979).

However, a number of recent studies (McLean and Jerzykwiewicz, 1978; Friend, 1978) have reported sequences where overbank deposits form a large proportion of ancient braided fluvial deposits. These have been interpreted both as (1) the result of extensive lateral movement of large active channels, where thick overbank deposits will form provided that sufficient lateral spread of suspended fine sediment occurs during flood events (Friend, 1978; Rust, 1978); (2) channel restriction on the floodplain accompanied by rapid subsidence (Miall, 1978).

Other controls that may result in the development of thick overbank sequences are source area and vegetation. In the present case erosion of a source area that contains a wide variety of rock type, with varying resistance to degradation, results in the release of a large scatter of grain sizes.

Calcretes within the sequence suggest an arid palaeoclimate. This and the absence of coal, carbonaceous or rootlet horizons, commonly recorded from 'tropical' alluvial fans (e.g. Heward, 1978a), indicate that vegetation was not abundant.

Given that the source area is capable of supplying a suitable range of grain sizes, it is suggested here that a combination of extensive lateral migration of the active areas of sedimentation accompanied by rapid subsidence were the major controls which led to deposition of thick overbank deposits. This is shown schematically in Fig. 4.31. Inherent in this model (modified after Friend, 1978) are the following features: (1) the lateral movement of the active

sedimentation area is consistently across the braidplain in one direction, until the active sedimentation area encounters the margin of the braidplain. It will then begin to migrate back in the opposite direction; (2) Most of the fine grained material is flushed out into overbank areas; (3) There is no tectonic tilt across the braidplain (cf computer models of Bridge and Leeder, 1980).

In this model rapid subsidence and constricted lateral movement result in only a limited thickness of overbank sediment, before the active area of sedimentation is superimposed on previously deposited active area units (Fig. 4.31a). Extensive lateral movement accompanied by very little subsidence results in superimposed active area sediments (Fig. 4.31b). Extensive lateral movement is accompanied by rapid subsidence resulting in thick overbank units (Fig. 4.31c).

Comparison of cyclic fluvial sequences characterised by abundant overbank sediments (McLean and Jerzykwiewicz, 1978; Friend, 1978) shows that they occur frequently in areas of tectonic activity associated with rapid subsidence.

McLean and Jerzykiewcz (1978) document a sequence that is primarily controlled by thrust emplacement; subsequent loading and subsidence, in front of the thrust sheets, occurs in response to isostatic adjustment (see 10.2.3, for a more detailed discussion).

In the present area, emplacement of the Lycian Nappes from the northwest in the Lower Miocene resulted in loading and subsequent subsidence of the carbonate platform onto which the thrust sheets were emplaced. Subsidence slowed during middle Miocene times as the sedimentary basin filled. Final emplacement of thrust sheets in the Upper Miocene, during which time the Kasaba Formation was deposited, again brought about rapid subsidence. Tectonic controls on regional sedimentation patterns are discussed more fully in 10.2.3.

In conclusion, thick overbank sequences are, in this case, the result of extensive lateral migration of the area of active sedimentation across the floodplain (autocyclic mechanism) accompanied by rapid subsidence (external control).

4.12 Vertical Mega-sequence trends

Superimposed on the small scale autocyclic fining-upward units is a large scale coarsening- and then fining-upward mega-sequence (Fig. 4.32). This is reflected in maximum clast size trends in the

Fig. 4.31

General model explaining cyclicity in fluvial sequence (in part after Friend, 1978).

(a) Rapid subsidence and restricted lateral migration of the active area of sedimentation result in only a limited thickness of overbank sediment before the active area of sedimentation is superimposed on previously deposited active area units.

(b) Extensive lateral migration accompanied by little subsidence results in superimposed active area sediments.

(c) Extensive lateral migration accompanied by rapid subsidence resulting in thick overbank sediments.

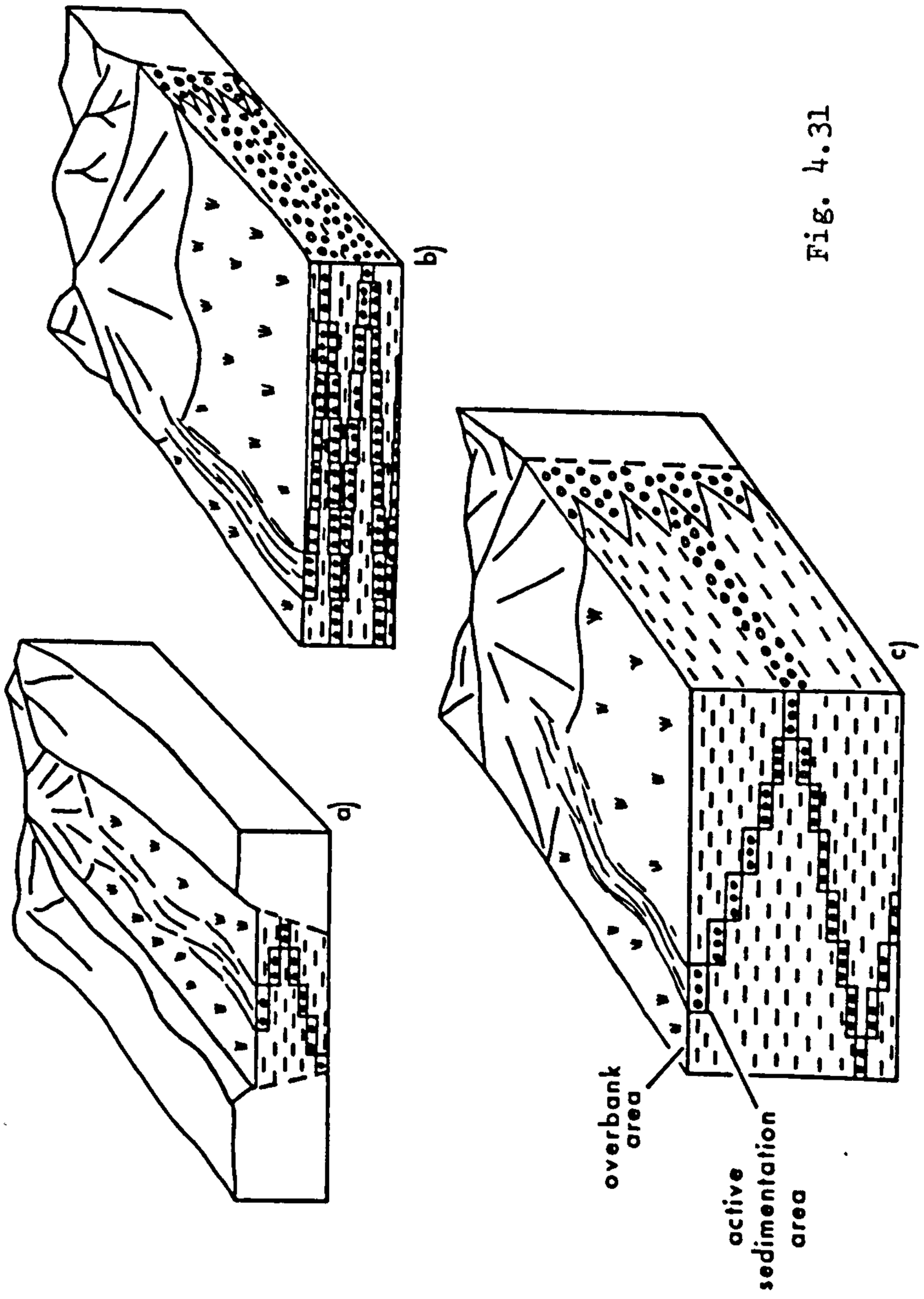

Fig. 4.31

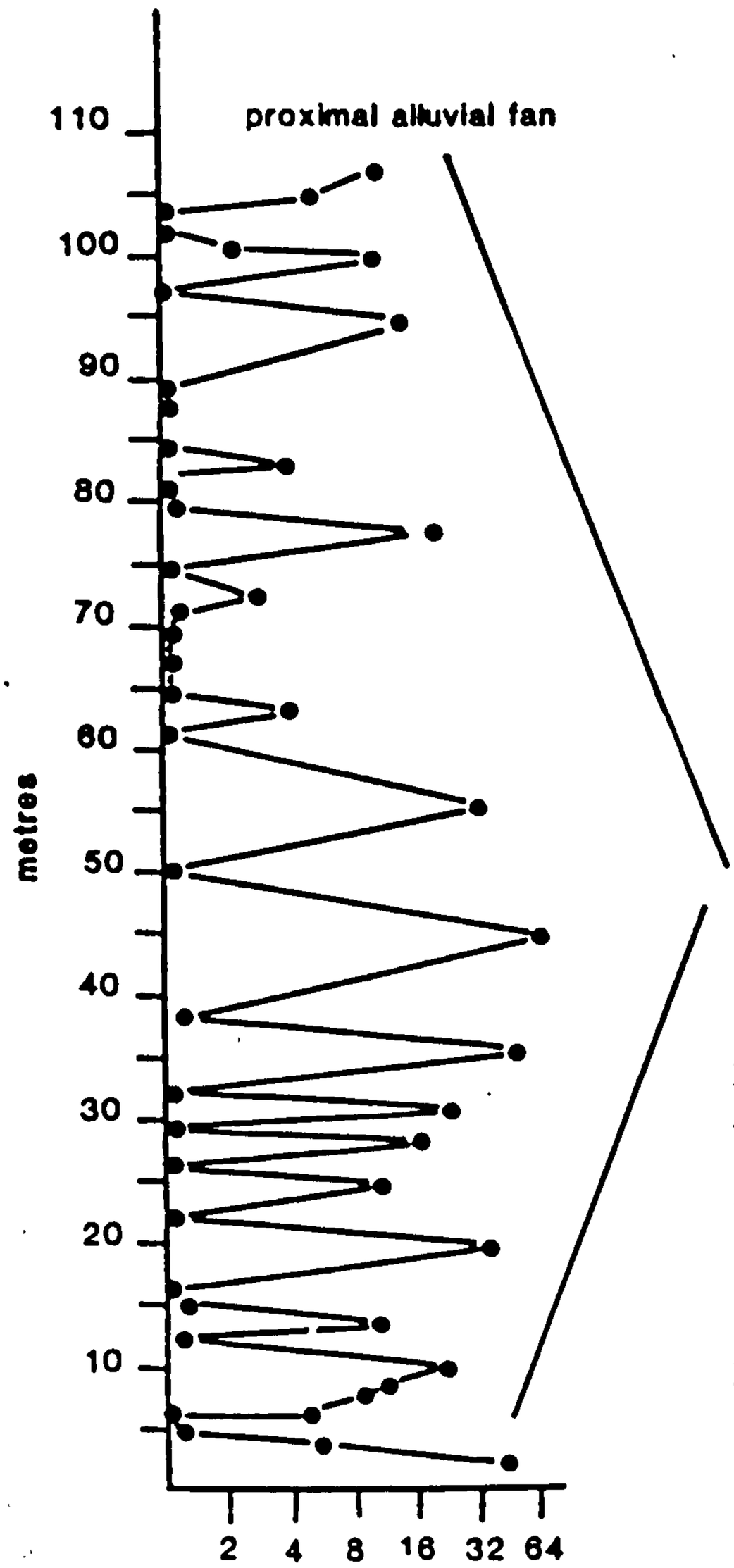

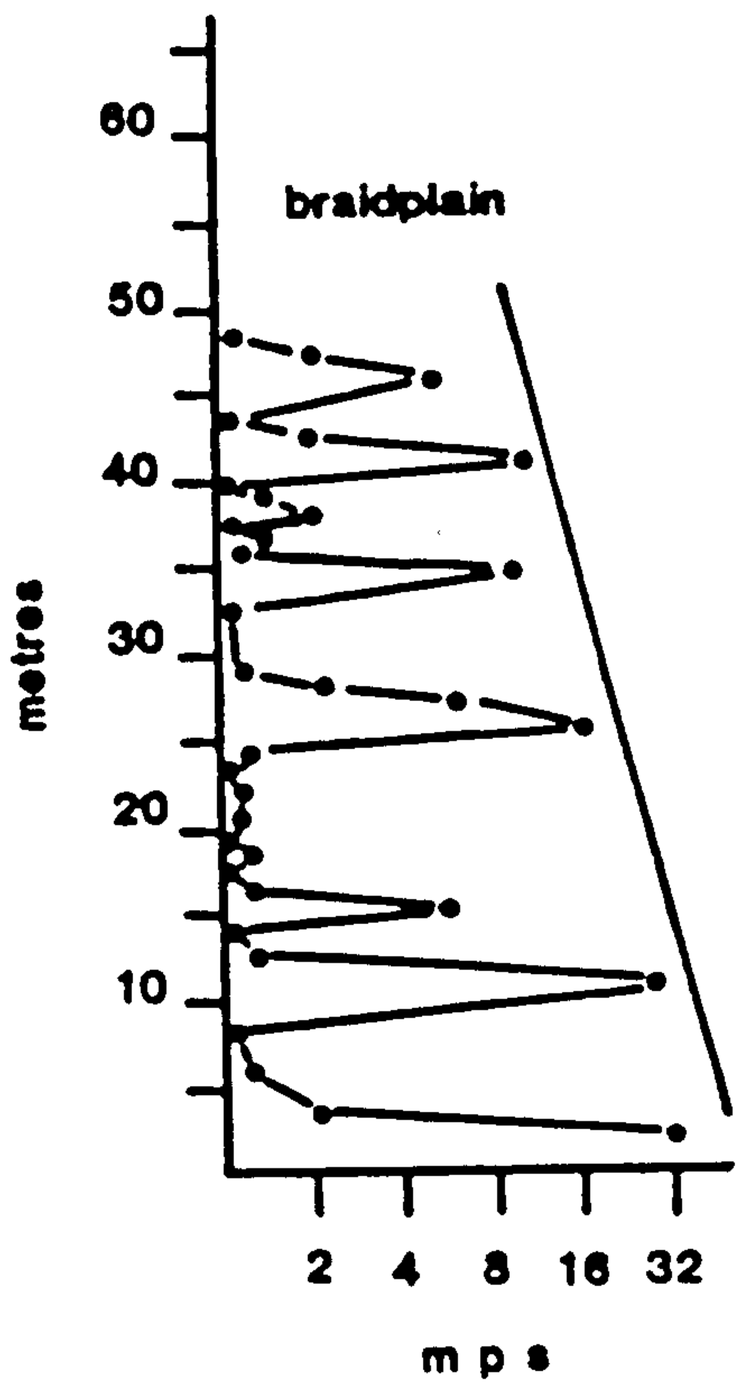

Fig. 4.32
Vertical mega-sequence trends, showing sequence scale coarsening- and then fining-upwards of the maximum particle size, Kasaba Formation (upper part of Doğantaş Member). This is interpreted to be the result of progressive uplift of the source area followed by scarp retreat.
See text for details.

conglomerate, and in the proportion of conglomerate units (Fig. 4.20).

The overall sequence represents initial uplift of the source area (final stage thrust emplacement, 10.2.4), producing a coarsening-upwards (cf Heward, 1978a) (Fig. 4.31); subsequent scarp retreat and lowering of relief resulted in deposition at progressively more distal locations, relative to the source, and a fining-upward sequence (Heward, 1978a; Wilson, 1980).

Clast size and proportion of conglomerate are consistent with source area retreat. However, upper parts of the sequence show evidence of small scale progradation. Non-marine sediments overly shallow marine sequences (Fig. 4.20). There is no evidence of within sequence disconformity indicative of syntectonic movements (Crowell, 1974). This, combined with the overall fining-upward trend, suggests that small scale progradation was the result of a fall in sea level. The Tortonian age of this sequence is consistent with the initial fall of sea level associated with the impending Messinian dessication event (Hsu *et al.*, 1973).

4.13 General Summary of the Western Margin

Sediments of the Kemer and Kasaba Formation were clearly derived from the Lycian Nappes. *Initial* emplacement of the nappes resulted in widespread subsidence of the carbonate platform (this is discussed in 10.2.3), from a previously shallow water carbonate depositing realm (9.2.5).

Initially fine grained, thin-bedded turbidites were deposited in both marginal (e.g. Sinekçibeli) and central areas of the basin. In marginal (proximal) areas, a coarsening-upward sequence reflects the progressive advance of the nappe front (rate of nappe movement is discussed in 10.2.2). The upper parts of the sequence in marginal (proximal) areas, represent deposition on the submarine area of a fan-delta (4.4.3). This passed basinward into a series of broad, shallow 'submarine fan' channels, within which thick conglomerate units were deposited (Fig. 4.18). The conglomerates passed down channel into an area of sandstone deposition. Away from the channels thin-bedded turbiditic sandstone and mudstone were deposited. Sequences in marginal (proximal) areas of the basin (e.g. Sinekçibeli, Fig. 4.3) were abruptly terminated in Langhian times by the continued southeastward thrusting of the nappe front.

In central areas of the basin sedimentation continued (e.g. Kasaba, Fig. 4.1), turbiditic sandstones and mudstones of Langhian age pass upwards into a mudstone dominated sequence (4.6.0). This general fining-upwards probably marks the end of the *initial phase* of nappe emplacement; relief in the source area had been lowered by erosion. Sedimentary facies suggest a general shallowing-upwards. This is probably related to both eustatic sea level changes during and towards the end of the Serravallian (Vail *et al.*, 1977; Hsu, 1973; Gwirtzman and Buchbinder, 1977), and more importantly (?) the progressive infilling of the sedimentary basin (see discussion 10.2.0). Upwards the sandstones and mudstones pass transitionally into the Kasaba Formation. This renewed influx of coarse grained material marks the *final* phase of Lycian Nappe emplacement. Alluvial fans deposited in proximal areas prograded over a fluvial braidplain into a shallow sea.

CHAPTER 5 EASTERN MARGIN SEDIMENTARY FACIES ASSOCIATIONS

CHAPTER 5

5.0 Eastern Margin Sedimentary Facies Association

5.1 Introduction

In this chapter facies models are developed from analysis of the sequential and spatial relationship between individual sedimentary facies along the eastern margin of the basin. Sedimentary sequences in this area, defined as the Salir Formation (2.3.0), crop out either side of the Finike anticline and along the centre of the Alaçadağ syncline (Fig. 5.1).

Initiation of clastic sedimentation. Over the area of the Salir Formation outcrop (Fig. 5.1) the initiation of clastic terrigenous sedimentation was abrupt (Fig. 5.3). Thin-bedded laterally continuous sandstone (Tde), mudstone and hemipelagic chalk lie with slight angular discordance on either green-grey calcareous marls of Oligocene age (Chapters 2 and 9) or limestones of Maastrichtian to Palaeocene age (Chapters 2 and 9).

5.2 Provenance

Composition. The composition of the sandstone and conglomerate, discussed more fully in Chapter 6, indicates a mixed igneous ophiolite, pelagic sedimentary (chert, pelagic limestone), carbonate platform (shallow water limestone), and quartzose sedimentary source area. Bioclastic content varies between 0% and 90%.

Palaeocurrents. Palaeocurrent measurements, summarised in Fig. 5.2, of sole marks, ripples, cross-stratification and imbrication indicate a general NE/E to SW/W sediment dispersal pattern. Slump folds, although often reflecting local slopes (Fig. 5.17), are consistent with a general ENE-SSW trending palaeoslope.

The Salir Formation was derived from the Antalya Complex to the east.

5.3 Lower Miocene

The Lower Miocene sequences of the Salir Formation are characterised by:

(I) The complete absence of shallow water indicators, including an almost complete absence of traction cross-bedding, and shallow marine faunas;

(II) Generally coarse grain size;

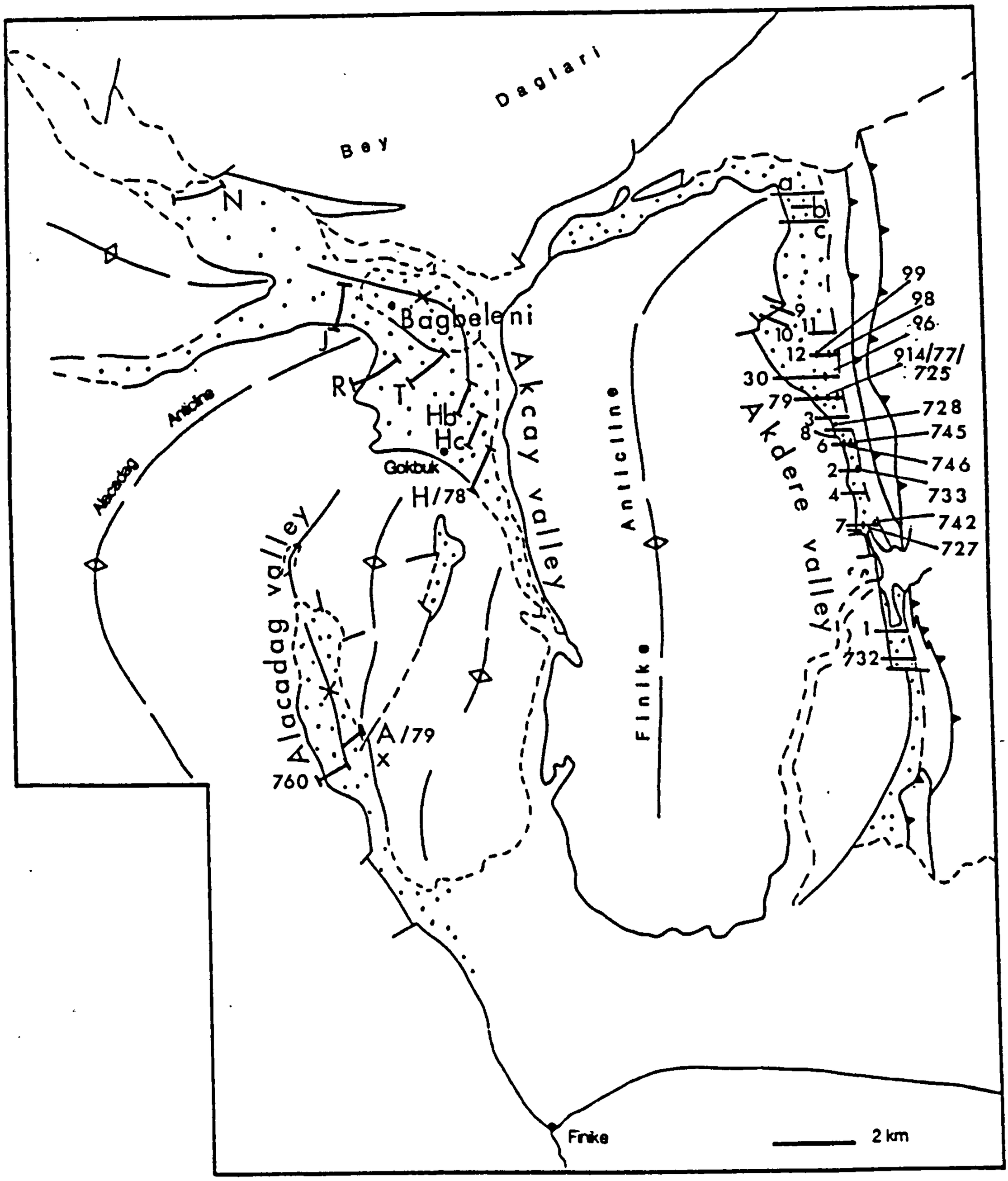

Fig. 5.1

Outcrop area of the Salir Formation, showing location of sedimentological sections and localities mentioned in text.

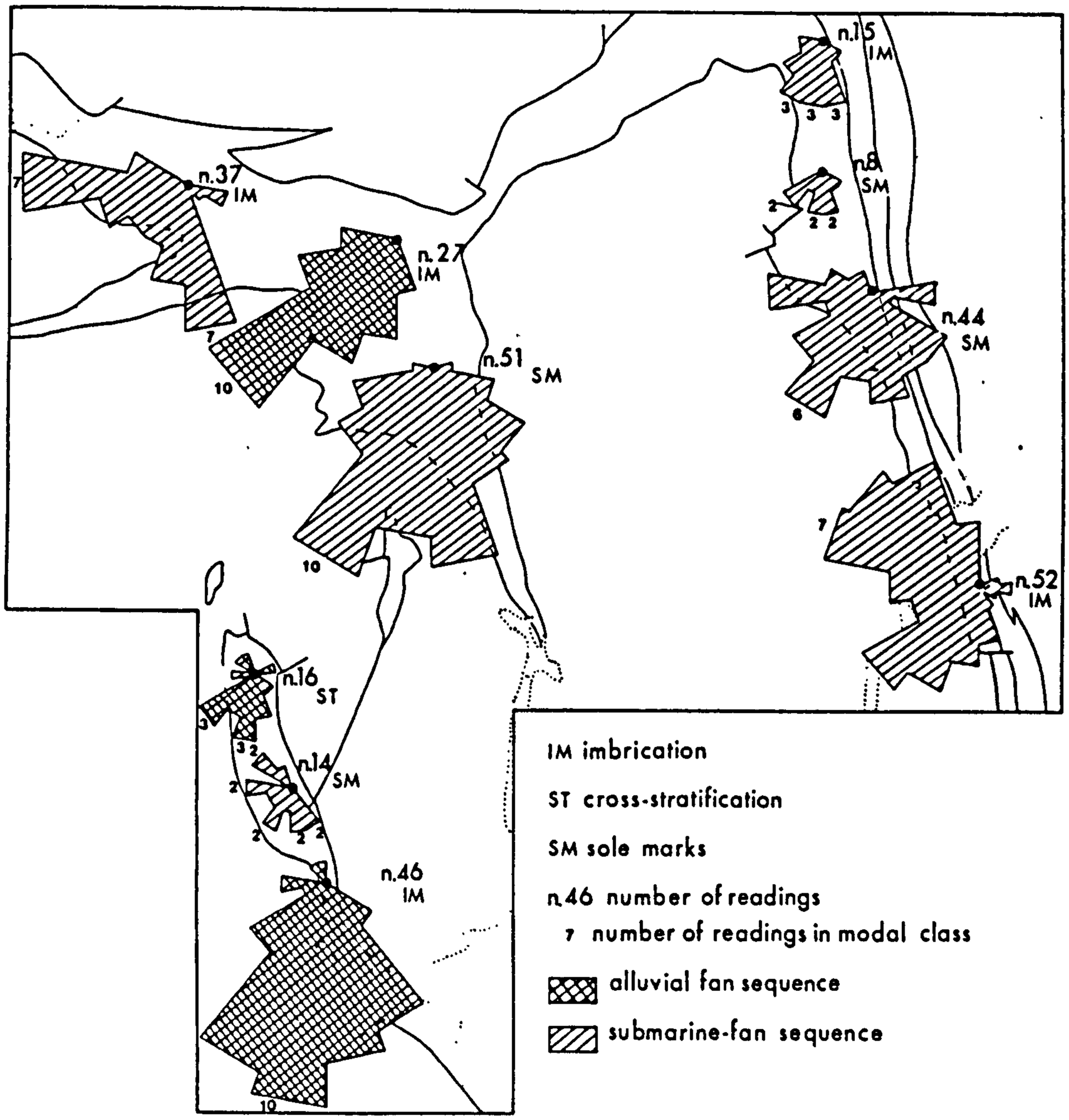

Fig. 5.2

Palaeocurrent data for the Salir Formation.

(III)Unidirectional palaeocurrents (Fig. 5.2);
(IV) Abundant pelagic chalk horizons;
(V) Channelled conglomerates and sandstone deposited by a variety of sediment gravity flows (3.4.0).

All of the above suggest deposition in a submarine fan environment. The sequence is initially subdivided into a number of 'proximal' facies associations (as determined from palaeocurrent data and clast size) and mid-distal facies associations.

5.4.0 Proximal Sequences

Proximal sequences are well exposed along the length of the Akdere valley. Several facies associations are recognised.

5.4.1 Conglomerate-Sandstone Association

Description. This facies is well exposed in the southern and central parts of the Akdere valley (Fig. 5.1). Amalgamated units of conglomerate and sandstone are between 5 m and 20 m thick; they are traceable over 500 m across palaeoslope. Bases are erosive, broad scours cut into the underlying mudstone-sandstone sequence are up to 5 m deep and 50 m across.

The units are dominated by pebble, cobble and boulder conglomerate (~75% average), consisting of disorganised conglomerate (Dsg, ~45%), graded conglomerate (Gg, ~25%), and matrix-supported conglomerate (Msp, ~10%, Ssp, ~15%). Average grain size varies up to .70 m, outsize clasts are up to 1.80 m. Massive structureless and graded sandstones form up to 25% of this association. Within the conglomerate-sandstone units interbedded thin mudstone, sandstone and chalk packets are volumetrically subordinate (~5%). On a scale of several hundred metres units of conglomerate and sandstone are interbedded with turbiditic sandstone, mudstone and pelagic chalk (see below and Figs. 5.3 and 5.4).

Conglomerate units are characterised by their complex internal geometry, consisting of channelled wedges, produced by repeated episodes of channel cutting and filling (Fig. 5.5). Individual beds are rarely laterally continuous over 50 m. Channel floors are generally regular and symmetrical or rarely irregular with occasional cobble conglomerate lags. In some of the conglomerate units (only two examples recorded) large scale cross-stratified pebble sandstone is present (Fig. 5.6). Facies transition analysis reveals no preferred sequential arrangement (Fig. 5.7). There is a tendency

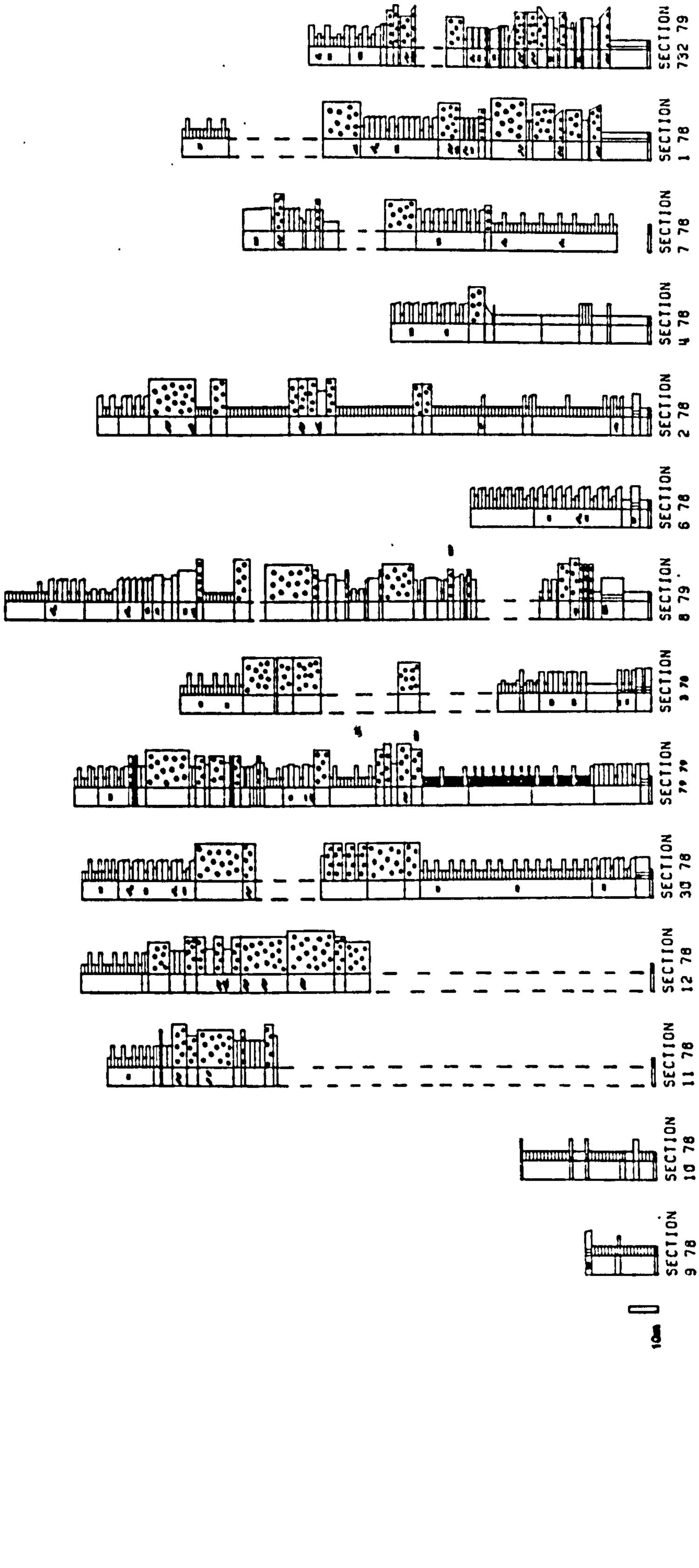

Fig. 5.3 Sedimentological logs measured in the south of the Akdere valley, Salir Formation (see Fig. 5.1 for location of sections). The sequence is interpreted as an inner submarine fan depositional environment. Sections are transverse to palaeoslope.

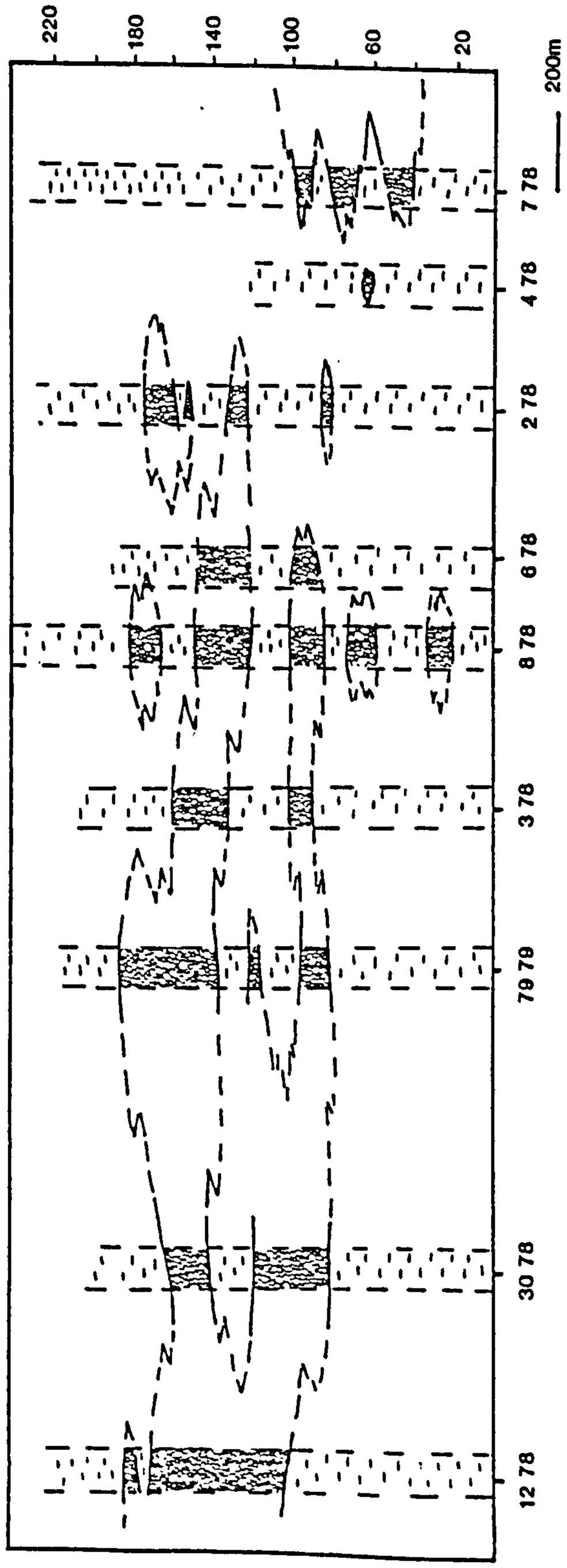

Schematic fence diagram showing inter-relationship (interconnectedness) of main conglomerate channel-fills from the inner fan facies association. Salir Formation. Logs much simplified from Fig. 5.3. Sections are transverse to palaeoslope.

Fig. 5.4

for all beds to occur randomly interbedded with massive structureless coarse sandstone. Fining- and thinning-upward cycles are recorded from several conglomerate-sandstone units (Figs. 5.8, 5.11); elsewhere there is a random variation in grain size (Fig. 5.10). Shale and mudstone rip-up clasts often decrease in frequency up a fining-upward unit. Where exposed, channel margins are not abrupt, conglomerate-sandstone units interfinger with the surrounding mudstone-sandstone. There is no evidence of any significant channel relief.

In several instances (Fig. 5.9), conglomerate units show an initial fining-upward fill which is capped by a thick disorganised cobble or boulder conglomerate (Fig. 5.11). Within this facies association occasional large (4.5 m long) sandstone-mudstone intraclasts occur (Fig. 5.12).

5.4.2 Interpretation : Inner-fan channel

Palaeocurrent dispersal patterns (Fig. 5.2) and the coarse grain size indicate this sequence to be the most proximal. The geometry and presence of channels suggests deposition in an inner submarine fan environment (Fig. 5.34). Main channels, orientated in a broadly E-W trend, were of the order of 300-700 m across, comprising a complex small scale braided channel system (Fig. 5.34). The term inner fan channel in this context does not imply a large canyon-like channel, rather an area of active sedimentation. The channels are inferred to have had little or no relief.

Deposition was by a variety of sediment gravity flows, from the facies types present density modified grain flows and turbulent events were dominant. Wedge geometry within channels is the result of continued cut-and-fill superimposed channels. Thinning- and fining-upward cycles are the result of progressive channel abandonment, depositing successively thinner and finer flows (Ricci Lucchi, 1969, 1975a, b; Mutti and Ghibaudo, 1972). Truncated fining-upward cycles overlain by massive disorganised conglomerate indicate deposition in the channel was terminated by the effective blocking of the channel by an outsize flow. Large intraclasts were derived from up-channel slumping.

5.4.3 Sandstone-Mudstone Association

Description. Amalgamated sandstone packets between 5 and 15 m thick, form lenticular units up to 500 m across. Bases are erosive

Fig. 5.5

Inner submarine fan channel-fill conglomerate sequence. Normally graded conglomerate (a) and normally graded sandstone (b) with conglomerate lag at base deposited by turbulent flows. Disorganised conglomerate (c) deposited by debris flow mechanism.
Note scoured bases(s), wedge geometry and truncation by successive depositional units (t).
Salir Formation. GR. 519385.

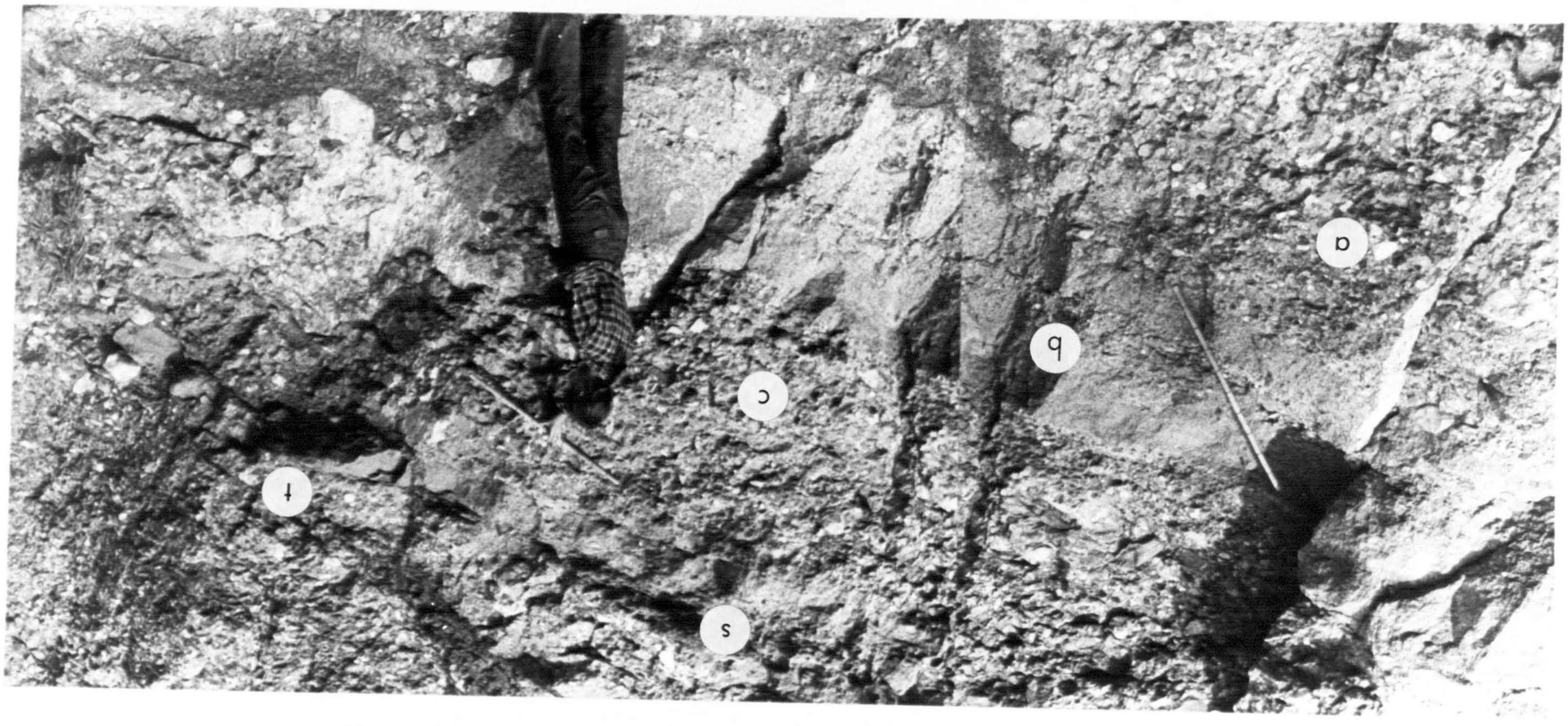
a
b
c
s
t

Fig. 5.6

Large scale cross-stratified sandstone (s) overlying disorganised conglomerate (Dsg) deposited by debris flow mechanism. The cross-stratified unit is interpreted to have formed by traction current reworking and deposition at the base of a later turbidity current. Confined within an inner fan channel. Note the apparent dune geometry, downcurrent transition to plane laminated beds (flow was left to right) and alignment of pebble conglomerate clasts along foresets. Salir Formation inner fan facies association. GR 510401. Face is 5 m high.

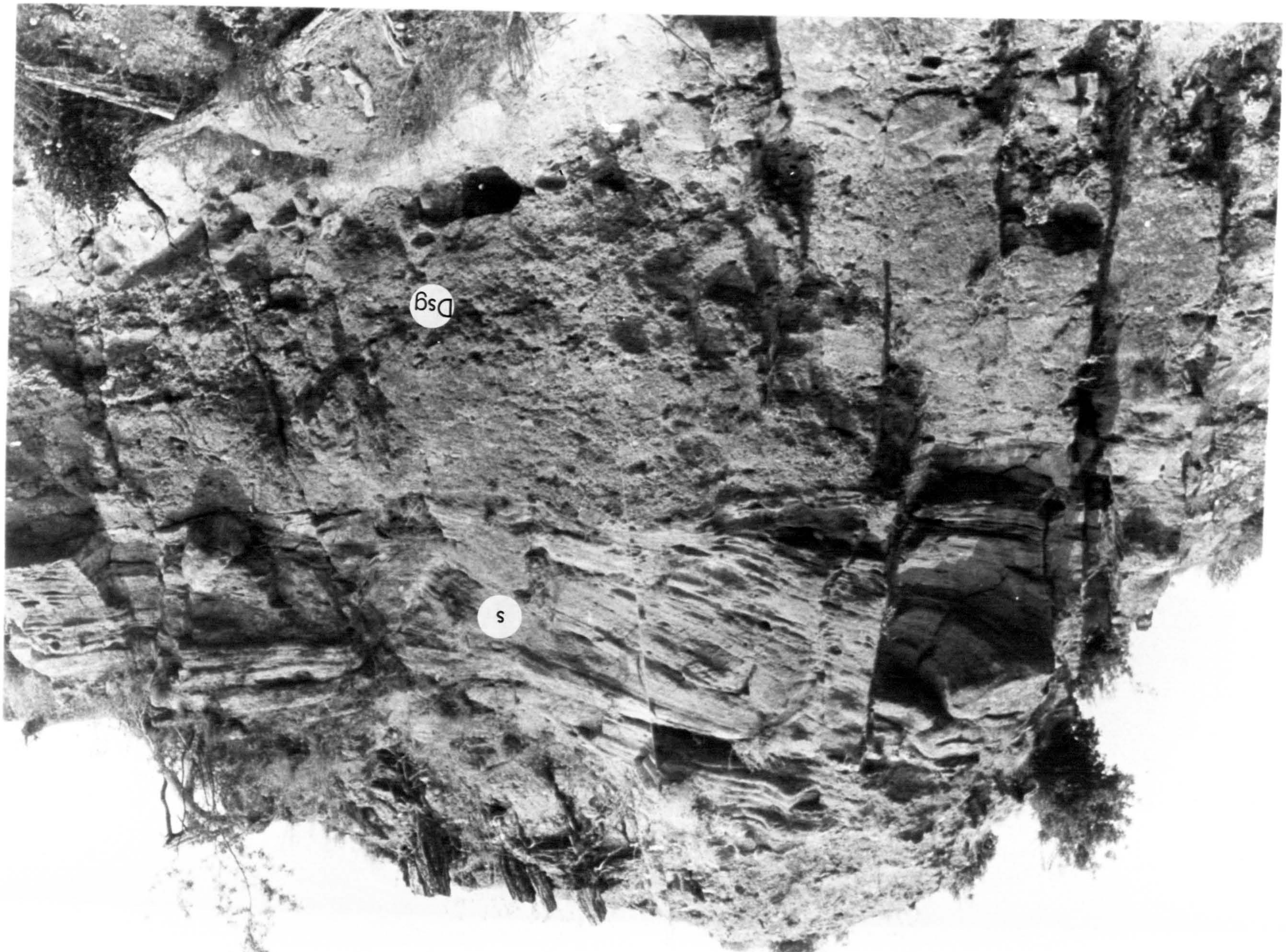
Dsg
S

Observed Transitions

	Dsg	Gg	Msp	Ssp	Sst	T_{AB}	T/M	M/C	TOTAL
Dsg	-	7	2	2	30	7	4	7	59
Gg	7	-	0	1	19	2	4	0	31
Msp	4	0	-	0	5	1	3	0	13
Ssp	3	0	0	-	1	0	0	1	5
Sst	34	8	7	1	-	2	3	2	57
T_{AB}	6	4	0	0	3	-	5	9	27
T/M	7	2	3	0	4	8	-	2	26
M/C	2	1	0	0	3	5	2	-	13
									231 TOTAL

Preferred Transitions

(observed minus random transitions
expressed as probabilities)

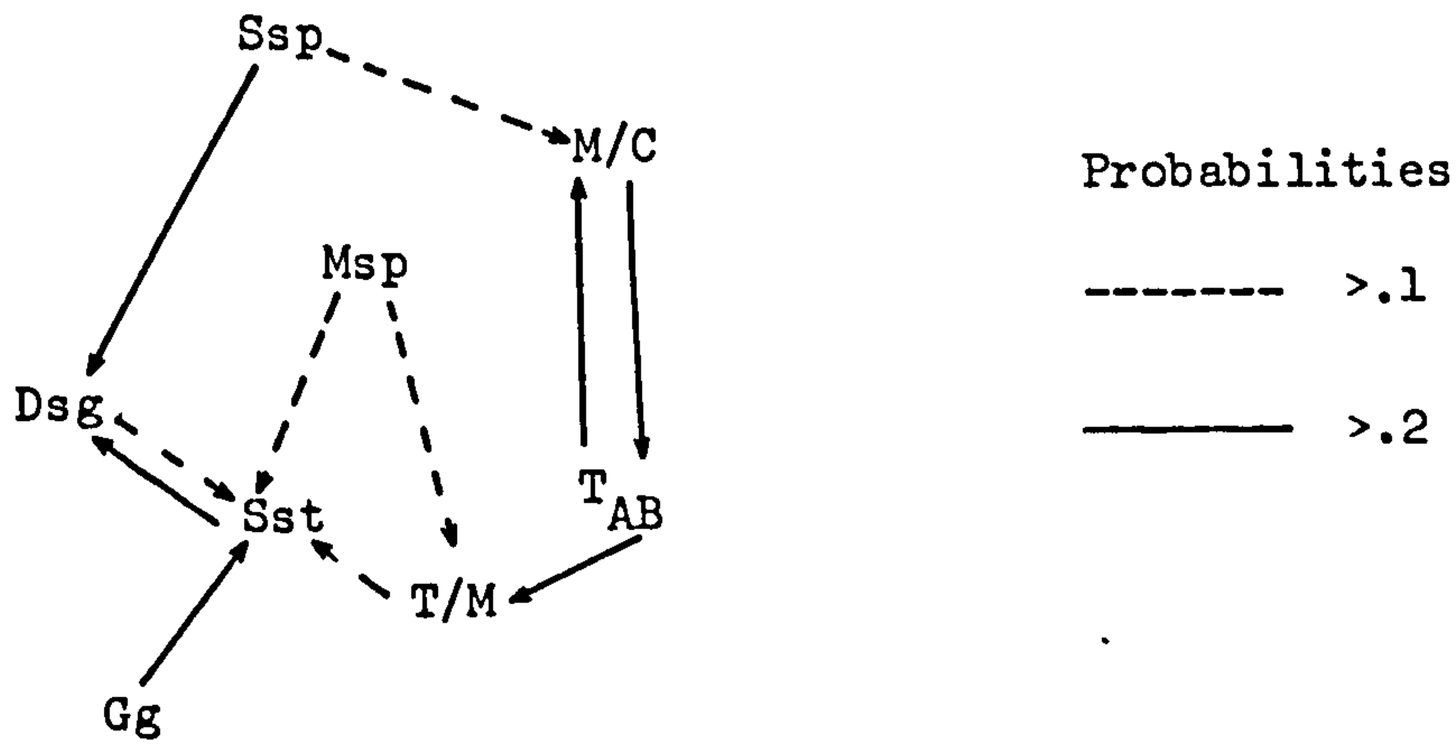

Fig. 5.7
Vertical facies transition analysis for inner fan channel association. Salir Formation. Calculated from 231 transitions.
Dsg - disorganised conglomerate; Gg - graded and graded stratified conglomerate; Msp - mud-supported conglomerate; Ssp - sand-supported conglomerate (pebbly sandstone); Sst - structureless coarse sandstone; T_{AB}- turbiditic sandstone (Tab); T/M - turbiditic sandstone, mudstone, chalk; M/C - mudstone, chalk.

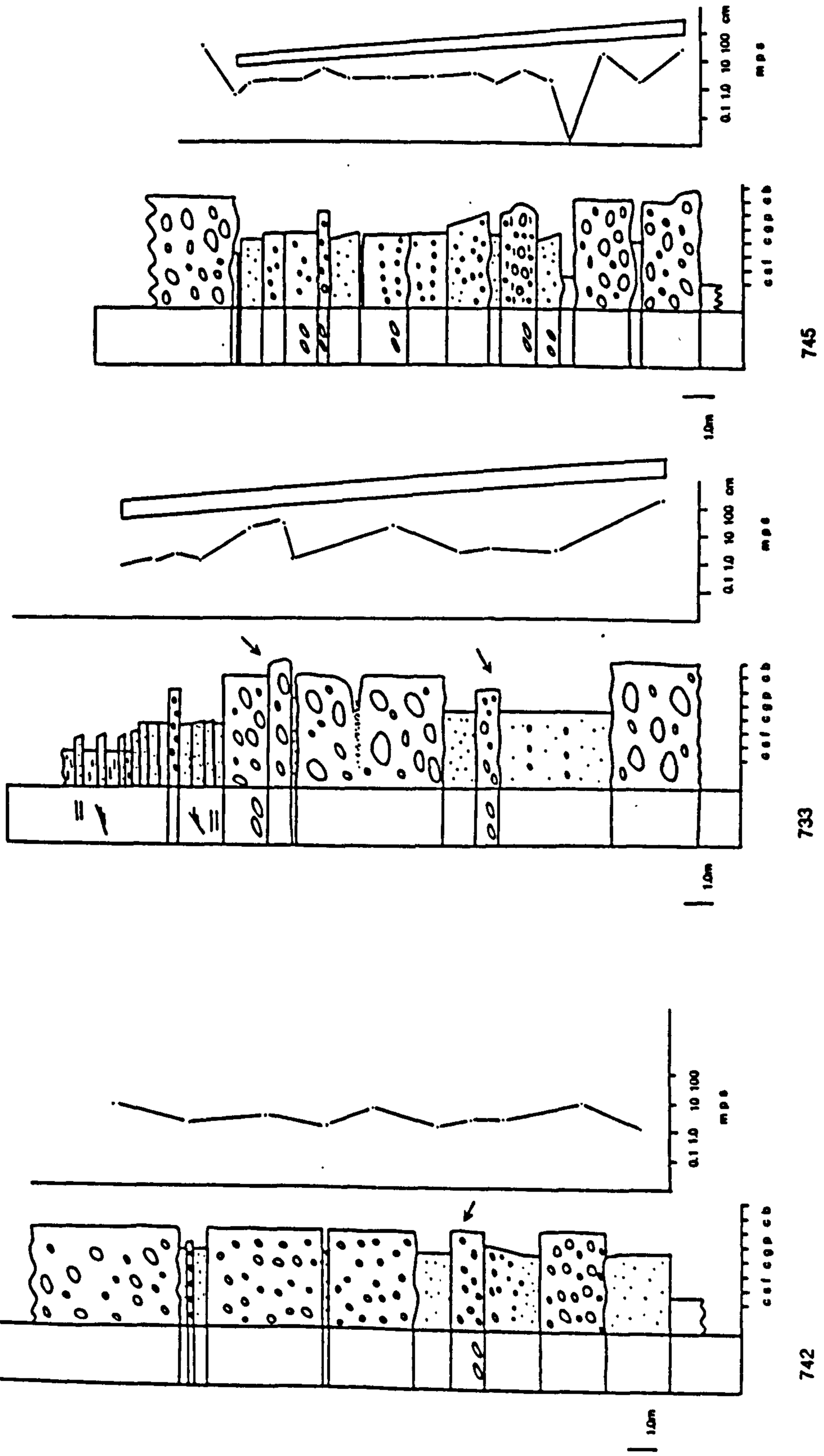

Fig. 5.8 Detailed sedimentological logs in conglomerate-sandstone facies association (inner submarine fan channels). Note presence of poorly defined fining-upward cycles. Salir Formation. See Fig. 5.1 for location of logs (Appendix C for key).

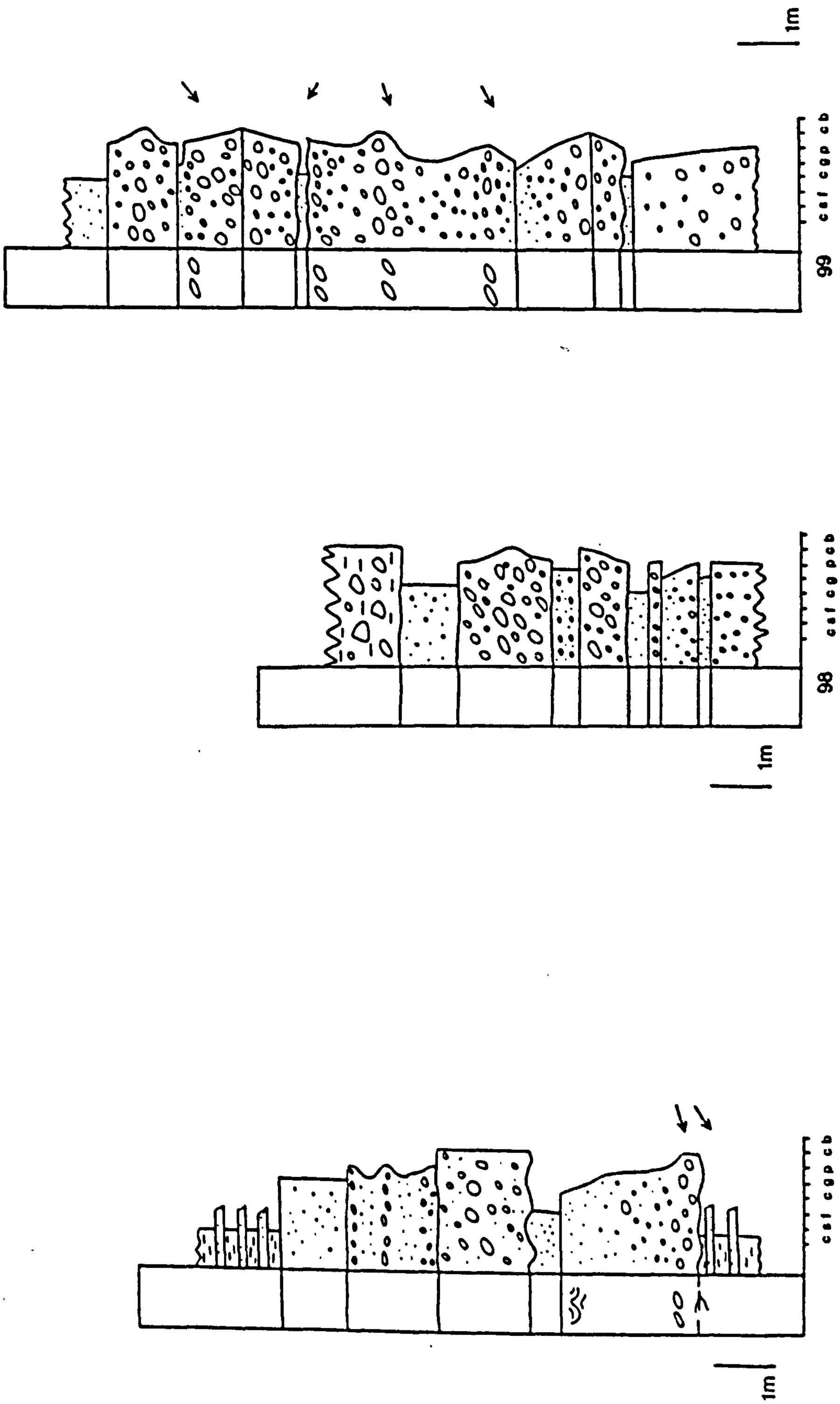

Fig. 5.9 Detailed sedimentological logs in conglomerate-sandstone facies association (inner submarine fan channels). Units are non-cyclic. For location of logs see Fig. 5.1 (Appendix C for key).

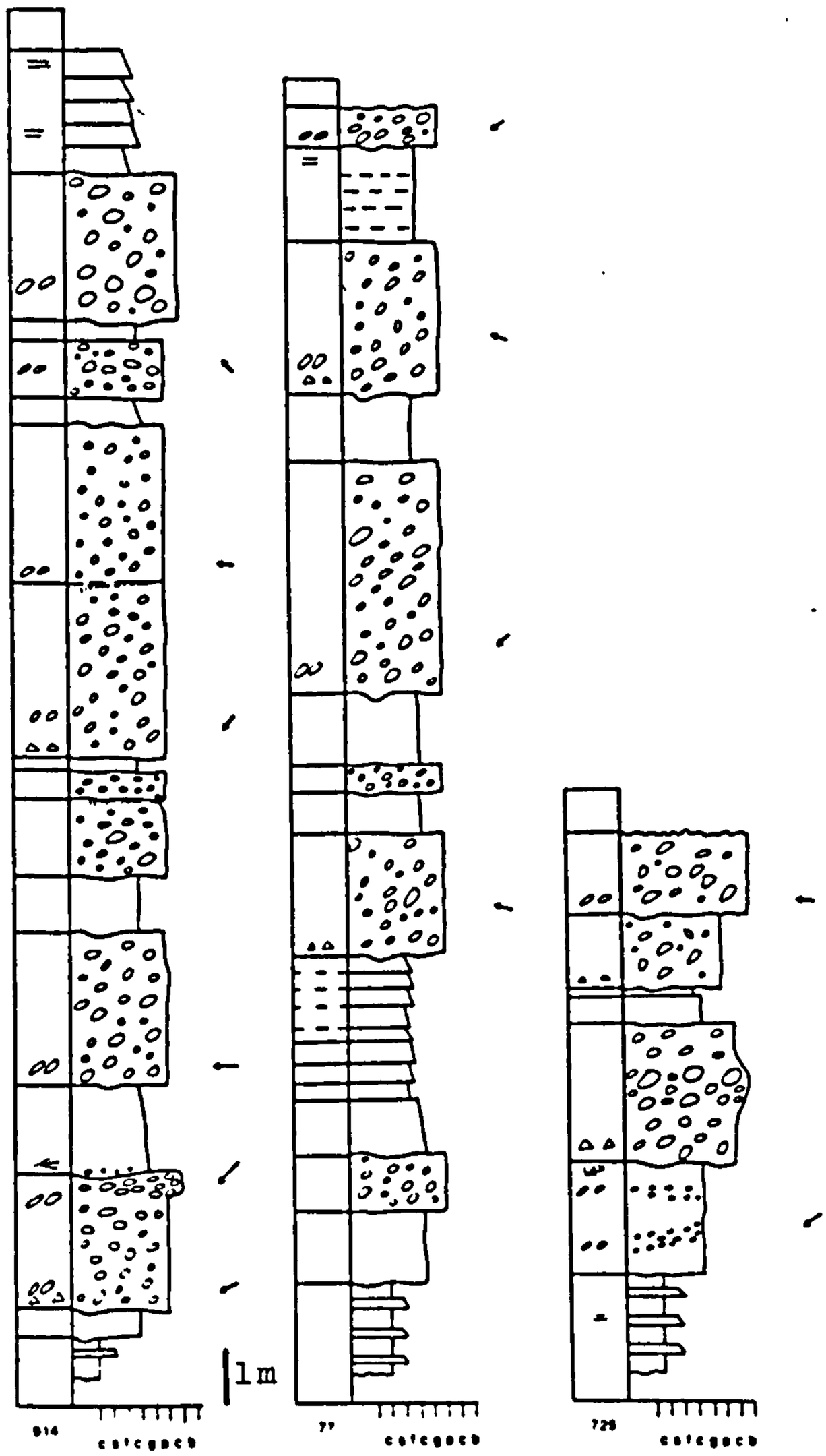

Fig. 5.10
Detailed sections in conglomerate-sandstone facies association (inner submarine fan channels). Units are non-cyclic.
For location of sections see Fig. 5.1 (Appendix C for key).

Fig. 5.11

Fining- and thinning-upwards channel-fill sequence. Conglomerate → very coarse sandstone → coarse sandstone, with associated decrease in bed thickness. This is interpreted to be the result of thinner and finer flows as the result of the gradual abandonment of a submarine fan channel. This is overlain and truncated (compare line emphasised by triangles) by a massive disorganised conglomerate unit. Inner fan facies association. Salir Formation. GR. 517385. Stick is 1 m long.

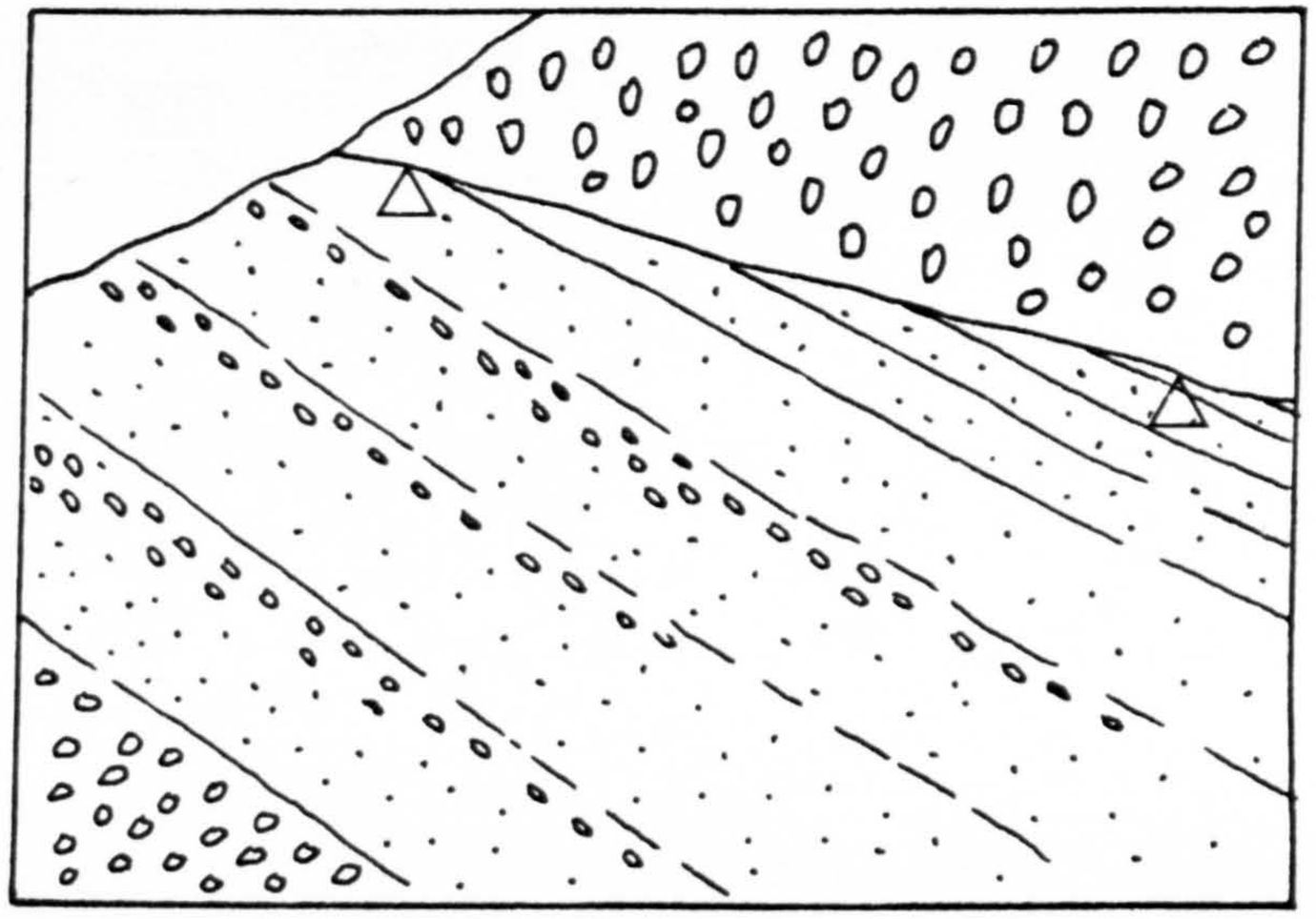

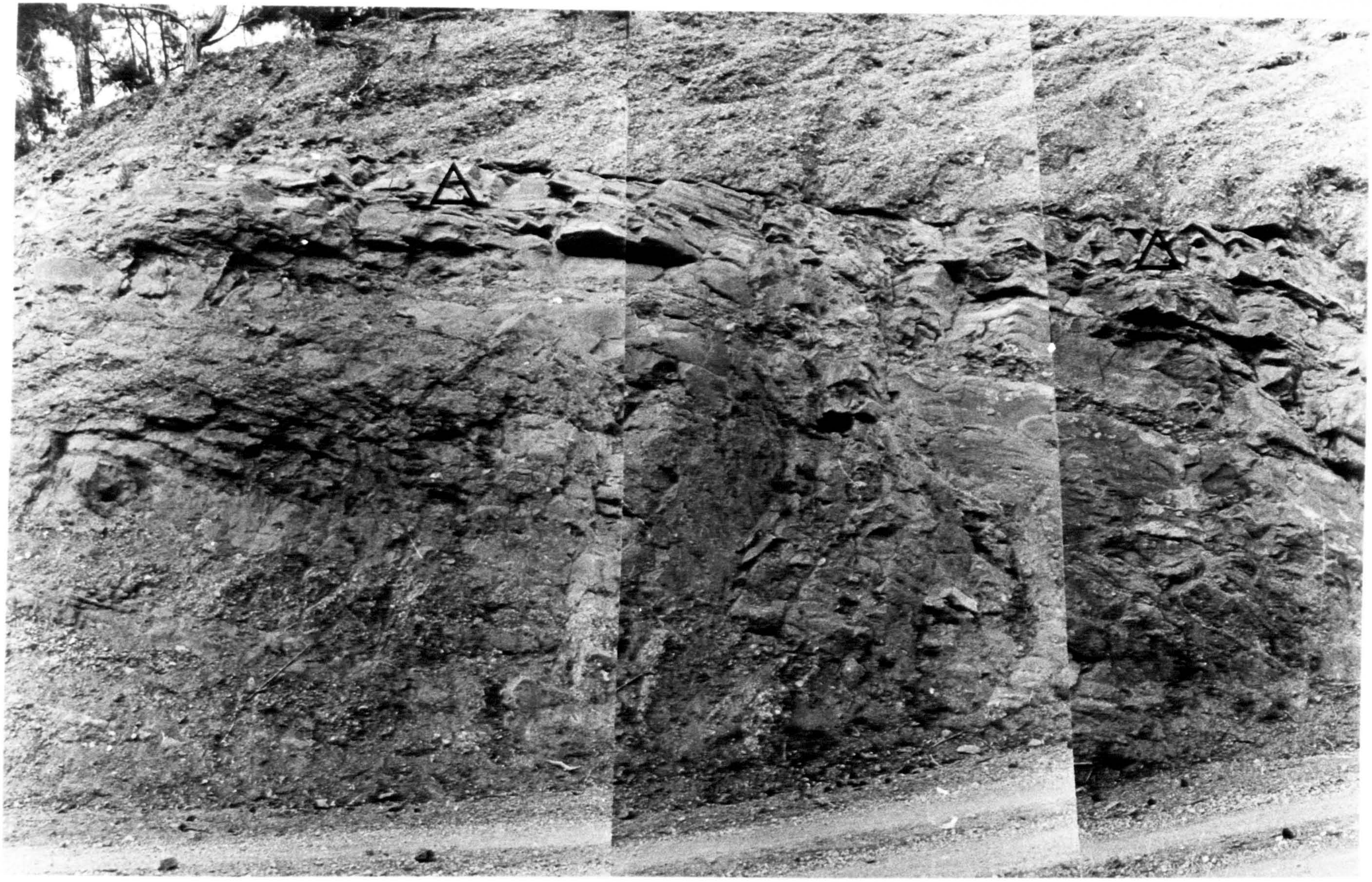

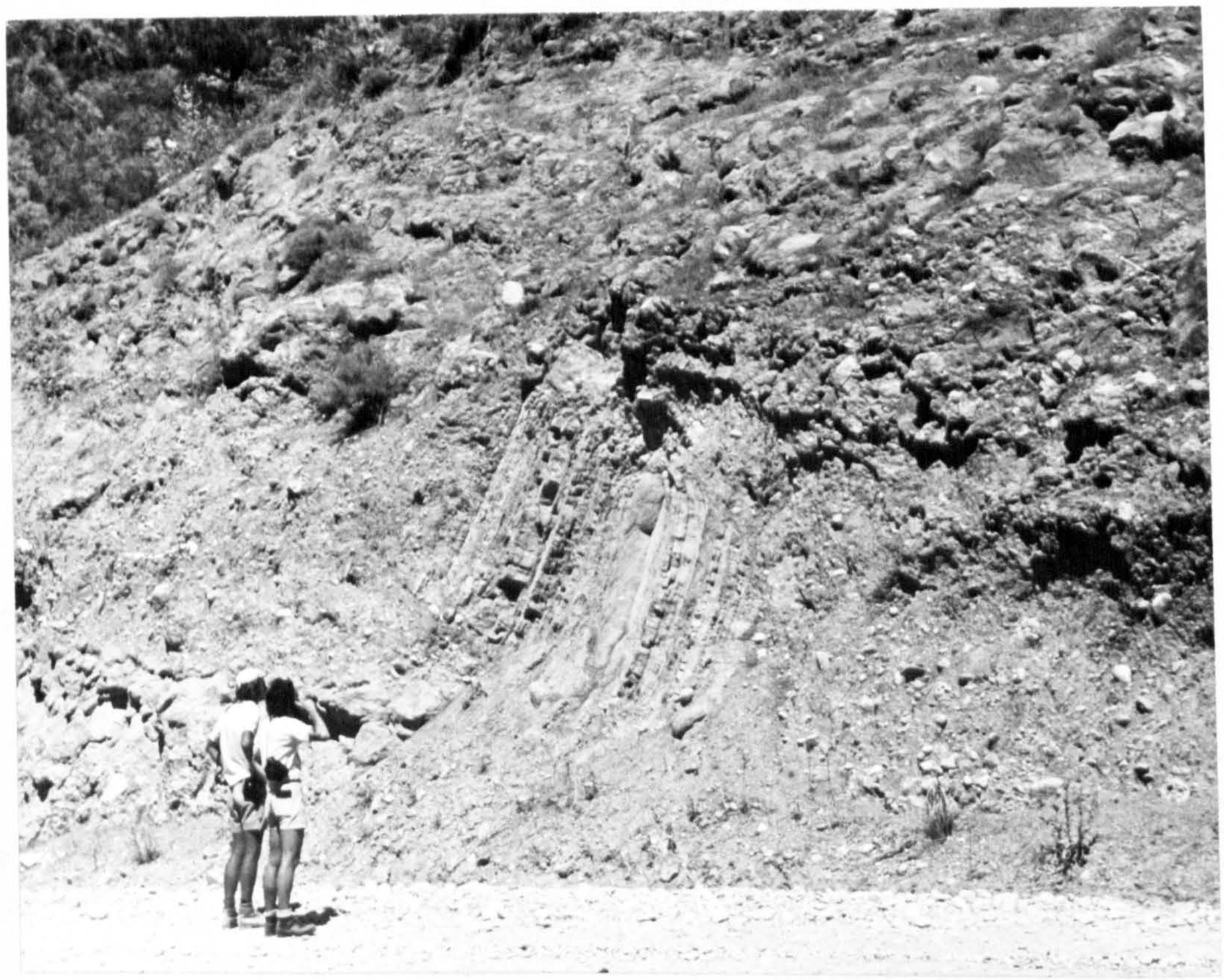

Fig. 5.12

Large sandstone-mudstone intraclast within mud-supported conglomerate deposited by debris flow mechanism. Clast is the result of slumping of partially consolidated strata.
Inner fan facies association, Salir Formation. GR. 532340.

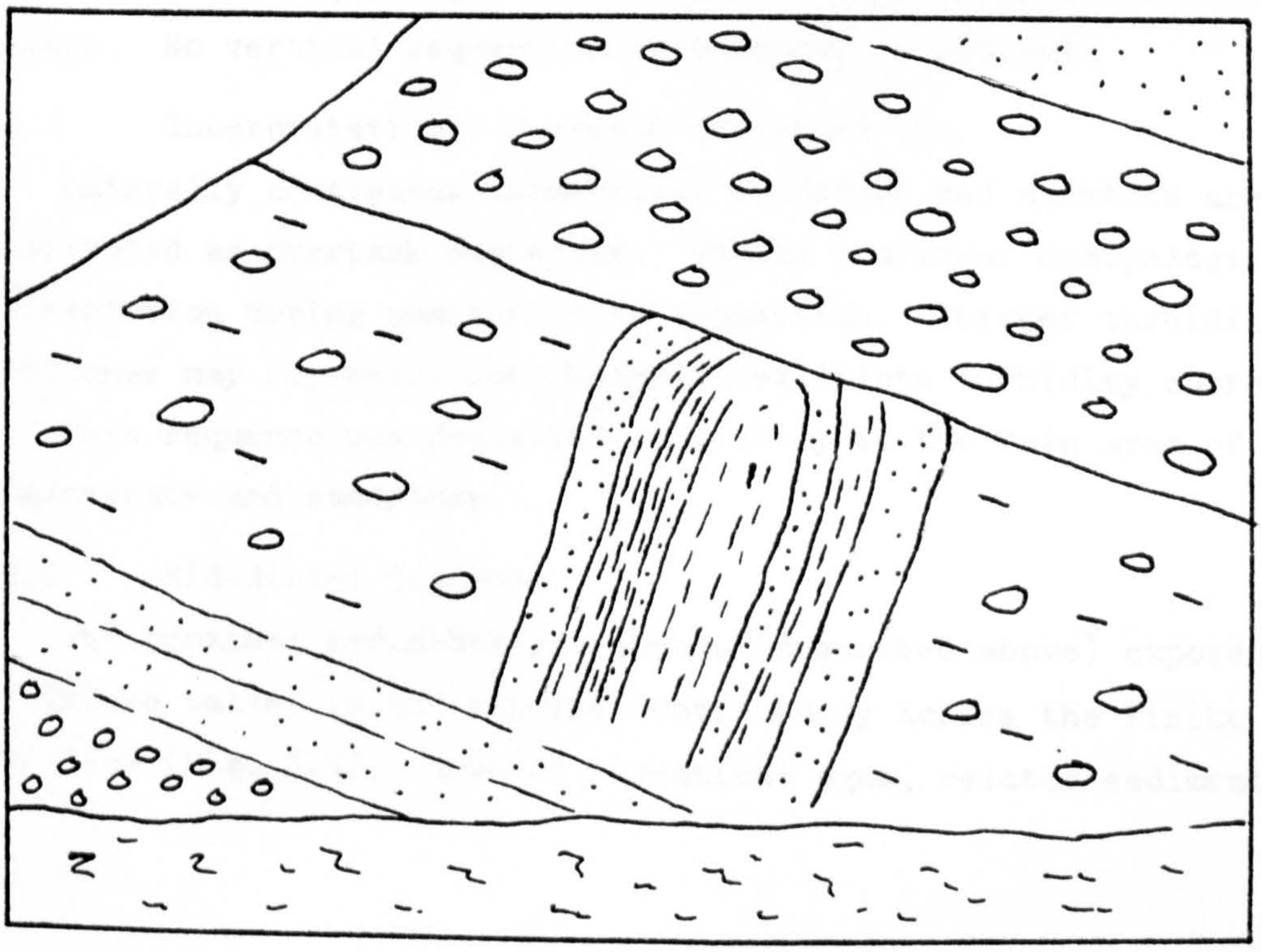

into the underlying sediment to a depth of 4 m. Massive structureless and turbiditic (Tabc) sandstones dominate (Fig. 5.13). Bases to individual beds are erosive and channelled. The channels are shallower (1-3 m) and internal structure is less complex than in the former association; channels are often symmetrical or only slightly truncational. Rare steep-sided scours show an aggradational offlapping fill (Fig. 5.14). Thin mud and chalk drapes within channel fills are laterally discontinuous as a result of erosional truncation. Tops to channels are often capped by mudstone, chalk, fine sandstone or siltstone.

5.4.4 Interpretation : Subsidiary Inner Fan Channel

This facies association is interpreted as being deposited in the inner fan region (Fig. 5.34). The scale of channel and grain size suggests deposition in a subsidiary channel located adjacent to, or more distal to, a larger channel. Turbidity currents were the main depositional process. Mud drapes indicate periods of slow deposition and possible channel switching. Gradual channel abandonment is indicated by well developed fining- and thinning-upward cycles (Fig. 5.13).

5.4.5 Thin Sandstone-Mudstone-Chalk Association

This association, which forms units between .50 m and 4.5 m thick, is characterised by thin laterally continuous fine to medium sandstone, mudstone and chalk. Sandstones are graded, sharp based, parallel laminated (Tde) or structureless. Mudstones are laminated with silt horizons, pelagic chalks show fade-out ripples and silt flasers. No vertical sequential arrangement is present.

5.4.6 Interpretation : Overbank Sedimentation

Laterally continuous thin-bedded sandstone and mudstone are interpreted as overbank sequences. Chalks represent hemipelagic sedimentation during non-turbidite deposition. Thicker turbiditic sandstones may represent non-channellised dilute turbidity currents.

This sequence was deposited marginally to the main area of conglomerate and sandstone.

5.5.0 Mid-distal Sequence

The proximal sedimentary sequence (described above) exposed in the Akdere valley is not exposed continuously across the Finike anticline (Fig. 5.1). However, identical ages, related sedimentary

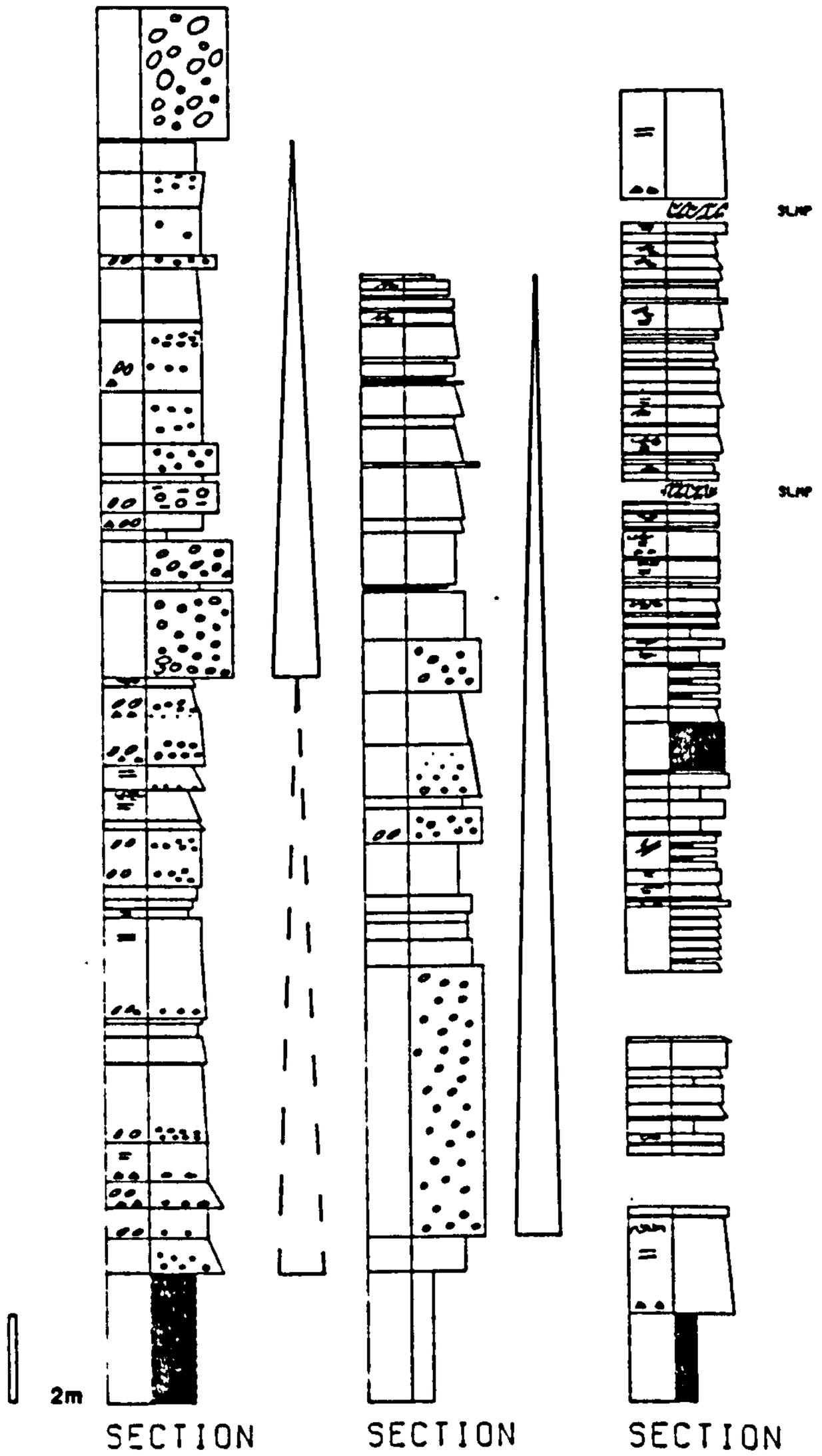

Fig. 5.13

Detailed sedimentological logs in sandstone dominated channel-fill sequences. Inner submarine fan facies association, Salir Formation. Note presence of fining- and thinning-upward cycles. See Fig. 5.1 for location of sections (Appendix C for key).

Facies Association	Bouma Divisions	Cycles	Mean sst bed thickness	Mean sst:mdst ratio within unit	% of total sequence
Channelled sst.	Tabc, Tab	fining-and thinning-upwards	~1.30 m	~50:1	~10%
Bundles of thick sst.	Tab, Tabc Tbc	variable, some fining-, some coarsening-upward cycles	~1.80 m	~2:1	~15%
Turbiditic sst. mudst, chalk	Tcde, Tde	irregular non-cyclic	~ .90 m	~2:3	~65%
mudst, pel.	-	irregular non-cyclic	-	-	~10%

TABLE 5.1 Summary Table of Mid-Fan Facies Associations.

facies and palaeocurrent dispersal patterns (Fig. 5.2) indicate the clastic sequence exposed in the Akçay and Alaçadağ valleys (Fig. 5.1) can be correlated with the sequence to the east in the Akdere valley and was originally a continuous sedimentation system. Sequences in the west represent the development of a more distal facies association. Abundant hemipelagic chalk horizons and a benthonic foraminiferal assemblage suggest a water depth of greater than 500 m (G. Adams, pers. comm., 1980). Within this sequence four facies associations are recognised, based on sandstone:mudstone ratio, bed thickness and vertical sequence textures (cf Ricci Lucchi, 1975a,b). The main features of each association are summarised in Table 5.1.

5.5.1 Channelled Sandstone Association

Channelled turbiditic (Tabc, Tab) sandstones occur as individual beds between 1.20 and 3.0 m thick (Fig. 5.15), or as amalgamated packets of up to four beds which form poorly defined fining- and/or thinning-upward units, typically 4-5 m thick. Bases are erosive into the underlying mudstone to a depth of 2-3 m over a distance of 100 m. Typical across channel variations in thickness and sedimentary structure are shown in Fig. 5.16. Thin mudstone drapes are rare within the units, sandstone:mudstone ratio is high, often in excess of 50:1. This association forms only a small part (10%) of the total sequence.

5.5.2 Bundles of Thick Sandstones

Bundles of thick (>.30 m) sandstone beds are restricted to the base and middle of the sequence in the Akçay valley (Fig. 5.17a, b). Bundles are composed of between 2 and 5 (mean 3) thick to very thick (Tab, Tabc, Tbc) sandstones interbedded with thin fine grained sandstone (Tde), mudstone and hemipelagic chalk. Individual sandstone beds are between .45 and 3.20 m thick (mean 1.80 m) with non- or slightly erosive bases. Bundles are between 3 and 15 m thick and laterally continuous over hundreds of metres. Fining- and coarsening-upward cycles between 3 and 15 m thick are present in some bundles, others show no ordered sequential arrangement. This association forms approximately 15% of the total sequence.

5.5.3 Turbidite Sandstone-Mudstone-Chalk Association

This association is the most abundant in the Akçay and Alaçadağ sequences, forming approximately 65% of the succession. Thickness ranges from .90 m to 30 m. Laterally continuous, flat-based sharp-

Fig. 5.14

Aggradational off-lapping coarse sandstone fill to small scoop shaped scour feature. Inner submarine fan channel facies association. Salir Formation.
Hammer is 34 cm long. GR. 516385.

Fig. 5.15

Channelised turbiditic sandstone bed, sandstone is parallel- and ripple-laminated and grades from coarse to medium. Interbedded pelagic chalks (white) and thin sandstones and mudstones are structureless.
Salir Formation, mid-fan association.
Stick is 1 m long. GR. 417397.

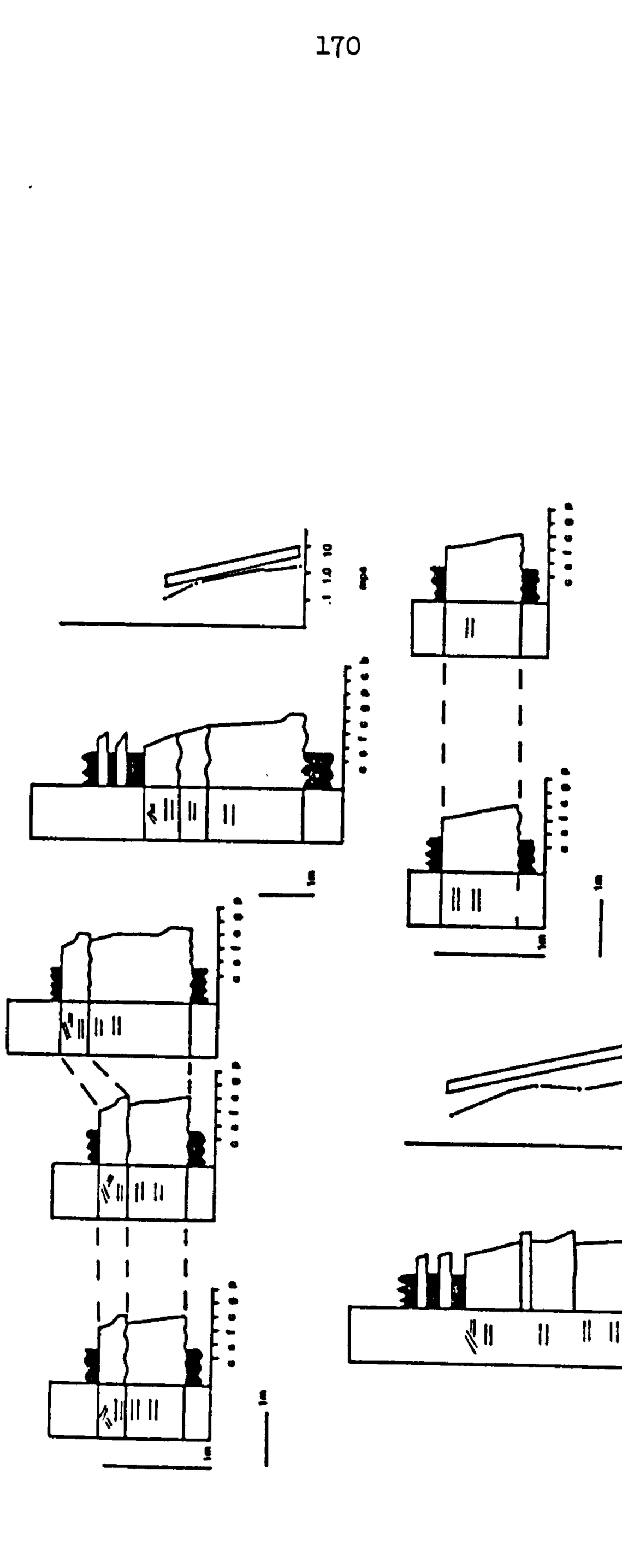

Fig. 5.16 Typical lateral and vertical variations in sedimentary structures and bed thickness in sandstone channels, mid-fan sequence, Salir Formation.

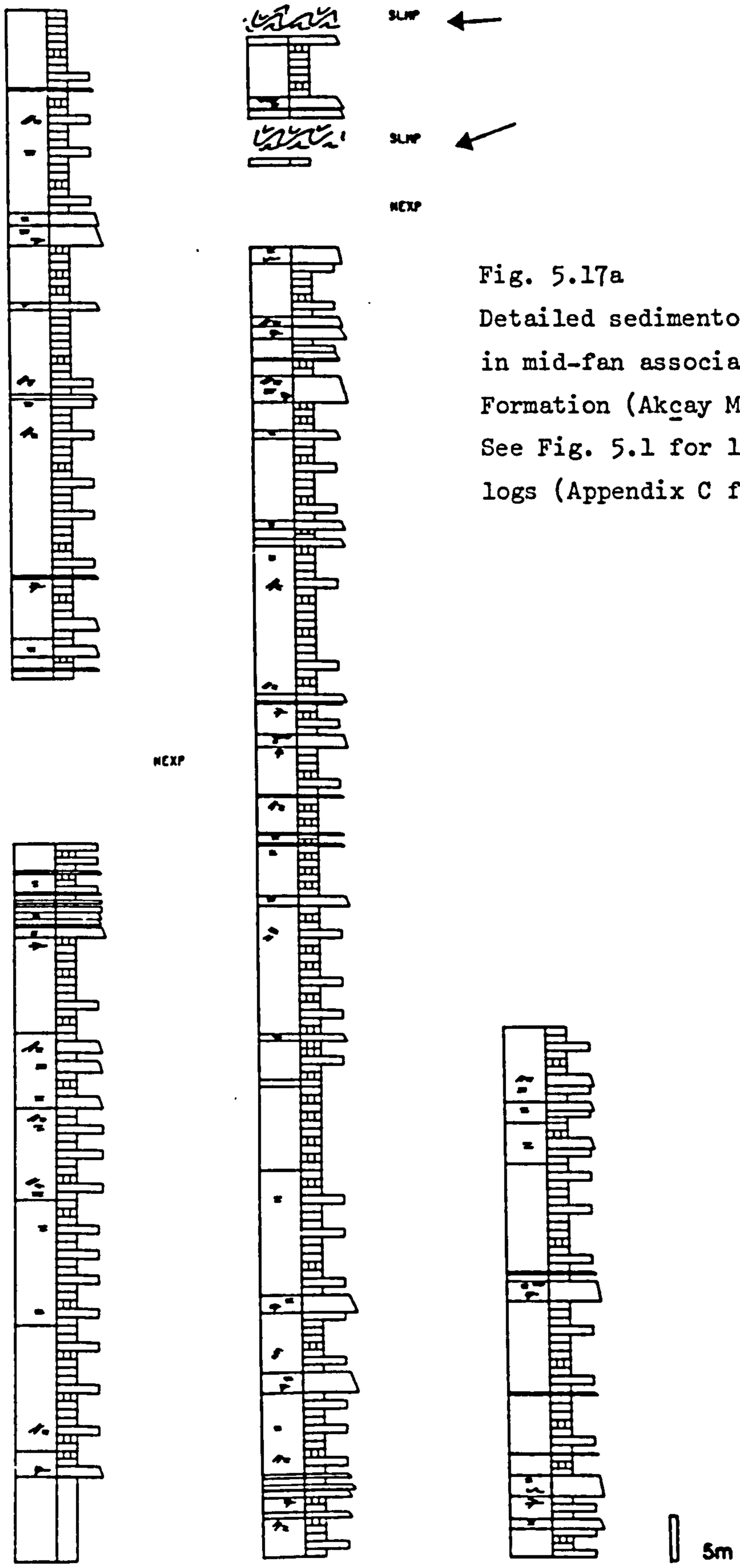

Fig. 5.17a
Detailed sedimentological logs in mid-fan association, Salir Formation (Akçay Member). See Fig. 5.1 for location of logs (Appendix C for key).

Fig. 5.17b
Detailed sedimentological logs in mid-fan sequence, Salir Formation (Akçay Member). See Fig. 5.1 for location of logs (Appendix C for key).

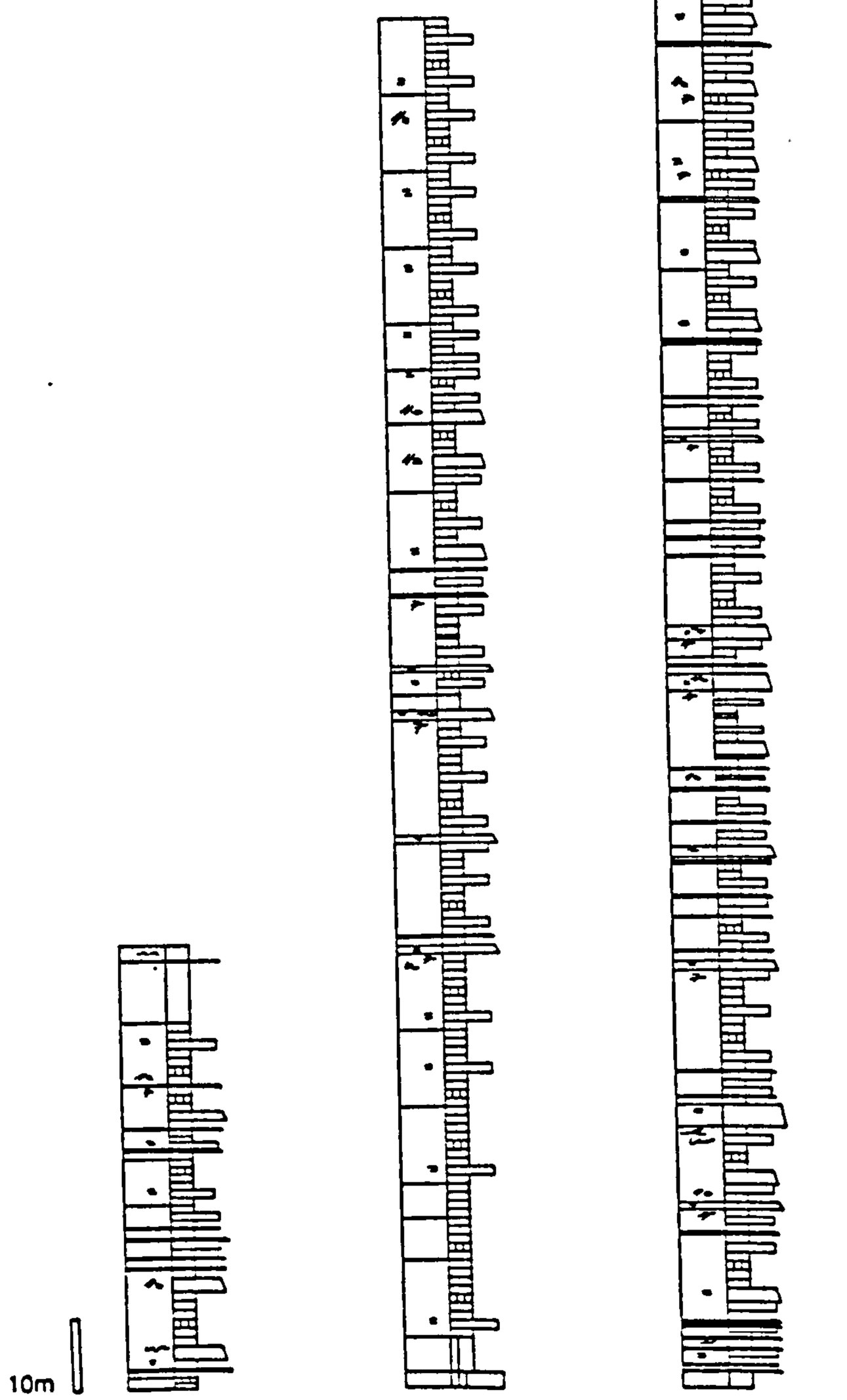

topped turbiditic sandstones (Tcde, Tde), are .02 to .50 m thick, mean .09 m, form 10-60% of individual units. Mudstones have a mean thickness of .05 m, form 20-80% of units. Pelagic chalks up to .04 m thick form 10-50% of individual units.

Layer thickness plots for this association show an irregular non-cyclic distribution with no tendency for sandstones to be segregated into packets (Fig. 5.18).

5.5.4 Mudstone-Pelagic Chalk Association

This association forms 10% of the sequence in the Akçay and Alaçadağ valleys. Comprising of units between .20 m and 3.5 m thick of interbedded finely laminated and massive mudstone (2-12 cm thick, mean 5 cm) and hemipelagic chalk horizons (0.5-4 cm thick, mean 1.5 cm). Mudstone generally forms greater than 60% of a unit.

5.5.5 Slump Structures

Description. Soft sediment intraformational slumping is confined largely to the mid-distal sequences of the Salir Formation (exposed in the Akçay and Alaçadağ valleys) but does occur rarely in the proximal sequence. Sporadically distributed, both laterally and vertically, horizons are 0.90 to 10.0 m thick.

Slump folds are restricted to thin sandstone-mudstone sequences in both areas. They have wavelengths and amplitudes of a few centimetres (Fig. 5.20) to several metres. Axial planes are inclined or recumbent. Folds are often disharmonic and range from isolated hinges to laterally persistent trains of folds. They are rarely exposed along strike, where exposed axes are discontinuous, die out and are replaced over ten to several tens of metres. Interlimb angles vary from 120 to 0°, the majority of folds are close to tight or isoclinal. Hinges are rounded to angular. Axial planes are inclined or roughly parallel to bedding.

Orientation. Over most areas slump folds have a variably N-S orientation and, where observable, a westerly asymmetry. Locally as in the Bağbeleni area (Fig. 5.1) folds with an amplitude and wavelength of several metres are orientated WNW-ESE and are asymmetric to the south (see 5.7.5).

Interpretation. The following features distinguish these folds as slump horizons formed at or near the sediment water interface:

(1) Common occurrence of chaotically deformed strata interstratified with undeformed strata.
(2) Association of slump horizons with other soft sediment deformation structures such as injection dykes.
(3) Erosional truncation of slump horizons by overlying strata (Fig. 5.20).

5.5.6 Layer-Thickness Analysis

The detailed study and analysis of vertical trends in layer-thickness and grain size in submarine fan sequences has revealed the presence of both thinning- and fining- and thickening- and coarsening-upward cycles (Mutti and Ghibaudo, 1972; Mutti and Ricci Lucchi, 1972; Mutti, 1974; Ricci Lucchi, 1975a, b). In the models produced by these authors, fining- and thinning-upward cycles represent the initiation, filling and gradual abandonment of submarine fan channels; coarsening- and thickening-upward cycles are thought to represent the gradual progradation of depositional lobes on the margin of a submarine fan.

Subsequent studies on other submarine fan sequences (e.g. Hiscott, 1980; Waldron, 1981) has revealed that asymmetric cycles of both types are far less common in many submarine fan sequences than implied by the Ricci Lucchi (1975a) model.

In the sequence studied here, only cycles within association 1 (channellised amalgamated sandstone) were recognised in outcrop. Taken as a whole the sequence is characterised by its generally acyclic or irregular layer-thickness variations (Fig. 5.19). This lends further support to the case that the recognition of thickening- or thinning-upward cycles can be rather subjective, particularly if the base is not marked by a very thick erosive sandstone (in the case of thinning-upward) or a thick mudstone unit (coarsening-upward). Many of the "cycles" published in the literature have been shown to be anomalous (Hiscott, 1980, 1981; Waldron, pers. comm. 1980).

5.5.7 Interpretation : Mid-Fan Depositional Environment

The following points indicate deposition on the mid-fan area of a submarine fan:

(I) Palaeocurrent analysis (Fig. 5.2) clearly indicates that this sequence is a more distal equivalent of the inner-fan facies association (above) exposed in the Akdere valley (Fig. 5.3). Soft sediment slump horizons in this sequence are consistent with a broadly

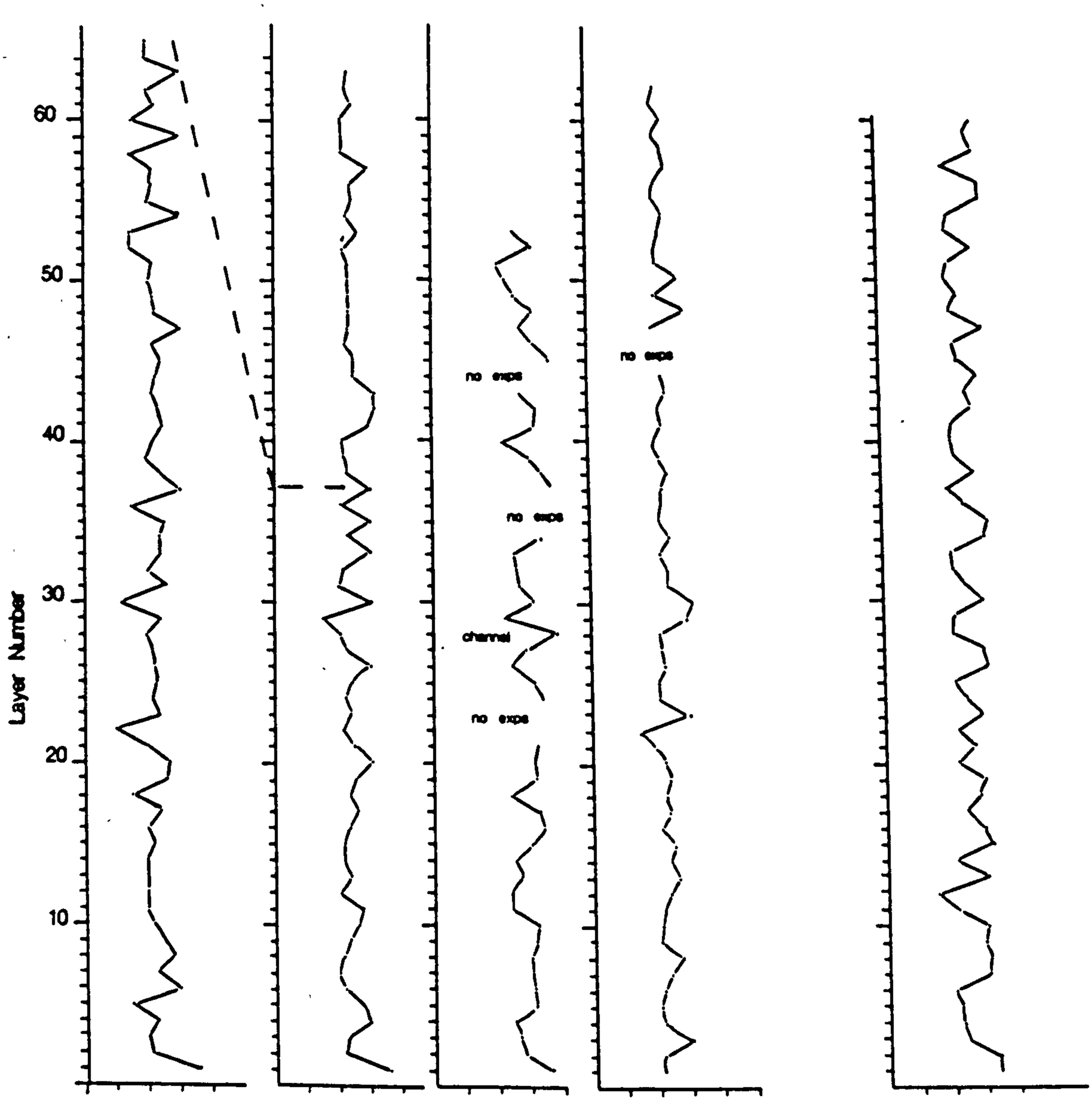

Fig. 5.18

Layer thickness plots for turbiditic sandstone-mudstone-chalk facies association, mid-fan sequence Salir Formation (Akçay Member). This association which comprises greater than 65% of the mid-fan sequences is non-cyclic. Sections in lower part of log H78 (Fig. 5.17a). Log scale for thickness.

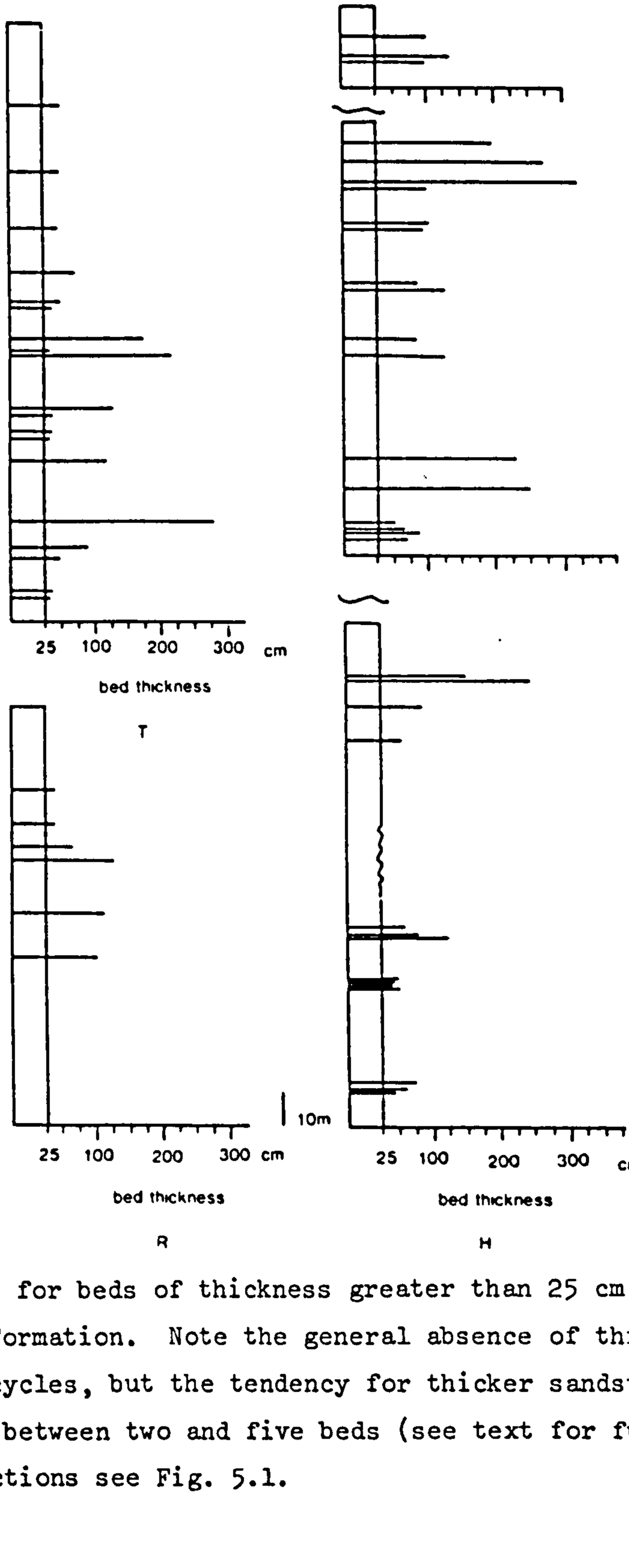

Fig. 5.19

Bed thickness plots for beds of thickness greater than 25 cm, mid-fan association Salir Formation. Note the general absence of thinning- or thickening-upward cycles, but the tendency for thicker sandstone beds to form packets of between two and five beds (see text for full discussion). For location of sections see Fig. 5.1.

ENE to WSW palaeoslope, local variations are described below (5.7.5). (II) The presence of broadly channelled amalgamated sandstone units and thick sandstone beds (Tab, Tabc) are not consistent with deposition on the lower fan or basin plain (Walker, 1979b; Reading, 1978a).

Amalgamated channelled sandstone units are attributed to deposition in broad shallow channels, 2-3 m deep and several hundred metres wide, on the upper parts of the mid-fan. Individual channellised sandstone beds represent small scale "one event" channels that are cut and filled by the same turbidite event.

Bundles of thick sandstone beds show both complex coarsening- and fining-upward cycles. Fining-upward cycles are the more dominant, they may represent broad (several kilometres wide) shallow channels. Alternatively, they may be the result of the gradual decrease in the volume of turbidity current released from the source area (Walker, 1970). Poorly defined coarsening-upward cycles may be the result of lobe progradation.

Facies association 3 is characterised by its lack of cyclicity and occasional sporadically interspersed, thick isolated sandstone beds. The lack of coarsening upward cycles, considered indicative of the non-channellised mid-fan environment, suggests either deposition marginal to a depositional lobe, or the result of the interaction of two lobes, producing an irregular sequence. Alternatively, depositional sites in this system may have undergone irregular limited progradation. The latter two seem more likely as facies association 3 comprises greater than 60% of the exposed sequences in the Akçay valley.

Facies association transitions. Analysis of facies transitions (Fig. 5.22) shows no preferred ordered sequential arrangement. All facies associations are interbedded with association 2. There is a tendency for amalgamated channel sandstones or sandstone bundles to pass upwards into pelagic chalks and mudstone (association 1). This is consistent with the latter association representing overbank sediments, that encroach on the channel as it migrates laterally.

The detailed sedimentary model is returned to in 5.11 after consideration of other data outlined below.

Fig. 5.20

Thin slump horizon in pelagic chalk-mudstone unit, truncated by overlying sandstone bed. Orientation indicates palaeoslope to the west. Salir Formation inner submarine fan sequence.
Pencil is 20 cm long. GR. 508394.

Fig. 5.21

Folded and chaotically disturbed strata beneath detached limestone block. Disharmonic folds are related to emplacement of the limestone block. Sequence is locally near vertical (youngs to the left). Salir Formation (Akçay Member) mid-fan sequence.
Face is approximately 5 m high. GR. 409406.

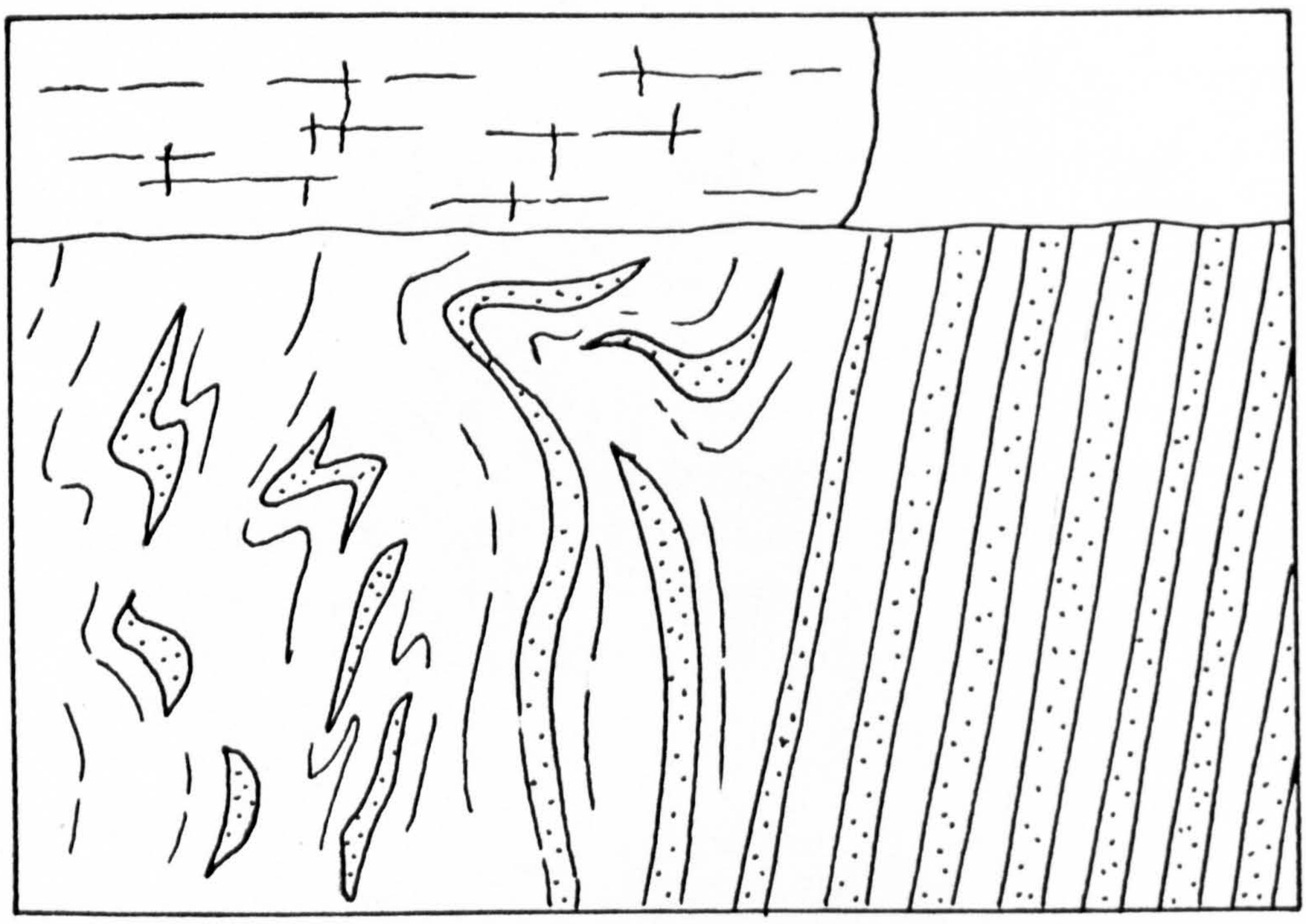

Observed Transitions

	1	2	3	4	5	6	TOTAL
1	-	11	2	1	0	0	14
2	3	-	5	6	0	15	29
3	1	10	-	0	2	0	13
4	2	4	0	-	0	0	6
5	0	3	1	0	-	1	5
6	6	11	0	0	0	-	17
							84 TOTAL

Preferred Transitions

(observed minus random transitions
expressed as probabilities)

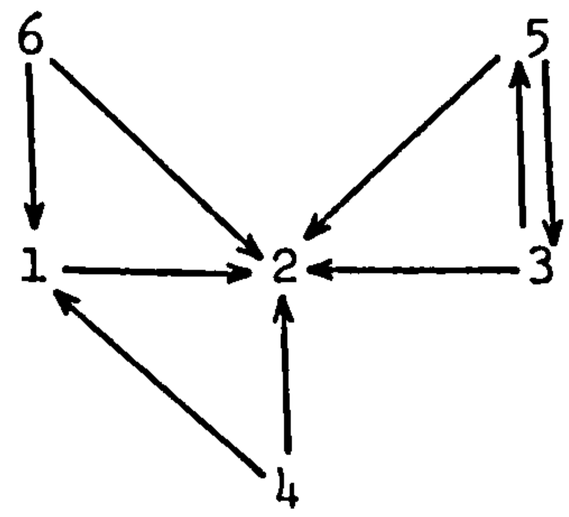

Probability >.1

Fig. 5.22

Vertical facies transition analysis for mid-fan sequence.
Based on 84 transitions.
1 - mudst/pelagic chalk; 2 - mudst/sst/pelagic chalk;
3 - sst bundles; 4 - channel sst; 5 - slumps; 6 - thick ssts.

5.5.8 Alaçadağ Area

Further west, in the Alaçadağ area (Fig. 5.1) the poorly exposed Lower (?) Miocene sequence comprises medium-to thick-bedded, dominantly flat based, turbiditic sandstones (Tabc, Tb-e), mudstones and pelagic chalks (Fig. 5.23). The sequence has a high sandstone: mudstone ratio and a more proximal aspect than much of the Akçay valley sequence. It cannot be explained by a simple E-W transition from inner fan to mid-fan. There are three possible explanations for this rather anomalous sequence:

(I) Biostratigraphic control is poor in the area and the sequence may not be exactly coeval with mid-fan sequences in the Akçay valley. The sequence may be related to the Mid to Upper Miocene fan-delta sequence (see below, 5.9.0).

(II) Another source area to the southwest. There is no evidence for this, petrographically the sandstones of this sequence are identical to other Lower Miocene sandstones of the eastern margin (Chapter 6). Rare palaeocurrent measurements are consistent with a source to the east.

(III)The sequence may represent a suprafan lobe association (Fig. 5.35). There is no direct evidence for this, although channellised sandstone bodies form less than 5% of the sequence. If the latter is correct, this sequence is likely to have been fed by one of the many E-W trending sandstone channels in the mid-fan sequence in the Akçay valley.

5.6 Pelagic Chalk Beds

Estimates of sedimentation rates. Pelagic chalk horizons are interpreted as being the result of hemipelagic "rain type" sedimentation (Chapter 3.3). The frequency and thickness of these horizons can be used to give a relative estimate of sedimentation rates throughout the sequence. In particular detailed bed-by-bed measured sections can be used to estimate the mean turbidity current frequency.

Pelagic carbonate sedimentation rates for Miocene sequences of the Pacific, Atlantic and Indian oceans vary between 1 and 2 cm/1000 years (Davies *et al.*, 1977). For the Lower Miocene the mean is around 1 cm. It is likely that similar rates of pelagic sedimentation can be applied to this sequence. Hemipelagic chalk horizons throughout most of the sequence vary between 0.5 and 4.0 cm thick, with a

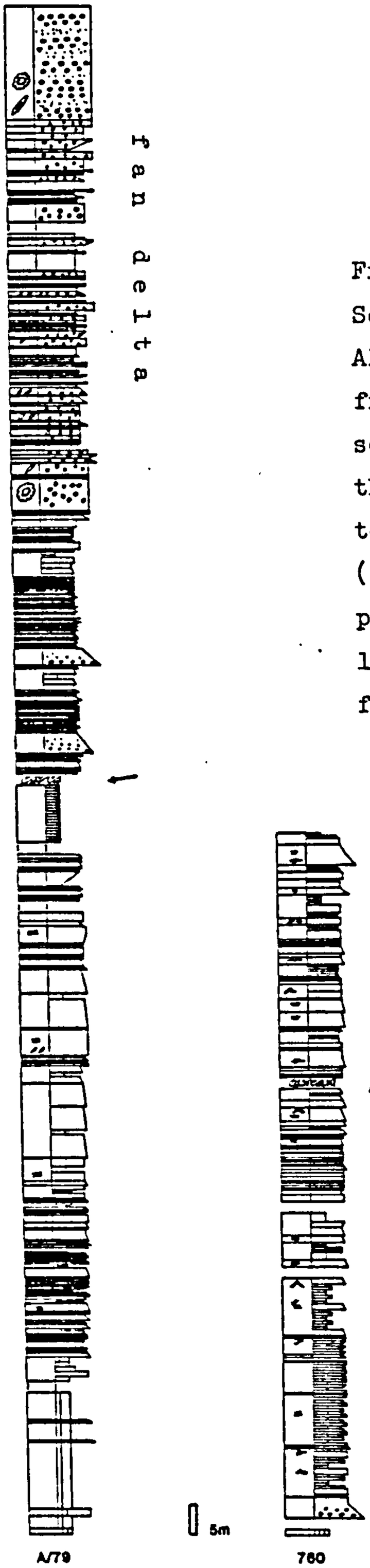

Fig. 5.23
Sedimentological logs in the Alaçadağ area showing transition from submarine fan to fan-delta sequence. Note proximal aspect of the submarine fan sequence (see text for discussion). Slump horizons (arrowed) indicate a general E→W palaeoslope. See Fig. 5.1 for location of sections (Appendix C for key).

mean of 1 cm. Assuming interbedded sandstone and mudstone to be the product of one instantaneous turbidite event, it is calculated that one turbidite (mudstone or sandstone) occurred approximately every 1,000 years. By removing the interbedded mudstone and summing the pelagic intervals between sandstone turbidite events, it is possible to calculate the time interval between successive *sandstone* turbidites (Fig. 5.24).

Well exposed mid-fan inter-depositional lobe sites (?) in the lower and middle parts of the Salir Formation (sections a, b, c, Fig. 5.17a) give periodicities of 45,000 to 75,000 years for the time interval between the deposition of thick (>.30m) sandstone turbidites. Smaller sandstones occur every 2-5,000 years (Fig. 5.24).

Indicators of submarine fan sub-environments. Pelagic chalks reach thickest development and greatest frequency in areas of low net and periodic deposition. In a submarine fan model these areas are unlikely to be located on the basin plain or outer fan as might be expected. In a mid-fan depositional lobe a turbidity current dumps its load over a limited area located closest to the distributary channel open at the time. On other parts of the mid-fan lobe or overbank areas, long time gaps occur during depositional events, allowing the accumulation of thick pelagic horizons. However, as the current moves distally it spreads out, so that on the outer fan and basin plain it covers a much larger area restricting the frequency and thickness with which pelagic horizons occur. Pelagic chalk horizons in some sequences may prove useful in delineating submarine fan sub-environments. By calculating the upward transition between sandstone, mudstone and chalk, two transition probability indices can be derived:

P_1 sst/mdst → pel chalk - a parameter expressing the probability of long periods of time between successive turbidite events. A high index is characteristic of overbank areas, in this case associated with channelled sandstone units.

P_2 sst/mdst → mdst/sst - a parameter expressing the probability of "continuous" deposition. A high index is characteristic of depo-centres such as active depositional lobes and outer fan environments. Caution must be exercised in the application of this approach, as inactive lobes may produce a similar high P_1 as an overbank channel area. In the former pelagic chalks are likely to be thicker with fewer turbidites.

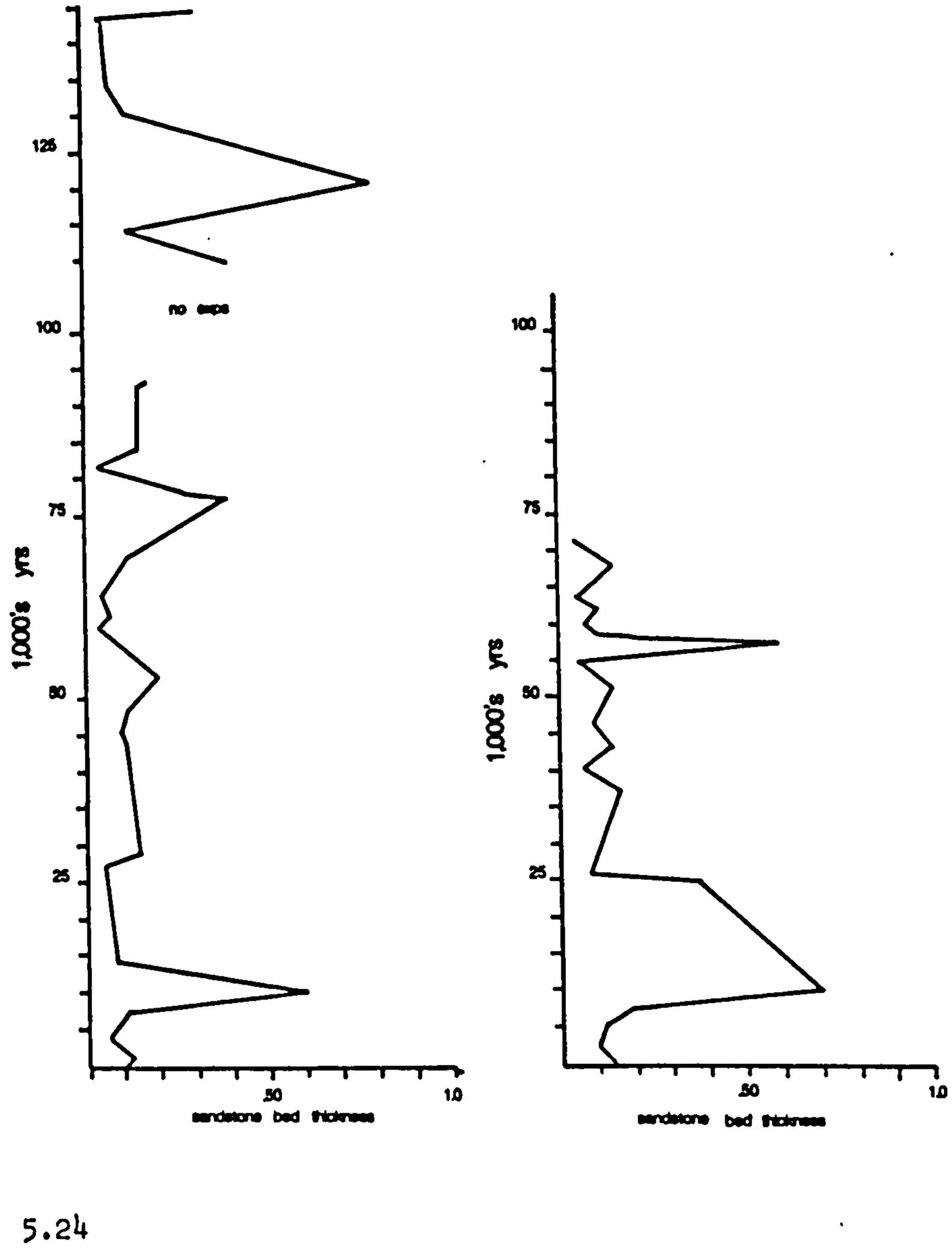

Fig. 5.24

Sandstone layer thickness (in metres) against time (based on pelagic chalk accumulation rate of 1 cm/1,000 years). Well exposed mid-fan sequence. Salir Formation (Log H78, Fig. 5.17a).

5.7.0 Syndepositional Tectonism

Several exotic facies types within the Salir Formation suggest syndepositional tectonic activity.

5.7.1 Debris Flow "Olistostrome"

This facies is well exposed in the north of the Akdere valley, where it interfingers with the inner fan sequences and in a narrow belt in the Akçay valley interbedded with mid-fan sequences (Fig. 5.25). In the north of the Akdere valley (Fig. 5.1) turbiditic sandstone (Tbce, Tcde), mudstone and chalk are overlain by approximately 350 m of interbedded matrix-supported conglomerate, thin sandstone (Tde), mudstone and pelagic chalk (Fig. 5.26).

Matrix-supported boulder conglomerates consist of clasts of *Halobia* limestone, basalt, radiolarian chert, mafic cumulates, gabbros and dolerites supported in a green-grey mudstone matrix. Clast proportions range from 5-35%. Tabular rafts of sandstone and mudstone, up to 1.5 m long, are also present. Clasts range in size from a few millimetres to several metres, modal size is around 0.50 m. Smaller clasts are poorly to moderately rounded (R1-3), larger clasts are angular (A3-4) and frequently lozenge shaped or, in the case of chert, tabular bed fragments. Bed thickness ranges from 0.70 to 8.0 m, amalgamated beds form units up to 60 m thick (Fig. 5.26). Both normal and inverse grading and rigid plugs are recognised.

The above textural features are indicative of a debris flow mechanism of deposition (3.4). Interbedded turbiditic sandstone and pelagic chalks are consistent with this interpretation. No sequential upward transition in bed thickness, clast size or composition is observed.

5.7.2 Detached Blocks of Ophiolite Affinity

Large blocks up to 500 m long and 100 m thick were not emplaced within a debris flow, but as gravity slid masses. Most of the blocks are tabular, approximately parallel to bedding. Larger blocks are restricted to *Halobia* limestone. Chert, basalt and serpentinite form blocks up to 8 m long and several metres thick. In one instance a block comprises of basalt overlain by radiolarian chert.

In the Akçay valley a 13.50 m thick debris flow unit of similar lithology occurs in the central part of the sequence (Fig. 5.25) in association with detached limestone blocks and carbonate breccias

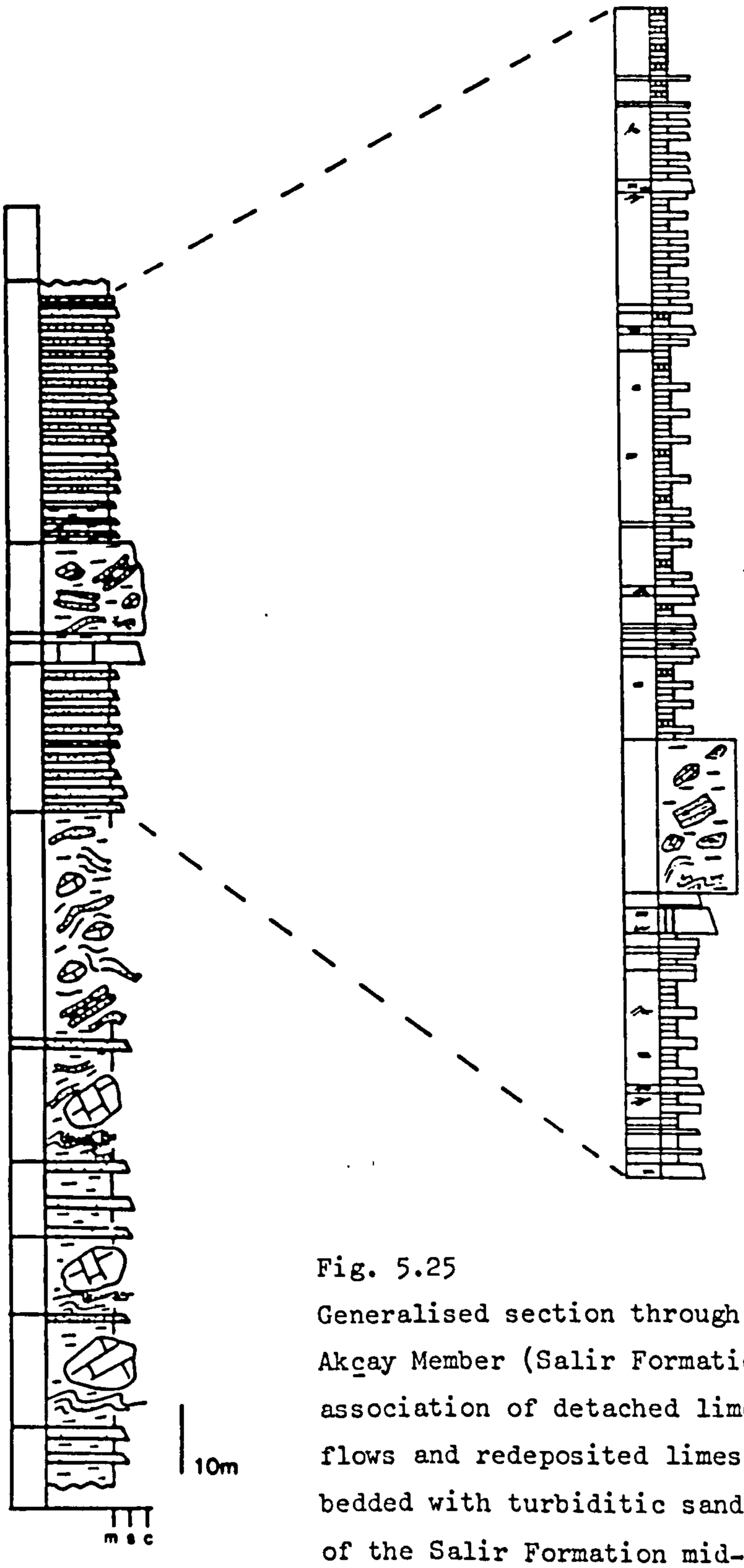

section J

Fig. 5.25
Generalised section through central parts of the Akçay Member (Salir Formation). This shows the association of detached limestone blocks, debris flows and redeposited limestone breccias, interbedded with turbiditic sandstones and mudstones of the Salir Formation mid-fan sequence.
See Fig. 5.1 for location of section.
(Appendix C for key).

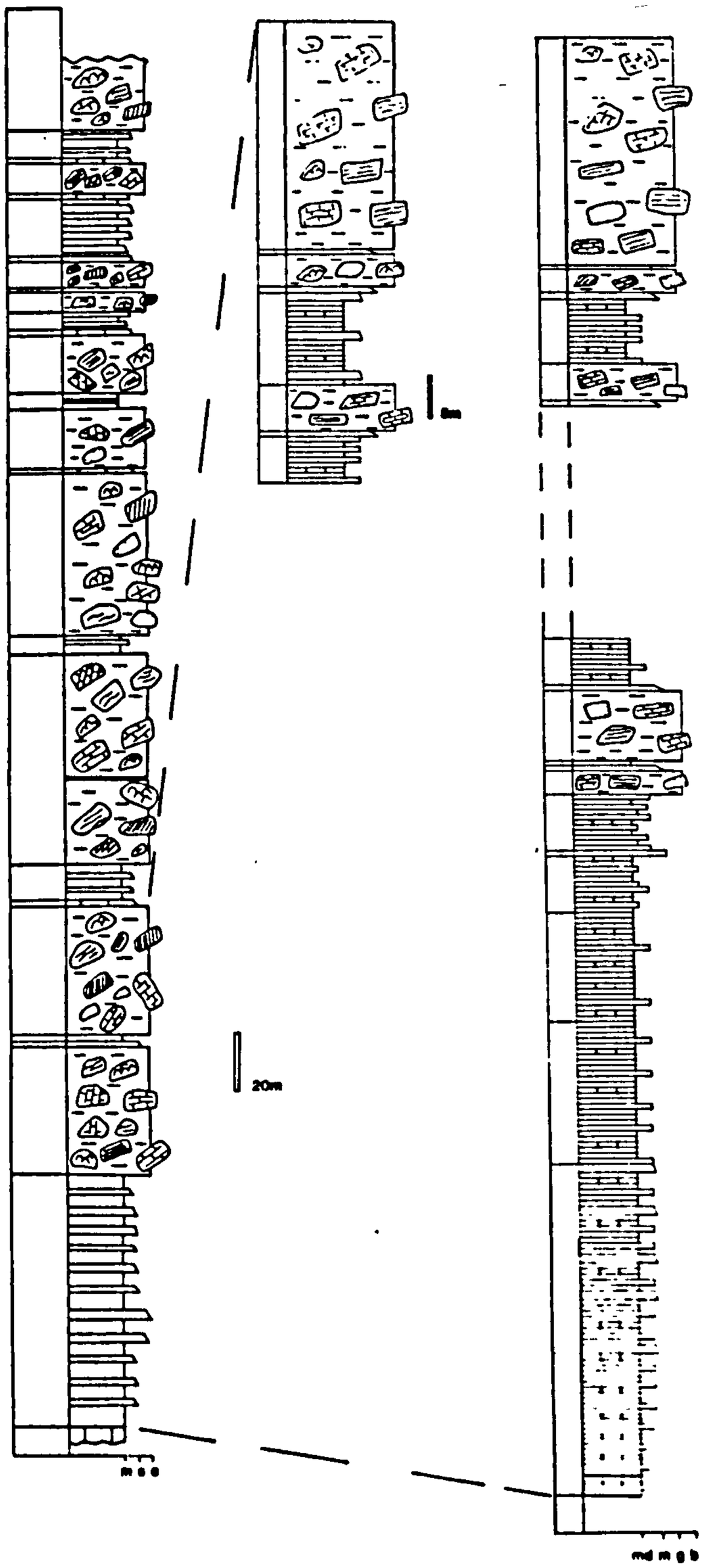

Fig. 5.26

Generalised sections in debris flow olistostrome sequence in the north of the Akdere valley (Salir Formation). See Fig. 5.1 for key (Appendix C for key).

(see below, 5.7.3).

Angular clasts of ophiolite derived material and foundered sandstone-mudstone rafts are supported in a mud matrix. The proportion of clasts ranges from 15-20%.

Clast lithologies are consistent with derivation exclusively from the Antalya Complex. Angular non-abraded clasts in the debris flows suggest that the clasts have not been transported through a high energy, fluvial or shallow marine environment prior to redeposition (cf inner fan debris flow, 5.4.1). The lack of current abraded clasts and local extent of this facies is consistent with derivation from submarine fault scarps (see below, 5.7.5).

5.7.3 Detached Limestone Blocks

Isolated blocks of partially recrystallised limestone occur within the mid-fan sequence in the Akçay valley. The blocks range in size between 5 and 20 m long and up to 20 m across. They comprise a variety of platform carbonate lithologies ranging in age from Maastrichtian (?) to Miocene (Şenel, pers. comm. 1979). Internally the blocks are little or undeformed. Detailed mapping (Fig. 5.27) reveals the blocks to be restricted to a central belt in the Salir Formation, well exposed along the middle of the Akçay valley between Çatallar and Akçay (Fig. 5.27). The belt is approximately 100 m in vertical thickness and thins to the southeast. Associated with this belt are several chaotic soft sediment slump horizons, debris flows (above) and carbonate breccias described below.

Direction of emplacement. The majority of long axes of the blocks are orientated NW-SE (Fig. 5.28); bedding is variably inclined to the NE (Fig. 5.27).

Studies of olistostromes in Italy and Cyprus have indicated that olistoliths can be treated as pebbles in debris flows or stream gravels. The direction of emplacement lies opposite to the direction of dip in most olistoliths (Gorler, 1976; Robertson, 1977a). Below and adjacent to the blocks sedimentary layering is extensively disturbed (Fig. 5.21). Deformed horizons are between 10 m and 20 m thick, depending on the size of the detached block. They are generally completely disrupted with no indication of emplacement direction. Occasional sense of overturn in the underlying sediments indicates a broadly NE to SW direction of emplacement, consistent with the orientation of the blocks (Fig. 5.28).

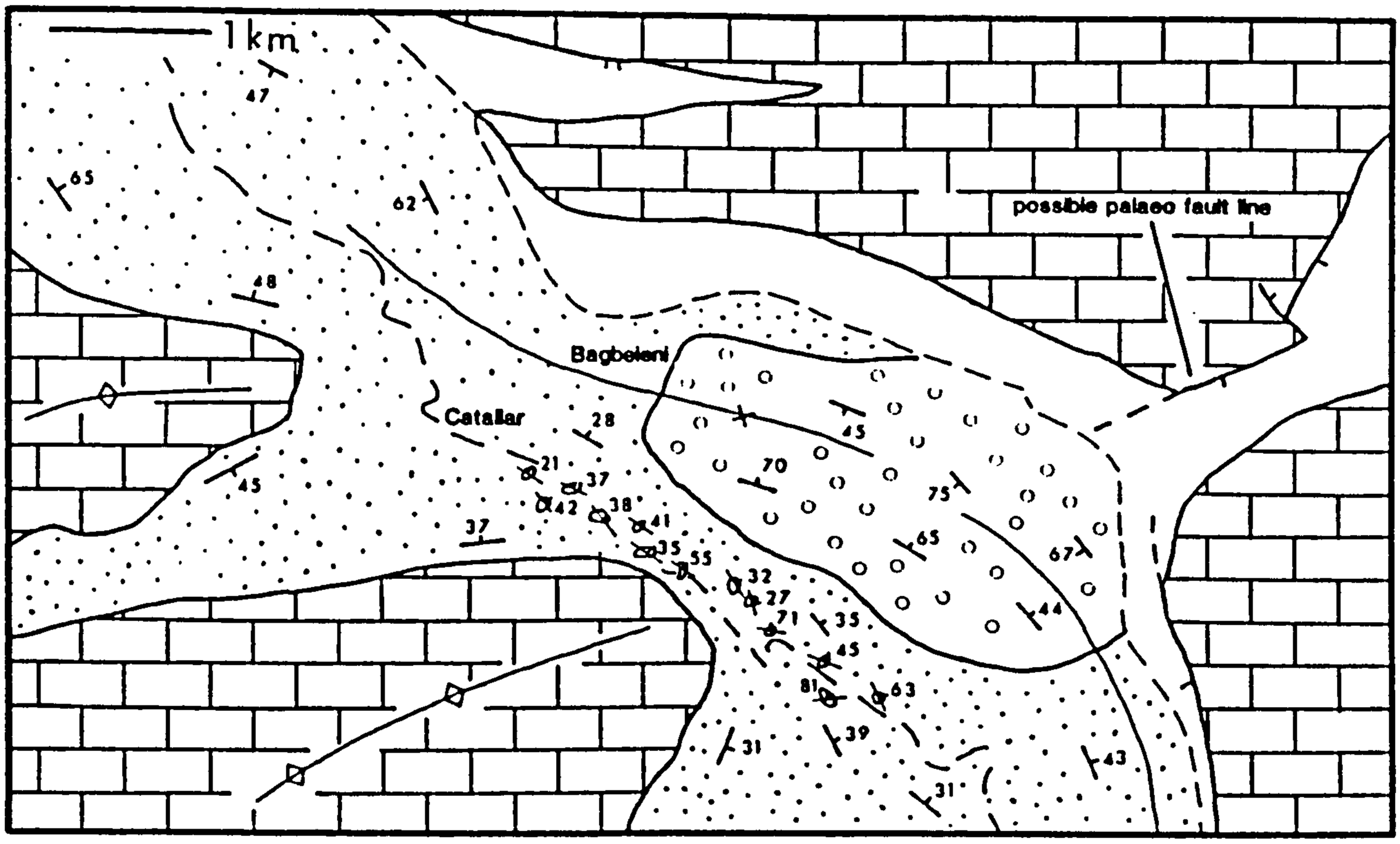

Fig. 5.27 Distribution of detached limestone blocks within the Salir Formation (Akçay Member, dotted). Carbonate platform - hatched, Bağbeleni Member - open circles.

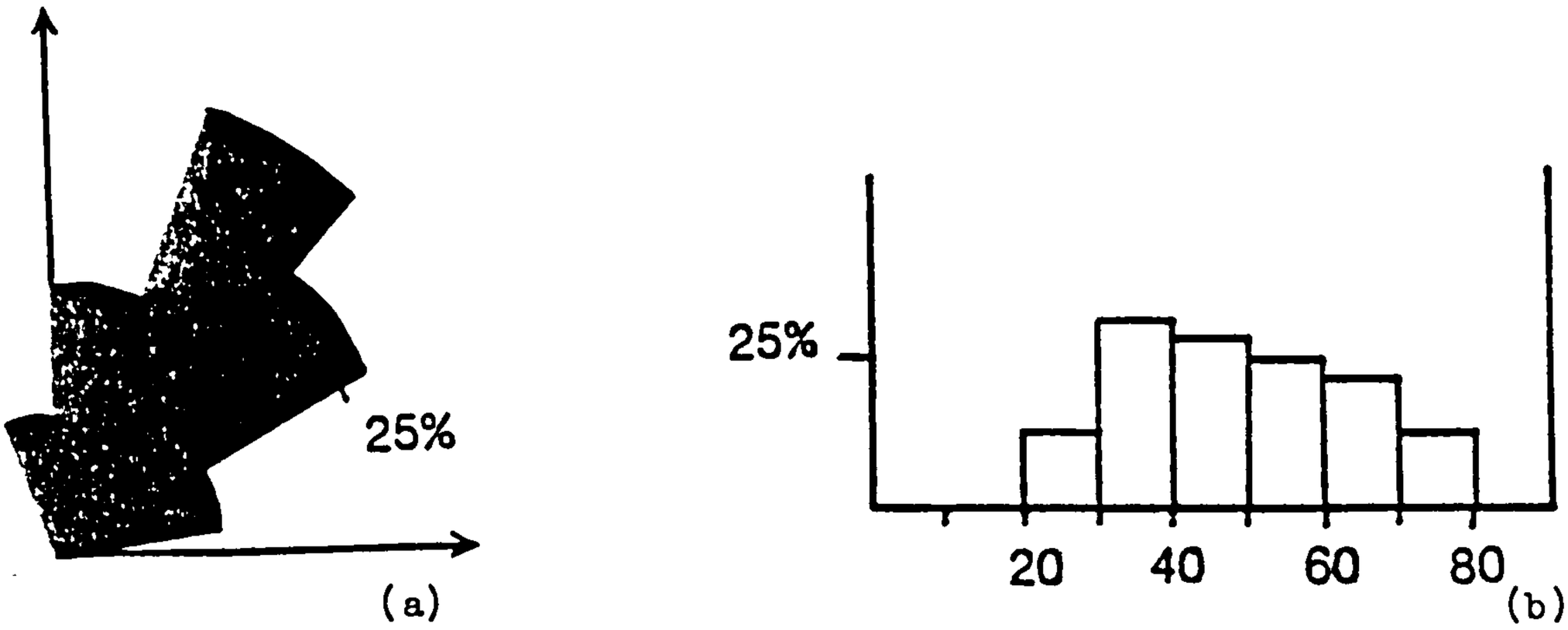

Fig. 5.28 Orientation of detached limestone blocks in the Salir Formation (Akçay Member).

(a) direction of dip of detached block long axis.

(b) angles of dip of strata (bedding) within block.

From sediment deformation below blocks and by analogy with olistolith orientation in olistostromes, the direction of emplacement was generally from NE to SW.

The blocks were emplaced by a combined process of sliding and rafting downslope from the NE to SW. Their orientation suggests release from uplift along a fault, located to the northeast of Bağbeleni (Fig. 5.27), thought to have been active at the time (see below, 5.7.5).

5.7.4 Bioclastic Carbonate Breccias

Spatially associated and interbedded with the two facies described above, in both the Akdere and Akçay valleys (Fig. 5.1) are bioclastic limestone breccias between 1.0 m and 4.50 m thick. Beds commonly consist of the A and B division of the Bouma cycle. In the Akdere valley individual beds thin consistently southwards. Imbrication of shale rip-up clasts at the base of beds is consistent with generally north to south palaeocurrents. Lithologically the breccias consist of an admixture of carbonate platform lithoclasts, mainly calcilutite and abundant bioclastic debris, often greater than 70%, comprising mainly algal, foraminiferal and shell debris. The composition indicates a mixed carbonate platform limestone, bioclastic source. Southwards thinning and the association with detached limestone blocks suggests they may have been derived from small carbonate build-ups situated along syndepositional fault scarps which exposed the underlying carbonate platform sequence (see below, 5.7.5).

5.7.5 Summary of Syndepositional Tectonic Activity

Syn depositional tectonic activity affecting this sequence can be subdivided into two components: (1) submarine faults affecting the Antalya Complex; (2) faulting in the carbonate platform that may be related to fault movements in the Antalya Complex.

Evidence outlined above suggests that during the deposition of the Lower Miocene sequence of the Salir Formation the carbonate platform was exposed along a probable NE-SW trending fault, situated northeast of Gökbuk (Fig. 5.1). Large detached limestone blocks were released off the fault scarp, bioclastic breccias may have been derived from small carbonate build-ups situated along the fault. Very angular platform limestone clasts suggest that the fault was not subaerially exposed.

Mid-fan sedimentary sequences with broadly similar palaeocurrent trends and sequence styles, either side of a line extended from the present fault into the basin (Fig. 5.17b, Sections T and N) indicate that the fault was not present in the centre of the basin. Although slump horizons locally orientated to the southeast approximately along strike from the fault line indicate some tectonic instability.

In the south of the Akdere valley the Antalya Complex was clearly subaerially exposed from L. Miocene times onwards, as evidenced from the well rounded ophiolite-derived sediments. In the extreme north the sequence lacks the abundant well rounded, turbiditic sandy conglomerate, typical of the inner fan environment. Instead ophiolite-derived debris flows form an olistostrome type sequence. Evidence outlined above suggests derivation from a submarine fault scarp and indicates that in this area the Antalya Complex was locally not subaerially exposed. The location of this facies and associated submarine fault coincides with a possible fault line in the carbonate platform (Fig. 5.1). This is further discussed in 5.11.

5.8.0 Coarsening-Upwards Transition

In the Akdere valley (Fig. 5.1) lower parts of the Salir Formation are transitional upwards into a melange produced during the final stage of emplacement of the Antalya Complex (10.6.3).

In the Akçay valley (Fig. 5.1) the transition upwards into the Bağbeleni Member is abrupt. Thin-bedded turbiditic sandstone, mudstone and chalk of the Akçay Member are overlain by a sequence of conglomerates (Figs. 5.29, 5.30). The transition occurs over approximately 20 m (Fig. 5.29). Thin sandstones are progressively replaced by thick-bedded, coarse massive sandstone and matrix- and clast-supported conglomerate interbedded with mudstone and chalk.

In the Alaçadağ area the upwards transition to the Bağbeleni Member is gradual and less marked. Thick coarse sandstone, granule conglomerate mudstone and chalk are progressively replaced over approximately 50 m by interbedded coarse sandstone and conglomerate (Fig. 5.23).

5.8.1 Bağbeleni Member

The Lower Miocene submarine fan sequence above is overlain by a thick (ca. 250 m) sequence of conglomerate and sandstone, the Bağbeleni Member of Middle Miocene (Serravallian?) age (Chapter 2).

Fig. 5.29 General section showing coarsening-upward trend in Bağbeleni Member (fan-delta sequence). A, B, C and D refer to position of sedimentological logs in Fig. 5.30.

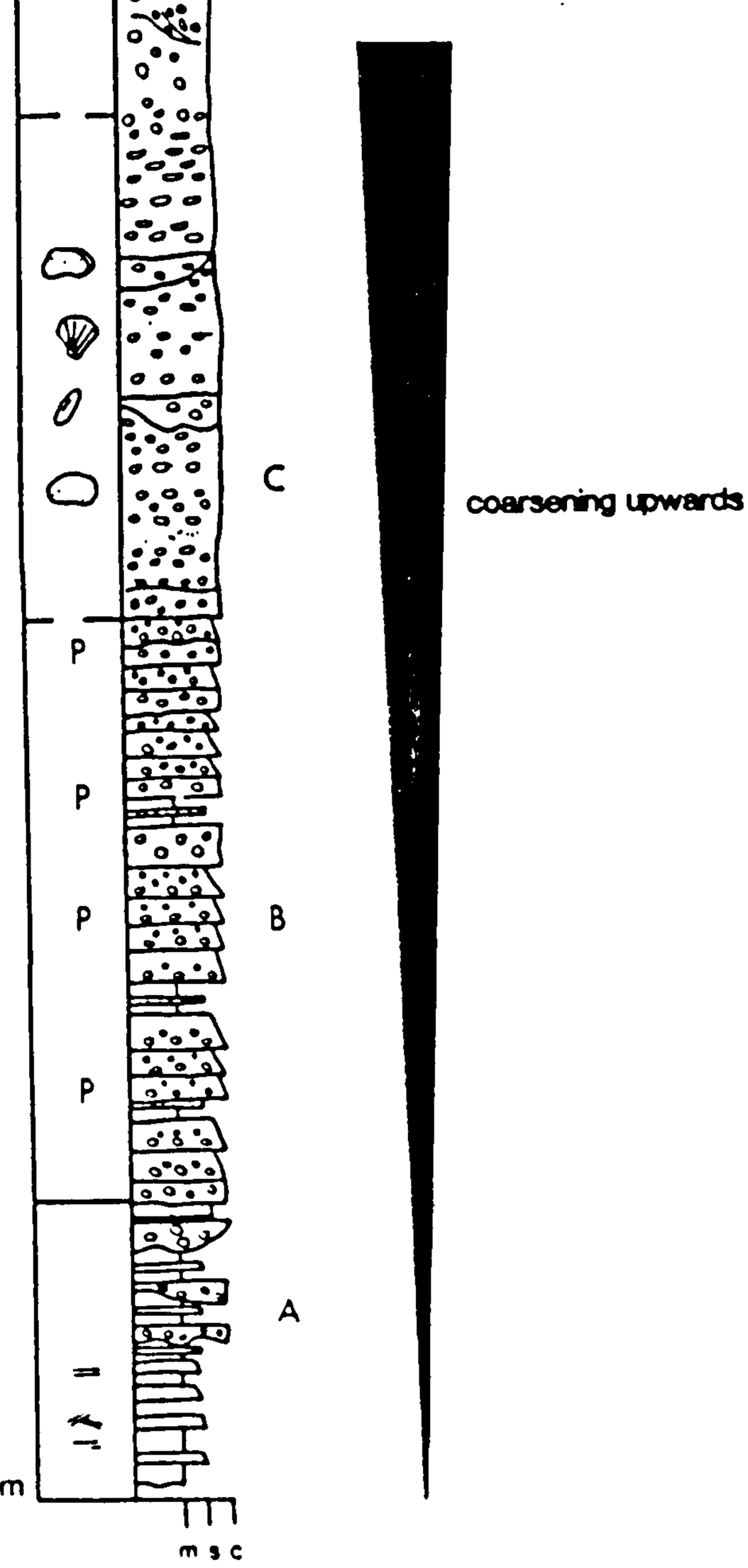

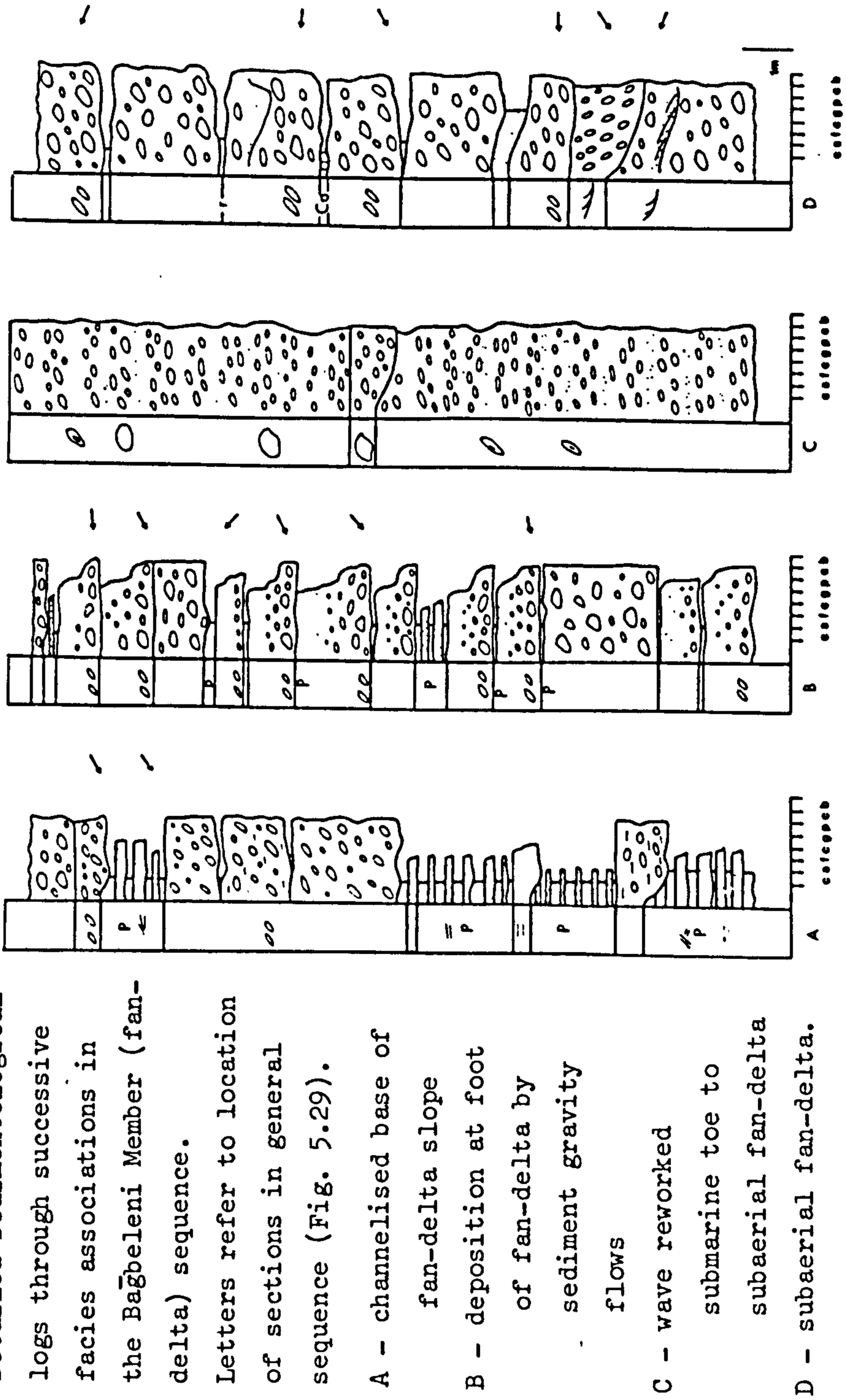

Fig. 5.30
Detailed sedimentological logs through successive facies associations in the Bagbeleni Member (fan-delta) sequence.
Letters refer to location of sections in general sequence (Fig. 5.29).
A - channelised base of fan-delta slope
B - deposition at foot of fan-delta by sediment gravity flows
C - wave reworked submarine toe to subaerial fan-delta
D - subaerial fan-delta.

This sequence represents the second major incursion of coarse terrigenous sediment along the eastern margin of the basin.

5.8.2 Provenance

Composition. The sediments of this sequence consist of a complete admixture of rock types. Clast types in the conglomerate (Chapter 6) consist of well rounded (R3-4) dolerite, gabbro, chert and ultrabasic cumulates with subordinate serpentinite and basalt. Poorly rounded platform limestone clasts generally form less than 5%. Sandstones are poorly sorted, rock fragments predominate. Dolerite, basalt, serpentinite, chert, quartz and feldspar are poorly cemented by carbonate (Chapter 6). Bioclastic content is low, 0-20%, comprising mainly foraminiferal and algal fragments.

Palaeocurrents. Cross-stratification in sandstone and conglomerate and imbrication in the latter indicate that for the most part palaeocurrents were variably from east to west (Fig. 5.3).

5.9.0 Sedimentary Facies Association

Limited outcrop and poor exposure restricts the discussion of these sediments to a vertical sequence type of analysis.

The sedimentary sequence can be subdivided into four associations that occur vertically stacked in the following sequence:

conglomerate-sandstone (1) → conglomerate-chalk (2) → stratified conglomerate-sandstone (3) → conglomerate-calcrete (4).

5.9.1 Conglomerate-Sandstone Association

Description. This association marks the transition upwards from the Akçay Member to the Bağbeleni Member of the Salir Formation.

Massive matrix-supported conglomerate between 0.70 m and 11.0 m thick are interbedded with normally graded conglomerate, disorganised conglomerate and coarse to very coarse sandstone (Fig. 5.30). Conglomerates are often lenticular over several metres and erosive into the underlying sediment. Turbiditic sandstone (Tab, Ta) are successively replaced by massive and graded sandstone upwards (Fig. 5.30). Interbedded mudstone and pelagic chalk units are between 0.30 and 3.50 m thick.

Interpretation

Turbiditic sandstone deposits at the base are gradually replaced

by conglomerates deposited by sandy debris flows and turbulent sediment gravity flows (Chapter 3). The marked upward coarsening reflects progradation of a coarse grained sediment body.

This sequence represents dominantly channellised deposition below wave base, at the foot of a fan-delta slope.

5.9.2 Conglomerate-Chalk Association

Description. This association is well developed in the Akcay valley (Fig. 5.1). It comprises normally graded clast-supported conglomerate between 0.50 and 1.20 m thick, interbedded with thin (~1 cm) chalk horizons, lenticular coarse sandstone and rare mudstone. Conglomerate beds are laterally continuous over 200+ m, bases are only slightly scoured and non-channelled (Fig. 5.30). Maximum clast size is 0.35 m. Units between 5m and 15 m thick are interstratified with disorganised conglomerate beds up to 10.5 m thick (Fig. 5.30). Throughout this sequence a gradual upward increase in grain size is observed.

Interpretation

Pelagic chalk horizons are consistent with deposition in a marine environment below wave base. Conglomerate textures indicate deposition by sediment gravity flows. Moderately sorted graded conglomerates were deposited by turbulent events, disorganised conglomerates by sandy debris flows transitional to density modified grain flows. Chalks accumulated between depositional events. The upward increase in percentage of conglomerate and grain size (Fig. 5.29) indicates progradation of a coarse sediment body. This association is interpreted to have been deposited at the foot of a fan-delta (coastal alluvial fan slope). High-gradient gravel-bedload streams that remain braided to the coast, in times of flood, transport a very high coarse sediment load. On entering the sea they will either dump the majority of their bedload at the river mouth or develop density underflows (Bates, 1953). In the former, slumping of poorly consolidated gravitationally unstable sediment may result in redeposition down the delta front (Collinson, 1969; Carter and Norris, 1977). In the latter case, with the development of density underflows, composed dominantly of conglomerates, similar sequences may be developed at the foot of a fan-delta. Redeposition of coarse grained material down the delta slope is by a combined process of sliding, saltation and turbulent flow.

5.9.3 Stratified Conglomerate-Sandstone Association

Description. This association consists of stratified cobble-pebble conglomerate between 0.30 and 0.70 m thick, interbedded with subordinate pebbly sandstone (Fig. 5.30). Well rounded clasts are up to 0.50 m in diameter. Rare disorientated coral blocks are up to 0.40 m in length. Silty medium to coarse sandstone, which forms lenticular horizons less than 0.05 m thick, contains foraminiferal fragments.

Interpretation

Although lacking in abundant marine fauna, coral blocks and foraminiferal fragments indicate a marine environment. High energy is suggested by:

(I) coarse grain size, complete lack of sediment finer than medium sand;

(II) absence of pelagic chalk horizons;

(III) absence of fossil remains.

Stratified conglomerate is consistent with wave reworking in a shallow marine environment (Clifton, 1973, see 3.3.2).

This association represents shallow marine reworking of the submarine toe to an alluvial fan or fan-delta top. The lack of cross-stratification is a result of the coarse grain size and low tidal current influence (high energy).

5.9.4 Conglomerate-Calcrete Association

Description. This association consists of poorly to moderately sorted red to green clast-supported conglomerate (Gm), subordinate lenticular, structureless, sandstone, green-grey mudstone, rootlets and rare calcrete horizons.

The conglomerate which comprises greater than 90% of the association, consists of moderate to well rounded (R2-4) pebbles, cobbles and boulders with a maximum clast size of 0.15 to 0.40 m. The conglomerates are entirely clast-supported, massive conglomerate (Gm) dominates forming 70% of the sequence (Fig. 5.32). Subordinate matrix-rich (Gmr), planar (Gp) and trough-cross-stratified (Gt) conglomerate also occur. Massive conglomerate forms units up to 50 m thick, with discontinuous clay, silt and sandstone lenses. Individual depositional units cannot be delineated. Planar and trough-cross sets form lenticular wedge-shaped units several metres thick and up to 20 m across (Fig. 5.31).

Fig. 5.31

Planar-cross-stratified conglomerate (Gp) passing down current (to the left) into cross-stratified sandstone. In this instance this facies is probably the result of migrating bedforms at high-flood stage. The cross-stratified unit overlies massive conglomerate (Gm) which shows well developed imbrication. Alluvial fan sequence (subaerial fan-delta) Salir Formation (Bağbeleni Member). Stick is 1 m long. GR 394290.

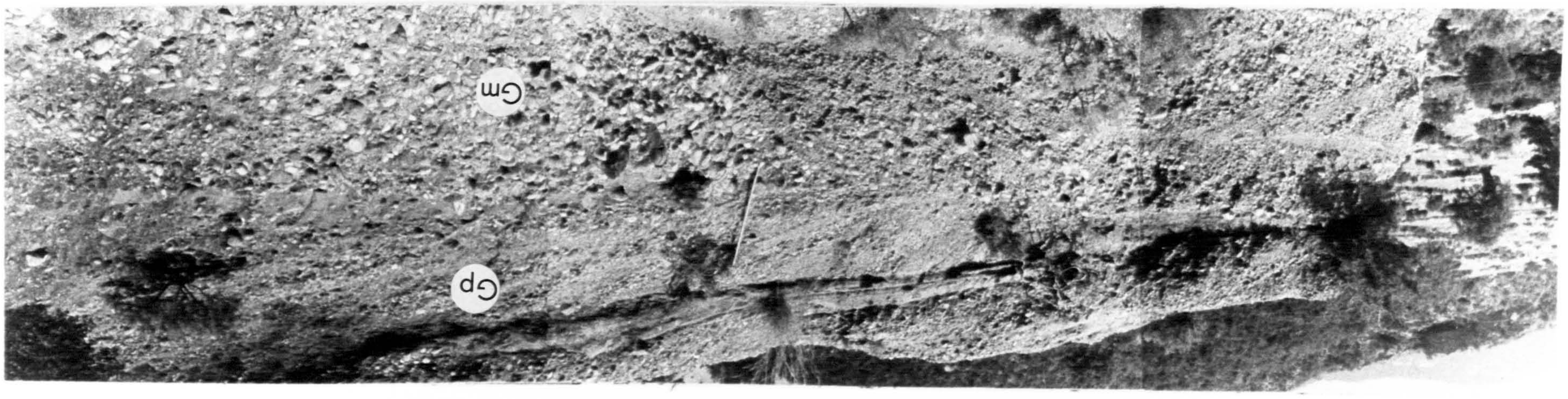
Gm
Gp

Fig. 5.32

Poorly stratified massive conglomerate (Gm) with well developed clast framework. Bedding delineated by dashed line dips steeply to the left. Alluvial fan (subaerial fan-delta) sequence, Salir Formation (Bağbeleni Member). Facies is 25 m across. GR 384313.

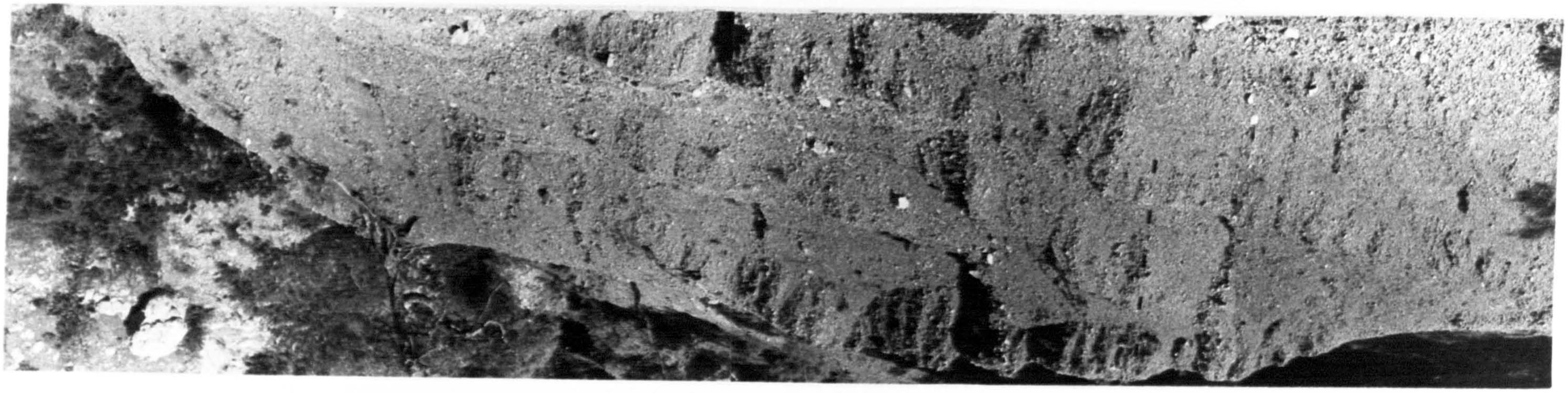

Trough-cross-sets often infill basal scours. Palaeocurrents measured from cross-stratification and imbrication were variably to the west (Fig. 5.2). Massive and planar-cross-stratified sandstone occurs as lenticular concave upwards wedge and box shaped units up to 1.50 m thick and 3.4 m across. Calcretes form laterally continuous rubbly horizons 10-30 mm thick, silt and fine sand are dispersed in a micrite matrix. In some instances they appear to drape depositional bed forms. Carbonaceous "rootlet" horizons are associated with lenticular discontinuous grey-green mudstone.

Interpretation

Calcrete and rootlet horizons indicate subaerial deposition. Bed lenticularity and poor segregation of sand and gravel is consistent with a fluvial origin (see 3.2.0). The high proportion of conglomerate suggests deposition on an alluvial fan. Lenticular sandstone bodies represent minor channel fill deposits (Howell and Link, 1979). The absence of debris-flow deposits precludes deposition on the upper parts of an alluvial fan. This association is interpreted as being the result of dominantly unconfined sheet flood and minor channel deposition on the mid to distal parts of a stream flow dominated alluvial fan (Fig. 5.35).

5.9.5 Coarsening-Upward Sedimentary Model : Summary

Facies associations and palaeocurrent evidence throughout this sequence (Fig.5.2) suggests that the coarsening-upward sequence is a result of the progradation of a fan-delta (coastal alluvial fan) system westwards into the basin.

Channellised, redeposited conglomerate and sandstone deposited in the pro-delta pass upwards into a sequence of interbedded redeposited conglomerate and chalk. This association represents deposition below wave base at the base of the fan-delta slope.

This sequence is overlain by stratified conglomerate and sandstone with shallow water aspects, probably deposited in the submarine delta-top environment. Overlying conglomerates with calcrete and rootlet horizons were deposited on an alluvial fan.

The lack of obvious transition zone features such as strand lines or seaward dipping imbrication (Cailleaux, 1945; Bluck, 1967) suggests a low energy micro-tidal environment. Shallow marine sequences with no significant palaeocurrent divergence from the subaerial sequences (compare 5.2), or deeper marine sequences, are

consistent with a low energy environment. Additionally, and importantly, the preservation potential of 'strand line type' features is likely to be low in an actively prograding environment.

The association of alluvial fans passing directly into a standing body of water has been described from the western margin of the sedimentary basin (4.9). In the sequence described here the subaerial parts of the system are not well exposed and downslope transitions and geometry of the sediment body cannot be accurately determined. In this case the general term fan-delta is applicable.

5.10 Fault Scarp Features

The coarsening-upward sequence described and interpreted above is well exposed in the Akçay valley and in the north of the Alaçadağ valley (Fig. 5.1). However, in the south of the Alaçadağ valley (Fig. 5.1, Locality x) crudely stratified conglomerate rests with strong angular unconformity on calcilutites of U. Cretaceous or Palaeocene age (Fig. 5.33).

The plane of unconformity dips variably between 65° and 75° to the northwest, bedding in the limestone dips between 20° and 24° to the northwest, ophiolite-derived conglomerate banked against the unconformity surface (Fig. 5.33) dips at between 20° and 22°.

Clast-supported conglomerate (Gm) is poorly stratified with interbedded lenticular coarse sandstone and mudstone lenses. It is interpreted as subaerially deposited alluvial conglomerate (3.2.5). Average clast size is 0.10-0.15 m. Large angular limestone blocks between 0.40 and 1.50 m in length occur restricted to distinct horizons (Fig. 5.33). The limestone is of identical lithology to the adjacent calcilutite.

This feature is interpreted as a subaerial palaeofault scarp, large limestone blocks derived of the scarp face attest to its syndepositional activity. Away from the fault limestone blocks decrease in size and frequency. Adjacent to the fault surface sediments are disrupted and sheared, indicating the fault was active during and after deposition.

Dissolution fissures in the fault surface are filled with ophiolite-derived material, forming neptunean dykes up to 10 m deep and 0.20 m across (Fig. 5.33).

Poor exposure prevents the mapping of this feature over a larger area. It is interpreted as a local fault scarp resulting from

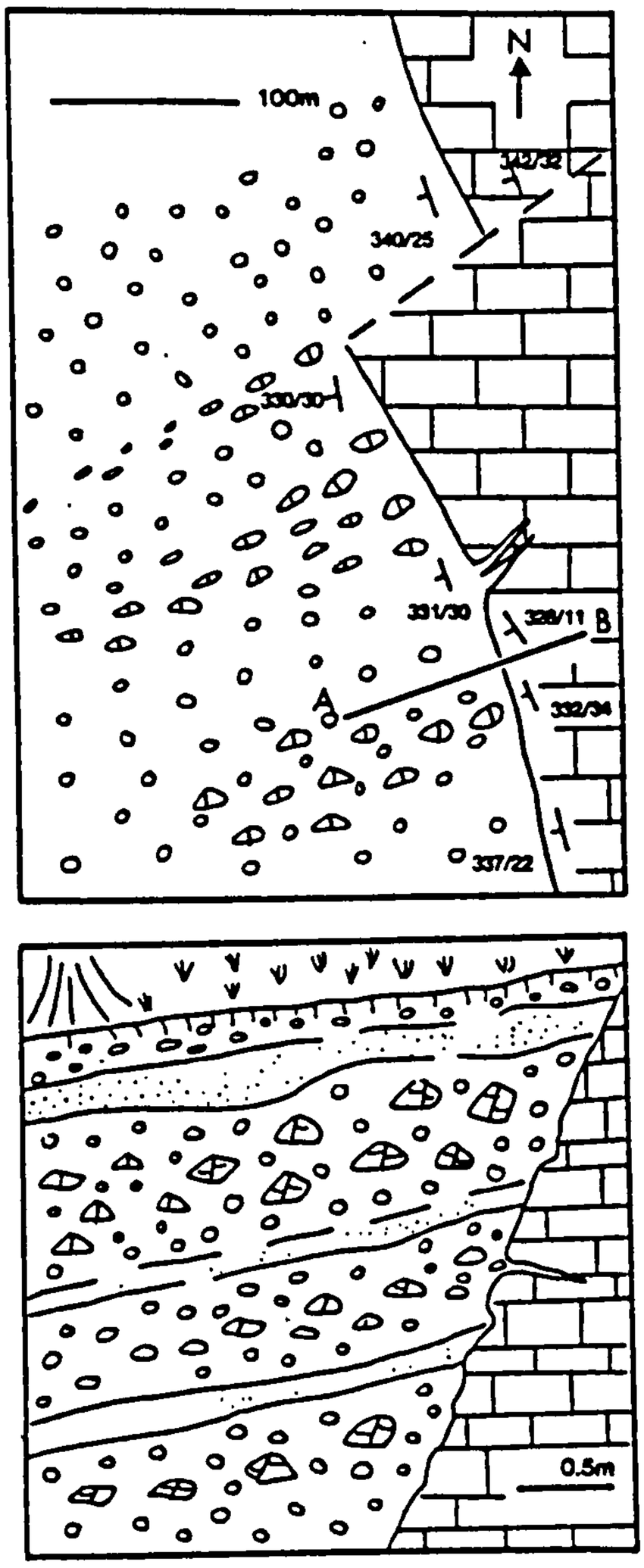

Fig. 5.33

Sketch map and section of fault scarp unconformity between alluvial fan sequence (Bagbeleni Member) and carbonate platform of Palaeocene age. Section along A-B.

Note presence of abundant carbonate platform derived clasts (shaded) and neptunean dykes (Locality X on Fig. 5.1).

tectonic uplift of the underlying carbonate platform following the final emplacement of the Antalya Complex.

5.11 General Sedimentary Model for the Eastern Margin

Sediments of the Salir Formation were clearly derived from the Antalya Complex to the east. Palaeocurrent orientations (Fig. 5.2), slump horizons and grain size trends are consistent with a broadly ENE-WSW trending palaeoslope. Facies associations and downslope transitions in Lower Miocene sequences indicate deposition on a series of small submarine fans, passing from inner fan to mid-fan regions from east to west. Palaeocurrents indicate several point sources along the basin margin in what is now the south Akdere valley. A northerly source from outside the area of current exposure (Fig. 5.1) is also indicated for some of the finer grained mid-fan sediments. The general sedimentary model is shown in Fig. 5.34.

The inner-fan area consists of amalgamated conglomerate-sandstone units formed in a low relief braided, broadly channelled area. Interbedded overbank sediments consist of thin sandstone, mudstone and chalk.

The well rounded nature of the clasts in the conglomerate implies derivation via a high energy shallow marine or fluvial environment. The lack of a well defined inner-fan canyon and broad channel areas suggests derivation from a series of coarse sediment lobes dumped by high gradient streams at or near the toe of a coastal alluvial fan or fan-delta. The absence of any well defined sequence-scale cyclicity produced by ordered channel migration is probably the product of several closely related sediment sources (Fig. 5.34). This results in the complex interaction of several channel areas. A steep palaeoslope is indicated by mega-intraclasts (Fig. 5.12), produced from large scale slumping, and the presence of very large, up to 2.50 m diameter, boulders. In the north debris flow olistostromes were derived from the submarine faulting of the Antalya Complex. Irregular subsidence and faulting associated with emplacement of the Antalya Complex resulted in shallow water carbonate deposition on areas of upfaulted carbonate platform. Large detached limestone blocks were derived off the fault scarp.

To the west, the mid-fan environment consists of amalgamated sandstone units deposited in shallow distributary channels, larger

Fig. 5.34

General depositional model for Lower Miocene, Salir Formation sequence.
Small fan-deltas (not exposed) pass downslope into a series of coalescing small submarine fans. Inner fan (proximal) sequences are dominated by conglomerates deposited by sediment gravity flows. This sequence passes basinwards into a mid-fan association that shows no well developed bed-thickness cyclicity. Fault scarps produced by irregular subsidence of the carbonate platform shed large detached blocks, and bioclastic breccias derived from small carbonate build-ups.
In the north debris flow olistostromes are derived from submarine faulting of the Antalya Complex (see text for details).

Fig. 5.35

General depositional model for the Upper Miocene Salir Formation (Bagbeleni Member) sequence.
Inner fan sequence is overthrust by emplacement of the Antalya Complex.
Fan-deltas prograde into a shallow sea. Rare patchreefs develop on their seaward margin (see text for details).

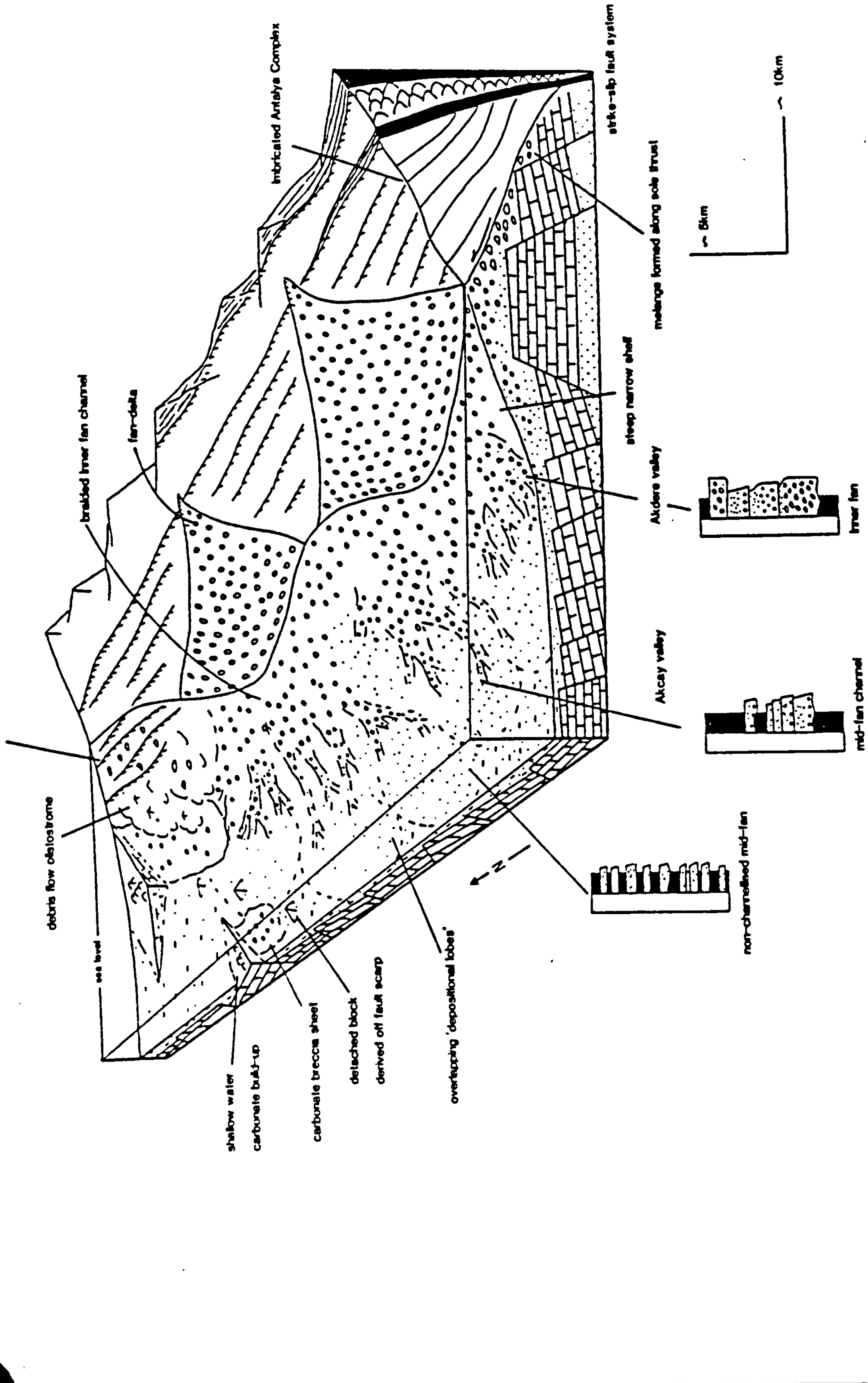
Imbricated Antalya Complex
strike-slip fault system
~ 8km
~ 10km
melange formed along sole thrust
braided inner fan channel
fan-delta
steep narrow shelf
Akdere valley
inner fan
Akcay valley
mid-fan channel
debris flow obstostrome
sea level
non-channelled mid-fan
shallow water carbonate build-up
carbonate breccia sheet
detached block
derived off fault scarp
overlapping 'depositional lobes'

Fig. 5.34

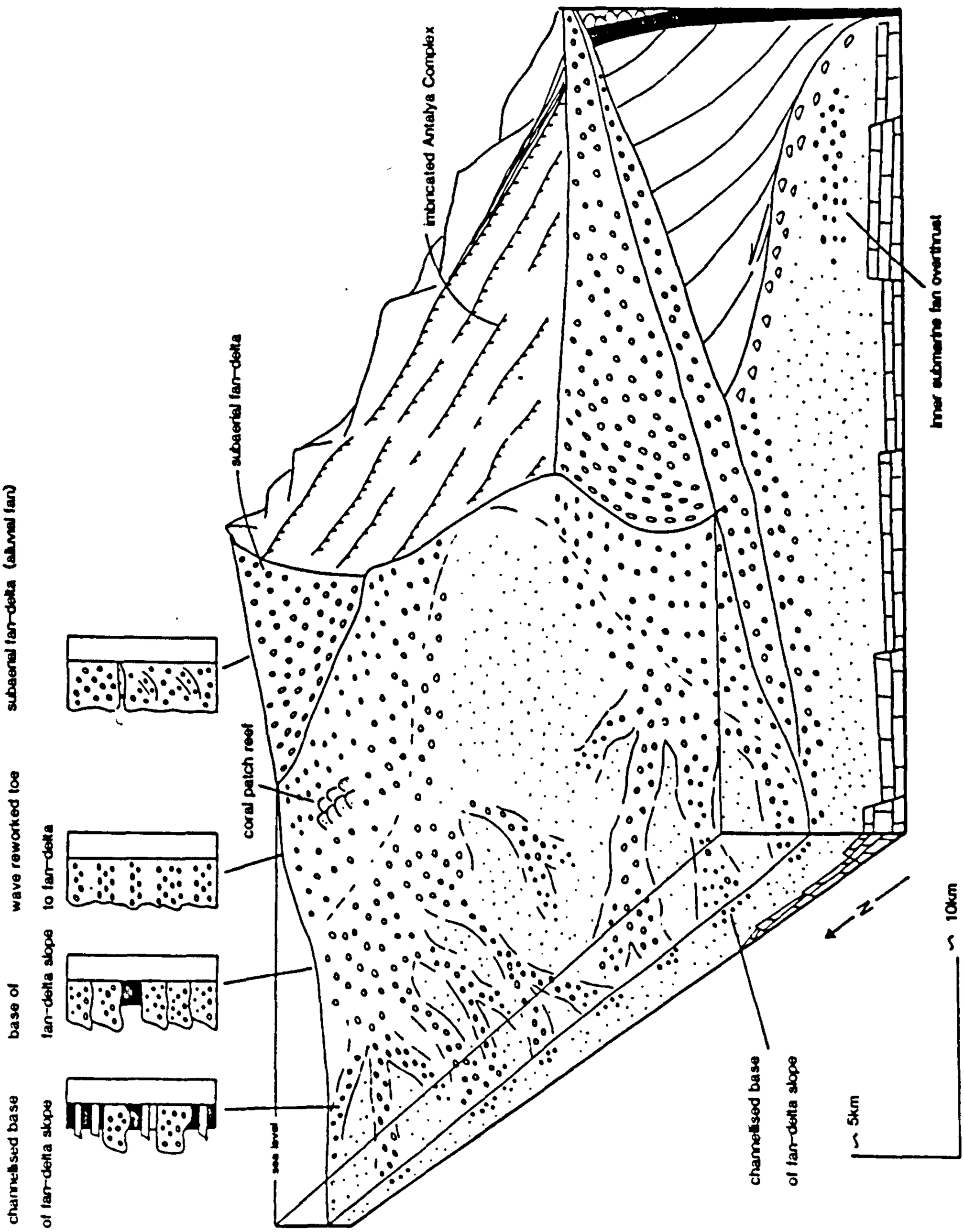
imbricated Antalya Complex
subaerial fan–delta
coral patch reef
inner submarine fan overthrust
subaerial fan–delta (alluvial fan)
wave reworked toe
to fan–delta
base of
fan–delta slope
channelised base
of fan–delta slope
sea level
channelised base
of fan–delta slope
N
~ 5km
~ 10km

Fig. 5.35

scale fining upward sandstone-mudstone units may represent large, very shallow, channel features. The majority of the sequence, interpreted to have been deposited in the mid-fan depositional 'lobe' area, is essentially non-cyclic probably as the result of the interaction of several lobes (Fig. 5.36).

Further west in the Alaçadağ area, the sequence is thinner, but has a higher sandstone:mudstone ratio. This may be the result of an input of sediment from a south westerly source, or more probably this area may represent a suprafan depositional lobe. Palaeocurrent evidence (5.2) is inconclusive.

Small immature submarine fan systems such as this (see brief discussion below, 5.12.0) are characteristically developed in basins, with narrow or non-existent shelves, located adjacent to high relief areas. Coastal alluvial fans prograding into standing water dump large volumes of sediment in gravitationally unstable positions. It is subsequently redeposited into the centre of the basin, down anastomosing broadly channelled active sedimentation areas.

In Middle Miocene times inner submarine fan sequences along the margin of the basin were abruptly truncated by the westward directed overthrusting of the Antalya Complex. In more central areas (e.g. Akçay valley) a general coarsening- and shallowing-upward sequence marks the progradation of a fan-delta (fan-delta complex) westwards into the basin (Fig. 5.35). The shallowing upwards sequence is probably in response to both eustatic sea level changes towards the end of the Serravallian (Vail *et al.*, 1977, Hsu *et al.*, 1973) and progressive infilling of the sedimentary basin. Coarsening-upwards reflects the uplift and final emplacement of the Antalya Complex (Fig. 5.35, see also 10.6.3).

5.12 Comparison with other Submarine Fan Models

The generally accepted model for many submarine fan sequences (e.g. Ricci Lucchi, 1975a, b; Normark, 1978; Walker, 1978, 1979) is based primarily on studies of modern, small, deep water fans on the continental margin of California (Normark, 1970, 1974, 1978) and field studies of ancient sequences of Tertiary flysch formations in the Northern Apennines and Southern Pyrenees (Mutti and Ricci Lucchi, 1972, 1974, 1975; Ricci Lucchi, 1975a, b; Mutti, 1977). Elements of these two studies have been combined by Walker (1978, 1979b) into the model shown in Fig. 5.36.

Currently there are two models for mature, small to medium sized (10's to several 100's of kilometres long axis dimension) fans developed in a stable tectonic environment at the base of continental slopes (Fig. 5.36). The primary difference is whether depositional lobes are connected to the inner fan area by a series of 'braided' mid-fan channels, as in the original Normark model based on modern fans (e.g. Normark, 1970, 1974, 1978), or whether the depositional lobes are separated from the inner fan by a zone of muddy by-passing. For an outline of this and other problems surrounding submarine fan nomenclature the reader is referred to a discussion by Nilsen (1980) and reply by Walker (1980).

In addition to these models, some very large fans have been described from the deep ocean basins. These include the Bengal fan (Curray and Moore, 1971), the Indus Cone (Jipa and Kidd, 1974), the Mississippi Cone (Huang and Goodell, 1970), the Amazon Cone (Damuth and Kumar, 1975) and the Laurentian fan (Stow, 1979, 1980; Uchapi and Austin, 1979). A recent model by Surlyk (1975a, b, 1978) describes submarine fans formed along scarps on antithetically rotated fault blocks in a failed spreading rift zone. The fans overlap to form a continuous sediment apron along the base of the fault scarp (Fig. 5.36). This model has been recently applied to submarine fans of Tertiary age in the North Sea (Stow *et al.*, in press). In more recent studies of Tertiary submarine fan sequences in Italy (e.g. Mutti, 1979; Mutti and Johns, 1979; Ricci Lucchi and Valmori, 1980; Mutti and Ricci Lucchi, 1981) the distinction has been drawn between "highly efficient" submarine fan systems which contain a large proportion of fine grained material and result in turbidites that spread thin units of sand over large areas (e.g. the classical Tertiary flysch sequences of the Northern Apennines) and "poorly efficient" systems which contain a low proportion of fine grained material and result in turbidites and other sediment gravity flows depositing relatively thick units of sand and gravel over a small area.

None of these models outlined above and discussed in more detail by Stow *et al.* (in press) and Nilsen (1980) can be easily applied to the small, very laterally variable submarine sequence of the Salir Formation. Although some similarities do exist, in that from proximal to distal areas there is a general decrease in the

Fig. 5.36

Submarine fan models (sandstone stippled, open circles for conglomerates).

(a) The 'Italian' model of Mutti and Ricci Lucchi (1972, 1974, 1975). Five environments and a number of subenvironments are distinguished The inner fan is leveed and splits into a number of small distributaries. They comprise a coarse grained thinning- and fining-upwards channel fill sequence, interbedded with bundles of thin sandstones and thick mudstones of the interchannel environment. The mid-fan transitional area consists of a number of braided and meandering channels with a channel fill facies, a sandy channel mouth bar and a zone of muddy by-passing. The outer fan is characterised by flow aligned convex lobes of sediment, fed by a distributary channel, and composed of classical turbidites arranged in thickening- and coarsening-upwards units. Interlobe deposits are finer grained, thin-bedded sandstones and mudstones. Both the fan fringe and basin plain comprise fine grained thin-bedded 'distal' turbidites.

(b) Model of Surlyk (1975a, b; 1978a, b). In this model the fans overlap to form a continuous sediment apron along fault scarps. Fan wedges can be divided into base of slope breccias and conglomerates, inner fan channels and lobes comprising thick conglomerates, graded and non-graded sandstones; inner fan interchannel and mid-fan thick sandstones and mudstones; outer fan interlaminated fine sandstones and mudstones with scattered thicker graded and non-graded sandstones and basinal mudstones. The basin fill is arranged in fining-upwards mega-cycles, corresponding to major phases of fault activity. Internally the mega-cycles are composed of fining-upward cycles that reflect channel filling and abandonment.

(c) Fan model of Walker (1979). Essentially a combination of the early models of Normark (1970, 1974, 1978) and those of the Italian school. In this model depositional lobes are connected to the distributary channels and there is no zone of by-passing. The model emphasises the distribution of conglomerate and sandstone within the system.

(d) Model developed from this study, it has similarities with both the Surlyk and Walker models. Fan-deltas feed a complexly channelised inner fan area, comprising fining-upward channel fill units. This passes abruptly into a series of coalescing mid-fan lobes, which are not characterised by any vertical arrangement of bed thickness or grain size (see text for more details).

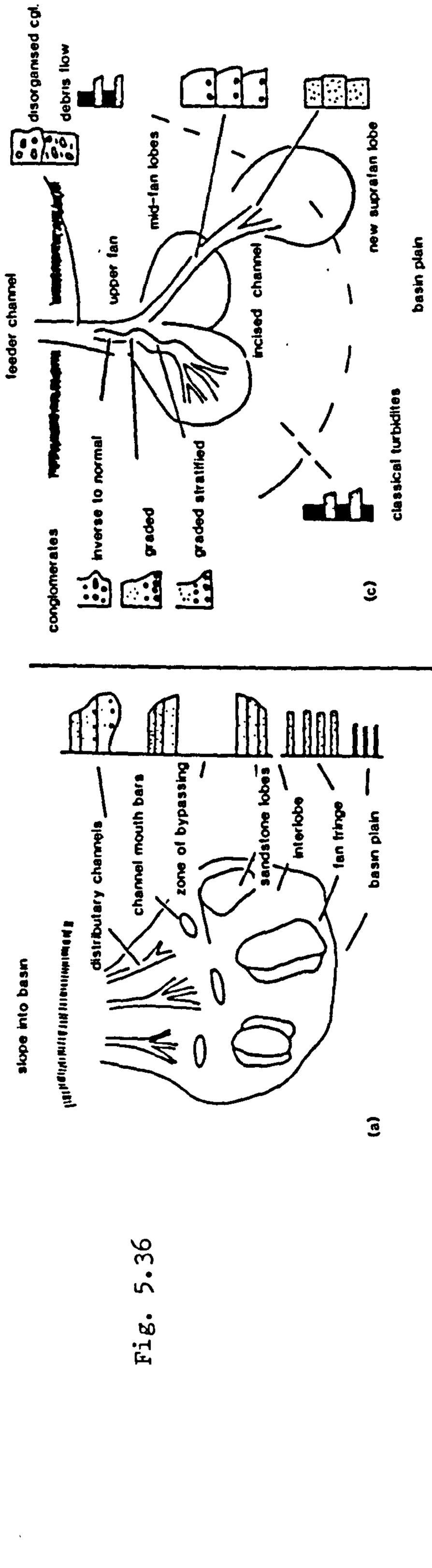
slope into basin
distributary channels
channel mouth bars
zone of bypassing
sandstone lobes
interlobe
fan fringe
basin plain
(a)
alluvial fan/fan delta
slope breccias
inner fan
mid-fan
outer fan
basin
continent source
rapid wedging out
shallow/emergent
outer fan
mid-fan
inner fan
scarp breccia
(b)
conglomerates
inverse to normal
graded
graded stratified
disorganised cgl.
debris flow
feeder channel
upper fan
mid-fan lobes
incised channel
new supralan lobe
basin plain
classical turbidites
(c)
alluvial fan/fan delta
braided inner fan channel
outer fan
overlapping mid-fan lobes
(d)

Fig. 5.36

proportion of channelled sandstone and conglomerate and decrease in the sandstone:mudstone ratio. A fundamental difference is the presence of a very broad complexly channelled inner fan area and absence of a well defined inner fan channel.

Downslope transitions are more rapid but broadly similar. The mid-fan is not generally characterised by an upper channelled area, suggesting that inner fan channels give way rapidly to non-channellised depositional lobes. In the mid-fan depositional lobe site there is an absence of well developed coarsening-upward cycles. This is attributed to tectonic control restricting the ordered progradation and abandonment of individual lobes, and the lack of a well defined inner fan channel resulting in the interaction of several depositional lobe sites fed by different parts of the inner fan and active at the same time.

Similar sequences have been described by Stanley (1980), Carter and Norris (1977) and Cazolla *et al.* (1981), in all cases, as in the Salir Formation, the submarine fan system was apparently fed by a fan-delta prograding directly into the basin over a very narrow or non-existent shelf.

CHAPTER 6 PETROGRAPHY OF THE OPHIOLITE-DERIVED SEDIMENTS

CHAPTER 6

6.0 Petrography of the Ophiolite-Derived Sediments

6.1 Introduction

In this chapter the petrography and diagenesis of the ophiolite-derived sediments are described. This chapter is subdivided into two parts, the first deals with the western margin sequences (Kemer and Kasaba Formations), and the second with the eastern margin sequences (Salir Formation). Lateral and vertical variations in petrography are described and discussed within related sequences (i.e. western margin) and between the two margins. Petrographic methods employed are outlined in Appendix A.

6.2.0 Western Margin

6.2.1 Conglomerates

Kemer Formation. The conglomerates of the Kemer Formation are variably sorted and moderately to well rounded. Sedimentary facies type exerts strong control on textural maturity (Chapter 4). Clast types are dominated by basic and ultrabasic igneous rocks along with chert and limestone. The main clast types are summarised in Table 6.1. Clast composition from point-counts is shown in Fig. 6.1.

Kasaba Formation. Conglomerates of the Kasaba Formation are similarly moderately to well rounded; textural maturity is again controlled dominantly by sedimentary facies. The conglomerates are composed of an admixture of pelagic sedimentary (chert and limestone) and igneous (mainly gabbro, dolerite and basalt) rock types, as well as considerable (up to 45%) shallow water limestone clasts. Typical compositions from point-counts are shown in Fig. 6.1.

Variations in conglomerate composition. Palaeocurrent data (Chapter 4) clearly indicate that the conglomerates and sandstones of the Kemer and Kasaba Formations were derived from the *west*, from the area of the Lycian Nappes. The nappes (1.3.2) comprise an assemblage of passive margin sediments, igneous ophiolitic rocks and the pelagic sedimentary cover of an ophiolite. Within the nappe pile no other rocks are known and the *petrography* of the conglomerates and sandstones clearly indicate an *ophiolitic source*.

Vertical variations in petrography may indicate periods of tectonic activity in the source area, or at least reflect the gradual unroofing of the nappe unit as it was emplaced.

Fig. 6.1

(a) Triangular composition plot for the conglomerates of the western margin.
This illustrates the marked increase in the percentage of shallow water limestone clasts (carbonate platform derived - CP) in the Kasaba Formation. Point counts of 100 clasts were taken from conglomerates throughout the sequence. (UL - upper levels of an ophiolite, LL - lower levels of an ophiolite, CP - shallow water limestone clasts, carbonate platform derived.

(b) Plots of conglomerate composition against stratigraphic thickness for the western margin sequences. Note the upward increase in shallow water limestone lithoclasts (1), marked decrease in clasts from the upper parts of an ophiolite (and related sedimentary cover - mainly radiolarian chert and pelagic limestone)(2). Clasts derived from the lower levels of an ophiolite (3) increase only slightly.

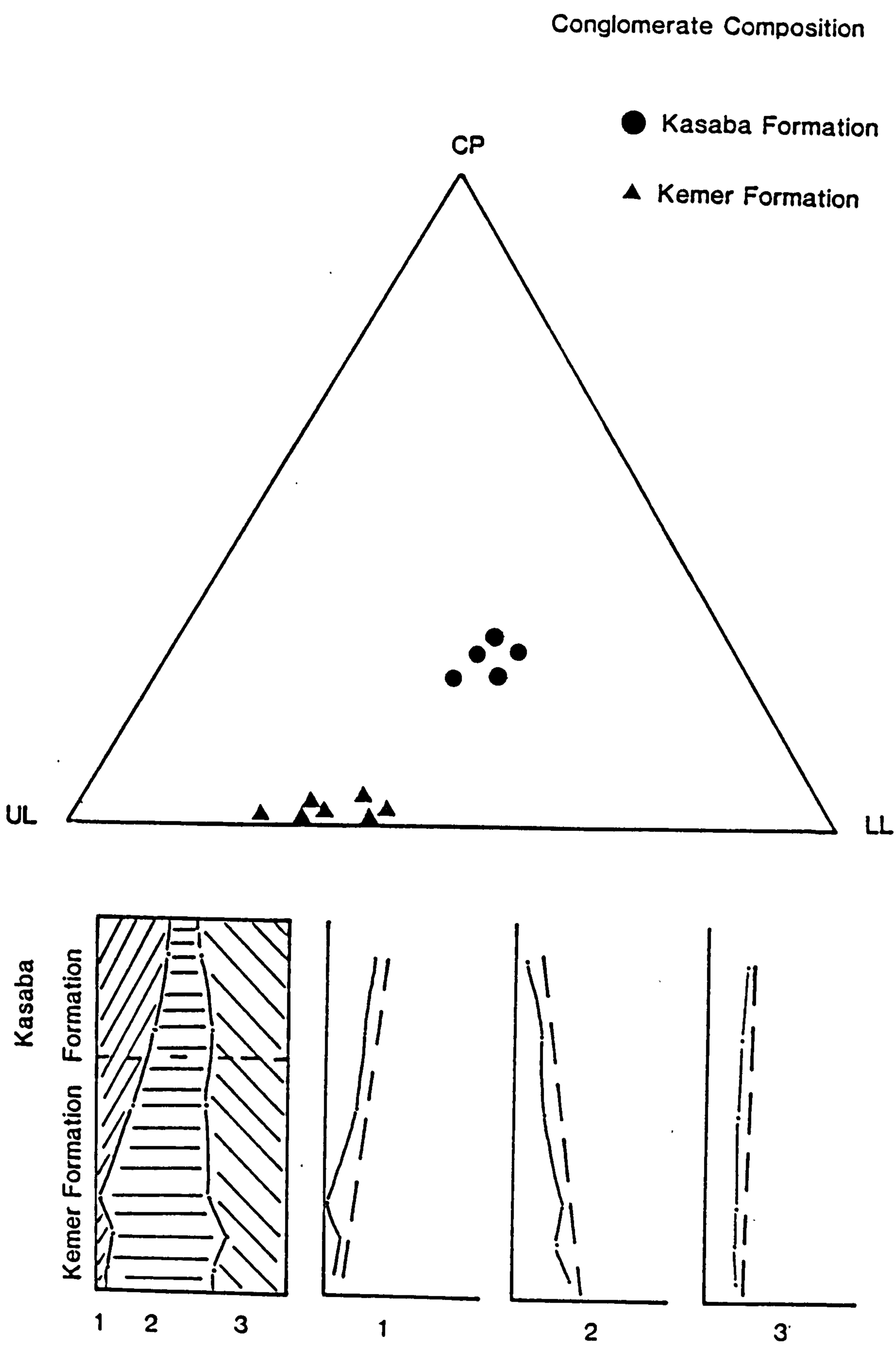
Conglomerate Composition
Kasaba Formation
Kemer Formation
CP
UL
LL
Kasaba Formation
Kemer Formation
1
2
3
1
2
3

Fig. 6.1

CLAST	INFERRED SOURCE
Serpentinite	LL
Hartzburgite	LL
Peridotite	LL
Pyroxenite*	LL
Norite	LL
Olivine gabbro*	LL
Gabbro	LL
Layered gabbro	LL
Cumulate textured gabbro*	LL
Norite*	LL
Diorite	LL/UL
Basalt	UL
Variolitic basalt*	UL
Red radiolarian chert	UL
Green chert	UL
Grey chert	?
Black chert	?
Vein quartz	?
Recrystallized sparite	?
White calcilutite with planktonic foraminifera*	UL?
Pink calcilutite	UL
Bioclastic limestone breccia	CP
Nummulitic calcarenite	CP
Bioclastic calcarenite	CP
Brecciated sparite	?
Green marl	UL?

Table 6.1

Main clast types in Kemer Formation conglomerates.
Identified from hand specimens and in some cases (*) thin sections.
See Fig. 6.1 for an idea of relative abundance.
LL - Lower levels of the Lycian Nappe ophiolite unit
UL - Upper levels of the Lycian Nappe ophiolite unit
CP - shallow water limestone lithoclast, carbonate platform derived.

Plots of clast composition against stratigraphy for both formations indicate two upward trends (Fig. 6.1):.

(1) A general decrease of clasts from the upper levels of an ophiolite (e.g. basalt dolerite) and related pelagic sedimentary cover (pelagic carbonates, radiolarian chert etc.).

(2) A general upward increase in the proportion of shallow water limestone clasts, especially marked over the Kemer-Kasaba Formation boundary. These trends are discussed below (6.2.3).

6.2.2 Sandstone composition

The sandstones of both the Kemer and Kasaba Formations are texturally and mineralogically immature. They consist principally of moderately to poorly sorted litharenites (McBride, 1963; Folk, 1968) (Fig. 6.2). Principal terrigenous framework grains comprise serpentinite, mafic and ultramafic rock fragments (mainly gabbro, pyroxenite and peridotite) dolerite, chert and limestone with subordinate quartz, spinels and opaques (magnetite and chromite), often in heavy mineral concentrations (Fig. 6.5). The main petrographic features of the dominant terrigenous grains are summarised in Table 6.2. In sandstones from submarine parts of the sequence contemporaneous skeletal carbonate grains are abundant. In some instances they are bored and micritised. The most common grain types are benthonic foraminiferans, coralline algae, shell debris and echinoderm plates and spines. A complete list is given in Table 6.2. Non-skeletal carbonate grains, pelloids, ooids etc. are not common. Disseminated wood fragments, up to 3 cm long, are abundant in some sandstones, although uncommon in subaerial parts of the Kasaba Formation (Doğantaş Member). They are carbonized and flattened, appearing reddish-brown to opaque in thin section.

Matrix. The sandstones in both formations are mainly grain-supported, but contain variable amounts of matrix. A fine grained, dominantly serpentinite, matrix occurs in some sandstones; in others micritic calcite is the matrix, sometimes showing neomorphism to microspar.

Composition plots. The QRF diagrams of Folk (1968) and subordinate rock fragment diagrams do not adequately illustrate the wide range in composition of such mineralogically immature sediments (Fig. 6.2). To overcome this several diagrams are used that are more applicable to the source areas represented here. These are (Fig. 6.2):

Fig. 6.2

Point counts of sandstones from the Kemer and Kasaba Formations. The QRF plot illustrates their immature nature but does not show the range of compositions that exist. The remaining diagrams illustrate the wide range of compositions present.

UL - upper levels of an ophiolite

LL - lower levels of an ophiolite

Other - remaining terrigenous grains

CP - shallow water limestone clasts (carbonate platform derived in the main).

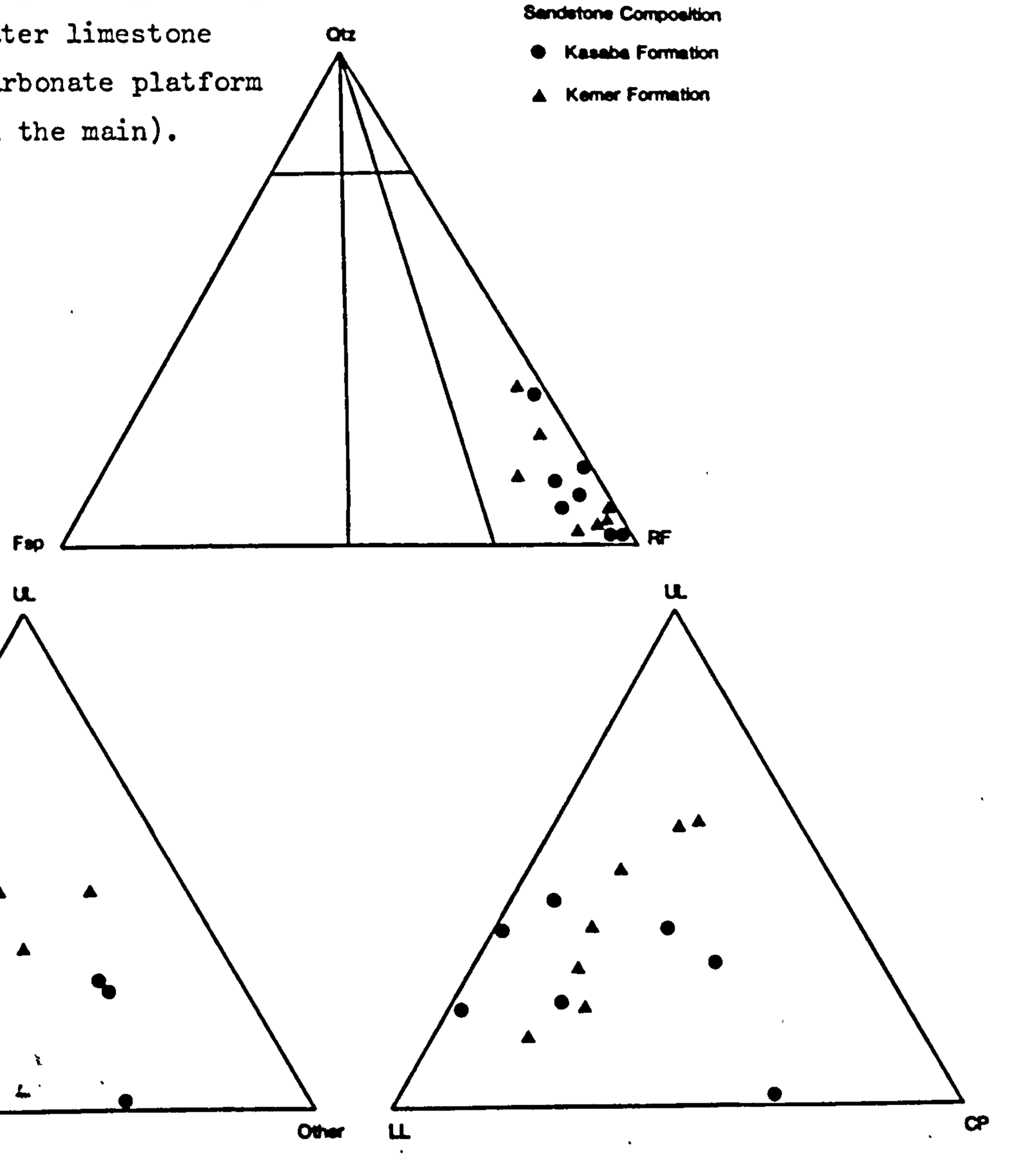

GRAIN FEATURES	SHAPE/ ROUNDNESS	ALTERATION AND DIAGENESIS	INFERRED SOURCE
Serpentinite			
I) fibrous lamellar antigorite, with abundant opaques II) mesh textured and concentrically banded with relict olivines and opx., opaques around crystal margins III) massive structureless	subangular to rounded, equant	extensive marginal replacement by calcite, bending and wrapping around harder grains, in subaerial sandstones alteration to Fe oxide	Lower levels of Lycian Nappe ophiolite unit
Gabbro			
cumulate texture opx., cpx., plag., fspar.	subrounded to rounded equant	fresh or partially altered to serpentinite, little *in situ* alteration	Lower levels of Lycian Nappe ophiolite unit
Peridotite	subrounded to rounded, equant	along margins replacement by calcite, alteration → Fe oxide in subaerial sandstones	Lower levels of Lycian Nappe ophiolite unit
Fe/Mg minerals			
opx., cpx., olivine	subangular to rounded, equant	in *subaerial* sandstones alteration → Fe oxide	Lycian Nappe ophiolite unit
Spinels (and other opaques)			
red and green spinel magnetite	angular to subangular	no alteration	Lycian Nappe ophiolite unit
Dolerite	subrounded to rounded, equant to elongate	little *in situ* alteration	Upper levels of Lycian Nappe ophiolite unit
Basalt			
I) variolitic II) glass III) flow aligned fspars.	subrounded to rounded, equant	alteration to fine grained clay aggregates, bending and wrapping around harder grains, in subaerial sandstones some alteration → Fe oxide	Upper levels of Lycian Nappe ophiolite unit
Plagioclase feldspar high An values	subangular to rounded, equant	no alteration	Lycian Nappe ophiolite unit
Chert			
I) microcrystalline chert II) red radiolarian chert with radiolarian 'ghosts'	angular to subrounded, equant	irregular replacement around margin by calcite, patchy wholesale replacement by calcite	Sedimentary cover to Lycian Nappe ophiolite unit
Quartz			
I) single, undulose and uniform extinction II) polycrystalline, stretched and sutured, with micas along grain boundaries	subangular to rounded equant to oblate	irregular replacement along margins by calcite	Passive margin sandstone sequences within Lycian Nappe allochthon

Table 6.2 Main framework grains of the Kemer and Kasaba Formation sandstones

GRAIN FEATURES	SHAPE/ ROUNDNESS	ALTERATION AND DIAGENESIS	INFERRED SOURCE
Limestone lithoclasts			
I) lime mudstone often with planktonic forams II) bioclastic boundstone III) bioclastic packestone IV) recrystallised sparite	subangular to rounded, elongate to equant	no *in situ* alteration, often pressure solution along grain margins	mainly reworked carbonate platform, sparite and some lime mudstone (pelagic limestone) from Lycian Nappe, sedimentary cover to ophiolite
Contemporaneous bioclastic debris			
I) benthonic forams II) planktonic forams III) algal debris IV) echinoid plates and spines V) bivalve and other shell fragments	angular, shape dependant on original form	often extensive pressure solution along grain margins	shallow water carbonate depositing area on margins of basin

Table 6.2 Main framework grains of the Kemer and Kasaba Formation sandstones.

(1) UL - LL - CP

UL - Upper level of an ophiolite 'stratigraphy', basalt, dolerite, and its related sedimentary cover (chert, pelagic limestone);

LL - Lower level of an ophiolite 'stratigraphy', serpentinite, mafic and ultramafic rock fragments, mafic minerals (clino-pyroxene, orthopyroxene, olivine), plagioclase, feldspar, opaque minerals;

CP - Shallow water limestone lithoclasts.

(2) UL - LL - OTHER

UL - as above;

LL - as above;

OTHER - all clasts not derived from the ophiolite suite or its sedimentary cover, in the present case this is predominantly shallow water limestones and quartz.

6.2.3 Source Area

The majority of the framework grains comprise rock fragments derived either from an *ophiolite* complex or from a *shallow water limestone* source area. Angular plagioclase feldspar (with high An values) which comprises greater than 90% of the feldspar component, is consistent with derivation from a basic igneous complex. The quartz component of the sandstone is dominated by well rounded, equant, polycrystalline stretched and sutured metamorphic grains and subordinate plutonic (?) quartz. This probably represents second or third cycle quartz derived from continental margin sandstone sequences within the Lycian Nappes. The low proportion of quartz from the western margin of the sedimentary basin is in marked contrast to those from the eastern margin of the basin (6.3.2). Abundant skeletal and rare non-skeletal carbonate grains were derived from areas of carbonate deposition around the margins of the basin.

6.2.4 Compositional Variations : Discussion

Variations, throughout the sequence, in the proportion of the six main components (grouped to related them to structural levels in an ophiolite complex and external source areas) are shown in Fig. 6.4. Trends observed, outlined below, are consistent with those recorded from changes in conglomerate composition.

(1) An initial abrupt increase in the proportion of mafic and ultramafic (lower levels of the ophiolite complex) rock fragments, followed by a gradual decrease (Fig. 6.4);

Fig. 6.3

Histograms of the six main terrigenous grain components in the Kasaba Formation sandstones. Feldspar shaded for reference (see Fig. 6.4 for key). Arrows indicate stratigraphic sequence, see Appendix D for location of specimens.

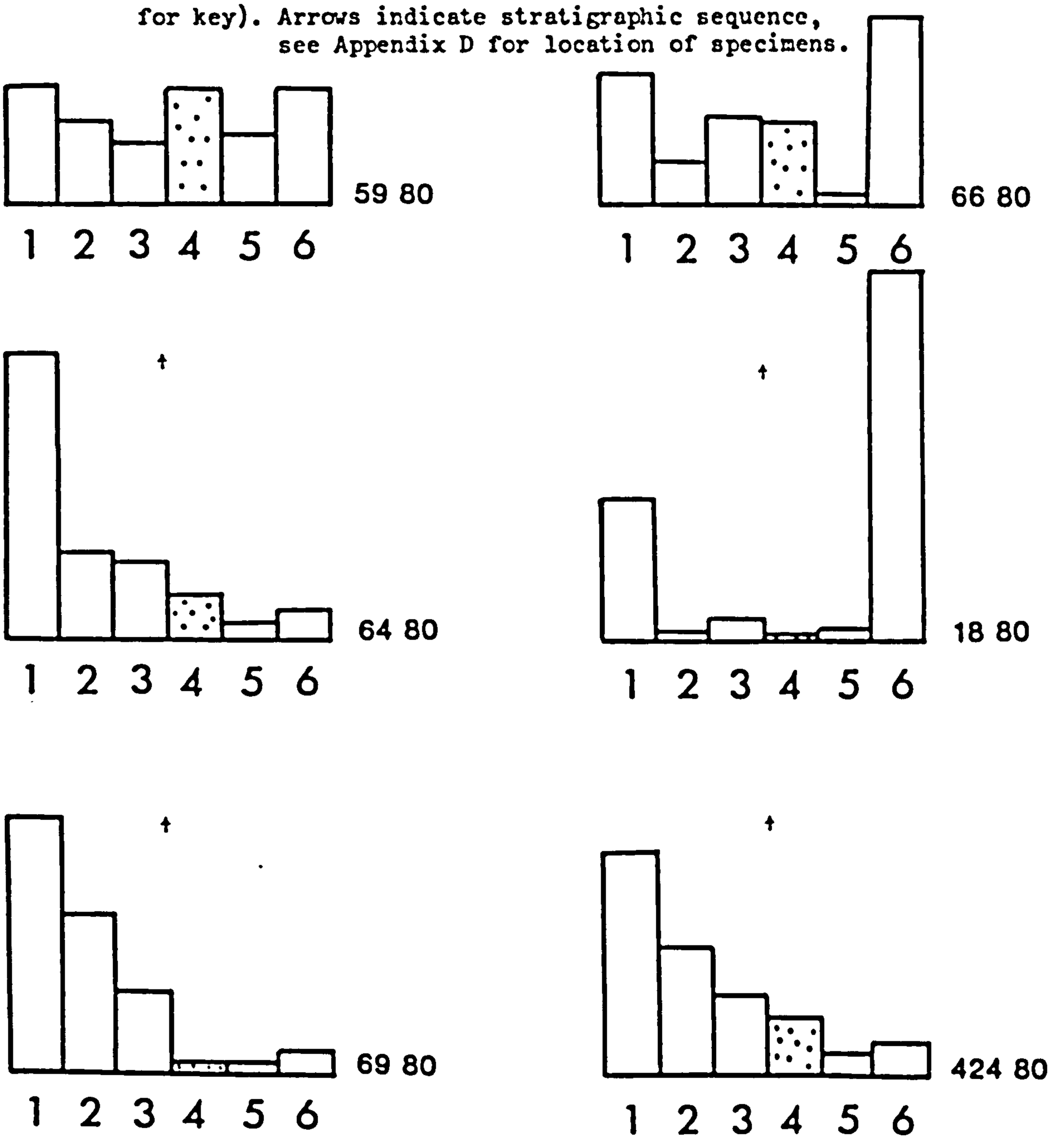

Proximal Sequence

Distal Sequence

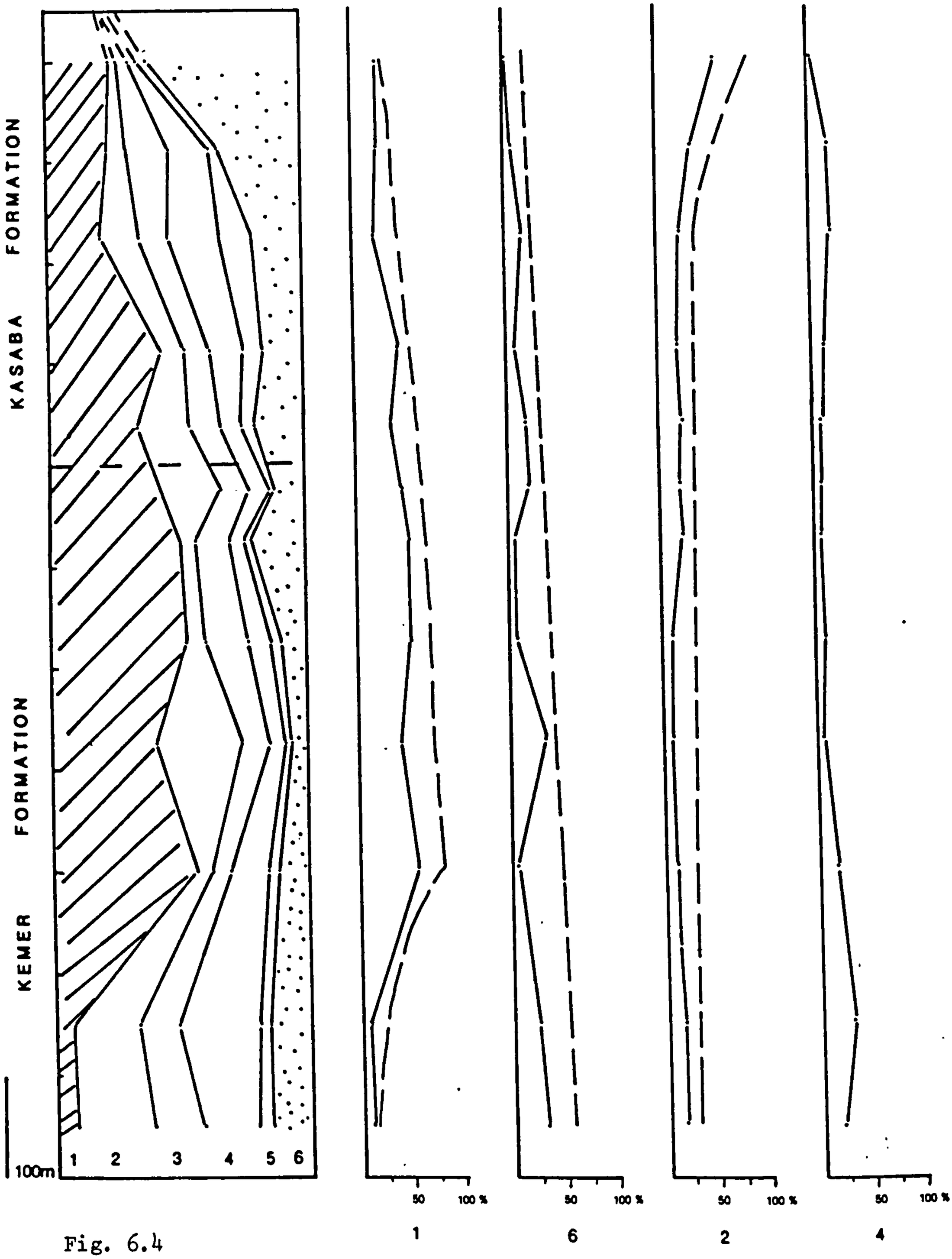

Fig. 6.4

Vertical variations in the petrography of the Kasaba and Kemer Formation sandstones (from 333 point counts). 1 - mafic and ultramafic rock frags and minerals. 2 - dolerite and basalt. 3 - chert. 4 - quartz. 5 - feldspar. 6 - limestone lithoclasts.

(2) A gradual upwards decrease in the proportion of dolerite, basalt and glass clasts (Fig. 6.4);
(3) A marked upward increase in the proportion of shallow water limestone lithoclasts, particularly noticeable from the base of the Kasaba Formation (Fig. 6.4). The first two reflect the gradual unroofing of the ophiolite during its emplacement. The presence of significant proportions of basalt and dolerite from the upper levels of the ophiolite complex, is in contrast to the rocks preserved in the Lycian Nappes today.

In the area west of Fethiye (Fig. 10.1) the igneous ophiolite assemblage comprises dominantly peridotite, pyroxenite, and hartzburgite, the upper levels having been removed by erosion during its emplacement.

The upward increase in the proportion of shallow water limestone lithoclasts (derived dominantly from the underlying carbonate platform) reflects the *tectonic disruption* of the carbonate platform during the *final* stages of ophiolite emplacement in the Middle to Upper Miocene (10.2.4), resulting in the faulting, uplift and subaerial exposure of the carbonate sequence and the introduction of a large proportion of limestone lithoclasts into the sediment.

Small-scale lateral and vertical variations can be attributed to several causes: (1) Depositional system - The coastal alluvial fans of both formations were fed by short, high gradient streams with a small drainage area. Sedimentary systems of this type are likely to result in locally different petrographies; (II) Small-scale tectonic disruption during emplacement of the ophiolite, revealing different levels of the ophiolite complex and associated sediments at different times in different areas.

6.2.5 Diagenesis

The various stages of diagenesis that are generally present in sandstones of both the Kemer Formation and submarine parts of the Kasaba Formation are outlined chronologically below.

(I) Deposition as poor to moderately-packed sediment, grains are often current aligned with heavy mineral concentrations (Fig. 6.5) of mainly magnetite, chromite and chrome spinels (identified by reflected light);

(II) Initial, preferential precipitation of non-ferroan carbonate cement on echinoderm fragments (Fig. 6.5);

Fig. 6.5

Photomicrographs of petrographic features of sandstones from the Salir and Kasaba Formations.

(a) Heavy mineral concentration of mainly chrome spinels and magnetite in the B division of a turbiditic sandstone.
Salir Formation. Spec 44/78.
The remainder of the grains are an admixture of ophiolite-derived and approximately 80% disseminated bioclastic skeletal material.
Field of view 1.0 cm. Plane polars GR. 518379

(b) Non-ferroan calcite overgrowth (O) on echinoid plate (e). Note later pressure solution, between echinoid plate and serpentinite (s). More pronounced pressure solution is seen between a coralline algal fragment *(Mesophyllum)* (m) and terrigenous grain (t).
Salir Formation. Spec. 40/78.
Field of view 1 cm. Crossed polars. GR. 517/379

(c) Cryptocrystalline haematite forming rims around terrigenous grains and infilling pore spaces.
Doğantaş Member, Kasaba Formation. Spec. 70/80.
Field of view 2 cm. Crossed polars. GR. 520357.

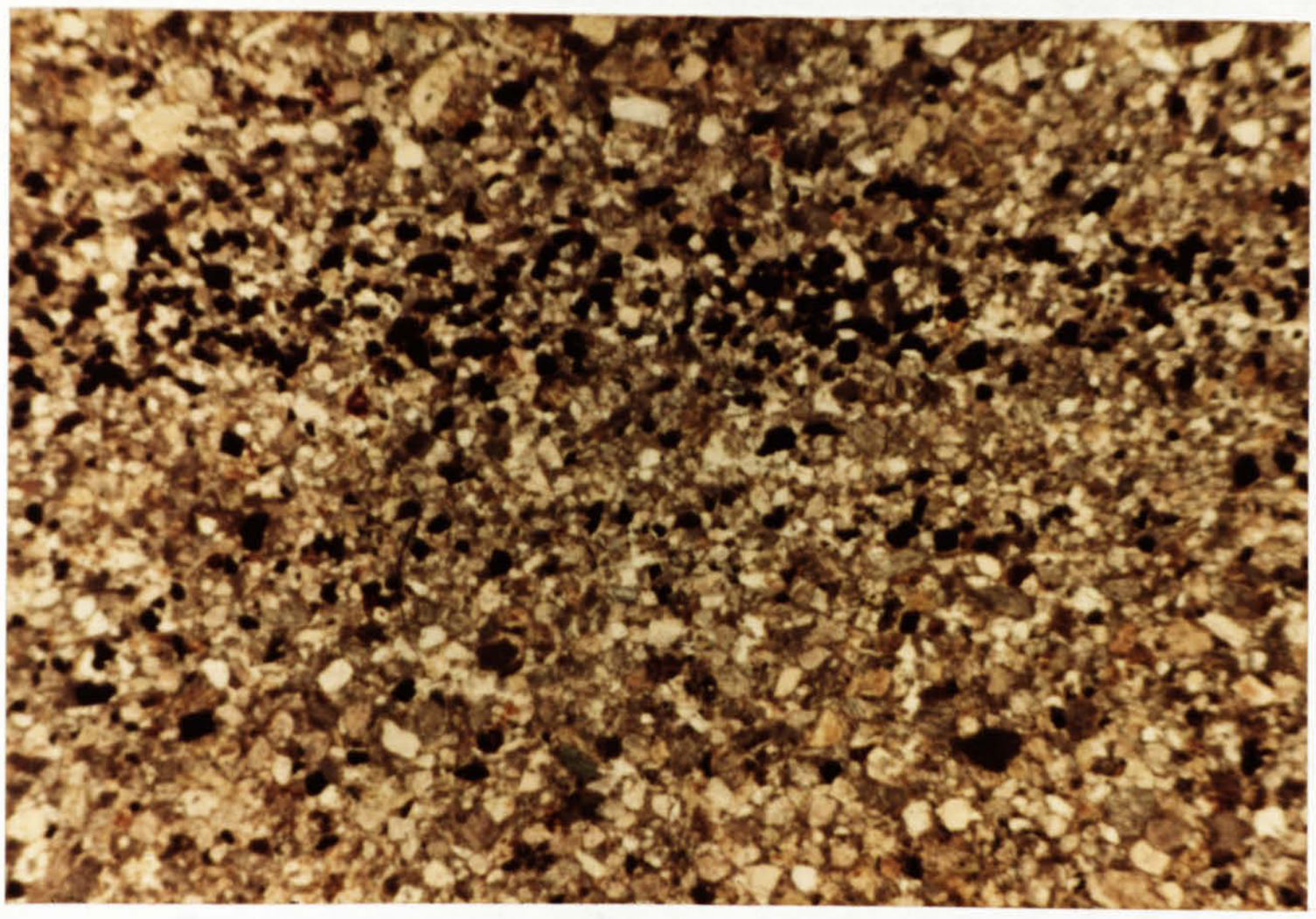

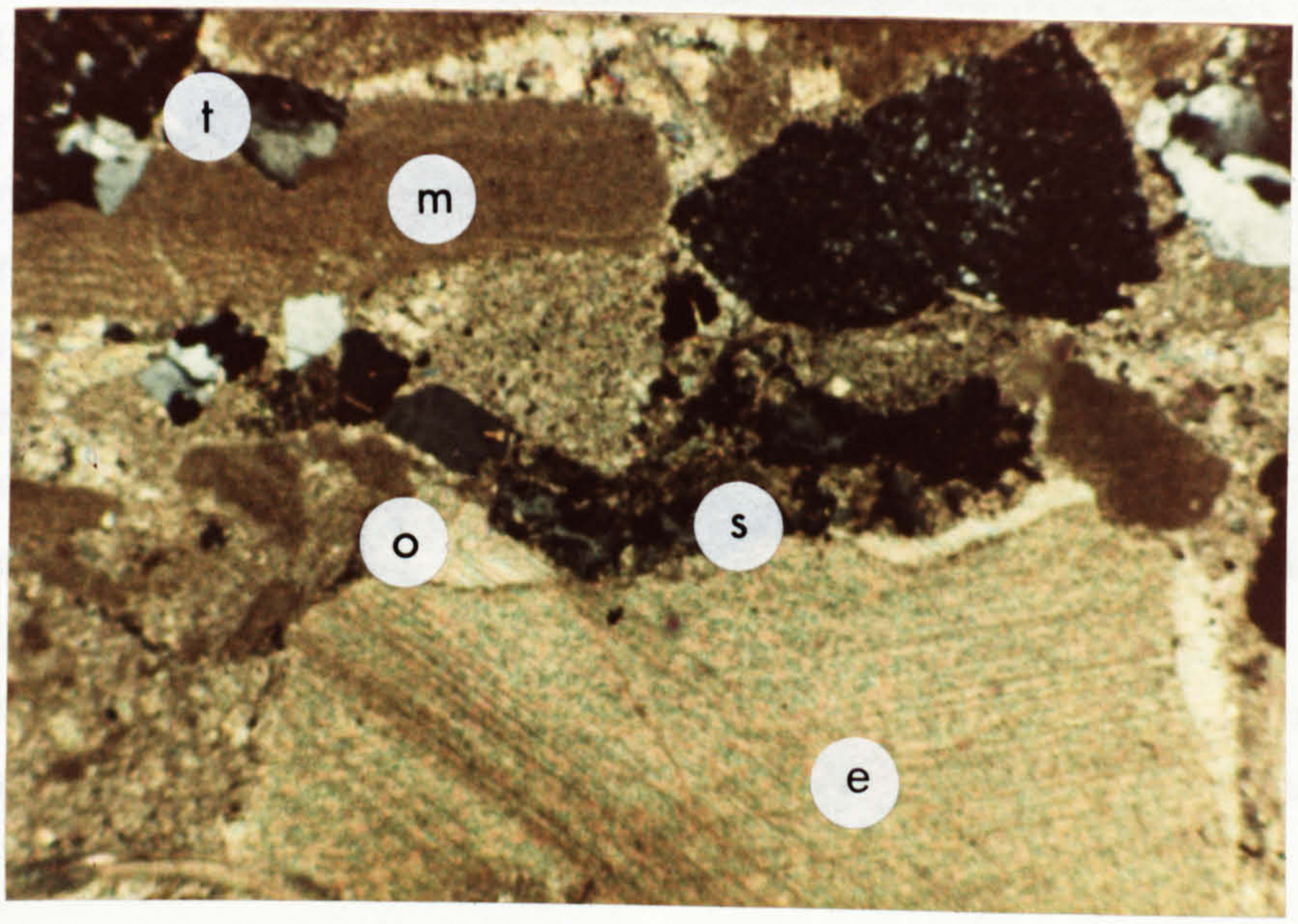
t
m
o
s
e

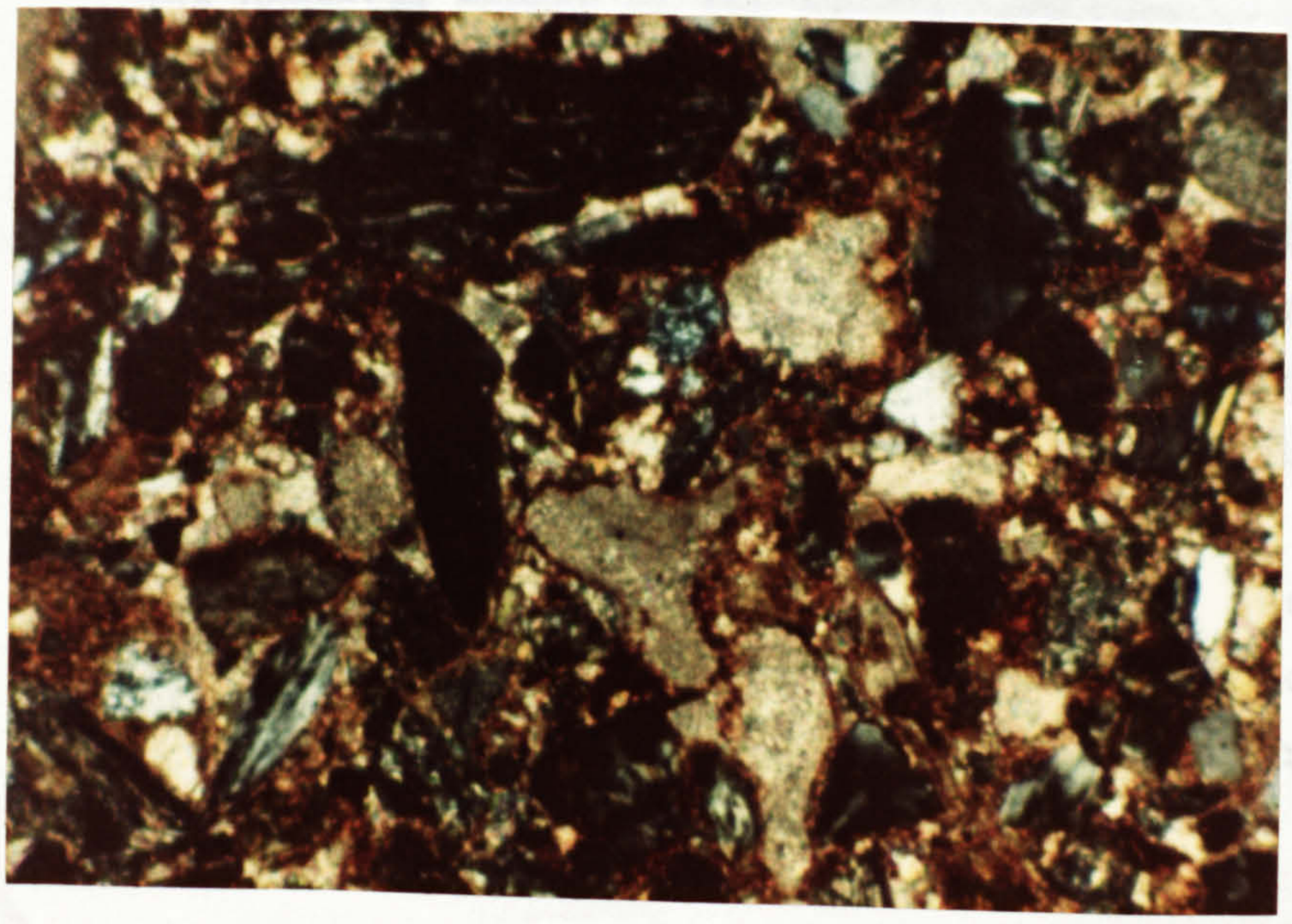

(III) Compaction resulting in irregularly distributed stress and fracturing of brittle terrigenous grains. Softer grains (e.g. serpentinite) are bent around harder grains (e.g. chert). Suturing of grains is generally along terrigenous/carbonate contacts and involves the preferential solution and displacement of carbonate;
(IV) Ferroan and non-ferroan carbonate infilled remaining pore spaces; this was accompanied by extensive corrosion and replacement around margins of chert, serpentinite and quartz by carbonate. Quartz and chert in particular are invaded from outside by stubby calcite crystals (Fig. 6.6);
(V) Late-stage authigenic overgrowths on quartz replacing calcite.

Subaerial parts of the Kasaba Formation show a significantly different diagenetic history, as outlined below:
(1) Deposition as poorly to moderately packed sediment, in a generally random orientation;
(2) Differential compaction results in areas of moderate to dense packing, grain contacts are long grain, concavo-convex, point and very rarely sutured;
(3) Patchy development of a haematite rim cement (see below, 6.2.6);
(4) Pervasive microsparite carbonate cement;
(5) Late-stage patchy void filling sparite. Patchy or wholesale replacement of chert and serpentinite. Corrosion of quartz and chert grain margins (Fig. 6.6). In calcretes extensive corrosion of quartz and invasion from the outside by stubby calcite crystals (Figs. 6.6 and 3.6).

6.2.6 Kasaba Formation Red Beds

The Doğantaş Member of the Kasaba Formation is a variegated red bed sequence, comprising interbedded red and non-red strata. Both sandstones and mudstones are variably reddened, red horizons comprise approximately 25% of the sequence. The reddening is produced by the presence of finely dispersed cryptocrystalline and euhedral haematite which forms rims to terrigenous rock grains (Fig. 6.5) and in patches infills pore spaces. The distribution and crystalline form indicate that the haematite is not detrital but formed *in situ*. In all cases haematite appears to have formed prior to micrite cement formation. Currently there are two hypotheses for the origin of haematite pigment in red beds. The first maintains

Fig. 6.6

Scanning electron micrographs of diagenetic features and terrigenous grains.

(a) Authigenic carbonate growing on detrital terrigenous grain and infilling pore space.
Spec. 97/78.
Salir Formation. GR. 527334.

(b) Close up of (a).

(c) Pitting and replacement of quartz (q) by carbonate in calcrete horizon.
Spec. 71/80.
Kasaba Formation. GR. 520357.

(d) Growth of authigenic clay mineral (c) has been followed by slight compaction resulting in the bending and fracturing of the clay.
Spec. 9291.
Kemer Formation. GR. 534295.

(e) Well rounded and pitted silt grains in Doğantaş Member (Kasaba Formation) sandstone. The roundness and pitted surface is consistent with aeolian activity.
Spec. 69/80. GR. 520357.

(f) Angular feldspar grain (f) in micrite matrix (m).
Surface of specimen polished then etched with dilute hydrochloric acid.
Spec. 191/78.
Salir Formation. GR. 331461.

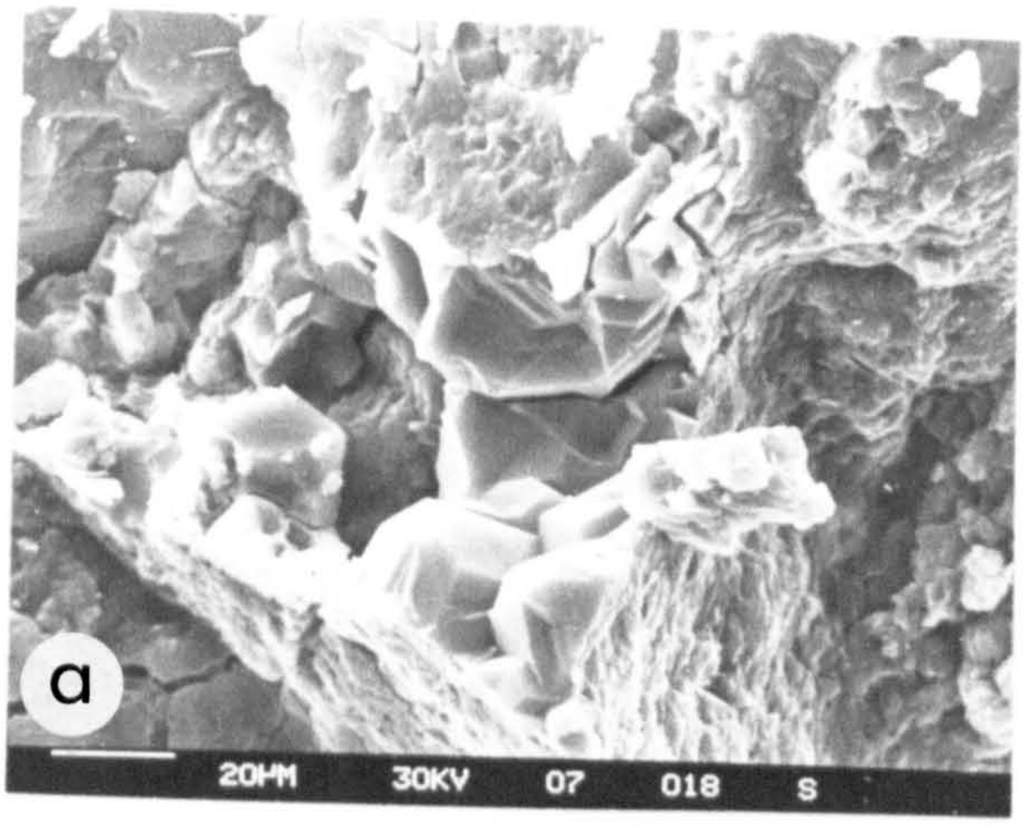
a
20HM 30KV 07 018 S

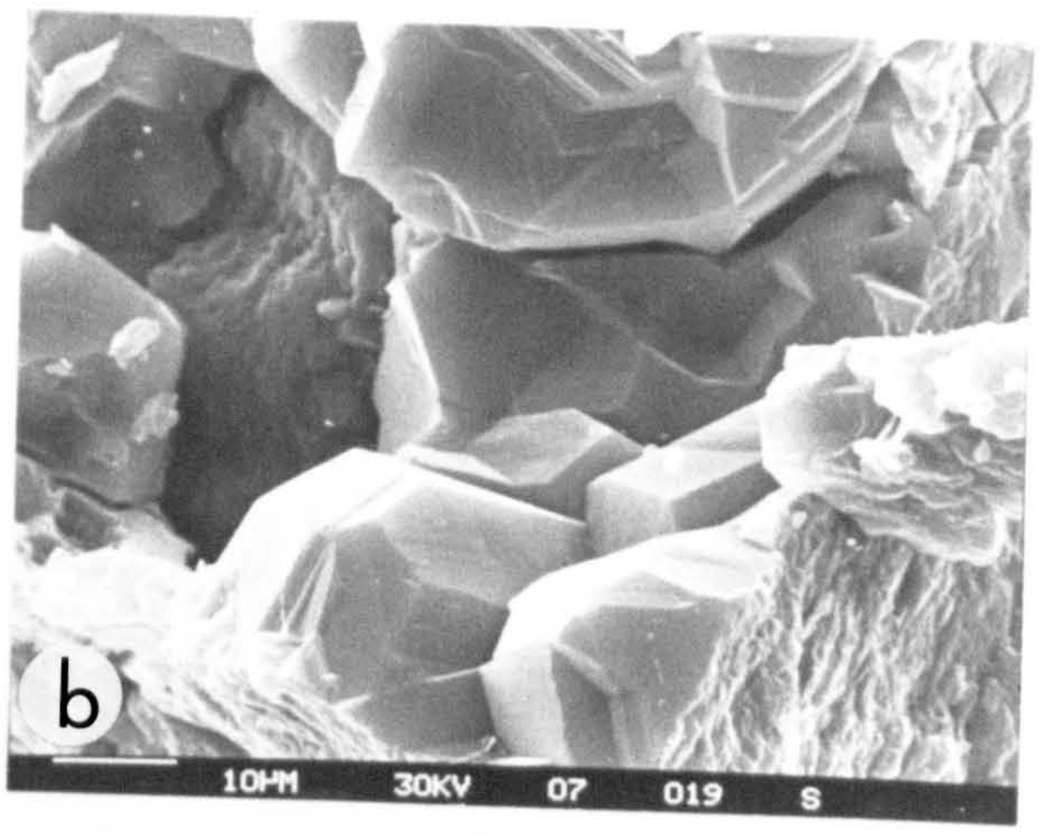
b
10HM 30KV 07 019 S

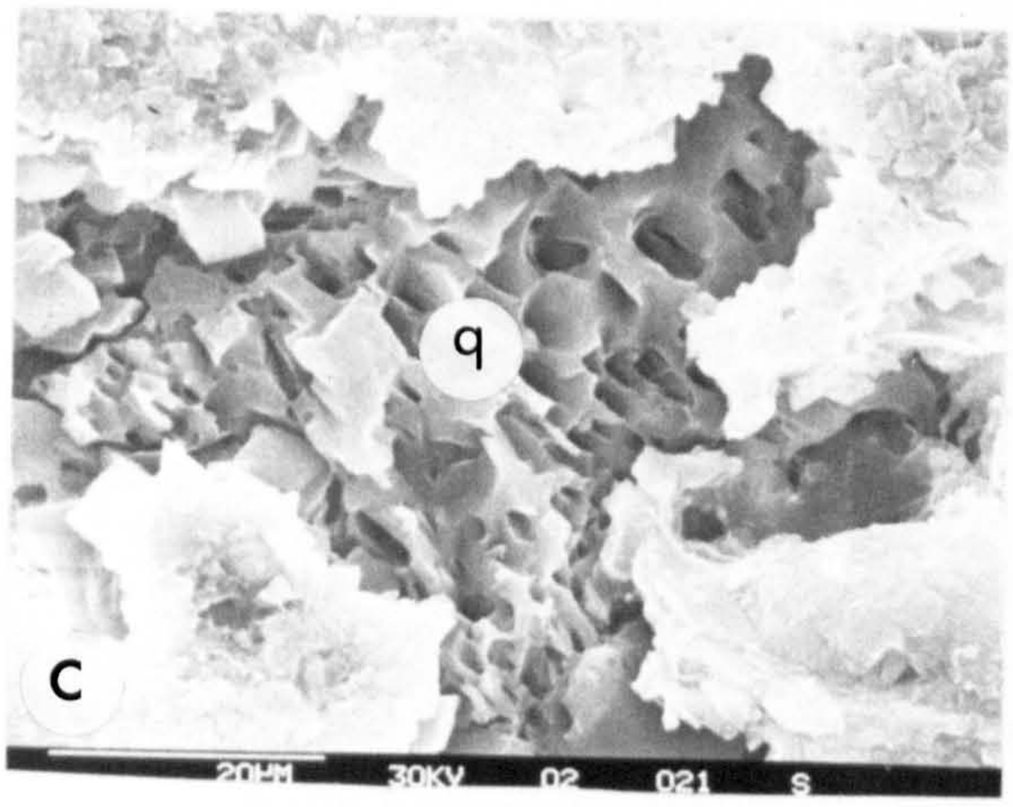
q
c
20HM 30KV 02 021 S

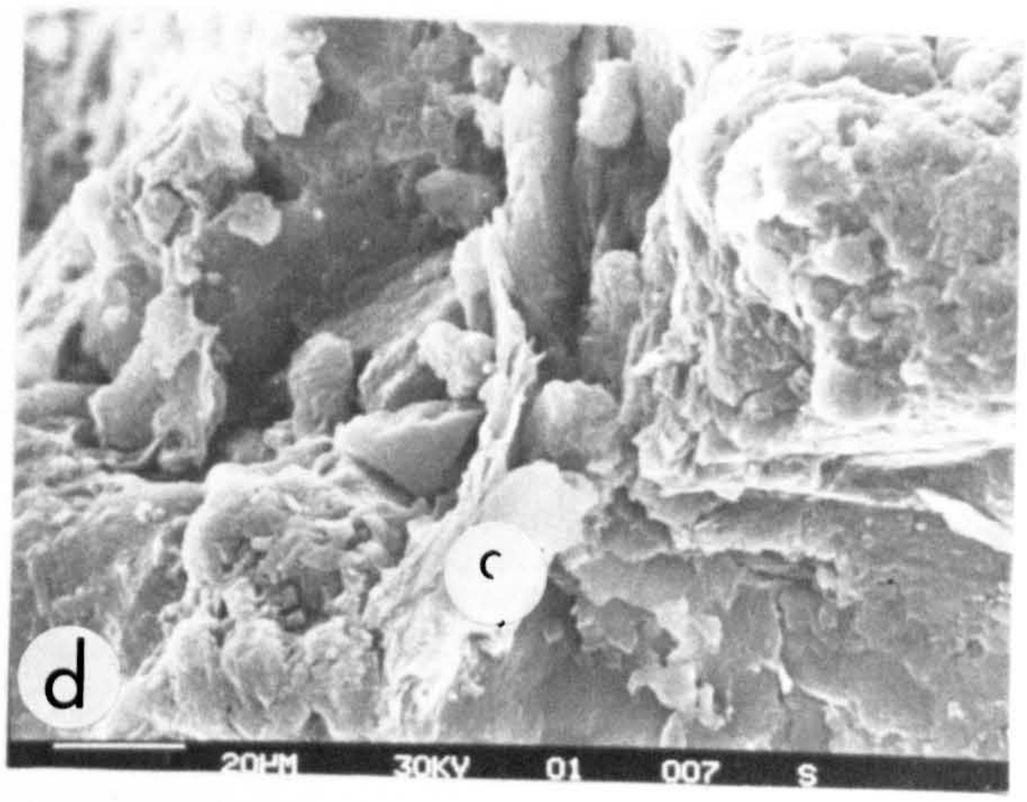
c
d
20HM 30KV 01 007 S

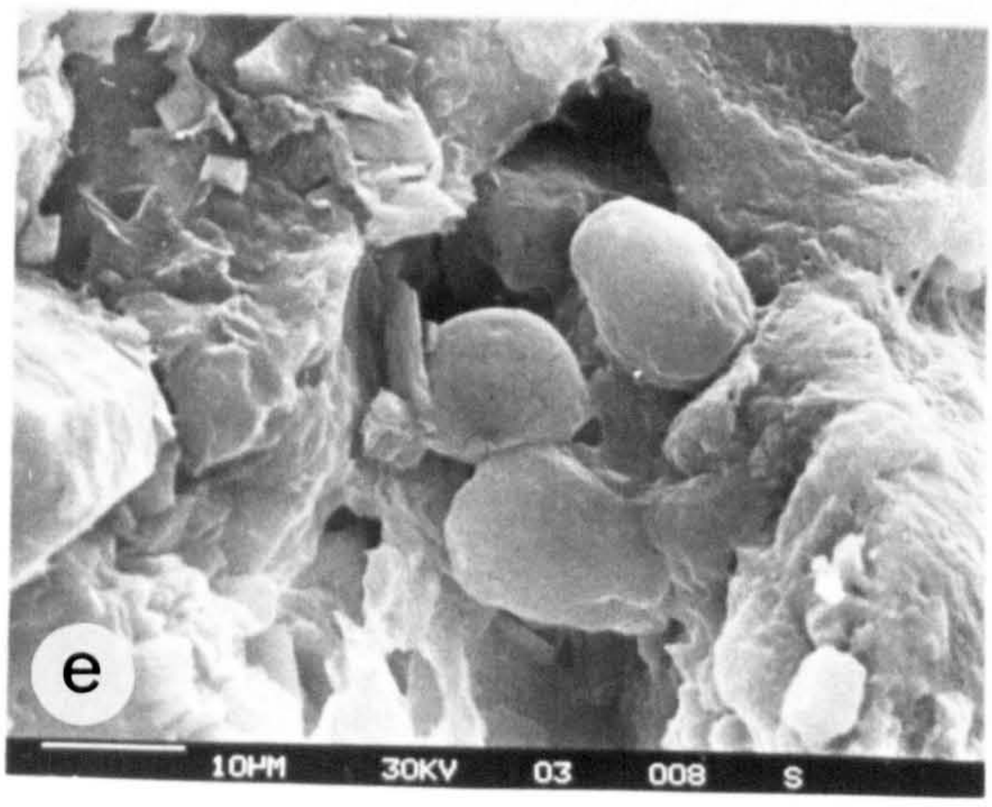
e
10HM 30KV 03 008 S

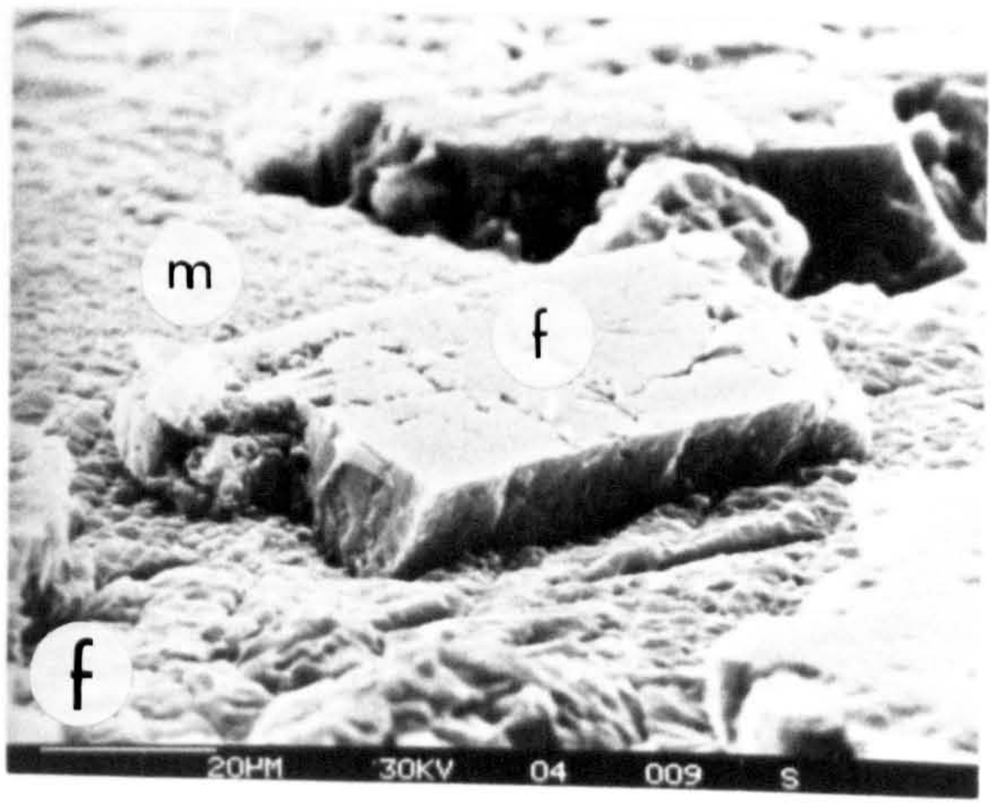
m
f
20HM 30KV 04 009 S

that haematite is from the *in situ* alteration of unstable iron bearing silicates and subsequent hydrated ferric oxide formation (e.g. Walker, 1967a, b; Turner, 1974). Where favourable post burial interstitial chemical and physical conditions persist the hydrated ferric oxides dehydrate and crystallise to haematite pigment.

The second hypothesis suggests the haematite is derived from the *in situ* post-depositional dehydration and crystallisation of detrital hydrated ferric oxides (van Houten, 1972; Friend, 1966; McPherson, 1980). The ferric oxides are produced as an amorphous substance by regolith weathering in upland areas. The subsequent reworking and transport results in an alluvium with abundant hydrated ferric oxides. Following deposition, providing the intrastratal conditions are favourable, the yellow/brown hydrated ferric oxide pigment is dehydrated and crystallises to haematite.

In summary, red beds may derive their colour either directly by intrastratal alteration of iron silicates or from the *in situ* dehydration and crystallisation of a detrital ferric oxide precursor. A detailed discussion of red bed formation is outside the scope of this thesis; a recent comprehensive review is provided by Turner (1981).

The Kasaba Formation was derived from a compositionally very immature source area. The presence of abundant unstable iron silicates that are readily altered (Fig. 6.5) strongly favours the former mechanism for the formation of red beds in this sequence. In support of this iron silicate minerals in the subaerial parts of the Kasaba Formation (Doğantaş Member, red bed sequence) are significantly *more* altered than iron silicates in the submarine parts of the sequence; in many instances they have been almost totally removed.

6.3.0 Eastern Margin

Overall composition (Fig. 6.7) and palaeocurrent orientations (Fig. 5.2) clearly indicate that the conglomerates and sandstones of the Salir Formation were derived from the Antalya Complex during its emplacement (Hayward and Robertson, in press) (10.2.1). Variations in composition are a potentially useful tool to aid in the understanding of the style and mode of emplacement.

6.3.1 Conglomerates

The conglomerates of the Salir Formation are variably sorted and

moderately to well rounded. Sedimentary facies exerts considerable control on textural maturity. Clast types are again dominated by basic and ultrabasic igneous rock fragments, along with chert, pelagic and shallow water limestone. Typical compositions determined from point-counts are shown in Fig. 6.7.

Vertical variations in composition. Conglomerates of the Salir Formation can be grouped by composition into three broad fields:
(1) Lower Miocene sequences, e.g. submarine fan sequences exposed in the Akdere valley (Fig. 5.1) consist of a wide spectrum of compositions (Fig. 6.7) with up to 42% shallow water limestone lithoclasts;
(2) Middle to Upper Miocene sequences, e.g. alluvial fan-shallow marine sequences of the Bağbeleni Member (Fig. 6.7) which have consistently less than 10% shallow water limestone lithoclasts;
(3) Some Middle to Upper Miocene sequences in the Alaçadağ area often have a very high proportion of clasts clearly derived from the carbonate platform. These sequences are located adjacent to syn-depositional fault scarps (described in detail in 5.10).

The general upward decrease in shallow water limestone clasts (carbonate platform derived), particularly from the base of the Bağbeleni Member upwards, reflects the progressive covering of the platform by terrigenous clastic material. The upper parts of the sequence were deposited after the main Miocene phase of emplacement of the Antalya Complex (5.11). The low proportion of limestone clasts suggest that in this area the carbonate platform was *not* involved in any *late-stage* tectonic movements.

6.3.2 Sandstone Composition

The sandstones of the Salir Formation are texturally and mineralogically immature. Moderately to poorly sorted, they consist of a complete admixture of basic igneous and sedimentary rock fragments (of variable derivation), quartz, feldspar and often abundant bioclastic material. The sandstones plot dominantly in the litharenite and sublitharenite fields of McBride (1963) and Folk (1968) (Fig. 6.7). Principal terrigenous framework grains and their characteristics are summarised in Table 6.3. Flattened, carbonised wood fragments are up to 4 cm long. Bioclastic material comprises dominantly algal, foraminiferal and shell debris, with rarely bored and micritised rims. A complete list of skeletal and non-skeletal carbonate grains is given in Table 6.4.

Fig. 6.7

Triangular composition plots for the conglomerates and sandstones of the Salir Formation (eastern margin). In the conglomerates; sed oph = pelagic limestone and radiolarian chert of "ophiolite" affinity. CP = shallow water limestone clasts (carbonate platform derived). Igneous ophiolite - igneous ophiolite clasts.

Note the grouping into three fields (see text for discussion).

The QRF plot shows a wide range in composition but a consistently low feldspar component.

The Qtz - Bioclastic carbonate (mainly skeletal) - Other plot demonstrates the high but widely varying percentage of bioclastic carbonate grains.

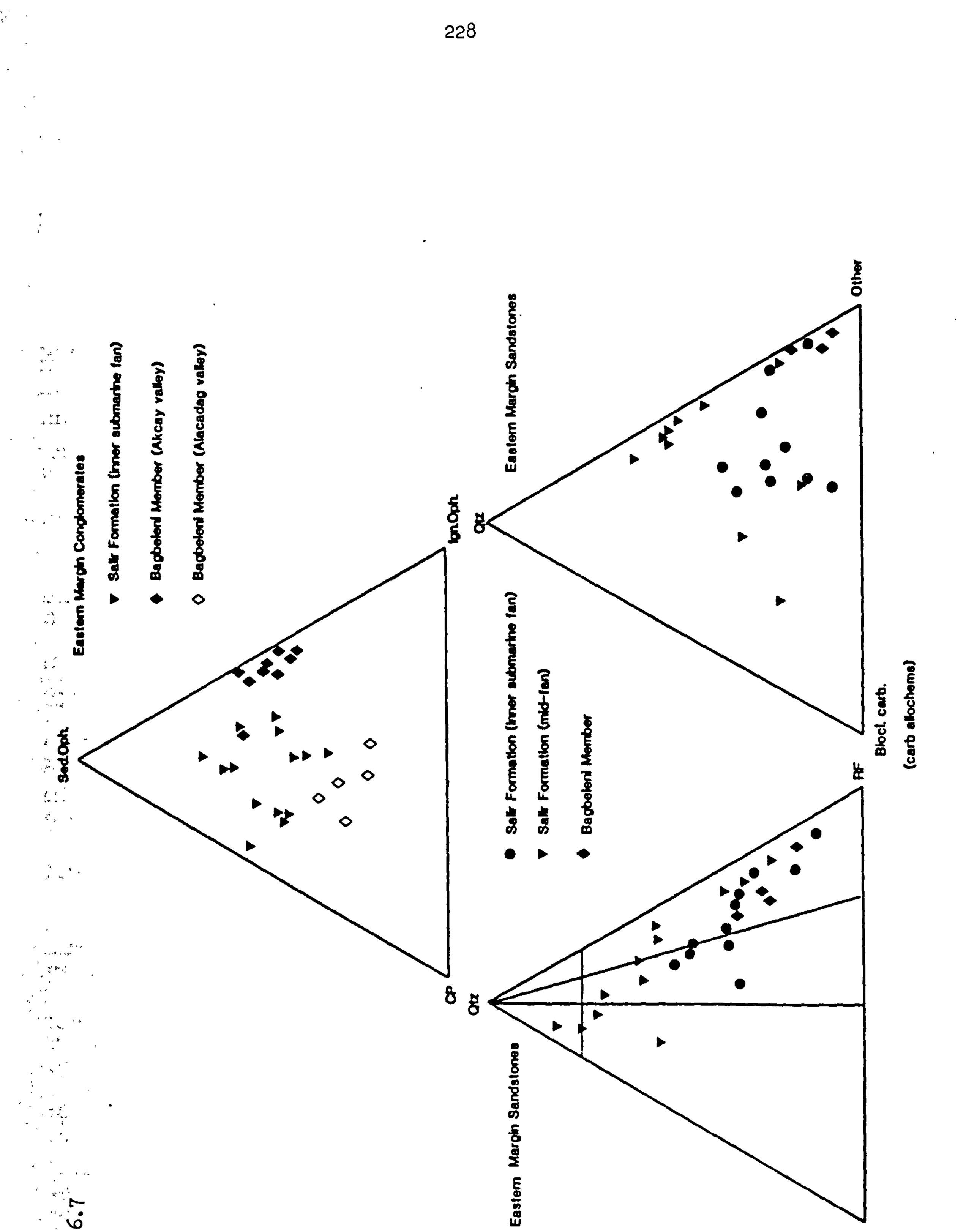
Eastern Margin Conglomerates
Salir Formation (inner submarine fan)
Bagbelent Member (Akcay valley)
Bagbelent Member (Alacadag valley)
Lgn.Oph.
Sed.Oph.
QP
Qtz
Eastern Margin Sandstones
Salir Formation (inner submarine fan)
Salir Formation (mid-fan)
Bagbelent Member
Bioci. carb.
(carb allochems)
RF
Fsp

Fig. 6.7

GRAIN FEATURES	SHAPE/ ROUNDNESS	ALTERATION AND DIAGENESIS	INFERRED SOURCE
Quartz			
I) single, undulose and uniform extinction, with inclusions II) polycrystalline, irregular, stretched and sutured boundaries inclusions of rutile, biotite and chlorite	subangular to rounded equant	irregular replacement around margin by carbonate, patchy wholesale replacement by carbonate	Mainly second cycle derived from Triassic passive margin sandstone sequence within the Antalya Complex
Feldspar			
I) plagioclase An_{35-70} II) patch perthites III) microcline	subangular to subrounded, equant to elongate	little or no *in situ* alteration	(I) from Antalya Complex ophiolite unit
Chert			
I) microcrystalline chert, green and black II) red radiolarian chert with radiolarian ghosts	angular to subrounded, equant	irregular replacement around margin by carbonate, patchy wholesale replacement by carbonate	(II) sedimentary cover to basalt of the Antalya Complex (1) as above minor input from replacement cherts in carbonate platform (?)
Basalt			
I) variolitic II) glass	subrounded to rounded, equant	alteration to chlorite, bent around and indented by harder grains	Basalts within the Antalya Complex
Serpentinite			
I) fibrous lamellar II) mesh textured and banded III) massive structureless	subangular to rounded, equant	marginal and patchy replacement by carbonate	"intrusions" within Antalya Complex
Fe/Mg minerals			
opx., cpx, olivine	subangular to rounded, equant	little *in situ* alteration	Antalya Complex ophiolite unit
Dolerite	subrounded to rounded, equant to elongate	little *in situ* alteration	Antalya Complex ophiolite unit
Spinels			
red and green	angular to subangular	no alteration	Antalya Complex ophiolite unit
Limestone lithoclast			
I) microspar II) lime mudstone with planktonic forams III) bioclastic packestone IV) bioclastic boundstone	subangular to rounded, elongate to equant	no alteration often extensive pressure solution along margins	mainly carbonate platform, some from sedimentary sequences within the Antalya Complex
Sandstone lithoclasts quartzose sandstone with quartz overgrowths	subrounded to rounded, equant	irregular replacement around margin by carbonate	Triassic passive margin sandstone sequence within Antalya Complex

Table 6.3 Main terrigenous framework grains of the Salir Formation.

Skeletal carbonate grains

Echinoderms

plates and spines

Bryozoan

several species

Shell fragments

bivalves

gastropods

Coralline algae

Mesophyllum

Archeolithothamnium

Lithothamnium

Lithophyllum

several additional species

Planktonic foraminifera

large number of species

Benthonic foraminifera

most commonly present are:

Miogypsina

Elphidium

Miliolidae

Amphistegina

Nephrolepidina

Eulepidina

Austrotrillina

Alveolina

Rotalia

Lepidocyclina

Neoalveolina

various agglutinating species

Non-skeletal carbonate grains

Pelloids

Table 6.4

Main skeletal and non-skeletal contemporaneous carbonate grains in Salir Formation sandstones.

6.3.3. Source Area

The ubiquitous high proportion of quartz reflects derivation in part from a Triassic continental margin sandstone sequence within the Antalya Complex (Hatip Formation of Robertson and Woodcock, 1981b). Well rounded grains of metamorphic quartz indicating second cycle derivation, are consistent with this. The low proportion of feldspar (generally less than 10%) reflects the lack of acidic igneous rocks in the source area. Marked variations in bioclastic content (5-60%) is shown in Fig. 6.7, and reflects irregular mixing with shallow water derived bioclastic debris from the margins of the basin.

Vertically there is very little systematic change in composition, most significant is a drop in the proportion of shallow water limestone clasts derived from the carbonate platform (also seen in the conglomerates of the Bağbeleni Member, Figs. 6.9, 6.10). Other principal components do not vary systematically. The *lack* of well defined trends in sandstone composition, reflecting the successive unroofing of the Antalya Complex, is consistent with its style of emplacement along a series of strike-slip faults (Woodcock and Robertson, 1981b), continuously exposing all levels of the ophiolite stratigraphy (Robertson and Woodcock, 1981a, b; Hayward and Robertson, in press) (see also Chapter 10).

6.3.4 Diagenesis

The main stages in sandstone diagenesis for submarine parts of the sequence are outlined chronologically below:

(1) Deposition as poor to moderately packed sediment with generally little matrix.

(2) Rarely skeletal carbonate clasts have an early isopachous fringe cement of probable marine origin.

(3) Formation of an early non-ferroan carbonate cement on echinoid plates.

(4) Compaction results in dense packing. Softer grains (e.g. serpentinite) are bent, wrapped around and indented by quartz and chert grains. In extreme cases serpentinite has been 'intruded' into fractures in limestone. Harder grains (e.g. chert) fracture and are subsequently veined by carbonate during later cementation.

(5) Associated with compaction is extensive pressure solution (grain margin dissolution, Hancock, 1978) of dominantly bioclastic

carbonate grains, particularly susceptible are foraminiferal and algal fragments (Fig. 6.8). Terrigenous grains now lie along sutured grain boundaries (Fig. 6.8).

(6) Corrosive replacement of chert and quartz grain margins and patchy replacement of chert and igneous rock fragments by calcite.

(7) Formation of ferroan and non-ferroan carbonate microsparite cement followed by occasional void filling spar.

The difference in principal diagenetic features of the sandstones reflects their varied composition. In sandstones with moderate to *high* bioclastic carbonate content (20-60%) compaction to a large degree is accommodated by the removal of carbonate by grain margin dissolution (pressure solution), resulting in a large proportion of sutured grain boundaries (Fig. 6.8). In sandstones with a *low* bioclastic content compaction is accommodated by the mechanical wrapping of softer grains (mainly serpentinite) around harder ones, in extreme cases serpentinite is 'intruded' into fractures developed in brittle grains.

Reducing conditions prevailed throughout the diagenetic history, allowing precipitation of ferroan calcite and preservation of wood fragments. Pyrite was precipitated locally within foraminifera tests.

6.4 Summary of Compositional Variations

The contrast in sandstone and conglomerate composition between the eastern and western margin sequences results principally from the different styles of tectonic emplacement (Chapter 10).

The most significant difference is the proportion of quartz present (Fig. 6.10). Although both allochthonous units contain broadly the same rock units (Chapter 1), i.e. they both represent a continental margin sequence and its associated ocean, they have been emplaced by vastly different processes (Chapter 10). The Kemer Zone of the Antalya Complex represents an imbricated continental margin sequence thrust onto its own margin (Woodcock and Robertson, 1981) (10.6.3). Triassic sandstones within the sequence are at a high structural level and provide a concentrated local source for the abundant quartz in the sediments of the eastern margin.

By contrast continental margin sandstone sequences within the Lycian Nappes have been extensively tectonised, are grossly allochthonous and tectonically intercalated within the Lycian Nappe pile.

Fig. 6.8

Photomicrographs of thin sections of mixed terrigenous-bioclastic sandstones. Salir Formation.

(a) Extensive pressure solution (grain margin dissolution) has resulted in irregular sutured grain boundaries between coralline algae (c) and quartz (q); echinoid plate (e) and coralline algae (c) and terrigenous grains, mainly serpentinite (s).
Salir Formation. Spec. 46/78. Field of view is 3 cm.
Crossed polars. GR. 512416.

(c) Fracturing followed by veining and extensive replacement of radiolarian chert by calcite.
Salir Formation. Spec. 147/78. Field of view is 1 cm.
Crossed polars. GR. 424368.

(c) Irregular 'needle' sutured grain boundary between coralline algae (c), echinoid plate (e) and skeletal carbonate clast (m).
Note the presence of terrigenous grains, mainly basalt and quartz, aligned along the grain boundaries; and the dramatic reduction in porosity purely as a result of pressure solution associated with compaction.
Salir Formation. Spec. 40/78. Field of view is 1 cm.
Crossed polars. GR. 517379.

(d) Pressure solution between radiolarian chert (r) and coralline algae (c). Other clasts present are serpentinite (s), feldspar (f) and altered basalt (b).
Salir Formation. Spec. 40/78. Field of view is 2 cm.
Crossed polars. GR. 517379.

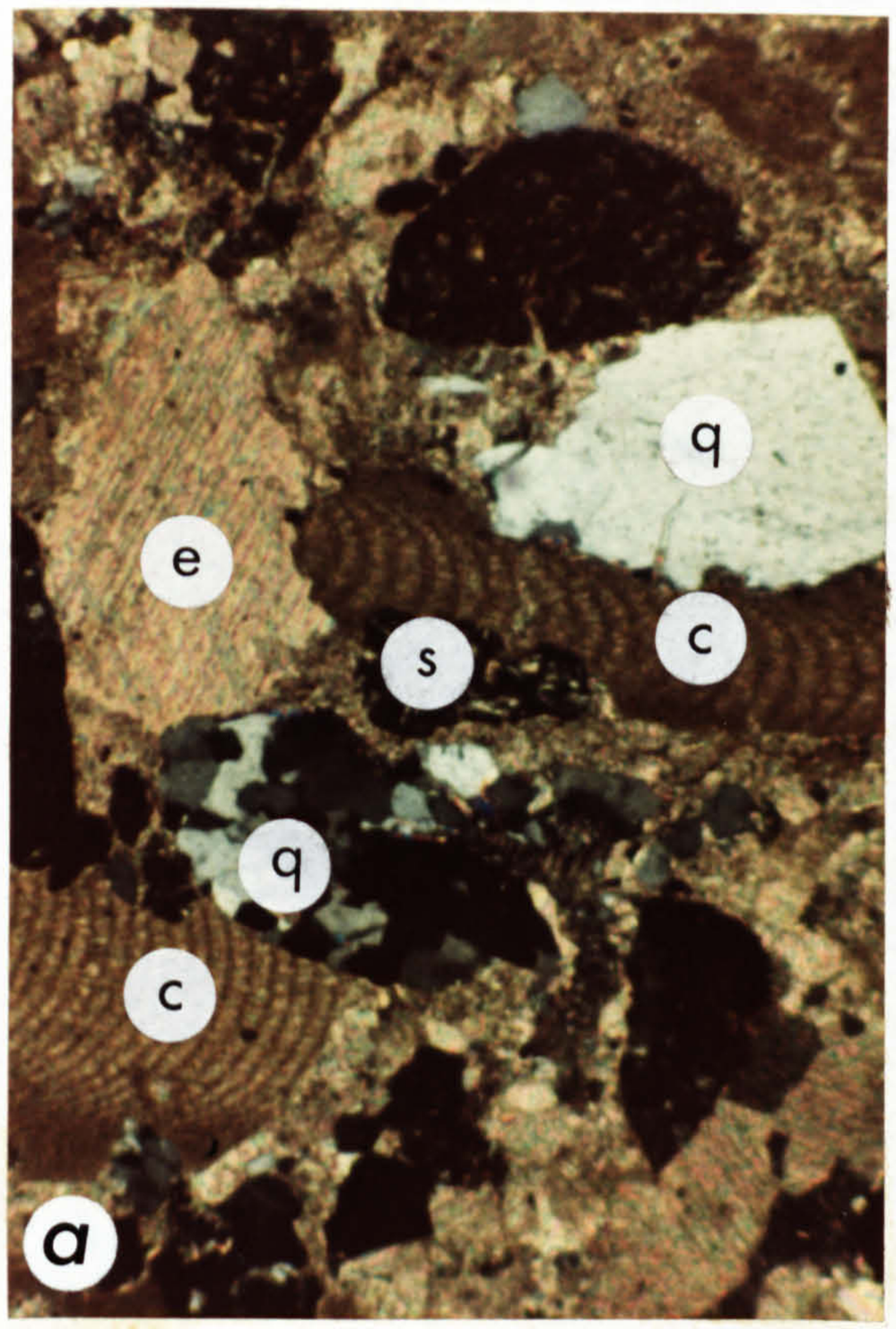
q
e
s
c
q
c
a

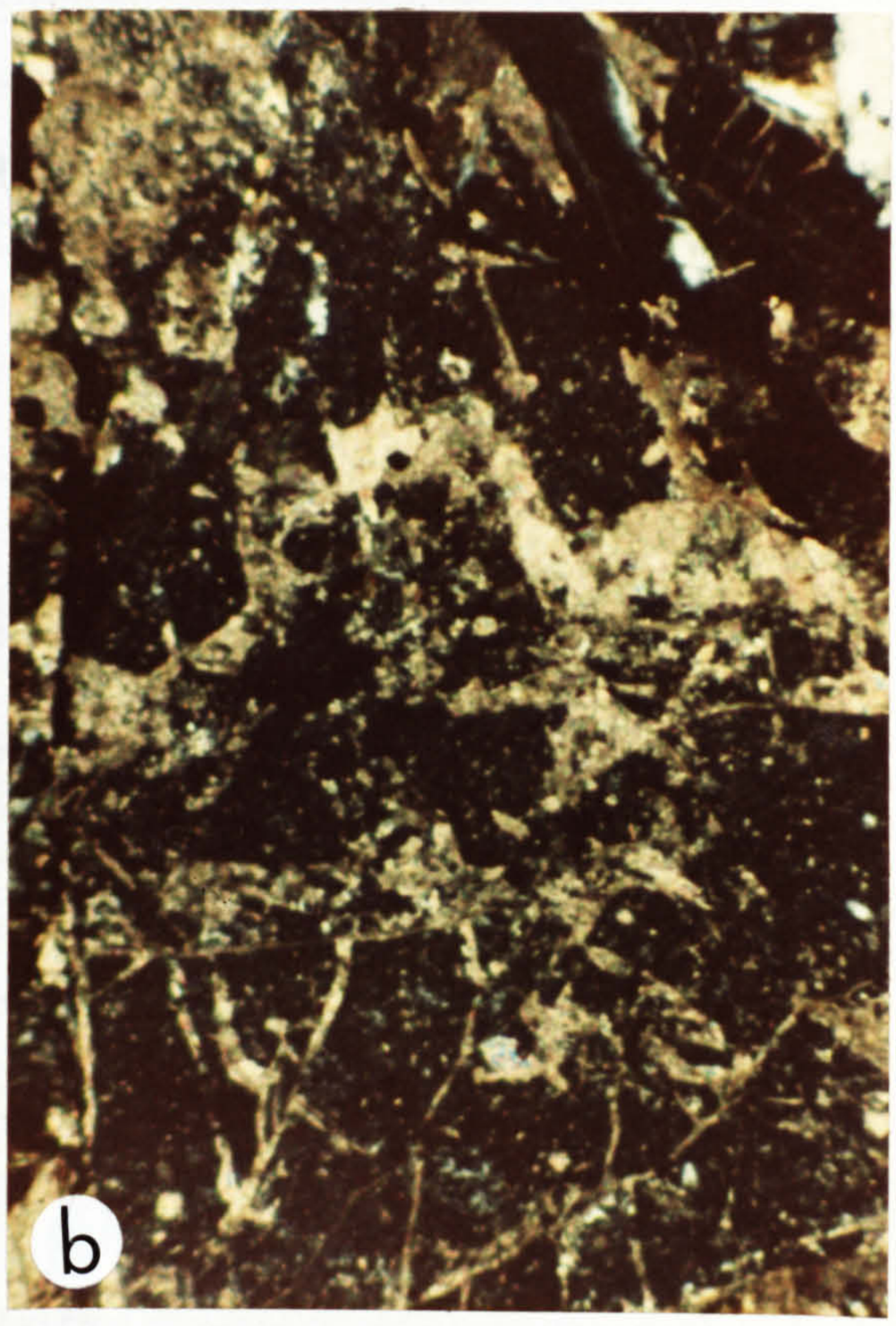
b

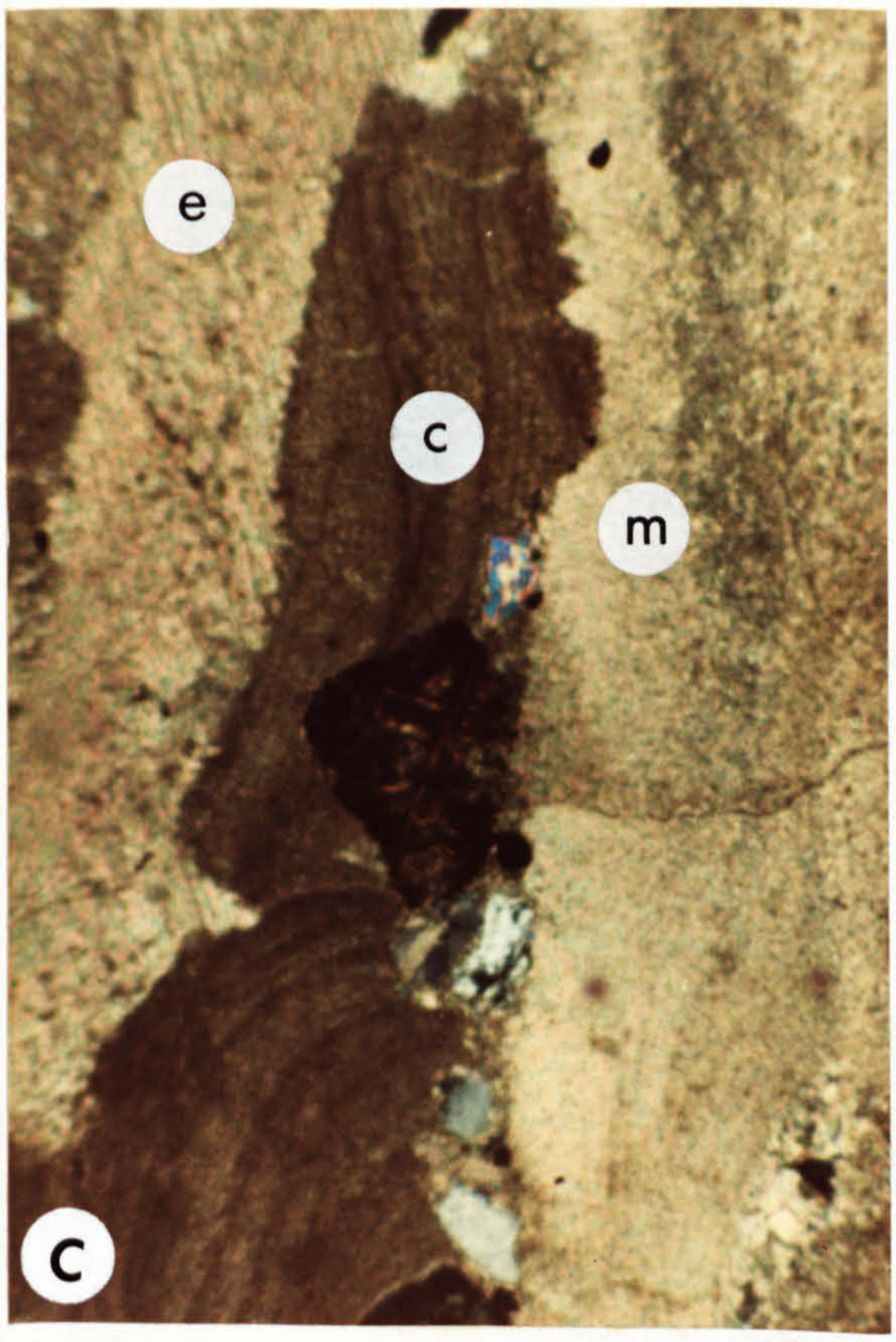
e
c
m
c

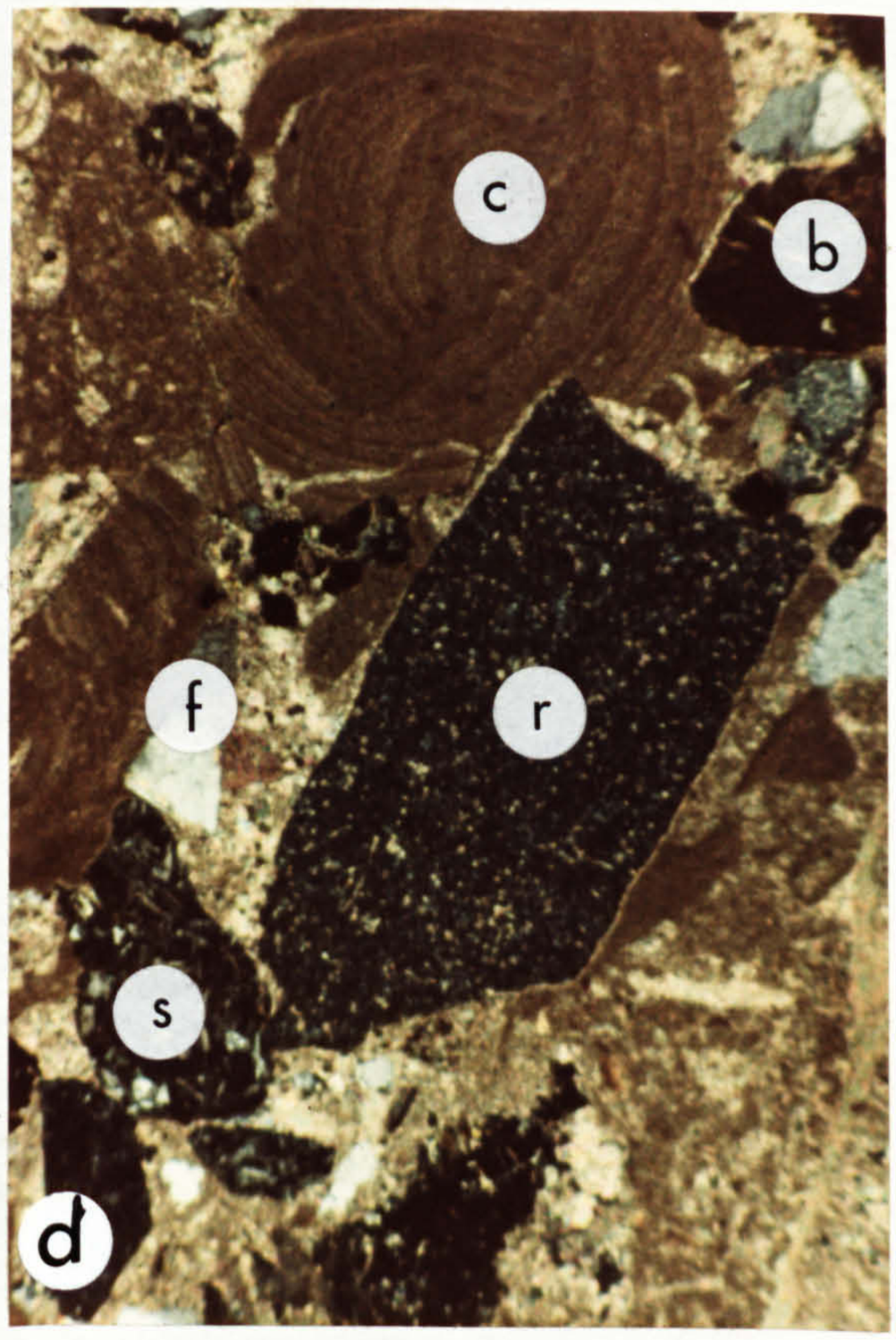
c
b
f
r
s
d

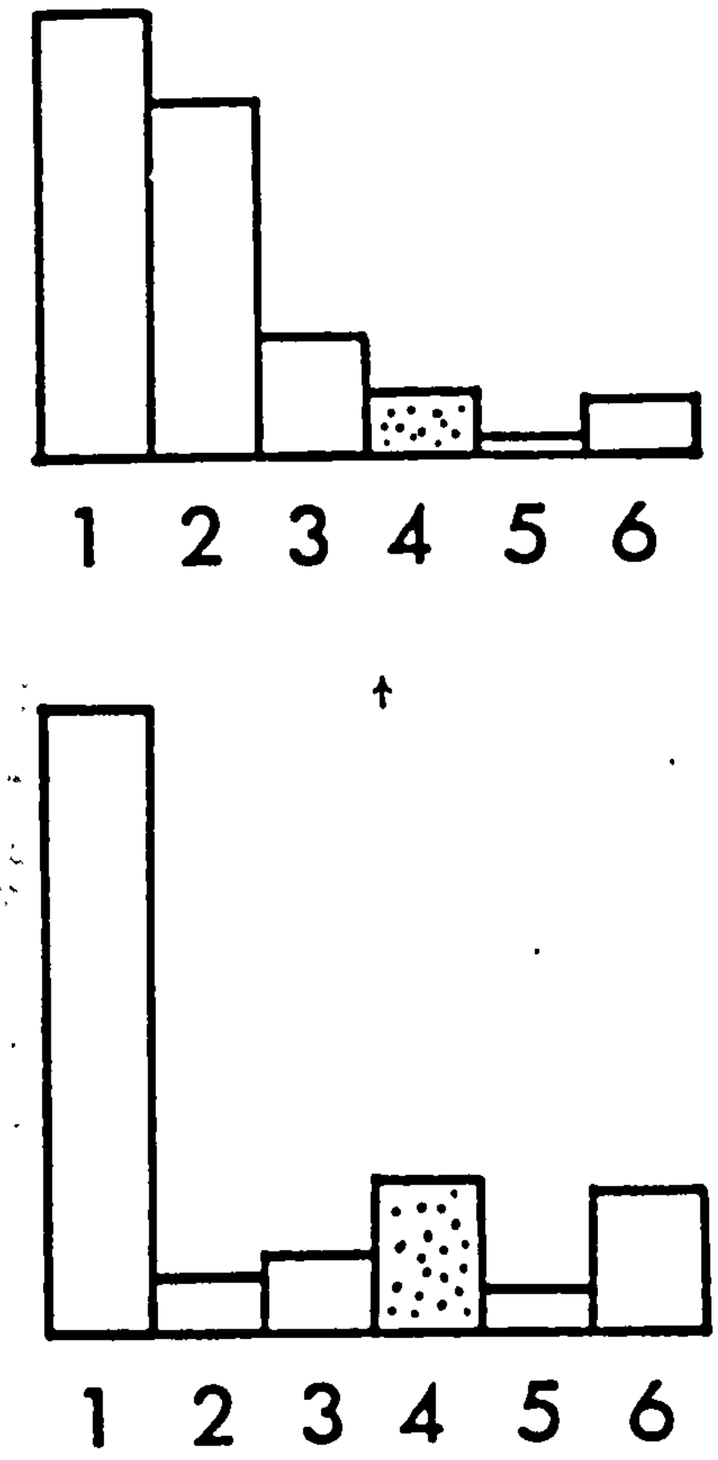

Fig. 6.9
Histograms of the six main terrigenous grain components in the Salir Formation (Akçay Member) sandstones.
Key as in Fig. 6.3. Quartz shaded for reference. For location of specimens see Appendix D. 1 is stratigraphically below 2.

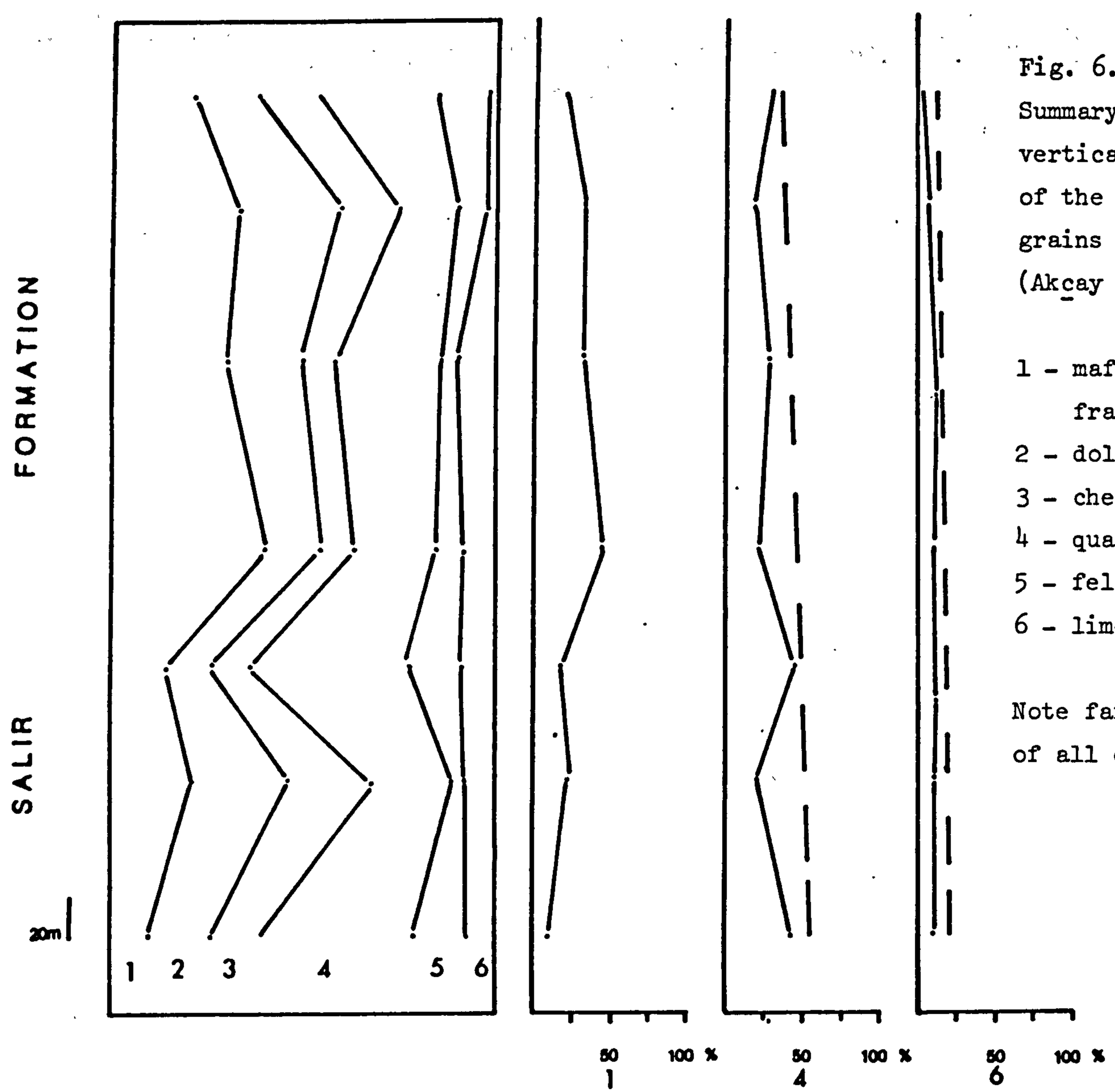

Fig. 6.10
Summary (from Fig. 6.9) of vertical trends in percentage of the six major component grains in the Salir Formation (Akçay Member) sandstones.

1 - mafic and ultramafic rock frags. and minls.
2 - dolerite and basalt
3 - chert
4 - quartz
5 - feldspar
6 - limestone lithoclasts

Note fairly uniform percentage of all clast types.

Fig. 6.11
QRF diagram demonstrating the difference in mineralogy of sandstones on either side of the sedimentary basin.
The eastern margin sandstones contain a significantly higher percentage of quartz derived from a localised continental margin turbidite sandstone sequence
(see text for full discussion).

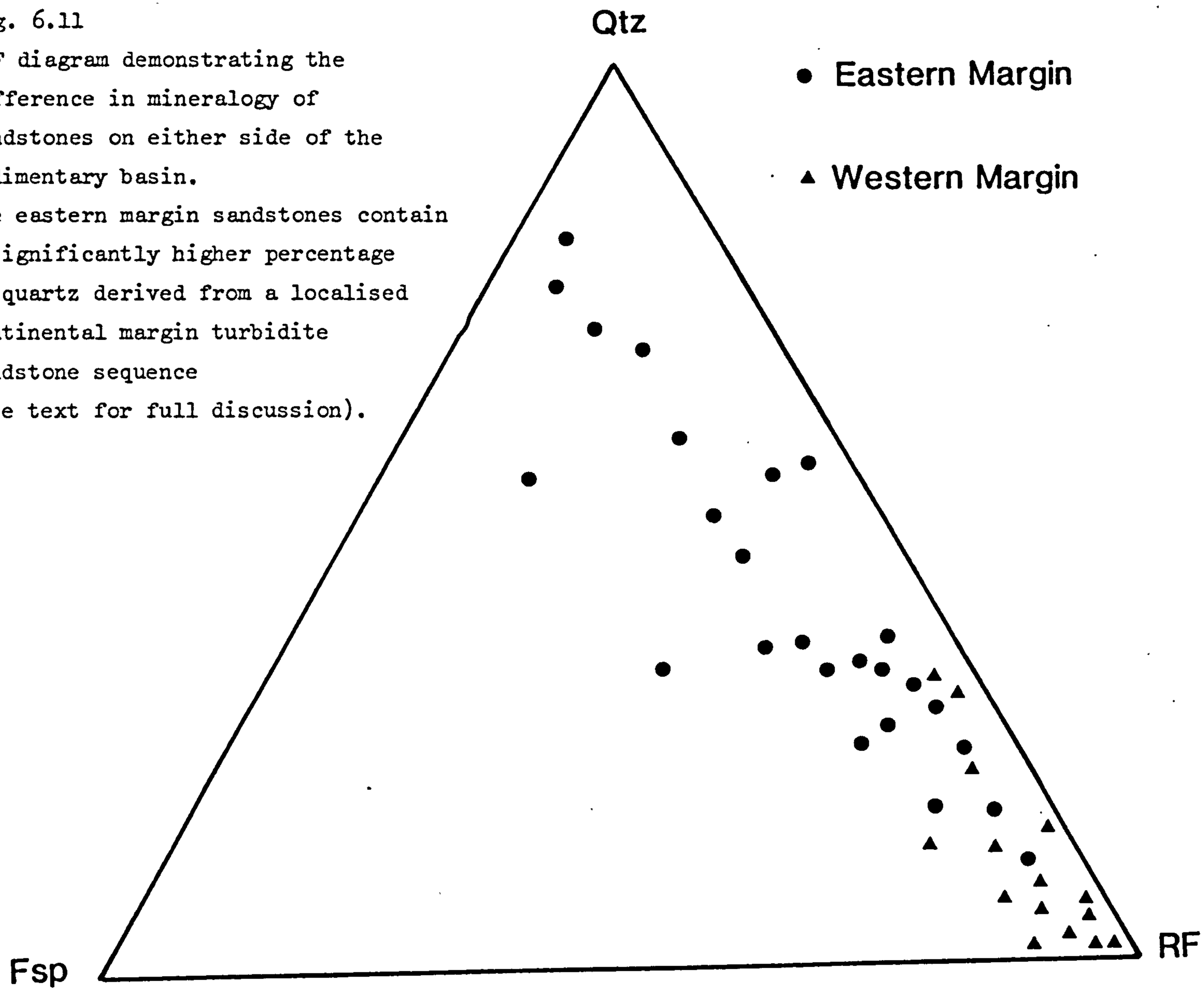

They do not provide a concentrated local source area.

On a smaller scale, subaerial parts of the sedimentary sequence (particularly the Kasaba Formation) show a wide variation in sandstone composition. This is directly related to sedimentary environment. In a subaerial alluvial fan environment clast components may not be subject to very effective mixing and sandstone composition may reflect one flood event derived from one small part of the source area.

PART III

CARBONATES

PART III

CARBONATES

CHAPTER 7 REDEPOSITED CARBONATES

CHAPTER 7

7.0 Redeposited Carbonates

7.1 Introduction

The Kemer Formation is subdivided lithostratigraphically into several members (2.4.0). Ophiolitic terrigenous clastic sediments derived from the Lycian Nappes to the northwest interfinger with carbonate sediments in the southwest in the Felenk Dağ area and to the northeast in the area around Çağman. These two limestone-dominated sequences are recognised as distinct, mappable, lithostratigraphic units (2.4.0). The sedimentology of these two members, their compositional differences and significance to the palaeogeographic and tectonic model for the sedimentary basin is outlined below.

7.2 Çağman Member

The Çağman Member crops out at the northeastern end of the Kasaba syncline, in the area between Kara Dağ and Çağman (Fig. 7.1). The sediments of this sequence are strikingly different from others of the Kemer Formation as they are dominantly composed of bioclastic carbonate material (carbonate allochems).

Initiation of Miocene sedimentation. In the type section (Fig. 7.2) the carbonate platform, which consists of shallow water limestone of Eocene age, is overlain by 40 m of homogeneous green calcareous marl with rare carbonate breccias up to .40 m thick. The platform top is extensively brecciated with a karstic surface, formed by subaerial exposure (9.2.3). As elsewhere in the basin, the marl sequence represents subsidence of the previously subaerially exposed carbonate platform, possibly to abyssal depths. The marls are overlain by a sequence of interbedded turbiditic sandstone (Tcde, Tde), calcareous mudstones and rare pelagic chalks. The sandstones are composed dominantly of bioclastic carbonate material, with generally less than 30% ophiolite-derived material, mainly red radiolarian chert. These cherts are always found in close association with pillow lavas in the Antalya Complex. The low proportion of ophiolite material (serpentinite, dolerite, basalt, etc.) and high proportion of quartz, up to 15%, suggests derivation from the Antalya Complex (6.3.2). Bed thickness ranges from .05 to rarely .35 m (mean .10 m). Sandstones form less than 30% of the sequence.

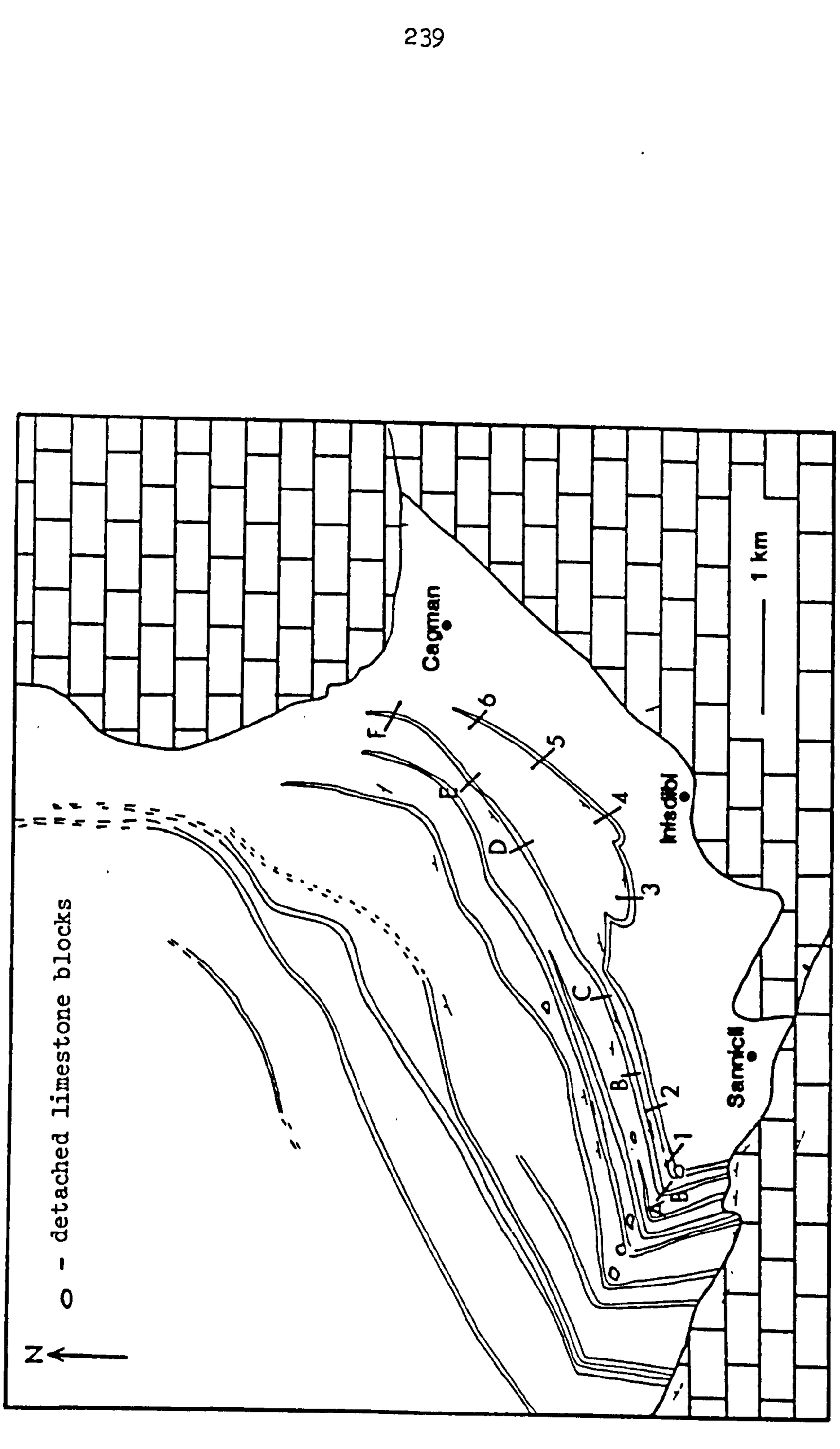

Fig. 7.1 Detailed map of the Cagman area showing extent of mega-breccia beds and consistent thinning to the northeast. Numbers and letters refer to sections in Figs. 7.5 and 7.6.

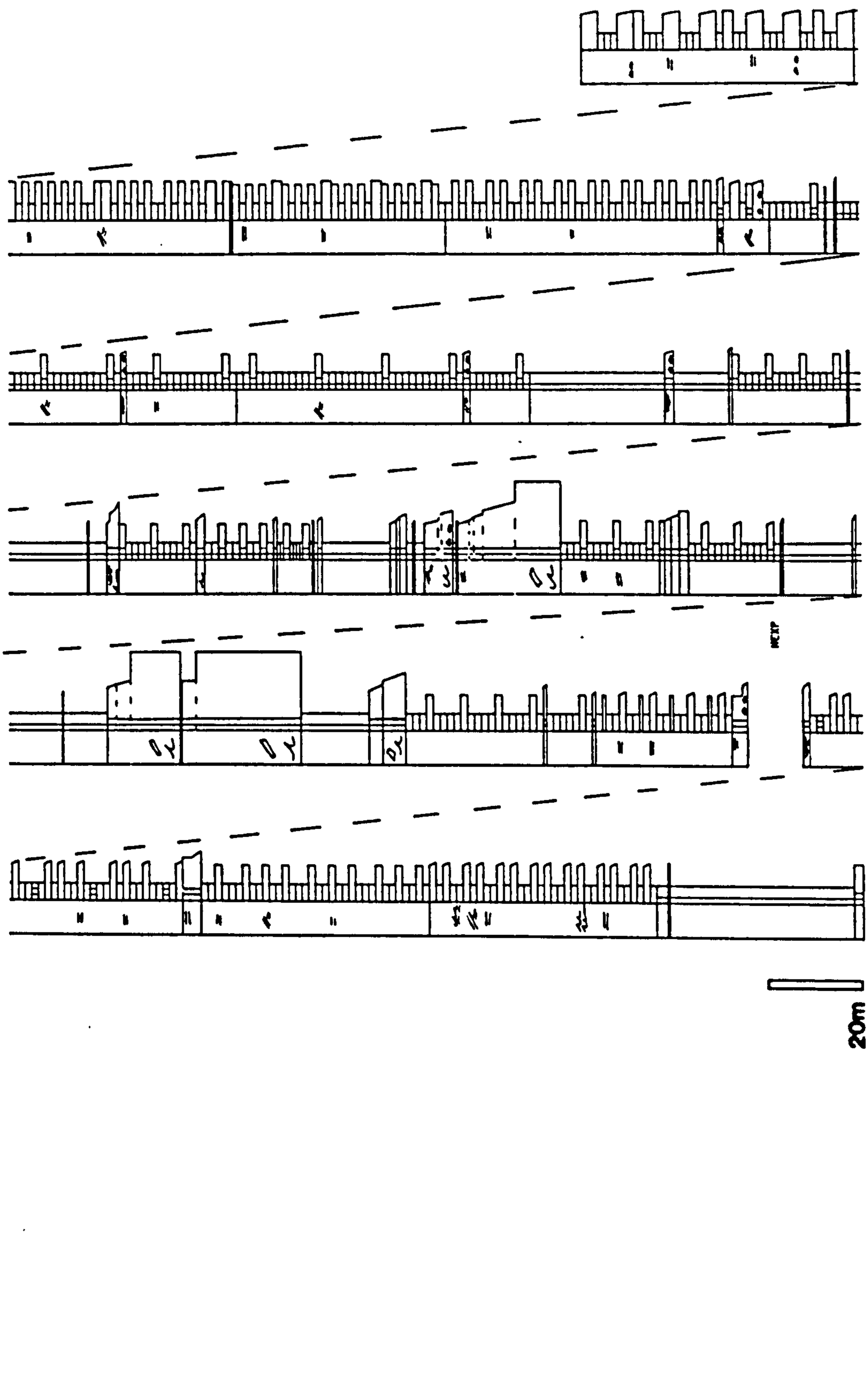

Fig. 7.2 Sedimentological log of the Cagman type section. Note upward increase and then decrease in percentage and thickness of mega-breccias and calcarenites (see Fig. 2.1 for location of section).

Although directional data (palaeocurrents etc.) are lacking petrographic evidence suggests this sequence probably represents a distal facies of the Salir Formation submarine fan system (5.5) deposited along the eastern margin of the basin. The sequence is approximately 100 m thick, the mudstone:sandstone ratio increasing upwards. The upper 50 m consists of very thin-bedded turbiditic sandstones (Tde), which form less than 10% of the sequence, interbedded with calcareous mudstone and calcarenites which become progressively thicker and more frequent upwards (Fig. 7.11). Rare pelagic chalk horizons are very thin (up to 5 mm). The paucity of chalk horizons in contrast to the rest of the basin, particularly the eastern area (Salir Formation), is probably the result of virtually continuous deposition of a "mud blanket" on the outer fan area of the Salir Formation submarine fan (5.5). In addition, fine grained sediment input from the western margin Kemer Formation ophioclastic fan system cannot be excluded.

The low number of pelagic horizons, results in a high P_2 index (sandstone-mudstone-sandstone upward transition) (see 5.6) and correlates well with the model of pelagic horizons as an indicator of submarine fan sub-environment postulated in 5.6.

Upwards the sequence passes into approximately 800 m of interbedded massive limestone breccias, calcarenites, calcareous mudstone and occasional pelagic chalk.

X-ray diffraction of the mudstone identifies serpentinite as the dominant mineral.

7.3.0 Carbonate Sedimentary Facies

Interbedded with the mudstones (above) are massive limestone mega-breccias and calcarenites. These are exotic to the submarine fan system and represent the interdigitation of sediments from a carbonate source, with terrigenous sediments of the submarine fan.

7.3.1 Calcarenites

Calcarenites vary from thick beds, up to 2.50 m thick, which grade from granule conglomerate to medium sandstone, to thin-bedded structureless or laminated medium to fine grained sandstone.

The calcarenites fall into two broad categories: (1) those deposited by dilute turbidity currents consist of Tcde and Tde Bouma sequences and are characterised by flat bases and sharp tops; (2) Those deposited by dense turbidity currents grade from granule

conglomerate and frequently consist of Tabc and Tbce Bouma sequences. These thicker beds are characterised by slightly erosive scoured bases with rare flutes, grooves and some load·structures. They are probably transitional to the mega-breccias described below.

7.3.2 Mega-breccias

Clast-supported mega-breccia beds are between 5 and 26 m thick and laterally extensive. Individual beds traced up to 5 km downslope (Fig. 7.1) display marked thickness variations (7.6.1 below). Internally each bed may be subdivided into three units.

Disorganised breccia (basal unit). The basal unit, between 2 and 22 m thick, consists of a completely disorganised, chaotic zone with random clast fabrics (Fig. 7.5). Clasts range between 1.2m and 5 mm in size, mean .10 m. Matrix consists of medium to coarse, muddy (lime mud) bioclastic sandstone. Intra clasts of mudstone and bedded mudstone-calcarenite are up to 5 m in length and 2 m wide. Many of the mudstone clasts are completely wrapped around or indented by carbonate clasts; indicating that they were in a semi-consolidated state when incorporated into the flow and subject to plastic deformation. Others were lithified and have remained as completely intact blocks. These are orientated parallel to bedding or with a-axes dipping upflow in upper parts of the basal unit.

Mudstone intraclasts form up to 40% (by volume) of the lower parts of this unit. In one of the thicker beds studied in detail, the percentage decreased markedly 3 m from the base to around 25% and then at approximately 18 m to 10%. No intraclasts are present above 22 m (Fig. 7.4). Intraclast and clast size decrease fairly uniformly up the flow with only very occasional larger clasts (to 1 m) in the upper parts of the flow (Fig. 7.4).

Sediments underlying the breccias are chaotically slumped and deformed (7.3.3, below). The basal 5 m show evidence of extensive incorporation of mudstone into the breccia by soft-sediment loading. Mudstone is injected as large dykes and flames up to 1.5 m across, between large clasts at the base of the flow. The transition upwards to the overlying organised breccia occurs over approximately .50 m. The contact is often very irregular, gently rounded irregularities up to 5 m across and 2 m deep were probably formed by soft-sediment loading of the denser overlying unit into the underlying mud-rich disorganised breccia, immediately following deposition.

Organised pebble-granule breccia (central unit). This unit consists of a more organised clast-supported breccia, with well developed normal grading, generally from pebble to granule or very coarse sand size. Grading is of the coarse-tail type. Clast a-axes imbrication, parallel to bedding or inclined upflow is occasionally present. Mudstone intraclasts are present only at the base of the unit. Thickness varies between 1 m and 8 m. The upper third of the unit frequently shows a rudimentary stratification parallel to bedding (Fig. 7.3).

Calcarenite cap (upper unit). The transition into the upper unit is gradational over .10-.30 m. This unit comprises normally graded calcarenite (90% of all occurrences) (Fig. 7.3) or rarely a complexly graded,stratified calcarenite (10% of all occurrences), between 1 and 3 m thick. Grading is again of the coarse-tail type. The base of the calcarenite consists of a massive division up to 2 m thick with well developed long-axis imbrication of occasional outsize clasts. This is commonly overlain by a parallel laminated division and more rarely a ripple laminated division (Fig. 7.3). These are directly equated with the A, B and C divisions of the Bouma cycle. Complexly graded, stratified calcarenites are overlain by a normally graded, structureless or parallel laminated unit up to .50 m thick (Fig. 7.5).

7.3.3 Slumped Horizons

In proximal areas (Fig. 7.1) where the breccias reach their thickest development (Figs. 7.5 and 7.6) underlying sediments which comprise calcarenites and mudstones are chaotically deformed. The slump horizons are between 3 and 10 m thick, the thickness varying irregularly over several tens of metres. Frequently the horizons are intensely deformed and slump-fold geometry is difficult to recognise. Where recognisable, slump folds have wavelengths and amplitude of typically 4-5 m. Axial planes are inclined to recumbent. Interlimb angles are rarely greater than 60° and the majority of folds are close to tight or isoclinal. Hinges are rounded and angular, frequently totally disrupted. Isolated hinges often occur in an otherwise disorganised 'sedimentary breccia'. Axial planes are inclined at low angles to bedding.

Fig. 7.3

Field photographs of the Cagman Member

(a) Mega-breccia bed (in proximal area); organised breccia (b) which fines upwards is overlain by a calcarenite cap (c). Note parallel orientation of mudstone intraclasts (m) parallel to bedding at base of calcarenite unit. Stick is 1 m long. GR. 606692.

(b) Mega-breccia bed in photograph (a) 5 km along strike. Organised breccia overlain by calcarenite cap which fines upwards. Stick is 1 m long. GR. 625313.

(c) Parallel- (B) and ripple-laminated (C) divisions of the Bouma cycle in a calcarenite cap to a mega-breccia bed. Note overall fining-upwards. GR. 591692.


c
m
b

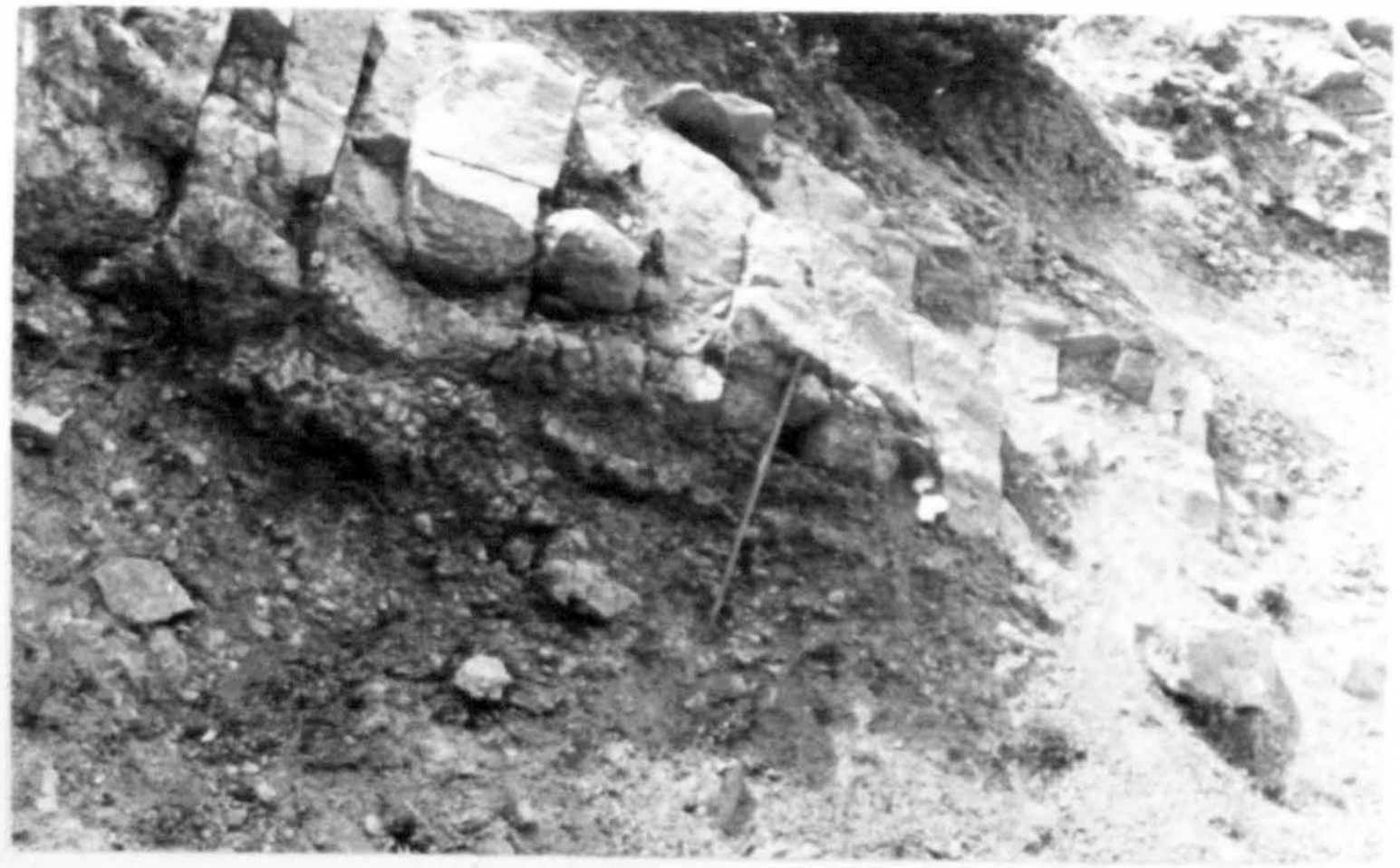

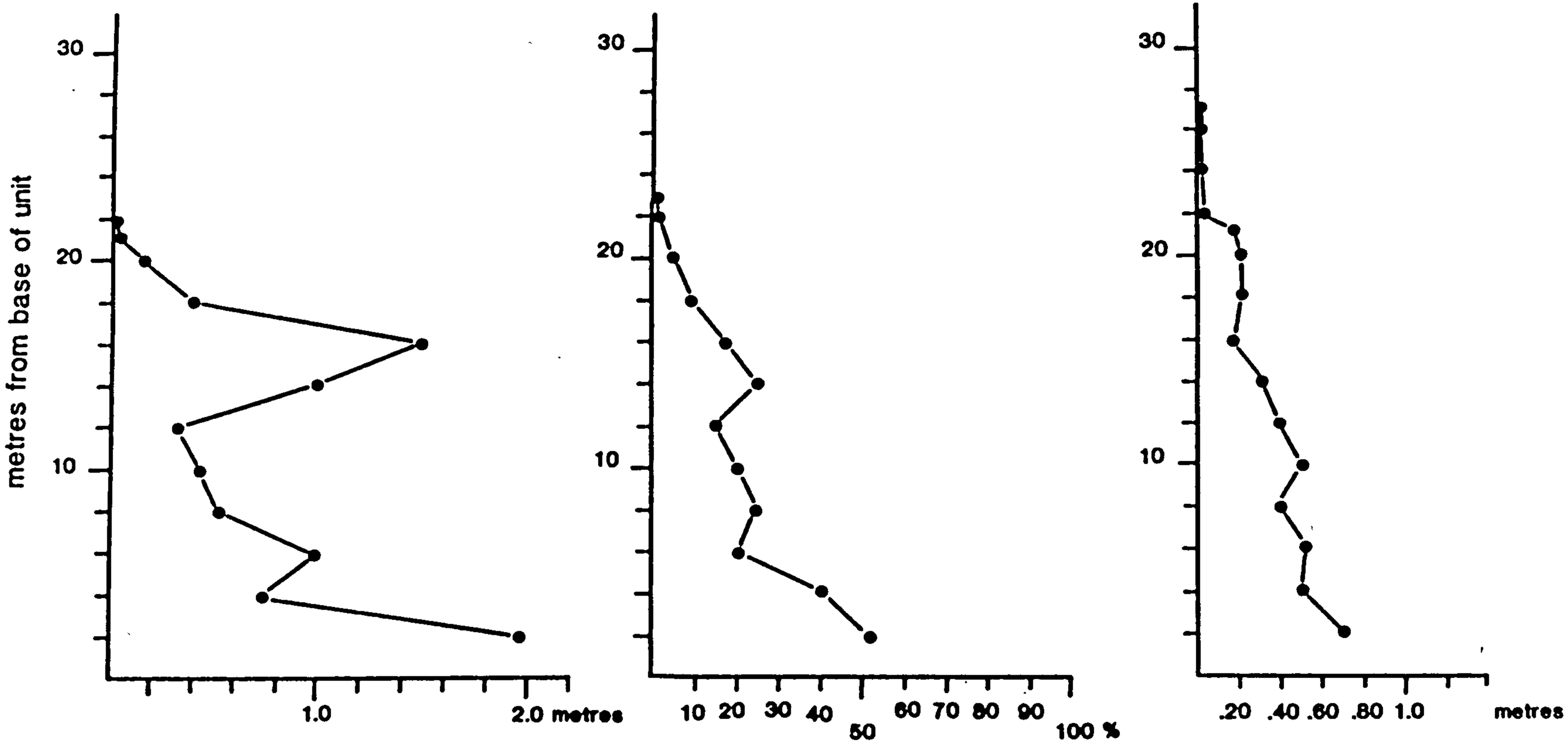

Fig. 7.4 Variation in clast and intraclast size through mega-breccia bed A in most proximal area (sectn. 1, Figs. 7.1, 7.5).

(a) Intraclast size.

(b) Percentage of intraclasts.

(c) Clast size variation.

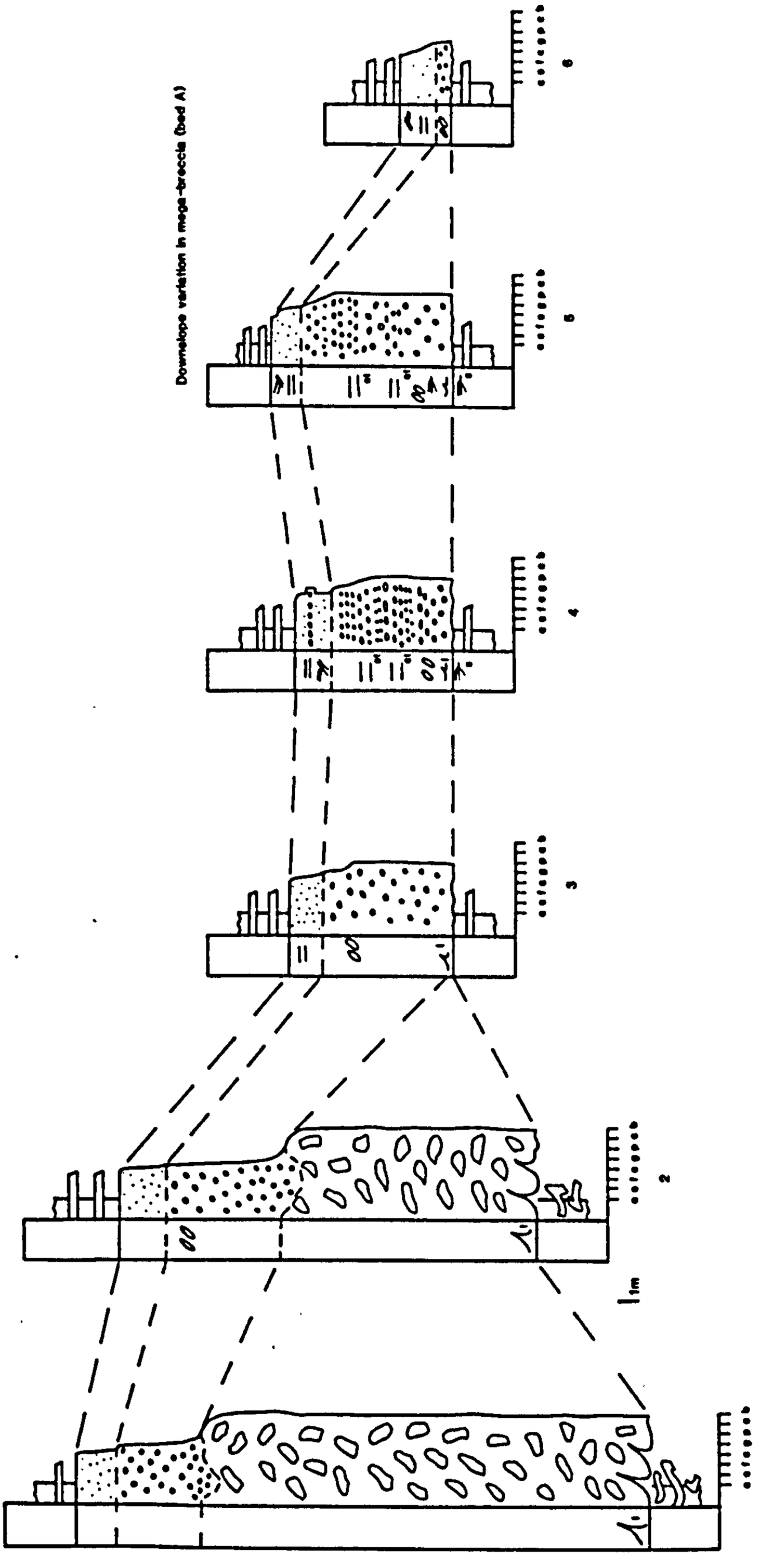

Fig. 7.5 Downslope variations in bed-thickness and sedimentary structure in mega-breccia bed A.
For location of sections see Fig. 7.1 (Appendix C for key).

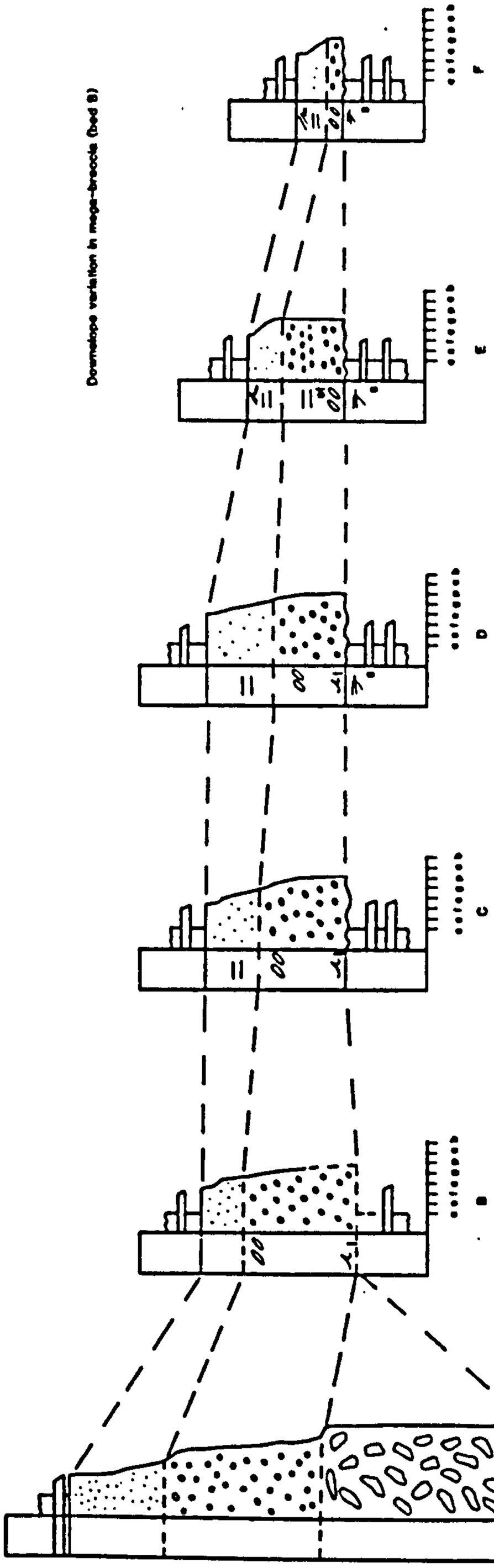

Fig. 7.6 Downslope variations in bed-thickness and sedimentary structure in mega-breccia bed B.
For location of sections see Fig. 7.1 (Appendix C for key).

Interpretation

The slump horizons are clearly genetically related to the mega-breccias. Three mechanisms possible for their formation are:
(1) Drag-shear as the breccia flowed over semi-consolidated sediment;
(2) Slump horizons were related to the initial movement of the breccia. Initially travelling ahead of the breccia, as the flow developed slump horizons were successively overriden by more distal parts of the flow, accounting for the localised occurrence of slump folds in proximal areas. In this mechanism slump folds would be truncated by the overriding flow, resulting in an erosional contact between the slump horizon and the overlying breccia;
(3) Slumping following deposition. Rapid deposition of a thick bed on semi-consolidated sediment results in the entire sediment pile becoming gravitationally unstable. Slumping occurs along a layer of unconsolidated sediment at the base of the flow (Fig. 7.7). The presence of large scale loading and soft sediment injection structures continuous upwards into the breccia from the underlying slump horizon, and absence of any erosional truncation between the slump and overlying breccia suggests that mechanism (3) is more likely.

The presence of extensive soft sediment loading features has often completely obliterated slump fold geometry. From the limited directional data obtained from fold axes, the palaeoslope was generally to the northeast. This is consistent with the general direction of thinning of the mega-breccias.

7.4 Detached limestone blocks

Detached, angular blocks of Eocene limestone are of the order of 10 x 20 m in size. They are confined to the most proximal parts of the sequence, associated stratigraphically with the mega-breccias (Fig. 7.1). Only five occurrences are recorded.

At one locality (Fig. 7.1, Locality S), northwest of Sannicli (Fig. 7.1) a very large block, ca. 50 x 50 x 30 m in dimensions, occurs associated with a thick mega-breccia. Poorly defined bedding in the block is inclined at steep angles (60^{o}) to bedding in the interbedded mega-breccias, calcarenites and mudstones. In this instance the block is partially incorporated into the breccia. Elsewhere randomly orientated blocks occur within interbedded mudstone-calcarenite sequences. In all cases poor exposure prohibits detailed examination of the surrounding sediment.

Fig. 7.7

Possible mechanism for the formation of slump horizons associated with mega-breccia beds. Following initial deposition, soft-sediment loading and continued downslope movement as the breccia finally comes to rest results in a chaotically deformed "slump" horizon immediately below the breccia. Rarely slump folds can be traced upwards into the base of the mega-breccia.

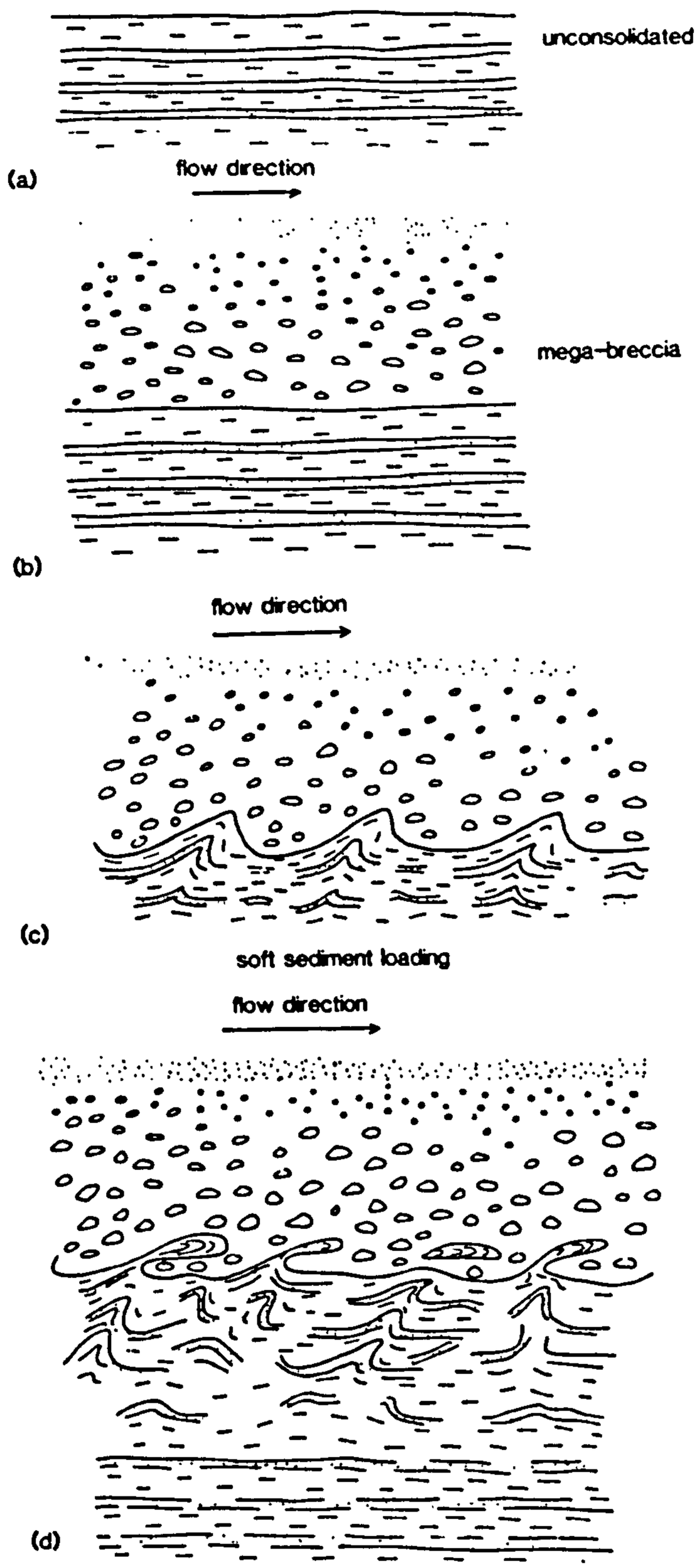
unconsolidated sediment
(a)
flow direction
mega-breccia
(b)
flow direction
(c)
soft sediment loading
flow direction
(d)
loading and continued movement

Fig. 7.7

Interpretation

The blocks were clearly derived from an area of uplifted carbonate platform that was located to the west. It is probable that they were derived from the wall of a syn depositional fault thought to have been active in Lower to Middle Miocene times (see discussion, 7.7.3). Emplacement was by downslope sliding under gravity. Srivastava *et al.* (1972) propose increased pore pressure beneath blocks resulting in a thin lubricating film maintained at high pressure as a mechanism for the emplacement of similar detached blocks derived from a carbonate reef complex of Devonian age in Alberta, Canada.

7.5 Composition

The breccias are characterised by very poorly sorted, angular to subangular fragments of bioclastic debris and limestone lithoclasts. Limestone lithoclasts, which form up to 20% (by volume) of the breccia, consist exclusively of nummulitic calcarenite of Eocene age. Angular to subrounded fragments are up to 1.2 m long, mean clast size is .10 m. Many of the smaller pebbles and cobbles have been bored by bivalves and subsequently encrusted by coralline algae.

Bioclastic debris is dominated by rhodoliths up to .10 m in diameter, (Fig. 7.12), coral blocks (to .30 m), shell debris (bivalves and gastropods), algal bound bioclastic clasts, and rare echinoderms. The calcarenites are composed of very angular comminuted algal clasts, bethonic foraminifera, shell debris and abundant reworked foraminifera of Eocene age (G. Adams, pers. comm. 1980).

Provenance. The abundance of bioclastic material indicates derivation from a shallow water carbonate build-up or reef complex. Rhodoliths which form the greatest proportion of the bioclastic debris are commonly found at the present day in depths of less than 100 m, in areas of slow sedimentation where there is intermittent agitation of the bottom by current action (Bosellini and Ginsburg, 1971). Reworked Eocene bioclastic debris and clasts of Eocene limestone indicate an area of uplifted carbonate platform. However, there is no evidence of subaerial exposure, such as carbonaceous material in the calcarenites or kaolinite, produced by subaerial weathering of limestone, in the associated mudstones.

The high angularity of many of the reworked nummulite fragments also indicates limited reworking.

Briefly, clast composition suggests derivation from a shallow water carbonate build-up, situated on a region of uplifted carbonate platform that was subject to limited reworking in the marine environment. The carbonate build-up is discussed in more detail below (7.9).

7.6.0 Geometry of Mega-breccias

The mega-breccia beds thin consistently to the northeast (Figs. 7.1, 7.5, 7.6) suggesting a general palaeoslope in this direction.

Good exposure and limited tectonic deformation enables individual beds to be traced up to 6 km down palaeoslope, allowing variation in sedimentary structure and bed thickness to be studied. In the most proximal area the breccias abut against a high-angle normal fault (Fig. 7.1). Evidence discussed below (7.7) suggests that this may have been active during Lower to Middle Miocene times.

7.6.1 Downslope Variation in Bed Thickness, Texture and Sedimentary Structure

Variations in sedimentary structure and texture for breccia beds A and B (Fig. 7.2) are shown in Figs. 7.5, 7.6, and 7.8. The following downslope trends are observed.

Disorganised breccia

(1) Dramatic thinning of the disorganised basal unit occurs over a distance of between 1 and 2 km. No systemmatic downslope variation in clast size or texture is recorded in this unit;

(2) Slump horizons occur only in proximal areas beneath disorganised breccia units. In 'distal' areas where the basal unit is absent, underlying sediments are only slightly disturbed by minor scouring and some loading.

Organised breccia

(3) Thickness of the organised breccia is relatively constant over 4-5 km, with only slight pinching and swelling, probably as a result of an irregular sea floor topography. Marked thinning occurs after 4-5 km.

(4) Downslope the following textural transition is recorded:

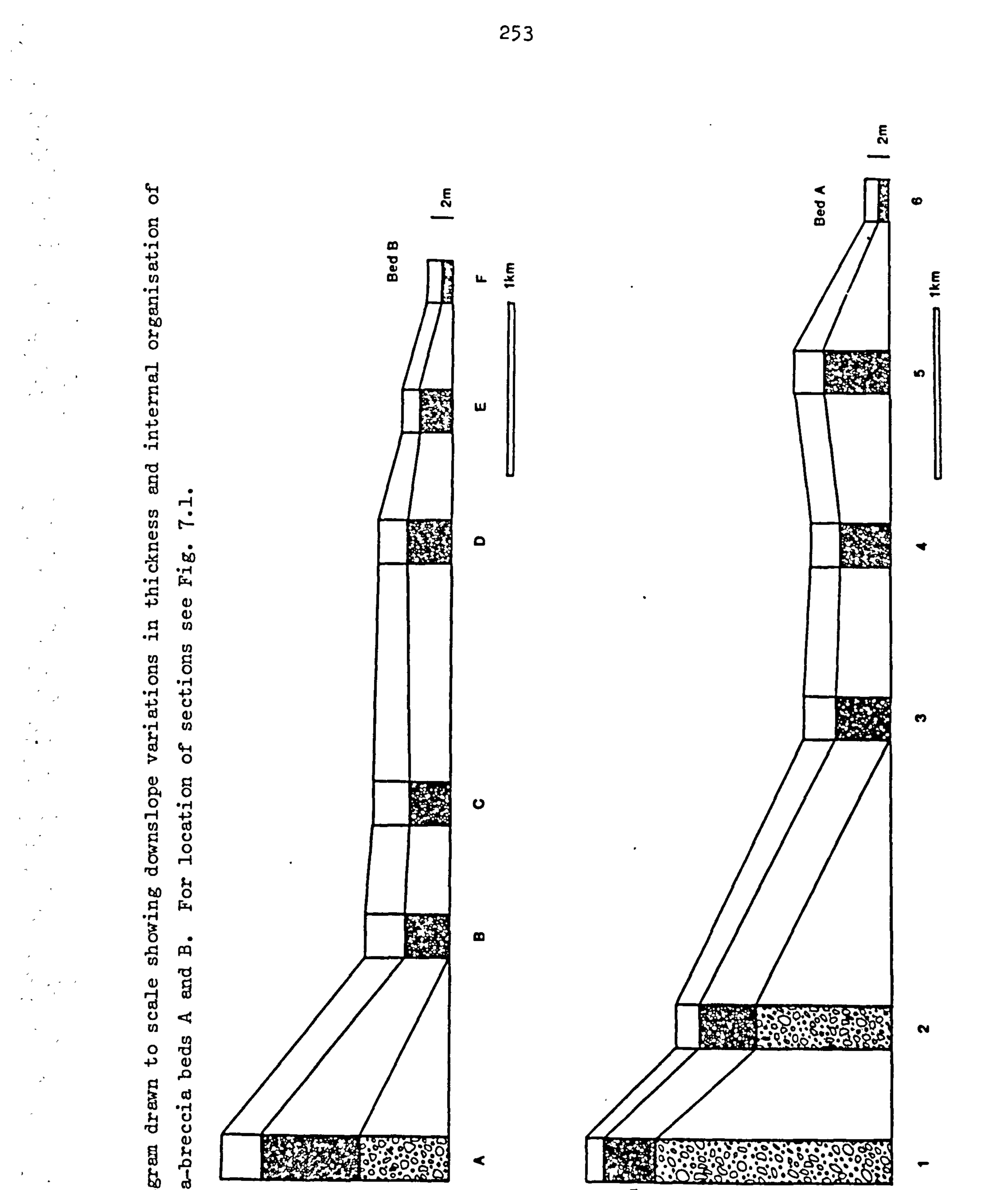

Fig. 7.8 Diagram drawn to scale showing downslope variations in thickness and internal organisation of mega-breccia beds A and B. For location of sections see Fig. 7.1.

massive slightly graded unit → distinctly graded units with some imbricated clasts → graded stratified units → thin, graded units with good clast imbrication at the base of calcarenite beds.

Calcarenite Cap

(5) Pinching and swelling in thickness can again be attributed to an irregular sea floor topography.

(6) Downslope the following textural transitions are observed:

(a) massive, structureless, graded unit → parallel-laminated, graded unit → cross-laminated, parallel-laminated, complexly graded unit → parallel-laminated and cross-laminated graded unit (Figs. 7.5 and 7.6);

(b) massive, structureless, graded unit → parallel-laminated, graded unit → parallel and cross-laminated graded unit (Figs. 7.5 and 7.6).

7.7.0 Mega-breccias : Depositional Mechanism

Interbedded turbiditic calcarenites and mudstones with abundant planktonic foraminifera are consistent with deposition in a marine environment by some form of subaqueous mass-flow mechanism.

In the *disorganised breccia* the lack of fabric and texture indicate that clasts moved little in relation to one another during transport. The absence of matrix support probably precludes deposition by a solely debris flow mechanism and deposition was by debris flow transitional to density modified grain flow, where matrix strength and clast-clast interaction were the main supporting mechanisms. For a full review of subaqueous mass-flow processes see 3.4.2.

In the overlying *organised breccia* normal grading indicates that the clasts moved freely in the flow and that vertical size segregation operated. These features are consistent with deposition by flows of lower sediment concentration, due to the effect of water intake into the flow (Walker, 1975; Middleton and Hampton, 1976). This unit was deposited by a flow intermediate between a debris flow and a fully turbulent flow.

The overlying *calcarenite cap* characterised by well developed Bouma cycles was deposited by a fully turbulent flow.

7.7.1 Evolution of a Tripartite Debris Flow

The development of this tripartite debris flow is explained in terms of the models of Hampton (1972) and Middleton and Hampton (1976). In this model based on experimental work (Hampton, 1972) sediment is eroded away along the front of the subaqueous debris flow by reverse shear and thrown upwards into the overlying water to produce a turbulent cloud (Fig. 7.9).

The mixing mechanism can be attributed to the pressure distribution around the front of the debris flow. In the area of reverse shear, at the front edge of the flow (Fig. 7.9) pressure is large enough to hold material to the debris flow surface. Behind the layer of reverse shear a low pressure zone exists where the flow direction of fluid along the surface of the debris flow is opposite to that in the layer of reverse shear. Material in the layer of reverse shear moves continuously into the region of low pressure, where it is lifted away from the debris flow surface into the overlying turbulent region resulting in a turbidity current cloud overlying the main part of the flow. In addition, introduction of water directly into the body of the flow itself may also aid in producing the overlying turbidite. In the debris flows discussed here the actual transition from debris flow to turbulent flow was apparently gradational. The central unit (organised breccia) of the flow in proximal areas has characteristics intermediate between debris flow and fully turbulent flow. The calcarenite cap represents the fully turbulent region.

7.7.2 Downslope Transitions

Downslope textural transitions for mass-flows have been predicted generally from the study of vertical sequences, by a number of authors, in particular Walker (1975, 1979b) and Krause and Oldershaw (1979). Although downslope transitions have been documented within individual turbidite beds (e.g. Contessa bed, Ricci Lucchi, 1975a; Ellis, pers.comm.1980), to the author's knowledge this sequence represents the first time that downslope textural transitions have been documented within one individual conglomerate mass-flow event that is laterally extensive and can be traced over 5 km downslope.

With increasing transport there is a *downslope transition* from disorganised-organised-calcarenite units to organised-calcarenite

Fig. 7.9

Evolution of a turbidity current above a debris flow. Based on the experiments of Hampton (1972), see text for details.

Fig. 7.10

(a) Hypothesised downslope transitions in siliciclastic redeposited conglomerates (after Walker, 1975).
Disorganised → inversely graded → normally graded → normally graded stratified.

(b) Hypothesised downslope transitions in carbonate breccias (after Krause and Oldershaw, 1979).
Disorganised → stratified-disorganised → stratified-normally-graded → stratified inverse to normally graded.

(c) Observed downslope transitions in carbonate mega-breccias from this study.
Disorganised-organised-calcarenite cap → organised-calcarenite cap → organised-calcarenite cap → calcarenite cap.

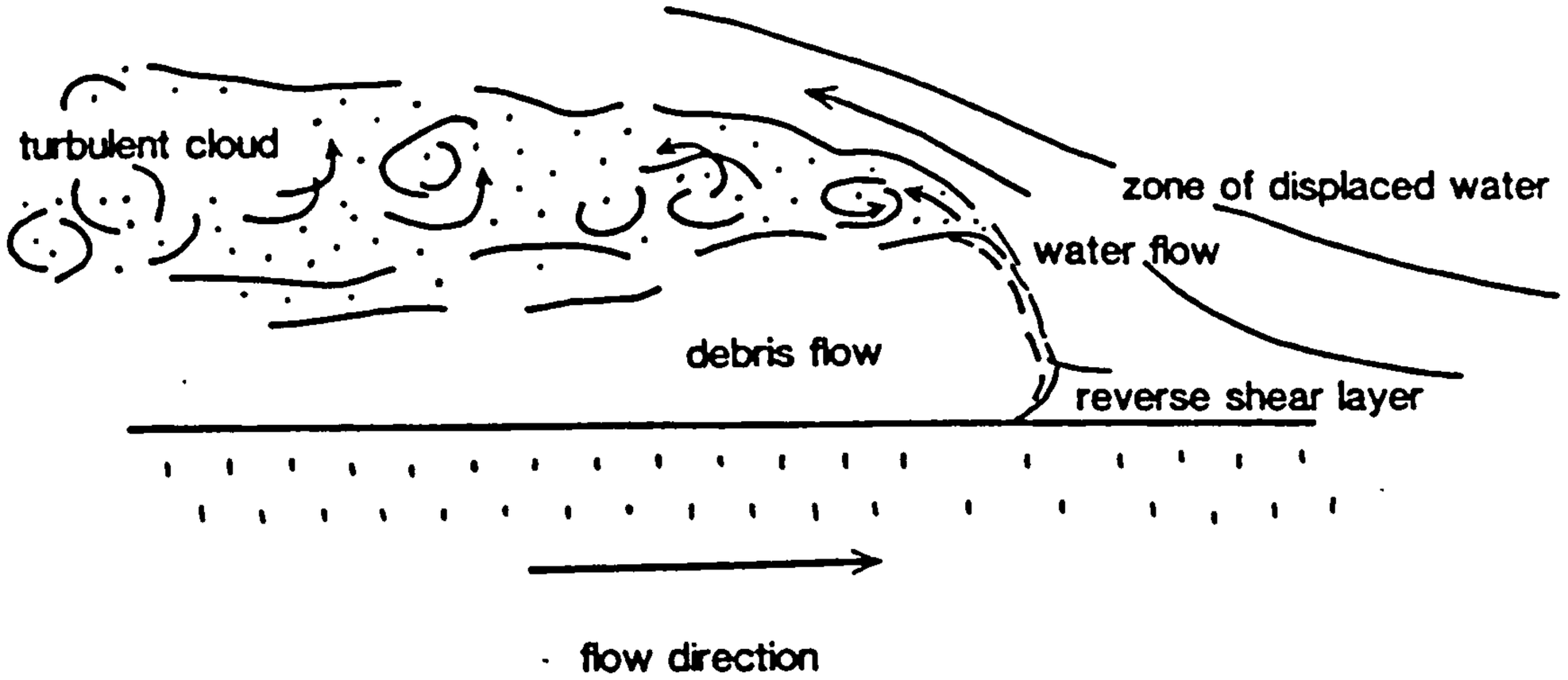

Fig. 7.9

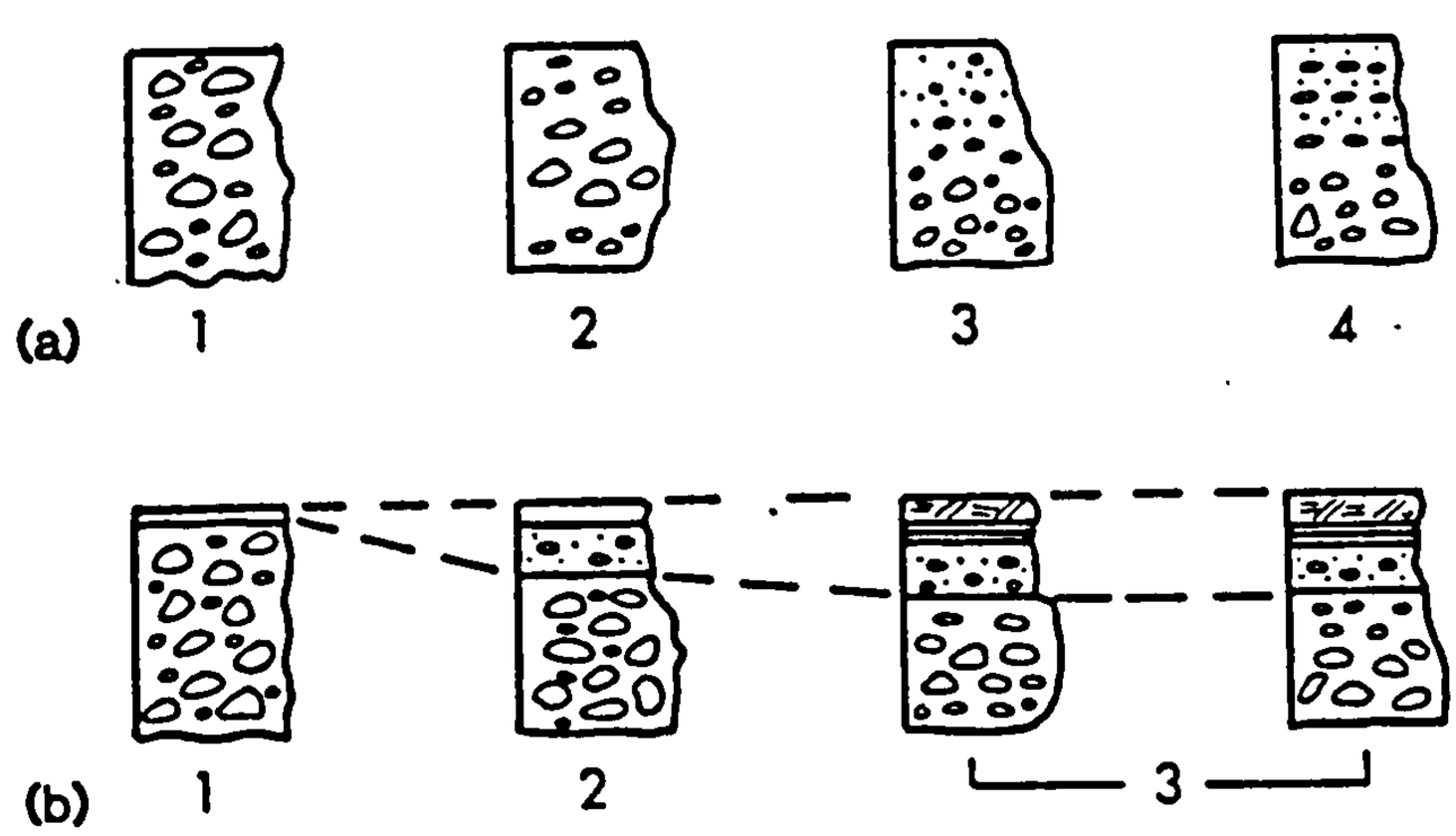

Fig. 7.10

units, to calcarenite units. The observed transition here is compared with the hypothesised transition of other authors in Fig. 7.10.

In *proximal areas* individual beds consist of disorganised breccia overlain by an organised graded breccia and calcarenite. Downslope the disorganised breccia wedges out and organised breccia is overlain by a calcarenite. This passes in most *distal areas* into a calcarenite unit. Within the organised breccia and calcarenite distinct downslope textural transitions are observed, massive only slightly graded breccia passing into well graded breccia and then into a graded stratified breccia. The calcarenite cap passes from a massive, structureless, graded bed downslope into a parallel-laminated bed and finally a parallel- and ripple-laminated bed (Figs. 7.5, 7.6).

From the downslope transition (Fig. 7.8) it is clear that only a small proportion of the initial mass flow event transformed into a fully turbulent flow, the majority remaining as a debris flow that came to rest probably within only 1-3 km of the flow initiation point (see below, 7.8), based on observed distance from source. At this point the overlying, partially turbulent flow overrode the debris flow and continued depositing downslope, gradually evolving from a flow intermediate between a debris flow and turbulent flow into a fully turbulent flow. It may be expected that there would be a non-depositing area beyond the end of the debris flow, before the overriding turbidity current began to deposit its load. However, the gradual transition (outlined above) may explain the downslope continuity from debris flow deposit to turbidite deposit.

7.7.3 Trigger Mechanism

The breccias clearly represent a large scale catastrophic event that affected the shallow water carbonate source area (reef complex) with the result that large volumes of material were redeposited downslope. Although not exposed in three dimensions, there is no evidence of any channelling and the breccias have an apparent sheet geometry. Assuming they are broadly equidimensional, the total volume of resedimented material represented by the largest flows is of the order of 0.5 km^3.

Analysis of vertical sequence trends in bed thickness show a broad upward increase in breccia bed thickness followed by a gradual

decline (Fig. 7.11). Associated with this is an upward increase and then decrease in the frequency of breccia and calcarenite beds.

In most proximal areas breccias abut against a high angle normal fault, and become progressively thinner and finer grained away from the fault line (Fig. 7.1). On the upthrown side Miocene sequences have been removed by erosion.

Mechanisms that may be invoked as a trigger mechanism are: (1) storms; (2) earthquakes; (3) oversteepening of slopes caused by crustal tilting; (4) oversteepening of slopes caused by undercutting; (5) slope instability caused by rapid deposition. Bed thickness variations are not consistent with derivation via periodic storm events in the source area, as in the Bahamas at the present day (McIlreath and James, 1979). In such a situation a much more random variation in bed thickness would be expected, as storms of differing magnitudes affected the carbonate source area. In addition the volume of material redeposited would require storms or tsunami of enormous magnitudes.

Recent carbonate flows in the Bahamas have been related to a lowering of sea-level producing undercutting, local sediment redistribution and instability on the upper steep part of the platform slope (Crevello and Schlager, 1980). However, there is no evidence of any sea-level fluctuations in this sequence, the breccias were deposited during the period Burdigalian to Langhian at a time when sea-level in this area was apparently stable (Gwirtzman and Buchbinder, 1977).

The upward increase and then decrease in bed thickness suggests a primary tectonic control. The presence of abundant reworked Eocene foraminifera and large limestone blocks of Eocene age indicate an area of uplifted carbonate platform (although not subaerially exposed) in the source area. It is suggested that a *syndepositional fault*, possibly along the lines of the present fault, resulted in an area of uplifted carbonate platform to the west. On the evidence of the bioclastic content of the breccias (mainly corals and rhodoliths, 7.9) water depth in the area was 100 m or less.

Tectonic tilting of this area and probable earthquake activity related to movement on the fault, resulted in the periodic redeposition of shallow water and reworked Eocene carbonate material into the basin. Large detached limestone blocks were derived from

Fig. 7.11

Layer thickness variation in Cağman Member type section,
(a) only mega-breccias
(b) mega-breccias and calcarenites.
Note upward increase followed by a decrease in the percentage and thickness of mega-breccias and calcarenites (see text for explanation).

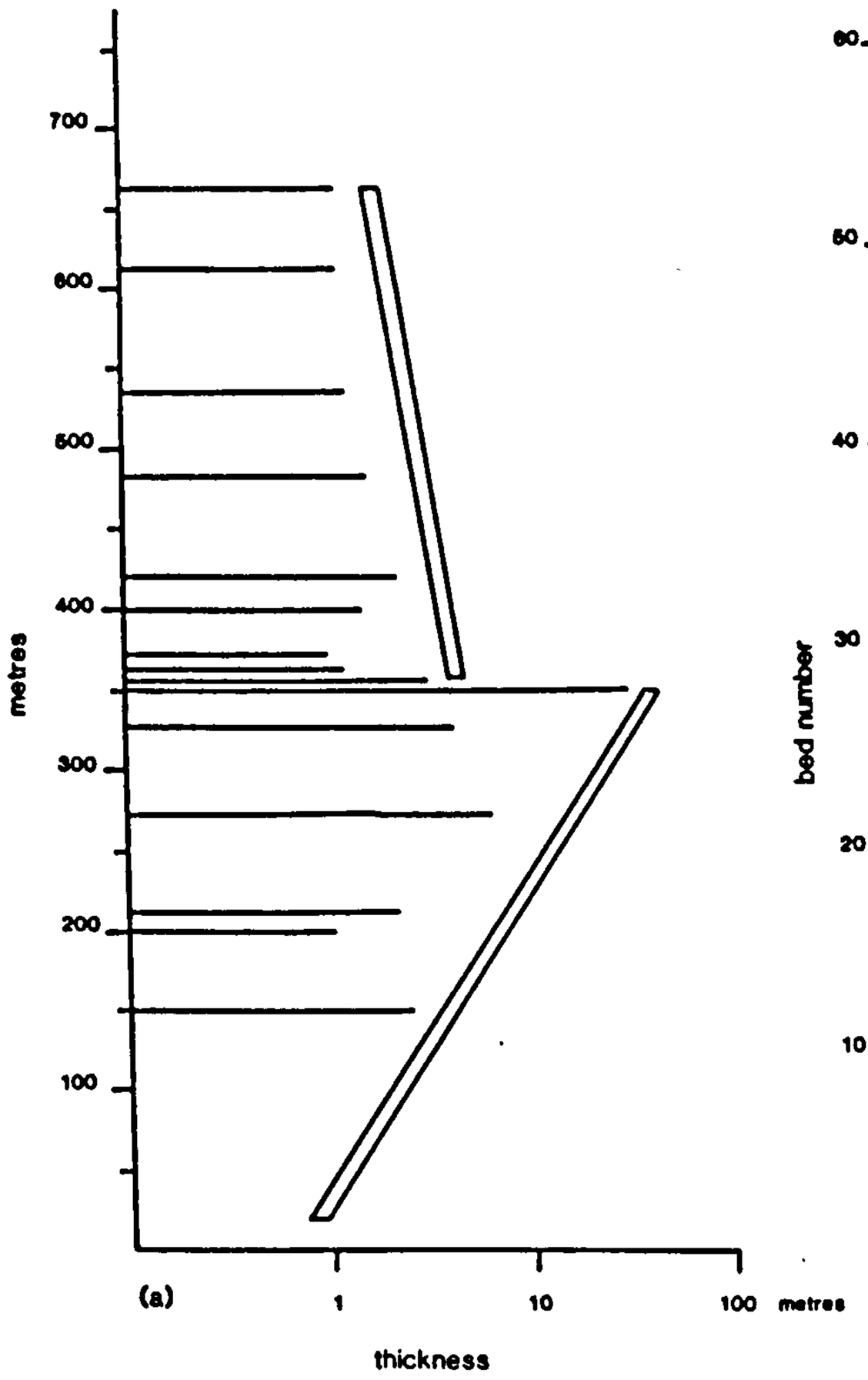

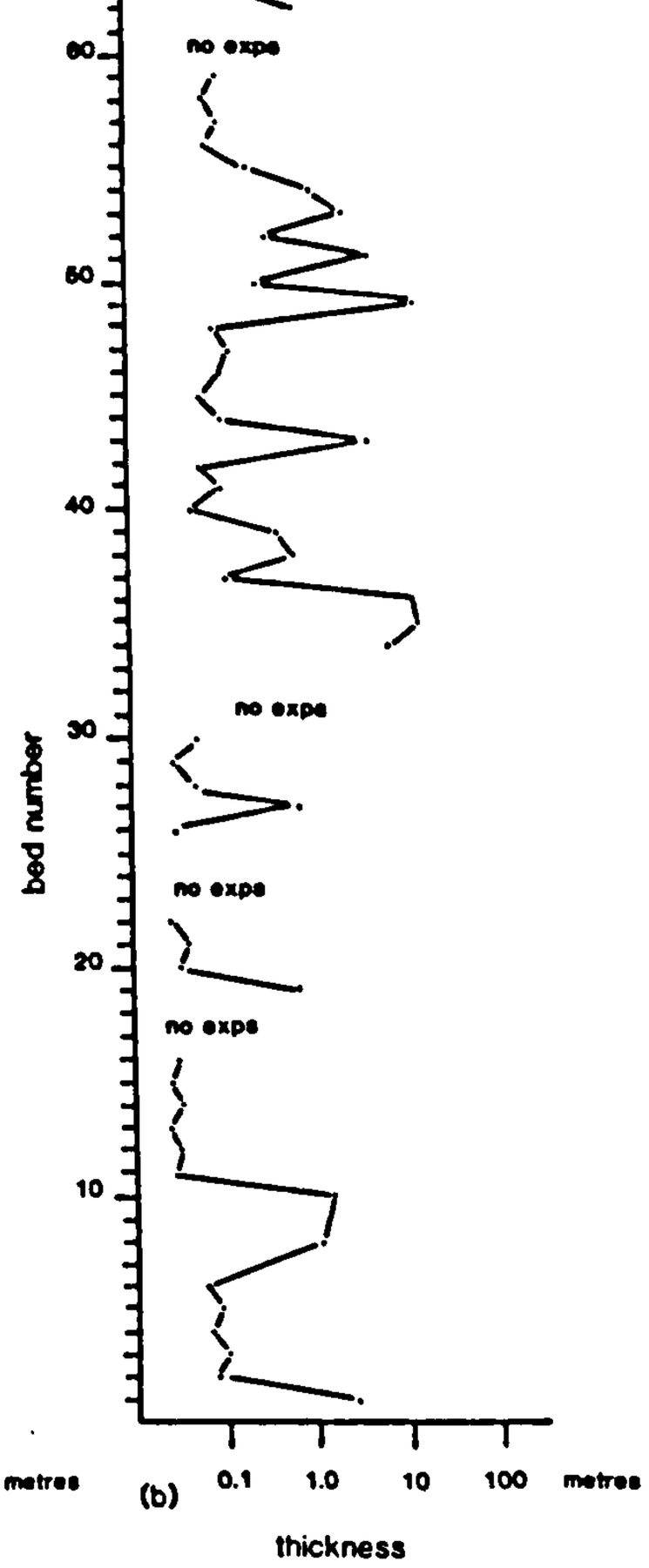

the wall of the fault. Thinner calcarenites with identical, although finer grained component clasts, record either small scale tectonic events or more probably are the result of storm activity affecting the carbonate depositing area.

The upward increase and then decrease in breccia bed thickness suggests an overall upward increase and then decrease in fault activity. By Middle Miocene times the fault appears to have become inactive.

7.8.0 Mass-Flow Carbonates : Discussion

Mass-flow carbonate breccias are known from numerous locations and stratigraphic horizons. They are generally taken to indicate the close proximity of a carbonate platform margin, reef complex or other form of shallow water carbonate-depositing area (e.g. Cook *et al.*, 1972; Mountjoy *et al.*, 1972; McIlreath and James, 1979).

A modern example of this type of deposit has been recently described from Exhuma Sound in the Bahamas (Crevello and Schlager, 1980). In this area a Recent carbonate breccia with a maximum thickness of 3 m can be traced over an area of 1500 km^2. The breccia comprises a pebbly mud-muddy rubble base up to 1 m thick, overlain by a graded sand unit up to 1.5 m thick. The flow resulted from the large scale failure of the carbonate platform upper slope and is probably related to undercutting associated with a lowering of sea level (Crevello and Schlager, 1980).

Comparison with redeposited siliciclastic conglomerates shows that many textural features of both types of deposit are very similar (see 3.4). However, the one striking difference is the occurrence of an overlying turbidite bed, genetically related to the underlying mass-flow. These 'cap beds' are common in redeposited bioclastic carbonates (e.g. see Kraus and Oldershaw, 1979, Table 3), but rare in redeposited siliciclastic sediments. Although advocated theoretically by Sanders (1965), Middleton (1967), Hampton (1972) and Middleton and Hampton (1973), the occurrence of siliciclastic redeposited disorganised conglomerate overlain by a related turbidite cap as reported from field observations, is rare (see 3.4). One or several of the following reasons may account for this difference: (1) source area; (II) mechanism; (III) slope; (IV) composition.

7.8.1 Source Area

The source area for bioclastic breccias such as those described here, commonly consists of some form of reefal framework and associated biota. Material derived from such a source varies from large blocks of reef frame-builders to micrite and fine disseminated carbonate produced by the bio-erosion of the reef. In many instances this material is frequently deposited directly downslope without any form of current reworking, resulting in a complete spread in grain size. In contrast terrigenous clastic material has frequently undergone several stages of transport and sorting prior to redeposition, normally through a fluvial and shallow marine environment. Even in the immature terrigenous clastic sedimentation systems discussed in this thesis, redeposited conglomerates are invariably better sorted than their bioclastic carbonate breccia counterparts. The poorly sorted sediment provides suitable material for the development of a debris flow - turbidite cap unit. The wide range of grain sizes present in bioclastic carbonate material has previously been used to explain the variation in turbidite sedimentary structures between silicous and bioclastic carbonate beds (Engel, 1970).

7.8.2 Mechanism

No field aspects of the sediments indicate that a fundamentally different mechanism is operating in the redeposition of bioclastic carbonate and siliciclastic material. The dominant transport mechanism, in both cases, is a combination of debris flow and grain flow (density modified grain flow, 3.4.2). However, at present no experimental work exists on sediments with lime mud or clay-lime matrix. All experiments to date have been carried out using clay-water mixtures (e.g. Hampton, 1972; Middleton and Hampton, 1973).

7.8.3 Slope

The slope down which a resedimented breccia is deposited may exert a strong control on the sorting and textures developed within the flow. The transition from shallow-water carbonate reef complex across the margin into the basinal area is often very abrupt, for example the Bahamas at the present day (Crevello and Schlager, 1980), and the models of McIlreath and James (1979) for various platform margin sequences. In contrast, terrigenous sediment is often channelled down fairly shallow submarine canyons and commonly

undergoes several stages of redeposition before it finally comes to rest. This is likely to result in progressively better sorting, with the end result that grain size variation is not sufficient for a turbidite cap to develop. By comparison, redeposited carbonates frequently come directly off the platform margin down very steep slopes, virtual cliffs in some instances and are commonly subject to only one stage of redeposition. In addition to this the angle of slope is inferred to produce different textures in resedimented conglomerates (e.g. Walker, 1975; Nemec *et al.*, 1980).

On a steep slope it can be expected that a debris flow will move at a greater velocity than on a low slope. This may result in more extensive 'erosion' at the head of the flow with the production of an overlying turbidite layer (outlined in 7.7.1), as proposed for the breccias discussed here and for other multi-layer carbonate breccia beds (Kraus and Oldershaw, 1979).

7.8.4 Density Contrast

The density difference between siliciclastic and bioclastic material, with high internal skeletal porosity and therefore low bulk density, is marked. This may result in low bulk-density carbonate material being susceptible to erosion from the head of the debris flow and more easily dispersed into the overlying turbidite layer. In support of this, the presence of large crinoidal fragments in some relatively distal bioclastic turbidites has been attributed to this difference in bulk density (Davies, 1977). In the present example the calcarenite caps are composed almost exclusively of comminuted foraminiferal and algal debris both of which have a relatively low bulk density.

In conclusion, it seems likely that source, slope and probably most importantly, differing *bulk densities* are the significant factors which result in carbonate mass-flows commonly occurring with a genetically related calcarenite cap, while their siliciclastic counterparts do not commonly exhibit this feature.

7.9 Carbonate Source Area

Composition of the breccias and calcarenites gives an indication of the type and style of carbonate build-up. Compound coral clasts (mainly *Favites sp.* and *Montastrea sp.*) up to .30 m long, provide evidence of a framework reef structure. Associated benthonic foraminifera (*Lepidocyclina, Operculina*) and echinoids (*Clypeaster sp.*) are consistent with a shallow water area.

Many of the breccias are composed of up to 80% (by volume) of coralline algal material, mainly in the form of algal nodules. Detached nodules of coralline algae are defined as rhodoliths (Barnes *et al.*, 1970; Adey and Macintyre, 1973). They can prove useful environmental indicators. At the present day rhodoliths actively form down to a depth of 60-70 m (McMaster and Conover, 1966; Adey and Macintyre, 1973), in areas of slow sedimentation where there is intermittent agitation of the bottom by waves or currents (Bosellini and Ginsburg, 1971). Strong water motion prevents the relatively light and fragile rhodoliths from forming, weak wave or current action leads either to their stabilisation through growth and coalescence of crusts or to burial beneath fine sediment that eventually kills the crustose corallines.

Particular genera are broadly indicative of the palaeoenvironment. The main genera present in this sequence are *Lithothamnium sp.*, *Pseudolithothamnium sp.* and *Lithoporella sp.* These all generally require strong light intensity to flourish and are thus indicative of shallow water environments (Adey and Macintyre, 1973).

Coralline algae form and rhodolith morphology also give an indication of energy conditions. Massive laminar nodules generally represent high energy conditions where the nodule was frequently overturned, whereas nodules characterised by open branched columnar algae indicate only periodic overturning and much lower energy conditions (Bosellini and Ginsburg, 1971, Adey and Macintyre, 1973). On Recent South Pacific atolls branching rhodoliths are found consistently in areas of *high tidal* current but *low wave* activity (T. Scoffin, pers. comm. 1981). In addition, rhodoliths developed in place by slow columnar growth have more encrusting organisms (foraminifera, bryozoan, etc.) incorporated into their structure than those whose laminar structure develops as a result of more or less continuous movement (Bosellini and Ginsburg, 1971).

In this sequence, although all forms occur, from massive laminar growths (Fig. 7.12) to delicate branching forms, the majority of nodules are characterised by intermediate growth forms (Fig. 7.12), with relatively few encrusters (Fig. 7.12), suggesting a moderate to low energy environment with only periodic overturning.

Calcarenites (Fig. 7.12) composed dominantly of comminuted algal, foraminiferal, bivalve and coral debris, with occasional echinoid

Fig. 7.12 Rhodoliths and bioclastic calcarenite from the Cağman Member

(a) Typical variation in rhodolith morphology passing from branching to massive laminar forms from left to right. All nodules are from the same horizon. Breccia bed A. Spec. CM4/80. GR. 606286.

(b) Internal structure of dominantly laminar rhodolith. A branching stage developed during an early period of growth. The way-up during the branching stage was to the right as indicated by the prominent geopetal fill (g). Abundant borings and other encrusting organisms present (mainly foraminifera) indicate a relatively slow rate of growth. Species present include; *Lithothamnium*, *Pseudolithothamnium* and *Lithoporella*.
Spec. CM4/80. Breccia bed A. GR. 606286.

(c) Internal structure of laminar rhodolith (left) and more branching form (right). In both cases the rhodoliths originated by encrustation on a shell fragment (s). The laminar rhodolith has a very regular morphology, evenly distributed layering throughout and relatively few other encrusting organisms. Two distinct stages of growth are marked by the change in colour and a prominent horizon of borings. The species are apparently similar in both parts of the nodule (mainly *Lithoporella* and *Lithothamnium*) and the reason for the colour difference is not obvious. The rhodolith on the right had a much slower growth rate as indicated by the more branching form, abundant borings and other encrusting organisms (foraminifera mainly).
Spec. CM4/80. GR. 606286.

(d) Bioclastic calcarenite from the calcarenite cap of a mega-breccia. Comprises dominantly benthonic foraminifera including reworked *Discocyclina* and *Nummulites* of Eocene age and contemporaneous Miocene forms (*Lepidocyclina*, *Miogypsina*) also echinoid plates (e) and other skeletal material.
Spec. 13.1.8.80. GR. 606286.
Field of view 4 cm.

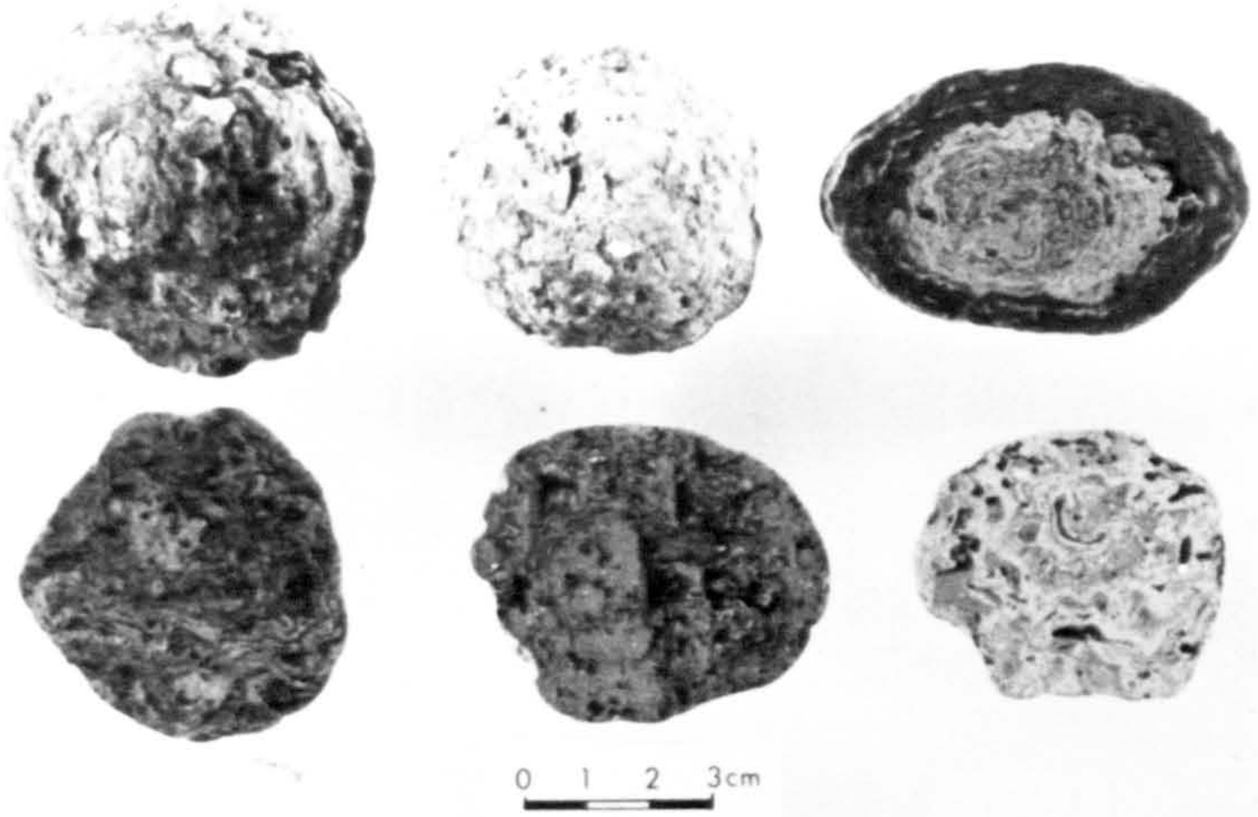

a

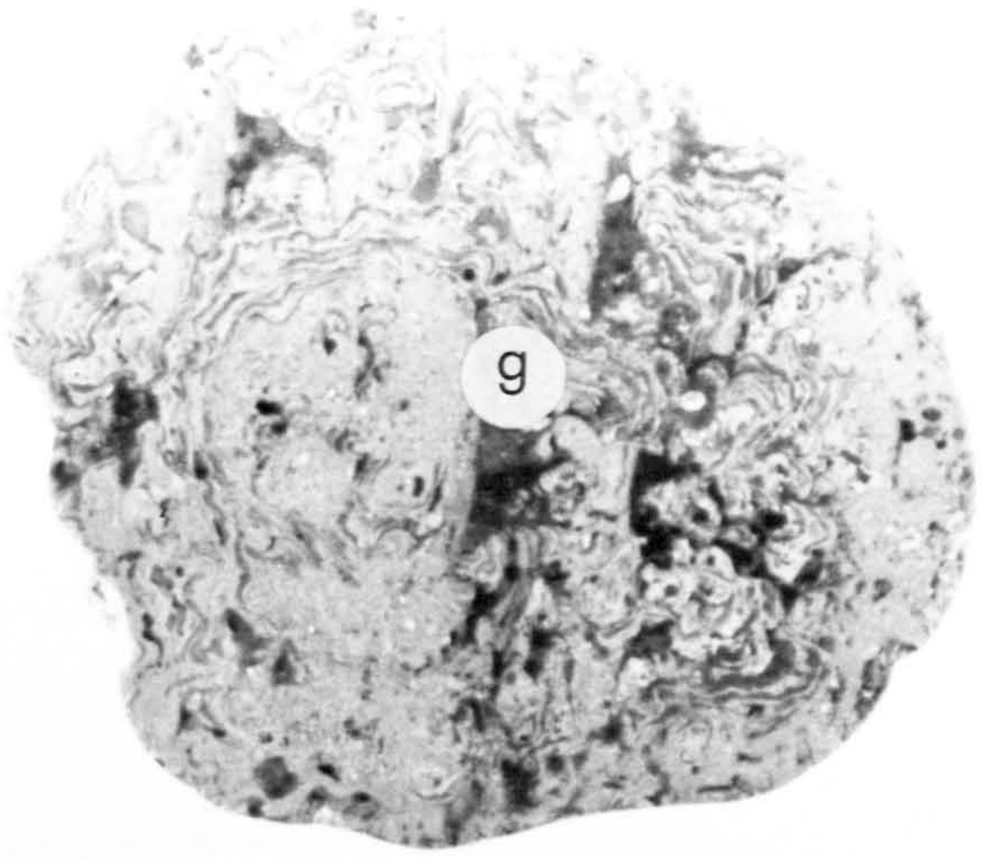

b

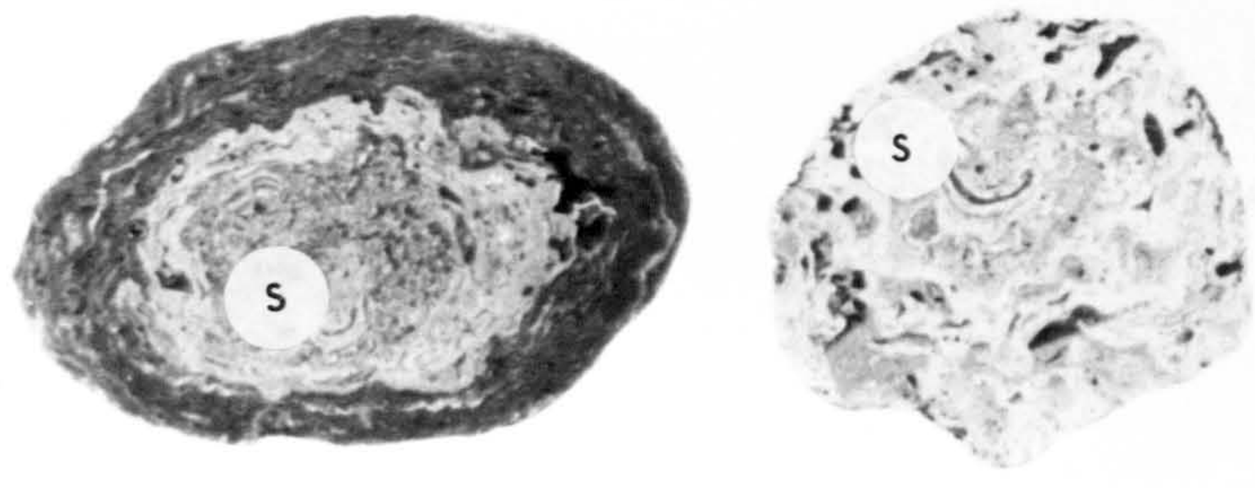

c

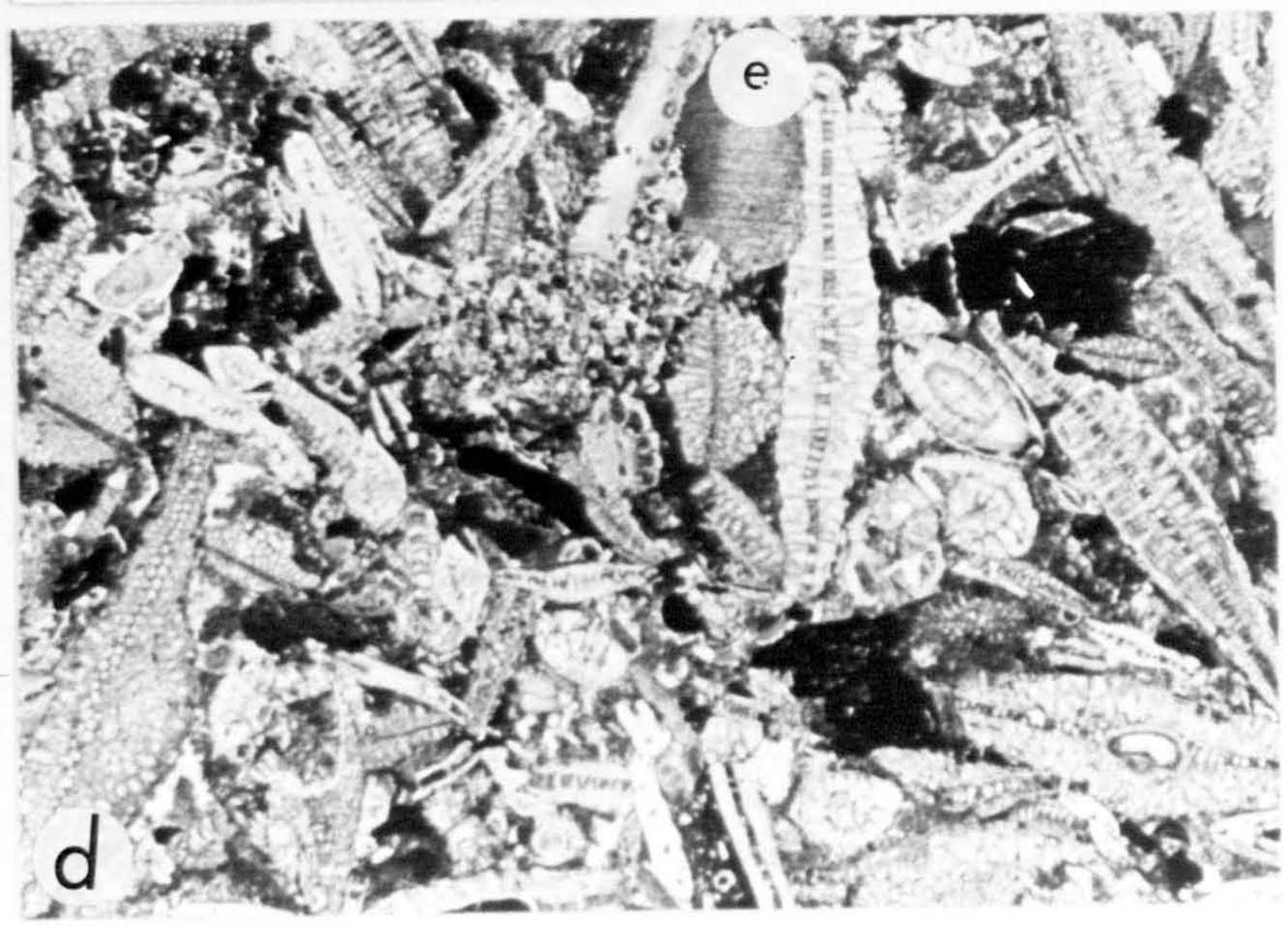

d

spines (Fig. 7.12) are consistent with a shallow marine 'reef' build-up.

In conclusion, the carbonate build-up consisted of a coral reef framework, with associated shallow water biota (benthic foraminifera, echinoids etc.). The percentage of algal material to coral debris suggests that the reefs were not very extensive, possibly formed along the break in slope along the margin (Fig. 7.13), and that most of the area was the site of extensive rhodolith formation. Depth of water was less than 50 m (probably less than 20 m) and the area was subject to periodic wave activity.

7.10 Margin type

The mega-breccia beds and associated facies represent the *marginal facies* to a carbonate build-up. The marginal facies being situated along the hinge line between a shallow water carbonate depositing area and deep water basinal area. Carbonate margins, such as this can be subdivided into a number of types (McIlreath and James, 1979). In this instance the carbonate build-up was situated along the top of a submarine fault scarp (Fig. 7.13). This is a by-pass margin of McIlreath and James (1979), so called because sediments are transported directly from shallow to deep water.

This style of margin is characteristic of many modern slope deposits, e.g. Belize (Ginsburg and James, 1973), Puerto Rico (Conolly and Ewing, 1967), Jamaica (Goreau and Land, 1974) and the Bahamas (Mullins and Neamunn, 1981). On the Belize margin (James and Ginsburg, 1979) where the fore-reef is gentle and flattens with depth grading into a relatively shallow basin, there is no evidence of downslope sediment transport. In contrast, where the fore-reef is steep and continuous to a great depth the profile is oversteepened and sediment accumulations are subject to episodic mass movements transporting material into deeper water.

7.11 Depositional Model : Summary

The Cayman Member sedimentary sequence represents the marginal facies to a shallow water carbonate build-up that was situated to the west of the present exposure (Fig. 7.1). The carbonate build-up developed on a submarine fault scarp produced by syndepositional faulting. The major components of the carbonate complex were crustose coralline algae and more subordinate coral reefs.

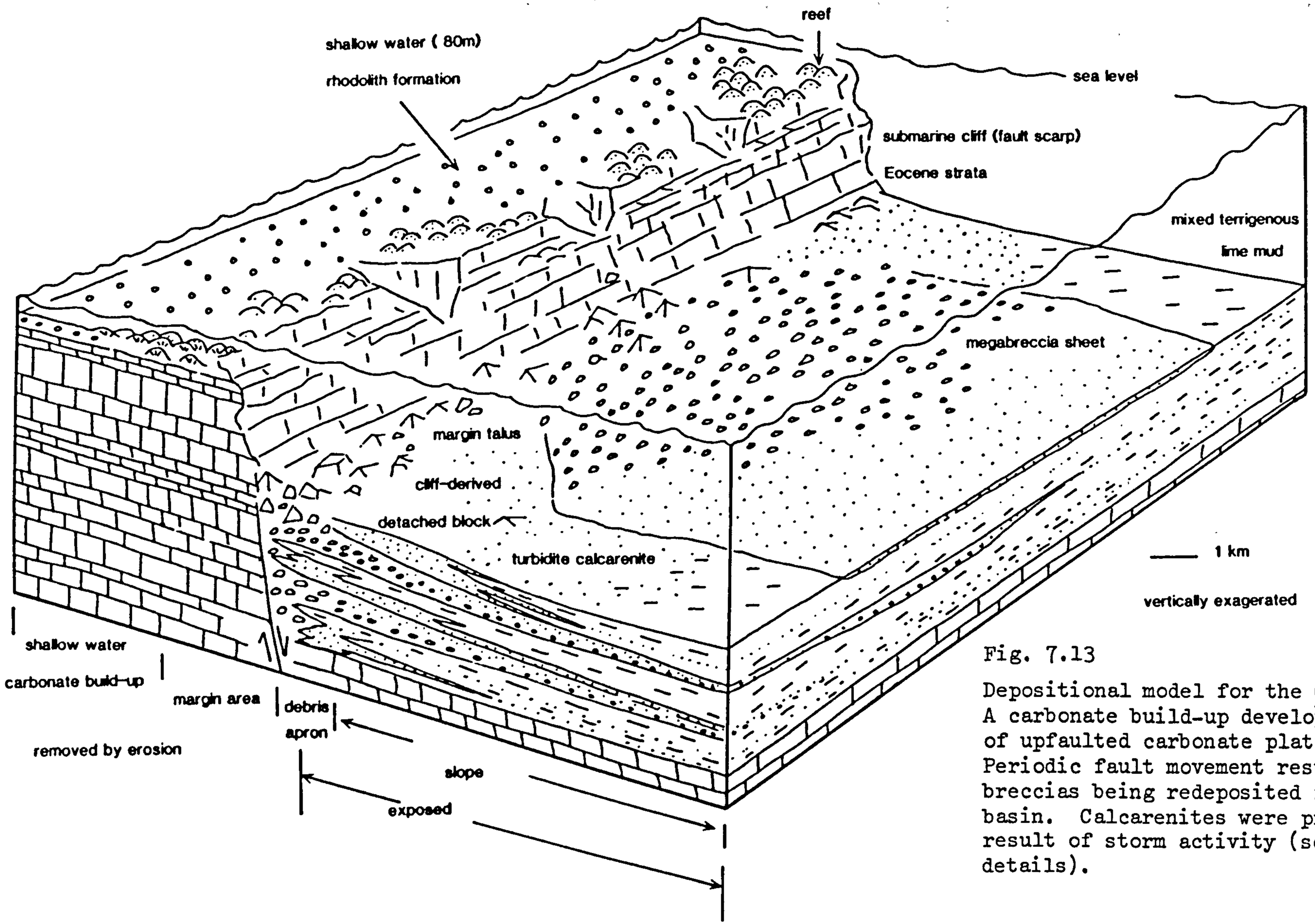

Fig. 7.13

Depositional model for the Cağman Member. A carbonate build-up developed on an area of upfaulted carbonate platform. Periodic fault movement resulted in megabreccias being redeposited into the basin. Calcarenites were probably the result of storm activity (see text for details).

Movements on the fault resulted in periodic earthquakes which redeposited large volumes of mixed bioclastic and reworked material from the underlying sediments downslope as a series of mega-breccias. The breccias show a progressive downslope change in texture and grain size, that can be related to the evolution of an individual mass-flow event. Large detached blocks of Eocene limestone were probably derived off the face of the fault, and slid into place under gravity. Periodic storms sweeping across the shallow water carbonate shelf resulted in the redeposition of finer grained calcarenites into the basin. The basinal sediments consist of very thinly bedded mixed terrigenous-lime mudstone and rare pelagic chalks. Terrigenous material being derived both from the northwest and east. The mega-breccias show a marked upward increase and then decrease in bed thickness, this is tentatively related to fault activity. By Middle Miocene times the fault had become inactive and bioclastic breccias are not present in the overlying terrigenous clastic sequence.

The margin model outlined above and shown schematically in Fig. 7.13, shows many of the features associated with present day reef-by-pass margins (McIlreath and James, 1979); for example the Bahamas (Crevello and Schlager, 1980; Mullins and Neamunn, 1981) and the Belize margin (James and Ginsburg, 1979).

7.12.0 Felenk Dağ Member

The Felenk Dağ Member crops out to the southwest of Kasaba, at the southwestern limit of the Kasaba syncline (Fig. 7.14). Sedimentary facies (described below, 7.14) are broadly similar to the ophiolite-derived sediments of the Kemer Formation, however, composition of the sediments is strikingly different.

7.12.1 Provenance

Composition. The conglomerates and sandstones of this member comprise a complete admixture of carbonate lithoclasts and carbonate bioclastic debris. For the most part the conglomerates are composed of moderately to well rounded (R2-3) lithoclasts of calcilutite, recrystallised calcarenite and more subordinate generally poorly rounded bioclastic material. Vertical variation in clast composition measured from point counts in conglomerates is shown in Fig. 7.15. This shows a general decrease in bioclastic material (from ~70% to ~10%) and increase in limestone lithoclasts up the succession. Only

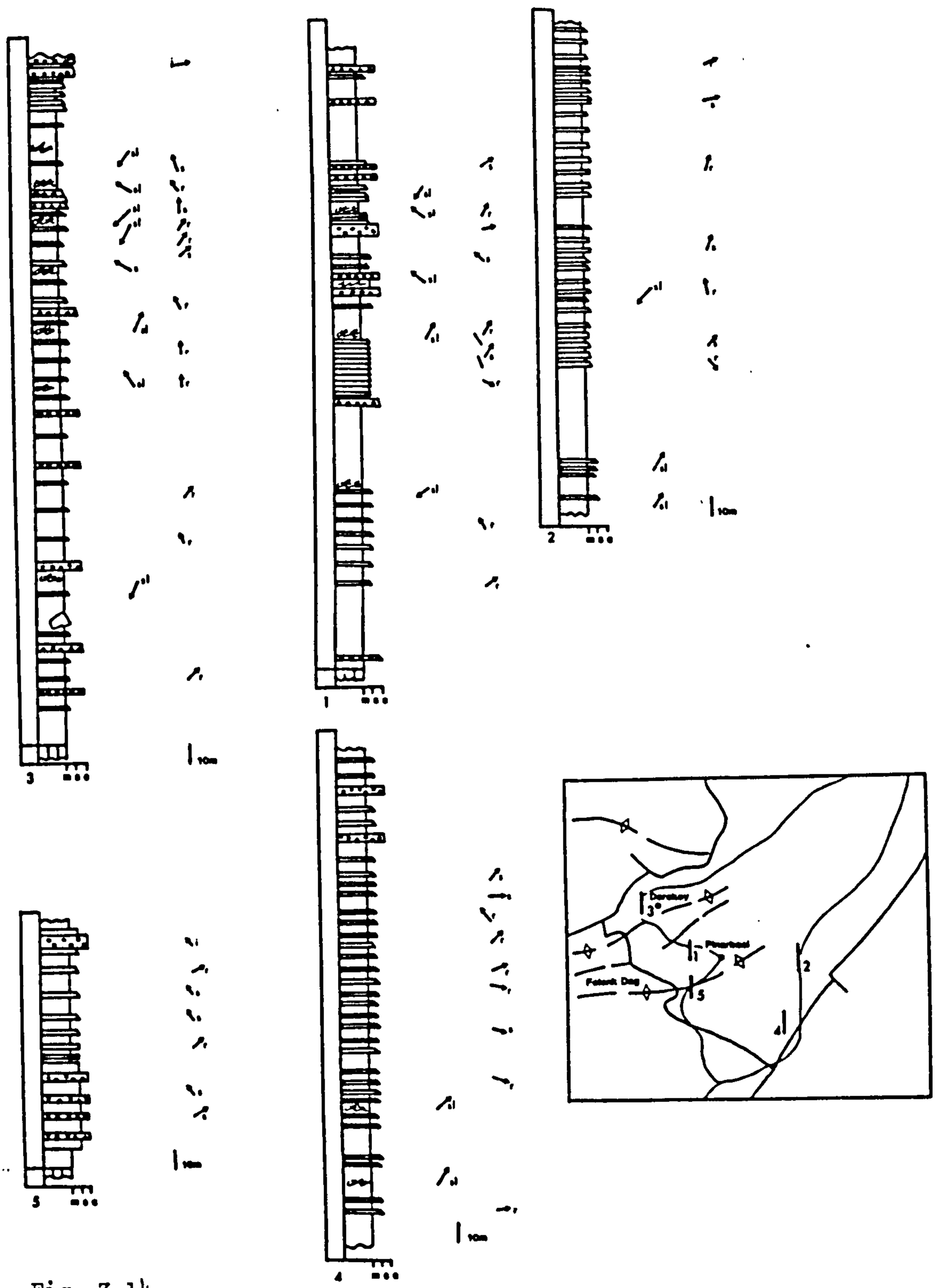

Fig. 7.14

Generalised sedimentological logs in the Felenk Dağ Member.
Note wide variation in orientation of slump horizons (sl),
compared with fairly consistent palaeocurrent trends
(r-ripple marks, s-sole marks)(see text for discussion).
Inset map for location of sections (Appendix C for key to logs).

in the upper parts of the sequence is ophiolite-derived material present. For example, in the Dereköy area conglomerates in the upper parts of the sequence consist of an admixture of ophiolite-derived material (20%), limestone lithoclasts (80%), and subordinate bioclastic debris.

The dominant limestone lithoclasts are:

(1) Bioclastic calcilutite - unknown age;
(2) Calcilutite with numerous nummulites of Eocene age;
(3) Stromatolitic and algal limestone of probable Cretaceous age;
(4) Recrystallised bioclastic calcarenite - unknown age.

Many of the limestone clasts within the conglomerates can be correlated palaeotologically and lithologically with Eocene rock units exposed in the underlying carbonate platform, indicating that substantial areas of the carbonate platform were uplifted and subjected to erosion during the deposition of this sequence. The high sphericity and roundness of many of the clasts is indicative of *subaerial erosion* with transport through a high energy shallow marine or fluvial environment prior to redeposition. The extent of platform exposure and erosion is discussed more fully below (7.19). Bioclastic clasts consist dominantly of algal fragments. Rare complete rhodoliths (forms akin to *Lithothamnium sp*) are between 1 and 6 cm in size. Fragmentary algal material and algal bound bioclastic material is also present. Rare blocks of scleractinian corals (*Montastrea sp., Favites sp.*) are 10-15 cm in length. Scattered shell debris (bivalves and gastropods) and echinoid fragments are also common, along with occasional ooids.

The sandstones consist of a complete admixture of limestone lithoclasts and bioclastic debris. They are generally poorly sorted immature calcarenites. Bioclastic content ranges from 5 to 85%. The dominant bioclastic components are angular algal fragments (*Lithophyllum* and *Lithothamnium*), foraminifera (encrusting, benthonic and rare planktonic forms) and shell debris. Lithoclasts generally comprise micritic limestone with planktonic and benthonic foraminifera of various ages, nummulitic calcarenites of Eocene age, and algal limestone clasts of probable Eocene age.

7.12.2 Mudstone Composition

X-ray diffraction analysis of the mudstone is consistent with a mixed ophiolitic-carbonate provenance. After removal of carbonate

(method outlined in Appendix A) the residual non-carbonate component in 'proximal' areas consists dominantly of kaolinite, illite, montmorillonite and mixed layer clays (Fig. 7.16). Kaolinite, indicative of subaerial weathering in a subtropical environment (Potter *et al.*, 1980) is consistent with subaerial exposure of the carbonate platform. In mudstone from "distal" areas (e.g. Fig. 7.14, Section 2) a significant proportion of serpentinite is present (Fig. 7.16), suggesting that much of the mudstone in distal areas is from the Kemer Formation ophiolite-derived sedimentary system to the northwest.

Palaeocurrents. Palaeocurrent measurements from bottom marks and ripples in sandstones indicate a general southwest to northeast radial dispersal pattern for this sequence (Fig. 7.17). Abundant soft sediment slump horizons are variably orientated (Fig. 7.14) and suggest marked *local* changes in palaeoslope orientation. This local variation may be attributed to tectonic activity in the form of small fault bounded blocks acting independantly to the main tectonic slope. This is discussed more fully below (7.14.3). In general terms the Felenk Dağ Member was derived from an area of uplifted carbonate platform and shallow water carbonate depositing area to the west and southwest of Kasaba (Fig. 7.14). Slump horizons, a good indicator of local palaeoslope (Woodcock, 1976), may not be reliable indicators of overall palaeoslope in this instance (see 7.14.3).

7.13 Initiation of Miocene Sedimentation

Over much of the area of the Felenk Dağ Member, the initiation of clastic sedimentation is similar to other areas in the Kemer Formation (4.3). However, in this area the Aquitanian shallow water limestone (Karabayir Formation) is absent (9.2.5), Eocene nummulitic limestone is overlain directly by up to 50 m of grey-green calcareous marl (Fig. 7.14) with abundant carbonaceous material and a sparse shallow marine fauna of gastropods and bivalves.

This passes upwards into a sequence of thin-bedded calcarenites (Tcde), calcareous mudstone and hemipelagic chalk horizons. The transition occurs abruptly over several metres (Fig. 7.14). Locally for example in the Pinarbaşi area (Fig. 7.14, Section 5), massive, structureless, extensively burrowed, medium to fine grained calcarenites rest with slight angular discordance (4^{o}) on the underlying nummulitic limestone of Eocene age.

Fig. 7.16

XRD traces of mudstones from the Felenk Dağ Member. Note the absence of serpentinite and the presence of kaolinite in proximal mudstones (see text for discussion).

Mo - montmorillonite
MC - mixed layer clays
Ka - kaolinite
serp- serpentinite
Il - illite
t - mounting tile

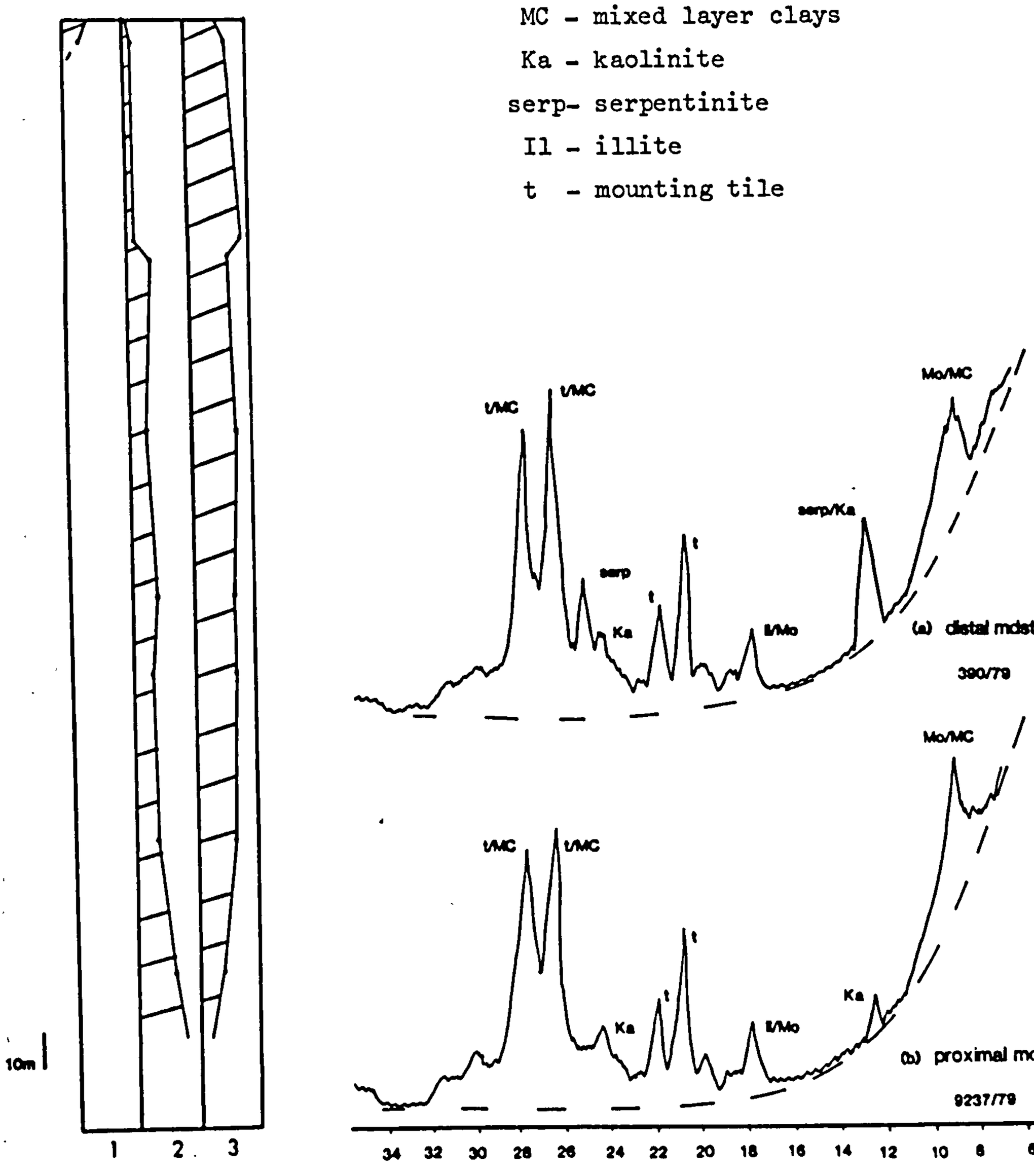

Fig. 7.15

Vertical variation in conglomerate composition from point counts of one hundred clasts at nine horizons through proximal sequences of the Felenk Dağ Member. 1 - ophiolite derived material, 2 - bioclastic material, 3 - limestone lithoclasts.

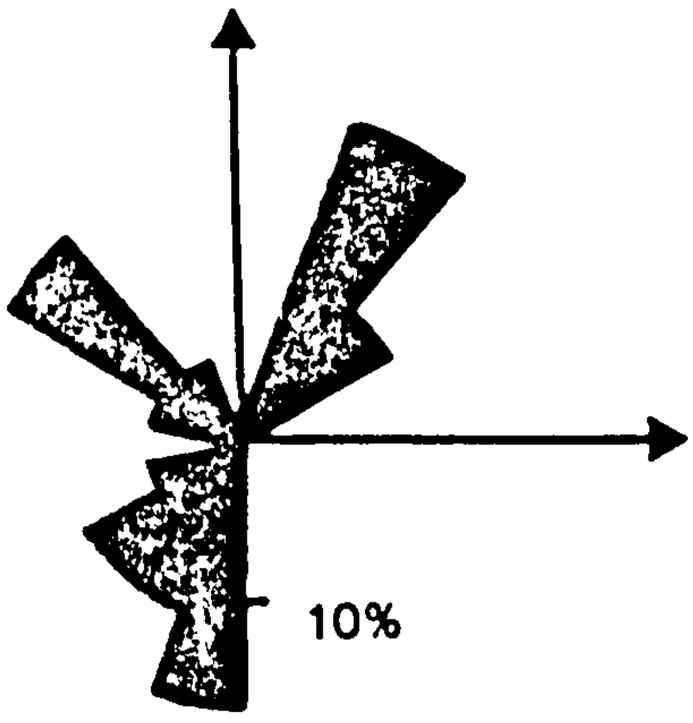

slump horizons N 19

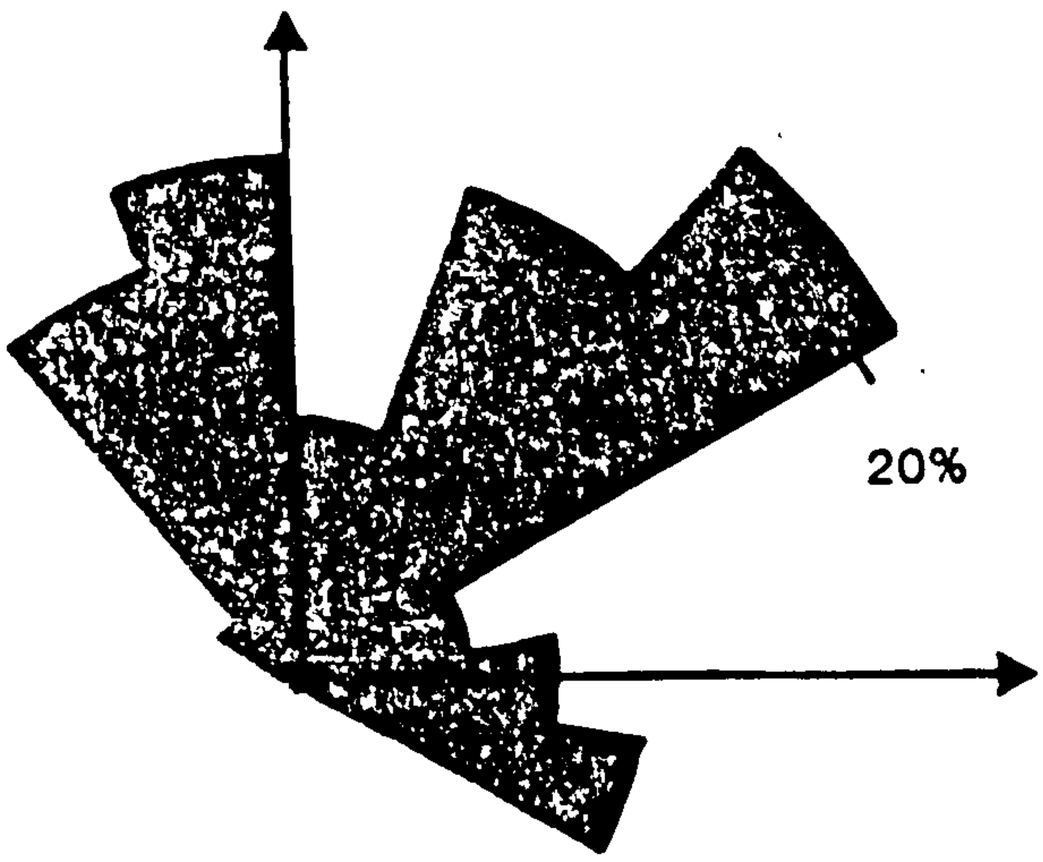

ripple lamination and sole marks N 37

Fig. 7.17
Summary diagram of palaeoslope (slump horizons) and palaeocurrent orientations for the Felenk Dağ Member.
Note fairly consistent trend in palaeocurrent orientation but wide variation in slump orientation, (see text for discussion).
N - number of readings, % - percentage of total readings.

Over most of the area the basal parts of the sequence consist of structureless, completely bioturbated sediment. Following deposition in a shallow marine environment, extensive biological reworking results in an homogeneous green calcareous mudstone, or in other areas, completely homogenised medium to fine grained calcarenite. Where preserved, bioturbation is dominated by horizontal branching networks of *Thallassonoides sp.* type burrow systems, along with subordinate vertical burrows.

This variation in sediment type at the base of the sequence indicates a diachronous introduction of coarse grained carbonate material.

Rare detached limestone blocks (only two occurrences known) are up to 15 x 15 m in size. Composed of nummulitic calcarenite of Eocene age, they were probably derived from syndepositional fault scarps.

Over the whole area the initial extensively bioturbated "shallow" marine sequence passes upwards into interbedded cobble and pebble limestone conglomerates, calciturbites, calcareous mudstones and pelagic chalks. As elsewhere along the western margin of the basin (4.3), the transition from subaerially exposed carbonate platform through a calcareous mudstone sequence deposited in a shallow marine environment, upwards, into a calciturbidite and redeposited limestone conglomerate sequence, reflects the subsidence of the carbonate platform, following emplacement of the Lycian Nappes (see discussion, 10.2.3).

7.14.0 Sedimentary Facies

On the basis of composition, grain size, texture and sedimentary structures, five sedimentary facies types are recognised, they are outlined briefly below and in Tables 7.1, 7.2 and 7.3.

7.14.1 Conglomerates

Description. Boulder, cobble, pebble and granule conglomerates are between 0.40 and 7.0 m thick. Three facies types are recorded (Table 7.2), textures are comparable to those described in 3.4.

Clast-supported conglomerates have a maximum clast size of 18 cm, contain very little fine grained matrix (less than 1% mud), are well indurated and generally show some form of internal organisation (Fig. 7.20) (frequently normal grading ~65%). The bases are often erosive and scoured. Rounded and abraided mudstone and sandstone rip-up

FACIES	BOUNDARIES	INTERNAL STRUCTURE	GEOMETRY	BED THICKNESS	INTERPRETATION
Normally graded clast-supported	U. transitional to sandstone L. erosional scoured	imbrication of a-axes, normal grading, matrix poor	sheet, lent. over 50 m		debris flow transitional to turbulent flow
Inverse to normally graded, clast-supported	U. transitional to sandstone, or sharp planar L. erosional or planar	inverse grading at base, matrix poor	sheet, lent. over 100 m		density modified grain flow (?)
Massive clast-supported	U. transitional to sandstone L. erosional, scoured	structureless, rare imbrication, sandy matrix	sheet, lent. over 100 m		density modified grain flow
Matrix-rich massive clast-supported	U. transitional to sandstone, or sharp planar L. non-erosional planar, rarely irregular erosional	structureless, rare imbrication, abundant mud-rich matrix	sheet		density modified grain flow transitional to debris flow
Matrix-supported massive conglomerate	U. transitional to sandstone, or sharp planar L. non-erosional, irregular erosional	structureless, rare imbrication of a-axes or alignment parallel to base	sheet		debris flow

TABLE 7.1 Summary Table of Conglomerate Facies in the Felenk Dağ Member.

clasts are common at the base of the bed. Tops frequently grade to coarse sandstone. Rarely the tops are sharp and planar.

Matrix-rich and *matrix-supported conglomerates* are poorly indurated, and rarely show any form of internal organisation. A complete gradation exists between these two facies types. The matrix is fine to very fine muddy calcareous sandstone. Bases to conglomerate beds are generally slightly erosive, the underlying sediment often shows soft sediment deformation in the form of slumps and load structures. Mudstone and sandstone intraclasts are common at the base of beds. Injection of mud intraclasts between limestone clasts indicates that the underlying sediment was only partly consolidated during deposition. Bed tops are frequently transitional to a medium or coarse grained calcarenite that may be ripple-or parallel-laminated (Fig. 7.19).

All conglomerates form lenticular units over 100's of metres. Clasts (a) long-axes are consistently aligned parallel to, or imbricated into the flow direction.

Interpretation

The presence of different grading types (Table 7.1), clast long (a) axes imbrication, general disorganised fabric and lack of features indicative of traction current transport of a bedload suggests deposition by a variety of subaqueous sediment gravity flow processes (Table 7.1).

Clast-supported conglomerates. Deposition was by a variety of mass-flow processes that were generally intermediate between full turbulent and density modified grain flow (see 3.4.2 for a full discussion of redeposited conglomerate textures).

Matrix-rich and matrix-supported conglomerates. Patches of matrix-support in matrix-rich conglomerates and areas of clast-support in matrix-supported conglomerates, suggest a continuous transition between these two facies. Matrix-support and clasts in gravitationally unstable positions is consistent with deposition by a debris flow mechanism. In the matrix-rich conglomerates deposition was by density modified grain flow transitional to debris flow, where the effects of dispersive pressure were aided by matrix strength and buoyancy. The relative effect of each supporting mechanism changed through time and from point to point in the flow.

7.14.2 Calcarenites

The calcarenites vary from thick (up to 3 m) beds which grade from pebble conglomerate to coarse sandstone, to thin-bedded structureless and laminated fine grained sandstones. Characterised by flat bases and sharp tops (Fig. 7.21) they are generally describable in terms of the Bouma sedimentary sequence of redeposited sandstones. The types of Bouma sequence observed, structures and associations are summarised in Table 7.2.

Interpretation

The majority of calcarenites fall into two categories: (1) those deposited by dilute turbidity currents, consist of Tcde and Tde divisions of the Bouma sequence; (2) those deposited by dense turbidity currents grade from pebble and granule conglomerate and frequently exhibit TA-E, TABCE and TAE Bouma sequences. They have scoured bases with flute and rare groove marks.

7.14.3 Slump Facies

Description. Soft sediment intraformational slump horizons, between 3.5 and .70 m thick, occur sporadically distributed throughout the sequence. They are more abundant in proximal sedimentary sequences and are generally restricted to thin-bedded calcarenite-mudstone-chalk units.

Slump folds typically have a wavelength and amplitude of .50 to 1.50 m. Axial planes are inclined or recumbent. Folds are frequently disharmonic ranging from isolated hinges to laterally persistent trains. In areas where they are exposed along strike, folds can often be traced into non-slumped strata, the transition from slumped to non-slumped strata is sharp. Interlimb angles vary from 120^{o} to 0^{o}, the majority of folds are close to tight or isoclinal. Hinges are rounded to angular, frequently totally disrupted. Axial planes parallel bedding or are inclined at low angles to bedding.

Interpretation

The following features distinguish these folds as soft sediment folds formed at or near the sediment water interface:

(1) Occurrence of chaotically deformed strata interstratified with non-deformed strata;

(2) Some folded horizons when traced laterally pass abruptly into non-deformed strata;

GRAIN SIZE	BED THICKNESS	BASE	TOP	INTERNAL STRUCTURE
gl. cgl.-vc.	vtk.-m.	flat, scoured flutes, grooves rip-ups	sharp	graded, struct.
gl. cgl.-vc -m.	vtk.-m.	flat, scoured, flutes, grooves rip-ups	sharp	graded, par. lams, ripple lams, pb., cgl. at base. Babce, Bbce.
m.-f.	tk.-tnb.	flat, slight scoured, flutes grooves, rip-ups some loading	sharp	graded, par. and ripple lams, conv. lams. Bcde, Bce.
m.-f.	tnb.-m.	flat, rare loading	sharp	graded, struct. or par. par. lam. Bde.
vc, c, m.	vtk.-m.	flat, sharp rare rip-ups	sharp	struct. some carb. lamellae at top
f.	vtnb.-m	flat	sharp	struct.
vc.	vtnb.-m	flat	sharp	struct. lent. over 10 m.

TABLE 7.2 Summary Table of Calcarenite Facies Types in the Felenk Dağ Member.

(3) The association with other soft sediment structures such as loading and injection structures.

Orientation. The folds show a wide range in orientation (Fig. 7.14) and indicate marked local changes in palaeoslope, both at any one stratigraphic horizon and through time (Fig. 7.14). This variation is probably related to fault activity in the underlying basement (carbonate platform) associated with subsidence of the platform following emplacement of the Lycian Nappes (10.2.3). It is suggested that fault bounded blocks in the platform, moving independantly produced marked variations in palaeoslope over relatively small areas.

Sedimentological features and interpretation of the fine grained facies (calcareous mudstone, hemipelagic chalk) are given in Table 7.3.

7.15.0 Facies Organisation

The Felenk Dağ sedimentary sequence is characterised by the following features;

(1) complete absence of shallow water indicators (including traction cross-bedding, and shallow marine faunas);

(2) broadly unidirectional radial palaeocurrents;

(3) abundant hemipelagic chalk horizons;

(4) channelled conglomerate and calcarenites deposited by a variety of sediment gravity flows (above and 3.4).

All of these are consistent with deposition in a submarine fan environment. Within the sequence several facies associations are recognised based on grain size, bed thickness, calcarenite:mudstone ratio and vertical sequence textures.

7.15.1 Conglomerate-Calcarenite-Calcareous Mudstone (association 1)

This association is well exposed in the Felenk Dağ and Pinarbaşi area (Fig. 7.18, Sections 7115, 7113). Individual conglomerate beds between .90 and 3.0 m thick, form packets of between one and three beds, up to 6.5 m thick. Bases to the conglomerate are erosive into the underlying sediment. Conglomerate packets are overlain by medium to thin-bedded turbiditic calcarenites (Tbcd, Tcde) forming overall fining- and thinning-upward cycles up to 8.5 m thick (Fig. 7.20). Where exposure permits, conglomerate packets are seen to thin markedly (up to 1-2 m) over several tens of metres, suggesting

FACIES	BED THICKNESS	BASE	TOP	INTERNAL STRUCTURE	COLOUR AND COMPOSITION	INTERPRETATION
Calcareous mudstone	individual beds 1-6 cm, amalgamated beds up to 1 m	planar, sharp or gradational	planar sharp	parallel and low-angle ripple-laminations, grading silt to clay (over 2-3 mm), rarely evid. of bioturbation	'proximal' areas white/light green very calcareous little clay, mainly kaolinite, illite and montmorillonite, 'distal' areas green/grey, with serpentinite and smectite	distal 'mud' turbidity current
Pelagic chalk	1-4 cm, mean 3 cm	planar, sharp rarely irregular and scoured (scale 2-3 mm)	planar sharp	struct. homogeneous, or rare silt flasers, and bioturbation, in thin section, cross and parallel lamination, micrograding and cut-and-fill struct.	white/grey planktonic and some benthonic forams, micrite matrix, carbonaceous plant fragments. coccoliths and planktonic foram fragments (S.E.M.)	initial deposition as hemipelagic rain-out sediment followed by limited reworking

Table 7.3
Summary Table of the sedimentary features of the Fine Grained Facies, Felenk Dağ Member.

a broadly channellised form. Organised matrix-poor conglomerates are markedly more channellised than the matrix-rich and matrix-supported beds.

Interbedded grey-green calcareous mudstones which comprise up to 60% of the sequence are homogeneous or rarely faintly laminated.

7.15.2 Packets of Amalgamated Calcarenites (association 2)

Thin- to thick-bedded, coarse to medium grained, graded calcarenites (Tbcd, Tbce) form amalgamated packets up to 5 m thick. Individual beds are .35 to 1.5 m thick (mean .70 m). Within 80% of the packets, which comprise of between three and six beds, distinct coarsening-upward sequences are present.

7.15.3 Calcarenite-Calcareous Mudstone-Chalk (association 3)

This association forms up to 80% of the sequence exposed in the area immediately southwest of Kasaba (Fig. 7.18, Section 7136). Laterally continuous, flat based sharp topped calcarenites (Tcde, Tde) between 0.03 and 0.25 m thick (mean 0.10 m), form between 10% and 60% of the sequence. Calcareous marls have a mean thickness of 0.08 m. Pelagic chalks, 1-5cm thick, form 2-15% of the sequence.

7.15.4 Calcareous Mudstone-Thin Calcarenite-Chalk (association 4)

This association comprises of thin to massive completely homogeneous green calcareous mudstones between 0.08 and 8.0 m thick. Interbedded with very thin pelagic horizons with a mean thickness of 4 cm. Chalks form between 2 and 30% of the sequence. Thin to very thin, coarse to medium grained, structureless or rarely graded calcarenites occur, interbedded with the mudstones.

7.16.0 Vertical and Lateral Variations in Facies Associations

Analysis of the vertical and lateral relationship of the facies associations outlined above enables the synthesis of a sedimentological (facies) model.

Lateral variations. Local lateral variations in sedimentary facies are difficult to demonstrate as a result of the poor exposure (generally confined to road cuttings) and localised folding.

Regional variations shown by a series of generalised sections in Fig. 7.14, indicate a general decrease in percentage of conglomerate, grain size and sandstone:mudstone ratio towards the east, southeast and north. This trend is broadly in agreement with palaeocurrent orientations which suggest a *point source* in the

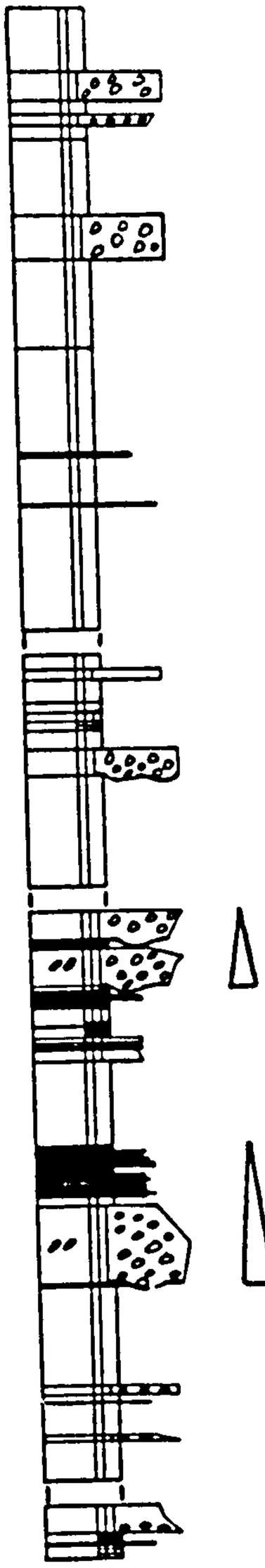

SECTION
FD 7115

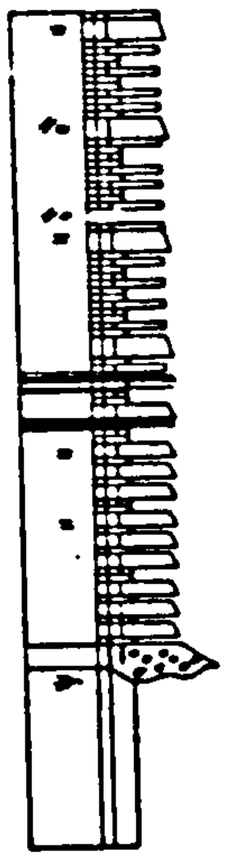

SECTION
FD 7130

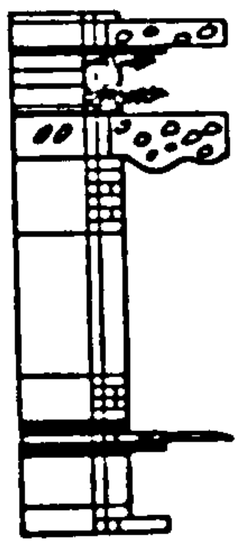

SECTION
FD 7113

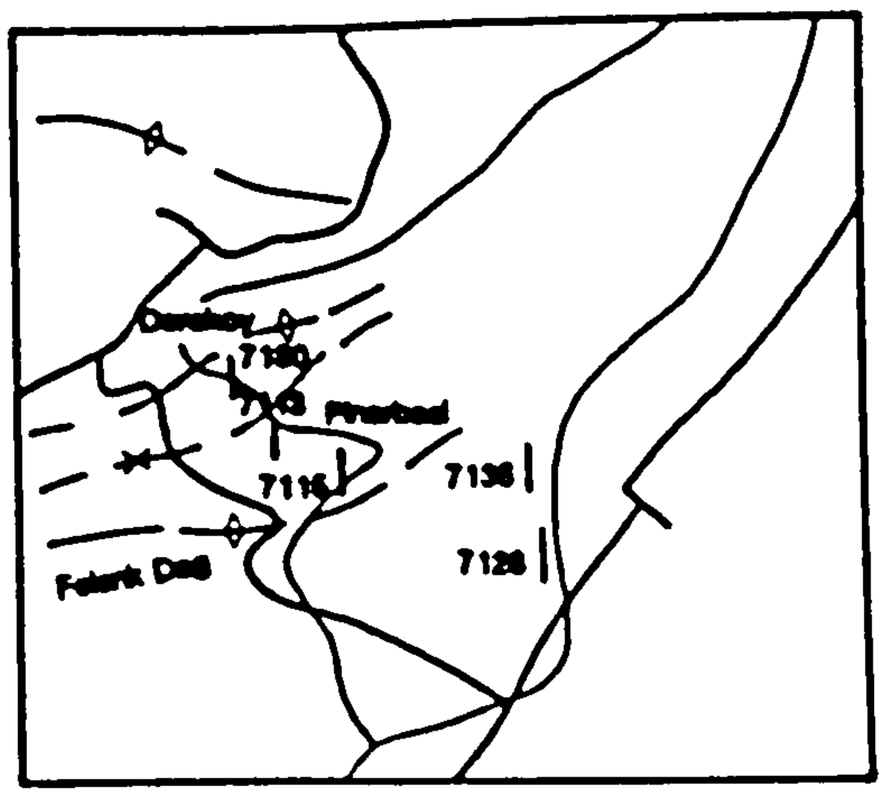

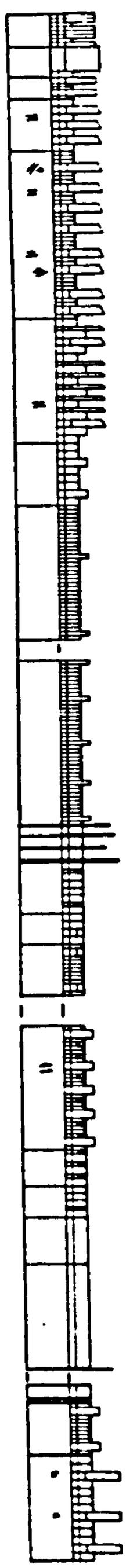

SECTION
FD 7128

6m

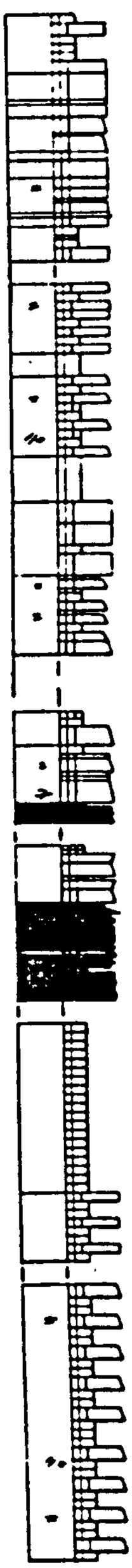

SECTION
FD 7136

Fig. 7.18

Detailed sections in the Felenk Dağ Member (inset map for the location of sections). Note presence of fining-upwards conglomerate-sandstone 'channel' units in proximal areas and thick generally non-cyclic sandstone sequences in more distal areas.

Felenk Dağ-Pinarbaşi area (Fig. 7.14). Dispersal of carbonate material radially away from this area results in the interdigitation of carbonate terrigenous sediment with ophiolitic terrigenous sediment in the area southwest and west of Kaş.

7.16.1 Inner Fan Depositional Environment

Palaeocurrent dispersal patterns and coarse grain size are consistent with the Felenk Dağ-Pinarbaşi area being considered *most proximal*. Sequences exposed in this area (Fig. 7.14, Sections 5 and 1) are dominated by facies association 1 (conglomerate-calcarenite) and 4 (calcareous mudstone-chalk-thin calcarenite). Although channel morphology is not always easily demonstrated (due to poor exposure), the presence of strongly erosive bases and fining- and thinning-upward cycles within packets of conglomerates and calcarenites (Fig. 7.20) suggest deposition in a submarine fan channel in the *inner fan area*. The channels appear to have been generally broad, shallow features in most of the sequences they have been plugged by one or, in some cases, two catastrophic mass-flow events (Fig. 7.18, Section 7115). The thinning- and fining-upward cycles to which the conglomerates form the base are the result of progressively thinner and finer flows (Ricci Lucchi, 1969, 1975b; Mutti and Ghibaudo, 1972). In some instances (e.g. Fig. 7.18, Section 7115) isolated channelled conglomerate horizons occur within a marl sequence with no associated calcarenites. In these cases "one event channels" are suggested, the channel being cut and filled by the same depositional event. Calcareous marls represent fine grained overbank material that in some parts of the sequence has been completely homogenised by bioturbation. Within the marls thin, laterally discontinuous coarse grained calcarenites are the result of spillover from the main channel into overbank areas.

Sequences exposed to the east, northeast and north of Felenk Dağ were deposited in a *more distal* sedimentary environment (Fig. 7.14, Sections 2 and 4). The following features suggest deposition on the *mid-fan area* of a submarine fan:

(1) visible channelling decreases in importance;

(2) absence of thick channellised conglomerates and calcarenites;

(3) the presence of coarsening-upward calcarenite packets is not consistent with deposition on the lower fan or basin plain (Walker, 1979b; Reading, 1978) but is more characteristic of deposition on

Fig. 7.19

Matrix-rich conglomerate interbedded with pelagic chalks, calcareous marls and rare thin calcarenites (c).
Inner submarine fan depositional environment.
Note thin 'turbiditic top' (t) to conglomerate bed and presence of cobble/boulder horizon through centre of bed.
Deposition was by debris flow mechanism.
Hammer is 34 cm long.
Felenk Dağ Member. GR. 399147.

Fig. 7.20

Amalgamated clast-supported conglomerate-calcarenite unit forming overall fining-upwards channel (?) sequence.
Inner submarine fan depositional environment.
Note presence of thin mud drapes (m) between successive conglomerate beds.
The basal conglomerate is slightly erosional into the underlying calcarenite/mudstone sequence.
Stick is 1 m long.
Felenk Dağ Member. GR. 406146.

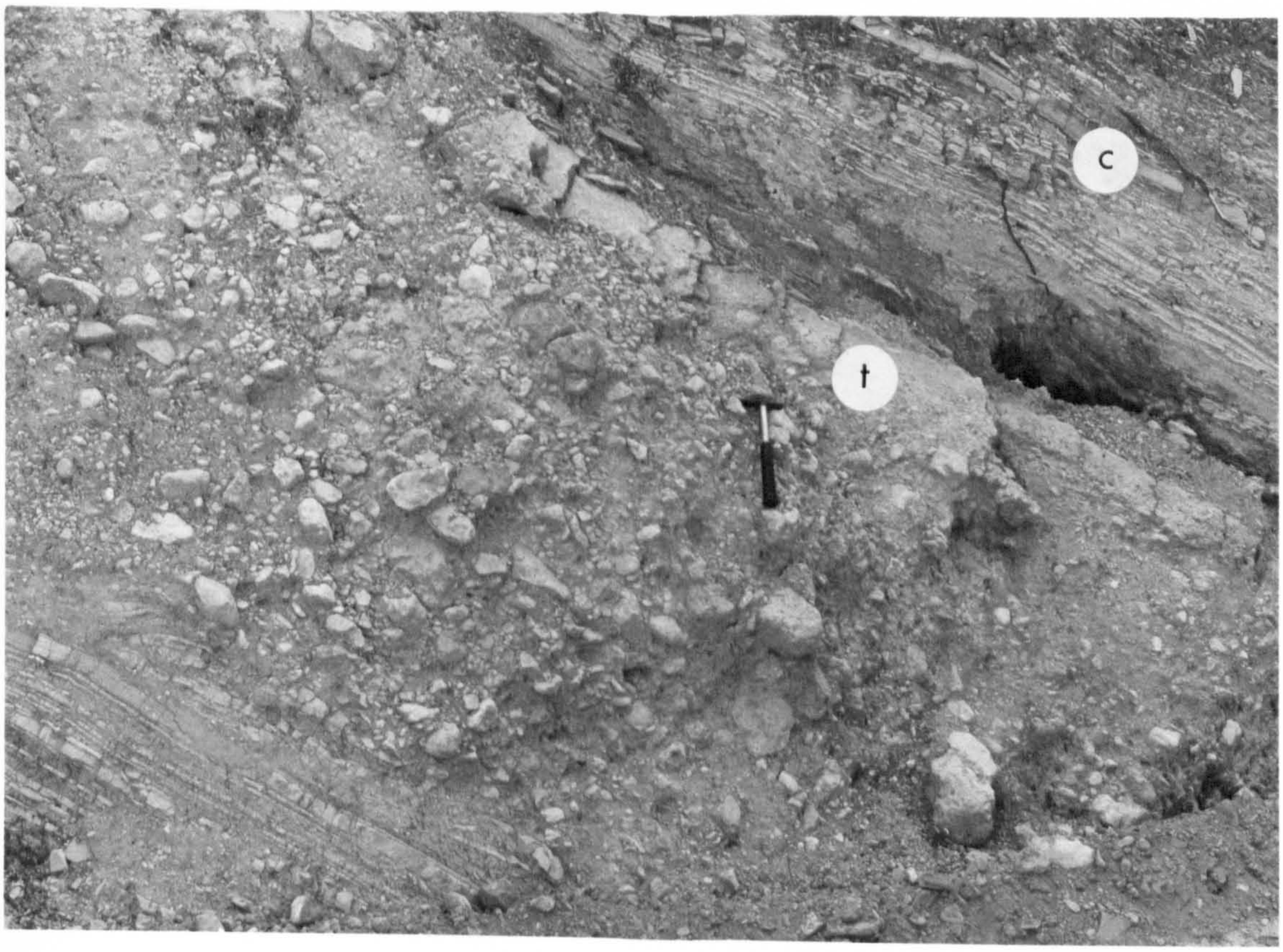
c
t

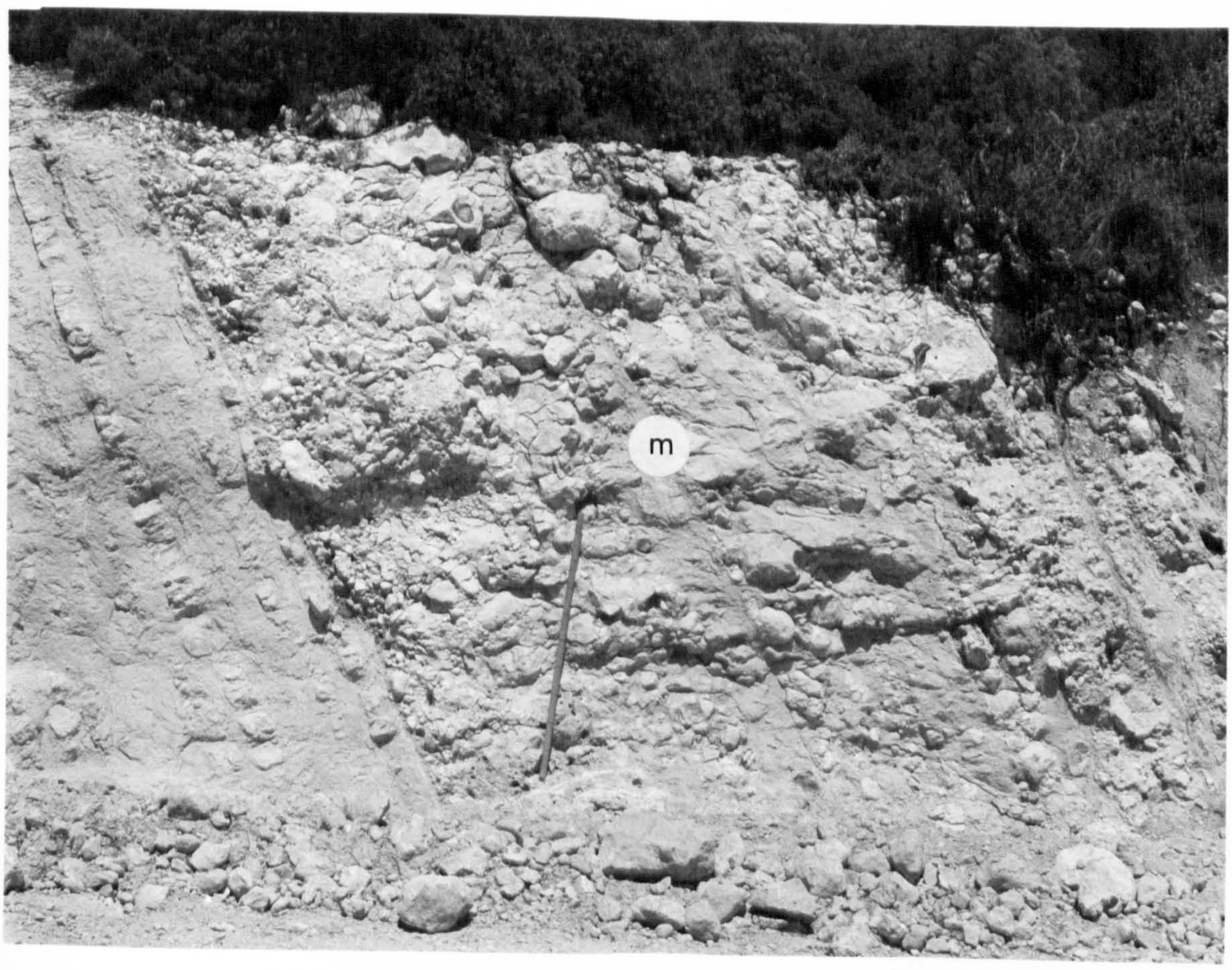
m

Fig. 7.21

Field photographs of the Felenk Dağ Member Sequence.

(a) Thin-bedded turbiditic calcarenite (t) with well developed normal grading, overlain by pelagic chalk horizon (p) and calcareous mudstones (m).
Note presence of slight bioturbation in top of the calcarenite bed (below lens cap).
Mid-fan association.
Lens cap is 7 cm in diameter. GR. 426143.

(b) Amalgamated thin- and medium-bedded, medium to fine grained turbiditic calcarenites.
Mid-fan association, layer thickness plots for this sequence show no ordered vertical arrangement.
Pen is 16 cm long. GR. 398170.

(c) Matrix-rich conglomerate interbedded with thin turbiditic calcarenites, calcareous mudstones and pelagic chalks.
Inner fan association.
Note presence of poorly developed inverse grading in conglomerate.
Hammer is 33 cm long. GR. 395154.

(d) Matrix-rich conglomerated interbedded with thin turbiditic calcarenite and calcareous mudstones.
Note lenticular (to the right) and erosive nature of base to conglomerate.
Inner fan association.
Hammer is 33 cm long. GR. 402152.

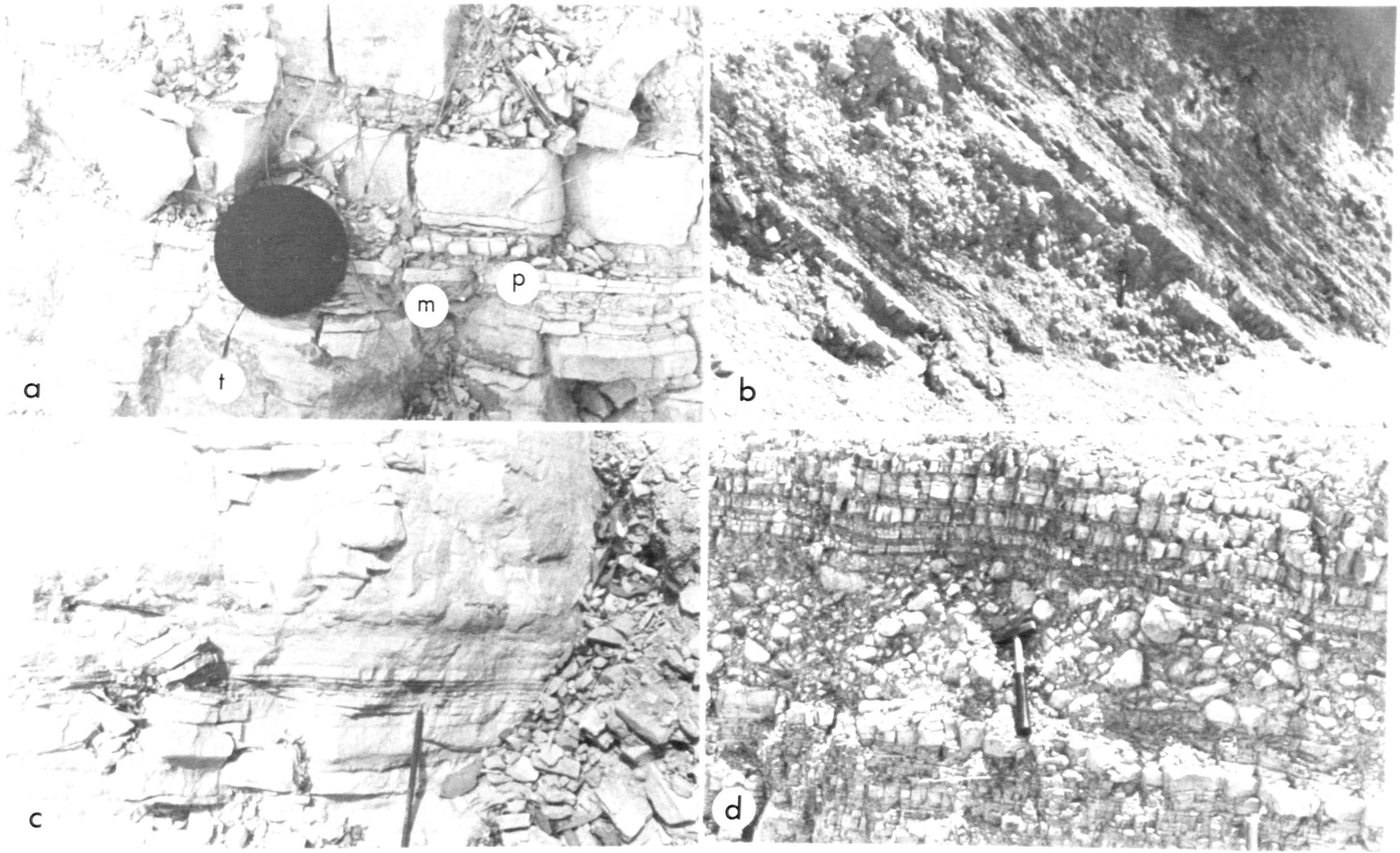
a
t
m
p
b
c
d

non-channellised mid-fan lobes.

Sequences in this area are dominated by facies associations 2 and 3. Packets of thick calcarenite beds which form distinct coarsening- and thickening-upward units account for only 20% of the sequence. These coarsening-upward cycles are attributed to progradation of mid-fan depositional lobes (Ricci Lucchi, 1975b; Walker, 1979b). The high percentage of interbedded calcarenites, mudstones and chalks (association 3) which are essentially acyclic (not characterised by either fining- or coarsening-upward cycles) should not be considered unusual. As discussed elsewhere (5.5.6) many sequences interpreted to have been deposited in a mid-fan submarine fan setting show no arrangement into well defined cycles. Possible explanations for this are numerous, some of the more likely ones are outlined below.

(1) *Tectonic events* either in the source area resulting in fluctuations in sediment supply to the entire sedimentary system or tectonic events within the basin that result in rapidly varying sediment dispersal paths.

(2) Tectonic events (above) may result in *irregular lobe progradation.*

(3) The interaction of *two overlapping depositional* lobes, derived from one or more channels.

Evidence outlined previously suggests that the Felenk Dağ sedimentation system was subject to marked tectonic control (7.14.3). In a small immature submarine fan setting such as this (Fig. 7.22) tectonic events exert a far greater control on fan geometry and changes with time, within the system, than are seen in many base of continental slope submarine fans (e.g. modern examples described by Normark, 1978; Stow, 1980). Present "facies models" (Walker and Mutti, 1973; Walker, 1979b) based partly on these systems developed in relatively stable tectonic areas can only be broadly applied to small submarine fans, developed in rapidly subsiding, tectonically unstable, ensialic basins. For fuller discussion of this see 5.12.

7.17 Sedimentation Rates

In areas of good exposure, chalk horizons produced by pelagic rain sedimentation enable approximate estimates of sedimentation rates to be made (e.g. 5.6). Pelagic carbonate sedimentation rates for the L. Miocene period in the Pacific, Atlantic and Indian Oceans varied between 1 and 2 cm/year (Davies *et al.*, 1977). When

considering sediments of the Salir Formation (5.6) an average of 1 cm/1,000 years was used in calculating sedimentation rates. Most of this sequence is characterised by two turbidite events interbedded with a pelagic chalk horizon averaging 3 cm, compared with 1 cm in the Salir Formation mid-fan environment (5.6). This suggests that sedimentation was consistently more intermittent in this sequence, allowing thicker pelagic interbeds to accumulate, when compared with the sedimentary sequence along the eastern margin of the basin (Salir Formation, 5.6). An alternative explanation is that in addition to the normal pelagic sedimentation, "pelagic horizons" in this sequence are composed of a significant proportion of very fine dispersed terrigenous carbonate resulting in substantially thicker pelagic beds.

7.18 Contrasts with other Redeposited Carbonate Sequences

The Felenk Dağ Member sequence is unusual in that it comprises a thick sequence of redeposited carbonate material derived from the uplift and erosion of a carbonate platform, in contrast to redeposited carbonate derived from the margins of steadily subsiding carbonate accumulations (e.g. in the Recent, Bahamas and Belize carbonate platforms; in the ancient, the Bey Dağlari, Chapter 9 and Robertson and Woodcock, 1981b). In all these, as in the Çağman Member (7.2), redeposition is down a steep slope along the entire margin. As a result an organised sedimentation system eminating from a point or series of points, is unlikely to develop. The Felenk Dağ Member system is in many aspects identical to a siliciclastic submarine fan sequence, the carbonate composition reflecting derivation from the uplifted carbonate platform. A similar sequence, although interpreted to have been derived from the submarine erosion of a carbonate platform, has been described from a Mesozoic continental margin in Greece (Price, 1977).

7.19 General Model : Summary

The Felenk Dağ Member clearly represents the introduction of carbonate terrigenous material, derived from an area of uplifted carbonate platform, to the southwest and west of Felenk Dağ, into the dominantly ophiolite-derived basin fill.

Abundant bioclastic material was derived from shallow water carbonate-shelf areas on the margins of the basin. Terrigenous carbonate material transported through this area, mixed with the

bioclastic carbonate material, resulting in a complete admixture of terrigenous carbonate and bioclastic carbonate clasts in the redeposited sediments. Well rounded limestone clasts, suggest transport through a high energy, fluvial or shallow marine environment prior to redeposition. A high percentage of carbonaceous plant material and kaolinite in some calcarenites indicates that the platform was sufficiently uplifted for soil and vegetation to develop. The immature nature of the sediments and abundance of conglomerates in proximal areas suggest that the submarine fan system was fed by a series of alluvial fans or fan-deltas that prograded across a shallow water carbonate shelf. These passed downslope into one or possibly several submarine fans. Poor exposure limits control on the sedimentological model. The area around Felenk Dağ and Pinarbaşi is characterised by interbedded conglomerates and marls. This sequence is interpreted as an inner fan channel. Homogeneous marls may be the result of extensive bioturbation, combined with high sedimentation rates, produced by ponding of fine grained material in fault-bound depressions. Inner fan sequences pass to the north, northeast and east, into a sequence of calcarenites, calcareous mudstones and chalks.

Coarsening-upward calcarenite packets in this area were deposited in prograding mid-fan lobes. The majority of this mid-fan sequence, however, is non-cyclic. In the area south and west of Kasaba (Fig. 7.14), calcarenites interdigitate with ophiolite-derived clastic sediments of the Kemer Formation. The general model for this sequence is shown in Fig. 7.22.

Uplift of the carbonate platform, probably along normal faults (10.2.3), was related to the initial emplacement of the Lycian Nappes onto the platform. Rare detached limestone blocks at the base of this sequence were probably derived off syndepositional fault scarps. Slump orientations which differ widely both vertically and laterally (Fig. 7.14) suggest that the underlying carbonate platform basement consisted of a number of fault bound blocks, acting more or less independantly, resulting in marked local variations in palaeoslope. If correct this may account for (1) thick sequences of homogeneous marls, produced by ponding in local fault-bound depressions; (II) irregular cyclicity of what is interpreted to be a mid-fan depositional site.

In conclusion, sedimentary facies analysis suggest that the Felenk Dağ Member represents a *small submarine fan* (or series of

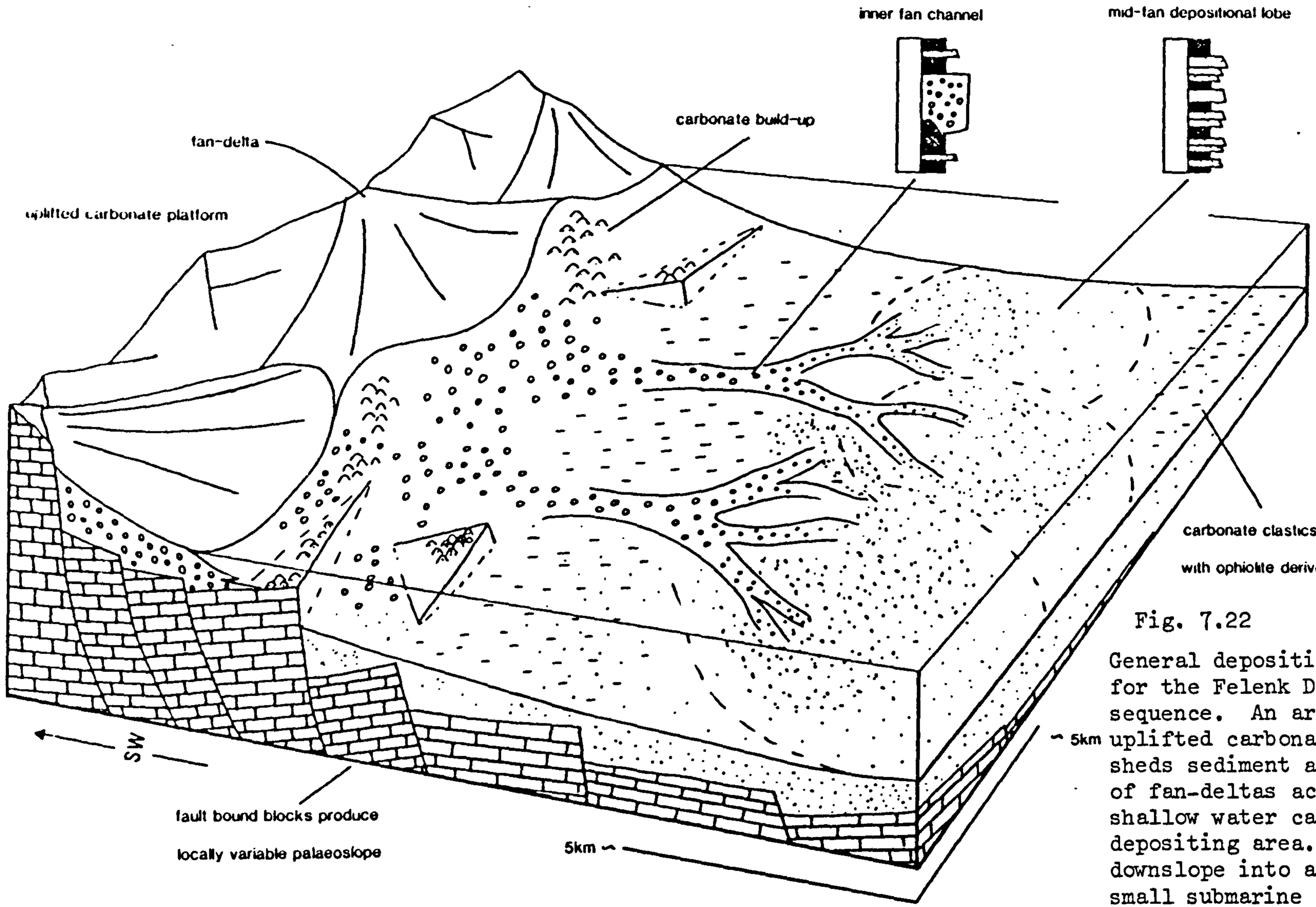

Fig. 7.22

General depositional model for the Felenk Dağ Member sequence. An area of uplifted carbonate platform sheds sediment as a series of fan-deltas across a shallow water carbonate depositing area. This passes downslope into a series of small submarine fans (see text for details).

fans) located on the southwestern margin of the basin. Carbonate terrigenous material derived from an area of *uplifted carbonate platform* to the west and southwest, was introduced into the basin via a series of fan deltas that prograded across a shallow water carbonate shelf (Fig. 7.22).

CHAPTER 8 REEF SEDIMENTOLOGY

CHAPTER 8

8.0 Reef Sedimentology

8.1 Introduction

Reefs have been identified from a number of stratigraphic horizons within the Kasaba Formation (Fig. 8.1). Disorientated reef blocks are also present in parts of the Kemer Formation (4.4.3), where preservation is very poor. The following chapter describes in detail only reefs from the Kasaba Formation.

8.2 Reef Morphology

The reefs are asymmetric mounds up to 8 m high and as much as 40-50 m across. They are generally oval or subspherical in plan morphology, with a bilateral symmetry. The basal surfaces of the reefs are roughly horizontal paralleling bedding in the underlying sediments. In some parts a depositional dip of up to 5° is observed. The exhumed tops are convex.

The reefs are not confined to one horizon, but are distributed throughout the sequence (Fig. 8.1). They are, however, restricted to the shallow near shore zone, seaward of the shoreface (Fig. 4.30, 4.8.2). Along strike it is seen that the reefs did not form a continuous fringing or barrier reef, but rather occurred as isolated build-ups paralleling the contemporary shoreline (Fig. 8.2), resulting in an approximate east-west alignment.

From the description of recent reefs (Stoddart, 1969; Logan *et al.*, 1969; James, 1972, 1979) the reefs most clearly resemble patch reefs, in that they are of limited size and are completely surrounded by coarse clastic terrigenous sediment (4.8.2).

8.3 Internal Structure and Facies Distribution

Corals form the major frame-building organisms, comprising between 50% and 90% by volume of the reef. Table 8.1 is a list of the dominant coral species, with an indication of their approximate abundance. Coralline algae are the other important frame-building organism.

The reefs can be subdivided into three facies types (Fig. 8.3):

Basal unit. All reefs overlie a cobble-pebble terrigenous conglomerate which passes gradationally into a very coarse calcarenite over a thickness of approximately 1.0 m. This passes rapidly upwards into a bioclastic breccia composed of coral fragments generally

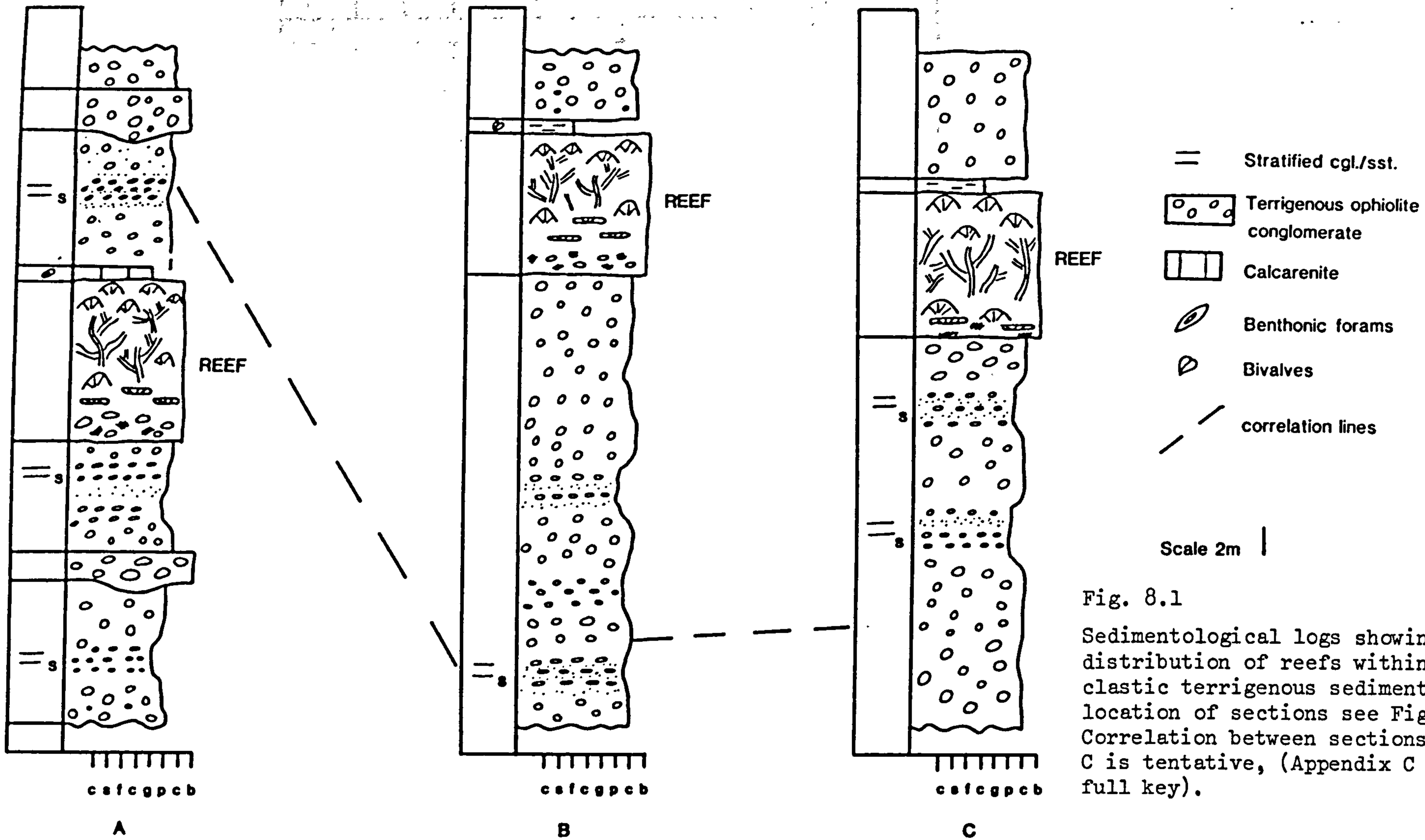

Fig. 8.1

Sedimentological logs showing distribution of reefs within coarse clastic terrigenous sediments (for location of sections see Fig. 8.2). Correlation between sections B and C is tentative, (Appendix C for full key).

Kasaba Formation

Kemer Formation

Carbonate Platform

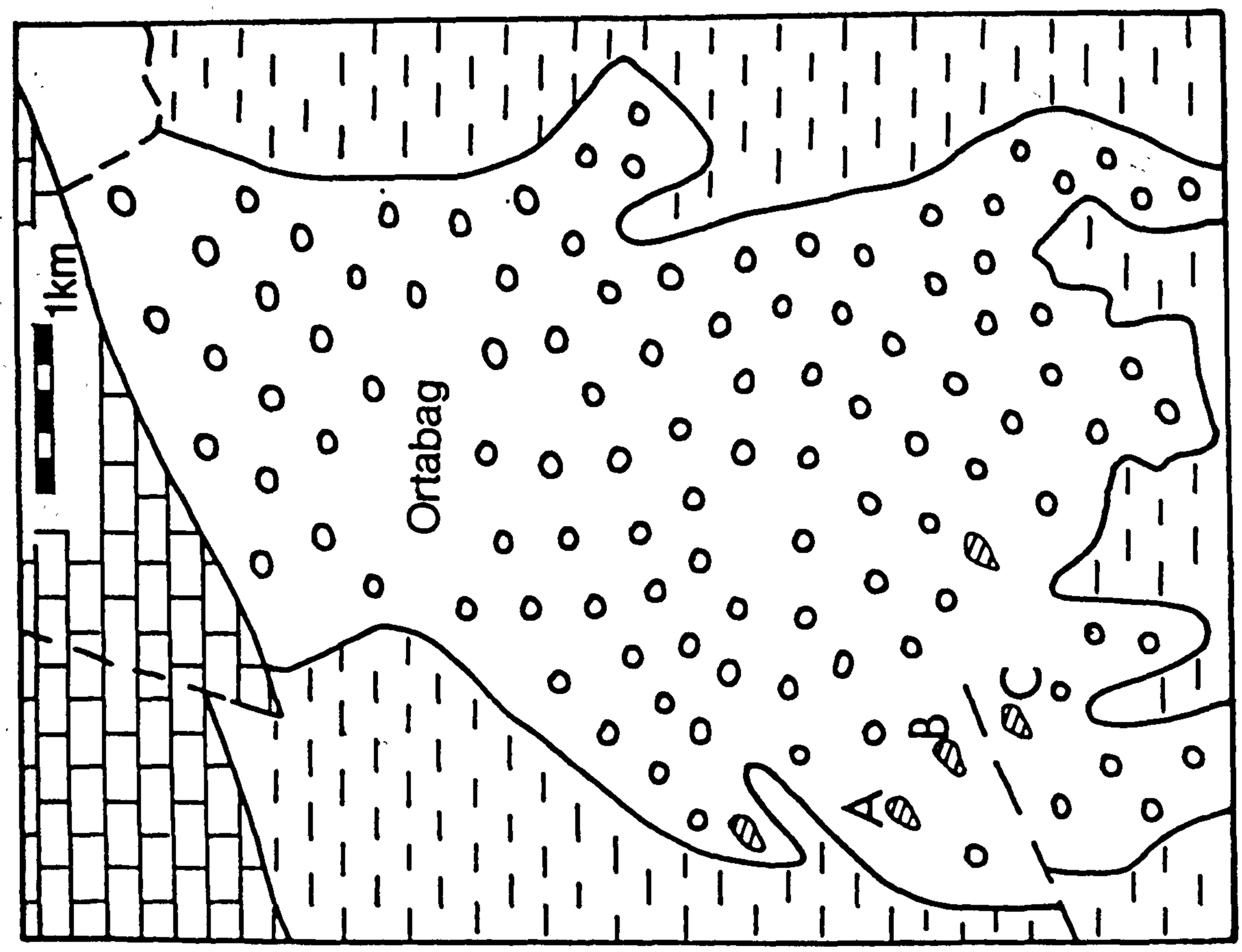

Fig. 8.2 Simplified geological sketch map showing area of Kasaba Formation and distribution of reefs.

CORAL SPECIES	APPROXIMATE ABUNDANCE IN REEFS
Montastrea spp	~30%
Tarbellastraea siciliae	~40%
Tarbellastraea spp	
Favites spp	~20%
Favites neglecta	
Favites neglecta (Michelotti)	
Porites spp.	<10%

TABLE 8.1 Coral Species and approximate abundances in the Kasaba Formation Reefs.

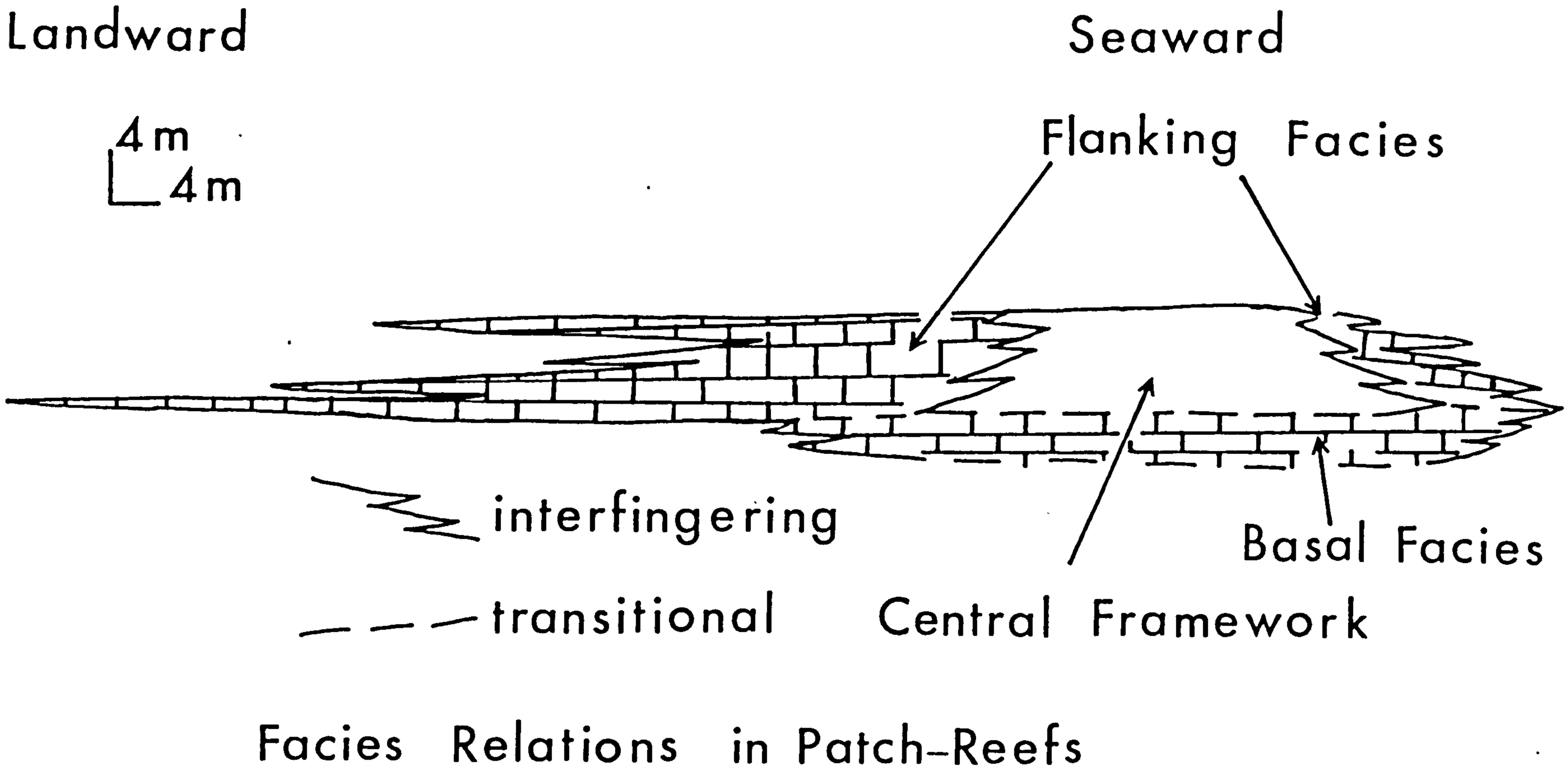

Fig. 8.3 Facies types in Kasaba Formation patch-reefs.

encrusted by algae, algal encrusted shell debris and foraminifera. The thickness of this bioclastic breccia varies between 0.50 and 1.0 m. The lowest unequivocably *in situ* corals are large (to 0.7 m across) dish tabulate forms mainly *Favites sp.* and *Montastrea sp.*, and a few scattered hemispherical forms. This zone dominated by tabulate compound forms is rarely greater than 1.0 m thick and passes laterally into poorly sorted coral calcarenite breccia (grainstone).

Central framework. The central framework of the reef is dominated by large branching reticulate colonies of *Tarballastraea sp.* The colonies have an average height of 1.5 m, maximum width of 3.0 m and commonly increase in width upwards. Individual branches are up to 1.0 m tall, 0.10 m in diameter and variably encrusted by algae (see below, 8.5.0). Tight packing of the structure in some areas is demonstrated by immature small branches wedged between larger ones. Voids between branches are often filled with terrigenous mudstone. The other main *in situ* components of the central framework are large hemispherical coral colonies. The original dimensions of these amalgamated colonies are difficult to estimate as they now grade transitionally into zones of coral breccia. Zonation in coral type and form are described below. Inter-colony areas are composed of a mixed breccia of coral fragments and algal-bound reef debris. Broken and disorientated coral fragments range from large foundered blocks of *Tarballastraea sp.* up to 2 m across, which have tumbled in locally, to small coral fragments 20-30 mm in size. Branches of *Tarballastraea sp.* form up to 70% of the inter-colony breccia; the remainder is composed of broken and disorientated coral heads, bivalves and blocks of algal-bound reef material. The latter attest to syngrowth brecciation and subsequent algal binding. The breccia is unstructured, large blocks being scattered randomly throughout.

Flanking facies. Laterally the margins of the reefs grade into talus breccias which themselves dovetail into the surrounding conglomerate and sandstone. The core facies to talus breccia transition typically occurs over a 4-5 m zone. Coral heads and colonies become progressively more disorientated away from the reef. The sides of the reef were apparently fairly steeply inclined at an angle of approximately 30-40°. Within the coarser, more proximal parts of the talus breccia, solitary corals and colonies are rarely

found in growth positions. Away from the core, over a distance of about 50 m, the breccias become thinner and finer grained, passing gradually into a very coarse calcarenite with weakly developed fining-upward grading and parallel laminations. Furthest from the reef (up to 70 m from the reef core), these calcarenites become progressively thinner and interfinger with a mixed terrigenous-bioclastic calcareous sandstone (Fig. 8.5). The percentage of coral debris within the flanking beds decreases away from the reef and is progressively replaced by more abundant algal and foraminiferal components. Analysis of geopetal sediment fills within orientated fragments suggest a depositional dip of between 10° and 15° for the flanking beds against the core areas, this decreases outwards over a distance of 10-20 m, to angles less than 4°.

The flanking beds are well developed only on the landward (back reef) margin of the reef (as determined from associated terrigenous clastic sedimentary facies and palaeocurrent analysis, 4.8). On the seaward (forereef margin) very coarse coral dominated breccias pass abruptly into terrigenous clastic material over distances of less than 15 m. The unsorted, coarse grained nature of the flanking beds and separation, in distal areas, into discrete depositional events suggest rapid transportation and deposition probably by periodic storms. The marked difference in flanking facies between seaward and leeward sides of the reef is probably the result of the prevailing environment. Wave and storm activity transported reef material into the lee of the reef where it remained relatively undisturbed. Similar asymmetrical development of reef-derived deposits have been described from the ancient by Lowenstam (1957) and, more recently, from studies of modern Australian reefs (Maiklem, 1968) and from the Bahamas (James, 1972). Deposition of the much coarser grained debris on the seaward margin of the reef was probably by the steady accumulation of fallen blocks. The asymmetric flank facies development of the Kasaba Formation reefs therefore suggests a dominantly northerly (onshore) wind.

In some areas reefs are overlain by a thin veneer of calcarenite composed of foraminiferal, algal and shell fragments and rare coral debris. Elsewhere, this calcarenite is absent and the reefs are overlain by very coarse terrigenous pebbly sandstone. The basal 0.5 m of the sandstone contains abundant reef derived material suggesting some minor reworking of the reef top. Above this the sandstone is devoid of reefal material.

Fig. 8.4

Field photographs of patch-reefs.

(a) Small patch-reef (r) overlying terrigenous conglomerate.(c). Note fore-reef breccia of mainly disorientated coral heads (b). Hammer is 34 cm long. GR. 505332.

(b) Central framework of reef, branching colony of *Tarballastraea sp* (t) overlain by more massive colonies of *Montastrea sp* (m). GR. 501331.

(c) Large colony of *Tarballastraea sp* (t) forming central framework to reef, overlain by *Montastrea sp* (m). Note presence of abundant mudstone in inter-colony areas. GR. 501331.

(d) Colony of *Montastrea sp* (m) intimately intergrown with *Tarballastraea sp* (t) upper part of central reef framework. GR. 501331.

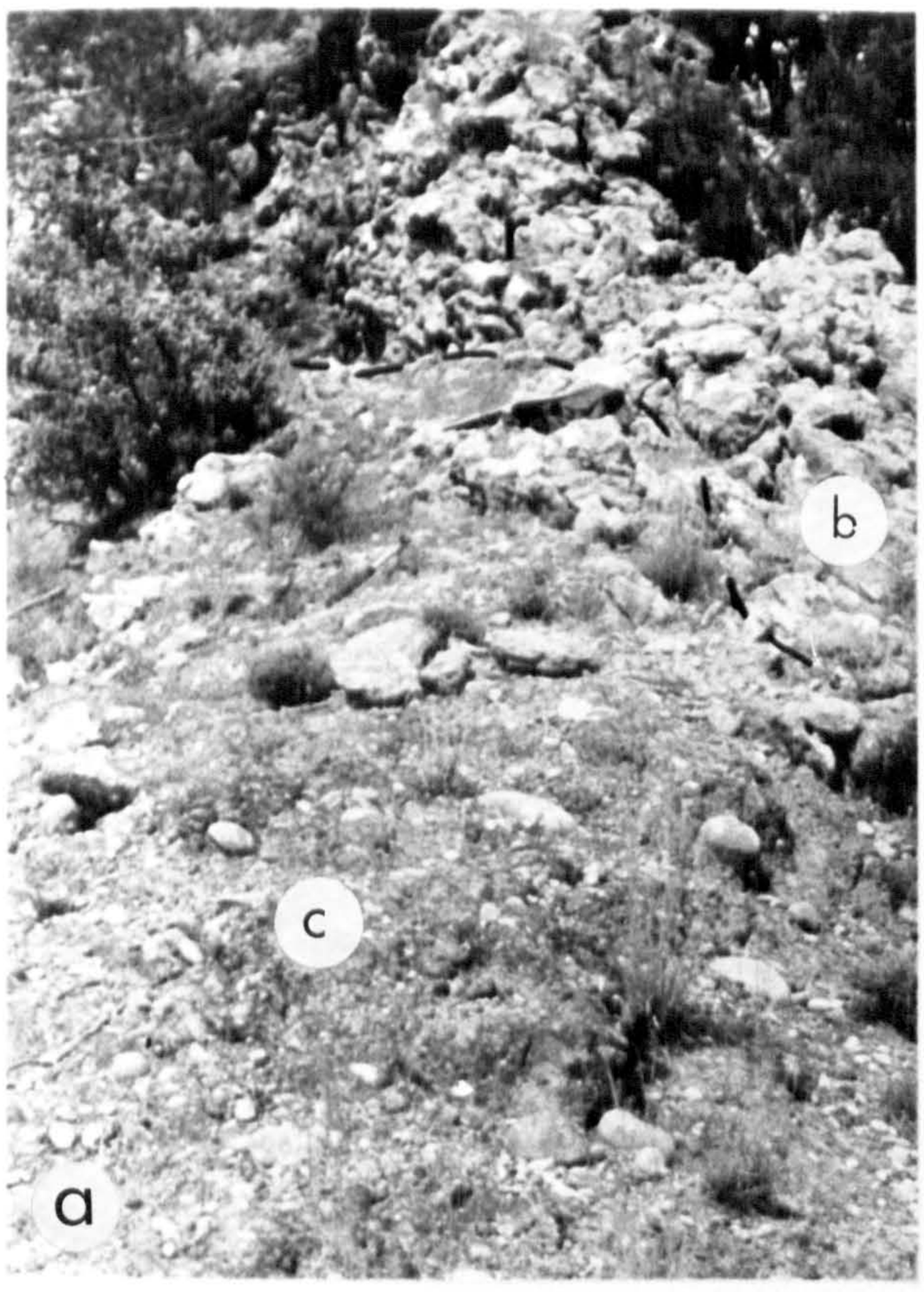
b
c
a

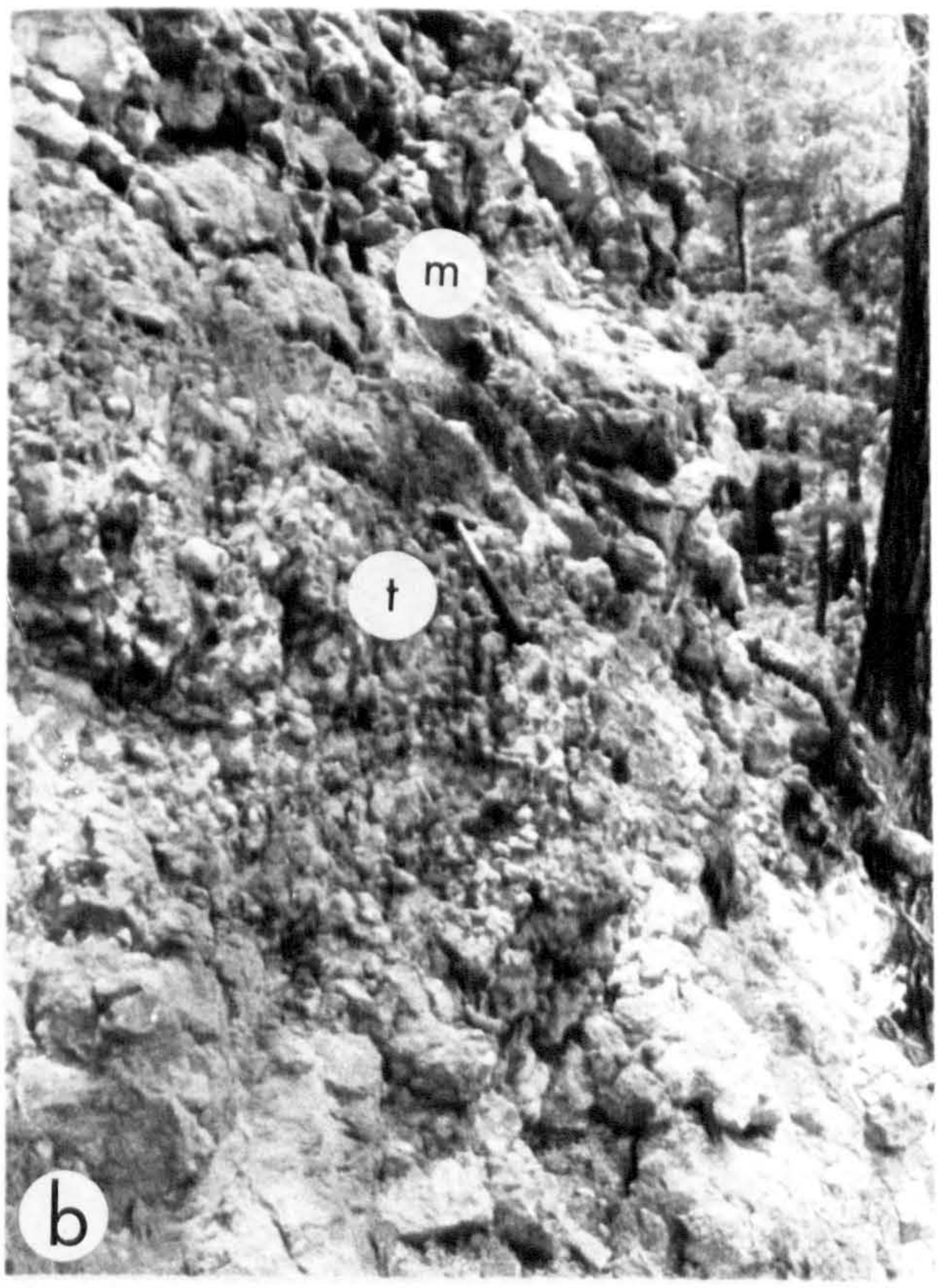
m
t
b

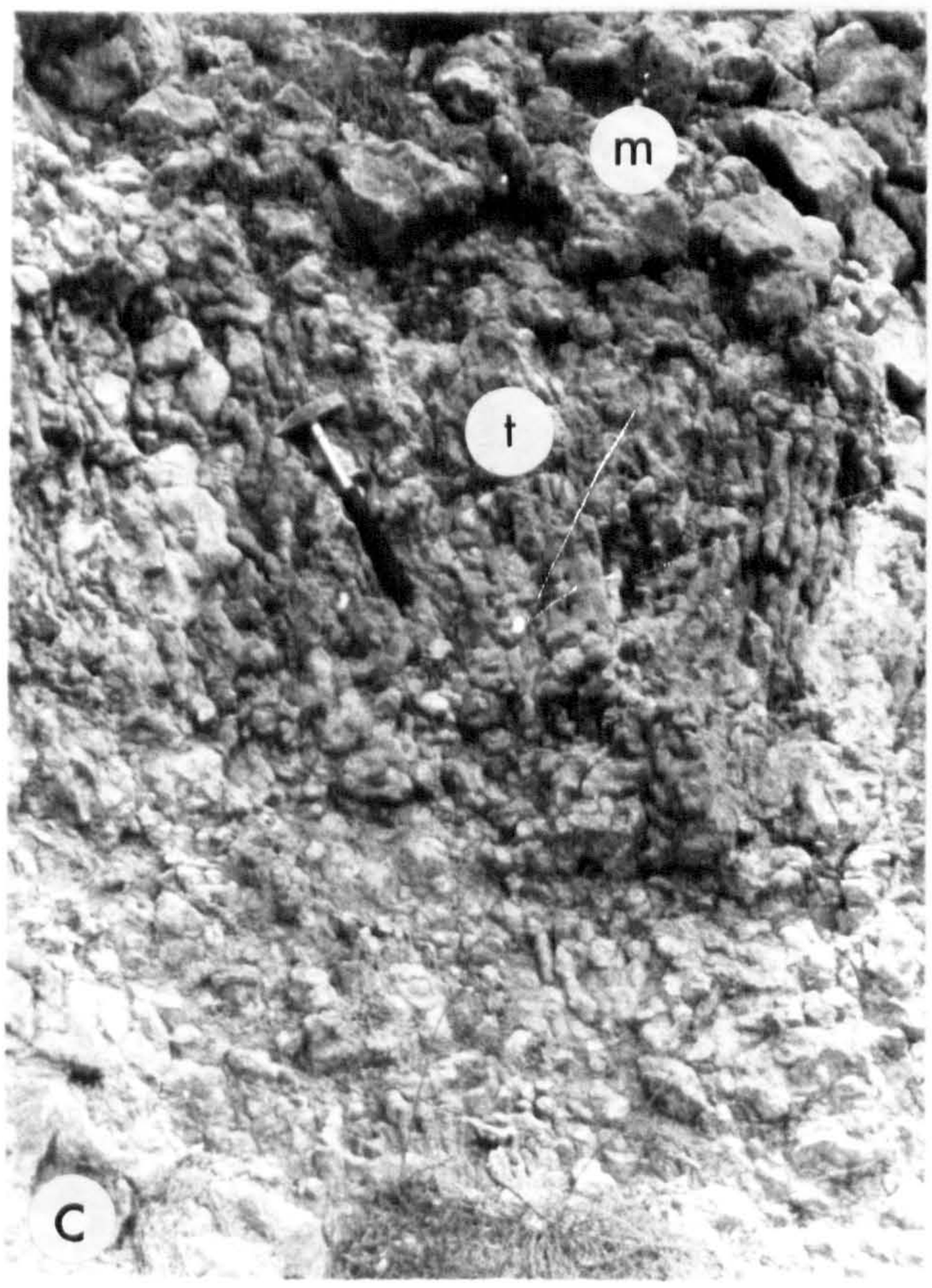
m
t
c

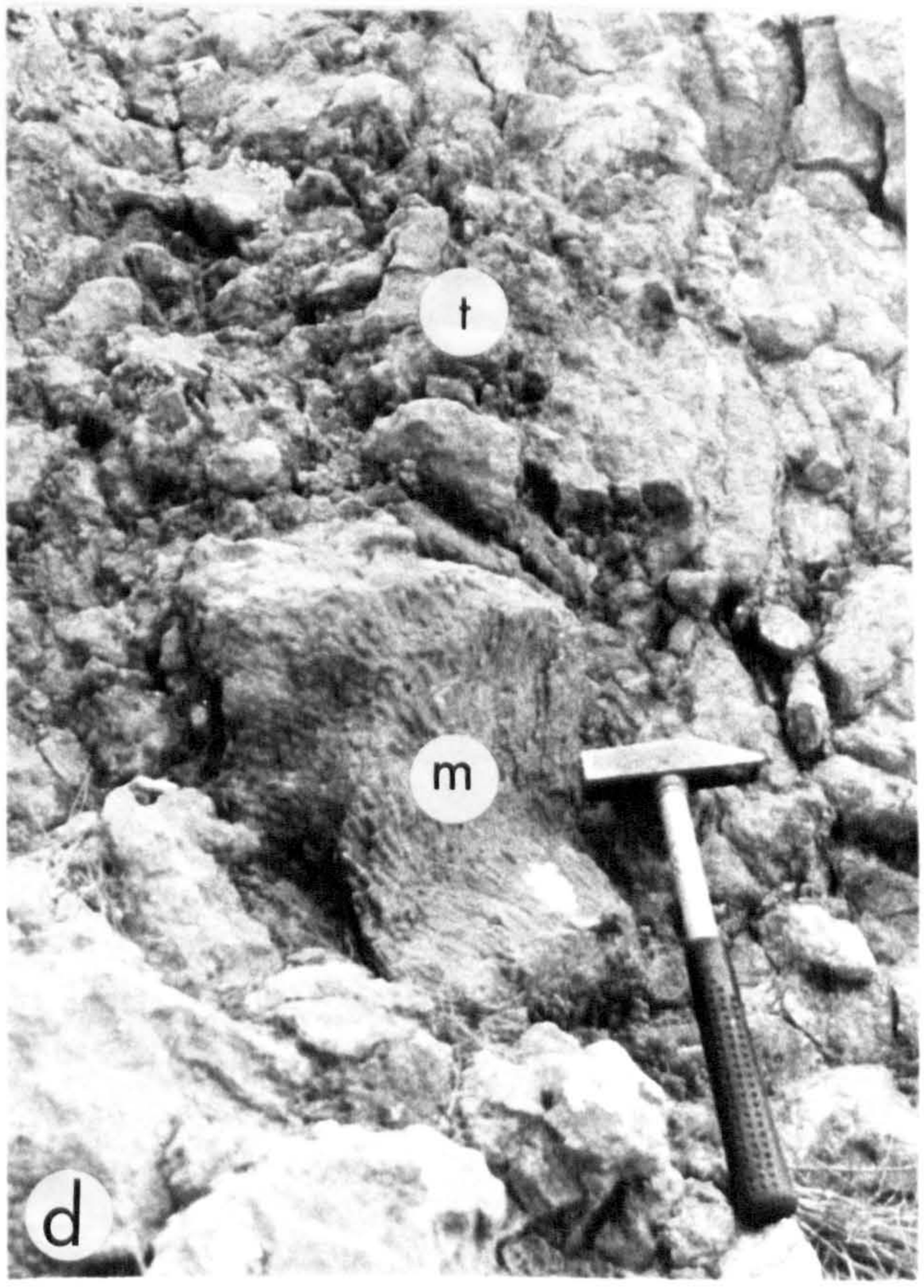
t
m
d

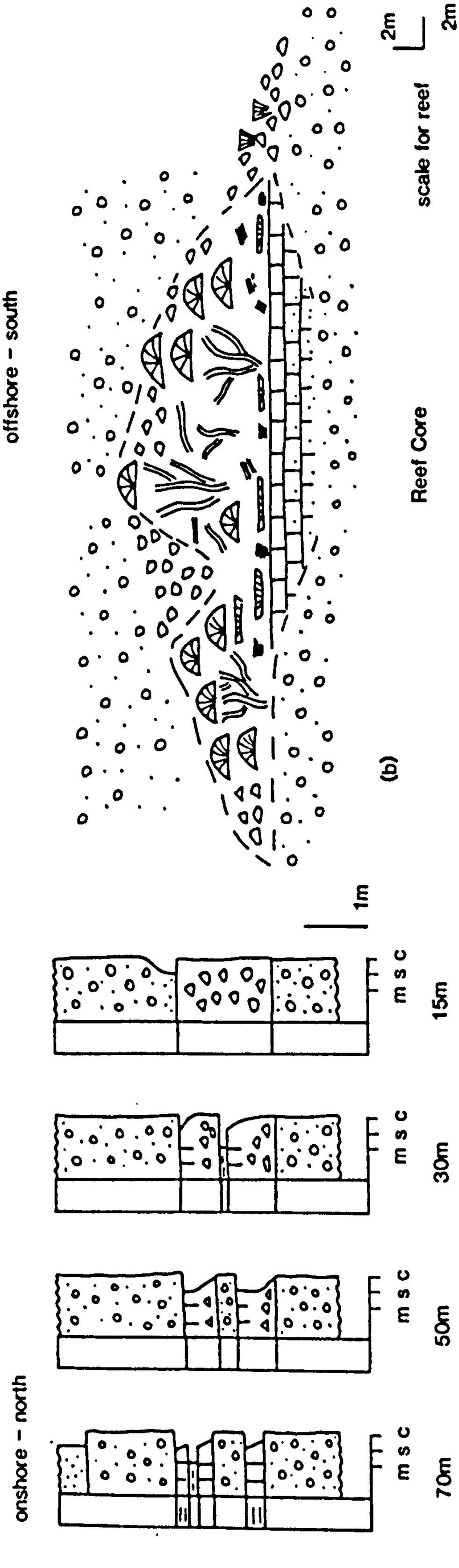

Fig. 8.5 Lateral variation in flanking facies away from reef core.
Bioclastic breccias pass progressively into coarse calcarenites that are normally graded.
Key as in Fig. 8.6.

8.4.0 Zonation in the Central Core

8.4.1 Introduction

Several studies of ancient reefs have noted and remarked on vertical zonation within the reef framework (Alberstadt *et al.*, 1974; Walker and Alberstadt, 1975; Frost, 1977). There is, however, very little known about the vertical zonation within modern reefs, although many studies have documented lateral zonations both lithologic and biologic, across the fore-reef, reef and back reef areas (Goreau, 1959; Logan *et al.*, 1969; Morton, 1974; Geister, 1977; Jaubert, 1977). From the studies of modern and ancient reefs various types of zonation are recognised.

8.4.2 Vertical Biotic Zonation

The study of Logan *et al.* (1969) of the Alacran Reefs off the coast of Yucatan is the most complete description of vertical zonation in modern reefs. However, the applicability of this zonation to ancient reefs is uncertain as the study described only the external zonation of the sides of the reef and not their internal zonation. From top to bottom, down the sides of the reef, the zonation is:

(1) *Acropora palmata* community

(2) *Diploria-Montastrea-Porites* community

(3) *Agarcia-Montastrea* community

(4) *Gypsina-Lithothamnium* community

(5) *Lithophyllum-Lithoporella* community

The *Gypsina-Lithothamnium* community (encrusting forams and algae, bryozoans, sponge and mollusc association) and the *Lithophyllum-Lithoporella* community (algal nodules, encrusting bryozoans, forams, molluscs and scattered corals) are believed to represent *pioneer communities* that formed on slight elevations of cemented limestone. Similar sequences have been described from Ordovician reefs (Alberstadt *et al.*, 1974), reefs of Oligocene age (Frost, 1977) and from patch reefs of Miocene age (Purdy, pers. comm. 1980). Alberstadt *et al.* (1974) suggest that one of the main functions of the pioneer community is the stabilization of the substrate.

The overlying reef can frequently be subdivided into a further three stages (James, 1979):

(i) *Colonization stage* : This is characterised by few species, generally branching lamellar forms. This stage reflects the initial colonization by reef-building metazoans.

(ii) *Diversification stage* : This stage provides the bulk of the reef mass. The number of reef building taxa reaches its greatest number and a large variety of growth forms are encountered.
(iii)*Domination stage* : This generally comprises a thin unit that overlies abruptly the bulk of the reef mass. It is characterised by a few taxa, generally lamellar encrusting forms, with evidence of surf effects.

Although well documented, the reasons for ecological successions similar to this in many reefs are poorly understood. Two theories are currently proposed:
(i) The sequence is extrinsic, reflecting a progressive replacement of deep water communities by shallow ones as the reef grows to sea level (e.g. Logan *et al.*, 1969).
(ii) The sequence is intrinsic, reflecting a natural succession as the organisms alter the substrate and change the energy flow and environment (e.g. Walker and Alberstadt, 1975; Frost, 1977).

8.4.3 Zonation in Coral Morphology

Vertical zonation in coral morphology has been described from a number of modern and ancient reefs (Garrett *et al.*, 1971; Mesolella *et al.*, 1970; Chappel, 1980).

In two Bermudian patch-reefs described by Garrett *et al.* (1971) corals (mainly *Montastrea* and *Diploria*) are the principal framework builders, forming between 40% and 80% of the central reef mass. The coral species show a limited degree of zonation, apparently controlled by water depth. Reef tops within 1-2 m of the surface consist of massive *Montastrea, Diploria* and *Porites*, whereas those within 4-5 m of the surface are covered by branching corals of *Oculina, Madracis* and *Millepora.*

The assemblage of massive *Montastrea-Porites-Diploria* is a high energy assemblage and the branched *Oculina-Madracis-Millepora* is a low energy assemblage. Coral species show little or no variation laterally, this is thought to be due to the absence of high energy conditions generated by waves moving across the top of the reef.

Pleistocene reefs of Barbados also show a zonation in coral type and form (Mesolella *et al.*, 1970). An early deep water stage composed primarily of *Montastrea annularis* followed by a shallow water stage of *Acropora palmata* and *Acropora cervicornis*.

8.4.4 Observed Zonation in Kasaba Formation Reefs

The Kasaba Formation reefs formed on a firm, although unlithified, substrate (cobble and pebble gravel) (Fig. 8.4). As a result they show no pioneer community that is significantly different from the overlying central framework of the reef. The only difference observed is an increase in the proportion of corals above the basal unit. The types and proportions of encrusting organisms and molluscs remain relatively constant throughout the reef core. In this respect these reefs are similar to those described from Barbados (Mesolella *et al.*, 1970), which developed on lithified Tertiary limestone and show no distinct pioneer community.

8.4.5 Coral Morphology

The reefs exhibit a distinct change in coral morphology from the base upwards (Fig. 8.6). The general overall zonation is from flat, tabulate dish forms (*Favites sp.*, some species of *Montastrea sp.*), through branching reticulate forms (*Tarballastraea sp.*) to massive domical forms (mainly *Montastrea*). In some reefs this zonation is particularly apparent. Elsewhere it is not so well developed and a complex relationship exists in the upper parts of the reef, branching and domical forms being intimately intergrown (Fig. 8.4).

No lateral variation in coral morphology is observed. This zonation is very similar to that described by Garrett *et al.* (1971) from Bermudan patch-reefs (see above). Recent work by Chappel (1980) has demonstrated that coral morphology will change in different ways in response to different environmental stresses. From the results of Chappel it is unclear which, if any, is the dominant environmental factor, and it is probable that all environmental stresses contribute to the form a coral will adopt.

Reefs developed in a similar environmental setting in southern Spain show a similar variation in coral morphology (Santibestan and Taberner, 1980). In this instance dish shaped corals pass into globate forms and then into *Tarballastraea* colonies in the upper part.

In conclusion, the *vertical zonation in coral forms* within the Kasaba Formation reefs is most consistent with the change due to *increasing hydrodynamic stress*. The *absence of a pioneer community reflects development on an already firm substrate*. Having become

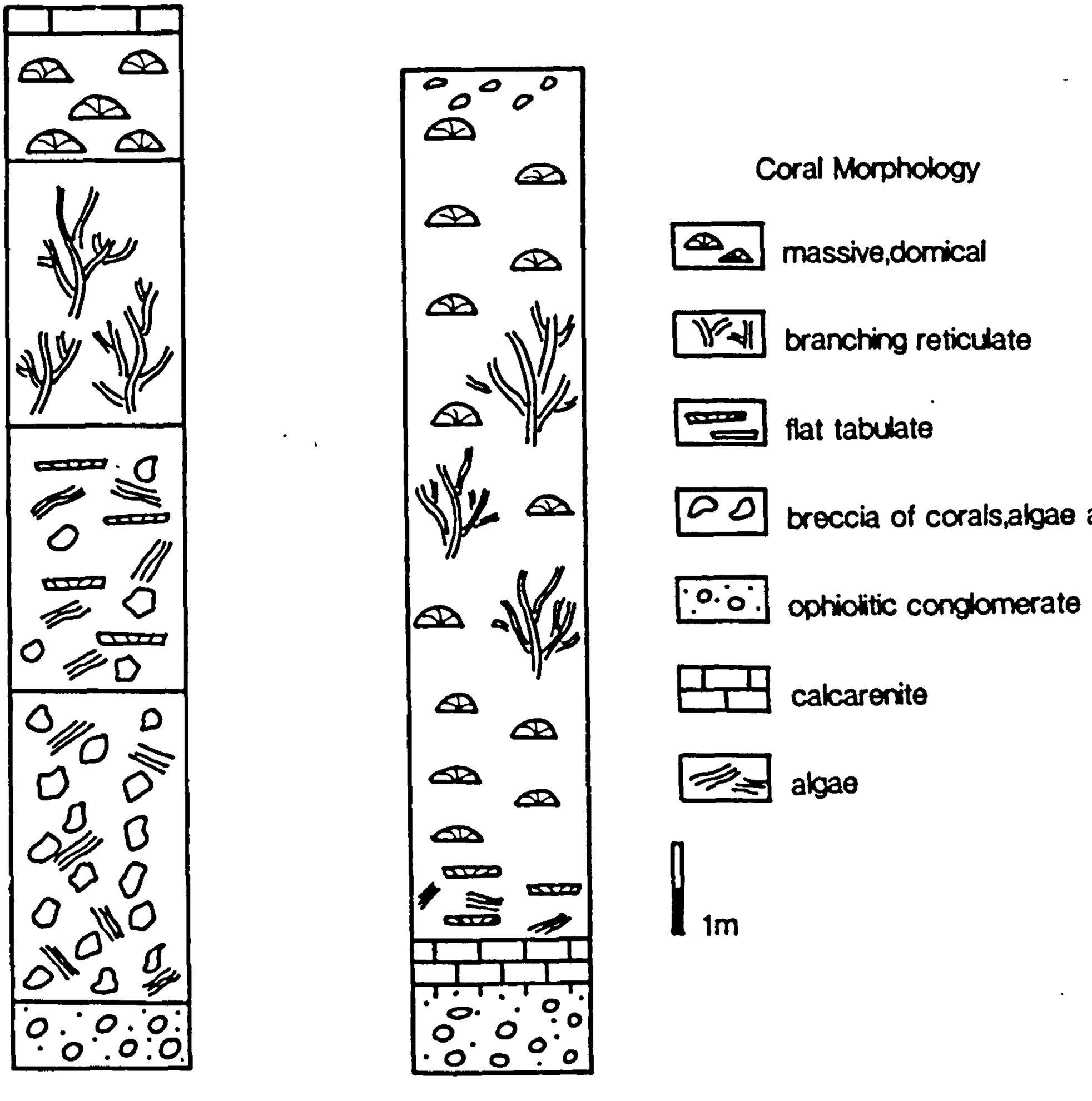

Fig. 8.6
Progressive change in coral morphology upwards through central reef framework (see text for details).

established, the gradual upward growth of the coral colonies resulted in increasingly shallow water and a corresponding increase in wave energy (hydrodynamic stress).

8.5 Internal Reef Structure and Alteration

A variety of processes complexly interact in the formation and preservation of a reef (Schroeder and Zankl, 1974; Scoffin and Garrett, 1974). The initial stage of primary framework building by corals is subject to later processes that are both constructional; the addition of a secondary framework by encrusting organisms, sedimentation and cementation, and destructional; boring rasping and grazing.

The manner and sequence in which these various processes interact is highly complex, it is related to the environment of growth of a particular part of the reef during an interval of time.

8.6.0 Calcareous Encrusting Organisms

8.6.1 Introduction

Calcareous encrusting organisms are defined as any organism, whether colonial or an individual, having a continuous (i.e. non spicular) calcareous skeleton which is permanently attached by a carbonate or an organic cement to the primary framework of a reef. Encrusters, so defined, can range from laminar to mound-like in form (Martindale, 1976).

The sequence of colonisation by encrusters on living reefs is dependant upon the environmental location of the substrate. Physical factors affecting this environment are, depth, amount of light, hydrodynamic exposure and abundance of sediment (Martindale, 1976).

8.6.2 Distribution in Recent Reefs

The detailed study of encrusting organisms and their distribution on recent reefs (e.g. Garrett *et al.*, 1971; Schroeder and Zankl, 1974; Scoffin and Garrett, 1974; Martindale, 1976) has shown that their development is strictly environmentally controlled.

Encrusting organisms and their environments of formation can be broadly subdivided into three associations:

(i) *Photophyllic* (light loving) association

This association consists solely of coralline algae and includes at the present day *Porolithon*, *Neogoniolithon* and *Lithophyllum*. In

present day reefs this association is restricted to shallow (0-8 m) well-lit areas.

(ii) *Photophyllic/sciaphyllic* association

In present day reefs this includes the coralline algae *Lithophyllum* and *Mesophyllum*, and encrusting foraminiferans such as *Homotrema rubrum*, *Planorbulina* and *Gypsina plana*, found in shaded environments at shallow and middle depths (to 20 m).

(iii)*Sciaphyllic* (shade loving) association

In present day reefs this includes coralline algae *(Mesophyllum, Lithothamnium, Archeolithothamnium)* and foraminiferans (*Homotrema rubrum, Gypsina plana*) along with numerous bryozoan and serpulid worms. This association is found only on the sediment free undersides of shaded and dim cavities and overhangs at shallow depths.

A transition therefore exists from photophyllic algae characteristic of shallow well-lit environments to sciaphyllic encrusters (e.g. forams, bryozoans, serpulids and some algae) typical of shaded areas (Martindale, 1976).

8.6.3 Encrusting Organisms within the Kasaba Formation Reefs

Within the Kasaba Formation reefs encrusting organisms form an important element of the framework. Prior to encrustation many coral substrates show evidence of having been extensively bored (8.7).

Several types of encrusting sequence are recognised and from comparison with the studies of modern reefs (outlined above), they can be directly related to their environment of formation.

8.6.4 Mixed Crusts

Description. Coral blocks taken from the base of colonies and inter-colony debris areas often show a thick (up to 8 mm) complex, crustal development.

An initial photophyllic crust of *Lithophyllum* is overgrown by successive encrustations of interlaminated *Mesophyllum* (and subordinate *Lithophyllum*) and encrusting foraminifera (*Gypsina plana, Planorbulina, Homotrema rubrum*) (Figs. 8.7, 8.8, 8.9). Away from the coral substrate *Mesophyllum* becomes progressively thinner and more contorted, supporting a number of encrusting foraminiferans (Fig. 8.7). The upper part of the encrusting sequence consists solely of foraminiferans which are overlain and interlaminated with reef sediment (biomicrite) (Fig. 8.7).

Interpretation

In recent reef environments (Schroeder and Zankl, 1974; Martindale, 1976) crusts of mixed composition record the progressive change from a photophyllic environment through photophyllic/ sciaphyllic to sciaphyllic environment.

Following initial encrustation by *Lithophyllum* in a photophyllic environment, upward and outward growth of the coral colony results in the lower (dead) areas of the colony becoming shaded. Cavities develop beneath the living reef surface by overgrowth, and within these cryptic environments, wave surge and currents prevent reef-derived sediment from being deposited. Such circulation aids the growth of intermediate crust types resulting in interlaminated *Mesophyllum* (and other photophyllic/sciaphyllic coralline algae) and foraminiferans.

Continued upward growth of the colony or an increase in reef debris overlying the cavity further decreases light intensity and the crusts become progressively more sciaphyllic. Ultimately there is insufficient light for the growth of crustose coralline algae and their position is taken by encrusting foraminiferan such as *Gypsina plana* and *Planorbulina*. The encrusting sequences are terminated by biomicrite reef sediment. A drop in the velocity of circulating water results in the cavities finally becoming choked with sediment and restricts growth. The similarity between sequences described from the Recent and those in the Kasaba Formation reefs indicates a very similar origin.

8.6.5 Constant Composition Crusts (a)

Description. Corals taken from presumed life position high within the reef core show a crust of variable thickness (0.40-2.5 mm) of the coralline algae *Lithophyllum sp.* Differential growth paths and rates of growth result in individual crusts frequently showing onlap and offlap relationships with adjacent crusts. Voids created by varying growth rates and borings are filled with reef sediment which occasionally forms discontinuous lenses, or by blocky microspar calcite cement. On the underside of coral colonies, crusts of *Lithophyllum* are absent or form discontinuous, very thin (40 μm) crusts. In some instances large *in situ* coral colonies do not have algal crusts on their upper surface.

Fig. 8.7

Photomicrographs of thin sections (a and c) and acetate peels (b and d) of encrusting sequences in the Kasaba Formation reefs.

(a) Crust of *Mesophyllum* (M) growing downwards into an intraskeletal void in a coral framework. This is overlain by a thin crust of *Planorbulina sp* (P). The void has been subsequently infilled by reef sediment (biomicrite)(b). In the remaining space a late stage equant blocky sparite cement (c) has developed.
Scale bar 2 mm. Plane polarised light. Spec. UM1.
GR. 501331.

(b) Crust of mixed composition:
Montastrea (M) encrusted by a thin crust of *Lithophyllum* (L), subsequent crusts consist of highly contorted, interlaminated *Mesophyllum* (Me) and an encrusting foraminifera *Planorbulina* (P). Crust growth has been terminated by reef sediment (biomicrite). Note extensive borings (b) in lower parts of crust. Scale bar 2 mm. Plane polarised light. Spec. U5.
GR. 501331.

(c) Mixed crust of interlaminated *Mesophyllum* (M), *Gypsina plana* (G) and *Planorbulina* (P). Much of the lower parts of the crust have been destroyed by borers and subsequently infilled with reef sediment (biomicrite). Scale bar 2 mm. Plane polarised light. Spec. UM6. GR. 501331.

(d) Crust of mixed composition. Coral substrate (c) is overlain by interlaminated *Lithophyllum* (L) and reef sediment (r). Successive crusts consist of interlaminated *Mesophyllum* (M) and *Homotrema rubrum (?)* (H). Crust growth was terminated by reef sediment. Scale bar is 2 mm. Plane polarised light. Spec. U.8.
GR. 501331.

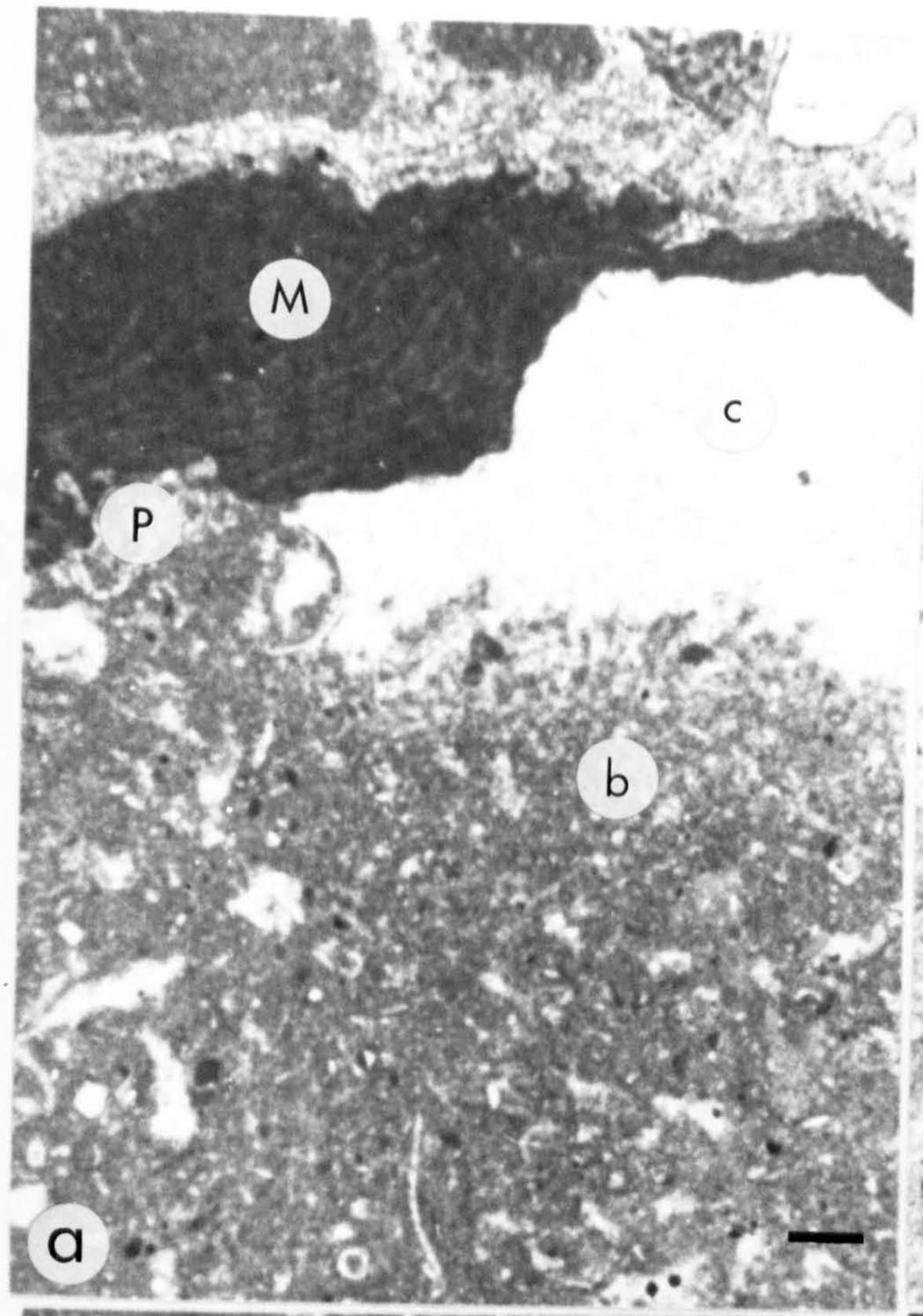
M
P
C
b
a

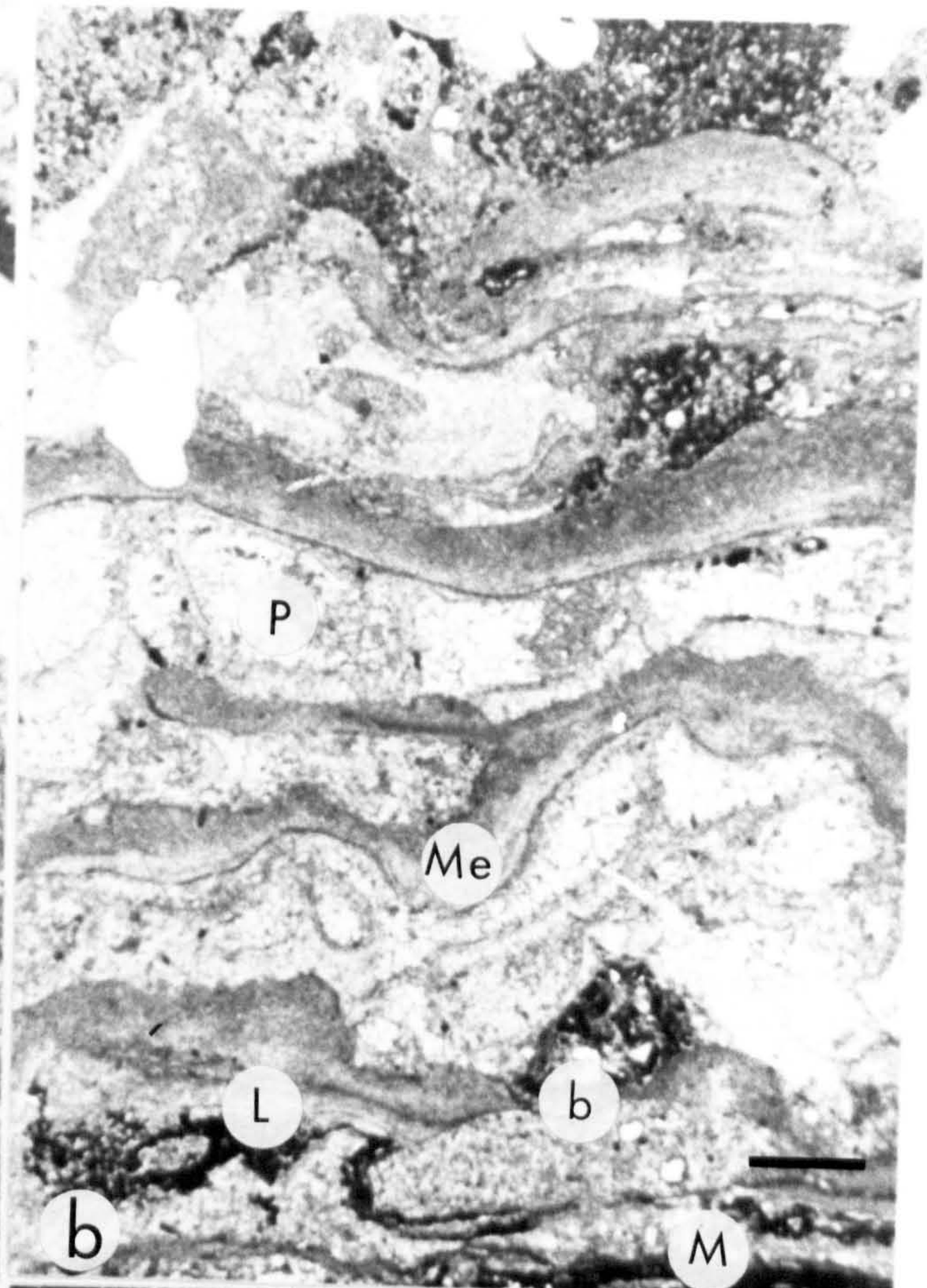
P
Me
L
b
b
M

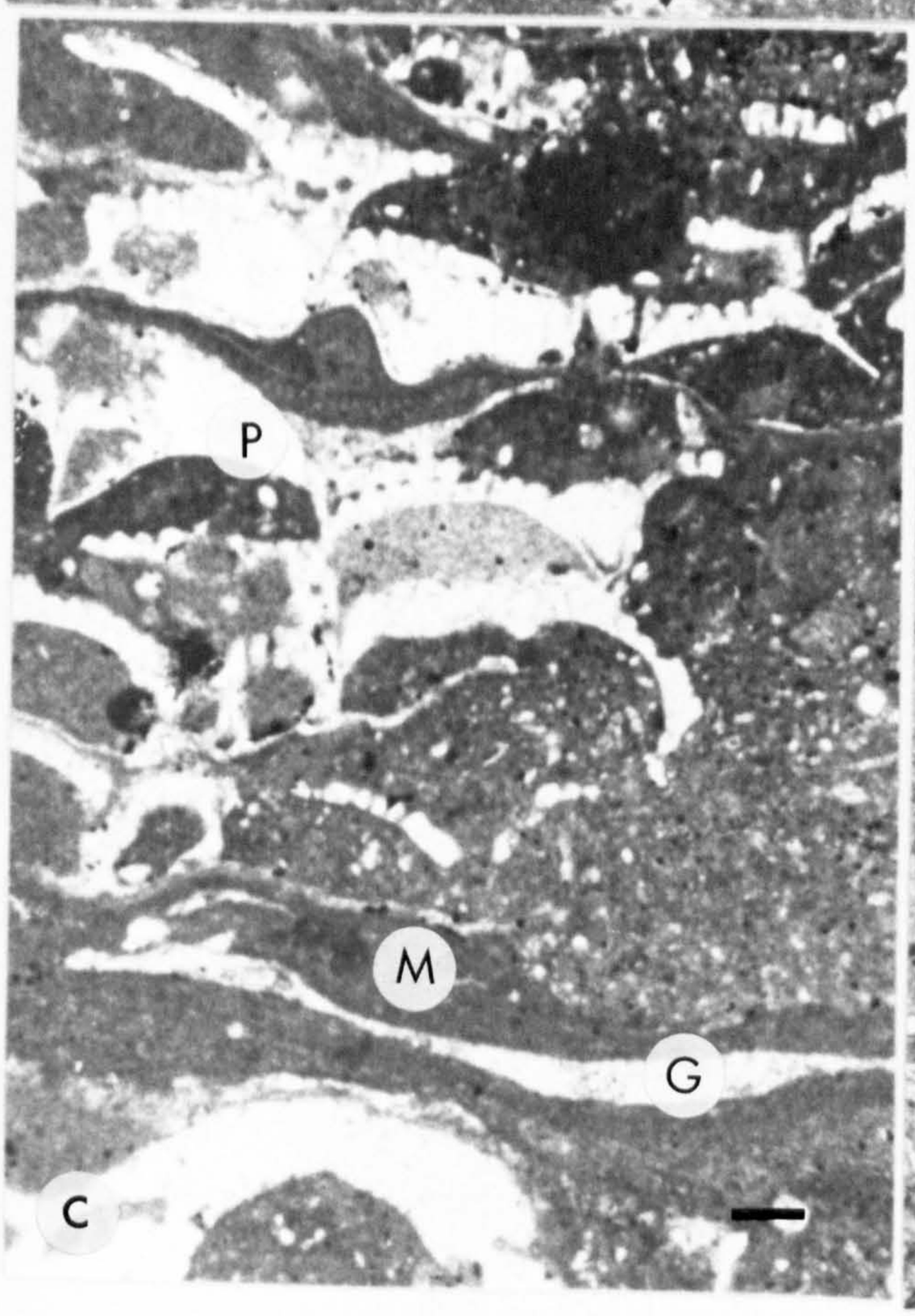
P
M
G
C

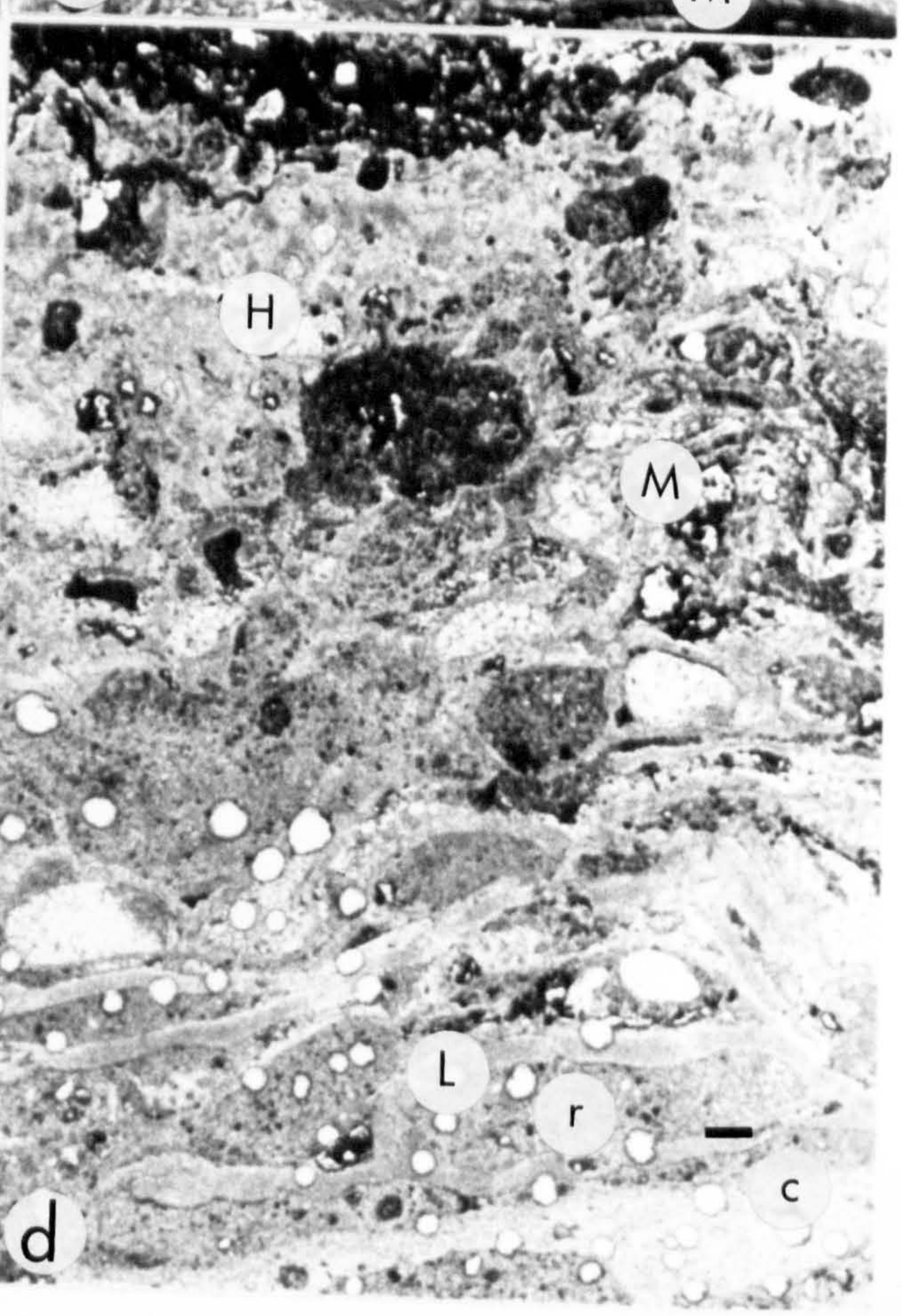
H
M
L
r
c
d

K E Y T O F I G U R E S 8.8 a n d 8.9

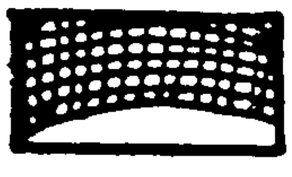
Mesophyllum


Lithophyllum


Lithothamnium

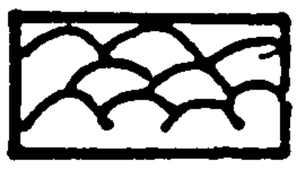
Gypsina plana

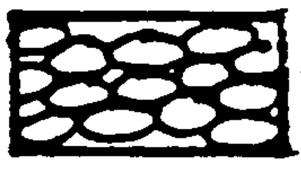
Planorbulina sp


Homotrema rubrum

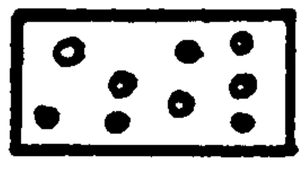
reef derived biomicrite


coral substrate


infilled borings within encrusting sequences


borings in coral substrate


internal cement

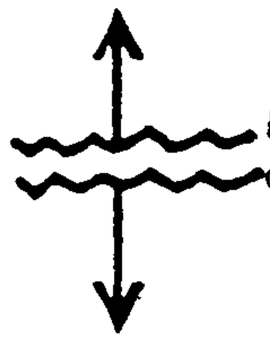
growth direction

Fig. 8.8

Diagrammatic cross sections of crusts of mixed composition.

(a) An initial thin photophyllic crust of *Lithophyllum* is overlain by interlaminated *Mesophyllum* and *Gypsina plana*. Crust growth was terminated by biomicrite reef sediment. Spec. 409/80. GR. 504333.

(b) An initial thin photophyllic crust is overlain by reef sediment and then by the encrusting foraminifera *Gypsina plana* and *Planorbulina*, with thin laterally discontinuous crusts of *Mesophyllum*. Spec. U18. GR. 504333.

(c) A thick photophyllic crust of *Lithophyllum* and *Lithothamnium* is overlain by interlaminated *Mesophyllum*, and the encrusting foraminiferans *Gypsina plana*, *Planorbulina* and *Homotrema rubrum*. Spec. 407/80. GR. 504333.

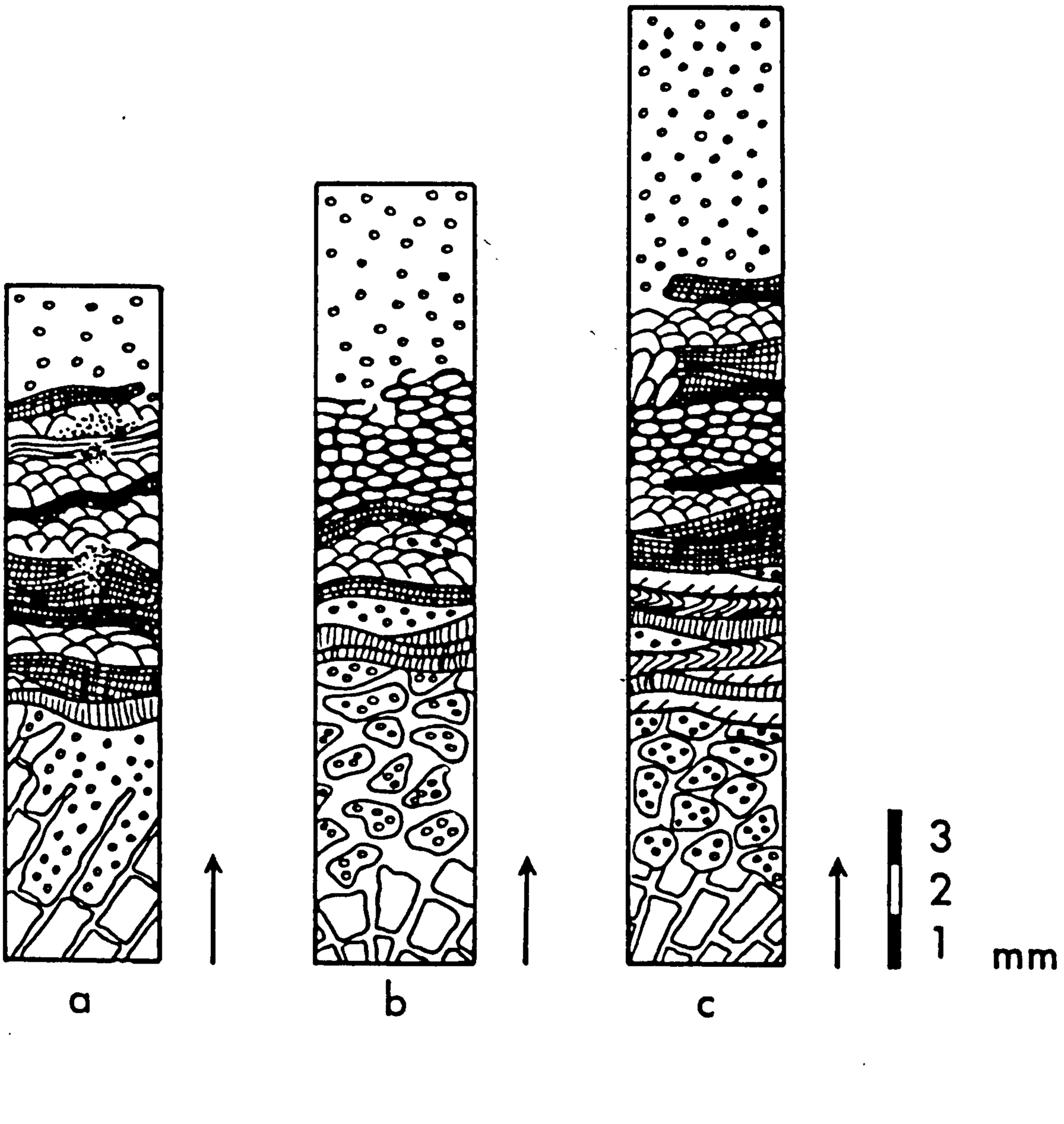

Fig. 8.8 Crusts of mixed composition

Fig. 8.9

Diagrammatic cross sections of constant composition crusts.

(a) An initial thick crust of *Mesophyllum* is overlain by interlaminated *Mesophyllum* and *Gypsina plana* and then by interlaminated *Mesophyllum* and reef sediment. Crust on *Favites neglecta* (Michelotti) from inter-colony debris area. Spec. U.10. GR. 504333.

(b) Constant composition crusts of interlaminated *Mesophyllum*, *Gypsina plana* and biomicrite reef sediment on both the top and underside of the disorientated *Montastrea* coral head from an inter-colony debris area.
Spec. UM19. GR. 504333.

(c) Thick photophyllic crust of *Lithophyllum* and *Lithothamnium* of top surface of *in situ Tarballastraea* branch. Lower surface comprises interlaminated *Mesophyllum*, *Gypsina plana* and *Homotrema rubrum*.
Spec. U4. GR. 501331.

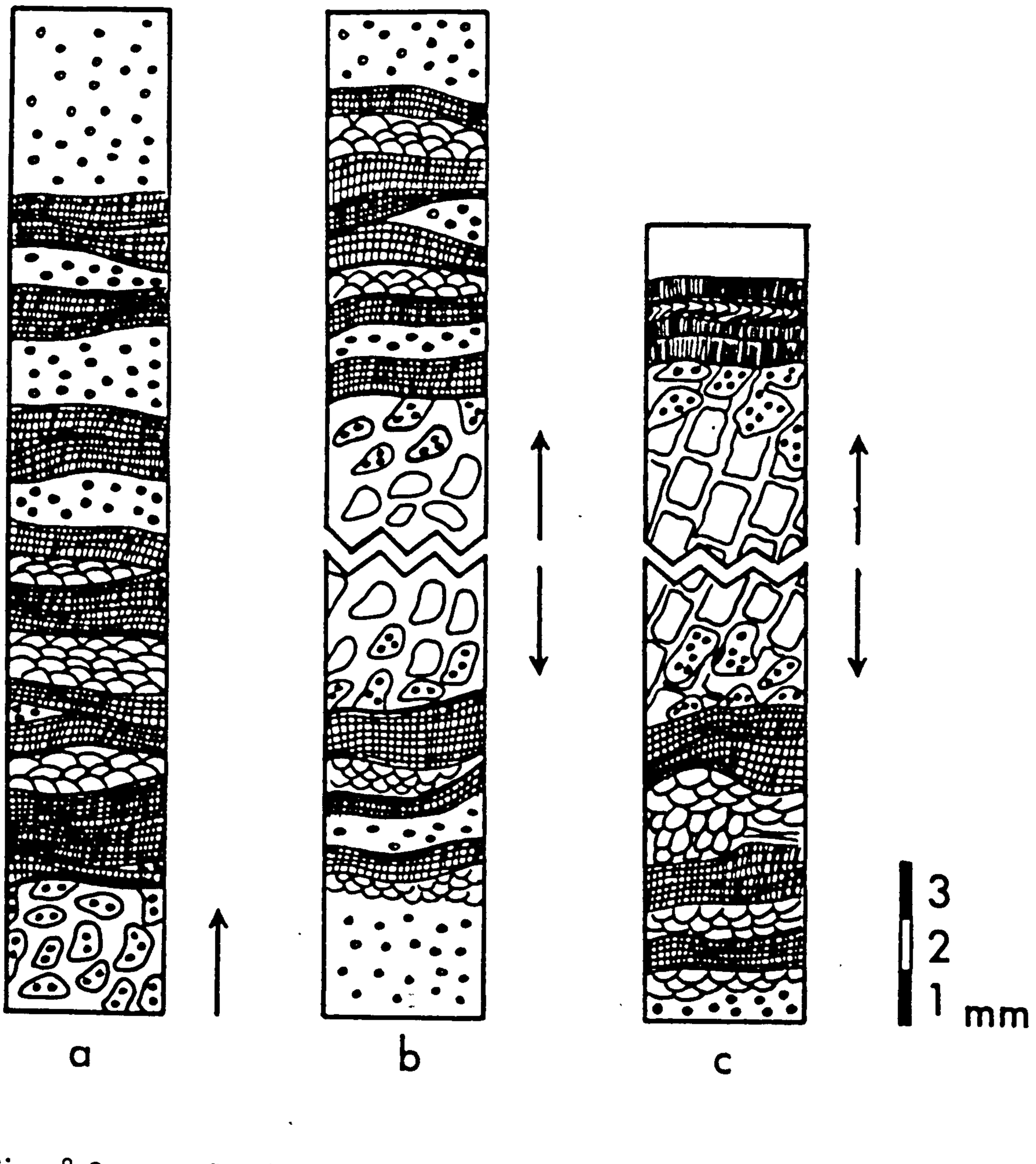

Fig. 8.9 Crusts of constant composition.

Interpretation

By comparison with Recent reefs, thick photophyllic crusts of *Lithophyllum* formed in a shallow well-lit environment. This is consistent with their position at the top of the reef. The thickness of the crust is related to the time spent in that environment and to the degree of illumination and hydrodynamic exposure to which the coral is subjected (Martindale, 1976). Algal crust growth was halted by an influx of terrigenous sediment terminating reef growth. Algal crusts are not present on some large corals suggesting that they were buried by terrigenous sediment prior to the establishment of any encrusting organisms. The absence of photophyllic crusts on the underside of corals is consistent with their shaded position in the colony during growth.

8.6.6 Constant Composition Crusts (b)

Description. Some *in situ* corals towards the base of the reef are encrusted by thick photophyllic crusts on their upper surface. The crusts, up to 6 mm thick, generally consist of one or two species of interlaminated coralline algae (e.g. *Mesophyllum*, *Lithophyllum*) and rarely encrusting foraminiferans (*Gypsina sp.*, *Planorbulina*). These crusts are always overlain by reef sediment.

Interpretation

Thick constant composition algal crusts, from lower areas of the reef core, indicate that upon death the coral remained in essentially the same environment and encrusting organisms were exposed to similar conditions through time. In present day reefs the destructive activity of boring organisms and rise in level of surrounding sediment results in burial of the coral (Martindale, 1976). A similar interpretation is favoured for the Kasaba Formation reefs.

8.6.7 Summary of Encrusting Sequences

A summary of the three basic types of encrusting sequences is shown in Figs. 8.8 and 8.9. Although no regular zonation occurs, several associations are present:

(1) Crusts of *mixed composition* occur dominantly in *inter-colony debris areas*.

(2) *In situ* corals towards the *base of the reef* are frequently encrusted by *thick photophyllic crusts* on their upper surface.

(3) *In situ* corals towards the *top of the reef* core are not encrusted, or only by a very *thin photophyllic* crust.

8.7 Bio-erosion

Borings are found both in the primary (coral) framework and within the overlying encrusting sequences. Borings within coral skeletons consist dominantly of two types: (i) rounded to oval, smooth walled cavities between 0.5 mm and 2.5 cm in diameter (Fig. 8.10) which rarely occupy greater than 15% of the coral. The activities are often lined with a microspar rim and invariably infilled with micrite reef sediment (Fig. 8.10). In shape and size they are similar to borings produced by Polychaeta and Bivalvia (Bromley, 1970). Apparent preserved shells within borings (Fig. 8.10) may be the actual bivalve responsible for the borings or the later occupant of a previously formed cavity (e.g. Yonge, 1958); (ii) Slightly irregular walled, ramose, branching networks, restricted to the outer 5 mm of the coral skeleton (Fig. 8.10). The borings are of variable length, up to 1mm in diameter. They often form a "bored skin" to the coral skeleton. They were probably produced by bryozoans. Cavities are now infilled with fine grained reef sediment.

Some rounded irregular cavities up to 5 mm in diameter, on the margin of coral skeletons, may be the result of grazing by sponges. In encrusting sequences, tubular, rounded, slightly irregular borings predominate. They are up to 1 mm in diameter with a variable density and distribution and probably result from bryozoan activity. Large, up to 5 mm, irregular rounded cavities occur sporadically within encrusting sequences (Fig. 8.10). They were probably produced by bivalves or sponges.

The types of boring do not differ significantly in corals taken from life position and those taken from inter-colony debris areas. However, the density of borings increases markedly in corals and crusts from inter-colony shaded environments where crust growth is slower and destructive processes are more dominant.

The boring activity of sponges, polychaetes, algae, bivalves and other organisms outlined briefly above (see Bromley, 1970 for complete review) within primary and secondary frameworks, results in formation of a variety of open and closed cavities. These, combined with non-bored skeletal and inter-skeletal voids, in both corals and encrusters, provide a suitable environment for the

Fig. 8.10

Borings and encrusting sequences in the Kasaba Formation reefs.
All scale bars 2 mm.

(a) Bivalve borings (b) infilled by reef sediment.
In (a) remains of the shell are clearly visible.
Spec. U.3. GR. 501331.

(b) Bored 'skin' (b) to margin of *Tarballastraea sp.* colony.
Note marked decrease in intensity of borers towards centre of colony. Boring was probably by polychaetes or bivalves.
Plane polarised light. Spec. U13. GR. 504333.

(c) Well developed geopetal sediment fills of biomicrite reef sediment in intraskeletal coral void. Overlain by equant sparite cement (c). A thin cement fringe (f) is probably of submarine origin. It is overlain by reef derived biomicrite.
Note presence of thin crust of *Mesophyllum* (M).
Plane polarised light. Spec. U.M.1. GR. 501331.

(d) Crust of mixed composition. *Lithophyllum* (L) encrusting bored coral substrate (c), this is overlain by interlaminated *Mesophyllum* (M) and *Gypsina plana* (G). Crust growth was terminated by reef sediment (r). Note presence of large borings (b).
Spec. UM.6. GR. 501331.

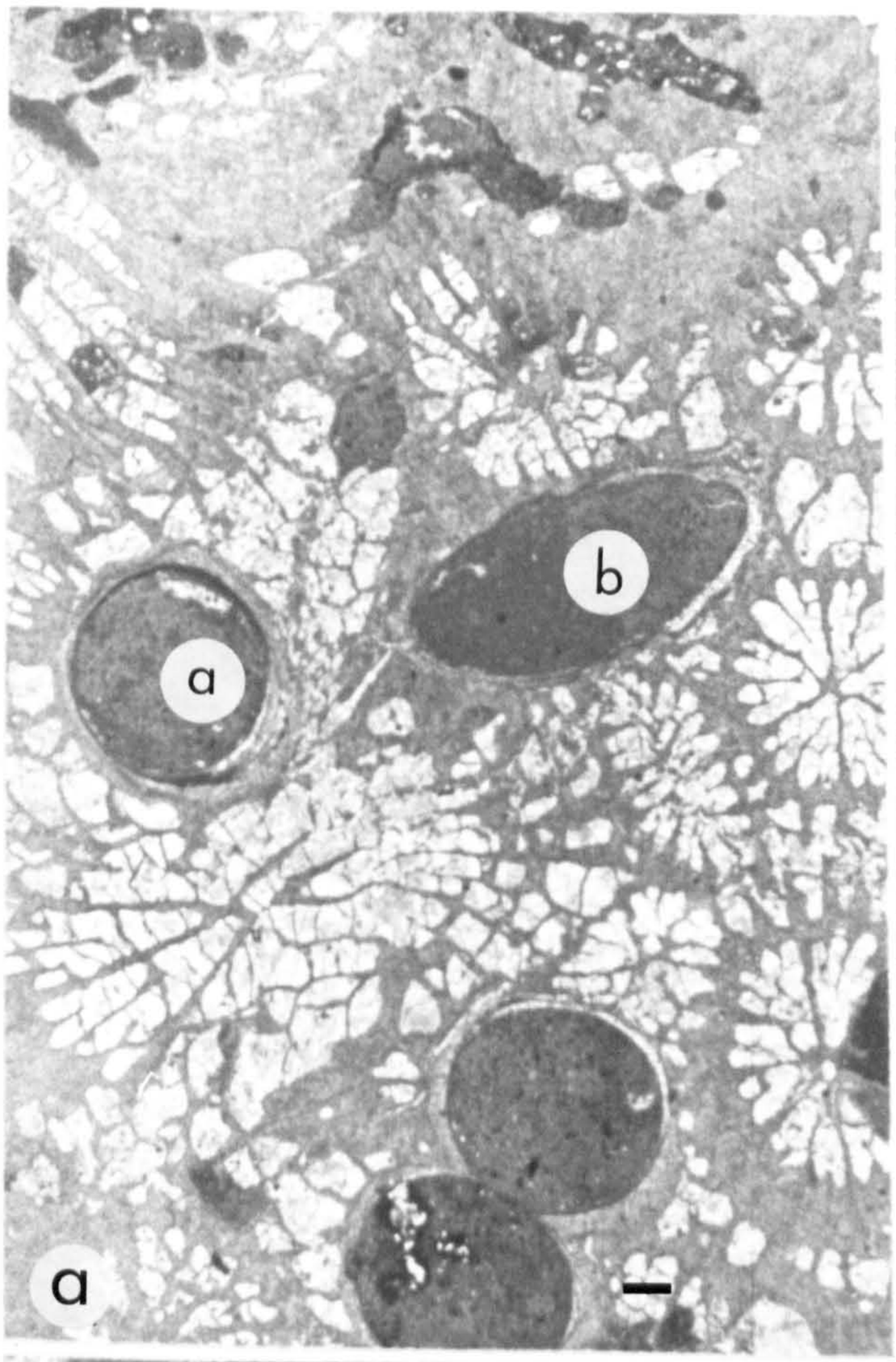
a
b
a

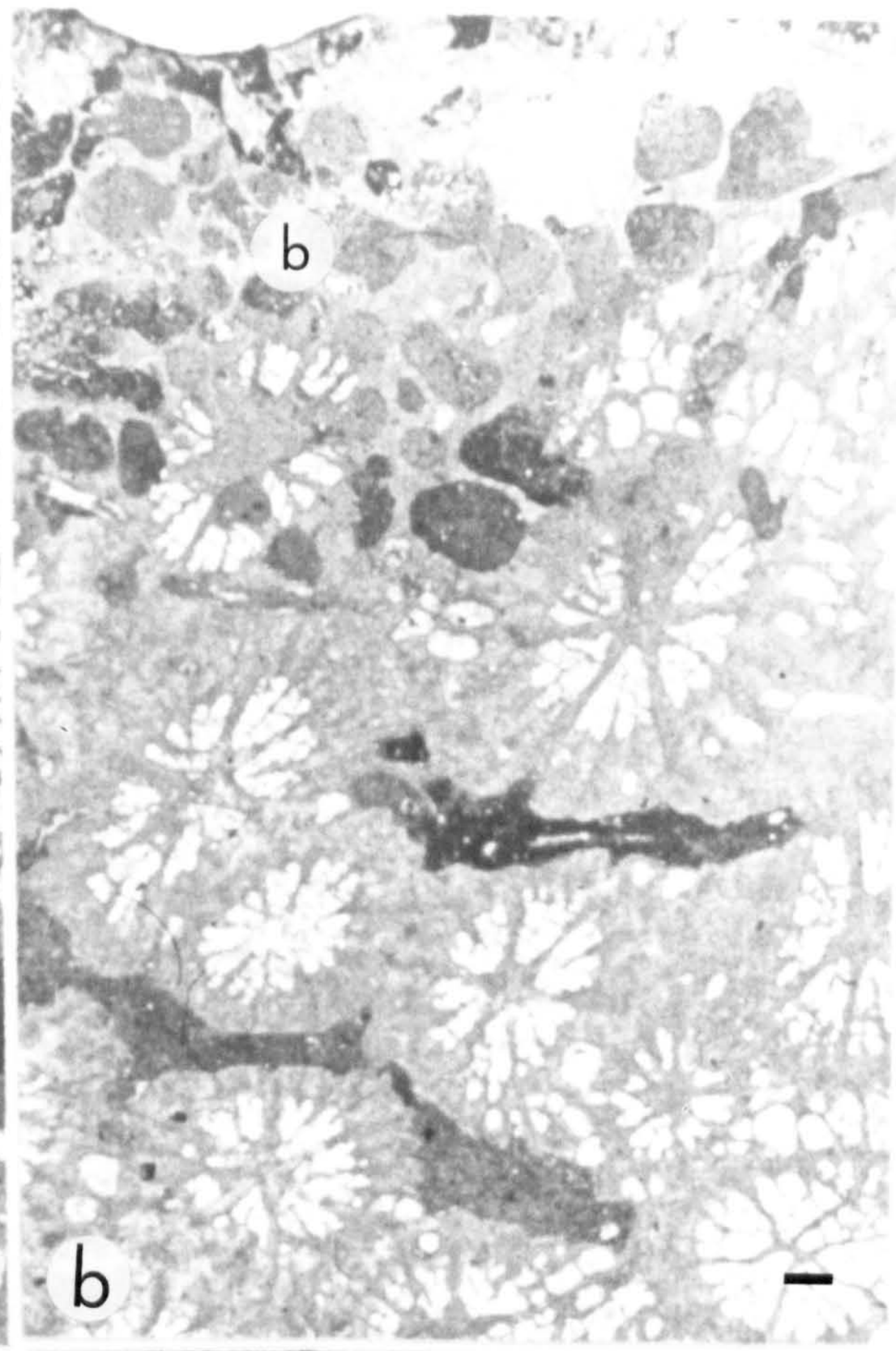
b
b


c
f
M
c

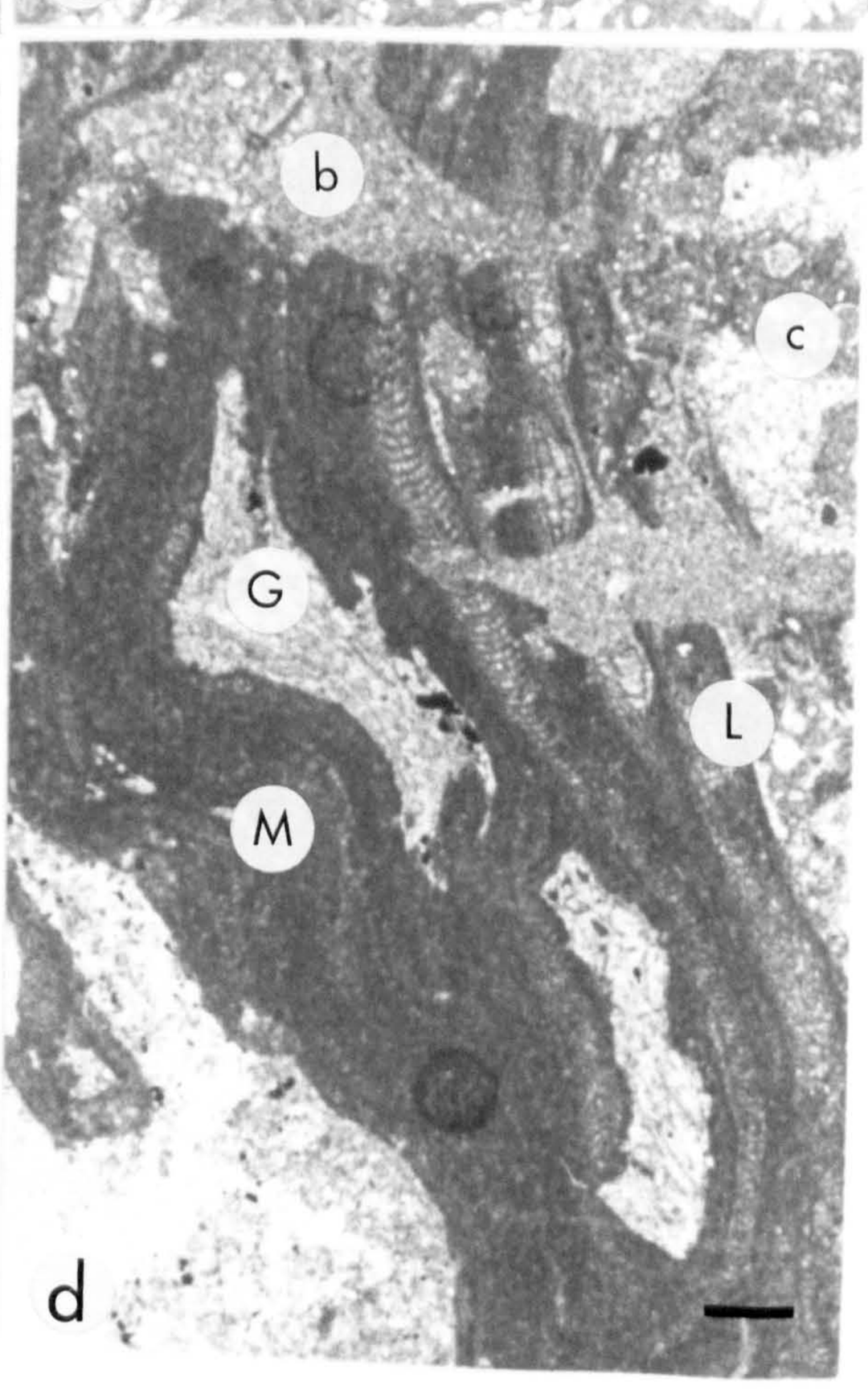
b
c
G
L
M
d

precipitation of carbonate cement and accumulation of reef-derived sediment.

8.8 Sedimentation

Reef sediment within cavities consists of subangular, generally poorly sorted fragments of coral, coralline algae, benthonic foraminiferans and shell fragments in a matrix of brown micrite (Fig. 8.10). Grain size varies from 10 μm to 5 mm. Micro-grading is rarely present. The sediment is essentially the same in cavities in both corals and encrusters.

The biomicrite sediment was probably produced by the organic breakdown of the frame. Wave action sucked water out of the cavities and voids, and the resultant turbulent inflow transported suspended sediment back into the frame (Ginsburg and Schroeder, 1973). In areas where the initial sedimentary fill has been subsequently bored by polychaetes or bivalves (Fig. 8.10) early synsedimentary cementation of the sediment must be invoked. These second generation borings are also frequently infilled with reef sediment (Fig. 8.10).

8.9 Submarine Cements ?

The recognition of submarine cements is dependant on the identification of an early cement, generally a fringing cement, preceeding reef sediment, or later void filling spar. Most marine cements consist of isopachous fibrous aragonite or high-Mg calcite fringes, the texture of which is often preserved despite neomorphism to calcite (Longman, 1980). A subsea cement is present as an isopachous fringe of calcite needles, up to 70 μm thick around the margins of some intraskeletal cavities and voids within coral skeletons. In some cases the cavity has been subsequently infilled by micrite reef sediment, confirming submarine cement formation.

The restriction of early cements to intraskeletal voids may indicate that interskeletal sedimentation was too high to allow the formation of aragonite or high-Mg calcite cements, on surfaces exposed to external processes. The formation of subsea cements in intraskeletal voids devoid of reef sediment occurs at the present time 1-2 mm beneath the living surface of the reef framework in Barbados (Martindale, 1976).

8.10 Interaction and Sequential Development

Following establishment of the primary framework, encruster growth, cementation and sedimentation are processes which continue the construction of the reef and reduce porosity by the addition of a secondary framework. At the same time boring organisms and mechanical breakdown by other physical mechanisms (wave action, turbulence, etc.) destroy both primary and secondary frameworks, creating new surfaces on which the sequence of events may be repeated.

Studies of modern reefs (Garrett *et al.*, 1971; Schroeder and Zankl, 1974; Scoffin and Garrett, 1974; Martindale, 1976) reveal that constructional processes dominate on the upper lighted surface, whereas on the undersurface destructive processes are frequently more important. Similar relationships are observed in the Kasaba Formation reefs. The detailed examination of several specimens from the underside of large colonies and inter-colony debris areas reveals the complex interaction of constructive and destructive processes during the growth and partial or complete destruction of the primary or secondary framework (Fig. 8.10). By comparison, corals taken from life position high in the reef framework, show only one generation of boring and subsequent photophyllic encrustation (Figs. 8.8, 8.9). The interaction of destructive and constructive processes continues until boring either completely destroys the primary framework and secondary frame, or until the frame is removed from the environment of growth (Martindale, 1976). In this case growth was terminated by the influx of terrigenous clastic material.

8.11.0 Burial and Diagenesis

Following burial the reefs were subject to a variety of diagenetic effects.

Primary framework. Coral skeletons which comprise the primary framework consist of either dusty, equant blocky calcite, or fibrous calcite that mimics aragonite crystal form (Fig. 8.10), both formed by the alteration of aragonite to calcite shortly after burial (Bathhurst, 1971; James, 1972). In the former the micro-architecture of the coral skeleton is completely destroyed. Alteration to low-Mg calcite takes place via a partial or complete void stage, resulting in the loss of skeletal structure (Friedman, 1964; Matthews, 1967;

James, 1972). The resultant structure is formed around a mould of voids and cavities filled with cemented micrite sediment. Where skeletal micro-architecture is partially preserved by fibrous calcite (Fig. 8.10) a gradual neomorphism of aragonite to calcite is suggested without an intermediary void stage.

Secondary framework. The encrusting sequences demonstrate well preserved skeletal micro-architecture (Fig. 8.7). This is because the skeletons of crustose coralline algae and foraminiferans consist of high-Mg calcite (Martindale, 1976). Alteration of the secondary high-Mg calcite frame takes place without a void stage, by exsolution of Mg from the crystal lattice (Friedman, 1964). As a result, the skeletal framework undergoes little or no structural alteration (Winland, 1968), and is preserved as the stable polymorph low-Mg calcite.

8.11.1 Cements

Excluding the initial submarine cement, which is patchily developed (see above), two generations of cement are present. The first consists of a patchily developed meniscus fringe of microspar approximately 40 μm thick. It is present lining the rims of voids and cavities (Fig. 8.10) and in some areas overlies reef sediment (Fig. 8.10). The second generation consists of equant blocky sparite that infills intraskeletal voids and cavities (Fig. 8.10), in both primary and secondary frameworks and also interskeletal voids (Fig. 8.10). Both these cements probably formed in the freshwater zone. The former may be the result of cementation in the vadose zone (Longman, 1980). Equant calcite cements can form in both the vadose and freshwater phraetic zones (Longman, 1980).

8.12 Reefs in a Coarse Clastic Sedimentary Environment : Comparison with Red Sea Reefs

Classically reefs were not thought to be associated with areas of high terrigenous clastic sedimentation. However, studies of ancient and modern reefs and their environment of formation have shown that this is not necessarily the case. At the present day coral reefs are found in close association with terrigenous clastic sediments from a number of areas, e.g. Jamaica (Wescott and Ethridge, 1980), Red Sea (Gwirtzman and Buchbinder, 1978; Hayward, in press, a).

Hermatypic corals which form coral reefs are restricted by their symbiotic relationship with algae (dinoflagellates or

zooxanthallae). They generally require a minimum water temperature of 18° (ideally 25-29°) and are therefore restricted to shallow, well-lit, warm water. In addition, they require a good supply of oxygen and a firm substrate for the planulae to settle, although light is considered the most limiting factor (Clarkson, 1979).

Fringing coral reefs are extensively developed around the margins of coastal alluvial fans along the coast of the Red Sea and Gulfs of Elat and Suez. This area differs in its overall tectono-environmental setting from the Miocene sequence of S.W. Turkey, but does provide a useful modern analogue.

The coarse gravel sediments of coastal alluvial fans provide an ideal substrate for coral planulae to settle. In the Red Sea small coral colonies grow directly on non-lithified terrigenous pebble clasts greater than 60 mm in diameter. Material finer than this is not colonised by corals. However, material as fine as granule gravel may be initially bound by coralline algae, upon which coral colonisation can follow.

The grain size of a potential growth substrate therefore exerts a very strong control on reef location in the Red Sea. In the Kasaba Formation reefs are only found where claystone forms a minor part of the sequence, suggesting a similar control. The presence of claystone in the nearshore, back-reef sequences (Fig. 8.11) is probably the result of the protection of this area by the reef from wave action. Mud provides an unsuitable substrate for colonisation by coral planulae (or coralline algae) and thus landward progradation of the reef is prevented.

The Kasaba Formation was deposited just prior to the Messinian dessication event, recorded all over the Mediterranean area (Hsu *et al.*, 1973), in a semi-arid environment characterised by low precipitation and low seasonal run-off. The critical factor in reef development was the localised and episodic sedimentation patterns typical of semi-arid alluvial environments. In recent examples of this climate, sedimentation is restricted to one or two flash-flood events every year. In addition, these periodic sediment influxes are confined to the active portion of a fan and, depending on the prevailing marine currents, have little effect on the marine sediments adjacent to inactive areas of the fan. With low episodic sedimentation rates a reef would have ample opportunity to re-establish itself, should it be swamped by an influx of terrigenous material.

In the Red Sea catastrophic flood events during the winter result in terrigenous material being carried onto the reef. Marine currents, mainly longshore drift and waves, take up to ten days to move the finer material away from the living reef area. The effect of such influxes on the reef, however, is minimal (B. Buchbinder, pers. comm, 1981). Much of the terrigenous material coarser than pebble gravel is retained in the reef, coralline algae, other encrusting organisms and corals binding the clasts into the reef. In some areas, terrigenous material bound in this way forms up to 50% of the reef framework (Hayward, in press, a).

In the Kasaba Formation, scattered terrigenous cobbles and pebbles within the reef core suggest that clastic influx rarely produced swamping of reefs with enough debris to terminate growth. However, the scattered development of reefs within the clastic sequence indicates that conditions for growth were only satisfied sporadically, probably as the locus of terrigenous sedimentation switched. This type of control on reef location is also evident in the Red Sea, where entrenched fluvial channels formed during a Pleistocene low sea level stand pass seawards into narrow incised canyons. Reefs are developed away from the active fluvial-marine channels but are not growing in the channel areas as a result of the high sedimentation rates formed by lateral confinement of the fluvial system.

Having demonstrated that reefs can and do flourish in a coarse terrigenous clastic environment, how was reef growth terminated?

The Kasaba Formation sedimentary sequences were developed in a vastly different tectonic regime, to the Red Sea, which exerts strong primary control on sedimentation and hence reef development. Rapid subsidence following emplacement of the Lycian Nappes and extensive migration of the active sedimentation tract across the fan surface (4.11) resulted in relatively high sedimentation rates over the entire alluvial fan surface.

Although in the short term sedimentation rates were probably similar to the Red Sea, subsidence and active progradation of the alluvial fan in the Kasaba Formation sequences was far more extensive than in the Red Sea examples which are in a more or less equilibrium situation at the present day.

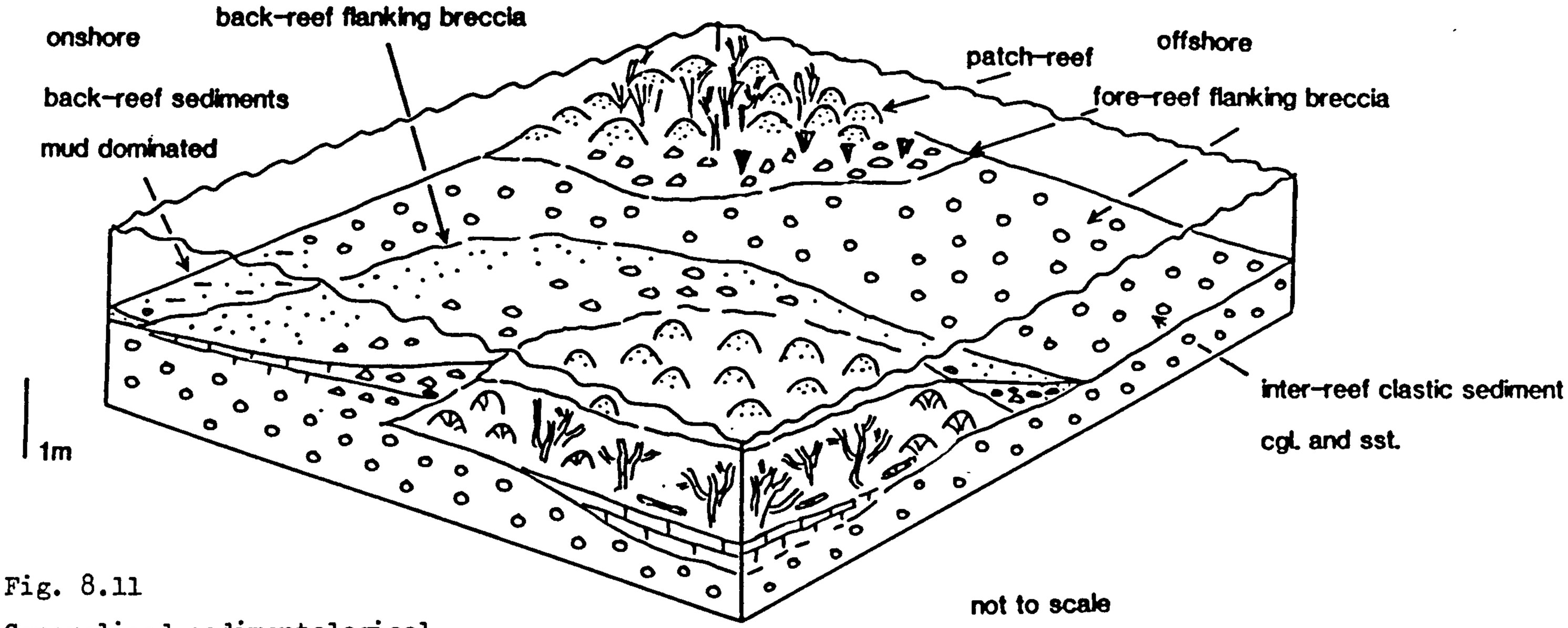

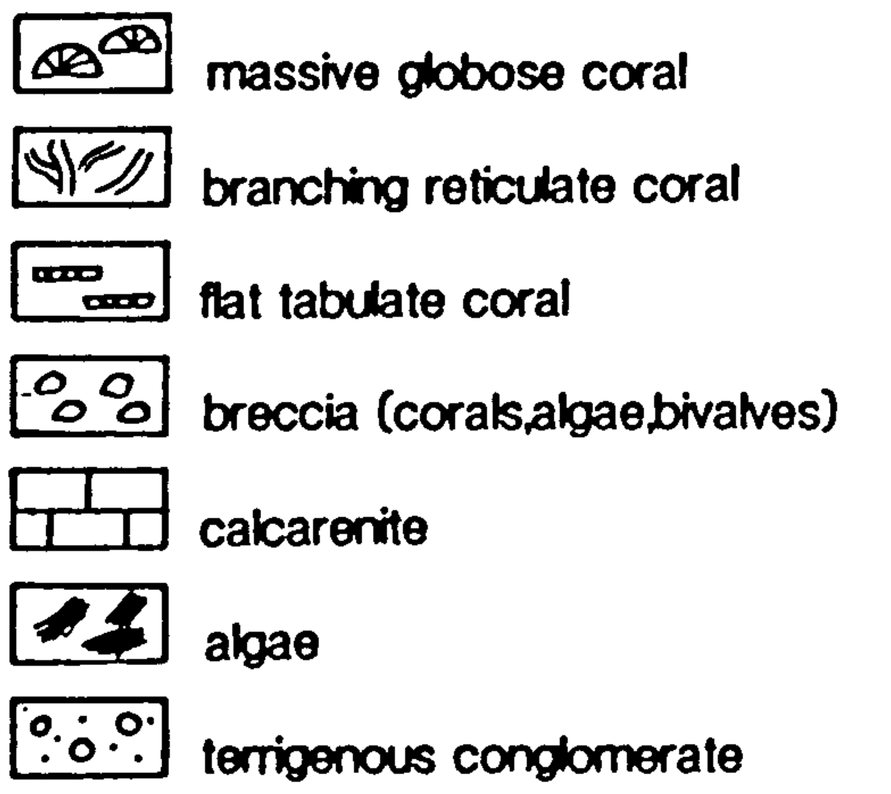

Fig. 8.11
Generalised sedimentological model for patch-reefs, showing greater development of flanking sediments on back-reef (landward margin). Inter-reef sediment is dominated by coarse terrigenous clastic sediment.

8.13 Summary of Reef Growth and Environment

Reefs developed parallel to the palaeoshoreline on the submarine toes to coastal alluvial fans. Gravel and coarse sand of the fans provide an ideal substrate on which coral planulae could settle and grow. As a result no pioneer community is present. Primary framework builders consisted dominantly of the corals *Favites sp.*, *Tarballastraea sp.*, *Montastrae sp.* and subordinate *Porites sp.* Coral morphology changed progressively as the reef grew upwards towards the surf zone. There is no evidence of subaerial exposure or surf effects at the top of the reef (e.g. rudstones, James, 1979) and the tops of the reefs were probably several metres below the sea surface. The lack of subaerial exposure combined with sedimentological data from the clastic sediments suggests a micro-tidal sea.

The primary framework was encrusted by a secondary framework of coralline algae and encrusting foraminiferans. The effects of boring and grazing by a number of organisms (bivalves, sponges, bryozoan) produced abundant debris which accumulated in inter-colony areas. Dominantly onshore wave and storm activity periodically redeposited some of this material landward into the lee of the reefs where it remained relatively undisturbed.

A close present day analogue of this environment are the fringing coral reefs developed along the margins of coastal alluvial fans in the Red Sea.

CHAPTER 9 CARBONATE PLATFORM

Colour Plate 2

The Bey Dağlari carbonate platform limestone massif viewed from the southern end of the Akdere valley. In the foreground carbonate platform limestones (C), on the eastern limb of the Finike anticline dip eastwards beneath Miocene clastic sediments (M). These are overthrust by a tectonic melange (T), Eocene redeposited limestones (E) and the imbricated Antalya Complex (A).


M
C
T
A
E

CHAPTER 9

9.0 Carbonate Platform

9.1 Introduction and Previous Work

Over the entire Bey Dağlari and Susuz Dağ, Miocene clastic sediments overlie a regionally extensive sequence of dominantly massive to thick-bedded limestones. The limestones contain a wide variety of bioclastic carbonate material, typically algae, benthonic foraminifera, rudists, corals, ooids and pelletoids. Previous regional studies (e.g. Brunn *et al.*, 1971; Poisson, 1977) recognised this sequence as an autochthonous carbonate platform unit, forming part of the Taurus autochthon (1.3.2, Fig. 1.2). The northern area of the Bey Dağlari, and to a much lesser extent, the southern Bey Dağlari and Susuz Dağ, was the subject of a detailed bio-stratigraphic study by Poisson (1977). Relative to their large area of exposure in the mapped area, the carbonate platform sequences were only briefly studied. This reconnaisance study was carried out to give a broad understanding of the platform history prior to the Miocene nappe emplacement events and to compliment the early work of Poisson.

The approach adopted here is one of examining large scale regional lateral variations in sedimentary facies as the platform evolved. Stratigraphic data used is a combination of results from this study together with those of Poisson (1977) and Onalon (1980).

The earlier parts of this chapter outline in detail the history of the S. Bey Dağlari and Susuz Dağ, based mainly on results from the present study. The concluding sections compare and contrast the S. Bey Dağlari and Susuz Dağ platform with the northern Bey Dağlari. Data for the northern Bey Dağlari is based almost exclusively on the work of Poisson (1977). The final section is a brief summary of the evolution of the Bey Dağlari and Susuz Dağ carbonate platform from its inception in early Liassic times to its termination by tectonic events in Lower to Upper Miocene times.

9.2.0 Southern Bey Dağlari and Susuz Dağ

9.2.1 Cretaceous

Over the Susuz Dağ and S. Bey Dağlari the stratigraphically lowest sequences are of Upper Cretaceous (mainly Cenomanian) age.

The *Cenomanian* sequence consists of thick to massive white or grey, limestone beds interbedded with finely laminated (scale of

several mm's) units up to 2 m thick. Cross-bedding and other indicators of current activity (basal scours etc.) are not seen. Bedding planes are often extensively stylotised. Non-laminated limestone frequently contains rudist debris.

Micro-facies. In thin section, several micro-facies are distinguished, terminology used follows that of Dunham (1962).

Finely laminated units comprise *algal-laminated boundstone* consisting of micrite layers with an irregular clotted texture separated by discontinuous lenses of slightly coarser micrite (Fig. 9.2). Uneven lamination results in small bulbous stromatolites. Layers of unlaminated *pelletoidal wackestone* are interbedded with the algal laminated units.

Massive to thin-bedded limestone comprise the following two micro-facies:

(1) *Lime mudstone*: uniformly fine grained limestone with, rare, scattered silt sized foram fragments and abundant dispersed carbonaceous material.

(2) *Pelletoidal-bioclastic-wackestone*: pellets are rounded to irregular in shape. Bioclastic material consists mainly of rudist debris, foraminifera, mainly *Miliolids*, *Discocyclids* and *Valvulinids* and rare bryozoan.

Interpretation

Stromatolitic algal boundstones of the type described here are found at the present day as algal mats in supratidal to intertidal environments (e.g. Shark Bay in Australia, Bahamas, Persian Gulf, James, 1979). Rudists represent higher energy fully marine environment, they may have formed low relief reefs. Benthonic forams also attest to open marine conditions. *Cenomanian* sequences over most of the Susuz Dağ and S. Bey Dağlari represent *shallow marine* supra- to subtidal environments of a stable carbonate platform.

Over the Susuz Dağ the remainder of the Upper Cretaceous is marked by a hiatus in sedimentation, Cenomanian limestone is overlain by shallow water limestone of Palaeocene age (below) (Fig. 9.1).

In the central area Cenomanian shallow water sequences are overlain by ca. 10 m of *pelagic limestone* of *Senomanian* (Maastrichtian) age.

Along the eastern flank of the S. Bey Dağlari the shallow water Cenomanian rocks are overlain by a similar sequence of *pelagic*

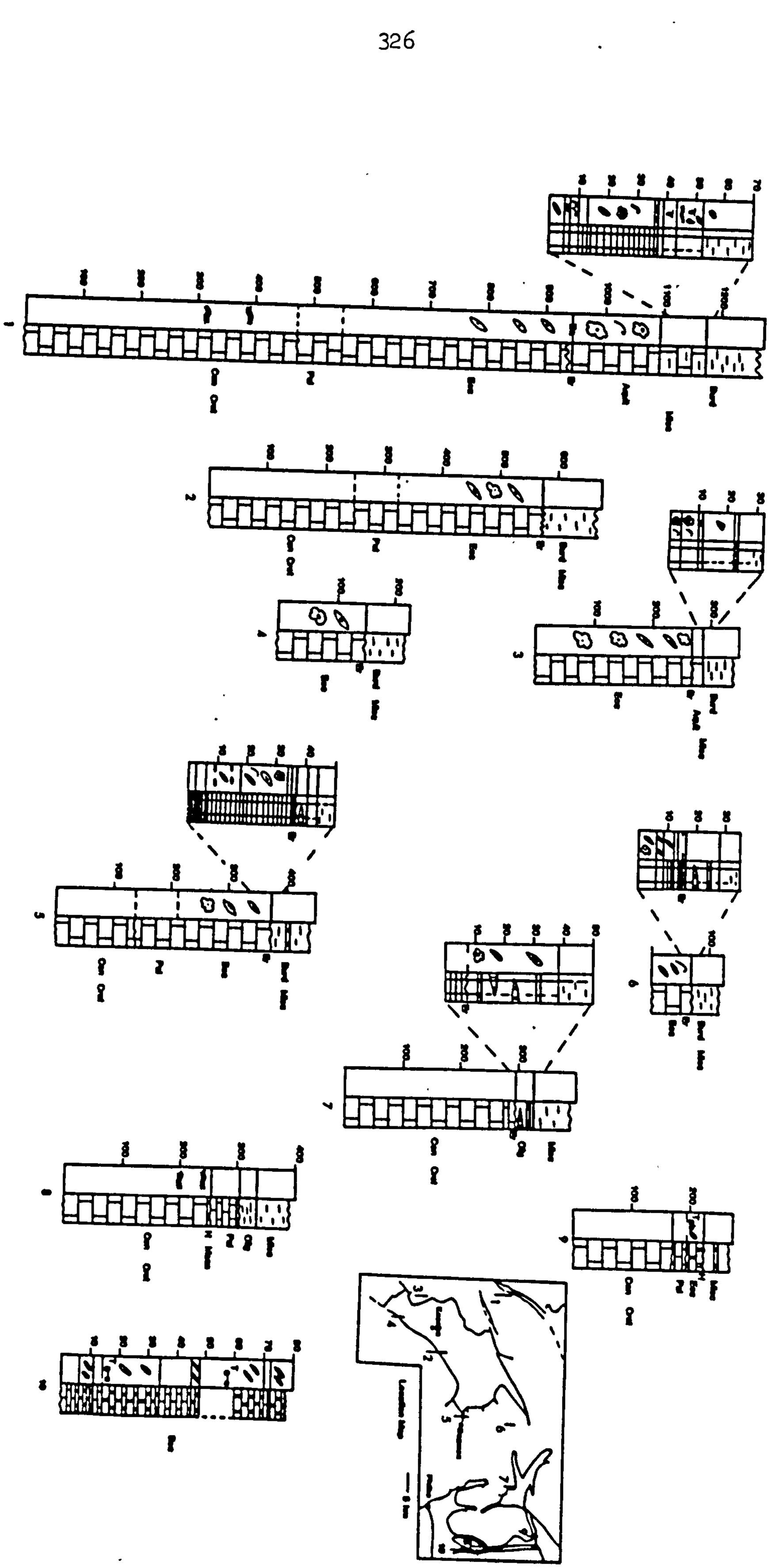

Fig. 9.1 Stratigraphic sections in the carbonate platform sequence over the Susuz Dağ and southern Bey Dağlari.
Map shows location of sections (thickness in metres, Appendix C for key).

Fig. 9.2

Photomicrographs and field photographs of the carbonate platforms.

(a) Cretaceous (Cenomanian) limestone. Algal laminated limestone consisting of micrite layers (m) with an irregular clotted texture separated by layers of coarser micrite (c).
Field of view 2.5 cm.
Plane polars. Spec. 435/80. GR. 521350.

(b) Maastrichtian pelagic limestones (M) overlain by thin silicified red ferrugenous limestone (f), representing a prolonged hiatus in sedimentation, this is overlain by calcareous marls and calcarenites of Oligocene age (O).
GR. 394392.
See Fig. 9.1, sect. 7 for location.

(c) Muddy limestone (calcareous marl) of Miocene (Aquitanian) age contains abundant planktonic foraminifera.
Spec. 251/80. GR. 368395.
See Fig. 9.1, sect. 1 for location.

(d) Redeposited Eocene limestone containing large benthonic foraminifera derived from a contemporaneous shallow water area and abundant planktonic foraminifera.
Spec. 153/78. GR. 385526.
See Fig. 9.1, sect. 10 for location.

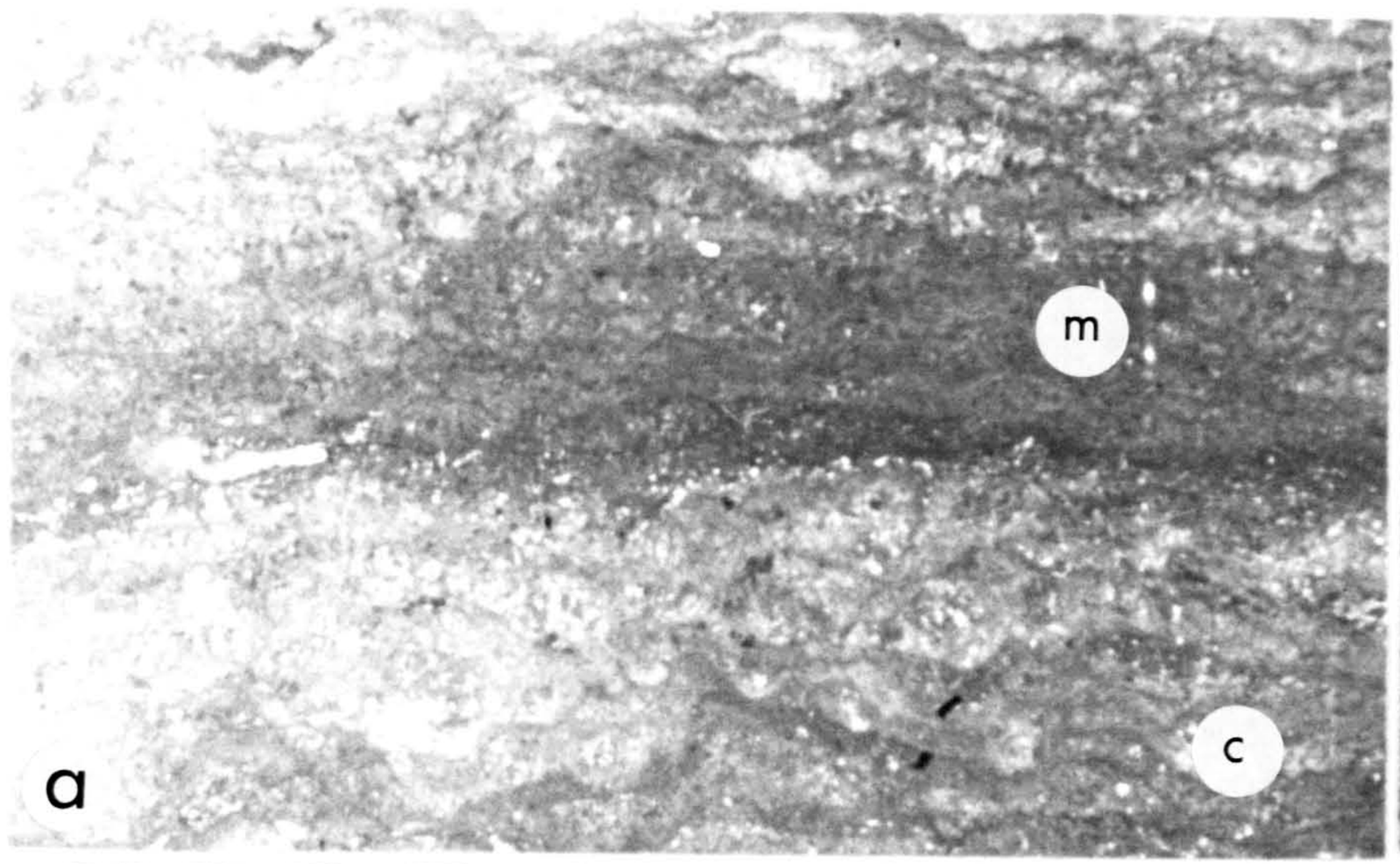
m
c
a

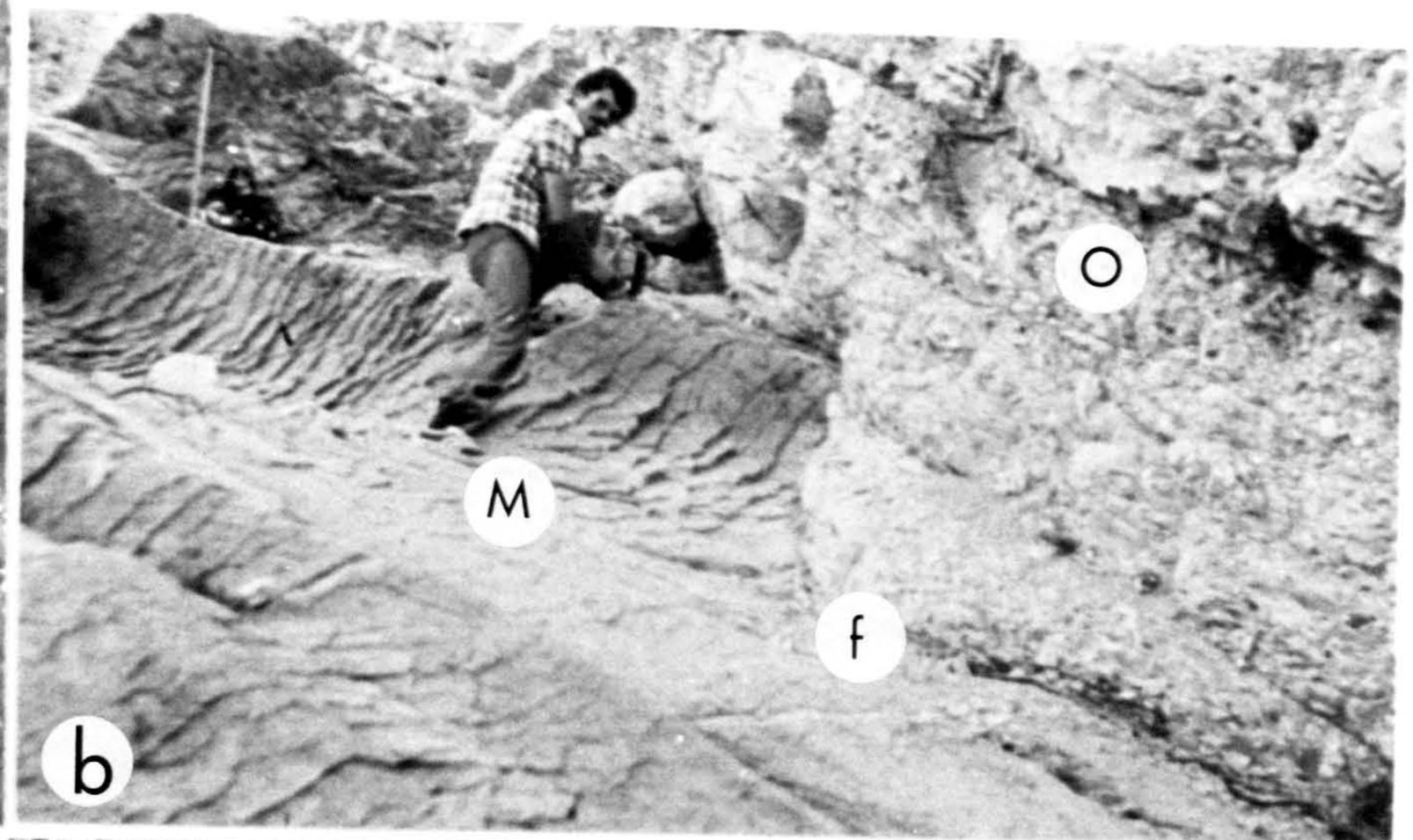
O
M
f
b

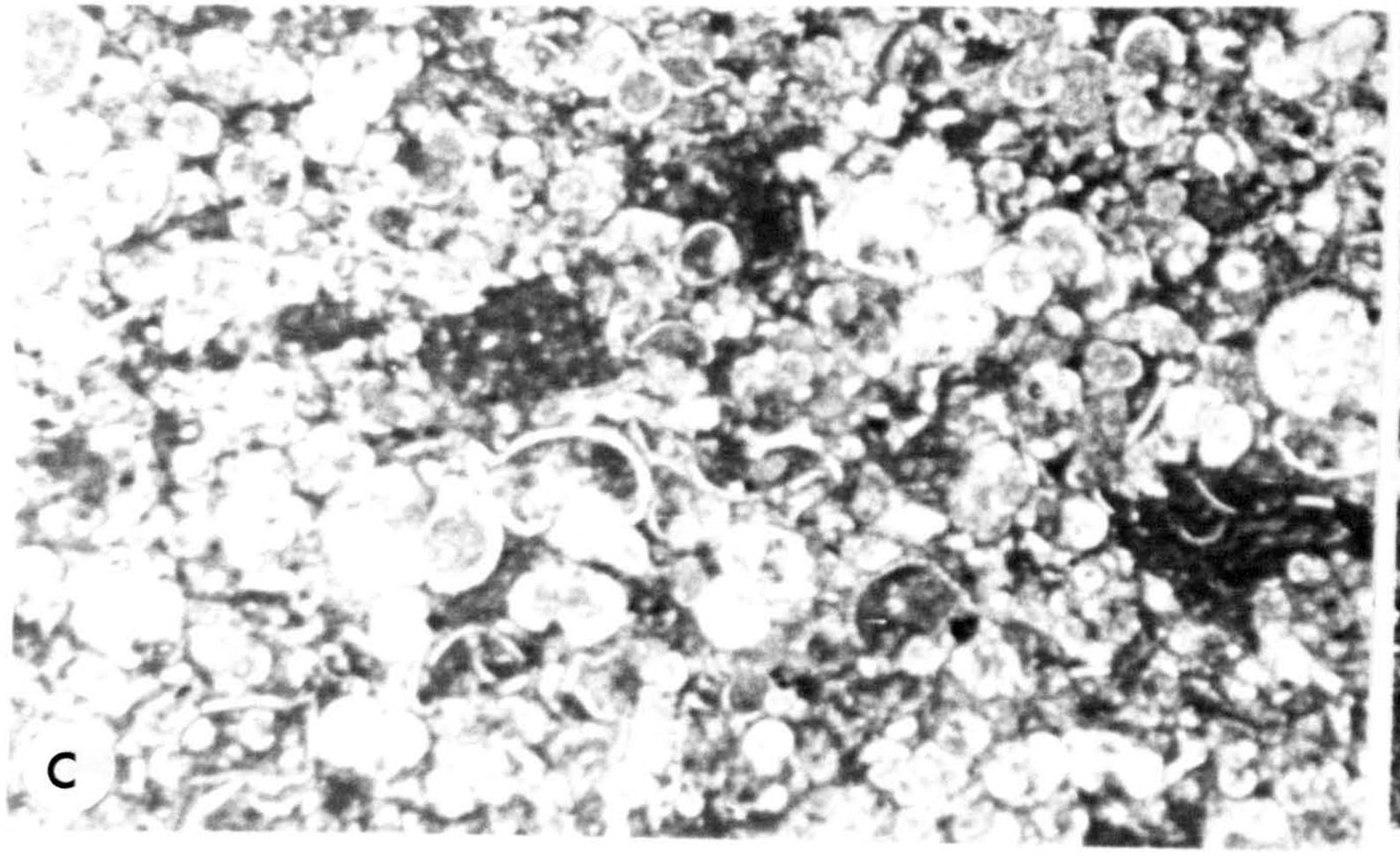
c

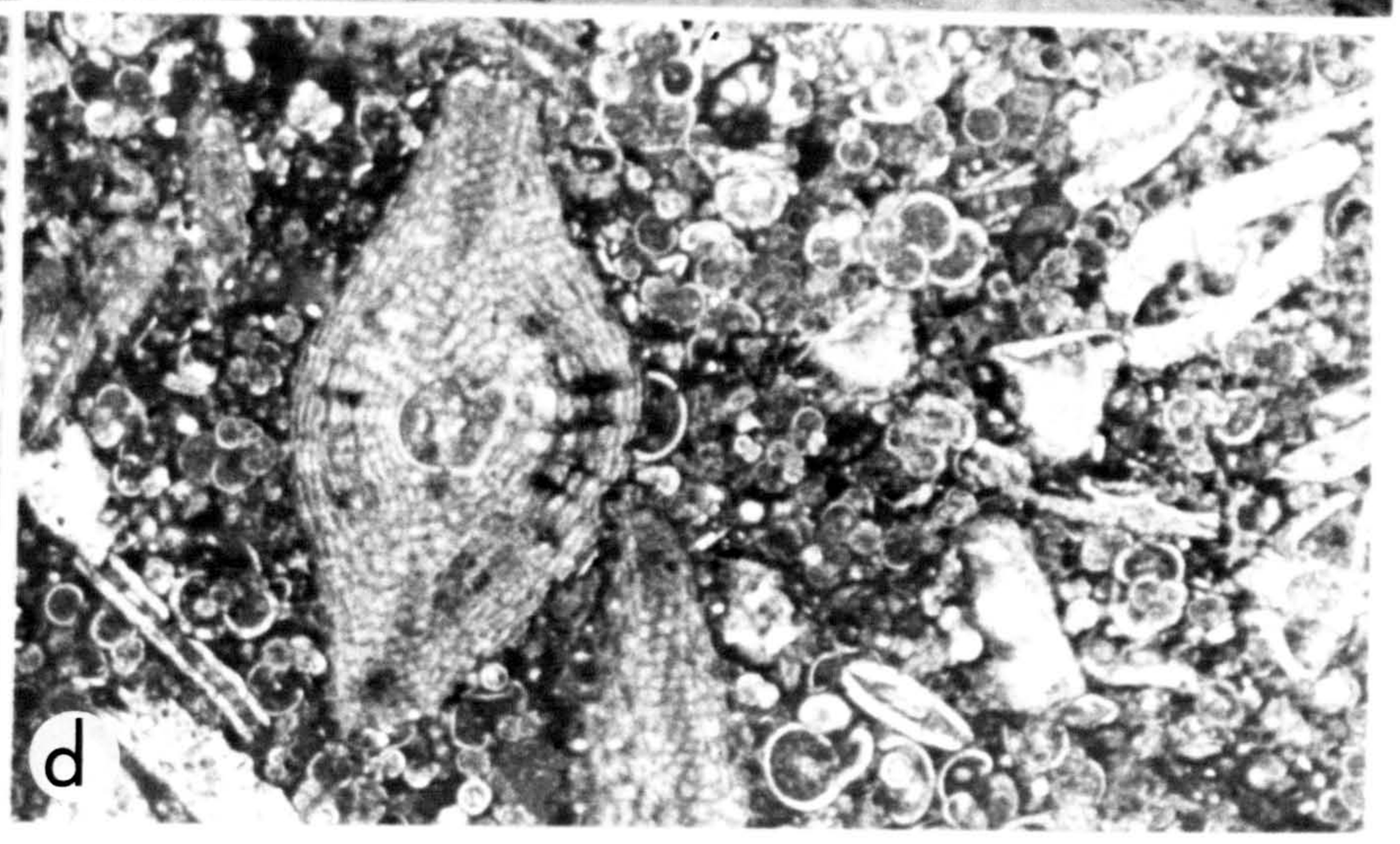
d

limestones of *Maastrichtian* age. The limestones comprise of thick- to thin-bedded *lime mudstones*, which are often partially silicified. Petrographically the rocks consist of planktonic foraminifera, including *Globotruncana* and calcite replaced Radiolaria in a micrite matrix. This sequence is continuous up into overlying Palaeocene (Danian) pelagic limestones (below).

This late Cretaceous (Maastrichtian) sequence signals the end of the stable, shallow marine, open platform carbonate realm that had existed with some breaks in sedimentation through the Cretaceous. The Maastrichtian pelagic limestones represent subsidence of the platform along its eastern margin to pelagic depths (ca. 500-1,000 m), and the development of a prominent north-south trending depositional hinge. To the west of this hinge in the Susuz Dağ area (Fig. 9.1, Sections 1-6) late Cretaceous sequences are absent, indicating either a prolonged hiatus in sedimentation or possibly subaerial exposure. In this respect there is no evidence of any well developed karstic surface.

9.2.2 Palaeocene

Marked regional lateral variations in the carbonate platform that had begun to develop in the Upper Cretaceous become more evident in the Palaeocene (Hayward and Robertson, in press).

In the area around Sinekçibeli, along the northwestern flank of the Susuz Dağ, the Palaeocene sequence comprises approximately 75 m of thin- (.10 m) to thick-bedded (1 m) fine grained monotonous white-grey limestone. Cross-bedding and other current structures are not seen.

Pellet-foram-bioclastic packestone/wackestone is the most common micro-facies. Pellets are rounded to irregular with a clotted texture and up to 3 mm in diameter. Forams are benthonic types mainly *Miliolidae*, *Rotalidae*, *Alveolina* and *Textularia*. Disseminated bioclastic material comprises angular shell (bivalves?), algal and rare echinoderm fragments. Some of the clasts show evidence of boring. Matrix comprises poorly sorted carbonate silt and mud. Other less common micro-facies are *bioclastic-pellet-wackestones* and *lime mudstones* (fine grained unlaminated limestone) with rare (5%) silt sized bioclastic debris.

Interpretation

The absence of algal boundstones (stromatolites) in this sequence

probably indicates a slightly deeper environment of deposition than the underlying Cretaceous sequence. The bioclastic component, particularly benthonic forams, suggests an open platform environment. The abundance of lime mudstone and absence of current structures suggests quiet water conditions.

By contrast, in the central southern areas of the Bey Dağlari, Palaeocene deposits are absent or restricted to only several centimetres of silicified red ferruginous limestone (e.g. Gokbuk, Fig. 9.1, Section 7; Fig. 9.2). Rare rounded clasts, up to 250 mm in diameter, of the underlying Maastrichtian pelagic limestone, are also present. In thin section angular fragments of silicified nummulites, algae and bivalves are dispersed in a dark brown ferruginous micrite matrix.

Interpretation

This highly condensed unit represents a prolonged hiatus in sedimentation. Diagenetic silicification of bioclastic debris and rounded clasts of the underlying Maastrichtian pelagic limestone (Fig. 9.2) may indicate subaerial exposure.

Along the eastern margin of the S. Bey Dağlari (e.g. southwest of Salir, Fig. 9.1 Section 8), the Palaeocene sequence comprises thick- to thin-bedded lime mudstones (chalks) interbedded with micro-conglomerates and grey-organic rich calcareous mudstone. White or cream coloured lime mudstones are often porcellenous as a result of slight silicification. Many of the beds are massive but some show parallel lamination and small micro-cross-lamination, which is attributed to weak bottom currents. Petrographically the chalks consist largely of densely packed foraminifera and calcified Radiolaria in a micrite matrix.

Interpretation

This sequence represents pelagic deposition in deep water (ca. 500-1,000 m).

Summary. The Palaeocene saw marked topographical differentiation over the Susuz Dağ and S. Bey Dağlari. A shallow water carbonate depositing realm in the west, passed eastwards into a central area that was possibly subaerially exposed. This was bordered to the east by an area of pelagic deposition (Fig. 9.4).

9.2.3 Eocene

The topographic differentiation in the carbonate platform that developed in the Palaeocene continued into the Eocene.

Over the area of the Susuz Dağ massif the Eocene sequence is between 200 and 400 m thick (Fig. 9.1, Sections 1 and 2). Beds range from thin (.10 m) to massive (4.0 m) and contain numerous intact non-abraded nummulites. Cross-bedding and other current structures are absent. The *lack* of graded bedding and associated sedimentary structures precludes redeposition by sediment gravity flows (turbidites, etc.).

The following micro-facies are distinguished:

(1) *Algal-bioclastic-pellet-packestone/wackestone.* Algal and disseminated bioclastic material comprise between 20 and 80% (by volume) dispersed in a lime mud/silt matrix. All clasts are angular, fragmented and randomly orientated. Forams are benthonic types (*Discocyclids, Nummulites, Alveolinids*). Pellets are rounded to irregular and up to 0.5 mm in size. Coralline algae are dominated by forms akin to *Mesophyllum* and *Archeolithithamnium.*

(2) *Foram-bioclastic-packstone/wackestone.* Similar to above, with greater abundance (up to 80%) of forams. The forams comprise benthonic forms to 10 mm long. Micrite matrix is patchily distributed. Intergranular pore space is filled with a sparite cement.

(3) *Lime mudstone.* Comprises very rare (less than 5%) foram fragments dispersed in a fine grained micrite matrix.

(4) *Foram-algal-boundstone.* Consists of intergrown encrusting foraminifera and coralline algae. Rare benthonic foraminifera are incorporated into the framework. Borings up to 1 mm in diameter are filled by sparite cement.

Interpretation

Micro-facies present suggest a shallow water open platform environment of deposition. The paucity of grainstones, angularity of bioclastic debris and absence of current formed sedimentary structures suggests low energy quiet water conditions. Encrusting foraminifera and coralline algae are probably indicative of a higher energy environment. They may have formed small reef knolls.

The top of the Eocene sequence is marked by a karstic or extensively brecciated surface. In a section exposed southeast of Sinekcibeli, pockets of bauxite, up to 1.5 m deep, are present in a

deep karstic surface (Fig. 9.1, Section 1). Erosion gullies and the presence of bauxite indicate a prolonged period of subaerial exposure prior to the deposition of the overlying Miocene (Aquitanian) algal limestone.

Elsewhere (e.g. Çağman, Demre Çay, Fig. 9.1, Sections 5 and 2) the top .10-.15 m of the sequence is characterised by extensive brecciation marking a hiatus in deposition and probable subaerial exposure.

Over a large area of the central and southern Bey Dağlari, Eocene sequences are completely absent (Fig. 9.1, Section 8). Where present, as at the northern end of the Finike anticline (Fig. 9.1, Section 9), the sequence consists of calcarenites and calcirudite breccias interbedded with pelagic chalks and mudstones. Very similar facies are seen in the area southwest of Salir (Figs. 9.1 Section 10, and 9.3), where they form a highly deformed tectonic slice sandwiched between the sole thrust of the Antalya Complex and the structurally underlying Miocene sediments of the Bey Dağlari.

Limestone breccias up to 3.5 m thick grade upwards into calcarenite. Interbedded medium to thick calcarenites show good Bouma sequences (Tabc, Ta-e). Thin-bedded pelagic chalks form between 10-50% of the sequence. The breccias and calcarenites are petrographically heterogeneous, containing fragmented shell, algal material (some micro-oncolites), echinoderm debris and numerous large benthonic foraminifera, including *Miliolines* and *Nummulites*, diagnostic of an Eocene age (M.T.A. determination). There are also numerous lithoclasts of partially silicified pelagic chalk containing *Globotruncana* and Radiolaria including forms akin to *Dictyomitra* and *Pseudoaulophacus* (suggesting a Cretaceous age). In addition the upper parts of redeposited beds often contain up to 80% comminuted planktonic foraminifera debris.

Pelagic chalk interbeds comprise of lime mudstone with abundant scattered, mainly intact, planktonic foraminifera and calcified Radiolaria tests. Diagenetic silicification is common throughout this sequence.

This sequence clearly represents the redeposition of bioclastic debris from a contemporaneous shallow water carbonate build-up across a marginal area into a deeper water basinal realm. The presence of abundant planktonic foraminifera within turbidite beds suggests redeposition via or through a pelagic depositing area. This implies

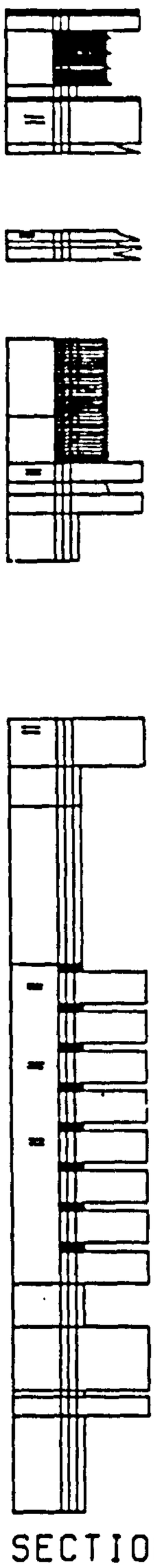

Fig. 9.3

Detailed sedimentological logs through redeposited Eocene limestone sequence, tectonically intercalated between the Miocene clastic sediments and Antalya Complex, along the eastern margin of the Finike anticline.
Sections are located north and south of section 10 on Fig. 9.1 (Appendix C for key).

that the margin was probably not one large scarp (fault?), but rather several steps on top of which pelagic chalks accumulated (Fig. 9.4).

Summary. The Eocene thus records a west to east transition from an elevated platform area across a N-S trending depositional hinge into a basin located east of the present edge of the Bey Dağlari. Inner areas underwent shallow water carbonate deposition or were subaerially exposed. Along the depositional hinge material as old as Cretaceous (as evidenced by limestone lithoclasts) was eroded during breaks in sedimentation. To the east basinal facies accumulated rapidly by a combination of mass-flow and turbidity currents.

9.2.4 Oligocene

Over the entire Susuz Dağ Oligocene sequences are absent. In the central area of the S. Bey Dağlari the Oligocene sequence comprises ca. 20 m of marls interbedded with lenticular, rarely graded bioclastic calcarenites (Fig. 9.1, Section 7). Petrographically the calcarenites consist of bioclastic debris, mainly benthonic foraminifera (*Discocyclines*, *Nummulites*), coralline algae (small rhodoliths) and *bryozoan* in a micrite matrix. The marls contain abundant planktonic foraminifera of Oligocene age (Poisson, 1977).

Along the eastern flank of the S. Bey Dağlari (e.g. southwest of Salir, Fig. 9.1, Section 8) the Oligocene sequence comprises ca. 20 m of marls with abundant planktonic foraminifera.

Interpretation

The calcarenites represent the probable localised redeposition of bioclastic debris from areas of minor shallow water carbonate build-ups. Marls are the result of continued hemipelagic deposition.

The N-S depositional hinge line which developed through the Palaeocene-Eocene continued into the Oligocene. Over vast areas of the platform the Oligocene is marked by a hiatus in deposition and in some areas subaerial exposure (?). Central areas were characterised by small shallow water carbonate build-ups. This material was transported basinward by sediment gravity flows (Fig. 9.3). Meanwhile, more basinal conditions existed along the eastern flank of the S. Bey Dağlari, as shown by continued hemipelagic deposition.

9.2.5 Miocene (Aquitanian, Karabayir Formation)

Over the S. Bey Dağlari, Aquitanian limestone is absent. Oligocene marls are overlain by terrigenous clastic sediments of Lower Miocene age (Salir Formation, Chapter 5). Westwards in the Susuz Dağ area, a sequence of thick to massive, white-grey limestone, of Miocene (Aquitanian) age, overlie unconformably the Eocene sequences (e.g. Fig. 9.1, Section 1). This sequence is defined as the Karabayir Formation by Poisson and Poignant (1974). The type section, located in the north of the Bey Dağlari at the village of Karabayir south of Korkuteli (Fig. 9.5), is over 300 m thick.

In the Susuz Dağ area the sequence shows marked lateral variations in thickness, from ca. 150 m on the northwestern flank of the Susuz Dağ (Fig. 9.1, Section 1) to only 25 m on the southeastern flank (Fig. 9.1, Section 3). The base of the sequence comprises thick- to massive-bedded *algal-bioclastic-packestones* containing algal rhodoliths between 3 and 150 mm in size. The larger nodules comprise nodular branching coralline algae, often formed around a nucleus of a shell fragment. Algal species are dominated by *Lithothamnium pseudoromassissimium poignant* with subordinate *Solenomenis dowilli Pfender* and *Lithoporella melobesoides* (Orszay-Spender *et al.*, 1977). Smaller, smoother, well rounded laminated nodules comprise the following species (Orszay-Spender *et al.*, 1977), *Lithophyllum capedeni, Lithophyllum lacroisi, Lithophyllum microsporum, Lithothamnium* cf *microsporangium, Pseudolithothamnium album, Dermitholithon, Lithoporella* and fragments of *Archeolithothamnium intermedium.*

Bioclastic debris comprises, gastropods, bryozoan, encrusting forams, echinoids (mainly *Clypeaster sp.*) and benthonic foraminifera. Intergranular space is filled by a micrite matrix.

Massive limestones at the base are overlain by a sequence of beige-white limestones with abundant bioclastic debris interbedded with white-grey argillaceous limestone and grey-green calcareous marl, both contain abundant planktonic foraminifera and rare bivalve and echinoid debris. The former limestones consist of *bioclastic-algal packestones* and *grainstones*, often with well developed normal grading. Bioclastic debris is identical to the underlying massive limestones. The percentage of limestones decreases upwards and is progressively replaced by marls, terrigenous mudstones and finally by interbedded mudstones and sandstones of the Kemer Formation (Chapter 4).

Interpretation

The faunal assemblage in the massive limestones at the base of the sequence suggests a shallow open marine moderate to high energy environment. Rhodoliths are found in similar conditions at the present day in water depths of less than 80 m (Bosellini and Ginsburg, 1971).

The sequence thickens to the west, suggesting a gradual marine transgression, over the previously exposed carbonate platform, from the west (Poisson, 1977). Upwards there is a gradual transition to deeper water as evidenced by the incoming of hemipelagic marls with abundant planktonic foraminifera. Interbedded graded limestones were deposited by turbidity currents and other sediment gravity flows eminating from the shallow water areas along the margin of the basin.

This sequence passes transitionally upwards into thin-bedded terrigenous clastic turbidites of the Kemer Formation (Chapter 4).

Summary. Along the western margin of the S. Bey Dağlari and Susuz Dağ, the Miocene is marked by a transgression that prograded gradually eastwards (Poisson, 1977). In central areas Burdigalian sandstones and mudstones rest disconformably on limestones of Eocene age (Fig. 9.1, Section 5) suggesting that central areas of the platform remained subaerially exposed. Along the eastern margin hemipelagic marls of Oligocene age pass upwards without a break into Lower Miocene sandstones and mudstones (Salir Formation, Fig. 9.1, Section 8). The progressive evolution of the *southern area* of the Bey Dağlari-Susuz Dağ carbonate platform from Upper Cretaceous times, is outlined in Fig. 9.4.

9.3 Comparison with the Northern Bey Dağlari

This section is based mainly on the study of Poisson (1977) summarised in Fig. 9.5, and on data collected during this study.

The history of the platform until the end of the Cenomanian is very similar over the entire Bey Dağlari and Susuz Dağ. A shallow marine carbonate platform with intertidal and supratidal areas and reefal build-ups of Rudists and corals, continued to the end of the Cenomanian. The presence of abundant planktonic foraminifera indicates an open marine environment.

In the *north* the platform underwent irregular subsidence throughout the Upper Cenomanian. Hemipelagic and pelagic limestone sequences pass conformably upwards into Maastrichtian pelagic

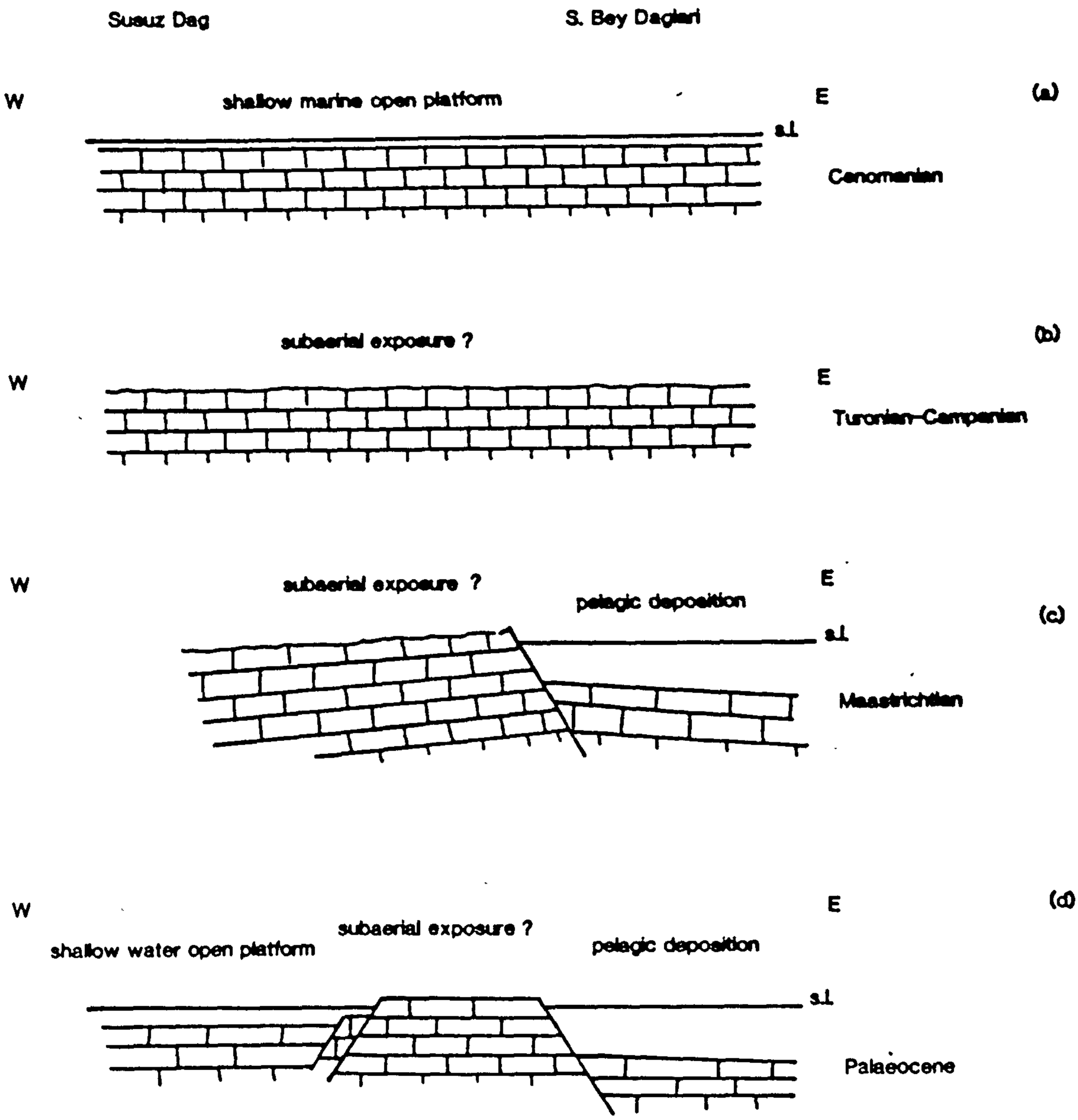

Fig. 9.4

Schematic evolution of the *southern* area of the carbonate platform. Important points to note are the development of a *depositional hinge line* in the Maastrichtian, continued shallow water deposition in the Eocene followed by subaerial exposure in the west. This was followed by the Miocene emplacement of the Antalya Complex from the east (see text for more details).

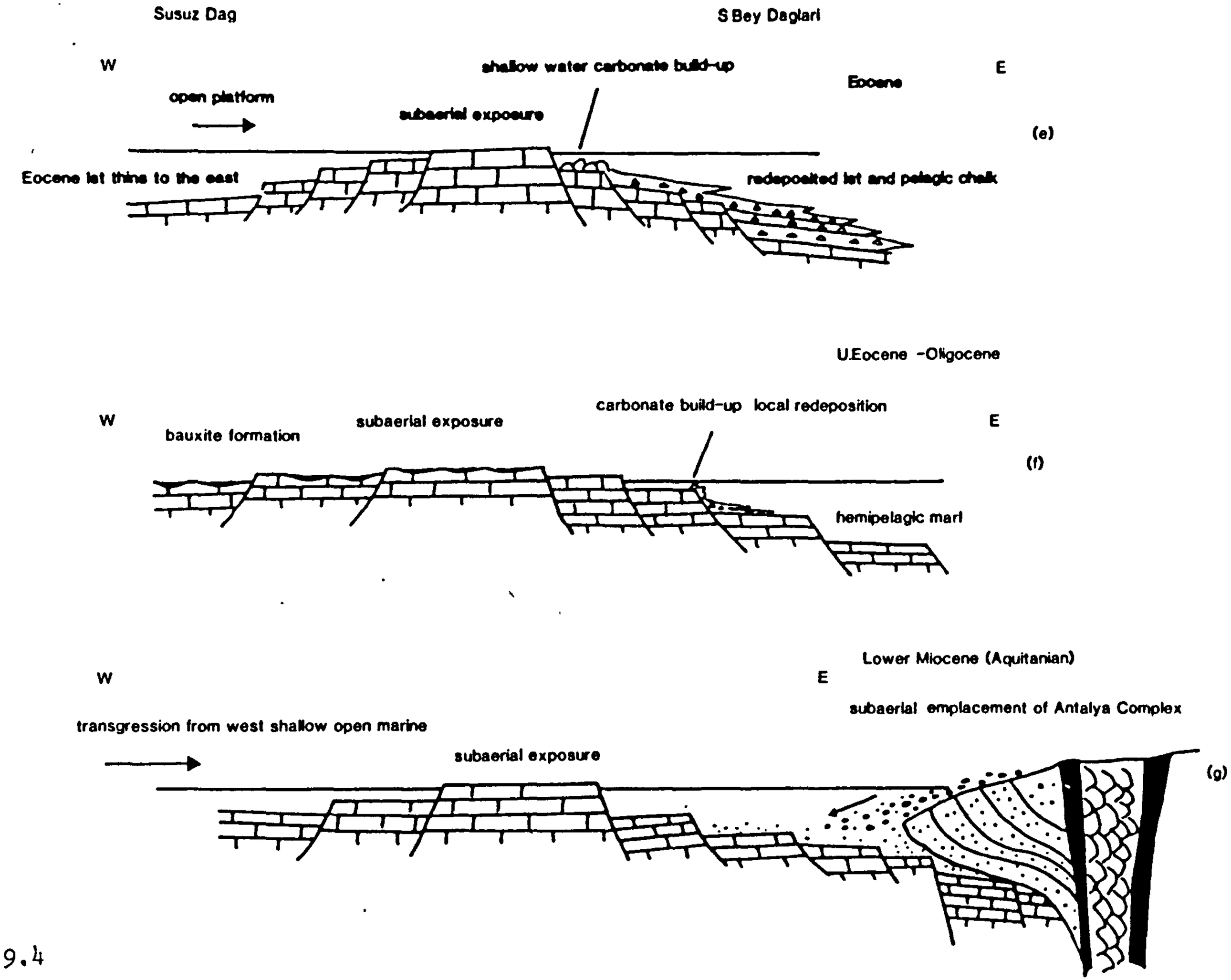
Susuz Dag
S Bey Daglari
W
E
shallow water carbonate build-up
Eocene
open platform
subaerial exposure
(e)
Eocene let thins to the east
redeposited let and pelagic chalk
U.Eocene -Oligocene
W
E
carbonate build-up local redeposition
subaerial exposure
bauxite formation
(f)
hemipelagic marl
Lower Miocene (Aquitanian)
W
E
subaerial emplacement of Antalya Complex
transgression from west shallow open marine
subaerial exposure
(g)

Fig. 9.4

limestones. On upfaulted blocks this period is marked by an hiatus in sedimentation and possible subaerial exposure. In the *south* this period is marked by a widespread hiatus and possible subaerial exposure. By Maastrichtian times pelagic and hemipelagic limestone sequences are widespread in the N. Bey Dağlari (Fig. 9.5). In some areas (e.g. Fig. 9.5, Section 12), breccias were redeposited from local fault bound highs (Fig. 9.6). In contrast pelagic limestones are only present along the eastern margin of the S. Bey Dağlari, central areas of the platform remained uplifted and possibly subaerially exposed (Fig. 9.4).

Along the eastern margin of the S. Bey Dağlari pelagic deposition continues unbroken into the Palaeocene (Fig. 9.1, Section 8). By contrast, in the N. Bey Dağlari, U. Cretaceous and Palaeocene (Danian) pelagic carbonates are overlain by olistostrome melange of Palaeocene and early Eocene age. This influx of terrigenous clastic sediment marks the initial tectonic break-up and emplacement of the Antalya Complex (Poisson, 1977; Hayward and Robertson, in press; Robertson and Woodcock, in press). Terrigenous clastic sediments (turbidites and olistostrome melange) are interbedded with pelagic limestones and calcarenites. The calcarenites contain a shallow marine bioclastic fossil assemblage and lithoclasts of platform limestone (Poisson, 1977). Turbidite sedimentary structures suggest they were derived from carbonate build-ups located on upfaulted blocks (Fig. 9.6).

Olistostrome melange reaches greatest development in early Eocene times (Fig. 9.5, Section 56). At the same time thick sequences of redeposited bioclastic calcarenites (e.g. Fig. 9.5, Section 51) suggest extensive shallow water carbonate build-ups. Redeposited calcarenite of Eocene to Oligocene age are seen both sides of the N. Bey Dağlari (Fig. 9.5, Sections 14 and 60). Along the eastern margin up to 150 m of redeposited calcarenites interbedded with pelagic micrites accumulated (Hayward and Robertson, in press). In the north these Eocene sequences are *in situ* beneath the basal thrust of the Antalya Complex (Hayward and Robertson, in press, Robertson and Woodcock, in press). Identical facies in the south are tectonically intercalated between Miocene sequences of the adjacent autochthon and the allochthonous Antalya Complex (Fig. 9.3). Open marine, shallow water carbonate deposits accumulated over the entire Susuz Dağ massif and on top of fault bound blocks in central areas of the N. Bey Dağlari.

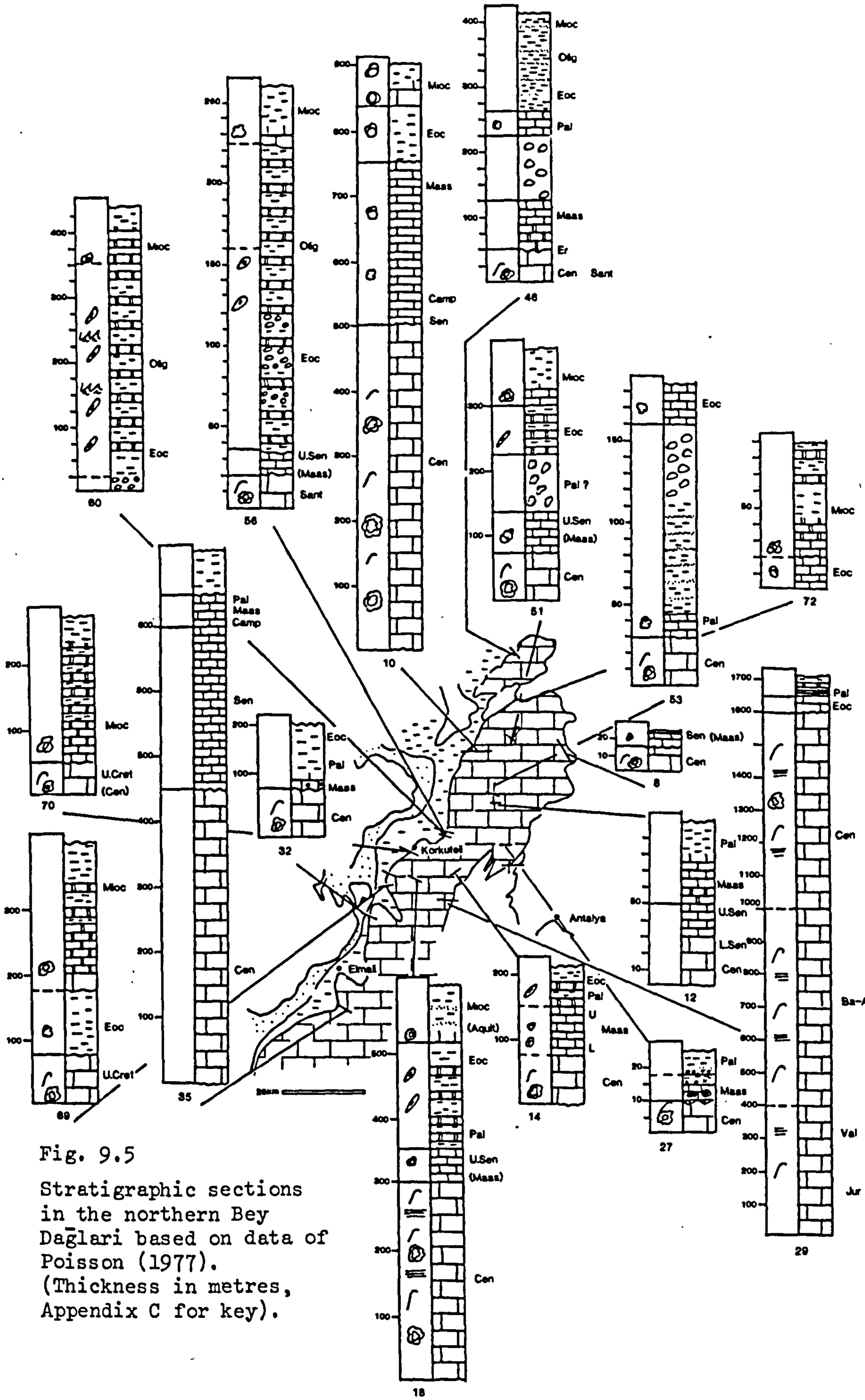

Fig. 9.5

Stratigraphic sections in the northern Bey Dağlari based on data of Poisson (1977). (Thickness in metres, Appendix C for key).

N.Bey Daglari

W E

shallow marine open platform

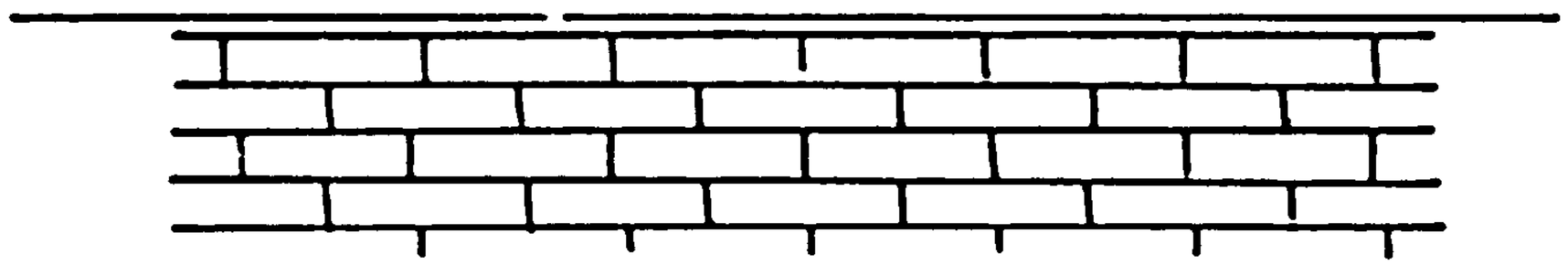

U.Jurassic–Cenomanian

(1)

W mainly pelagic deposition E

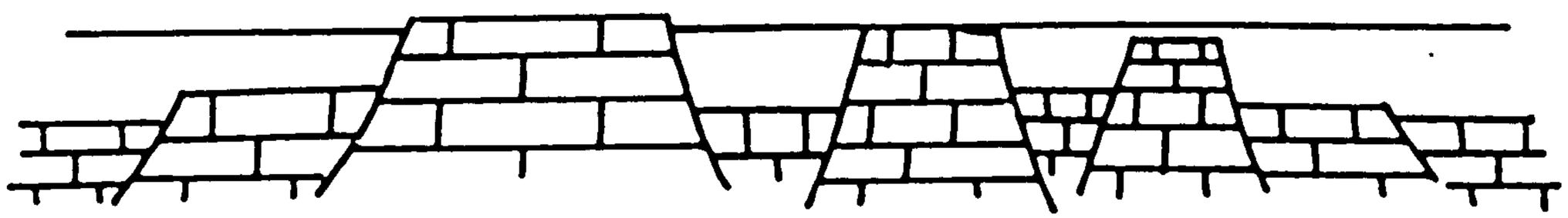

U.Senonian–Maastrichtian

(2)

W E

some redeposition pelagic sedimentation

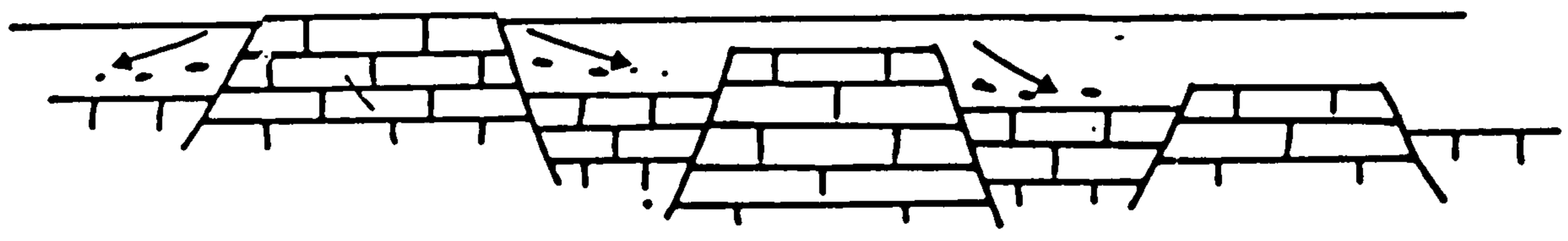

Maastrichtian

(3)

Fig. 9.6 (for explanation see over)

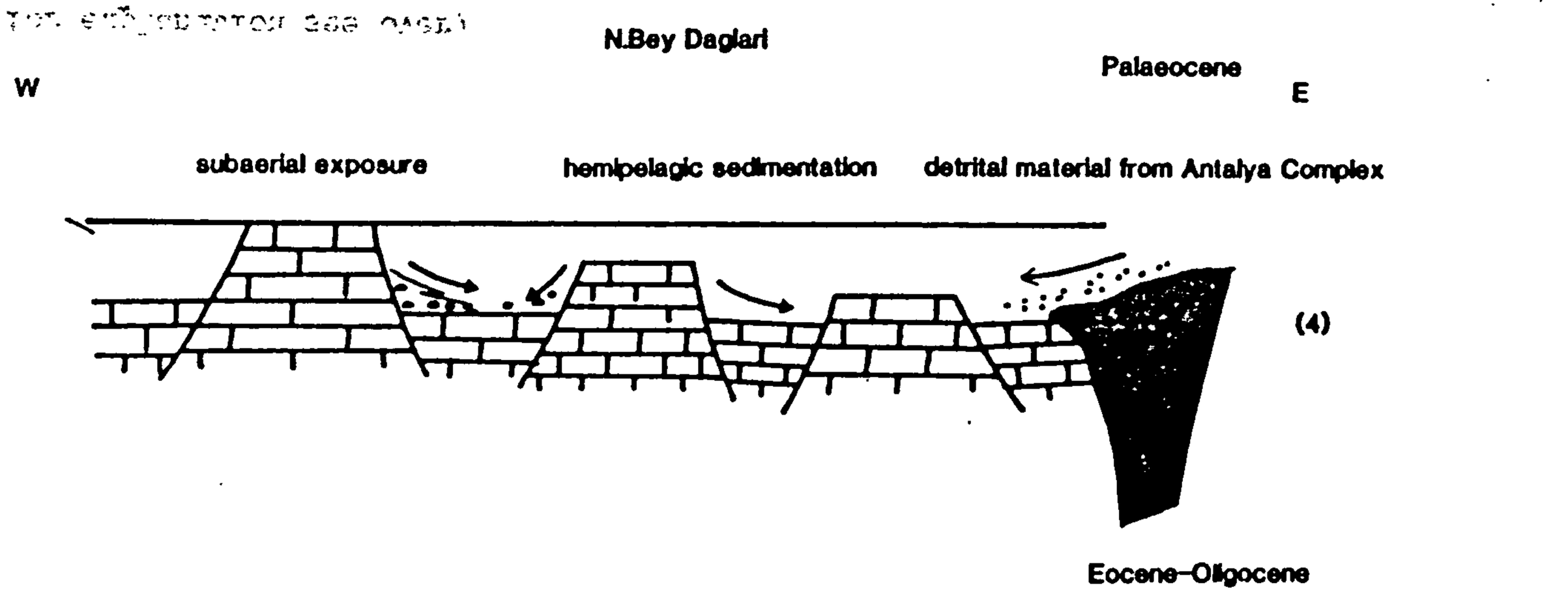

Fig. 9.6

Evolution of the Northern Bey Dağlari.

Important points are the widespread, irregular subsidence from Upper Senonian times onwards and initial submarine emplacement of the Antalya Complex in the Palaeocene (see text for more details).

The Oligocene marks the most enigmatic period in the carbonate platform history. In central and northern areas of the N. Bey Dağlari Eocene deep water redeposited facies pass upwards into Oligocene sequences of a similar type (Fig. 9.5, Sections 46, 56, and 60) indicating basinal areas of hemipelagic marl deposition and upfaulted areas on which shallow water carbonates accumulated. Elsewhere in the N. Bey Dağlari Oligocene sequences are absent and Eocene sediments are overlain by shallow water (<100 m, based on the presence of Rhodoliths) limestones and marls of Miocene (Aquitanian) age.

Over most of the N. Bey Dağlari Aquitanian limestone lies disconformably on underlying sequences that range from Cenomanian to Oligocene in age, indicating a general period of subsidence (see further discussion in 10.2.0). Limestones and marls at the base pass upwards into thin-bedded sandstones and mudstones of Lower Miocene (Burdigalian) age.

9.4 Carbonate Platform History : Summary

Over the S. Bey Dağlari and Susuz Dağ exposed sequences span U. Cretaceous to Miocene, in the N. Bey Dağlari a slightly lower erosion level exposes sequences as old as Jurassic (Fig. 9.5, Section 29). The early history of the carbonate platform can only be elucidated by study of redeposited carbonate sequences originally in areas marginal to the carbonate platform and now found within thrust slices in the adjacent Antalya Complex.

Within the Antalya Complex large detached blocks of reef limestone first occur in late Triassic times (Robertson and Woodcock, in press). They are found associated with redeposited calcirudites and calcarenites interpreted as a platform edge facies association. An extensive fauna of corals, sponges, algae, ammonites, gastropods and benthonic foraminifera indicates a late Triassic (Carnian-Norian) age (Cuif, 1974). This sequence is evidence that by latest Triassic times the carbonate platform had become fully established. A shallow marine open platform enviroment continued from late Triassic times, through the Jurassic, to U. Cretaceous times. Progressive subsidence during this interval was balanced by the deposition of up to 2,000m of shallow water carbonates (Poisson, 1977).

Regional variations in sedimentary facies first become apparent in the carbonate platform in U. Cenomanian times. During the U. Cenomanian northern areas undergo subsidence while southern areas

remain exposed, suggesting a general N-S tilting and irregular block faulting of the northern margin, to pelagic depths (ca. 500-1,000 m). This is followed in the Maastrichtian by continued subsidence in the north and development of a depositional hinge along the southeastern margin. Through the Palaeocene, Eocene and Oligocene subsidence and faulting continued in the north and east, in south central areas periods of emergence are interspersed with shallow water carbonate deposition. In the north initial tectonism of the Antalya Complex during this time resulted in an incursion of terrigenous clastic sediment.

The Miocene is marked by regional subsidence of the entire carbonate platform possibly as a result of thrust loading associated with emplacement of the Lycian Nappes in the west (see discussion, 10.2.3). Carbonate deposition gives way to terrigenous clastic sediments derived from both the Antalya Complex to the east and the Lycian Nappes to the west.

PART IV

CONCLUSIONS

PART IV

CONCLUSIONS

CHAPTER 10 BASIN SUMMARY AND REGIONAL IMPLICATIONS : CONCLUSIONS

CHAPTER 10

10.0 Basin Summary and Regional Implications : Conclusions

10.1 Introduction

This chapter discusses sedimentary models for the entire Miocene sedimentary basin, from its inception in earliest Miocene (Aquitanian) to its termination in Late Miocene times (Tortonian), in which sedimentary facies and sediment distribution are related to tectonic events. This is followed by a brief discussion of the implications of this study for the regional geology of southwestern Turkey and the Eastern Mediterranean area in general.

10.2.0 Summary of the Southern Area

The Kasaba sedimentary basin clearly extended a considerable distance outside the present study area, the approximate dimensions are discussed below (10.3). This section summarises and relates the various sedimentary systems into a basin model for the study area (S. Bey Dağlari and Susuz Dağ.)

10.2.1 Eastern Margin

Along the entire eastern margin of the Bey Dağlari pelagic deposition is continuous from Maastrichtian times into the Oligocene (9.2, Fig. 9.1). Ophiolite-derived clastic sediments are absent in the carbonate platform sequences in the southern area of the Bey Dağlari prior to the Miocene; indicating that during this period (U. Cretaceous-Oligocene) the Antalya Complex formed a low lying submarine area to the east of the partially subsided carbonate platform margin (Fig. 10.8).

By *early Miocene* times the Antalya Complex formed an *elevated landmass* to the *east* of the already subsided eastern margin of the Bey Dağlari carbonate platform (9.2.5). As the Complex was emplaced the carbonate platform continued to subside possibly as a result of flexural loading associated with thrusting (see discussion below, 10.2.3). The Antalya Complex was rapidly eroded, rivers supplied the conglomerates to *fan-deltas* which in turn fed a series of small *submarine fans*. Palaeocurrent orientations and grain size variations are consistent with a broadly ENE-WSW palaeoslope (5.2). Irregular subsidence and faulting in the underlying carbonate platform resulted in considerable volumes of carbonate clastics, and fault-derived detached blocks, being shed into the basin (5.7). In the north of

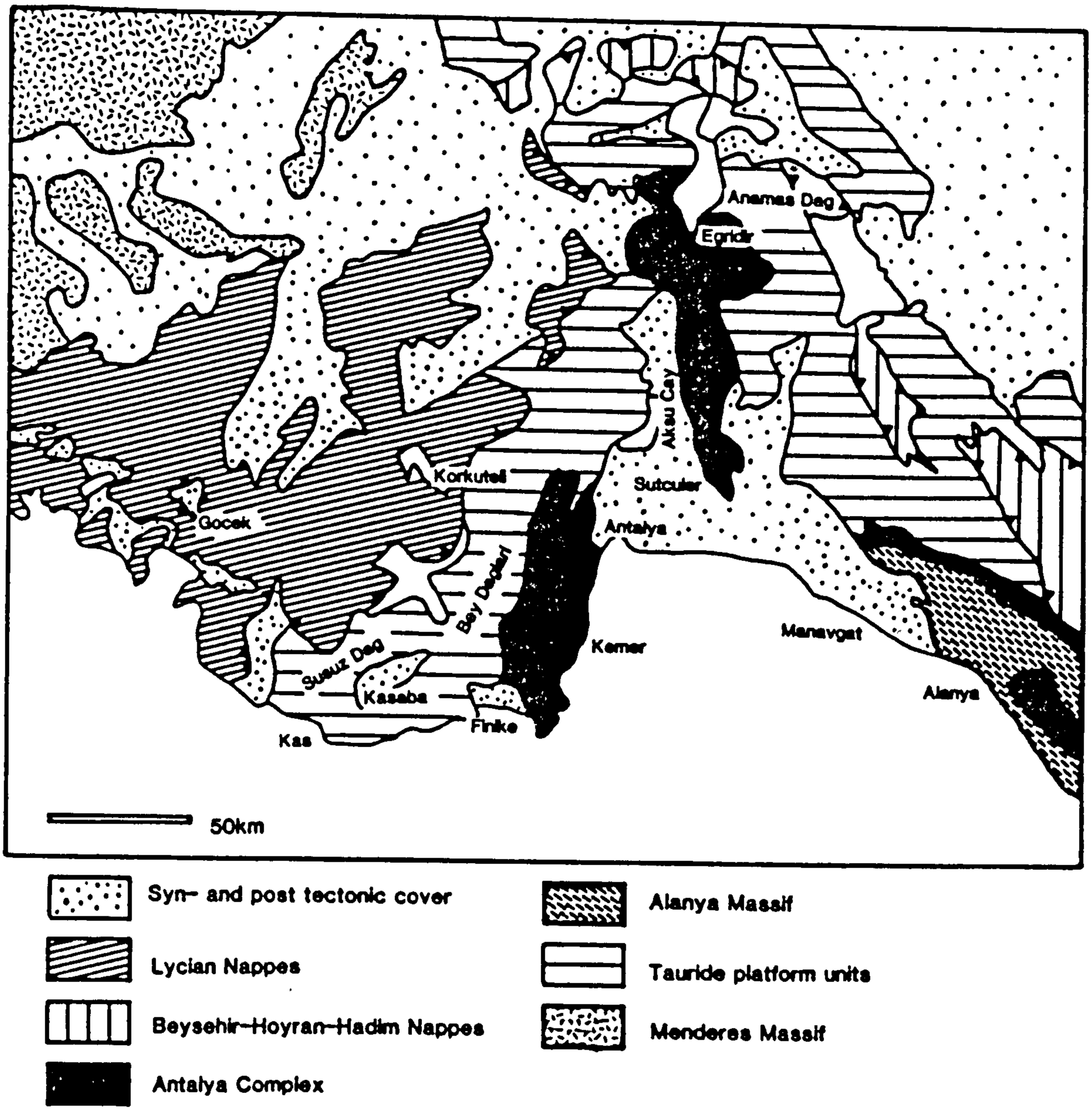

Fig. 10.1

Geological map of southwestern Turkey showing main structural units and localities mentioned in text.

the Akdere valley submarine faulting and *local submarine* impingement of the Antalya Complex against the platform is indicated by a very thick sequence of *debris flow olistostromes* and very large olistoliths derived off the front of the Antalya Complex as it advanced (5.7.1).

The submarine fan phase of sedimentation was abruptly terminated in *mid-Miocene* times by the *westward thrusting* of the Antalya Complex near to its present position. In the east, the Antalya Complex overrode the earlier Miocene submarine fan sequence forming a basal tectonic melange and preventing further deposition. Slivers of marginal, Eocene, Bey Dağlari limestone sequences (9.2.3) were stripped off and entrained along the sole thrust of the Antalya allochthon (Hayward and Robertson, in press). To the west *alluvial fans* prograded over the autochthon (5.11), where coarse grained ophiolite-derived deposition continued until Upper Miocene times (5.11, Fig. 5.35, and Fig. 10.8).

Distance of overthrusting. The distance the Antalya Complex has been thrust over the Miocene clastic sediments cannot be determined accurately from structural analysis of the allochthonous units (Woodcock and Robertson, 1981a; Woodcock, pers. comm., 1980). An alternative approach is to examine the *in situ* sedimentary facies transitions. The distance between the coastline (hinterland) and inner fan area on small submarine fans, in present day areas, varies from less than 8 km in the Red Sea, to distances of greater than 50 km where a significant continental shelf is present. Similar small immature submarine fan systems, for example along the coast of California at the present day typically have an inner fan to shoreline extent of ca. 10-40 km. The indications from sedimentary facies associations (5.0) are that the small submarine fans of the eastern margin sequences (Salir Formation) were fed over a narrow relatively high gradient shelf by a series of fan-deltas. In a sedimentation system such as this it is unlikely that the coastline-inner fan transition was more than 10-15 km. This suggests that the *autochthon has been overthrust by the order of 15 km* and that the Bey Dağlari extends beneath the Antalya Complex more than half the distance to the present day coastline. The presence of mid-Upper Miocene alluvial fan deposits in the Akçay area (Bağbeleni Member, 5.8) prohibits overthrusting of the Antalya Complex onto central

areas of the autochthon more than 6 km from its *present* position. Total overthrusting was therefore probably of the order of 20 km.

Comparison with the northeastern margin of the Bey Dağlari. In the north, ophiolitic olistostromes and turbidites were first shed into the Bey Dağlari carbonate platform in Palaeocene to early Eocene times (9.2.2, Fig. 9.6). This influx of terrigenous sediment marks the *initial* impingement of the Antalya Complex against the carbonate platform. Earlier (U. Cretaceous, Maastrichtian) tectonic events in the Antalya Complex are recorded by ophiolite-derived olistostrome debris flows in offshore carbonate build-ups in the Godene Zone (Robertson and Woodcock, 1981b, c). Ophiolite-derived sediments in the N. Bey Dağlari are related to the major phase of *northeastward directed thrusting* recognised by Waldron (1981) in Coubre d'Isparta area. At the same time the Antalya Complex was undergoing extensive tectonic movement along *strike-slip* faults (Robertson and Woodcock, 1980a, in press), see also discussion below (10.6.3). The olistostromes and turbidites are consistent with a submarine derivation and as in the southern area of the Antalya Complex there is no evidence of subaerial exposure at this time.

Along the northeastern margin of the Bey Dağlari the sole thrust of the Antalya Complex overlies redeposited Eocene limestones (9.2.3). This absence of ophiolite-derived sediments beneath the Antalya Complex implies that the area was tectonically overriden relatively early, prior to the subaerial exposure of the Antalya Complex, or that the basin along the northeastern margin formed a narrow trough and any ophiolite-derived sediments of Miocene age have been over-thrust.

10.2.2 Western Margin

Palaeocurrents and downslope sedimentary facies transitions (Chapter 4) clearly indicate that the ophiolite-derived sediments of the western margin (Kemer and Kasaba Formations) were derived from the Lycian Nappes. Shallow water limestones of Aquitanian age are overlain by thin-bedded turbiditic sandstones and mudstones with abundant planktonic foraminifera. This sequence of Burdigalian age marks the *initial* phase of nappe emplacement and *rapid subsidence*, probably to depths of ca. 500-1,000 m, of the carbonate platform. In order to understand fully the role of the Lycian Nappes in the formation of the sedimentary basin and to estimate their rate of

movement it is necessary to look outside the immediate study area.

The Lycian Nappes extend from the western margin of the Susuz Dağ for approximately 130 km to the border of the Menderes Massif (Fig. 10.1, 1.3.2). In the area of Gocek (Fig. 10.1) a tectonic window in the nappe pile reveals an autochthonous carbonate platform sequence overlain by Miocene clastic sediments of Burdigalian age (Graciansky, 1972) (Fig. 10.2). The sediments are very comparable both in petrography and facies types to those described from the Susuz Dağ. Shallow water Aquitanian limestones are overlain by ca. 75 m of shallow marine conglomerates, sandstones and mudstones (Graciansky, 1972), of Lower to Upper Burdigalian age. This sequence is overlain by approximately 20 m of melange above which lie the Lycian Nappes (Fig. 10.2). The melange comprises of large blocks of all lithologies from the overlying nappe pile, along with chaotically slumped, deformed sandstones and conglomerates from the underlying sedimentary sequence. It is interpreted by Graciansky (1972) as a sedimentary melange related to nappe emplacement. The shallow marine conglomerates and sandstones are here interpreted to represent the proximal (marginal) sequence of thin-bedded mudstones and sandstones of Lower to Upper Burdigalian age that overlie Aquitanian limestone in the Susuz Dağ area (e.g. Sinekçibeli, Fig. 4.3).

Rate of nappe movement. The sequence exposed at Gocek, as well as documenting the gross allochthonous nature of the Lycian Nappes, allows an estimate of the rate of nappe movement during Burdigalian to Langhian times to be made. In the Gocek window the sedimentary sequence is truncated by nappe emplacement in Upper Burdigalian times (Graciansky, 1972). By contrast, along the western margin of the Susuz Dağ the sedimentary sequence is not truncated by nappe emplacement until Langhian times (4.1, Fig. 10.2). The Gocek window lies approximately 70 km to the west of the Susuz Dağ, indicating that in a period of approximately 3 myrs. the Lycian Nappes were translated ca. 70 km at an average rate of 2.5 cm/yr.

10.2.3 Thrust-Loading as a Mechanism for Basin Formation

The subsidence of the carbonate platform and subsequent basin formation (at least in the western area, Susuz Dağ etc.) are clearly closely related to the emplacement of the Lycian Nappes. Beaumont (1981) has recently proposed a model whereby sedimentary basins form in response to the lateral transfer of a rock mass over an adjacent

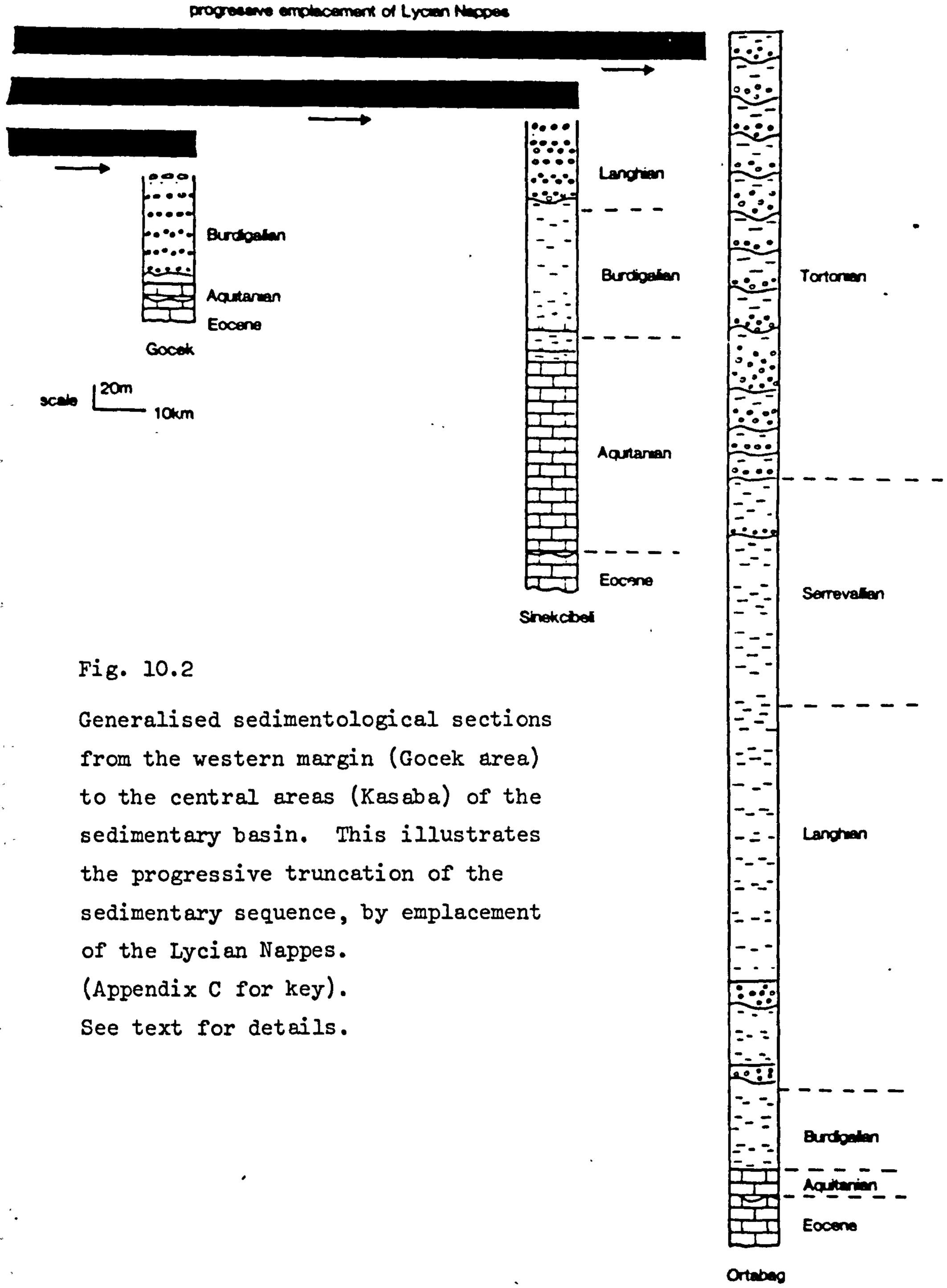

Fig. 10.2

Generalised sedimentological sections from the western margin (Gocek area) to the central areas (Kasaba) of the sedimentary basin. This illustrates the progressive truncation of the sedimentary sequence, by emplacement of the Lycian Nappes.
(Appendix C for key).
See text for details.

part of the lithosphere. The lithosphere responds by downward flexure in response to passive loading of the supralithospheric mass. This results in a *coupled trough* being created in front of the fold-thrust belt in which sediments can accumulate (Fig. 10.3). Although the basins discussed by Beaumont (1981) are in some cases an order of magnitude larger than the present one, similar physical principles probably apply.

An interesting aspect of the flexural loading model for basin formation is the *flexural upwarp* predicted (and observed in areas such as the Rocky Mountains, Beaumont, 1981) along the margin of the basin opposite the thrust belt (Fig. 10.3). This may be applicable in the present area. Initial emplacement of the Lycian Nappes and subsequent loading of the carbonate platform in Lower Burdigalian times was west of Gocek (Fig. 10.1) in the area adjacent to the Menderes massif. This resulted in the formation of a sedimentary basin that extended for greater than 150 km west to east (see also 10.3). Over most of this area the *Lower Miocene* (Burdigalian to Langhian) is a period of very *rapid subsidence*, in some areas up to 1,000 m of sediment accumulated during this period (e.g. Korkutelli area, N. Bey Dağlari, Fig. 10.1). However, in the area southwest of Kaş the *carbonate platform* was *uplifted* and thick sequences of platform derived conglomerate and sandstone (Felenk Dağ Member, 7.2.0) accumulated along the southeastern margin of the basin. Evidence of uplifted carbonate platform is also seen at this time in the Çağman area (Çağman Member, 7.1.0).

The Felenk Dağ Member in particular may be related to a peripheral upwarp formed as a result of thrust loading (Fig. 10.3).

Subsidence and sedimentation rates. In the Kasaba area and further north at Korkuteli (Fig. 10.1), subsidence of the carbonate platform during Burdigalian to Langhian times was extremely rapid (Fig. 10.4). In the Kasaba area ca. 750 m of sediment accumulated in 5 myrs. at an average rate of 15 cm/1,000 yrs. Sedimentation slowed during the Serravallian, when only ca. 200 m of sediment accumulated. This period could represent a pause in nappe movement. The overlying Tortonian sequence (Kasaba Formation) again marks a period of rapid subsidence, over 350 m of sediment accumulating in approximately 4 myrs. at an average rate of 7 cm/1,000 yrs.

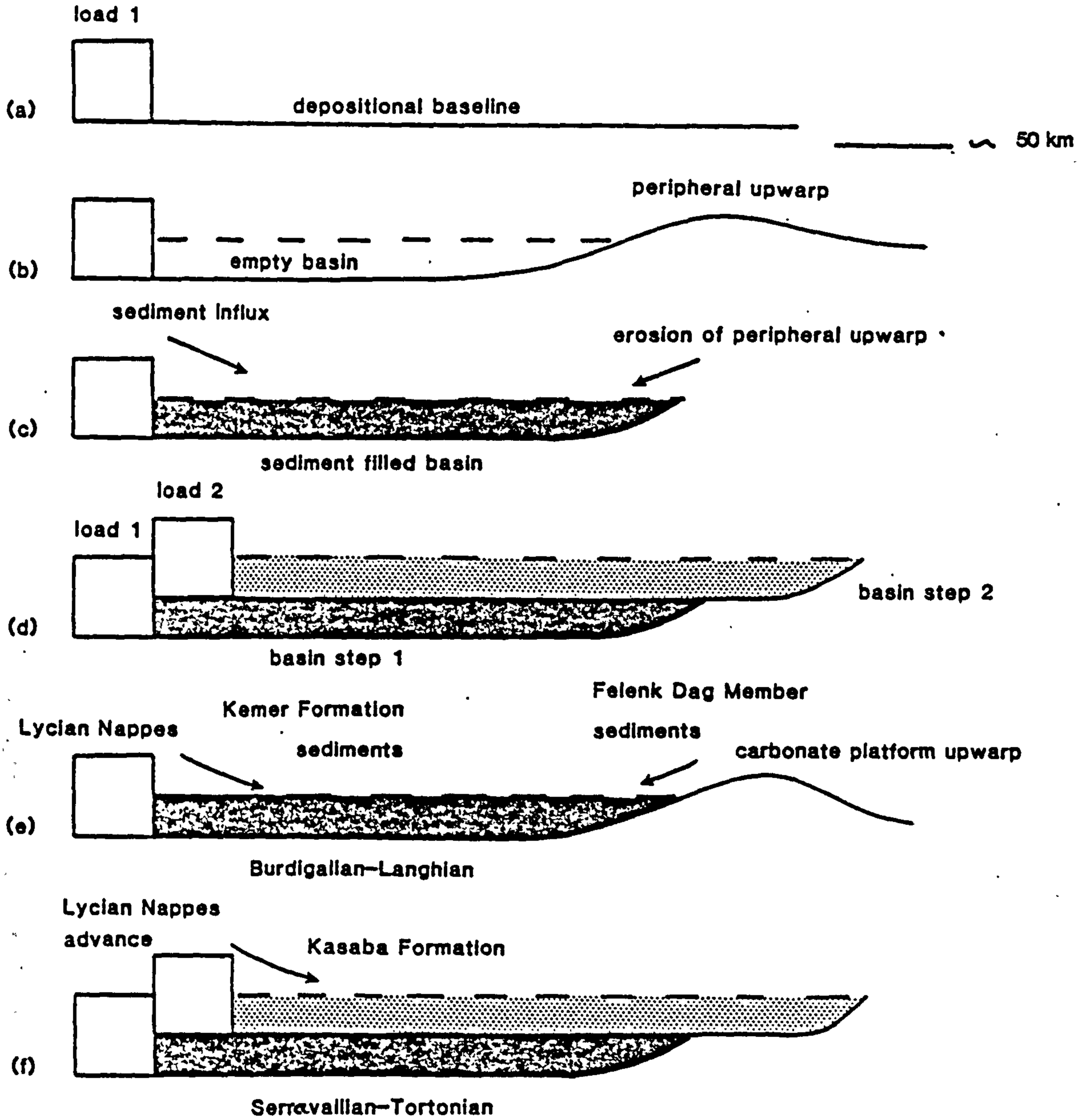

Fig. 10.3

The flexural model for basin formation (after Beaumont, 1981).
The loads of the thrust belt induce a foredeep that is subsequently filled with sediment (as in a, b and c, see text for details).
In d and e the model is applied to the Miocene sedimentary basin (see text for details).

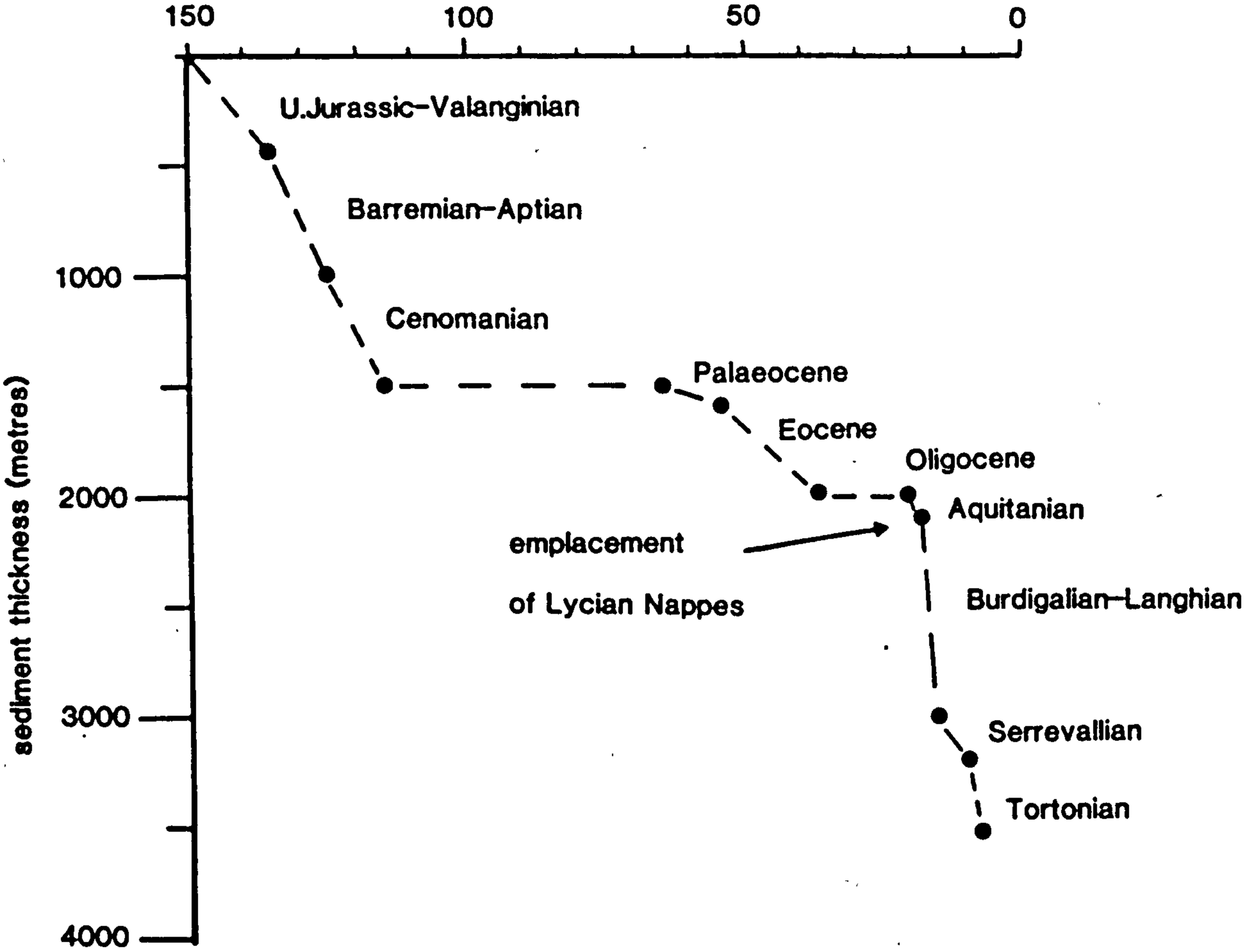

Fig. 10.4

General subsidence curve for the Susuz Dağ area (computed by plotting sediment thickness against time). The early parts (Jurassic-Aptian) are calculated from the data of Poisson (1977) from the northern Bey Dağlari. This is probably valid for the southern area (Susuz Dağ) as during this period the platform behaved uniformly.
Note the dramatic increase in subsidence rate following emplacement of the Lycian Nappes.

10.2.4 Summary of the Western Margin and Central Areas of the Basin

Nappe loading in Lower Burdigalian times resulted in rapid subsidence and the formation of a sedimentary basin that extended westwards from the Susuz Dağ at least as far as Gocek (Fig. 10.5). In this area shallow marine conglomerates and sandstones accumulated at the foot of *fan-deltas* and passed eastwards into a thin-bedded (distal) turbidite sequence. At the same time irregular subsidence and uplift of the carbonate platform southwest of Kaş, possibly related to a peripheral upwarp, resulted in a thick sequence of carbonate-derived clastic sediments being deposited along the southwestern margin of the basin (Felenk Dağ Member, Kemer Formation, 7.12.0) The Çağman area also records evidence of irregular subsidence and syndepositional fault activity in the underlying carbonate platform. *Eastward thrusting* of the Lycian Nappes terminated deposition in the Gocek area in U. Burdigalian times. Along the western flank of the Susuz Dağ (Fig. 10.5 Sinekçibeli) a coarsening-upward sequence reflects the progressive approach of the nappe front. In this area during Langhian times *fan-deltas* derived off the nappe front passed downslope into a small *'submarine fan'* system. In U. Langhian times the *marginal areas* of the basin (e.g. Sinekçibeli area, Fig. 10.5) were *overthrust from the west.* Deposition continued in central areas of the basin. During Serravallian times subsidence slowed and coarse terrigenous clastic sediment input was minimal. This period probably represents a hiatus in nappe emplacement. A *final phase* of *southwestward thrusting* in Tortonian times, was again accompanied by rapid subsidence, resulting in a thick coarse grained clastic wedge (Kasaba Formation) which prograded into a shallow sea. The petrography of the Kasaba Formation (6.0) suggests that the carbonate platform may have been involved in this last phase of thrusting, possibly along high angle reverse faults, present on the southwestern limb of the Susuz Dağ anticline (1.5.1, see also map 2 in backcover).

10.2.5 Comparison between West and Eastern Margins of the Sedimentary Basin

The two margins are broadly similar in that they were both supplied with coarse grained terrigenous ophiolitic material, derived off a tectonically active allochthonous unit.

Along the western margin fan-deltas derived from the Lycian

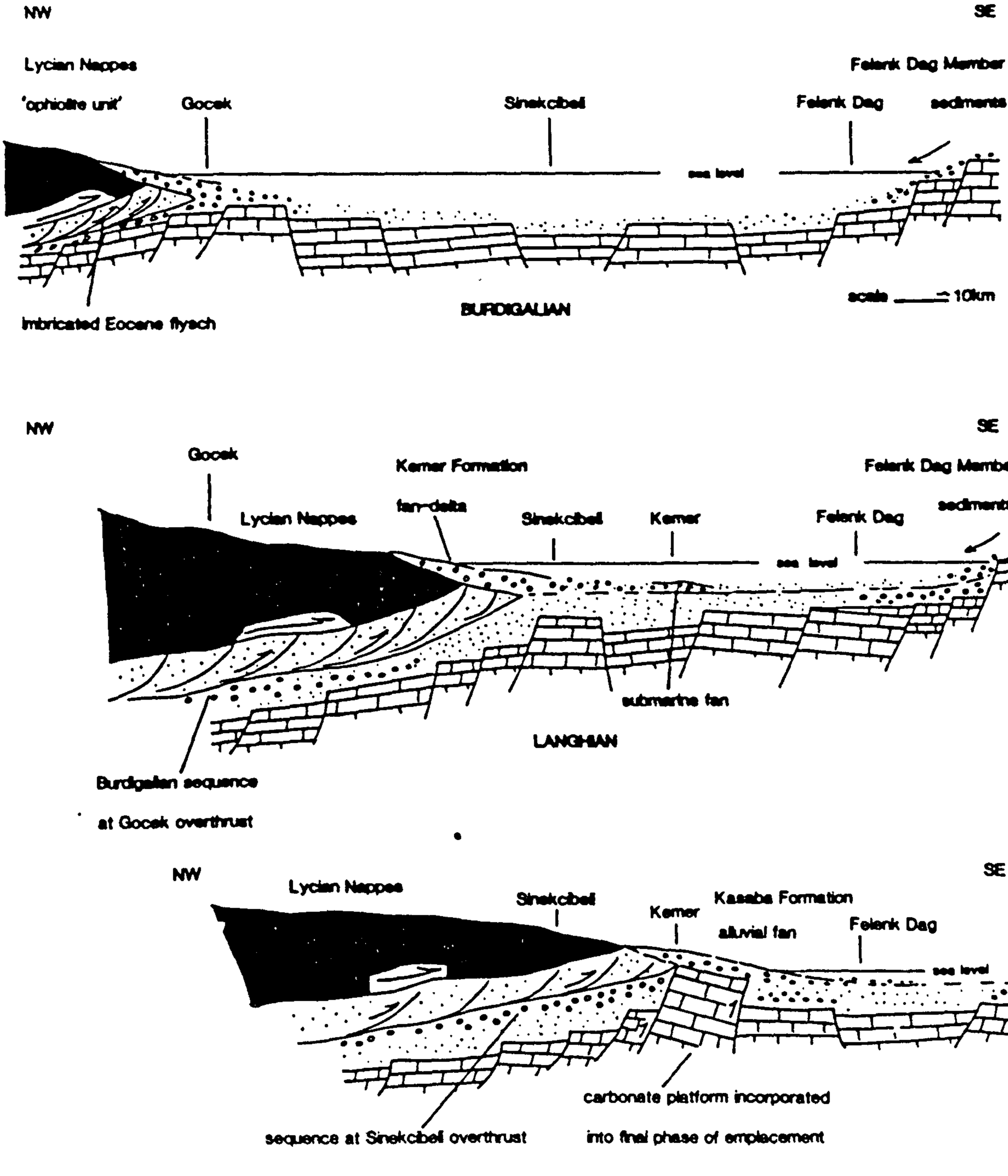

Fig. 10.5

Model for the Miocene emplacement history of the Lycian Nappes. This shows the progressive overthrusting of the sedimentary basin formed in front of the thrust pile. The carbonate platform only becomes involved in the very last stages of nappe emplacement (see text for details).

Nappes prograded into a shallow sea with a 'wide' (several kilometres) shelf and apparently low slope. The fan-delta fed a large submarine inner-fan channel. Migration of the submarine fan channel was related to the active area of sedimentation on the fan-delta(s) (Fig. 4.18) and for long periods of time the submarine fan system was located in one area.

On the eastern margin the Antalya Complex was uplifted along strike-slip faults, a complex of fan-deltas prograded directly into deep water onto the previously subsided and dissected carbonate platform. Gravel and sand were redeposited down a large number of adjacent channels (5.11).

On both margins the initial phase of sedimentation was terminated in proximal areas by overthrusting of the allochthonous units. In the east submarine fan sequences are overlain abruptly by deposits of a fan-delta. In the west the upward transition is more gradual, reflecting a probable pause in nappe movement at this time and a low relief source area. The absence of coarse material, derived from the eastern margin of the basin, within sequences of the western margin, during this period (mid-Miocene, U. Langhian-Serravallian) suggests that the two may not have been connected at this time. Along the western margin of the basin the final stage of nappe emplacement in the U. Miocene results in a coastal alluvial fan sequence overlying a shallow marine sequence.

In the eastern area the uppermost parts of the sequence have been removed by erosion. However, in the west the sequence is continuous up until the Tortonian. Throughout this sequence there is *no* direct evidence of any *large scale* eustatic sea-level changes. Studies of Miocene sequences in the Levant and Red Sea area (Gwirtzman and Buchbinder, 1977) suggest a grouping of relative sea-level changes to two time periods in the Miocene. The first *minor* change occurred during the Middle Miocene, the second *major* change recorded over the entire Mediterranean area during the Messinian. Although there is some evidence for the Middle Miocene event in the general shallowing-upwards recorded in the sedimentary sequence, *sedimentation patterns* are more clearly *related* to *tectonic events* and progressive infill of the sedimentary basin. The Messinian dessication event seen over the whole Mediterranean (Hsu *et al.*, 1973) is reflected in the semi-arid palaeoclimate in the Upper Miocene (Tortonian) Kasaba Formation sequences. Sedimentation in the area was terminated by the dramatic

drop in base sea-level associated with the Messinian dessication event.

10.3 Dimensions of the Sedimentary Basin and Comparison with Sequences in the Northern Bey Dağlari

The original dimensions of the sedimentary basin can be approximately estimated by removing the thrust sheets that have been emplaced on either side. To the west the basin extended at least to Gocek and probably slightly further in Burdigalian times. In the east the Antalya Complex has been thrust ca. 20 km over the Miocene clastics to its present position. In the southeast (Fig. 10.1) there is some evidence of a shallow water area in Lower to Middle Miocene times (e.g. the source area for the Cağman area, 7.9). However, the size of this is unknown. The presence of small fault bound outliers of Lower Miocene sandstones and mudstones in this area of the carbonate platform (e.g. southeast of Kasaba) suggest that the basin extended to the present day coastline and possibly beyond. In the south, around Felenk Dağ, lithoclastic carbonates are indicative of an area of uplifted carbonate platform, probably located in the area around Kas, and delineate the southern extremities of the basin.

In the Northern Bey Dağlari Miocene ophiolite-derived clastic sediments are widespread along the northwestern limb of the Bey Dağlari (Fig. 10.1). In the area around Korkuteli (Fig. 10.1) a thick sequence (ca. 800 m) of turbiditic sandstones, redeposited conglomerates and mudstones pass upwards into a sequence, approximately 250 m thick, of conglomerates and sandstones within which large reef-derived limestone blocks are found. This sequence is essentially the same as in the Susuz Dağ area and represents the gradual infilling of the sedimentary basin. Submarine fan sequences are overlain by the deposits of a fan-delta. The presence of extensive channellised conglomerate horizons suggests a local point source. In central areas of the N. Bey Dağlari, erosion has reached a deeper structural level than in the S. Bey Dağlari and Miocene sequences which were presumably deposited in this ares have been subsequently eroded.

In the extreme north of the Bey Dağlari sequences of Miocene terrigenous clastic are very poorly exposed. Thin, turbiditic, fine sandstones and mudstones of U. Aquitanian to Burdigalian age reach an exposed thickness of 75 m (Poisson, 1977, p. 159). The absence of any coarse grained sediment in this area precludes a source area

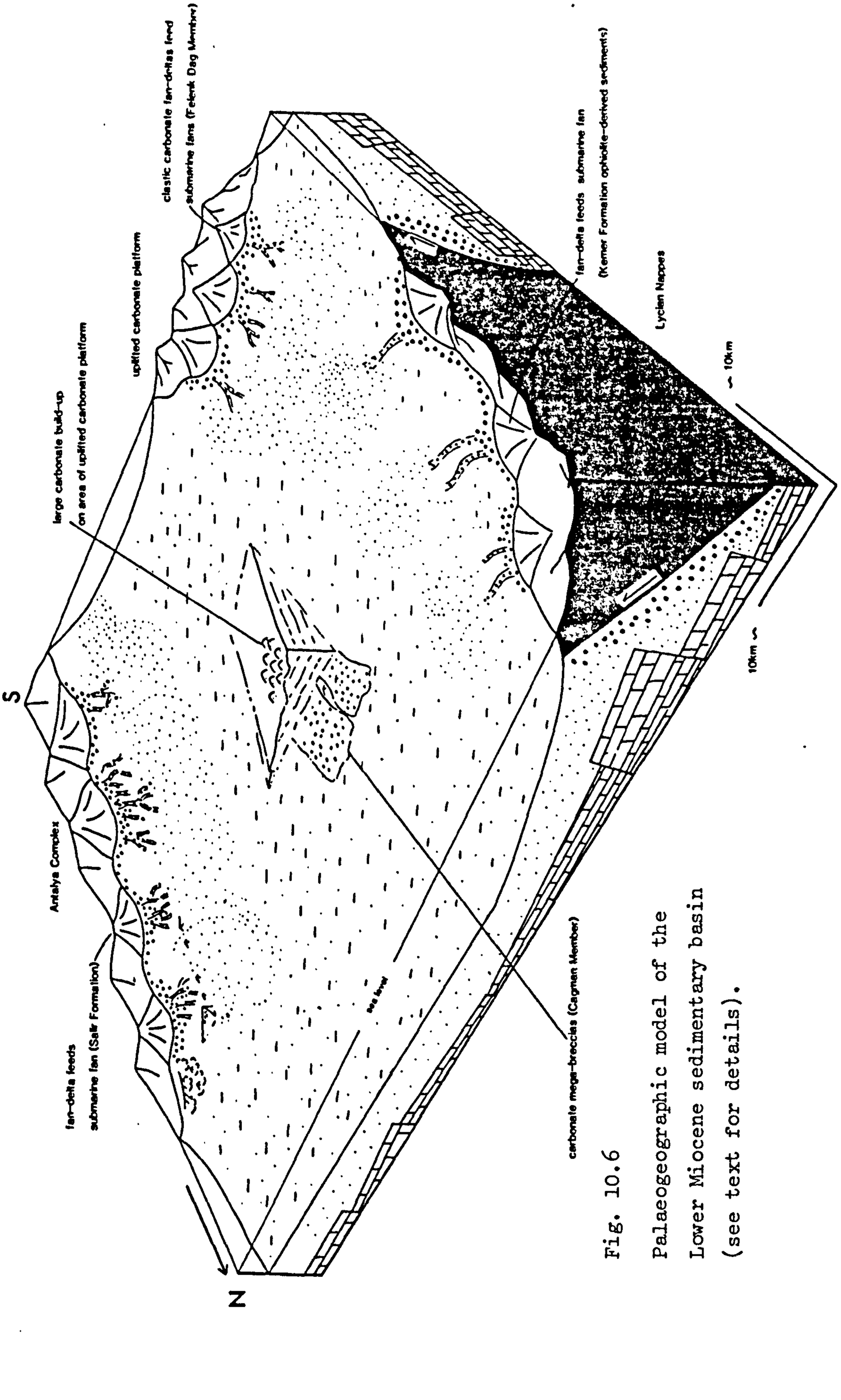

Fig. 10.6

Palaeogeographic model of the Lower Miocene sedimentary basin (see text for details).

to the north. The original northward extent of the Miocene basin is poorly controlled and unknown, although ophiolite-derived Lower Miocene sediments are not present anywhere in the centre of the Coubure d'Isparta (Gutnic, 1977; Waldron, 1981 and pers. comm.). Fig. 10.6 summarises the Lower Miocene model for the sedimentary basin.

10.4.0 Implications for the Original Location of the Antalya Complex

10.4.1 Earlier Work

Lefevre (1967) first recognised the Antalya Complex as a series of allochthonous thrust sheets, prior to this the radiolarites, other thin-bedded sediments and igneous rocks had been considered essentially autochthonous (e.g. Blumenthal, 1963). Initial work assumed that the Complex formed a series of outlying tectonic klippen related to the other major ophiolitic nappe units (Lycian Nappes, Beysehir-Hoyran-Hadim Nappes) in southwest Turkey, thrust southward over the autochthonous carbonate platform sequences during the Tertiary era. Following this the stratigraphic studies of Brunn *et al.* (1970, 1971) demonstrated that continuous sequences in northern areas of the carbonate platform, up to Eocene times, prevented emplacement prior to this date, whereas parts of the Antalya Complex are known to have been emplaced in Late Cretaceous to Palaeocene times. In the light of this evidence Dumont *et al.* (1972a, b) postulated a *southern external* origin for the Complex, suggesting an original location south of the carbonate platform autochthon, in an area that they defined as the Pamphyllian basin which lay between the Tauride platform and the African continental margin, separated from the main Tethys ocean.

In recent years the *"internalist"* hypothesis has again found favour with a number of geologists (Ricou *et al.*, 1974, 1975, 1979; Ricou and Marcoux, 1980; Monod, 1976b; Dumont, 1976b; Dumont *et al.*, 1980). The most recent model proposed by Ricou *et al.* (1979) necessitates that large areas of the Tauride carbonate platform hitherto regarded as autochthonous, or para-autochthonous, be regarded as far travelled allochthonous sheets. In this model the Bey Dağlari is made up of two separate tectonic units, a "Western Bey Dağlari" and an "Eastern Bey Dağlari", supposedly separated by a major trending thrust which runs into the Miocene basal thrust of the Antalya Complex along the S.E. flank of the Bey Dağlari (Figs. 1.2, 10.1).

10.4.2 Evidence for an External Origin

The *sedimentological* results from this study are *unequivocal* in indicating a *southern, external origin for the Antalya Complex.* The following points, outlined by Hayward and Robertson (in press) are critical:

(1) The N-S trending Maastrichtian to Eocene depositional hinge along the eastern margin of the Bey Dağlari shows *no* sign of an offset;

(2) *Sedimentary features* in terrigenous clastic sequences (Salir Formation) related to the emplacement of the Antalya Complex show quite unambiguously that *supply was from the east*, from the direction of the Antalya Complex.

(3) *Sedimentary sequences* in *central areas* of the autochthon (e.g. Kasaba area) (Fig. 10.2) are *continuous until Upper Miocene times.* Whereas the Antalya Complex and Bey Dağlari in the north near Antalya have an unconformable cover of Middle to Upper Miocene age. The Antalya Complex cannot therefore have been emplaced over the western Bey Dağlari during Middle Miocene times as required by the "internalist" hypothesis of Ricou *et al.* (1979).

In addition, structural evidence from the Bey Dağlari also refutes the Ricou hypothesis, in particular:

(1) the *lack* of a penetrative tectonic fabric in the supposedly overthrust 'Western Bey Dağlari'; (II) the absence of any major mapped thrust cutting the Bey Dağlari as opposed to numerous high angle faults.

This evidence is in agreement with recent detailed structural and sedimentological work within the Antalya Complex (Robertson and Woodcock, 1980a; Woodcock and Robertson, 1981a, b; Robertson and Woodcock, 1981a, b, c; Waldron, 1981). Studies of the Antalya Complex adjacent to the Bey Dağlari indicate a simple westward thrusting and imbrication against the platform margin (Woodcock and Robertson, 1981a, b) (1.5.3). The polarity of sedimentary facies within the imbricated sediments confirms this interpretation (Robertson and Woodcock, 1981a, b).

In the Eğridir area, north of Antalya, the sense of thrusting and fold asymmetry is consistently to the north (Waldron, 1981) indicating an original position for the Antalya Complex to the south.

In conclusion, *all* available *field evidence* indicates an *original 'external'* location for the Antalya Complex to the *south and east* of the major platform units of the Western Taurides, as originally proposed

by Dumont *et al.* (1972a, b) and more recently by Robertson and Woodcock (1981a, b), Woodcock and Robertson (1981a, b), Waldron (1981) and Hayward and Robertson (in press).

10.5.0 Miocene Sequences from elsewhere in Southwestern Turkey and Related Areas

10.5.1 Sequences within the Antalya Complex

Unfossiliferous, subaerially deposited, ophiolite-derived, clastic sediments are present as deformed intercalations within the ophiolitic rocks of the Godene Zone (Robertson and Woodcock, 1980a). The sediments range from well stratified ophiolite-derived sandstones to volumetrically abundant conglomerates. The conglomerates are dominated by massive to poorly stratified matrix-supported units. Clast composition records all levels of an ophiolite suite and its former sedimentary cover. Sedimentary features indicate rapid deposition from a series of ephemeral fault scarps. Often the clast composition bears little relation to presently adjacent rocks. The sequences are interpreted by Robertson and Woodcock (1980a) to record deposition in a series of small transtension basins formed during strike-slip faulting of the Antalya Complex.

Age. The age cannot be determined accurately as the sediments are completely unfossiliferous. However, the absence of ophiolite-derived sediments in the platform sequences (apart from submarine-derived olistostromes in the N. Bey Dağlari) appears to preclude subaerial exposure of the Antalya Complex before Lower Miocene times. These sequences most probably represent the *subaerial equivalent* of the ophiolite-derived sediments of the *Salir Formation*.

The only dated Miocene rocks within the Antalya Complex are small outcrops of Miocene limestones overlying the Tekirova ophiolite south of Kemer (Fig. 10.1). The contact with the underlying ophiolitic rocks is not well exposed, but appears to be faulted. The sequence is ca. 70 m thick. At the base thin, laterally continuous (sheet), fine grained calcarenites are interbedded with very thin calcareous silt horizons. The tops of the calcarenites are extensively bioturbated. Upwards, coarse grained, tabular cross-bedded calcarenites interbedded with thin bioclastic siltstones become dominant. The calcarenites contain abundant comminuted bivalves and other bioclastic debris. The sequence represents deposition in an open, high energy, shallow marine environment.

A prominent N-S trending cleavage in these sediments, a feature not generally seen in the rocks of the Antalya Complex, suggests this area may have been a site of intense late Miocene deformation, possibly related to strike-slip faulting (see 10.6.3).

On the Antalya-Kemer road a poorly exposed, steeply dipping sequence, ca. 250 m thick, consists of stratified dominantly clast-supported conglomerates, intercalated with beds of unfossiliferous brown calcareous mudstone. In the conglomerates limestone and replacement chert clasts are well rounded. Ophiolite-derived material is conspicuous by its absence. The sequence represents deposition on a stream-flow dominated alluvial fan. It is tentatively given a Miocene age on the basis that it overlies the deformed Antalya Complex and has itself been deformed.

10.5.2 Other Areas in Southwestern Turkey

Over the remainder of the western Taurides Miocene sequences are only patchily distributed. North and east of Antalya thick sequences of Middle to Upper Miocene sediments are preserved. In the Aksu-Çay area, north of Antalya (Fig. 10.1) a thick conglomeratic sequence (ca. 1,500 m) is dated as Middle to Upper Miocene (Poisson, 1977; Aksu Çay Formation Akbullut, 1977). Interbedded reef limestones and a shallow marine fauna suggest deposition in a fan-delta setting. Similar sequences have also been recorded by Dumont (1976a) in the Kesme area further east. In all cases composition of the conglomerates indicates derivation from the Antalya Complex to the northwest. In the east, near Sutculler, Akbullut (1977) records a Middle Miocene unconformable cover overlying the Antalya Complex, indicating that only parts of the Complex were remobilised during Upper Miocene tectonic events (below, 10.6.1).

Further east in the Manavgat area (Fig. 10.1) conglomerates, sandstones and shallow water limestones span Burdigalian to Tortonian (Monod, 1977a). Limestones of Burdigalian to Langhian age mark an initial transgression that has been correlated with the Aquitanian transgression in the Bey Dağlari and Susuz Dağ (Monod, 1977a). Overlying conglomerates and sandstones, that become finer grained to the southwest, record the gradual uplift and unroofing of the Taurus Occidental.

10.5.3 Evidence from Cyprus

The Kyrenia range of northern Cyprus is a critical link in the history of the Eastern Mediterranean (Baroz, 1980). A recent reconnaissance study (Robertson and Woodcock, pers. comm. 1981) suggests that the Kyrenia range consists of a continental sliver composed of Triassic to Cretaceous shallow marine carbonate build-up lithologies, overlain by Maastrichtian to Eocene pelagic carbonates interbedded with submarine shonshonitic and calc-alkaline volcanics (Baroz, 1980; Rocci *et al.*, 1980). The overall stratigraphy is in many aspects similar to large off-margin massifs in the Kemer Zone of the Antalya Complex (e.g. Tahtali Dağ, Teke Dağ). After tectonic disruption in the late Eocene, the Kyrenia Range is overlain by a thick 'flysch' sequence which spans Upper Eocene to Upper Miocene (Weiler, 1970). The basal, ca. 30 m of the sequence comprises ophiolite-derived fluvial conglomerates with palaeocurrents which indicate a northward derivation (Robertson and Woodcock, pers. comm. 1981). This passes rapidly upwards into a thick sequence (ca. 500 m) of interbedded turbiditic sandstones, mudstones and pelagic chalks, which span Lower to Upper Miocene. Palaeocurrents indicate a dominantly NE-SW trending basin with derivation from the NE, from the area of Adana (Weiler, 1970). Overlying undeformed Messinian evaporites indicate deformation of this sequence in latest Miocene times. Along the southern margin of the Kyrenia range, the flysch sequence (Ovgas Formation, Weiler, 1970) contains material clearly derived from the Troodos Complex (Weiler, 1970). This, and the absence in the field of any structural discontinuity between the Kyrenia range and the Troodos ophiolite complex (Robertson and Woodcock, pers. comm. 1981), suggests that the Kyrenia range and the Troodos ophiolite may be essentially one tectonic unit.

Following the palaeomagnetic studies of Moores and Vine (1971) it is widely accepted that Troodos, and by implication (as outlined above), the Kyrenia range, has been rotated approximately 90° in an anticlockwise direction since its formation in the Cretaceous. However, available palaeomagnetic results from Africa, the Levant and Eastern Turkey (Hadzi *et al.*, 1976; Orbay and Bayburdi, 1979) indicate that these areas have also rotated, although by a lesser amount. Recent work (Shelton and Gass, 1980) suggests that this rotation may have been as late as Middle Miocene.

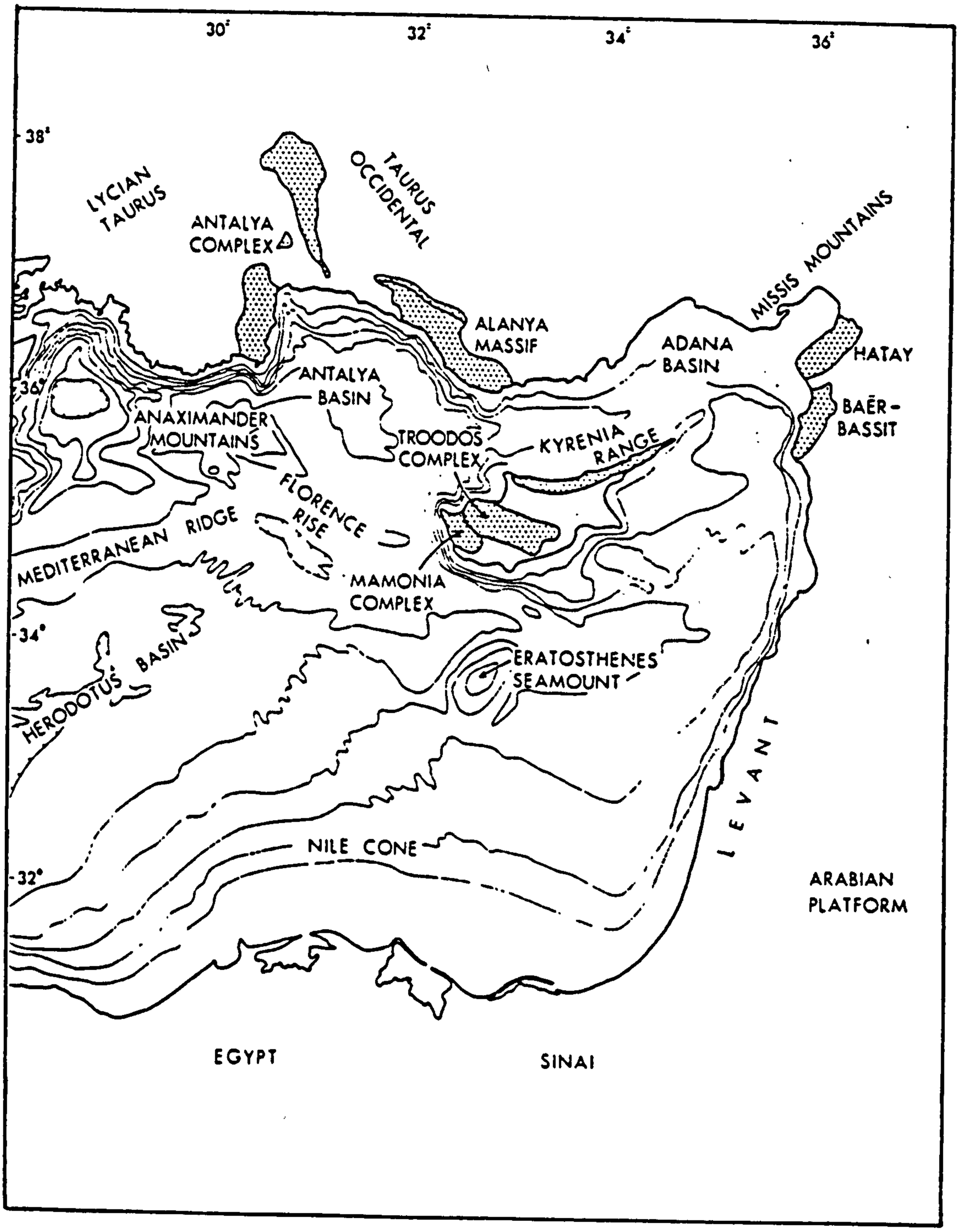

Fig. 10.7

Outline map of the east Mediterranean showing bathymetric contours at 500 m intervals and areas and features mentioned in the text (after Robertson and Woodcock, 1980b).

10.6.0 Destruction of the Antalya Complex Ocean

In this section the results of this study are put into the broader framework of Tertiary tectonic events in the Eastern Mediterranean.

10.6.1 Original Ocean (Troodos Ocean)

The ophiolites of Antalya, Cyprus, Hatay and Baer Bassit (Fig. 10.3) occur in a relatively *external* position in the Tauride mountain belt to the south of major Mesozoic to Tertiary carbonate platforms. Ricou *et al.* (1974, 1975, 1979) and Monod (1976b) propose a tectonic explanation for this phenomenon, in which the external ophiolites and pelagic sediments of Antalya, Cyprus and Baer Bassit are interpreted as klippen of the late Cretaceous nappes transported southwards over the carbonate platform. *Results of this* and other recent studies (e.g. Robertson and Woodcock, 1980a; Waldron, 1981) clearly *preclude such an origin for the Antalya Complex* (see 10.4.2). In Cyprus the presence of a continuous pelagic sedimentary sequence above the Troodos ophiolite (Robertson and Hudson, 1974) precludes Cretaceous long distance nappe transport from the north. The *"external" ophiolites* must therefore have *originated* in an ocean basin *between* the northern Tauride *carbonate platform autochthon* (Bey Daglari, Anamas Dag, Akseki) and the *continental massif of Africa and Arabia.* This basin has been termed the Troodos ocean (Robertson and Woodcock, 1980a) although it is in part equivalent to the "Pamphyllian basin" of Dumont *et al.* (1972a, b), "Tethys 2" of Dewey *et al.* (1973) and to parts of the Mesogea of Biju-Duvaal *et al.* (1977).

10.6.2 Constructive Phase

Rifting in the Troodos ocean was initiated in early to Mid Triassic times (Robertson and Woodcock, 1980a; Waldron, 1981). At present there are very few constraints on rift geometry, most authors (e.g. Biju-Duvaal *et al.*, 1977; Robertson and Woodcock, 1980a; Waldron, 1981) favour a N-S orientated rift zone with the Bey Dağlari placed adjacent to the Levant margin. Small continental slices were rifted off the main margins forming off margin highs on which carbonate build-ups developed (e.g. in the south adjacent to the Bey Dağlari margin, Tahtali Dağ and Teke Dağ, Robertson and Woodcock, 1981a, b, c). The early rift phase was accompanied by limited subsidence and eruption of great thicknesses of lava (e.g. Godene Zone, Robertson and Woodcock, 1981c; Cyprus, Phasoula lava, Swarbrick,

Fig. 10.8 (a and b)

Evolution of the Antalya Complex (after Robertson and Woodcock, in press)

(a) Triassic - Jurassic

In the early Triassic initial continental separation produces a small basin. Large slivers of continental basement are detached from the parent margin. This is followed in the late Triassic by erosion of continental basement and subsidence. Shallow submerged areas are colonised by reefal build-ups.

(b) Jurassic to Late Cretaceous

Passive margin conditions persist through the Jurassic to mid-Cretaceous. Subsidence along with shallow water carbonate deposition results in the formation of a major 'Bahamian type' carbonate platform (Bey Dağlari) and a series of coral atolls on the rifted off-margin continental blocks. In basinal areas pelagic radiolarites, mudstones and redeposited carbonate sediments accumulate. True ocean floor spreading is initiated in late Jurassic to early Cretaceous times, this is followed by subsidence of the carbonate platform and off-margin build-ups.

Fig. 10.8a

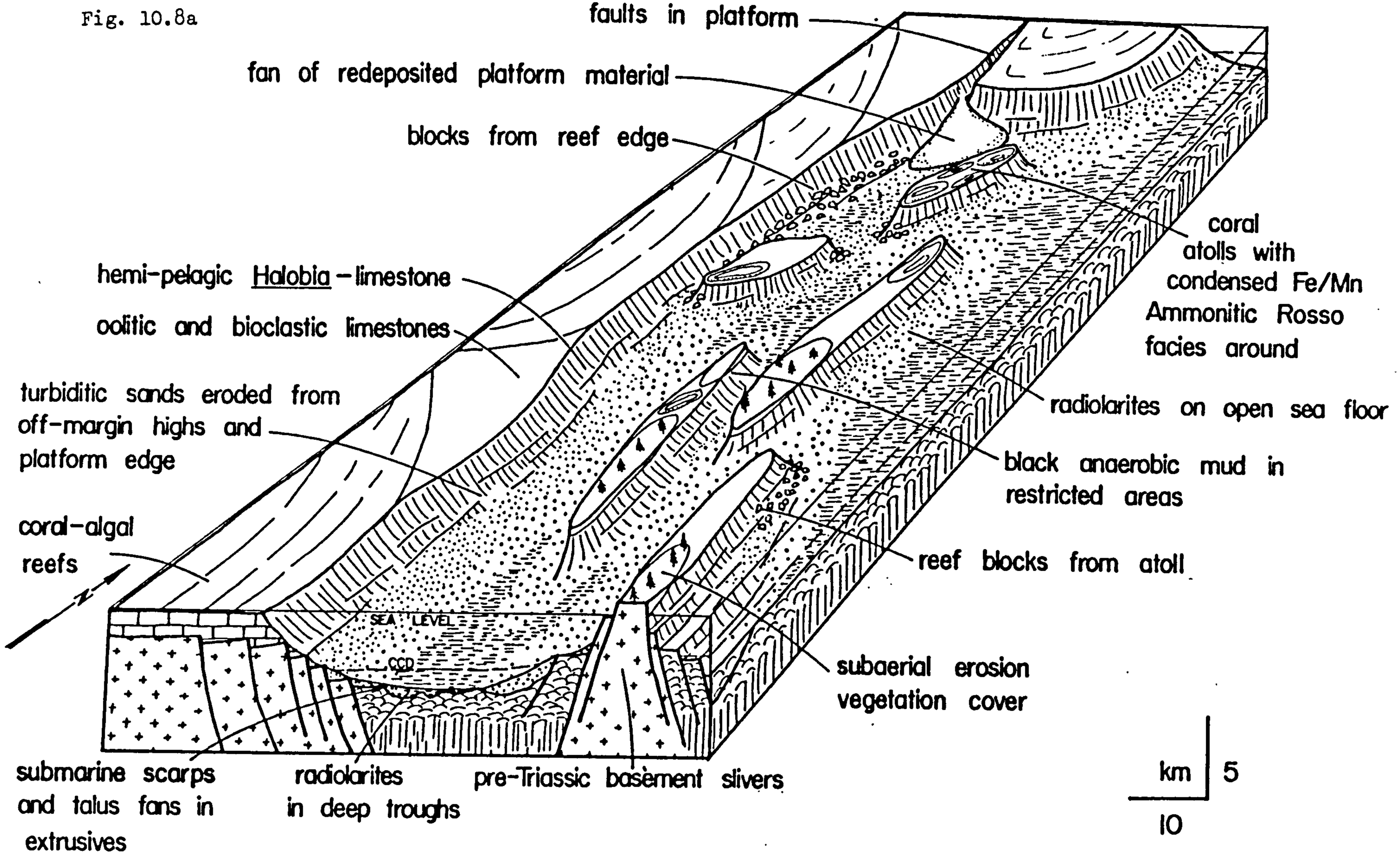
faults in platform
fan of redeposited platform material
blocks from reef edge
hemi-pelagic Halobia-limestone
oolitic and bioclastic limestones
turbiditic sands eroded from off-margin highs and platform edge
coral-algal reefs
coral atolls with condensed Fe/Mn Ammonitic Rosso facies around
radiolarites on open sea floor
black anaerobic mud in restricted areas
reef blocks from atoll
subaerial erosion vegetation cover
SEA LEVEL
CCD
submarine scarps and talus fans in extrusives
radiolarites in deep troughs
pre-Triassic basement slivers
km 5
10

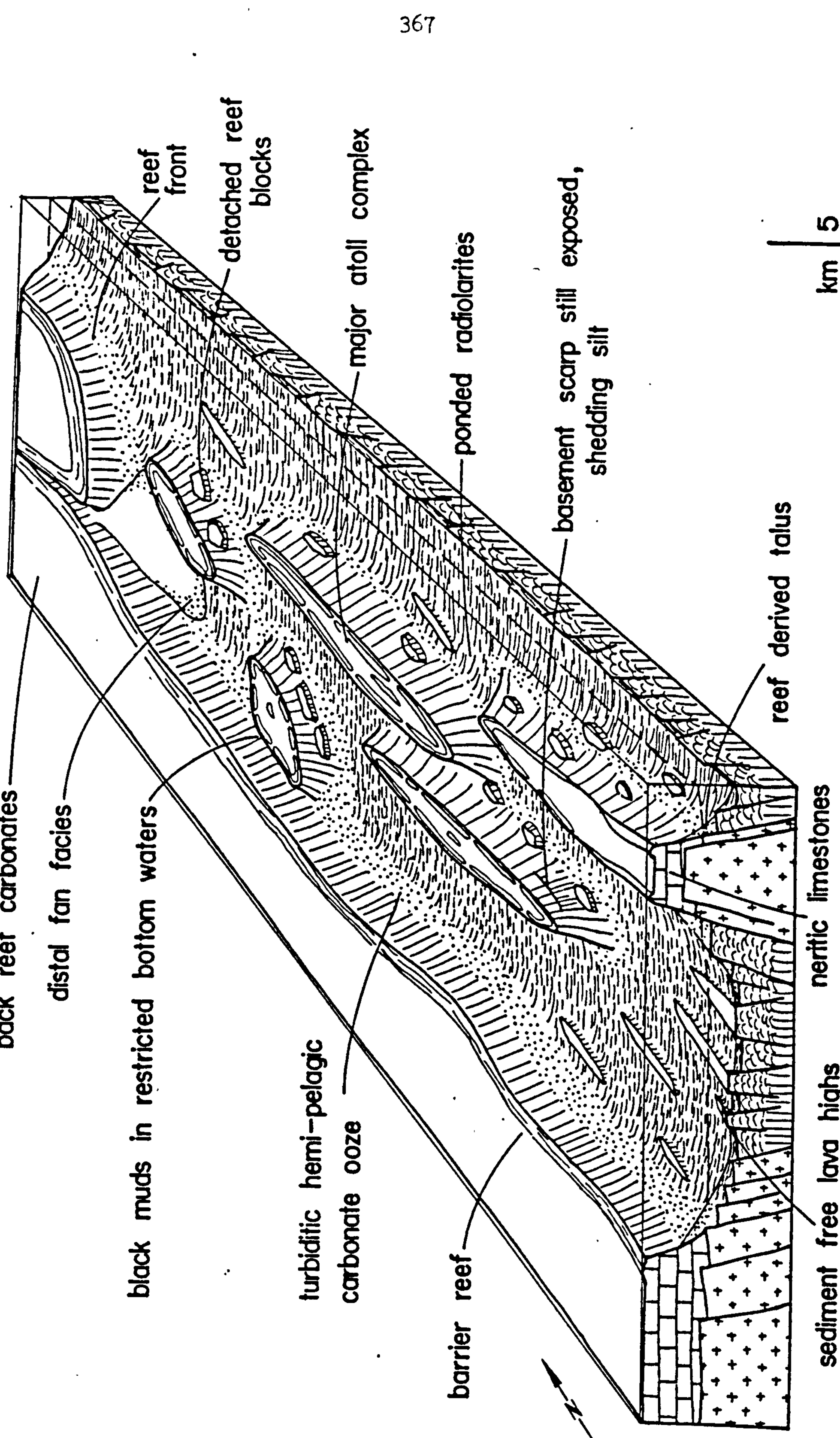
reef front
detached reef blocks
major atoll complex
ponded radiolarites
basement scarp still exposed, shedding silt
reef derived talus
nertitic limestones
km 5 10
back reef carbonates
distal fan facies
waters
black muds in restricted bottom
turbiditic hemi-pelagic
carbonate ooze
barrier reef
free lava highs
sediment free

Fig. 10.8b

1980). Renewed extension began in late Jurassic to early Cretaceous times as recorded by rapid subsidence of the platform edge zone (e.g. Anamas Dağ, Waldron, 1981), widespread deposition of manganiferous hydrothermal sediments (Robertson, 1981, Waldron, 1981) and the formation of the Antalya, Troodos, Hatay and Bäer Bassit ophiolites (Fig. 10.7).

By mid-Cretaceous times the Bey Dağlari formed a large carbonate platform bounded to the north and east by open ocean. The extent of the ocean eastwards is unknown, in the north an ocean of at least 100 km width, between the Bey Dağlari and Anamas Dağ platform units, and possibly much greater, is suggested by a recent palinspastic reconstruction of the imbricated margin and ophiolite units (Waldron, 1981). This northern arm of the Troodos ocean may have connected with the Pindos, Othrys or Vardar ophiolite zones of Greece (Auboin *et al.*, 1963; Smith, 1973). There is no evidence to indicate whether the Bey Dağlari was connected to Africa or separated by an oceanic zone at this time.

10.6.3 Late Cretaceous to Tertiary Destruction

The *late Cretaceous* change in relative motion of Africa and Europe (Pitman and Talwani, 1972; Smith, 1973) resulted in *thrusting* in the continental margin sequences of Antalya in the west and Hatay, Baer Bassit and Oman in the east (Robertson and Woodcock, 1980b). In more central areas of the ocean basin late Cretaceous to Palaeocene calc-alkaline and shoshonitic volcanism in Cyprus (Baroz, 1980), volcanoclastic sediments in Cyprus (Kannaviou Formation, Robertson, 1977b) and glaucophane schist in the Alanya massif, suggest the initiation of an island arc associated with intra-oceanic subduction, at this time, along the northern margin of the Troodos basin (Fig. 10.9).

Within the Antalya Complex initial tectonism in Maastrichtian times is marked by ophiolitic siltstones and sandstones within off margin carbonate massifs, by olistostrome melanges in the Godene Zone and ophiolite-derived conglomerate with an Upper Cretaceous marine fauna in the Tekirova Zone (Robertson and Woodcock, in press). The eastern margin of the Bey Dağlari, at this time, is marked by subsidence along a N-S trending hinge line. Structural studies (Woodcock and Robertson, 1981a, b) suggest that in this area, E-W shortening was accommodated by broadly N-S *strike-slip* fault movement. This continued through the late Cretaceous to Palaeocene. The

culmination of this episode in the Eocene is marked by the presence of thick, ophiolite-derived olistostrome debris flows, and turbiditic sandstones in the northern Bey Dağlari and continued subsidence of the eastern margin. In the north, along the southern margin of the Anamas Dağ, carbonate platform emplacement of the Antalya Complex was towards the northeast as a series of thrust slices.

This led Waldron (1981) to suggest that the Bey Dağlari has been rotated through 45° since Eocene times and was originally orientated as in Fig. 10.9. This enables strike-slip faulting along the eastern margin of the Bey Dağlari to be accommodated by a NW-SE trending thrust front along the southern margin of the Anamas Dağ platform (Fig. 10.9).

At the same time, a thick sequence of Eocene flysch that overlies the Anamas Dağ carbonate platform marks the final phase of emplacement from the northeast of the Beyşehir-Hoyran Nappes (Brunn *et al.*, 1971). West of the Bey Dağlari at this time, the Lycian Nappes underwent tectonism and subaerial exposure (?) resulting in a thick sequence of Eocene flysch which now lies structurally beneath the ophiolitic unit of the Lycian Nappes (Poisson, 1977).

In *early Miocene* times continued convergence resulting from the northwestward movement of Africa was accommodated by the *Lycian Nappes*, together with its Eocene flysch sequence being emplaced onto the *western margin* of the Bey Dağlari (Fig. 10.9). Subsidence of the Bey Dağlari, as a result of thrust emplacement, resulted in a coupled basin being formed in front of the advancing nappe pile. Material shed from the nappes was deposited as the Kemer and Kasaba Formations. Marginal areas of the basin were successively overthrust throughout the Miocene, the nappes finally coming to rest in Middle to Upper Miocene times. The amount of overthrusting along the western margin of the Bey Dağlari is in excess of 70 km, probably nearer 100 km. At the same time, along the *eastern margin* of the Bey Dağlari, the Antalya Complex existed as a deeply dissected landmass. Small tear-apart basins within the Complex, produced by wrench faulting, were infilled by subaerial clastic sediments (Figs. 10.9, 10.8). Terrigenous material derived off the Antalya Complex prograded into carbonate platforms as a series of small submarine fans (Salir Formation, Chapter 5) (Fig. 10.8).

Evidence outlined above (10.5.3) indicates that Cyprus (Troodos

Fig. 10.8 (c and d)

Destruction of the Antalya Complex (see text, 10.2.1 and 10.6.3 for more details)

(c) Lower Miocene

First phase of *subaerial* emplacement following initial submarine tectonism in Maastrichtian to Eocene times. Extensive N-S orientated strike-slip faulting in the Antalya Complex results in its subaerial exposure and impingement against the subsided eastern margin of the Bey Dağlari carbonate platform. The marginal facies is imbricated and coarse clastic ophiolite-derived sediment is shed onto the carbonate platform as a series of fan-deltas, these pass downslope into small submarine fans. Within the Antalya Complex small tear-apart basins are initiated. Shallow water limestones are deposited in an open sea to the east.

(d) Middle - Upper Miocene

Continued strike-slip faulting results in the margin of the sedimentary basin being overthrust and fan-deltas prograde into a shallow sea.

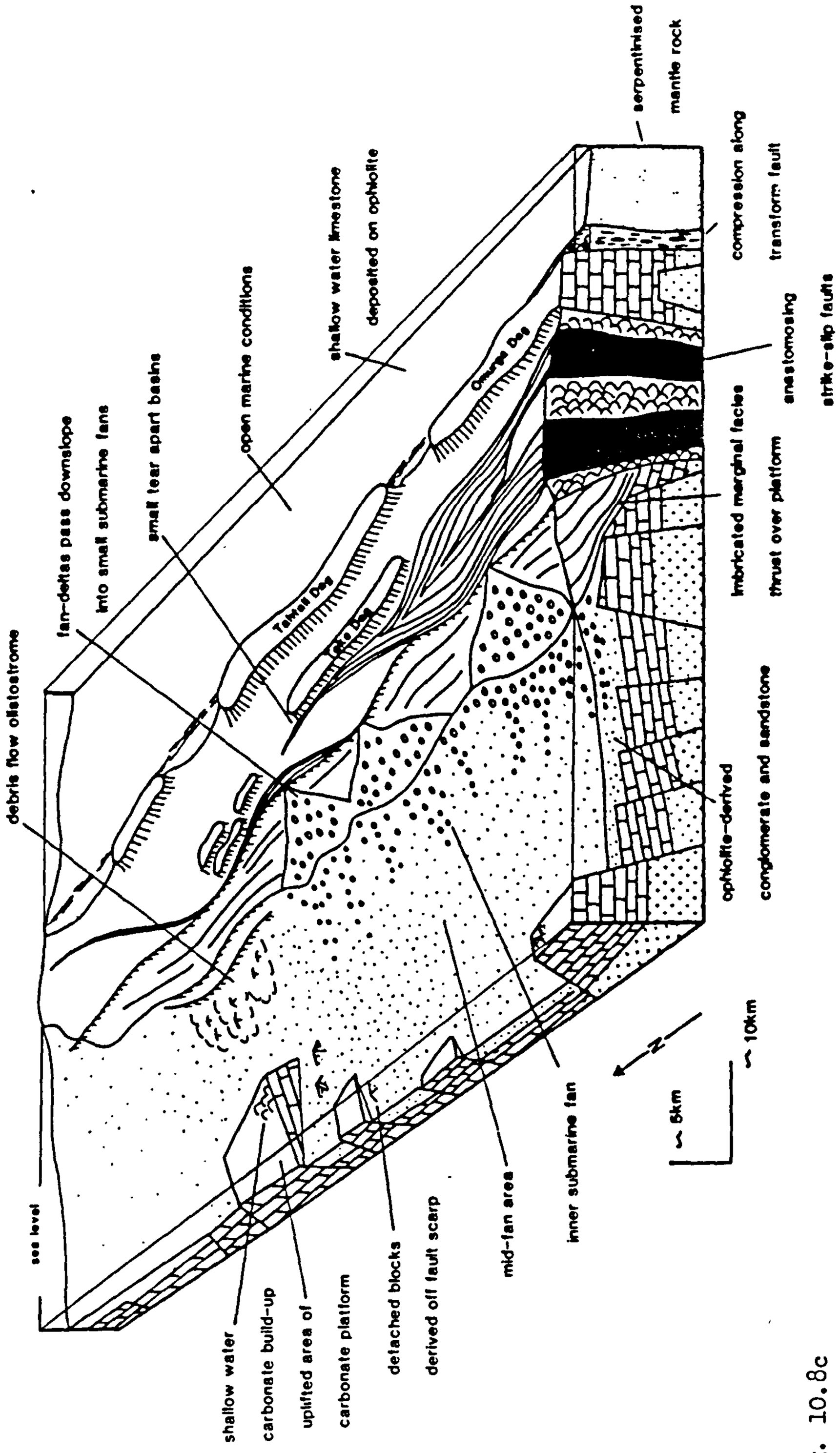
serpentinised
mantle rock
compression along
transform fault
shallow water limestone
deposited on ophiolite
open marine conditions
small tear apart basins
into small submarine fans
fan-deltas pass downslope
debris flow olistostrome
Ghaba Deg
Takhat Deg
Qaisha Deg
anastomosing
thrust over platform
imbricated marginal facies
strike-slip faults
ophiolite-derived
conglomerate and sandstone
~ 10km
~ 5km
N
inner submarine fan
mid-fan area
detached blocks
derived off fault scarp
uplifted area of
carbonate platform
carbonate build-up
shallow water
sea level

Fig. 10.8c

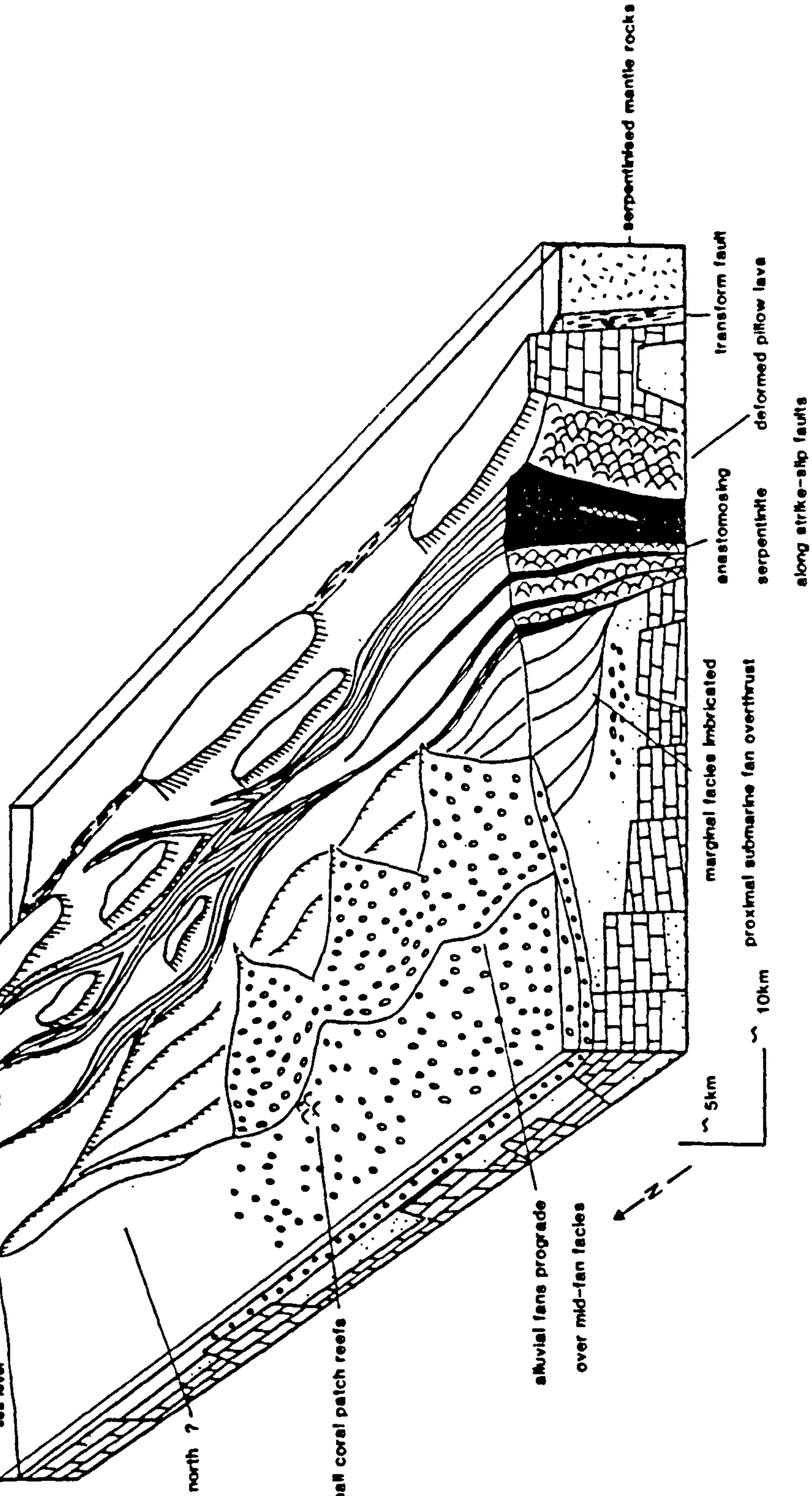
serpentinised mantle rocks
transform fault
deformed pillow lava
anastomosing
serpentinite
along strike-slip faults
marginal facies imbricated
proximal submarine fan overthrust
~ 10km
~ 5km
N
alluvial fans prograde
over mid-fan facies
small coral patch reefs
no Miocene clastics in north ?

Fig. 10.8d

and possibly the Kyrenia range) has rotated by 90° since Cretaceous times. In a recent reconstruction Robertson and Woodcock (1980b) suggest rotation away from the mainland area of SW Turkey out of the Gulf of Antalya (Fig. 10.9). This is supported by recent field evidence that suggests that the Kyrenia range is composed essentially of a basement sliver overlain by a carbonate massif, and is in fact very comparable to limestone massifs constructed on off-margin highs in the Kemer Zone of the Antalya Complex. It therefore seems likely that the Kyrenia massif and the Troodos ophiolite complex originated adjacent to the Antalya Complex.

Upper Eocene, fluvial, ophiolite-derived sediments overlying the Kyrenia limestone sequences represent tectonism of the Antalya Complex possibly associated with extensive strike-slip fault movement (10.2.1, Fig. 10.9). The Kyrenia Range could have been rotated anticlockwise away from the coast of mainland Turkey along strike-slip faults during Oligocene to Lower Miocene times. By Middle Miocene times it was probably in approximately its present position as fluvial ophiolite-derived sediments are overlain by a flysch sequence derived from a granite/metamorphic terrain in the Adana area to the northeast (Weiler, 1970). The rotation was concomitant with dextral strike-slip faulting in the Antalya Complex and localised strong uplift and subsidence in southern Cyprus (Robertson, 1977c). During Lower Miocene times an open sea probably existed to the east of the Antalya Complex. Shallow marine limestones of Miocene age (10.5.1) exposed at Kemer (Fig. 10.1) were probably deposited on highs or in marginal areas away from the main influence of terrigenous clastic sedimentation.

In *mid-Miocene* the submarine fan phase of sedimentation along the eastern margin of the Bey Dağlari was abruptly terminated by the *westward overthrusting* of the Antalya Complex to near its present position. Alluvial fans prograded westward over the autochthon where deposition continued until Upper Miocene times (Fig. 10.8).

The rotation of Cyprus out of the Gulf of Antalya may have created a tear-apart basin in the centre of the Isparta angle (Aksu Çay area) (Fig. 10.9). This was filled by a thick sequence of Upper Miocene conglomerates and sandstones (Aksu Çay Formation) of fan-delta affinity. A final phase of E-W compression took place in latest Miocene times (Aksu phase of Poisson, 1977). Along the Aksu thrust (Fig. 10.9) the southeastern segment of the Antalya Complex was thrust

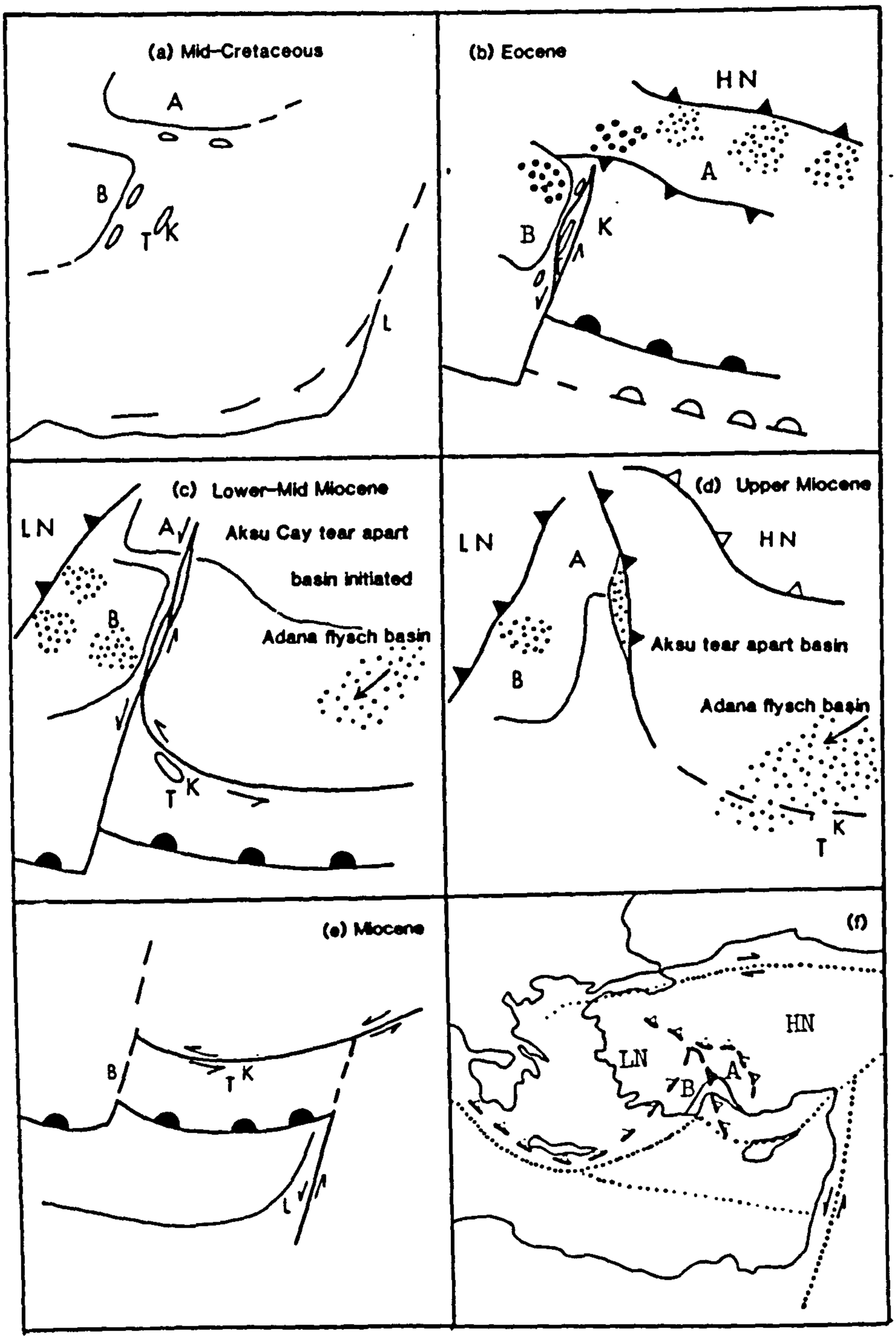
(a) Mid-Cretaceous
A
B
T
K
L
(b) Eocene
HN
A
B
K
(c) Lower-Mid Miocene
LN
A
B
Aksu Cay tear apart
basin initiated
Adana flysch basin
T
K
(d) Upper Miocene
LN
A
HN
B
Aksu tear apart basin
Adana flysch basin
T
K
(e) Miocene
B
T
K
(f)
HN
LN
A
B

Fig. 10.9

Fig. 10.9

Schematic plate model for the destruction of the Antalya Complex ocean (Troodos Ocean). See text for more details.

(a) Mid-Cretaceous, palaeogeography based principally on the data of Waldron (1981) and Robertson and Woodcock (1980a). The Bey Dağlari (B) and Anamas Dağ (A) form carbonate platforms bounded by open ocean.

(b) Late Cretaceous to Eocene, initial destructive phase. Thrusting of the Antalya Complex onto the Anamas Dağ platform (A) in the north is accommodated by N-S strike-slip faulting along the eastern margin of the Bey Dağlari (B). In central areas of the ocean an intra-oceanic subduction zone is initiated. N-S shortening is also taken up along the northern margin of the Anamas Dağ resulting in emplacement of the Beysehir-Hoyran-Hadim Nappes (HN).

(c) Lower Miocene. Dextral strike-slip faulting continues along the eastern margin of the Bey Dağlari resulting in initial subaerial emplacement of the Antalya Complex onto the subsided carbonate platform. At the same time the Troodos massif and Kyrenia Range are rotated, along strike-slip faults out of the Gulf of Antalya. A possible mechanism for initiation of this strike-slip belt is the collision of the mid-ocean ridge with the subduction zone, forming a strike-slip belt and resulting in subsequent initiation of a subduction zone further south. Shortening is also accommodated by the initial emplacement of the Lycian Nappes onto the northern margin of the Bey Dağlari.

(d) Lower to Upper Miocene. Strike-slip faulting results in the formation of the Aksu tear-apart basin. A last phase of thrusting results in the final emplacement of the Lycian Nappes; and parts of the Antalya Complex along the Aksu thrust.

(e) Miocene plate model for the Eastern Mediterranean (after Robertson and Woodcock, 1980a).

(f) Present day configuration showing traces of thrust fronts and plate boundaries (in part after McKenzie, 1977).

Key to Maps

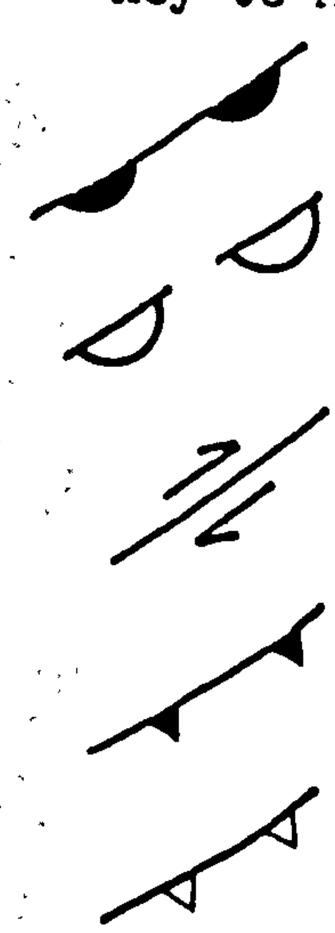

subduction zone

incipient subduction zone

strike-slip fault zone

thrust active

thrust inactive

'flysch' sediments

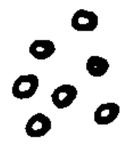

submarine olistostrome

A - Anamas Dağ; B - Bey Dağlari;

T - Troodos Massif; K - Kyrenia Range;

HN - Beysehir-Hoyran-Hadim Nappes;

LN - Lycian Nappes.

L - Levant Margin

southwestward over the margin of the Aksu basin. At the same time, further to the east (Manavgat area), regional uplift of the Taurus Occidental resulted in the progradation of a thick conglomerate wedge towards the southwest. The present day configuration is shown in Fig. 10.9, including the traces of the thrust fronts of the Lycian Nappes, Beysehir-Hoyran-Hadim Nappes and the Aksu thrust. North of Africa the continent-ocean boundary is imprecisely fixed, however, the area between Egypt and Cyprus is apparently floored by oceanic crust, whereas that between Crete and north Africa is floored by continental crust (J. Makris, pers. comm., 1979). Present day plate boundaries are located south of Cyprus and Crete (Fig. 10.9) (Mckenzie, 1977).

10.7 Comparisons and Modern Analogues

The western margin of the basin, related to the large scale overthrusting of the Lycian Nappes, is in many ways comparable to a 'foreland' basin type setting, although the overall orogenic regime and scale is rather different. The most thoroughly documented ancient example of basins forming in front of migrating fold and thrust belts is in the Rockie Mountains (Bally *et al.*, 1966; Eisbacher *et al.*, 1974; McLean and Jerzykiewicz, 1978; Beaumont, 1981). Modern analogues of this type of sequence are poorly documented. A possible example is the foothills of the Himalayas. In this area rapid subsidence of the Indogangetic plain is related to thrusting and loading along a series of thrust faults along the southern margin of the Siwalik hills (Johnson and Vondra, 1972).

The Antalya Complex strike-slip related margin has both ancient and modern analogues in the overall tectonic regime in New Zealand, where strike-slip tectonics have been occurring since Miocene times (Norris *et al.*, 1978; Norris and Carter, 1980; Sporli, 1980) and also in California along the San Andreas and related fault systems (Crowell, 1974; Howell *et al.*, 1980; Saleeby, 1977, 1979).

10.8 Sedimentological Studies as a means of resolving Regional Tectonic Controversies : a final word

In structurally complex terrains the approach of studying autochthonous sedimentary sequences is in many areas a far more reliable method than structural analysis of the allochthonous units. In such areas (e.g. see below) the largely unstudied autochthonous sequences may provide critical data on the direction, distance and

timing of emplacement of the allochthonous units.

Other areas where this approach may help to resolve outstanding regional geological problems are the Baer Bassit and Menderes massifs. Although it is widely agreed that the Lycian Nappes have been thrust over the Menderes massif, a detailed study of the autochthonous sequence within the Menderes massif would almost certainly provide data on the exact timing and nature of overthrusting. In the Baer Bassit area (Fig. 10.7) the regional geology is essentially the same as in southwestern Turkey, comprising an autochthonous carbonate platform either side of which lie two allochthonous ophiolite units (Delaune-Mayere and Parrot, 1976). A detailed study of the autochthonous sedimentary sequence, in particular the polarity of the carbonate platform margin facies (e.g. Chapter 9), would prove conclusively whether the ophiolites comprise one tectonic unit or are in fact the remnants of two small ocean basins separated by a carbonate platform.

REFERENCES

ADEY, W. H. and MACINTYRE, I. G. 1973. Crustose Coralline Algae: a re-evaluation in the Geological Sciences. Bull. Geol. Soc. Am. 84 883-904.

AKBULUT, A. 1977. Etude Géologique d'une partie du Taurus occidentale au sud d'Eğridir (Turquie). Thesis: Univ. Paris Sud, Orsay.

ALBERSTADT, L. P., WALKER, K. R. and ZUROWSKI, R. P. 1974. Patch reefs in the Carters Limestone (Middle Ordovician) in Tennessee, and vertical zonation in Ordovician reefs. Bull. Geol. Soc. Am. 85 1171-1182.

ALLASINAZ, A., GUTNIC, M. and POISSON, A. 1974. La formation de l'Isparta Cay: Calcaires à Halobies, Grès à plantes, et Radiolarites d'âge Carnien (?) - Norien (Taurides - Region d'Isparta - Turquie). Schr. Erdwiss. Komm. Oster. Akad. 2, 11-21.

ALLEN, J. R. L. 1963. The classification of cross-stratified units with notes on their origin. Sedimentology 2, 93-114.

ALLEN, J. R. L. 1964. Studies in fluviatile sedimentation: six cyclothems from the Lower Old Red Sandstone, Anglo-Welsh Basin. Sedimentology 3, 163-198.

ALLEN, J. R. L. 1965. A review of the origin and characteristics of recent alluvial sediments. Sedimentology (Special Issue) 5, 89-191.

ALLEN, J. R. L. 1970. Physical Processes of Sedimentation. Allen and Unwin, London.

ALLEN, J. R. L. 1974a. Studies in fluviatile sedimentation: implications of pedogenic carbonate units, Lower Old Red Sandstone, Anglo-Welsh outcrop. Geol. J. 9, 181-208.

ALLEN, J. R. L. 1974b. Studies in fluviatile sedimentation: lateral variation in some fining-upwards cyclothems from the Red Marls, Pembrokeshire. Geol. J. 9, 1-16.

ALLEN, J. R. L. 1978. Studies in fluviatile sedimentation: an exploratory quantitative model for the architecture of avulsion controlled alluvial suites. Sediment. Geol. 21, 129-147.

ARGYRIADIS, I. , MERCIER, J. L. and VERGELY, P. 1976. La fenetre d'Attique-Cyclades et les corrélations Hellenides-Taurides. C.r. Séances Acad. Sci. Paris 283, 599-601.

ARGYRIADIS, I. , GRACIANSKY, P. C. de, MARCOUX, J. and RICOU, L. E. 1980. The opening of the Mesozoic Tethys between Eurasia and Arabia-Africa. Int. geol. Congr. Paris 1980, Colloque C5 and Mém. Bur. Rech. géol. minières 115, 199-214.

AUBOUIN, J., BRUNN, J. H., CELET, P., DERCOURT, J., GODFRIAUX, I. and MERCIER, J. 1963. Esquisse de la géologie de la Grèce. *In* Libre à la mémoire du Professeur Paul Fallot. Mém. hors-serie Soc. géol. Fr., 583-610.

AUBOUIN, J., BONNEAU, M., DAVIDSON, J., LEBOULANGER, P., MATESCO, S. and ZAMBETAKIS, A. 1976. Esquisse structural de l'Arc égéen externe: des Dinarides aux Taurides. Bull. Soc. géol. Fr. 18(7), 327-336.

BAGNOLD, R. A. 1954. Experiments on a gravity-free dispersion of large solid spheres in a Newtonian fluid under shear. Proc. R. Soc. Lond. A225, 49-63.

BAGNOLD, R. A. 1956. The flow of cohesionless grains in fluids. Philos. Trans. R. Soc. Lond., A249, 315-319.

BALLY, A. W., GORDY, P. L. and STEWART, G. A. 1966. Structure, seismic data and orogenic evolution of the southern Canadian Rockies. Bull. Can. Petrol. Geol. 14, 337-381.

BARNES, J., BELLAMY, D. J., JONES, D. J., WHITTON, B. A., DREW, E. A. and LYTHGOE, J. N. 1970. Sublittoral reef phenomena of Aldabra. Nature 225, 268-269.

BAROZ, F. 1980. Volcanism and continent-island arc collision in the Pentadaktylos range, Cyprus. *In* Panayiotou, A. (ed). Ophiolites: Proceedings International Ophiolite Symposium Cyprus 1979. Geological Survey Department, Cyprus. 73-85.

BARTON, C. M. 1975. Mount Olympus, Greece: new light on an old window. Geol. Soc. Lond. Q. J. 131, 389-396.

BASSAGET, J. P. 1966. Contribution à l'étude de la région au Sud du Massif du Menderes entre Fethiye et Sandras Dağ (province de Muğla, Turquie). Thesis: Univ. Grenoble.

BATES, C. C. 1953. Rational theory of delta formation. Bull. Am. Assoc. Petrol. Geol. 37, 2119-2162.

BATH URST, R. G. C. 1966. Boring algae, micrite envelopes and lithification of molluscan biosparites. Geol. J. 5, 89-109.

BATHHURST, R. G. C. 1971. Carbonate Sediments and their Diagenesis. Elsevier. Amsterdam & New York. 620 p.

BEAUMONT, C. 1981. Foreland basins. Geophys. J. R. astr. Soc. 65, 291-329.

BEERBOWER, J. R. 1964. Cyclothems and Cyclic Depositional Mechanisms in Alluvial Plain Sedimentation. *In* Merriam, D. F. (ed) Symposium on Cyclic Sedimentation. Kan. Geol. Surv. Bull. 169, 31-42.

BERNOULLI, D., GRACIANSKY, P. D. de and MONOD, O. 1974. The extension of the Lycian Nappes (S. W. Turkey) into the southeastern Aegean islands. Eclog. geol. Helv. 67, 39-90.

BIJU-DUVAL, B., DERCOURT, J. and LE PICHON, X. 1977. From the Tethys Ocean to the Mediterranean Seas: a plate tectonic model of the evolution of the western Alpine system. *In* Biju-Duval, B. and Montadert, L. (eds) Structural History of the Mediterranean Basins. Technip Paris. 143-164.

BLACKWELDER, E. 1928. Mudflow as a geologic agent in semi-arid mountains. Bull. Geol. Soc. Am. 39, 465-483.

BLISSENBACH, E. 1954. Geology of alluvial fans in semi-arid regions. Bull. Geol. Soc. Am. 65, 175-190.

BLUCK, B. J. 1967. Sedimentation of beach gravels: examples from S. Wales. J. Sediment. Petrol. 37, 128-156.

BLUCK, B. J. 1979. Structure of coarse-grained braided stream alluvium. Trans. R. Soc. Edinburgh, 70, 181-221.

BLUMENTHAL, M. 1963. Le système structural du Taurus sud-Anatolien. *In* Livre à la mémoire du Professeur Paul Fallot. Mém. hors-série Soc. géol. Fr., 611-662.

BORAY, A., AKAR, V., AKDENIZ, N., AKÇOREN, Z., ÇAĞLAYAN, A., GUNEY, E., KORKMAZER, B., ÖZTURK, E. M. and SAV, H. 1973. Some geological problems and their possible solutions along the southern border of Menderes Massif. Geological Congress: 50th Anniversary of Turkish Republic. M.T.A. and D.S.I. Ankara.

BOSELLINI, A. and GINSBURG, R. N. 1971. Form and internal structure of Recent algal nodules (Rhodolites) from Bermuda. J. Geol. 79, 669-682.

BOUMA, A. H. 1962. Sedimentology of some flysch deposits. A graphic approach to facies interpretation. Elsevier, Amsterdam. 168 p.

BOUMA, A. H. and SHEPHARD, D. 1966. Large rectangular box cores from submarine canyons and fan valleys. Bull. Am. Assoc. Petrol. Geol. 48, 225-31.

BOOTHROYD, J. C. and ASHLEY, G. M. 1975. Processes, bar morphology and sedimentary structures on braided outwash fans, northeastern Gulf of Alaska. *In* Jopling, A. V. and McDonald, B. C. (eds), Glaciofluvial and Glaciolacustrine sedimentation. Soc. Econ. Palaent. Mineral. Spec. Pub. 23, 193-222.

BOOTHROYD, J. C. and NUMMEDAL, D. 1978. Proglacial braided outwash: a model for humid alluvial-fan. *In* Miall, A. D. (ed), Fluvial Sedimentology. Mem. Can. Soc. Petrol. Geol. 5, 641-667.

BREMER, H. 1971. Geology of the coastal regions of southwestern Turkey. *In* Campbell, A. S. (ed). Geology and History of Turkey. Petroleum Exploration Society of Libya. Tripoli. 257-274.

BRIDGE, J. S. and LEEDER, M. R. 1979. A simulation model of alluvial stratigraphy. Sedimentology 26, 617-644.

BRINKMANN, R. 1976. Geology of Turkey. Elsevier, Amsterdam, 158 p.

BROMLEY, R. G. 1970. Borings as trace fossils and *Entobea cretocea* Portlock as an example. *In* Crimes, J. P. and Harper, J. C. (eds), Geol. J. Spec. Issue 3, 49-90.

BRÖNNIMAN, P., POISSON, A. and ZANINETTI, L. 1970. L'unité du Domuz Dağ (Taurus Lycien, Turquie). Microfaciès et foraminifères du Trias et du Lias. Riv. Ital. Paleontol. 76, 1-36.

BRUNN, J. H. 1974. Le problème de l'origine des nappes et leurs translations dans les Taurides occidentales. Bull. Soc. géol. Fr. 16(7), 101-106.

BRUNN, J. H. 1976. L'arc concave zagro-taurique et les arcs convexes taurique et égéen: collision et arcs induits. Bull. Soc. géol. Fr. 18(7), 553-567.

BRUNN, J. H., GRACIANSKY, P. C. de, GUTNIC, M., JUTEAU, T., LEFEVRE, R., HARCOUX, J., MONOD, O. and POISSON, A. 1970. Structures majeurs et corrélations stratigraphiques dans les Taurides occidentales. Bull. Soc. géol. Fr. 12(7), 515-551.

BRUNN, J. H., DUMONT, J. F., GRACIANSKY, P. C. de, GUTNIC, M., JUTEAU, T., MARCOUX, J., MONOD, O. and POISSON, A. 1971. Outline of the geology of the western Taurides. *In* Campbell, A. S. (ed), Geology and History of Turkey. Petroleum Exploration Society of Libya, Tripoli. 225-257.

BRUNN, J. H., ARGYRIADIS, I., MARCOUX, J., MONOD, O., POISSON, A. and RICOU, L. E. 1973. Arguments pour et contre l'origine méridionale des nappes à ophiolites d'Antalya. Geological congress: 50th Anniversary of Turkish Republic. M.T.A. & D.S.I. Ankara. 58-73.

BRUNN, J. H., ARGYRIADIS, I., RICOU, L. E., POISSON, A., MARCOUX, J., and GRACIANSKY, P. C. de. 1976. Éléments majeurs de liaison entre Taurides et Héllénides. Bull. Soc. géol. Fr. 18(7), 481-497.

BULL, W. B. 1964. Geomorphology of segmented alluvial fans in Western Fresno County, California. Prof. Pap. U.S. geol. Surv., 352-E. 89-129.

BULL, W. B. 1972. Recognition of alluvial-fan deposits in the stratigraphic record. *In* Rigby, J. K. and Hambin, W. K. (eds) Recognition of Ancient Sedimentary Environments. Spec. Publ. Soc. econ. Palaeontol. Mineral. Tulsa 16, 63-83.

CAILLEAUX, A. 1945. Distinction des galet marins et fluviatiles. Bull. Soc. géol. Fr. 15, 375-404.

COLIN, H. J. 1962. Geologische untersuchungen in raume Fethiye-Antalya-Kaş-Finike (S. W. Anatolien). Bull. Miner. Res. Explor. Inst. Turkey 59, 19-61.

CANT, D. J. 1978. Development of a facies model for sandy braided river sedimentation: comparison of the South Saskatchewan River and the Battery Point Formation. *In* Miall, A. D. (ed), Fluvial Sedimentology. Mem. Can. Soc. Petrol. geol. 5, 627-639.

CANT, D. J. and WALKER, R. G. 1976. Development of a braided-fluvial facies model for the Devonian Battery Point Sandstone, Quebec. Can. J. Earth Sci. 13, 102-119.

CANT, D. J. and WALKER, R. G. 1978. Fluvial processes and facies sequences in the sandy braided South Saskatchewan River, Canada. Sedimentology 25, 625-649.

CARTER, R. M. 1975. Discussion and classification of subaqueous mass transport with particular application to grain flow, slurry flow and fluxoturbidites. Earth Sci. Rev. 11, 145-177.

CARTER, R. M. and NORRIS, R. J. 1977. Redeposited conglomerates in a Miocene flysch sequence at Blockmount, Western Southland, New Zealand. Sediment. Geol. 18, 289-319.

CAZOLLA, C., FONNESU, F., MUTTI, E., RAMPONE, G., SONNINO, B. and VIGNA, B. 1981. Geometry and Facies of Small Fault-controlled Deep-sea Fan Systems in a Transgressive Depositional Setting (Tertiary Piedmont Basin, N. W. Italy). *In* Ricci Lucchi (ed) Excursion Guidebook. Intl. Assoc. Sediment. 2nd European Regn'l Meeting.

CHAPPEL, J. 1980. Coral morphology, diversity and reef growth. Nature 286, 249-252.

CHURCH, M. 1972. Baffin Island sandurs: a study of arctic fluvial processes. Bull. Can. geol. Surv. 216.

CHURCH, M. and GILBERT, R. 1975. Proglacial fluvial and lacustrine environments. *In* Jopling, A. V. and McDonald, B. C. (eds), Glaciofluvial and Glaciolacustrine Sedimentation. Spec. Publ. Soc. Econ. Palaeontol. Mineral. Tulsa 23.

CLARKSON, E. N. K. (ed). 1979. Invertebrate Palaeontology and Evolution. George Allen and Unwin, London.

CLIFTON, H. E. 1973. Pebble segregation and bed lenticularity in wave-worked versus alluvial gravel. Sedimentology 20, 173-189.

CLIFTON, H. E. 1976. Wave-formed sedimentary structures - a conceptual model. *In* Davis, R. A. Jr., and Ethington, R. L. (eds), Beach and Nearshore Sedimentation. Soc. Econ. Palaeontol. Miner. Spec. Pub. 24, 126-148.

CLIFTON, H. E. 1981. Progradational Sequences in Miocene Shoreline Deposits, Southeastern Caliente Range, California. J. Sediment. Petrol. 51, 165-184.

CLIFTON, H. E., HUNTER, R. E. and PHILLIPS, R. L. 1971. Depositional structures and processes in the non-barred high energy nearshore. J. Sediment. Petrol. 41, 651-670.

CALELLA, A. 1979. Medium-scale tractive bedforms and structures in the Gorgolione Flysch (Lower Miocene; Southern Apennines, Italy). Bull. Soc. Geol. Ital. XCVIII, 483-494.

COLLINSON, J. D. 1969. The sedimentology of the Grindslow Shales and the Kinderscout Grit: a deltaic complex in the Namurian of northern England. J. Sediment. Petrol. 39, 194-221.

COLLINSON, J. D. 1978. Alluvial sediments. *In* Reading, H. G. (ed), Sedimentary Environments and Facies. Blackwell Sci. Publ. Oxford, 15-60.

CONOLLY, J. R. and EWING, M. 1967. Sedimentation in the Puerto Rico Trench. J. sediment. Petrol. 37, 44-59.

COOK, H. E., MCDANIEL, P. N., MOUNTJOY, E. W. and PRAY, L. C. 1972. Allochthonous carbonate debris flows at Devonian Bank (reef) margins Alberta, Canada. Bull. Can. Petrol. Geol. 20, 439-497.

CREVELLO, P. D. and SCHLAGER, W. 1980. Carbonate Debris Sheets and Turbidites, Exhuma Sound, Bahamas. J. Sediment. Petrol. 50, 1121-1147.

CROWELL, J. C. 1974. Sedimentation along the San Andreas Fault California. *In* Dott, R. H. and Shaver, R. H. (eds), Modern and Ancient Geosynclinal Sedimentation. Spec. Publ. Soc. econ. Palaeont. Miner. 19, Tulsa.

CUIF, J. P. 1974. Recherches sur les Madneporaines du Trias, 1 Famille des Stylophillidae. Bull. Mus. natl. Hist. nat. Paris 17, 211-291.

CURRAY, J. R. and MOORE, D. G. 1971. Growth of the Bengal deep-sea fan and denudation in the Himalayas. Bull.Geol. Soc. Am. 82, 563-572.

CURRY, R. R. 1966. Observations of an Alpine mudflow in the Tennile Range, Central Colorado. Bull. Geol. Soc. Am. 77, 771-6.

DABRIO, C. J. 1975. La sedimentaciai arrecifal Neogena en la region del rio Almonzana. Esteidiois Geologicas 41, 285-296.

DAILY, B., MOORE, P. S. and RUST, B. R. 1980. Terrestial-Marine transition in the Cambrian rocks of Kangaroo Island, South Australia. Sedimentology 27, 379-399.

DALY, R. A. 1936. Origin of submarine 'canyons'. Am. J. Sci. 31, 401-420.

DAMUTH, J. E. and KUMAR, P. 1975. Amazon cone: morphology, sediments age and growth patterns. Bull. Geol. Soc. Am. 86, 863-878.

DAVIDSON-ARNOTT, R. G. D. and GREENWOOD, B. 1974. Bedforms and structures associated with bar topography in the shallow water wave environment, Kanchibougvac Bay, New Brunswick, Canada. J. sediment. Petrol. 44, 698-704.

DAVIES, G. R. 1977. Turbidites, debris sheets and truncation structures in Upper Palaeozoic deep-water carbonates of the Sverdrup basin, Arctic Archipelago. *In* Soc. Econ. Palaeont. Miner. Spec. Publ. 25, 221-247.

DAVIES, T. A., HAY, W. W., SOUTHAM, J. R. and WORSLEY, T. R. 1977. Estimates of Cainozoic Oceanic Sedimentation Rates. Science 197, 53-55.

DAVIES, I. C. and WALKER, R. G. 1974. Transport and deposition of resedimented conglomerates: the Cap Enragé Formation Cambro-Ordovician, Gaspé, Quebec. J. sediment. Petrol. 44, 1200-1216.

DELAUNE-MAYERE, M. and PARROT, J. F. 1976. Evolution du Mésozoique de la Marge Continentale Meridionale du Bassin Tethysien Oriental d'après L'étude des séries sedimentaires de la Region Ophiolitique du N. W. Syrien. Cah. O.R.S.T.O.M., sér. Géol. VIII, 173-183.

DELAUNE-MAYERE, M., MARCOUX, J., PARROT, J. F. and POISSON, A. 1977. Modèle d'évolution mésozoique de la paléo-marge tethysienne au niveau des nappes radiolaritiques et ophiolitiques du Taurus lycien, d'Antalya et du Baër-Bassit. *In* Biju-Duval, B. and Montadert, L. (eds), Structural History of the Mediterranean Basins. Technip Paris, 79-94.

DE RAAF, J.F.M., READING, H. G. and WALKER, R. G. 1965. Cyclic sedimentation in the Lower Westphalian of North Devon, England. Sedimentology 4, 1-52.

DEWEY, J. F., PITMAN, W. C., RYAN, W. B. F. and BARIN, J. 1973. Plate tectonics and the evolution of the Alpine system. Bull. Geol. Soc. Am. 84, 37-80.

DICKSON, J. A. D. 1965. A modified staining technique for carbonates in thin section. Nature 205, 587.

DUFF, P. McL. D., HALLAM, A. and WALTON, E. K. 1967. Cyclic Sedimentation, 280 p. Elsevier, Amsterdam.

DUMONT, J. F. 1972. Découverte d'un horizon cambrien à Trilobites dans le Taurus de Pisidie (Turquie). C.r. Séances Acad. Sci. Paris 274, 2435-2438.

DUMONT, J. F. 1976a. Études géologiques dan les Taurides Occidentales: Les formations paléozoiques et mésozoiques de la coupole de Karacahisar (Province d'Isparta, Turquie). Thesis: Univ. Paris-Sud, Orsay. 213 p.

DUMONT, J. F. 1976b. La courbure d'Isparta et l'origine des nappes d'Antalya; hypothèse d'un décrochement majeur, l'accident trans-taurique, qui a dédouble le dispositif structural Taurique établi par la tectogènèse du Crétacé supérieur. Bull. Miner. Res. Explor. Inst. Turkey 84, 57-68.

DUMONT, J. F., GUTNIC, M., MARCOUX, M., MONOD, O. and POISSON, A. 1972a. Le Trias des Taurides Occidentales (Turquie). Définition du bassin pamphylien: Un nouveau domaine à ophiolithes à la marge externe de la chaine taurique. Z. Deutsch geol. Ges., 123, 385-409.

DUMONT, J. F., GUTNIC, M., MARCOUX, J., MONOD, O. and POISSON, A. 1972b. Essai de reconstitution d'un bassin triasique à ophiolites à la marge externe des Taurides: le bassin pamphylien. C.r. Somm. Soc. géol. Fr. 2, 73-74.

DUMONT, J. F., UYSAL, S. and MONOD, O. 1980. La série de Zindan: un élément de liason entre plate-forme et bassin à l'Est d'Isparta (Taurides occidentales, Turquie). Bull. Soc. géol. Fr. 22(7) 225-232.

DUNHAM, R. J. 1962. Classification of carbonate rocks according to depositional texture. *In* Ham, W. E. (ed), Classification of Carbonate Rocks. Mem. Am. Assoc. Petrol. Geol. 1, 108-121.

DURR, S. 1976. Ueber das Menderes-Kristallin und sein aequivalent in Greichenland. Bull. Soc. géol. Fr. 18(7), 429.

DURR, S., ALTHERR, R. and KELLER, J. 1977. The median aegean crystalline belt: stratigraphy, structure, metamorphism, magnetism. *In* Closs, H. *et al.* (eds), Mediterranean Orogens. Stutgart.

EISBACHER, G. H., CARRIGY, M. and CAMPBELL, R. B. 1974. Palaeodrainage patterns and late-orogenic basins of the Carodian Cordillera *In* Tectonics and Sedimentation, Dickson, W. R. (ed) Soc. econ. Geol. Palaeont. Spec. Pub. 22, 143-166.

ELLIOT, R. E. 1968. Facies, sedimentation successions and cyclothems in productive coal measures in the East Midlands, Great Britain. Mercian. Geol. 2, 351-372.

EMBLEY, R. W. 1976. New evidence for occurrence of debris flow deposits in the deep sea. Geology 4, 371-374.

ENGEL, W. 1970. Die Nummuliten-Breccien im Flyschbecken von Ajdovscina in Slowenien als Beispiel karbonatischer Turbidite. Verh. Geol. B.-A. H4, 570-582.

ENOS, P. 1977. Flow Regimes in Debris Flows. Sedimentology 24, 133-142.

EYNON, G. and WALKER, R. G. 1974. Facies relationships in Pleistocene outwash gravels, southern Ontario: a model for bar growth in braided rivers. Sedimentology 21, 43-70.

FLEUTY, M. J. 1964. The Description of Folds. Proc. Geol. Assoc. London 75, 461-492.

FOLK, R. L. 1968. Petrology of Sedimentary Rocks. Hemphills, Austin Texas, 170 p.

FOREL, F. A. 1885. Le ravin sous-lacustre du Rhône dans le lac Leman. Bull. Soc. Vaudoise Sci. Nat. 23, 85-107.

FRIEDMAN, G. M. 1964. Early Diagenesis and Lithification in Carbonate Sediments. J. sediment. Petrol. 34, 777-813.

FRIEDMAN, G. M. and SANDERS, J. E. 1978. Principles of Sedimentology. New York, John Wiley and Sons, 792 p.

FRIEND, P. F., 1966. Clay fractions and colours of some Devonian red beds in the Catskill Mountains. Geol. Soc. London. Q. J. 122, 273-292.

FRIEND, P. F. 1978. Distinctive features of some ancient river systems. *In* Miall, A. D. (ed), Fluvial Sedimentology. Mem. Can. Soc. Petrol. Geol. 5, 531-542.

FROST, S. H. 1977. Ecologic controls of Caribbean and Mediterranean Oligocene reef coral communities. *In* Taylor, D. L. (ed), Proc. 3rd Int. Coral Reef Symp., Miami, Florida, 367-375.

GARRETT, P., SMITH, D. L., WILSON, A. O. and PATRIGUIN, D. 1971. Physiography Ecology and Sediments of Two Bermuda Patch Reefs. J. Geol. 79, 647-668.

GEISTER, J. 1977. The influence of wave exposure on the ecological zonation of Caribbean coral reefs. *In* Proc. 3rd Int. Coral Reef Symp. Miami, 1, 23-29.

GILBERT, G. K. 1885. The topographic features of lake shores. Ann. Rep. U.S. geol. Surv. 5, 69-123.

GILBERT, G. K. 1890. Lake Bonneville. M .. U.S. geol. Surv. 1.

GILE, L. H., PETERSON, F. F. and CROSSMAN, R. B. 1966. Morphological and genetic sequences of carbonate accumulation in desert soils. Soil Sci. 101, 347-360.

GILE, L. H. 1970. Soils of the Rio Grande Valley Border in southern New Mexico. Proc. Soil Sci. Soc. Am., 34. 466-472.

GINSBURG, R. N. and SCHROEDER, J. H. 1973. Growth and Submarine Fossilisation of Algal Cup Reefs, Bermuda. Sedimentology 20, 575-614.

GOREAU, T. F. 1959. The Ecology of Jamaican Coral Reefs, Pt. 1: Species Composition and Zonation. Ecology 40, 67-90.

GOREAU, T. F. and LAND, L. S. 1974. Fore-reef morphology and depositional processes, North Jamaica. *In* Reefs in Time and Space: Selected Examples from the Recent and Ancient. Soc. Econ. Palaeontol. Miner. Spec. Publ. 18, 77-89.

GORLE , K. 1976. The determination of former mudflow-directions in olistostromes. 9th Intl. Congr. Sediment. Nice, 163-169.

GOUDIE, A. S. 1973. Duricrust in Tropical and Subtropical Landscapes. Clarendon Press, Oxford.

GRACIANSKY, P. C. 1967. Existence d'une nappe ophiolitique à l' éxtrémite occidentale de la chaîne sud-anatolienne; relations entre les autres unites chariées et avec les terrains autochtones (Turique). C.r. Séances. Acad. Sci. Paris 264, 2876-2879.

GRACIANSKY, P. C. 1968. Stratigraphie des unités superposées dans le Taurus Lycien et place dans l'arc dinaro-taurique. Bull. Miner. Res. Explor. Inst. Turkey 71, 42-62.

GRACIANSKY, P. C. de 1972. Recherches géologiques dans le Taurus Lycian Occidental. Thèse, Universite de Paris-Sud, 571 p.

GRACIANSKY, P. C. 1973. Le probleme des "coloured mélanges" a propos de formations chaotiques associées aux ophiolites de Lycie occidentale (Turquie). Rev. Géogr. phys. Géol. dyn. Paris 15, 556-566.

GRACIANSKY, P. C. and LYS, M. 1968. Présence d'une microfaune d'âge Ladinien probable dans l'une des unités alloctones du Taurus occidental (Turquie). C.r. Séances Acad. Sci. Paris 267, 36-38.

GRACIANSKY, P. C., LEMOINE, M., LYS, M. and SIGAL, J. 1967. Une coupe stratigraphique dans Paléozoique supérieur et Mésozoique à l'éxtrémité occidentale de la chaîne sud-anatolienne (nord de Fethiye). Bull. Miner. Res. Explor. Inst. Turkey 69, 10-33.

GRACIANSKY, P. C., LORENZ, C. and MAGNE, J. 1970. Sur les étapes de la transgression du Miocène inférieur observée dans les fenêtres de Göcek (Sud-Ouest de la Turquie). Bull. Soc. géol. Fr. 12(7), 557-564.

GRIGGS, G. B. and KULM, L. D. 1970. Sedimentation in Cascadia deep sea channel. Bull. Geol. Soc. Am. 81, 1361-1384.

GUTNIC, M. 1977. Géologie du Taurus pisidien au Nord d'Isparta (Turquie). Principaux resultats extraits des notes de M. Gutnic entre 1964 et 1971 par O. Monod. Publ. Faculté des Sciences, Univ. Paris-Sud, Orsay, 130 p.

GUTNIC, M. and POISSON, A. 1970. Un dispositif remarquable des chaînes tauriques dans le sud de la courbure d'Isparta. C.r. Séances Acad. Sci. Paris 270, 672-675.

GUTNIC, M., MONOD, O., POISSON, A. and DUMONT, J. F. 1979. Géologie des Taurides occidentales (Turquie). Mém. Soc. géol. Fr. 58(137), 1-112.

GWIRTZMANN, G. and BUCHBINDER, B. 1977. The Dessication events in the Eastern Mediterranean during Messinian times as compared with other Miocene dessication events in basins around the Mediterranean. *In* Biju-Duval, B. et Montadent, L. (eds) Structural History of the Mediterranean Basins, Editions Technip Paris, 411-420.

GWIRTZMANN, G. and BUCHBINDER, B. 1978. Recent and Pleistocene Coral Reefs and Coastal Sediments of the Gulf of Elat. *In* Post congress Guidebook, Tenth Int. Congr. sediment, Jerusalem, 163-189.

HADZI, E., PANTIC, N., ALEKSIC, V. and KALENIC, M. 1976. Un modèle préliminaire de l'évolution tectonique de la peninsule balkanique dans le cadre du developpement de la Mediterranée entière au cours du cycle alpin. Bull. Soc. géol. Fr. 18(7), 199-203.

HAMPTON, M. A. 1972. The role of subaqueous debris flow in generating turbidity currents. J. sediment. Petrol. 42, 775-793.

HAMPTON, M. A. 1975. Competence of fine-grained debris flow in generating turbidity currents. J. sediment. Petrol. 45, 834-844.

HANCOCK, N. J. 1978. Discussion on pressure solution. J. geol. Soc. Lond. 135, 134.

HARMS, J. C. and FAHNESTOCK, R. K. 1965. Stratification, bedforms and flow phenomena (with an example from the Rio Grande) *In* Middleton, G. V. (ed), Primary Sedimentary Structures and their Hydrodynamic Interpretation. Spec. Publ. Soc. econ. Palaeontol. Miner., Tulsa 12, 84-115.

HARMS, J. C., SOUTHARD, J. B., SPEARING, D. R. and WALKER, R. G. 1975. Depositional Environments as Interpreted from Primary Sedimentary Structures and Stratification. Short Course, Soc. econ. Palaeont. Miner. Tulsa 2.

HAYWARD, A. B. 1981. Depositional processes on Red Sea alluvial fans and their modification by marine processes. Weir Fund Report, Univ. Edinburgh, unpubl. 15 p.

HAYWARD, A. B. in press (a). Reefs in a coarse clastic sedimentary environment, Miocene, Turkey. Quaternary Red Sea. J. Coral Reef. Soc.

HAYWARD, A. B. in press (b). Alluvial fans and associated marine facies, Miocene, southwest Turkey. *In* Collinson, J. D. (ed), Fluvial Sedimentology, Int. Assoc. sediment. Spec. Publ.

HAYWARD, A. B. and ROBERTSON, A. H. F. in press. Direction of ophiolite emplacement inferred from Cretaceous and Tertiary sediments of an adjacent autochthon, the Bey Dağlari, S. W. Turkey. Bull. Geol. Soc. Am.

HEDBERG, H. D. (ed), 1976. International Stratigraphic Guide. John Wiley, New York, 200 p.

HEEZEN, B. C. and EWING, M. 1952. Turbidity currents and submarine slumps and the 1929 Grand Banks earthquake. Am. J. Sci. 250, 849-873.

HEEZEN, B. C. and HOLLISTER, C. D. 1964. Deep-sea current evidence from abyssal sediments. Mar. Geol. 1, 141-174.

HEIN, F. J. and WALKER, R. G. 1977. Bar evolution and development of stratification in the gravelly, braided, Kicking Horse River, British Columbia. Can. J. Earth Sci. 14, 562-570.

HENDRY, H. E. 1973. Sedimentation of deep water conglomerate in L. Ordovician rocks of Quebec, composite bedding produced by progressive liquefaction of sediment. J. sediment. Petrol. 43, 125-137.

HESSE, R. 1975. Turbiditic and non-turbiditic mudstone of Cretaceous flysch sections of the East Alps and other basins. Sedimentology 22, 387-416.

HEWARD, A. P. 1976. Sedimentation patterns in coal bearing strata, Northern Spain and Great Britain. D.Phil. thesis, Univ. Oxford.

HEWARD, A. P. 1978a. Alluvial fan sequence and megasequence. *In* Miall, A. D. (ed), Fluvial Sedimentology. Mem. Can. Soc. Petrol. Geol. 5, 669-702.

HEWARD, A. P. 1978b. Alluvial fan and lacustrine sediments from the Stephanian A and B (La Magdalena, Crinera Matallara and Sabero) coalfields, Northern Spain. Sedimentology 25, 451-488.

HISCOTT, R. N. 1980. Depositional framework of sandy mid-fan complexes of Tourelle Formation, Ordovician, Quebec. Bull. Am. Assoc. Petrol. Geol. 64, 1052-1077.

HISCOTT, R. N. 1981. Deep-sea Fan deposits in the Macigno Formation (Middle-Upper Oligocene) of the Gordana Valley, Northern Apennines Italy: Discussion. J. sediment. Petrol. 51, 1015-1020.

HOLMES, A. 1965. Principles of Physical Geology. Publ. Nelson, London, 1288 p.

HOWELL, D. G. and LINK, M. H. 1979. Eocene conglomerate sedimentology and basin analysis, San Diego and the southern California borderland. J. sediment. Petrol. 49, 517-540.

HOWELL, D. G., CROUCH, J. K., GREENE, H. G., McCULLOCH, D. S. and VEDDER, J. G. 1980. Basin development along the Late Mesozoic Cainozoic California margin: a plate tectonic margin of subduction, oblique subduction and transform tectonics. *In* Ballance, P. F. and Reading, H. G. (eds), Sedimentation in Oblique-slip Mobile Zones. Int. Assoc. Sediment. Spec. Publ. 4, 43-62.

HSU, K. J. 1973. The dessicated deep-basin model for the Messinian events. *In* Drooger, C. W. (ed), Messinian Events in the Mediterranean. North Holland, Amsterdam, 60-67.

HSU, K. J., RYAN, W. B. F. and CITA, M. B. 1973. Late Miocene dessication of the Mediterranean. Nature 242, 240-244.

HUANG, T. C. and GOODALL, H. H. 1970. Sediments and sedimentary processes of the eastern Mississippi Cone, Gulf of Mexico. Bull. Am. Assoc. Petrol. Geol. 54, 2070-2100.

IZDAR, E. 1976. Geotectonic developments of Western Anatolia and the comparison with geological units of western parts of Aegean Region (abstract). Bull. Soc. géol. Fr. 18(7), 476.

JACOBI, R. D. 1976. Sediment slides on the northwestern continental margin of Africa. Mar. Geol. 22, 157-174.

JAFFREZO, J., POISSON, A. and AKBULUT, A. 1978. Les algues du Crétacé inférieur des Bey Dağlari (Taurides occidentales, Turquie). Bull. Miner. Res. Explor. Inst. Turkey 91.

JAMES, N. P. 1972. Late Pleistocene Reef Limestones, N. Barbados, West Indies. Ph.D. Thesis, McGill Univ. Montreal, 242 p.

JAMES, N. P. 1978a. Facies Models 13: Carbonate Slopes. Geoscience Canada 5, 189-199.

JAMES, N. P. 1978b. Facies models 10: Reefs. Geoscience Canada 5, 16-26.

JAMES, N. P. 1979. Facies Models 11: Reefs. *In* Walker, R. G. (ed), Facies Models, Geoscience, Canada, Reprint Series 1.

JAMES, N. P. and GINSBURG, R. N. 1979. The Seaward Margin of Belize Barrier and Atoll Reefs. Int. Assoc. Sediment. Spec. Publ. 3, 183 p.

JAUBERT, J. 1977. Light, metabolism growth forms of the hermatypic scleractinian coral Synaraea convera Verrill in the lagoons of Moorea (French Polynesia). Proc. 3rd Int. Coral Reef Symp., Miami 2, 483-488.

JIPPA, D. and KIDD, R. B. 1974. Sedimentation of coarser grained interbeds in the Arabian Sea and sedimentation processes of the Indus cone. Init. Reports DSDP XXIII, 471-492.

JOHNSON, D. 1938. The origin of submarine canyons. J. Geomorphology 1, 230-243.

JOHNSON, A. M. 1970. Physical Processes in Geology. Freeman, Cooper and Co., San Francisco.

JOHNSON, H. D. 1978. Shallow siliciclastic seas. *In* Reading, H. G. (ed), Sedimentary Environments and Facies. Blackwell Sci. Publ. Oxford, 207-258.

JOHNSON, G. D. and VONDRA, C. F. 1972. Siwalik sediments in a portion of the Punjab re-entrant: the sequence at Haritalyangar, District Bilaspur, H.P. Himalayan Geol. 2, 120-144.

JOPLING, A. V. 1965. Hydraulic factors controlling the shape of laminae in laboratory deltas. J. Sediment. Petrol. 35, 777-791.

JOPLING, A. V. 1966. Some applications of theory and experiment to the study of bedding genesis. Sedimentology 7, 71-102.

JUTEAU, T. 1975. Les ophiolites des nappes d'Antalya (Taurides occidentales, Turquie). Mém. Sci. Terre Nancy 32.

JUTEAU, T., NICOLAS, A., DUBESSY, J., FRUCHARD, J. C. and BOUCHEZ, J. L. 1977. The Antalya ophiolite complex (Western Taurides, Turkey): a structural model for an oceanic ridge. Bull. Geol. Soc. Am. 88, 1740-1748.

KALAFATÇIOĞLU, A. 1973. Geology of the western part of Antalya Bay. Bull. Miner. Res. Explor. Inst. Turkey 81, 31-84.

KELLING, G. and HOLROYD, J. 1978. Clast size, shape and composition in some ancient and modern fan gravels. *In* Stanley, D. J. and Kelling, G. (eds), Sedimentation in submarine Canyons, Fans and Trenches. p. 138-162. Dowden, Hutchinson and Ross Inc. Pennsylvania.

KOMAR, P. D. 1970. The competence of turbidity current flow. Bull. Geol. Soc. Am. 81, 1555-1562.

KRAUSE, F. F. and OLDERSHAW, A. E. 1979. Submarine carbonate breccia beds: a depositional model for two layer sediment gravity flows from the Sekwi Formation (L. Cambrian), Mackenzie Mts, N. West Territories, Canada. Can. J. Earth Sci. 16, 189-199.

KRUMBEIN, W. C. and SLOSS, L. L. 1963. Stratigraphy and Sedimentation. W. H. Freeman, San Francisco, 660 p.

KUENEN, Ph. H. 1950. Marine Geology. John Wiley, New York.

KEUNEN, Ph. H. and MIGLIONI, C. I. 1950. Turbidity currents as a cause of graded bedding. J. Geol. 58, 91-127.

LEEDER, M. R. 1975. Pedogenic carbonates and flood sediment accretion rates: a quantitative model for alluvial arid-zone lithofacies. Geol. Mag. 112, 257-270.

LEEDER, M. R. 1978. A quantitative stratigraphic model for alluvium with special reference to channel deposit density and interconnectedness. *In* Miall, A. D. (ed). Fluvial Sedimentology. Mem. Can. Soc. Petrol. Geol. 5, 587-596.

LEFEVRE, , 1967. Un nouvel élément de la géologie du Taurus lycien: les nappes d'Antalya (Turquie). C.r. Séances Acad. Sci. Paris 265, 1365-1368.

LEOPOLD, L. B. and WOLMAN, M. G. 1957. River channel patterns: braided meandering and straight. Prof. Pap. U.S. geol. Surv. 282-A, 39-85.

LEWIS, G. L. 1953. Turkish. Teach Yourself Books. Kodder and Stoughton, Sevenoaks, Kent, 175 p.

LOGAN, B. W., HARDLING, J. L., ALM, W. M., WILLIAMS, J. D. and SWORD, R. G. 1969. Carbonate sediments and reefs in Yucatan Shelf, Mexico. Am. Assoc. Petrol. Geol. Mem. 11, 1-196.

MIALL, A. D. 1970. Devonian alluvial fans, Prince of Wales Island, Arctic Canada. J. sediment. Petrol. 40, 556-571.

MIALL, A. D. 1977. A review of the braided river depositional environment. Earth Sci. Rev. 13, 1-62.

MIALL, A. D. 1978. Lithofacies types and vertical profile models in braided river deposits: a summary. *In* Miall, A. D. (ed), Fluvial Sedimentology. Mem. Can. Soc. Petrol. Geol. 5, 597-604.

MIDDLETON, G. V. 1967. Experiments on density and turbidity currents III. Deposition of sediment. Can. J. Earth Sci. 4, 475-505.

MIDDLETON, G. V. 1969. Turbidity currents and grain flows and other mass movements down slopes. *In* Stanley, D. J. (ed), The New Concepts of Continental Margin Sedimentation. GM-A-1 to GM-B-14, Am. geol. Inst. Short Course Notes.

MIDDLETON, G. V. 1970. Experimental studies related to problems of flysch sedimentation. *In* Lajoie, J. (ed), Flysch sedimentology in North America. Geol. Assoc. Can. Spec. Pap. 7, 253-272.

MIDDLETON, G. V. 1973. Johannes Walther's law of correlation of facies. Bull. Geol. Soc. Am. 84, 979-988.

MIDDLETON, G. V. and HAMPTON, M. A. 1973. Sediment gravity flows: mechanics of flow and deposition. *In* Turbidites and Deep-Water Sedimentation. Short Course Soc. econ. Paleontol. Mineral. Tulsa 1, 1-38.

MIDDLETON, G. V. and HAMPTON, M. A. 1976. Subaqueous sediment transport and deposition by sediment gravity flows. *In* Stanley, D. J. and Swift, D. J. P. (eds), Marine sediment transport and environmental management. Wiley, New York. 197-218.

MONOD, O. 1976a. Carte géologique du Taurus occidental au sud de Beysehir. Centre National Recherche Scientifique. Univ. Paris-Sud, Orsay. 2 sheets.

MONOD, O. 1976b. La courbure d'Isparta: une mosaique de blocs autochtones surmontés de nappes composites à la jonction de l'arc héllénique et de l'arc taurique. Bull. Soc. géol. Fr. 18(7), 521-531.

MONOD, O. 1977a. Recherches géologiques dans le Taurus occidental au sud de Beysehir (Turquie). Thesis: Univ. Paris-Sud, Orsay.

MONOD, O. 1977b. Towards a tectonic connection between Hellenides and Taurides. Abstracts 6th Colloquium Geology Aegean Region. Izmir, Turkey.

LONG, D. G. F. 1977. Resedimented conglomerates of Huronian (lower Aphebian) age from the north shore of Lake Huron, Ontario, Canada. Can. J. Earth Sci 14, 2495-2509.

LONGMAN, M. W. 1980. Carbonate diagenetic textures from nearsurface diagenetic environments. Bull. Am. Assoc. Petrol. Geol. 64, 461-487.

LOWE, D. R. 1976a. Grain flow and grain flow deposits. J. sediment. Petrol. 46, 188-199.

LOWE, D. R. 1976b. Subaqueous liquified and fluidized sediment flows and their deposits. Sedimentology 23, 285-308.

LOWENSTAN, H. A. 1957. Niagarian reefs in the Great Lakes area. *In* Hedgepeth, J. W. and Lodd, H. S. (eds), Treatise on marine ecology and palaeoecology 2. Palaeoecology Geol. Soc. Am. Mem 67, 215-248.

LUSTIG, L. K. 1965. Clastic sedimentation in Deep Springs Valley, California. Prof. Pap. U.S. geol. Surv. 352F, 131 p.

MAIKLEM, W. R. 1970. The Capricorn Reef Complex, Great Barrier Reef, Australia. J. sediment. Petrol 38, 785-798.

MAITRE, D. 1967. Contribution a l'étude géologique de la bordure sud du massif du Menderes dans la region située à l'Est de Köycegiz (province de Muğla) Turquie. Thesis: Fac. Sci. Grenoble.

MARTIN, J. H. 1981. Quaternary glaciofluvial deposits in central Scotland: sedimentology and economic geology. Ph.D. Thesis Univ. of Edinburgh, 242 p.

MARTINDALE, W. 1976. Calcareous Encrusting Organisms of the Recent and Pleistocene Reefs of Barbados, West Indies. Ph.D. Thesis Univ. of Edinburgh, 141 p.

MARTINI, I. P. 1977. Gravelly flood deposits of Irvine Creek, Ontario, Canada. Sedimentology, 24. 603-622.

MATTHEWS, R. K. 1967. Diagenetic Fabrics in Biosparites from the Pleistocene of Barbados, W. Indies. J. sediment. Petrol 37, 1147-1153.

MERRIAM, D. F. (ed). 1964. Symposium on Cyclic Sedimentation. Kan. Geol. Surv. Bull. 169.

MESOLELLA, K. J., SEALEY, H. A. and MATTHEWS, R. K. 1970. Facies Geometrics within Pleistocene reefs of Barbados, West Indies. Bull. Am. Assoc. Petrol. Geol. 54, 1899-1917.

MATZNER, A. B. and WHITLOCK, M. 1958. Flow behaviour of concentrated dilutant suspensions. Trans. Soc. Rheology 2, 234-254.

MONOD, O. 1978. Güzelsu Akseki bölgesindeki Antalya Naplari üzerine aciklama (Orta Bati Toroslar - Turkiye). Precisions upon the Antalya Nappes in the region of Guzelsu-Akseki (Western Taurus, Turkey). Bull. geol. Soc. Turkey 21, 27-29.

MONOD, O., MARCOUX, J., POISSON, A. and DUMONT, J. F. 1974. Le domaine d'Antalya, temoin de la fracturation de la plate-forme africaine au cours du Trias. Bull. Soc. géol. Fr. 16(7), 116-127.

MOORES, E. M. and VINE, F. J. 1971. The Troodos Massif, Cyprus, and other ophiolites as oceanic crust: evaluation and implications. Philos. Trans. R. Soc. London A268, 443-466.

MORTON, J. 1974. The coral reefs of the British Solomon Islands. A comparative study of their composition and ecology. Proc. 2nd Intl. Coral Reef Symp. II, Gt. Barrier Reef Comm., Brisbane, 55-69.

MOUNTJOY, E. W., COOKE, H. E. and McDANIEL, P. N. 1972. Allochthonous carbonate flows worldwide indicators of carbonate reef complexes, banks or shelf margins. 24th Int. geol. Congr. sect. 6, 172-189.

MULLINS, H. and NEUMANN, A. C. 1981. Carbonate bank margin sediments. *In* Doyle, L. J. and Pilkey, O. H. Geology of Continental Slopes. Spec. Pub. Soc. Econ. Palaeont. Miner. 27, 165-192.

MUTTI, E. 1974. Examples of ancient deep-sea fan deposits from circum-Mediterranean geosynclines. *In* Dott, R. H. and Shaver, R. H. (eds), Modern and ancient geosynclinal sedimentation. Spec. Publ. Soc. econ. Paleontol. Mineral. Tulsa 19, 92-105.

MUTTI, E. 1977. Distinctive thin-bedded turbidite facies and related depositional environments in the Eocene Mecho Group (south central Pyrenees, Spain). Sedimentology 24, 107-131.

MUTTI, E. 1979. Turbidites et cônes sous-marins profounds. *In* Sédimentation détritique (fluviatile, littorale et marine). Homewood, P. (ed). Inst. Géol. Univ. Fribourg, 353-419.

MUTTI, E. and GHIBAUDO, G. 1972. Un esempio di torbiditi di conoide sottomarina esterna: le Arenarie di San Salvadore (Formazione di Bobbie, Miocene) nell' Appennino di Piacenza: Mem. Acc. Sci. Torino, Cl. Sci. Fis. Mat. Nat. S.4, 40 p.

MUTTI, E. and JOHNS, D. R. 1979. The role of sedimentary by-passing in the genesis of basin plain and fan fringe turbidites in the Hecho Group System (south-central Pyrenees). Mem. Soc. geol. Ital. 18, 15-22.

MUTTI, E. and RICCI LUCCHI, F. 1972. Le torbiditi den "Apennino settentrionale" introduzione all' avalisi de facies. Soc. Geol. Italiana Mem. 11, 161-199.

MUTTI, E. and RICCI LUCCHI, F. 1974. La signification de centaines unites sequentielles dans les series a turbidites. Bull. Soc. géol. Fr. XVI, 577-582.

MUTTI, E. and RICCI LUCCHI, F. 1975. Examples of turbidite facies and facies associations from selected formations of the Northern Apennines. Field Trip Guidebook A-11, IX Int. Congr. Sedim., Nice, 21-36.

MUTTI, E. and RICCI LUCCHI, F. 1981. Introduction to the excursions on siliciclastic turbidites. *In* Ricci Lucchi, F. (ed), Excursion Guidebook, 2nd Europ. Reg. Meet. Int. Assoc. Sediment, 1-3.

McBRIDE, E. F. 1963. A classification of common sandstones. J. sediment. Petrol. 33, 664-669.

McDONALD, B. C. and BANERJEE, I. 1971. Sediments and bedforms on a braided outwash plain. Can. J. Earth Sci. 8, 1282-1302.

McILREATH, I. A. and JAMES, N. P. 1979. Facies Models 12. Carbonate Slopes. *In* Walker, R. G. (ed) Facies Models. Geoscience Canada, Reprint Series 1.

McKENZIE, D. 1977. Can plate tectonics describe continental deformation. *In* Biju-Duval, B. and Montadert, L. (eds), Structural History of the Mediterranean Basins. Technip, Paris, 189-196.

McLEAN, R. J. and JERZKIEWICZ, T. 1978. Cyclicity, Tectonics and Coal: some aspects of fluvial sedimentology in the Brazean-Pashapoo Formations, Coal Valley area, Alberta, Canada. *In* Miall, A. D. (ed), Fluvial Sedimentology. Mem. Can. Soc. Petrol. Geol 5, 441-468.

McMASTER, R. L. and CONOVER, J. T. 1966. Recent algal stromatolites from the Canary Islands. Geol. J. 74, 647-652.

McPHERSON, J. G. 1979. Calcrete (caliche) palaeosols in fluvial redbeds of the Aztec siltstone (Upper Devonian), southern Victoria Land, Antarctica. Sediment. Geol. 22, 267-285.

McPHERSON, J. G. 1980. Genesis of variegated redbeds in the fluvial Aztec Siltstone (Late Devonian), Southern Victoria Land, Antarctica. Sediment. Geol. 27, 119-142.

NAYLOR, M. A. 1978. A geological study of some olistostromes and mélanges. Thesis: Cambridge University.

NAYLOR, M. A. 1981. The origin of inverse grading in muddy debris flow deposits - a review. J. sediment. Petrol. 50, 1111-1116.

NELSON, C. H,, MUTTI, E. and RICCI LUCCHI, F. 1975. Comparison of proximal and distal thin-bedded turbidites with current-winnowed deep sea sands. IXme Congres International de Sedimentologic, Nice, 1975.

NEMEC, W., PAREBSKI, S. J. and STEEL, R. J. 1980. Texture and Structure of resedimented conglomerates: Examples from Ksiaz Formation (Fammenian-Tournasian), southwestern Poland. Sedimentology 27, 579-538.

NELSON, C. H. and KULM, L. D. 1973. Submarine fans and deep sea channels. *In* Middleton, G. V. and Bouma, A. H. (eds), Turbidites and Deep Water Sedimentation. Soc. Ec. Palaeont. Miner. Tulsa. Pacific Sectn. Short Course Lecture Notes 39-78.

NILSEN, T. H. 1980. Modern and Ancient Submarine Fans: Discussion of Papers by R. G. Walker and W. R. Normark. Am. Assoc. Petrol. Geol. 64, 1094-1112.

NORMARK, W. R. 1970. Growth patterns of deep sea fans. Bull. Am. Assoc. Petrol. Geol. 54, 2170-2195.

NORMARK, W. R. 1974. Submarine Canyons and fan valleys: factors affecting growth patterns of deep-sea fans. Spec. Pub. Soc. Ec. Palaeont. Miner. 19, 56-68.

NORMARK, W. R. 1978. Fan valleys, channels and depositional lobes on modern submarine fans: characters for the recognition of sandy turbidite environments. Bull. Am. Assoc. Petrol. Geol. 62, 912-931.

NORMARK, W. R., PIPER, D. J. W. and HESS, G. R. 1979. Distributary channels, sandstone lobes and mesotopography of Navy submarine fan, California Borderland, with applications to ancient fan sediments. Sedimentology 26, 749-774.

NORRIS, R. J. and CARTER, R. M. 1980. Offshore sedimentary basins at the southern end of the Alpine Fault, New Zealand. *In* Ballance, P. F. and Reading, H. G. Sedimentation in Oblique-slip Mobile Zones. Spec. Publ. Int. Assoc. Sediment. 4, 237-265.

NORRIS, R. J., CARTER, R. M. and TURNBULL, I. M. 1978. Cainozoic sedimentation in basins adjacent to a major continental transform boundary in southern New Zealand. J. geol. Soc. Lond. 135, 191-205.

ODELL, J. 1977. Description in the geological sciences and the litho-stratigraphic description system. L.S.D.Ø2. Geol. Mag. 114, 81-114.

ONALON, M. 1980. Elmali-Kas (Antalya) Arasirdaki Bolgerin jeolojisi. Istanbul Universitesi, Fen Fakultesi Monografileri, Sayi 29. 140 p.

ORBAY, N. and BAYBURDI, A. 1979. Palaeomagnetism of dykes and tuffs from the Mesudiye region and rotation of Turkey. Geophys. J. R. astron. Soc. 59, 437-444.

ORSZAG-SPENBER, F., POIGNANT, A. F. and POISSON, A. 1977. Palaeogeographic Significance of Rhodolites: Some examples from the Miocene of France and Turkey. *In* Flügel, E. (ed), Fossil Algae. Springer-Verlag, New York, 286-294.

OZGUL, N. and ARPAT, E. 1973. Structural units of the Taurus orogenic belt and their continuation in neighbouring regions. Bull. geol. Soc. Greece 10, 156-164.

PIPER, D. J. W. 1975. Late Quaternary deep-water sedimentation off Nova Scotia and the western Grand Banks. Can. Soc. Petrol. Geol. Mem. 4, 195-204.

PIPER, D. J. W. 1978. Turbidite muds and silts on deep sea fans and abyssal plains. *In* Submarine Canyon and Fan Sedimentation, D. J. Stanley and G. Kelling (eds). Dowden, Hutchison and Ross, Stroudsburgh, Pa., 163-176.

PIPER, D. J. W. and BRISCO, C. D. 1975. Deep water continental margin sedimentation. Initial reports of the Deep-sea Drilling Project Leg 28, Antarctica. *In* Initial Reports of the Deep-sea Drilling Project (ed. D. Hayes, L. A. Fralves, *et al.*), 727-755.

PISONI, C. 1967. Contribution a l'Etude Geologique de la Region de Kas (Vilayet D'Antalya). Bull. Miner. Res. Explor. Inst. Turkey 69, 44-51.

PITMAN, W. C. and TALWANI, M. 1972. Sea-floor spreading in the north Atlantic. Bull. Geol. Soc. Am. 83, 619-649.

POISSON, A. 1967a. Données nouvelles sur le Crétacé et le Tertiaire du Taurus occidental au Nord-Ouest d'Antalya (région du Korkuteli, Turquie). C.r. Séances Acad. Sci. Paris 264, 218-221.

POISSON, A. 1967b. Présence d'un Trias supérieur de faciès récifal dans le Taurus lycien au Nord-Ouest d'Antalya (Turquie). C.r. Séances Acad. Sci. Paris 264, 2443-2446.

POISSON, A. 1968a. Le Crétacé supérieur détritique de l'unité de Yeleme (Taurus lycien, Turquie). C.r. Somm. Soc. géol. Fr. 196 , 188.

POISSON, A. 1968b. L'unité inférieur du Domuz Dağ (Taurus lycien, Turquie), série sédimentaire avec intercalation de coulées sous marines en coussins. Bull. Miner. Res. Explor. Inst. Turkey 70, 100-105.

POISSON, A. 1974a. Chronologie des événements tectoniques depuis le Crétacé supérieur sur la bordure nord-occidentale du golfe d'Antalya, Turquie. Proceedings 24th Congress, Commision Internationale pour l'exploration scientifique de la Méditerranée. Monaco.

POISSON, A. 1974b. Présence de Jurassique et de Crétacé inférieur à faciès de type plateforme dans l'autochtone lycien près d'Antalya (Bey Daglari) Turquie. C.r. Séances Acad. Sci. Paris 278, 835-838.

POISSON, A. 1974c. Schéma structural des environs de Termessos. Éléments pour une chronologie des événements tectoniques posterieurs à la mise en place des nappes d'Antalya (Turquie). C.r. Séances Acad. Sci. Paris 279, 1983-1986.

POISSON, A. 1976. Essai d'interprétation d'une transversale Korkuteli-Denizli (Taurus ouest anatolien, Turquie). Bull. Soc. géol. Fr. 18(7), 499-510.

POISSON, A. 1977. Recherches géologiques dans les Taurides occidentales (Turquie). Thesis: Univ. Paris-Sud, Orsay, 795 p.

POISSON, A. and POIGNANT, A. F. 1974. La formation de Karabayir base de la transgression miocene dans la région de Korkuteli (Antalya-Turquie). *Lithothamnium pseudoramossissimum* nouvelle espèce d'Algue rouge de la formation de Karabayir. Bull. Miner. Res. Explor. Inst. Turkey 82, 67-71.

POTTER, P. E. 1967. Sand Bodies and Sedimentary Environments: A Review. Bull. Am. Assoc. Petrol. Geol. 51, 337-365.

POTTER, P. E., MAYNARD, J. B. and PRYOR, W. A. 1980. Sedimentology of Shale. Springer-Verlag, New York, 306 p.

PRICE, I. 1977. Deposition and derivation of clastic carbonates on a Mesozoic continental margin. Othris Greece. Sedimentology 24, 529-546.

READING, H. G. (ed) 1978a. Sedimentary Environments and Facies. Blackwell Sci. Publ. Oxford.

READING, H. G. 1978b. Facies *In* Reading, H. G. (ed) 1978. Sedimentary Environments and Facies. Blackwell Sci. Publ. Oxford.

REES, A. I. 1968. The production of preferred orientation in a concentrated dispersion of elongated and flattened grains. J. Geol. 76, 457.

REEVES, C. C. 1970. Origin, classification and geologic history of caliche on the southern High Plains, Texas and eastern New Mexico. J. Geol. 78, 352-362.

REINECK, H.-E. and SINGH, I. B. 1975. Depositional Sedimentary Environments. Corrected reprint of 1st edn. Springer-Verlag, Berlin.

REYNOLDS, D. L. 1954. Fluidization as a geological process and its bearing on the problem of intrusive granites. Am. J. Sci. 252, 577-614.

RICCI LUCCHI, F. 1969. Channelised deposits in the middle Miocene flysch of Romagna (Italy). Giorn. Geol. S.2. 36, 203-282.

RICCI LUCCHI, F. 1975a. Sediment dispersal in turbidite basins: examples from the Miocene of the Northern Apennines. IX Congres International de Sedimentologie, Nice.

RICCI LUCCHI, F. 1975b. Depositional cycles in two turbidite formations of the northern Apennines (Italy). J. sediment. Petrol. 45, 3-43.

RICCI LUCCHI, F. 1981. (ed) Excursion Guidebook. 2nd Europ. Regnl. Meet. Int. Assoc. Sediment. Bologna.

RICCI LUCCHI, F. and VALMENI, E. 1980. Basin wide turbidites in a Miocene over supplied deep sea plain: a geometrical analysis. Sedimentology 27, 241-270.

RICOU, L. E., ARGYRIADIS, I. and LEFEVRE, R. 1974. Proposition d'une origine interne pour les nappes d'Antalya et le massif d'Alanya (Taurides occidentales, Turquie). Bull. Soc. géol. Fr. 16(7), 107-111.

RICOU, L. E., ARGYRIADIS, I. and MARCOUX, J. 1975. L'axe calcaire du Taurus, un alignement de fenêtres arabo-africaines sous des nappes radiolaritiques, ophiolitiques et metamorphiques. Bull. Soc. géol. Fr. 17(7), 1024-1043.

RICOU, L. E., MARCOUX, J. and POISSON, A. 1979. L'allochtonie des Bey Dağlari orientaux. Reconstruction palinspastique des Taurides occidentales. Bull. Soc. géol. Fr. 21(7), 125-134.

RICOU, L. E. and MARCOUX, J. 1980. Organisation générale et rôle structurale des radiolarites et ophiolites le long du systèm alpine-méditerranéen. Bull. Soc. géol. Fr. 22(7), 1-14.

ROBERTSON, A. H. F. 1977a. The Moni Melange Cyprus: an olistostrome formed at a destructive plate boundary. J. Geol. Soc. 133, 447-466.

ROBERTSON, A. H. F. 1977b. The Kannoviou Formation, Cyprus, volcaniclastic sedimentation of a probable late Cretaceous volcanic arc. J. Geol. Soc. 134, 269-292.

ROBERTSON, A. H. F. 1981. Metallogenesis on a Mesozoic continental margin, Antalya Complex, S.W. Turkey. Earth. planet. Sci. Lett. 54, 323-345.

ROBERTSON, A. H. F. and HUDSON, J. D. 1974. Pelagic sediments in the Cretaceous and Tertiary history of the Troodos Massif, Cyprus. *In* Hsu K. J. and Jenkyns H. C. (eds). Pelagic sediments: on land and under the sea. Spec. Publ. Int. Assoc. Sedimentol. 1, 403-436.

ROBERTSON, A. H. F. and WOODCOCK, N. H. 1980a. Strike-slip related sedimentation in the Antalya Complex, S.W. Turkey. *In* Ballance, P. F. and Reading H. G. (eds) Sedimentation in Oblique-Slip Mobile Zones. Spec. Publ. Int. Assoc. Sediment. 4, 127-145.

ROBERTSON, A. H. F. and WOODCOCK, N. H. 1980b. Tectonic setting of the Troodos Massif in the east Mediterranean. *In* Panayiotou, A. (ed). Ophiolites: proceedings International Ophiolite Symposium, Cyprus, 1979. Geological Survey Department, Cyprus. 36-49.

ROBERTSON, A. H. F. and WOODCOCK, N. H. 1981a. Alakir Çay Group, Antalya Complex, S.W. Turkey: deposition on a Mesozoic passive carbonate margin. Sediment. Geol. 30, 95-131.

ROBERTSON, A. H. F. and WOODCOCK, N. H. 1981b. Bilelyeri Group, Antalya Complex, S.W. Turkey: deposition on a Mesozoic passive continental margin. Sedimentology 28, 381-399.

ROBERTSON, A. H. F. and WOODCOCK, N. H. 1981c. Gödene zone, Antalya Complex, S.W. Turkey: volcanism and sedimentation on Mesozoic marginal oceanic crust. Geol. Rdsch.

ROBERTSON, A. H. F. and WOODCOCK, N. H. in press. Sedimentary History of the S.W. segment of the Mesozoic-Tertiary Antalya Continental Margin, S.W. Turkey. J. Geol. Soc. Lond.

ROCCI, G., BAROZ, F., BEBIEN, J., DESMET, H., LAPIERRE, D., OHNENSTETTER, M. and PARROT, J. F. 1980. The Mediterranean ophiolites and their related Mesozoic volcano-sedimentary sequences. *In* Panayiotou, A. (ed) Ophiolites: proceedings International Ophiolite Symposium, Cyprus, 1979. Geological Survey Department, Cyprus, 36-49.

RODINE, J. D. and JOHNSON, A. M. 1976. The ability of debris, heavily freighted with coarse clastic materials, to flow on gentle slopes. Sedimentology 23, 213-234.

RUPKE, N. A. 1977. Growth of an ancient deep-sea fan. Geol. J. 85, 725-744.

RUPKE, N. A. and STANLEY, D. J. 1974. Distinctive properties of turbiditic and hemipelagic mud layers in the Algero-Balearic Basin, Western Mediterranean Sea. Smithsonian Contributions to the Earth Sciences 13, 40 p.

RUST, B. R. 1972a. Structure and process in a braided river. Sedimentology 18, 221-245.

RUST, B. R. 1972b. Pebble orientation in fluvial sediments. J. sediment. Petrol. 42, 384-388.

RUST, B. R. 1975. Fabric and structure in glaciofluvial gravels. *In* Jopling, A. V. and McDonald, B. C. (eds), Glaciofluvial and Glaciolacustrine Sedimentation. Spec. Publ. Soc. econ. Paleontol. Mineral. Tulsa 23, 238-248.

RUST, B. R. 1978. Depositional models for braided alluvium, *In* Miall, A. D. (ed) Fluvial Sedimentology. Mem. Can. Soc. Petrol. Geol. 5, 605-625.

RUST, B. R. 1979. Coarse alluvial deposits, *In* Walker, R. G. (ed) Facies Models. Geoscience Canada, Reprint series 1, Geological Association of Canada, 9-22.

SALEEBY, J. B. 1977. Fracture zone tectonics, continental margin fragmentation and emplacement of the Kings-Kaweah ophiolite belt southwest Sierra Nevada. *In* Coleman, R. G. and Irwin, W. P. (eds) North American ophiolite volume, Oregon. Dept. Geol. Min. Indust. Bull. 95, 141-160.

SALEEBY, J. B. 1979. Kaweah serpentinite melange, southwest Sierra Nevada foothills, California. Bull. Geol. Soc. Am. 90, 29-46.

SANDERS, J. E. 1965. Primary sedimentary structures formed by turbidity currents and related sedimentation mechanisms. *In* Middleton, G. V. Primary Sedimentary Structures and their Hydrodynamic Interpretation. Spec. Publ. Soc. econ. Palaeont. Miner. 12, Tulsa, 192-219.

SANTIBESTAN, C. and TABERNER, C. 1980. Reefs in the U. Miocene of S.E. Spain, Reefs Past and Present. Meeting, Cambridge, 1980, Abstr. only.

SARP, H. 1976. Etude géologique et mineralogique du corrège ophiolitique de la région située en NW de Yesilova (Burdur, Turquie). Thesis: Univ. Geneva.

SAUNDERSON, H. C. 1975. Sedimentology of the Brampton Esker and its associated deposits: an empirical test of theory. *In* Jopling, A. V. and McDonald, B. C. (eds), 1975, Glaciofluvial and Glaciolacustrine Sedimentation. Spec. Pub. Soc. econ. Palaeont. Miner., Tulsa 23.

SHELTON, A. W. and GASS, I. G. 1980. Rotation of the Cyprus microplate. *In* Panayiotou, A. (ed), Ophiolites: proceedings International Ophiolite Symposium, Cyprus, 1979. Geological Survey Department, Cyprus, 61-65.

SCHROEDER, J. H. and ZANKL, H. 1974. Dynamic Reef Formation: A Sedimentological Concept based on Studies of Recent Bermuda and Bahama Reefs. Proc. 2nd Intl. Coral Reef Symp. 11, Gt. Barrier Reef Comm., Brisbane, 413-428.

SCOFFIN, T. P. and GARRETT, P. 1974. Processes in the Formation and Preservation of Internal Structure in Bermuda Patch Reefs. Proc. 2nd Intl. Coral Reef Symp. 11, Gt. Barrier Reef Comm., Brisbane, 429-449.

SELLWOOD, B. W. 1972. Tidal-flat sedimentation in the Lower Jurassic of Bornholm, Denmark. Palaeogeogr. Palaeoclim. Palaeoecol. 11, 93-106.

SENEL, M. Teke Toroslavi, 1980. Güneydoğusunun jeologisi, Finike-Kumluca-Kemer (Antalya). M.T.A. Enstitüsü jeologi dairesi, unpubl. Rep. Anhara, 106 p.

SENGOR, A. M. C. and YILMAZ, Y. 1980. Tethyan evolution of Turkey: a plate tectonic approach. Tectonophysics 75, 181-242.

SHARP, R. P. and NABLES, L. H. 1953. Mudflow of 1941 at Wrightwood, Southern California. Bull. Geol. Soc. Am. 64, 547-560.

SHEPHARD, F. P. and DILL, R. F. 1966. Submarine Canyons and Other Sea Valleys. Rand McNally, Chicago, 381 p.

SINGH, I. B. 1977. Bedding structures in a channel sand bar of the Ganga River near Allahabad Uttar Pradesh, India. J. sediment. Petrol. 47, 747-753.

SMITH, A. G. 1971. Alpine deformation and the oceanic areas of the Tethys, Mediterranean, and the Atlantic. Bull. Geol. Soc. Am. 82, 2039-2079.

SMITH, A. G. 1973. The so-called Tethyan ophiolites. *In* Tarling, D. and Runcorn, S. (eds). Implications of Continental Drift to the Earth Sciences. London: Academic Press. 977-986.

SMITH, N. D. 1970. The braided stream depositional environment: comparison of the Platte River with some Silurian clastic rocks, North-central Appalachians. Bull. Geol. Soc. Am. 81, 2993-3014.

SMITH, N. D. 1974. Sedimentology and bar formation in the Upper Kicking Horse River, a braided outwash stream. J. Geol. Chicago 82, 205-223.

SNEH, A. 1979. Late Pleistocene fan-deltas along the Dead Sea Rift. J. Sediment. Petrol. 49, 541-552.

SPORLI, K. B. 1980. New Zealand and oblique-slip margins: tectonic development up to and during the Cainozoic. *In* Ballance, P. F. and Reading, H. G. (eds), Sedimentation in Oblique-slip Mobile Zones. Spec. Publ. 4, Int. Assoc. Sediment. 147-170.

SRIVASTAVA, P., STEARN, C. W. and MOUNTJOY, E. W. 1972. A Devonian megabreccia at the margin of the Ancient Wall carbonate complex, Alberta. Bull. Can. Petrol. Geol. 20, 412-438.

STANLEY, D. J. 1974. Pebbly Mud Transport in the Head of the Wilmington Canyon. Marine. Geol. 16, M1-M8.

STANLEY, D. J. 1980. The Saint-Antonin Conglomerate in the Maritime Alps: A Model for Coarse Sedimentation on a Submarine Slope. Smithsonian Contributions to Marine Science 5, 25 p.

STEEL, R. J. 1974. New Red Sandstone flood plain and piedmont sedimentation in the Hebridean Province. J. Sediment. Petrol. 44, 336-357.

STODDART, D. R. 1969. Ecology and morphology of Recent coral reefs. Biol. Rev. 44, 433-498.

STOW, D. A. V. 1977. Late Quaternary Stratigraphy and Sedimentation on the Nova Scotian Outer Continental Margin. Ph.D. Thesis, Dalhousie Univ.

STOW, D. A. V. 1979. Distinguishing between fine grained turbidites and contourites on the Nova Scotia deep water margin. Sedimentology 26, 371-387.

STOW, D. A. V. 1980. The Laurentian Fan: morphology, sediments, processes and growth patterns - models for hydrocarbon exploration. Bull. Am. Assoc. Petrol. Geol. 65, 375-393.

STOW, D. A. V. and SHANMUGEN, S. 1980. Sequence of structures in fine grained turbidites: comparison of recent deep sea and ancient flysch sediments. Sediment. Geol. 25, 23-42.

STOW, D. A. V., BISHOP, C. D. and MILLS, S. J. in press. Fan Models for hydrocarbon exploration with examples from the North Sea, N.W. European Shelf. Bull. Am. Assoc. Petrol. Geol.

SURLYK, F. 1975a. Fault controlled marine fan-delta sedimentation at the Jurassic-Cretaceous boundary, East Greenland. IXth Int. Congr. Sedimentology 4(2), 305-312.

SURLYK, F. 1975b. Block faulting and associated marine sedimentation at the Jurassic-Cretaceous boundary, East Greenland. NPF-Jurassic Northern North Sea Symposium 7, 1-31.

SURLYK, F. 1978. Submarine fan sedimentation along fault scarps on tilted fault blocks. Bull. Grønlands geol. Unders. 128, 108 p.

SWARBRICK, R. E. 1979. The Mamonia Complex of S.W. Cyprus and its relationship to the Troodos Massif. Ph.D. Thesis: Cambridge Univ.

SWARBRICK, R. E. 1980. The Mamonia Complex of S.W. Cyprus; a Mesozoic continental margin and its relationship to the Troodos Complex. *In* Panayiotau, A. (ed) Ophiolites: Proceedings of the International Ophiolite Symposium, Cyprus. Min. of Agric. and Nat'l. Res. Geol. Surv. Dept., Cyprus, 86-92.

TEICHERT, C. 1958. Concept of Facies. Bull. Am. Assoc. Petrol. Geol. 42, 1064-1082.

TERZAGHI, K. 1956. Varieties of submarine slope failures. Proc. 8th Texas Soil Mech. Found. Eng. Conf., 1-41.

THIUZAT, R. and MONTIGNY, R. 1979. K-Ar geochronology of three Turkish ophiolites. Abstracts, International Ophiolite Symposium. Geological Survey Department, Cyprus, 80-81.

TOLUN, N. 1965. 1/25,000 ölçekli Antalya P24 a2 ve a3 paftalarinin jeolojik incelemesi. M.T.A. Papor No. 3627.

TURNER, P. 1974. Origin of red beds in the Ringerike Group (Silurian) of Norway. Sediment. Geol. 12, 215-235.

TURNER, P. 1981. Continental Red Beds, Developments in Sedimentology, 29. Elsevier, Amsterdam.

UCHAPI, E. and AUSTIN, J. A. 1979. The stratigraphy and structure of the Laurentian cone region. Can. J. Earth Sci. 16, 1726-1752.

VAIL, P. R., MITCHUM, R. M. and THOMPSON, S. 1977. Global cycles of relative changes in sea level. *In* Payton, C. E. (ed). Seismic Stratigraphy - applications to hydrocarbon exploration. Am. Assoc. Petrol. Geol. Mem., 26, 83-97.

VAN HOUTEN, F. B. 1972. Iron and clay in tropical savanna alluvium, northern Colombia: a contribution to the origin of red beds. Bull. Geol. Soc. Am. 83, 2761-2772.

VAN HOUTEN, F. B. 1973. Origin of red beds - a review, 1961-1972. Earth Plant. Sci. Annu. Rev. 1, 39-61.

VISHER, G. S. 1965. Fluvial processes as interpreted from ancient and recent fluvial deposits. *In* Middleton, G. V. (ed), Primary Sedimentary structures and their Hydrodynamic Interpretation. Spec. Publ. Soc. econ. Palaeont. Miner. 12, Tulsa, 116-132.

WALDRON, J. W. F. 1981. Mesozoic sedimentary and tectonic evolution of the northeast, Antalya Complex, Egridir, S.W. Turkey. Ph.D. Thesis: Univ. of Edinb., 239 p.

WALKER, K. R. and ALBERSTADT, L. P. 1975. Ecological succession as an aspect of structure in fossil communities. Palaeobiol. 1, 238-257.

WALKER, R. G. 1965. The origin and significance of the internal sedimentary structures of turbidites. Proc. Yorkshire geol. Soc. 35, 1-32.

WALKER, R. G. 1967. Turbidite sedimentary structures and their relationship to proximal and distal depositional environments. J. sediment. Petrol. 37, 25-43.

WALKER, R. G. 1970. Review of the geometry and facies organisation of turbidites and turbidite bearing basins. *In* J. Lajoie (ed), Flysch Sedimentology in North America. Geol. Assoc. Can. Spec. Paper 7, 219-251.

WALKER, R. G. 1975. Generalized Facies Models for Resedimented Conglomerates of Turbidite Association. Bull. Geol. Soc. Am. 86, p. 737-748.

WALKER, R. G. 1976. Facies models 2 Turbidites and Associated coarse clastic deposits. Geoscience Canada 3, 25-36.

WALKER, R. G. 1977. Deposition of Upper Mesozoic resedimented conglomerates and associated turbidites in southwestern Oregon. Bull. Geol. Soc. Am. 88, 273-285.

WALKER, R. G. 1978. Deep-water sandstone facies and ancient submarine fans: models for exploration for stratigraphic traps. Bull. Am. Assoc. Petrol. Geol. 62, 932-966.

WALKER, R. G. 1979a. Facies and facies models. General introduction. *In* Walker, R. G. (ed) Facies Models. Geoscience Canada Reprint Series 1. Geological Association of Canada, 1-8.

WALKER, R. G. 1979b. Turbidites and associated coarse clastic deposits. *In* Walker, R. G. (ed) Facies Models. Geoscience Canada, Reprint Series 1. Geological Association of Canada.

WALKER, R. G. 1979c. Facies Models. Geoscience Canada, Reprint Series 1. Geological Association of Canada.

WALKER, R. G. 1980. Modern and Ancient Submarine Fans: Reply to Discussion by T. H. Nilsen. Am. Assoc. Petrol. Geol. 64, 1094-1112.

WALKER, R. G. and MUTTI, E. 1973. Turbidite facies and facies associations. *In* Middleton, G. V. and Bouma, A. H. (eds) Turbidites and deep water sedimentation. Pacif. section Soc. econ. Paleont. Miner. short course, Los Angeles. 119-157.

WALKER, T. R. 1967a. Formation of red beds in modern and ancient deserts. Bull. Geol. Soc. Am. 78, 353-368.

WALKER, T. R. 1967b. Colour of recent sediments in tropical Mexico: a contribution to the origin of red beds. Bull. Geol. Soc. Am. 78, 917-920.

WALTHER, J. 1894. Einleitung in die Geologie als Historische Wissenschaft. Bd 3. Lithogenesis der Gegenwert. Fischer Verlag, Jena, 535-1055.

WASSON, R. J. 1977. Last-glacial alluvial fan sedimentation in the Lower Derwent Valley, Tasmania. Sedimentology 24, 781-799.

WATTS, N. L. 1980. Quaternary pedogenic calcretes from the Kalahari (Southern Africa): mineralogy, genesis and diagenesis. Sedimentology 27, 661-686.

WEILER, Y. 1970. Mode of occurrence of pelites in the Kythrea flysch basin (Cyprus). J. Sediment. Petrol. 40, 1255-1261.

WENTWORTH, C. K. 1922. A scale of grade and class terms for clastic sediments. J. Geol. Chicago 30, 377-392.

WESCOTT, W. A. and ETHRIDGE, F. A. 1980. Fan-delta sedimentology and tectonic settings - Yallahs Fan-delta. Bull. Am. Assoc. Petrol. Geol. 64, 374-399.

WILLIAMS, P. F. and RUST, B. R. 1969. The sedimentology of a braided river. J. Sediment. Petrol. 39, 649-679.

WILSON, A. C. 1980. The Devonian sedimentation and tectonism of a rapidly subsiding semi arid fluvial basin in the Midland Valley of Scotland. Scot. J. Geol. 16, 291-313.

WINLAND, H. D. 1969. Stability of Calcium Carbonate Polymorphs in Warm, Shallow Sea Water. J. Sediment. Petrol. 39, 1579-1587.

WINN, R. D. and DOTT, R. H. 1977. Large-scale traction-produced structures in deep-water fan-channel conglomerates in southern Chile. Geology 5, 41-44.

WINN, R. D. and DOTT, R. H. 1979. Deep water fan channel conglomerates of Late Cretaceous age, Southern Chile. Sedimentology 26, 203-228.

WOODCOCK, N. H. 1976. Structural style in slump sheets: Ludlow series, Powys, Wales. J. geol. Soc. Lond., 132, 339-415.

WOODCOCK, N. H. and ROBERTSON, A. H. F. 1977a. Imbricate thrust belt tectonics and sedimentation as a guide to the emplacement of part of the Antalya Complex, S.W. Turkey. Abstracts, 6th Colloquim Geology Aegean Region, Izmir, Turkey.

WOODCOCK, N. H. and ROBERTSON, A. H. F. 1977b. Origins of some ophiolite related metamorphic rocks of the "Tethyan" belt. Geology 5, 373-376.

WOODCOCK, N. H. and ROBERTSON, A. H. F. 1981a. Wrench-related thrusting along a Mesozoic-Cenozoic continental margin, Antalya Complex, S.W. Turkey. *In* McClay, K. R. and Price, N. J. (eds) Thrust and Nappe Tectonics. Geol. Soc. London. 359-362.

WOODCOCK, N. H. and ROBERTSON, A. H. F. 1981b. Imbricate thrusting and wrench tectonics in the Antalya Complex, S.W. Turkey. J. geol. Soc. Lond.

YONGE, C. M. 1958. Observations on *Petricola carditoides* (Conrad). Proc. malac. soc. Lond. 33, 25.

ZARALIOĞLU, M. 1967. Finike veciraninda 1/25,000 ölçekli detay jeoloji harita aliminda bulunmustur. M.T.A. Papor. unpubl. Ankara.

APPENDICES

Appendix A

Methods and Techniques employed

Appendix B

Faunal list

Appendix C

Key to Sedimentological Logs

Appendix D

Specimen list of department collection

APPENDIX A

TECHNIQUES

A1 Petrographic methods

Most thin sections were stained for carbonate (method of Dick_son, 1965). Grain size was estimated in thin section and classified using the Wentworth (1922) scale. Sphericity, roundness and angularity were quantified using standard charts published by Odell (1977) (Fig. A1). Mineral abundances were determined by point counting. For each thin-section a point count spacing approximately equal to the grain size of the rock was chosen, and 333 points counted. As well as standard QRF plots (Folk, 1968), other plots that are more suited to the rock types described here are also employed.

A2 X-Ray Diffraction

Sample Preparation. Many of the finer grained 'mud' sediments contain a high percentage of carbonate which acts as a dilutent, reducing the diffraction intensity of the crystalline species, producing attenuation of the primary x-ray beam and increasing the level of scatter of the x-rays. To produce sharper and more well defined peaks samples were first treated for removal of carbonate. After crushing and grinding, the sample (~two spatulas) was dissolved in 100 ml of 15% acetic acid. It was left for 24 hours and then washed in distilled water and filtered. A small amount of sample was dispersed in water with a few drops of saturated magnesium hydrosulfate solution to prevent flocculation. The sample was then mounted on warmed (~35^{o}C) ceramic tiles.

A3 Transition Matrices

Transition matrices are used throughout this thesis for analysis of sequences of both facies associations and individual facies. The method used is that outlined by Walker (1979a).

A4 Palaeocurrent Measurements

In most areas palaeocurrents were measured from strata with a tectonic dip of between 20^{o} and 30^{o} and horizontal or locally horizontal fold-axes. In such strata tectonic dip results in angular errors of less than 3^{o} in palaeocurrent orientation (Ramsay, 1961) and can be ignored. Over most of the mapped area fold axes are broadly upright and horizontal, and in areas of tectonic dip of greater than

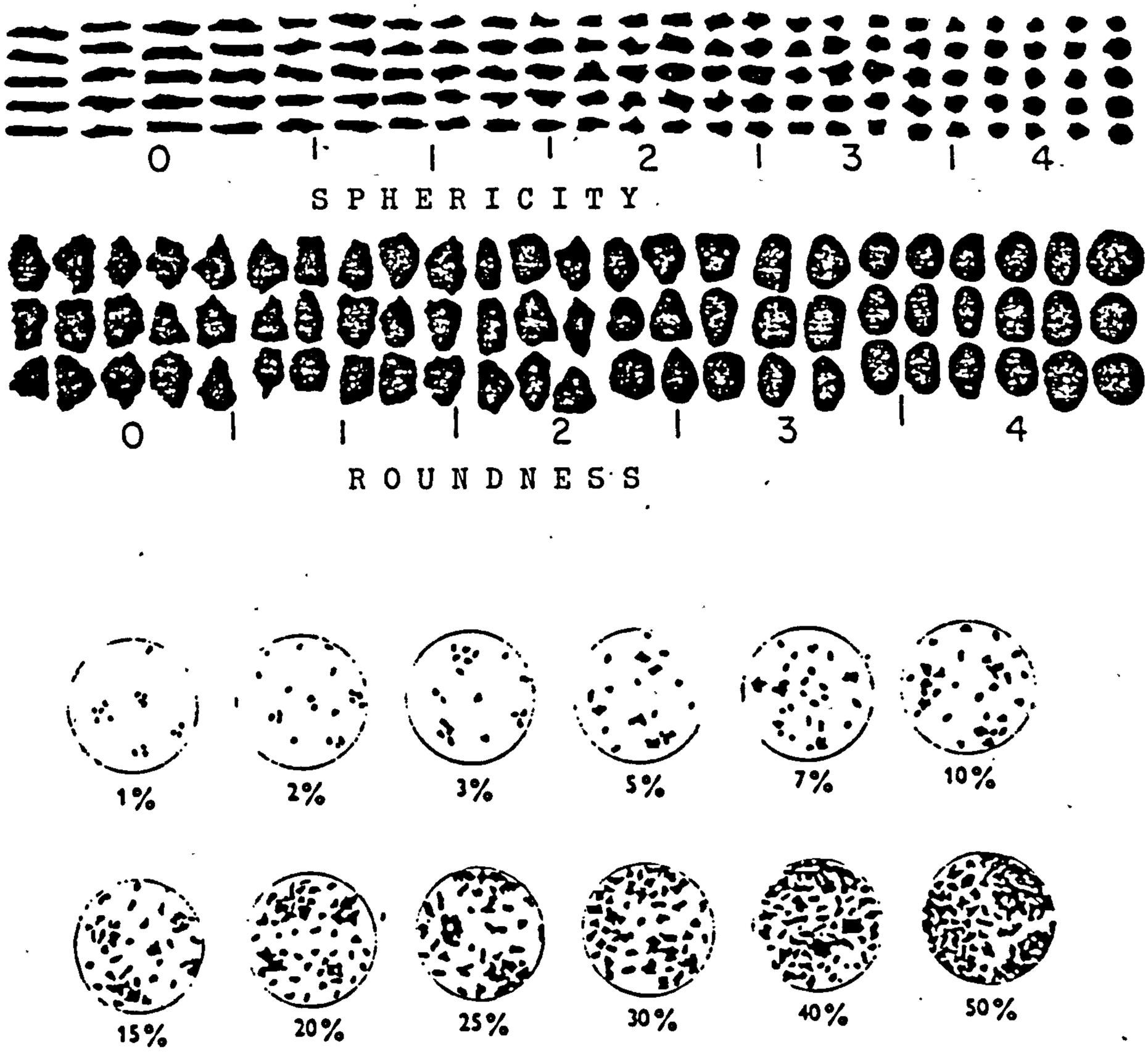

Fig. A1

Standard charts used for description of textures in conglomerates and sandstones (after Odell, 1977).

Letter		Name	Approximate pronunciation
A	a	a	as in French *avoir*, Northern English *man*
B	b	be	as in English
C	c	ce	*j* in *jam*
Ç	ç	çe	*ch* in *church*
D	d	de	as in English
E	e	e	as in *bed*
F	f	fe	as in English
G	g	ge	as in *goat*
•	ğ	yumuşak ge	lengthens a preceding vowel
H	h	he	as in *house*
I	ı	ı	*i* in *cousin*
İ	i	i	as in *pit*
J	j	je	as in French *jour*, like *s* in *leisure*
K	k	ke, ka	as in *king*
L	l	le	as in English
M	m	me	" "
N	n	ne	" "
O	o	o	like French *eau*
Ö	ö	ö	as in German *König*, French *eu* in *deux*
P	p	pe	as in English
R	r	re	as in *ribbon*
S	s	se	as in *sing*
Ş	ş	şe	*sh* in *shall*
T	t	te	as in English
U	u	u	as in *push*
Ü	ü	ü	as in German *Führer*, French *u* in *tu*
V	v	ve	as in English
Y	y	ye	as in *yet*
Z	z	ze	as in English

Fig. A2

Pronunciation of Turkish alphabet.

25° simple rotation back to horizontal is sufficient to restore sedimentary structures to their original position. Rarely in area of more intense folding, e.g. parts of the Salir Formation, the methods of Ramsay (1961) were employed.

A5 Graphic Logs

Many of the sedimentological sections were drawn on GEOLOG, a program written by Dr. J. W. F. Waldron.

(Note - references cited in Appendices are contained in the reference list as the back of the text.)

APPENDIX B

FAUNAL LIST

Specimens held in Thesis Collection

Kasaba Formation - Upper Miocene

Spec. No.	Fossil	Grid Reference
UM1	*Montastrea sp*	501 331
UM3	*Favites neglecta*	501 331
U3	*Tarbellastraea sp*	501 331
U4	*Tarbellastraea sp*	501 331
U5	*Montastrea sp*	501 331
UM6	algal encrusted reef breccia	501 331
U8	*Tarbellastraea sp*	501 331
U10	*Favites neglecta* (Michelotti)	504 333
U13	*Tarbellastraea sp*	504 333
U14	*Montastrea sp*	504 333
UM17	*Montastrea sp*	504 333
UM18	coralline algae encrusted breccia	504 333
UM19	*Tarbellastraea siciliae*	504 333
UM19a	algal encrusted coral	504 333
UM20	*Favia sp*	504 333
UM22	*Montastrea sp*	504 333
UM23	*Favites neglecta*	504 333
407/80	*Montastrea sp*	504 333
409/80	*Montastrea sp*	504 333
94/80	bivalves	502 337
95/80	solitary coral	502 337
96/80	*Turritella sp*	502 337
96a/80	*Turritella bicarinata*	502 337
96b/80	*Turritella turris*	502 337
97/80	*Strombus nodosus*	502 337
99/80	*Chlamys solarium*	502 337
100/80	gastropods (not identified)	502 337

Spec. No.	Fossil	Grid Reference
181/80	*Conus (Conospirus) diyardini* Deshayes	502 337
182/80	*Ancilla (Baryspina) glandiformis* Lamarch	502 337
97a/80	*Venus basteroti*	502 337
	Kemer Formation	
404/80	*Favites sp*	355 448
402/80	*Montastrea sp*	355 448
405/80	algal encrusted coral	355 448
406/80	*Montastrea sp*	355 448
410/80	*Montastrea sp*	355 448
92/80	*Montastrea sp*	355 448
9206	*Clypeaster sp*	441 287
	Felenk Dağ Member	
92/80	*Montastrea sp*	496 154
322/80	*Montastrea sp*	496 154
	Çağman Member	
CM1/80	corals from bioclastic breccia, *Montastrea sp, Favia sp.* several other scleractinian corals	599 288
CM3/80	rhodoliths, branching and encrusting forms, species present include *Lithothamnium sp, Pseudolithothamnium, Lithoporella*	599 288
CM4/80	rhodoliths	599 288
CM2/80	bioclastic breccia	599 288
CMa	algal calcarenite	604 287
CMc	algal breccia	604 287
9198	algal breccia	599 288
3.2.8.80	branching rhodolith	599 288
	Salir Formation	
10/78(3)	*Ostrea sp*	517 380
F1	*Clypeaster sp*	517 380

APPENDIX C

Appendix C (in the pocket at the back of the thesis) is a "pull out" key to the sedimentological logs.

APPENDIX D

List of specimens held in Thesis Collection

(*-refers to thin section)

Spec. No.	Description	Formation	Logged Section	Grid Reference
8/78	M.sst.carb.	Salir Formation	-	365 431
9/78	u.c. CRN	" "	-	510 362
11/78*	c.sst.	" "	-	520 367
29/78	F.sst	" "	7	518 364
30/78*	gl. cgl.	" "	7	518 364
32/78	M.sst	" "	7	518 364
33/78*	C.CRN	" "	7	519 364
35/78*	c.sst	" "	7	519 364
37/78*	c/t	Carbonate Plat. (Maast)		524 336
40/78*	c.sst.	Salir Formation	8	517 379
41/78*	F.sst.	" "	8	517 379
43/78	M.calc.sst.	" "	8	518 379
44/78*	c.sst.	" "	8	518 379
46/78*	c.sst.	" "	9	512 416
50/78	M.sst.	" "	DS	514 388
52/78	mudst + chordrites	" "	DS	514 388
57/78	M.sst.	" "	DS	515 388
63/78	chert nodule	Eoc. lst.		527 375
73/78	M.CRN	" "		527 375
74/78	M.sst.	Salir Formation	DS	515 388
79/78	pel.clt.	Eoc. lst		532 296
80/78	clt.	" "		532 296
81/78	M.CRN	" "		532 296
82/78	C.CRN	" "		532 296
83/78	clt.	" "		533 296
84/78	F.CRN	" "		533 296
85/78	F.CRN	" "		533 296
86/78	M.CRN	" "		533 296
89/78	M.sst.	Salir Formation	1	526 334
91/78	M.sst.	" "	1	526 334
95/78*	F.sst.	" "	1	527 334
97/78*	M.calc.sst.	" "	1	527 334
98/78	pel.chalk	" "	1	527 334
99/78*	F.sst	" "	1	528 334
100/78	F.sst	" "	1	529 334
103/78	F.sst	" "	A	454 446
106/78*	v.c.sst.	" "	B	442 441
107/78*	F.sst.	" "	B	442 441
107a/78*	v.c.sst.	" "	B	442 441
110/78	pel.chalk/mdst.	" "	B	442 441
115/78	F.sst.	" "	D	408 433
117/78	v.c. CRW	" "	E	434 346
118/78	C.CRN	" "	E	434 346
121/78*	v.c.CRN	" "	E	434 346
125/78*	F.sst.	" "	E	434 346
126/78*	M.sst.	" "	G	432 352
128/78	basalt clast	" "	G	432 352
131/78	F.sst.	" "	H	427 364

Spec. No.	Description	Formation	Logged Section	Grid Reference
140/78	M.sst.	Salir Formation	H	427 365
143/78*	pb.cgl.	" "	H	426 366
143a/78	c.sst.	" "	H	425 366
145/78	M.sst.	" "	H	425 367
147/78*	c.sst.	" "	H	424 368
149/78	F.sst.	" "	H	424 368
153/78*	M.CRN	Eoc. lst.	-	385 526
158/78	F.sst.	Salir Formation	J	383 428
160/78*	F.sst.	" "	J	383 428
161/78	Carb.M.sst.	" "	J	383 428
163/78	M.sst.	" "	K	408 414
169/78*	v.c.CRN	" "	M	396 394
172/78	lst.breccia	" "	M	396 394
174/78	clt.silicified	Carbonate Platform	-	394 392
176/78	red. numm.CRN	" "	-	394 392
181/78*	M.sst.	Salir Formation	N	348 451
183/78	M.sst.	" "	N	348 451
184/78	v.c.sst.	" "	N	347 451
186/78	pel.chalk	" "	N	347 451
191/78*	M.sst.	" "	O	331 461
194/78	pb.cgl.	" "	O	331 461
197/78	M.sst.	" "	P	412 382
199/78	F.sst.	" "	P	412 382
204/78*	silic.CRN	" "	Q	399 385
205/78*	chert nodule	Eoc. lst.	-	526 380
208/78	v.c.sst.	Salir Formation	R	389 415
210/78*	c.sst.	" "	R	389 415
211/78*	M.sst.	" "	R	389 415
212/78*	M.sst.	" "	R	389 415
222/78	lst.breccia	" "	T	406 407
223/78	M.calc.sst.	" "	T	410 408
225/78	c.sst.	" "	T	411 412
230/78*	c.sst.	" "	T	411 412
237/78	c.sst.	" "	T	408 414
239/78	M.sst.	" "	U	410 415
242/78*	c.sst.	" "	U	410 415
246/78*	M.sst.	" "	U	412 420
251/78	lst.breccia	" "	V	381 417
252/78	calc.mudst.	" "	V	381 417
270/78	gl.cgl.	" "	25	511 409
274/78	pel.lst.red clast	" "	25	511 409
277/78	lst.breccia	" "	26	505 410
279/78	M.calc.sst.	" "	26	510 412
286/78	c.sst.	" "	27	510 416
94	gl.cgl.	" "	99	517 389
917	lst.breccia	" "	716	514 398
918	gl.cgl.	" "	716	514 398
924	gl.cgl.	" "	724	517 384
925	lst.breccia	" "	724	517 384
929	v.c.sst.	" "	727	519 365
945	pel.clt.	" "	1	526 336
946*	pel.clt.	" "	1	527 336
970	v.c.sst.	" "	745	521 364
971	clt.	" "	745	522 364
974	gl.cgl.	" "	745	522 364

Spec. No.	Description	Formation	Logged Section	Grid Reference
9104	pel.chalk	Salir Formation	764	372 338
9118*	F.sst.	" "	775	425 368
9120	pel.clt.	" "	775	425 369
9122*	pel.clt.	" "	775	425 369
9126*	c.sst.	" "	-	356 308
9129*	M.sst.	" "	778	425 382
9131	pel.clt.	" "	778	425 382
9132	F.sst.	" "	778	425 382
9136*	C.CRN	" "	778	426 383
9137*	M.CRN	" "	778	426 383
9138*	gl.cgl.	" "	778	426 383
9139*	F.calc.sst.	" "	778	426 383
9142	c.sst.	" "	780	383 309
9144	pel.clt.	" "	-	415 405
9165*	M.sst.	" "	791	384 311
9166*	M.sst.	" "	791	384 311
9174*	M.calc.sst.	" "	791	384 311
9174a	lst.breccia	" "	791	383 311
9176	lst.breccia	" "	791	383 311
9177*	F.sst.	" "	791	383 311
9178	lst. breccia	" "	791	383 311
9179	pel.clt.	" "	791	383 311
9181	lst.breccia	" "	791	383 408
9184*	gl.cgl.	" "	791	383 408
9191	M.sst.	" "	792	422 392
9203	M.calc.sst.	Kemer Formation	799	442 305
9204	c.calc.sst.	" "	799	443 304
9205*	M.calc.sst.	" "	799	444 302
9210	pb.cgl.	" "	7100	440 300
9215*	M.CRN	Cağman Member	7105	627 298
9217*	M.CRN	" "	7105	627 298
9220*	v.c.CRN	Felenk Dağ Member	7107	396 153
9226*	F.CRN	" " "	7111	402 154
9227	pel.clt.	" " "	7112	396 153
9228	pel.clt.	" " "	7112	396 153
9229*	C.CRN	" " "	7113	393 156
9230*	pel.clt.	" " "	7113	393 156
9231*	C.CRN.	" " "	7113	394 156
9232	F.CRN carbonaceous	" " "	7114	407 148
9234*	F.CRN carbonaceous	" " "	7114	406 148
9235*	F.CRN	" " "	7114	405 147
9243	VF. CRN	" " "	7115	407 152
9244	pel.clt.	" " "	7115	407 152
9248	v.c. CRN	" " "	7115	407 153
9267	numm.lst.	Carbonate Platform (Eoc)	-	635 300
9275*	v.c.calc.sst.	Kemer Formation	7122	442 271
9278*	F.sst.	" "	7124	539 281
9280	c.sst.	" "	7124	538 283
9281*	F.sst.	" "	7124	537 284
9284*	c.sst.	" "	7124	536 290
9291*	M.sst.	" "	7124	534 295

Spec. No.	Description	Formation	Logged Section	Grid Reference
9292*	v.f.sst.	Kemer Formation	7124	530 302
9297	C.CRN	Cağman Member	7125	642 304
9305	calcrete	Şalir Formation	-	386 295
9310*	F.sst.	Felenk Dağ Member	7128	426 149
9313	M.sst	" " "	7128	426 140
9315*	SLST.calc.	" " "	7128	425 148
9317*	M.CRN	" " "	7128	425 148
9318*	M.sst.	" " "	7128	425 148
9338*	c.sst.	Cağman Member	7129	635 294
9339	F.sst.	" "	7129	634 295
9344*	F.CRN	" "	7129	634 295
9345	F.CRN	" "	7129	630 296
9348*	C.CRN	" "	7129	628 297
9355	lst.cgl.	" "	7129	627 298
9361	F.CRN	Felenk Dağ Member	7130	382 152
9364	lst.breccia	" " "	7130	385 153
9386	F.CRN	" " "	7136	428 142
9389*	F.CRN	" " "	7136	427 140
9394*	pel.clt.	" " "	7136	426 139
9400	C.CRN	" " "	7136	425 136
9405*	M.calc.sst.	Kemer Formation	7139	529 305
9411	c.sst.	Salir Formation	7143	390 278
9414	gl.CRN	Cağman Member	-	
9415*	M.calc.sst.	" "	7145	600 288
9417*	M.CRN	" "	7145	595 287
9419*	C.CRN	" "	7145	593 288
9420*	F.CRN	" "	7145	592 289
9422	M.CRN	" "	7145	588 290
9423*	M.calc.sst.	" "	7145	585 291
9425	F.CRN	" "	7145	583 291
9428	M.CRN	" "	7145	580 292
9431	M.sst.	Eocene flysch	-	385 450
9433	pel.clt.	Salir Formation	-	415 405
9436*	M.CRN	Cağman Member	-	606 288
9437*	F.CRN	" "	-	604 287
18/80*	v.c.sst.	Kasaba Formation	4	517 361
30/80	pel.clt	Kemer Formation	-	575 290
33/80	M.sst.	" "	-	574 292
38/80	M.calc.sst.	" "	-	572 292
43/80*	algal.lst.	Carbonate Platform(Mioc)	9.80	432 308
49/80*	lst.breccia	Kemer Formation	9.80	485 517
50/80*	lst.breccia	" "	9.80	485 517
52/80	lst.breccia	Kasaba Formation	11.80	518 368
53/80*	lst.breccia	" "	11.80	518 368
59/80	c.sst.green	" "	11.80	518 368
64/80*	c.sst.	" "	16.80	520 357
66/80*	M.sst.	" "	16.80	520 357
68/80	M.sst.(red)	" "	16.80	520 357
69/80*	c.sst.(red)	" "	16.80	520 357
70/80*	c.sst.(red)	" "	16.80	520 357
71/80*	calcrete	" "	16.80	520 357
72/80*	M.sst.	Kemer Formation	16.80	520 357
77/80*	clt.	Carbonate Platform	18.80	395 143

Spec. No.	Description	Formation	Logged Section	Grid Reference
79/80	F.CRN	Felenk Dağ Member	18.80	395 143
80/80*	C.CRN	" " "	18.80	396 143
81/80*	marl	" " "	18.80	396 143
82/80*	muddy clt.	" " "	18.80	396 143
107/80	lst.breccia	Cağman Member	-	627 301
113/80*	v.c.CRN	carbonate platform	22.80	634 297
118/80*	F.CRN	Cağman Member	22.80	634 297
121/80*	M.CRN	" "	22.80	633 298
124/80*	v.c.CRN	" "	-	620 287
126/80*	M.CRN	" "	-	623 288
127/80	lst.breccia	" "	-	624 289
128/80*	v.c.CRN	" "	-	624 289
129/80*	M.CRN	" "	-	624 289
130/80	lst.breccia	" "	-	630 300
131/80*	c.CRN	" "	-	630 300
132/80	M.CRN	" "	-	630 300
138/80	reworked numm.lst.	" "	23.80	635 305
139/80*	numm. lst.	Carbonate platform (Eoc)	24.80	650 304
140a/80*	clt.	" "	24.80	649 304
143/80*	clt.	" "	24.80	647 305
144/80	algal lst.	Carbonate Platform	24.80	647 305
145/80*	lst.breccia	" "	24.80	644 305
146/80*	clt.	" "	24.80	644 305
148/80	lst.breccia	Cağman Member	25.80	642 305
155/80	F.CRN	" "	25.80	617 284
156/80	lst.breccia	" "	25.80	616 284
160/80	algal lst.	Carbonate Platform (Mioc)	26.80	376 171
161/80	M.CRN	" "	26.80	378 170
162/80*	M.CRN	" "	26.80	380 168
163/80	clt.	" "	26.80	381 167
164/80	c.CRN	" "	26.80	381 166
166/80	lst.breccia	" "	26.80	381 166
169/80*	clt.clast	Felenk Dağ Member	-	389 160
171/80*	lst.breccia	" " "	27.80	398 154
174/80*	lst.breccia	" " "	27.80	398 154
178/80	c.sst	Kemer Formation	28.80	490 328
183/80	M.CRN	Kasaba Formation	29.80	501 332
186/80	F.sst	Cağman Member	30.80	594 288
190/80*	lst.breccia	" "	30.80	593 290
196/80	v.c.CRN	" "	30.80	592 291
197/80*	F.CRN	" "	30.80	585 291
199/80*	c.sst.	" "	30.80	583 293
203/80*	F.CRN	" "	30.80	583 292
205a/80*	calcrete	Kasaba Formation	-	521 360
209/80	M.CRN	Cağman Member	30.80	581 293
212/80*	F.CRN	" "	30.80	580 294
234/80	M.sst.	Eoc. flysch	38.80	370 437
237/80	gl.cgl.	" "	38.80	365 440
246/80	F.CRN	Carbonate platform (Mioc)	42.80	373 394
247/80*	algal lst.	" "	42.80	373 394
248/80	M.CRN	" "	42.80	372 395
249/80*	numm.lst.	" "	42.80	372 395

Spec. No.	Description	Formation	Logged Section	Grid Reference
250/80	clt.	Carbonate platform (Mioc)	42.80	370 395
251/80*	clt.	" "	42.80	368 395
252/80	clt.	" "	42.80	366 396
254/80*	clt.	" "	42.80	365 396
257/80	v.c.sst.	Kemer Formation	43.80	362 393
258/80	pb.cgl.	" "	43.80	362 393
262/80	M.sst.	" "	44.80	363 386
263/80	M.sst.	" "	44.80	363 386
263/80	M.sst.	" "	Korkuteli area	
264/80	gl.cgl.	" "	"	"
281/80*	M.sst.clast	" "	40.80	393 457
283/80	lst.breccia clast	" "	43.80	363 394
287/80*	peridotite clast	Kemer Formation	43.80	363 394
289/80*	pyroxenite clast	" "	43.80	363 394
290/80*	peridotite clast	" "	43.80	363 394
291/80	lst.breccia clast	" "	43.80	363 394
299/80*	lst.breccia	Salir Formation	-	382 430
301/80	clt.det.block	" "	-	410 401
312/80	v.c.CRN	Kemer Formation	-	398 454
315/80	c.sst.	Eoc. flysch	51.80	362 437
317/80	M.sst.	" "	51.80	360 438
318/80*	c.calc.sst.	" "	51.80	360 438
320/80*	c.sst.	Kemer Formation	Korkuteli area	
322/80*	M.CRN	" "	"	"
337/80	numm.lst.	Carbonate Platform (Eoc)	-	440 287
339/80	stromatolite	Carbonate Platform (Cret)	-	440 287
342/80*	peridotite clast	Kemer Formation	-	440 287
344/80	serp.clast	" "	-	440 287
345/80*	gabbro clast	" "	-	440 287
346/80*	dolerite clast	" "	-	440 287
346a/80	algal lst.clast	" "	-	440 287
347/80*	serp.clast	" "	-	440 287
348/80*	peridotite clast	" "	-	440 287
356/80*	algal lst.	Carbonate platform (Eoc)	59.80	505 250
358/80*	algal lst.	" "	59.80	530 246
363/80	algal lst.	" "	60.80	457 168
368/80	algal lst.	Carbonate (Mioc) "	61.80	380 165
377/80	c.CRN	Carbonate (Eoc) "	63.80	690 413
378/80*	v.c.CRN	" "	63.80	690 413
379/80*	c.CRN		63.80	690 413
385/80*	algal lst.	" "	64.80	660 408
386/80	muddy clt.		64.80	660 408
389/80	CRN	" "	-	609 412
394/80	m.sst.	Kemer Formation	70.80	530 304
400/80	c.CRN	Carbonate platform (Mioc)	-	387 258
403/80	c.sst.	Kemer Formation	-	394 253
403a/80	algal CRN	" "	-	445 446

Spec. No.	Description	Formation	Logged Section	Grid Reference
414/80*	c.sst.	Kemer Formation	74.80	532 318
416/80*	M.sst.	" "	74.80	532 319
418/80	c.sst.	Kasaba Formation	76.80	526 367
419/80	m.sst.red	" "	76.80	526 367
423/80*	F.sst.	" "	79.80	496 338
424/80*	m.sst.	" "	79.80	496 338
431/80	M.CRN	Miocene	Kalkan area	
433/80	lst.breccia	Eoc. lst.	-	532 290
435/80*	algal stromatilite	Carbonate platform (Cret)	-	521 350
436/80*	clt.	" "	-	520 350
439/80	pel.clt.	Salir Formation	-	420 400
446/80	pel.clt.	" "	-	420 400
457/80	F.CRN	Carbonate platform (Mioc)	-	Hordubek Yayli
458/80	algal CRN	" "	-	" "
459/80	algal lst.	" "	-	" "
936/80	algal lst.	carbonate platform	-	380 425
UM7	F.CRN	Kasaba Formation	-	501 331
4.0.80	lst.	Çağman Member	8.80	601 288
4.1.8.80	C.CRN	" "	8.80	601 288
6.1.8.80	clt.clast	" "	8.80	601 288
7.1.8.80	f.CRN	" "	8.80	601 288
7.1.1.80	lst.breccia	" "	8.80	601 288
9.1.8.80	v.c.CRN	" "	8.80	605 287
11.1.80	lst.breccia	" "	8.80	605 287
13.1.8.80*	c.CRN	" "	8.80	606 286
2.8.80	lst.breccia	" "	8.80	606 286
4.2.8.80*	c.CRN	" "	8.80	606 286
5.2.8.80*	c.CRN	" "	8.80	606 286
6.2.2.80	c.CRN	" "	8.80	606 286

Appendix C(I)

Pull-out Key to Sedimentological Logs

K E Y T O S E D I M E N T O L O G I C A L L O G S (Appendix C (1))

Lithologies and Grain Size

General Logs

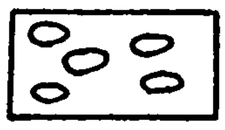

conglomerate (terrigenous)

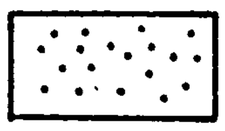

sandstone (terrigenous)

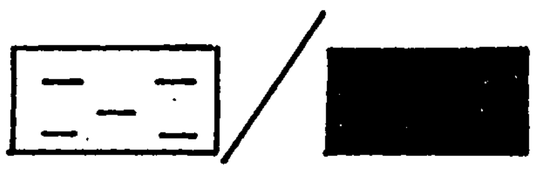

mudstone

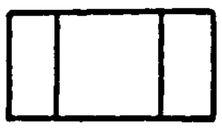

limestone

calcareous-terrigenous

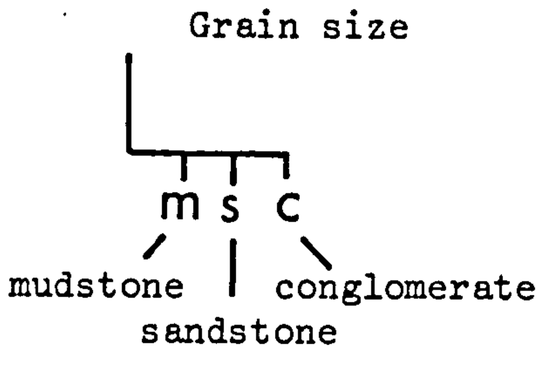

Logs in Limestone sequence

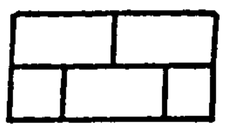

shallow water (neritic) limestone

pelagic limestone

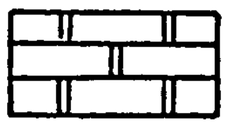

redeposited limestone

Detailed logs (as in general logs, in addition)

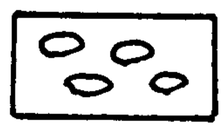

clast-supported conglomerate

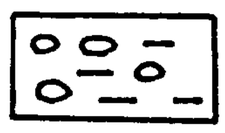

matrix (mud) - supported conglomerate

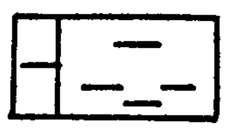

marl

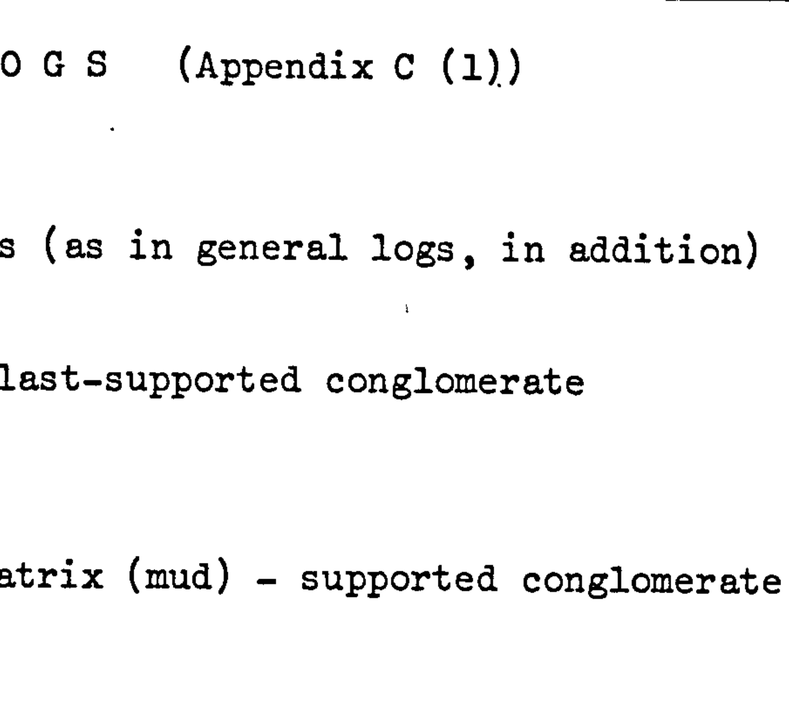

Computer drawn logs

Lithology

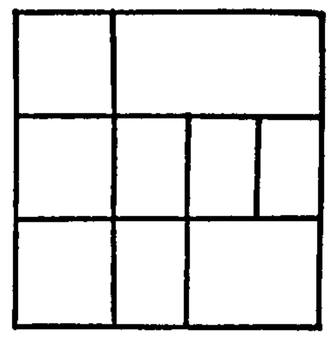

terrigenous

limestone

calcareous terrigenous

Grain size

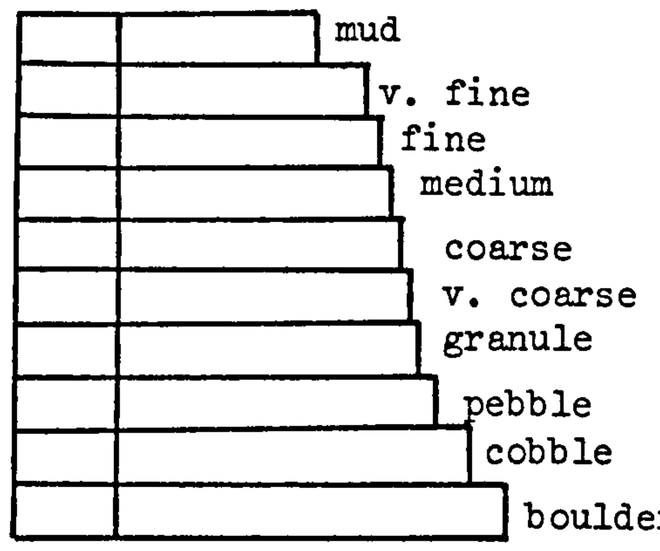

mud
v. fine
fine
medium
coarse
v. coarse
granule
pebble
cobble
boulder

Bed thickness for generalised intervals

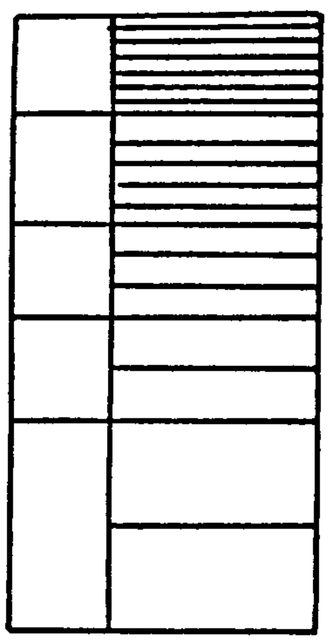

very thin (1-3 cm)

thin (3-10 cm)

medium (10-30 cm)

thick (30 cm - 1 m)

very thick (1- 3 m)

Appendix C(II)

Pull-out Key to Sedimentological Logs

KEY TO SEDIMENTOLOGICAL LOGS (Appendix C (II))

Symbols

Sedimentary structures

trough-cross-stratification

planar-cross-stratification

imbrication

ripple-cross-lamination

convolute lamination

wave reworked upper part of bed

$_s$ parallel stratified (shallow marine)

$_{st}$ parallel stratified (redeposited)

parallel lamination

small mudstone intraclasts (<5 cm)

large mudstone intraclasts (>5 cm)

flute or groove (sole) marks

soft sediment loading

slump horizon

Tab refers to Bouma division

P pelagic chalk

Cp calcrete

generalised palaeocurrent reading

Er erosion (unconformity) surface

Ba bauxite

fining-upwards

coarsening-upwards

Contacts (between beds)

erosive

irregular (sharp)

planar

gradational

Fossils

bivalves (intact)

bivalves (broken)

coral fragments

gastropods

stromatolites

coralline algal nodules (rhodoliths)

benthonic foraminifera

planktonic foraminifera

horizontal bioturbation

vertical bioturbation

CONTAINS

PULLOUTS